Pertanika Journal of

TROPICAL AGRICULTURAL SCIENCE

JTAS

VOL. 49 (5) OCT. 2026

PERTANIKA JOURNALS

A scientific journal published by Universiti Putra Malaysia Press

Pertanika Journal of Tropical Agricultural Science
Pertanika Journal of Tropical Agricultural Science

PERTANIKA JOURNAL OF TROPICAL AGRICULTURAL SCIENCE

About the Journal

Overview

Pertanika Journal of Tropical Agricultural Science is an official journal of Universiti Putra Malaysia. It is an open-access online scientific journal. It publishes the scientific outputs. It neither accepts nor commissions third party content.

Recognised internationally as the leading peer-reviewed interdisciplinary journal devoted to the publication of original papers, it serves as a forum for practical approaches in improving quality on issues pertaining to tropical agriculture and its related fields.

Pertanika Journal of Tropical Agricultural Science currently publishes 6 issues per year (*January, February*, *May*, *June, August*, and *November*). It is considered for publication of original articles as per its scope. The journal publishes in **English** and it is open for submission by authors from all over the world.

The journal is available world-wide.

Aims and Scope

Pertanika Journal of Tropical Agricultural Science aims to provide a forum for high quality research related to tropical agricultural research. Areas relevant to the scope of the journal include agricultural biotechnology, biochemistry, biology, ecology, fisheries, forestry, food sciences, genetics, microbiology, pathology and management, physiology, plant and animal sciences, production of plants and animals of economic importance, and veterinary medicine.

History

Pertanika was founded in 1978. Currently, as an interdisciplinary journal of agriculture, the revamped journal, *Pertanika* Journal of Tropical Agricultural Science now focusses on tropical agricultural research and its related fields.

Vision

To publish journals of international repute.

Mission

Our goal is to bring the highest quality research to the widest possible audience.

Quality

We aim for excellence, sustained by a responsible and professional approach to journal publishing. Submissions are guaranteed to receive a decision within 90 days. The elapsed time from submission to publication for the articles averages 180 days. We are working towards decreasing the processing time with the help of our editors and the reviewers.

Abstracting and Indexing of Pertanika

Pertanika Journal of Tropical Agricultural Science is now over 47 years old; this accumulated knowledge has resulted in *Pertanika* Journal of Tropical Agricultural Science being abstracted and indexed in Journal Citation Reports (JCR-Clarivate), SCOPUS (Elsevier), BIOSIS, National Agricultural Science (NAL), Google Scholar, MyCite, and ISC.

Citing Journal Articles

The abbreviation for *Pertanika* Journal of Tropical Agricultural Science is *Pertanika J. Trop. Agric. Sci*.

Publication Policy

Pertanika policy prohibits an author from submitting the same manuscript for concurrent consideration by two or more publications. It prohibits as well publication of any manuscript that has already been published either in whole or substantial part elsewhere. It also does not permit publication of manuscript that has been published in full in proceedings.

Code of Ethics

The *Pertanika* journals and Universiti Putra Malaysia take seriously the responsibility of all its journal publications to reflect the highest publication ethics. Thus, all journals and journal editors are expected to abide by the journal's codes of ethics. Refer to *Pertanika*'s **Code of Ethics** for full details, available on the official website of *Pertanika*.

Originality

The author must ensure that when a manuscript is submitted to *Pertanika*, the manuscript must be an original work. The author should check the manuscript for any possible plagiarism using any programme such as Turnitin or any other software before submitting the manuscripts to the Editorial Office, *Pertanika* Journal Publication Section.

All submitted manuscripts must be in the journal's acceptable **similarity index range**:
≤ 20% – *PASS*; **> 20%** – *REJECT*.

International Standard Serial Number (ISSN)

An ISSN is an 8-digit code used to identify periodicals such as journals of all kinds and on all media–print and electronic. All *Pertanika* journals have an e-ISSN.

Pertanika Journal of Tropical Agricultural Science: e-ISSN 2231-8542 (Online).

Lag Time

A decision on acceptance or rejection of a manuscript is expected within 90 days (average). The elapsed time from submission to publication for the articles averages 180 days.

Authorship

Authors are not permitted to add or remove any names from the authorship provided at the time of initial submission without the consent of the journal's Chief Executive Editor.

Manuscript Preparation

For manuscript preparation, authors may refer to *Pertanika*'s **INSTRUCTION TO AUTHORS**, available on the official website of *Pertanika*.

Editorial Process

Authors who complete any submission are notified with an acknowledgement containing a manuscript ID on receipt of a manuscript, and upon the editorial decision regarding publication.

Pertanika follows a **double-blind peer review** process. Manuscripts deemed suitable for publication are sent to reviewers. Authors are encouraged to suggest names of at least 3 potential reviewers at the time of submission of their manuscripts to *Pertanika,* but the editors will make the final selection and are not, however, bound by these suggestions.

Notification of the editorial decision is usually provided within 90 days from the receipt of manuscript. Publication of solicited manuscripts is not guaranteed. In most cases, manuscripts are accepted conditionally, pending an author's revision of the material.

The Journal's Peer Review

In the peer review process, 2 or 3 referees independently evaluate the scientific quality of the submitted manuscripts. At least 2 referee reports are required to help make a decision.

Peer reviewers are experts chosen by journal editors to provide written assessment of the **strengths** and **weaknesses** of the written research, with the aim of improving the reporting of research and identifying the most appropriate and highest quality material for the journal.

Operating and Review Process

What happens to a manuscript once it is submitted to *Pertanika*? Typically, there are 7 steps to the editorial review process:

Pertanika Journal of Tropical Agricultural Science
Pertanika Journal of Tropical Agricultural Science

1. The journal's Chief Executive Editor and Editor-in-Chief examine the paper to determine whether it is relevance to the journal's needs in terms of novelty, impact, design, procedure, language as well as presentation and allow it to proceed to the reviewing process. If it is not appropriate, the manuscript is rejected outright and the author is informed.

2. The Chief Executive Editor sends the article-identifying information having been removed, to 2 or 3 reviewers. They are specialists in the subject matter of the article. The Chief Executive Editor requests that they complete the review within 3 weeks.

   Comments to authors are about the appropriateness and adequacy of the theoretical or conceptual framework, literature review, method, results and discussion, and conclusions. Reviewers often include suggestions to strengthening of the manuscript. Comments to the editor are in the nature of the significance of the work and its potential contribution to the research field.

3. The Editor-in-Chief examines the review reports and decides whether to accept or reject the manuscript, invite the authors to revise and resubmit the manuscript, or seek additional review reports. In rare instances, the manuscript is accepted with almost no revision. Almost without exception, reviewers' comments (to the authors) are forwarded to the authors. If a revision is indicated, the editor provides guidelines to the authors to attend to the reviewers' suggestions and perhaps additional advice on how to revise the manuscript.

4. The authors decide whether and how to address the reviewers' comments and criticisms and the editor's concerns. The authors return a revised version of the paper to the Chief Executive Editor along with specific information describing how they have answered' the concerns of the reviewers and editor, usually in a tabular form. The authors may also submit a rebuttal if there is a need especially when the authors disagree with certain comments provided by the reviewers.

5. The Chief Executive Editor sends the revised manuscript out for re-review. Typically, at least 1 of the original reviewers will be asked to examine the article.

6. When the reviewers have completed their work, the Editor-in-Chief examines their comments and decides whether the manuscript is ready to be published, needs another round of revisions, or should be rejected. If the decision is to accept, the Chief Executive Editor is notified.

7. The Chief Executive Editor reserves the final right to accept or reject any material for publication, if the processing of a particular manuscript is deemed not to be in compliance with the S.O.P. of *Pertanika.* An acceptance notification is sent to all the authors.

   The editorial office ensures that the manuscript adheres to the correct style (in-text citations, the reference list, and tables are typical areas of concern, clarity, and grammar). The authors are asked to respond to any minor queries by the editorial office. Following these corrections, page proofs are mailed to the corresponding authors for their final approval. At this point, **only essential changes are accepted**. Finally, the manuscript appears in the pages of the journal and is posted online.

Pertanika Journal of

TROPICAL AGRICULTURAL SCIENCE

Vol. 49 (5) Oct. 2026

PERTANIKA JOURNALS

A scientific journal published by Universiti Putra Malaysia Press

PJTAS

***Pertanika* Journal of Tropical Agricultural Science**

AN INTERNATIONAL PEER-REVIEWED JOURNAL

UNIVERSITY PUBLICATIONS COMMITTEE

CHAIRMAN
Zamberi Sekawi

EDITOR-IN-CHIEF
Md Kamal Uddin
Agricultural technology, Agronomy, Plant Science, Soil Science

JOURNAL SECTION
Head of Section:
Navaneetha Krishna Chandran

Journal Officers:
Ain Haziqah Ab Razak
Nur Izni Shafiqah Mohd Hamidi
Saundarya Saran

Editorial Assistants:
Zulinaardawati Kamarudin

Pre-press Officers:
Aisyah Umairah Jasmin
Engku Erina Zahirah Engku Mohd Suhaimi
Ku Ida Mastura Ku Baharom

IT Officer:
Kiran Raj Kaneswaran

Journal Section Office
Putra Science Park
1st Floor, IDEA Tower II
UPM-MTDC Technology Centre
Universiti Putra Malaysia
43400 UPM Serdang
Selangor, Malaysia

General Enquiry
Tel. No: +603 9769 1622
E-mail:
pertanika.proceeding@upm.edu.my
URL:
http://www.pertanika.upm.edu.my/

PUBLISHER
UPM Press Centre
Universiti Putra Malaysia
43400 UPM Serdang
Selangor, Malaysia
Tel: +603 9769 3606
E-mail: dir.penerbit@upm.edu.my
URL: http://penerbit.upm.edu.my

EDITORIAL BOARD 2024-2026

Abd. Razak Alimon
Animal Production, Animal Nutrition
Universitas Gadjah Mada, Indonesia

Alan Dargantes
Veterinary Epidemiology and Surveillance, Disease Diagnostics and Therapeutics, Disease Ecology
Central Mindanao University, Philippines

Amin Ismail
Food Biochemistry
Universiti Putra Malaysia, Malaysia

Azamal Husen
Plant Stress Physiology, Nanoparticles, Plant Propagation, Tree Improvement, Medical Plants
Wolaita Sodo University, Ethiopia

Chye Fook Yee
Food Science and Nutrition, Food Microbiology, Food Biotechnology
Universiti Putra Malaysia, Malaysia

Faez Firdaus Jesse Abdullah
Ruminant Medicine
Universiti Putra Malaysia, Malaysia

Faridah Abas
Bioactive Compounds, Natural Products Chemistry, Metabolomics, LCMS, Functional Food
Universiti Putra Malaysia, Malaysia

Indika Herath
Soil Science, Environmental Impact, Crop Water Use, Water Footprint, Carbon Footprint
Wayamba University of Sri Lanka, Sri Lanka

Kadambot H. M. Siddique
Crop and Environment Physiology, Germplasm Enhancement
University of Western Australia, Australia

Kavindra Nath Tiwari
Plant Biotechnology, Natural Products
Banaras Hindu University, India

Khanitta Somtrakoon
Bioremediation, Phytoremediation, Environmental Microbiology
Mahasarakham University, Thailand

Lai Oi Ming
Esterification, Lipase, Fatty Acids, Transesterification
Universiti Putra Malaysia, Malaysia

Md. Tanvir Rahman
Antimicrobial Resistance/AMR, Virulence and Pathogenesis, Vaccine, Microbial Ecology, Zoonoses, Food Hygiene and Public Health
Bangladesh Agricultural University, Bangladesh

Mohammad Noor Amal Azmal
Fish Disease Diagnosis, Fish Disease Epidemiology, Development of Fish Vaccines
Universiti Putra Malaysia, Malaysia

Mohd Effendy Abdul Wahid
Immunology, Pathology, Bacteriology, Vaccine
Universiti Malaysia Terengganu, Malaysia

Najiah Musa
Bacteriology, Biopharmaceuticals, Disease of Aquatic Organisms
Universiti Malaysia Terengganu, Malaysia

Norhasnida Zawawi
Bichemistry, Food Science, Food Chemistry, Antioxidant Activity, Food Analysis
Universiti Putra Malaysia, Malaysia

Phebe Ding
Postharvest Physiology
Universiti Putra Malaysia, Malaysia

Saw Leng Guan
Botany and Conservation, Plant Ecology
Curator of Penang Botanic Gardens, Malaysia

Shamshuddin Jusop
Soil Science, Soil Mineralogy
Universiti Putra Malaysia, Malaysia

Sivakumar Sukumaran
Plant Breeding, Molecular Breeding, Quantitative Genetics
University of Queensland, Australia

Tan Wen Siang
Molecular Biology, Virology, Protein Chemistry
Universiti Putra Malaysia, Malaysia

Tati Suryati Syamsudin
Ecology, Entomology, Invertebrate, Fruit Fly management
Institut Teknologi Bandung, Indonesia

Vincenzo Tufarelli
Animal Science, Animal Nutrition, Poultry Science
University of Bari 'Aldo Moro', Italy

Zora Singh
Horticulture, Production Technology and Post-handling of Fruit Crops
Edith Cowan University, Australia

INTERNATIONAL ADVISORY BOARD 2024-2027

Banpot Napompeth
Entomology
Kasetsart University, Thailand

Graham Matthews
Pest Management
Imperial College London, UK

ABSTRACTING AND INDEXING OF PERTANIKA JOURNALS

The journal is indexed in Journal Citation Reports (JCR-Clarivate), SCOPUS (Elsevier), BIOSIS, National Agricultural Science (NAL), Google Scholar, MyCite and ISC.

The publisher of Pertanika will not be responsible for the statements made by the authors in any articles published in the journal. Under no circumstances will the publisher of this publication be liable for any loss or damage caused by your reliance on the advice, opinion or information obtained either explicitly or implied through the contents of this publication.
All rights of reproduction are reserved in respect of all papers, articles, illustrations, etc., published in Pertanika. Pertanika provides free access to the full text of research articles for anyone, web-wide. It does not charge either its authors or author-institution for refereeing/publishing outgoing articles or user-institution for accessing incoming articles.
No material published in Pertanika may be reproduced or stored on microfilm or in electronic, optical or magnetic form without the written authorisation of the Publisher.
Copyright ©2026 Universiti Putra Malaysia Press. All Rights Reserved.

Pertanika Journal of Tropical Agricultural Science
Vol. 49 (5) Oct. 2026

Contents

Foreword xiii
Md Kamal Uddin

Review Article 2115
Synergy of *Bradyrhizobium* spp. and Co-Inoculants to Enhance Fertiliser Efficiency and Soybean Yield in Acid-Stressed Soils: A Systematic Review
Josephine Alexa Mada, Stanislaus Adhi Pramudya, Mieke Rochimi Setiawati, Fairus Hisanah Hibatullah, and Tualar Simarmata

Physiological and Metabolic Responses of Early Juvenile Blue Swimming Crab, *Portunus pelagicus*, to Dietary Deficiency 2133
Jamali Muhammad-Firdaus, Ariffin Hidir, Donald Torsabo, Hon Jung Liew, Mhd Ikhwanuddin, and Noordiyana Mat Noordin

Review Article 2155
A Review on the Use of Spices in the Blending of Malaysian Curry Powder Matrix
Chon Lok Siaw, Nyuk Ling Chin, and Nor Amaiza Mohd Amin

Biofertilisers and Micronutrients Enhance Productivity and Land-Use Efficiency of Cereal-Legume Intercropping Systems on Indonesian Drylands 2171
Yanto Surdianto, Nana Sutrisna, Muhammad Iskandar Ishaq, Bambang Susanto, Yiyi Sulaeman, Eni Maftu'ah, Dwi Purnamawati Widiastuti, Jumakir, and Agus Nurawan

Ameliorative Effects of dbcAMP and des (1-3) IGF-1 on Myogenic and Adipogenic mRNA Expression in Transdifferentiated C2C12 Myogenic Cells 2197
Muhamad Faris Ab Aziz , Zoe C.T.R. Daniel, Andrew Salter, and Tim Parr

Gallic Acid-Loaded Graphene Oxide (GAGO) Nanocomposite Attenuates Inflammatory Response in LPS-Stimulated RAW 264.7 Macrophages 2217
Nur Hazwani Norjoshukrudin, Ida May Jen Ng, Seri Narti Edayu Sarchio, Masriana Hassan, Shafinaz Abd Gani, and Suhaili Shamsi

Integrating *Brassica* spp. Residues and Bioethanol to Mitigate Disease and Enhance Potato Seed Yield in Medium-Altitude Regions 2237
Andi Muhibuddin, Zulkifli Maulana, Fatmawati, Haris Mahmud, and Andi Tenri Fada

Comparative Shelf-Life Predictions of Packaged Paddy Using Water Mass-Transfer Modelling and Quality-Deterioration Kinetics Under Different Controlled Relative Humidities 2257
Astriella Awwali Maissy, Sri Rahayoe, and Hanim Zuhrotul Amanah

Visible-Near Infrared Spectroscopy for Predicting Carotenoid and Antioxidant Composition in Healthy and Bronzed Jackfruit (*Artocarpus heterophyllus* Lam. cv. Tekam Yellow) at Different Maturity Stages 2275
Kok Jeng Lim, Phebe Ding, Nazmi Mat Nawi, and Mashitah Jusoh

Review Article 2303
An In-Depth Analysis of Cottonseed Oil and Its Composition, Digestibility, Health-Promoting Properties, Industrial Relevance, Animal Feed Value, and Green Technologies
Savanam Chandra Sekhar, Degala Pushpa Sri, Mohammed Irfan, Meeravali Shaik, B. Vasantha Lakshmi, Krishna Babu Sambaru, and Palagiri Tejovathi

Comparative Phytochemical and Biological Properties of Unripe *Spondias pinnata* Fruit Extract 2323
Rattana Meekrasae, Noppadon Somphol, Wuttisak Kunu, and Supawadee Patathananone

Antioxidant Film Packaging from Red Tilapia Fish Scale Gelatin with Kesum (*Persicaria Odorata*) Powder 2343
Nur Syazwani Yusri, Roseliza Kadir Basha, Siti Nurnajihah Salahuddin, Nazatul Shima Azmi, Farah Saleena Taip, Noor Zafira Noor Hasnan, and Nor Amaiza Mohd Amin

Comparison of Plant Nutrient Requirements During the Annual Phenological Development of Young Rubber Trees (*Hevea brasiliensis* Mull. Arg.) Prior to the Rubber Tapping Process in Upland and Lowland Areas 2361
Surachart Pechkeo and Sayan Sdoodee

Integrated Effects of DAP Fertiliser, Soil Amendments, and Nano-Biostimulant Foliar Application on Growth and Yield of Wheat 2387
Maher Adhafa Drai'am Al-Aboudi, Hayyawi W. A. Al-Juthery, and Luma Abdalalah Sagban Alabadi

Microalgae for Anti-Aging Cosmeceuticals: Synergistic Bioactivities and Physicochemical Potential 2413
Felicia Stella Indarto, Sook Chin Chew, Fatimah Md Yusoff, Malinna Jusoh, and Norazira Abdu Rahman

Combination Effects of Cocopeat and Chicken Manure on the Vegetative Growth and Yield Performance of Eggplant 2439
Kahar, Rian Christian Sondakh, and Irmawati

Two New Localisation Records of *Priacanthus sagittarius* (Starnes, 1988) in the Westernmost Part of the Levant Sea 2461
Alper Yıldız, M. Tunca Olguner, Mehmet Gökoğlu, Jale Korun, and Mesut Yılmaz

The Effect of Number of Shoots of Sorghum in First and Second Ratoon System 2467
Avisema Sigit Saputro, Samanhudi, Puji Harsono, and Supriyono

Identification and Diversity Analysis of *Uromycladium* on *Paraserianthes lophantha* subsp. *montana* Using a Multilocus Molecular Approach 2483
I Made Mayun Maha Diputra, Sri Rahayu, Intan Berlian, and Tanaka Chihiro

Aquaponics as a Sustainable Food Security Solution: Global Scholarly Trends and Intellectual Structure Analysis 2499
Nor Azilah Husin, Amirul Syafiq Mohd Ghazali, Azni Abdul Rashid, Nurzalyna Mohamed Zaki, and Nasser Al Yahyaei

Evaluation of the Aqueous Extracts of *Celosia argentea* L. (Plumosa Group) as a Bioherbicide for Dominant Weeds in Soybean Cultivation 2523
Safira Nur Aini, Dyah Weny Respatie, Aziz Purwantoro, and Qurrotul Uyun

Growth, SPAD Index, and Nitrogen Use Efficiency of Two *Axonopus compressus* Variants Under Soil Mixture Ratios and NPK Fertiliser Regimes 2545
Ting Zeng, Abdul Shukor Juraimi, Nazatul Shima Naharudin, Mahmudul Hasan, and Muhammad Saiful Ahmad-Hamdani

Classification and Prediction of Chilli Powder (*Capsicum Annuum* L.) Colour Based on Near-Infrared Spectra and Random Forest 2565
Nafis Khuriyati, Anggoro Cahyo Sukartiko, Ririn Nur Alfiani, Tyasto Prima Ahmadi, and Avicenna Nur Kasih

Microbiological Quality, Antibiotic Susceptibility and Stability of Human Breast Milk Microbiota Stored at Refrigerated Temperature 2581
Nur Hanis Salim, Zulfa Zakuan, Rashidah Sukor, Aliah Zannierah Mohsin, Yaya Rukayadi, Nurul Hawa Ahmad, Yu Suet Li, Siti Nabilah Karim, and Anis Shobirin Meor Hussin

Maximising Growth and Quality of *Caulerpa lentillifera* Through Multilevel Cultivation with LED Approach 2603
Nur Amira Yasmin Mohd Nizar, Jamil Tajam, Non Daina Masdar, Zamzila Erdawati Zainol, Mohamad Niza Md Nor, Khairul Naim Abd Aziz, and Sharir Aizat Kamaruddin

Foreword

Welcome to the fifth issue of 2026 of the Pertanika Journal of Tropical Agricultural Science (PJTAS)!

PJTAS is an open-access journal for studies in Tropical Agricultural Science published by Universiti Putra Malaysia Press. It is independently owned and managed by the university for the benefit of the world-wide science community.

This issue contains 25 articles: three review articles and the rest are regular articles. The authors of these articles come from different countries namely China, India, Indonesia, Iraq, Japan, Malaysia, Oman, Thailand, Turkey, and United Kingdom.

The review article entitled "A Review on the Use of Spices in the Blending of Malaysian Curry Powder Matrix" synthesises current knowledge on the principal spices used in formulating Malaysian curry powder to provide a scientific basis for quality control and product optimisation. Examining the integrated spice matrix across popular commercial brands, the study details how common ingredients such as coriander, cumin, fennel, chilli, turmeric, black or white pepper, cinnamon, star anise, cardamom, cloves, nutmeg, fenugreek, and ginger, contribute distinct sensory and functional properties. It correlates specific volatile compounds, including linalool, cuminaldehyde, trans-anethole, turmerones, and zingiberene, with their botanical sources and flavor profiles, while distinguishing the robust, redder characteristics of meat curry powders from the milder, more aromatic, and yellowish profiles of fish curry powders. Furthermore, the review outlines essential processing operations, quality parameters, and compliance with the Malaysian Food Regulations 1985 requirements, such as maintaining at least 85% spice content and a minimum volatile oil limit. Further details of this study can be found on page 2155.

The regular article entitled "Microalgae for Anti-Aging Cosmeceuticals: Synergistic Bioactivities and Physicochemical Potential" evaluates the antioxidant and anti-aging properties of ethanol-water extracts derived from Thalassiosira weissflogii TRG10-P105 (Tw), Arthrospira platensis (Sp), Chlorella vulgaris (Cv), and a 1:1 Sp-Cv mixture (SC). Utilising 90% ethanol as an optimal extraction solvent, the study established that Tw possessed high carotenoid and flavonoid content, whereas the SC mixture exhibited superior total phenolic content,

featuring diverse bioactive compounds like catechin, quercetin, ferulic acid, and caffeic acid, alongside strong radical-scavenging activity and potent collagenase inhibition reaching 100% at 10 μg mL^{-1}. When formulated into anti-aging creams at concentrations of 1% and 2.5%, both Tw and SC extracts yielded stable, skin-compatible, smooth, and easily spreadable topical emulsions, highlighting their viability as natural bioactive ingredients for cosmeceutical applications. Full details of this study are available on page 2413.

The regular article entitled "Maximising Growth and Quality of Caulerpa Lentillifera through Multilevel Cultivation with LED Approach" evaluates a multilevel cultivation arrangement for the edible green macroalga Caulerpa lentillifera (Laktud) under white LED, pink LED, and natural sunlight over a 28-day period at Kubang Badak, Langkawi. Assessing parameters such as frond density, frond length, plate weight, daily growth rate (DGR), and biomass yield across nine cultivation plates, the study found that white-LED plate W2 achieved the highest plate weight (1,305 g), frond density (79.33 per 100 cm^2), daily growth rate (0.018551 day^{-1}), and biomass yield (247.76 g m^{-2} day^{-1}). While sunlight-exposed plate S1 yielded the longest individual fronds (4.628 cm), natural sunlight exhibited significant variability across shelf positions, with lower tiers declining, whereas LED lighting provided more consistent growth performance across the multilevel setup. Further details of this study can be found on page 2603.

We anticipate that you will find the evidence presented in this issue to be intriguing, thought-provoking and useful in reaching new milestones in your own research. Please recommend the journal to your colleagues and students to make this endeavour meaningful.

All the papers published in this edition underwent Pertanika's stringent peer-review process involving a minimum of two reviewers comprising internal as well as external referees. This was to ensure that the quality of the papers justified the high ranking of the journal, which is renowned as a heavily-cited journal not only by authors and researchers in Malaysia but by those in other countries around the world as well.

We would also like to express our gratitude to all the contributors, namely the authors, reviewers and Editorial Board Members of PJTAS, who have made this issue possible.

PJTAS is currently accepting manuscripts for upcoming issues based on original qualitative or quantitative research that opens new areas of inquiry and investigation.

Editor-in-Chief
Md Kamal Uddin

Pertanika J. Trop. Agric. Sci. 49 (5): 2115 - 2132 (2026)

PERTANIKA JOURNALS

TROPICAL AGRICULTURAL SCIENCE

Journal homepage: http://www.pertanika.upm.edu.my/

Review Article

Synergy of *Bradyrhizobium* spp. and Co-Inoculants to Enhance Fertiliser Efficiency and Soybean Yield in Acid-Stressed Soils: A Systematic Review

Josephine Alexa Mada, Stanislaus Adhi Pramudya, Mieke Rochimi Setiawati, Fairus Hisanah Hibatullah, and Tualar Simarmata*

Department of Soil Science and Land Resources, Faculty of Agriculture, Padjadjaran University, 45363 Sumedang, Indonesia

ABSTRACT

Bradyrhizobium spp., as nitrogen-fixing bacteria, when combined with plant growth-promoting rhizobacteria such as *Azospirillum*, *Bacillus*, and *Pseudomonas*, alongside arbuscular mycorrhizal fungi (AMF), can sustain soil health and enhance soybean yields by working together to improve fertiliser efficiency, this approach has an impact on sustainable agriculture. Soybeans are a vital crop for soil regeneration in tropical agriculture, especially in regions with acidic soils. This systematic literature review evaluates how *Bradyrhizobium* and co-inoculants enhance biological nitrogen fixation, root nodule formation, and soybean growth. PRISMA guidelines and bibliometric analysis were employed to maintain scientific transparency and stringency. During the initial screening process, 12 out of 1,463 articles met the criteria, focusing on Rhizobiaceae-based inoculants and co-inoculation approaches in acidic soils. The results show that strategic co-inoculation significantly increased soybean yields by 8-88%, reduced reliance on chemical nitrogen fertilisers by approximately 30-50%, and enhanced nutrient use efficiency and root nodule formation. In addition to enhancing productivity, this technology has an impact on long-term soil rehabilitation, making it a vital component of climate-resilient and sustainable agriculture.

Keywords: Arbuscular mycorrhizal fungi, acidic soils, biofertiliser, co-inoculants, fertiliser efficiency, PGPR, soybean, symbiotic N-fixer

ARTICLE INFO

Article history:
Received: 08 July 2025
Accepted: 12 August 2026
Published: 30 October 2026

DOI: https://doi.org/10.47836/pjtas.49.5.01

E-mail addresses:
josephine21002@mail.unpad.ac.id (Josephine Alexa Mada)
stanislaus21001@mail.unpad.ac.id (Stanislaus Adhi Pramudya)
m.setiawati@unpad.ac.id (Mieke Rochimi Setiawati)
fairus23002@mail.unpad.ac.id (Fairus Hisanah Hibatullah)
tualar.simarmata@unpad.ac.id (Tualar Simarmata)
* Corresponding author

e-ISSN: 2231-8542

© Universiti Putra Malaysia Press

INTRODUCTION

Soybean (*Glycine max* L.) is a legume crop which is highly beneficial due to its capability of enhancing soil fertility through symbiotic nitrogen fixation, supporting the sustainability of cropping systems by facilitating the improvement of soil quality. In addition to its agroecological role, soybean provides plant-based protein with high-quality, essential amino acids and vegetable oil, making it an important commodity for global food security, nutrition, and animal feed. Soybeans' position is strengthened by this role as a key element of both agricultural productivity and environmental sustainability. However, soybean productivity is frequently constrained by acid-stressed soils, which are widespread in tropical and subtropical regions. These soils are characterised by low pH, aluminium (Al) toxicity, phosphorus (P) fixation and deficiency, manganese toxicity, calcium and magnesium deficiencies, and impaired biological nitrogen fixation, all of which restrict root development, microbial activity, nutrient availability, and ultimately soybean growth and yield (Li et al., 2023; Zahran, 1999). Previous studies have reported that soybeans grown under acidic soil conditions exhibit significant reductions in root development, nodulation, nutrient uptake, and grain yield due to these combined stresses (Bedassa et al., 2022).

To overcome constraints on soybean production in acid-stressed soils, increasing research has focused on the synergistic use of nitrogen-fixing *Bradyrhizobium* spp. and microbial co-inoculants, particularly plant growth-promoting rhizobacteria (PGPR) such as *Bacillus, Azospirillum,* and *Pseudomonas*, as well as arbuscular mycorrhizal fungi (AMF). These microbial symbionts have synergistic roles in enhancing root growth habit, phosphorus and micronutrient solubilisation, and induction of plant hormones such as indole-3-acetic acid (IAA), which increases plant abiotic stress tolerance to aluminum toxicity, low pH, and phosphorus deficiency (Ahmad et al., 2018; Khan et al., 2023).

AMF, in particular, form symbiotic relationships with soybean roots and create a productive root surface area through networks of hyphae that facilitate water and nutrient uptake, especially under compacted, acidic soils or low-nutrient conditions. AMF also induce aggregation and cycling of soil organic matter, which helps overall soil health. In combination with PGPR and *Bradyrhizobium*, these microbial consortia create a more favorable rhizosphere, enhance nodulation efficiency, and significantly boost biological nitrogen fixation. Recent studies have shown that such co-inoculation practices significantly enhance soybean yields—reported increases of up to 40–80% depending on soil conditions, while reducing the reliance on chemical nitrogen fertilisers (Moretti et al., 2020). Region-specific strain identification, inoculant with optimally formulated inoculants, and validation on a field scale across various agroecological zones need to be focused on in future studies (Santos et al., 2019).

In their capacity to overcome the constraint of soybean (*Glycine max* L.) cultivation in acid-stressed soils, symbiosis between soybean roots and *Bradyrhizobium* species plays a critical role in sustaining biological nitrogen fixation (BNF). Through this symbiosis,

Bradyrhizobium infects root tissues and nodules, where atmospheric nitrogen is biologically converted to ammonia, supplying the plant with an available and renewable source of nitrogen. In acidic soils, *Bradyrhizobium* inoculant quality is generally impaired by its sensitivity to low pH, aluminum (Al) toxicity, and disrupted microbial communication, leading to weak nodulation and nitrogen fixing activity.

These problems have been resolved using co-inoculation methods involving *Bradyrhizobium* spp., plant growth-promoting rhizobacteria such as *Azospirillum, Bacillus,* and *Pseudomonas*, and arbuscular mycorrhizal fungi (AMF). These microbial combinations enrich the rhizosphere environment through phytohormone (auxin) synthesis, phosphorus solubilisation, siderophore production, soil aggregation, and promotion of root elongation. They also indirectly reduce abiotic stresses and increase the colonisation ability and nitrogen fixation capacity of *Bradyrhizobium*. Co-inoculation also improves root system architecture by enhancing nutrient and water uptake under stress. Different studies have proven the synergistic effect of such a microbial mixture. Jabborova et al. (2021) noted that co-inoculation improved nodulation by 56% and shoot biomass by 48% under drought stress. Wei et al. (2023) documented that combining PGPR with *Bradyrhizobium* enhanced soybean yield by 32% in long-term trials, while Marinković et al. (2024) observed a yield increase of 44% under both stressed and non-stressed conditions. On different soils and ecosystems, these findings all reveal quantitative yield boosts ranging from 20% to 56%. These benefits result not only from enhanced nitrogen fixation and nutrient mobilisation but also from enhanced tolerance to abiotic stress. Most importantly, by supplying a significant portion of the plant's nitrogen demand biologically, co-inoculation helps reduce inorganic nitrogen fertiliser use, minimise environmental impact, and lower input costs. Therefore, co-inoculation with PGPR and arbuscular mycorrhizal fungi (AMF) alongside *Bradyrhizobium* is a sustainable, scalable, and climate-resilient method to increase soybean productivity in tropical agroecosystems with varying conditions and stresses such as soil acidity.

Despite numerous studies evaluating the role of *Bradyrhizobium* spp. and a wide variety of co-inoculants in enhancing soybean growth, recent evidence remains disjointed across multiple combinations of microbes, measured agronomic parameters, and environmental conditions. The majority of research projects have focused on specific aspects of plant growth or single inoculant; on the other hand, a comprehensive synthesis of the synergistic effects of *Bradyrhizobium* spp. combined with plant growth-promoting rhizobacteria (PGPR), arbuscular mycorrhizal fungi (AMF), and other beneficial microorganisms under acid-stressed soil conditions is still lacking. Moreover, identification of the most effective microbial consortium approaches for enhancing nodulation efficiency, nutrient uptake, fertiliser use efficiency, and sustainable soybean production has received lack of attention. Therefore, a systematic synthesis of the current evidence is needed to bridge these knowledge gaps and provide evidence-based recommendations for future research and practical agricultural applications.

Despite the increasing number of studies investigating the application of *Bradyrhizobium* spp. and microbial co-inoculants for soybean cultivation under acid-stressed soil conditions, several important research problems remain unresolved. The present review addresses the following research problems: (1) The most effective microbial consortium combinations, particularly the synergistic interactions between *Bradyrhizobium* spp., plant growth-promoting rhizobacteria (PGPR), and arbuscular mycorrhizal fungi (AMF), have not been systematically evaluated with respect to nodulation efficiency, nutrient uptake, fertiliser use efficiency, and soybean productivity; (2) The lack of an integrated synthesis of current findings limits the development of evidence-based inoculation strategies to support sustainable soybean cultivation in acid-affected tropical agroecosystems.

This systematic literature review aims to critically evaluate and summarise recent research on the contribution of *Bradyrhizobium* spp. and co-inoculants to enhancing soybean (*Glycine max* L.) growth in acidic soil conditions. The study specifically examines the synergistic effects of co-inoculation on nutrient uptake, root nodule formation, and yield improvement, identifying the most effective microbial combinations and application strategies to enhance inoculant efficacy and fertiliser use efficiency. The supreme objective is to provide insights based on evidence to sustain long-term and resilient soybean cultivation in tropical agroecosystems affected by environmental adversity such as acidic soil pressure.

MATERIALS AND METHODS

Literature Search Strategy

Literature search was carried out comprehensively using Scopus and ScienceDirect. The search utilised combinations of keywords such as "*Bradyrhizobium*", "Symbiotic nitrogen fixation", "Co-inoculants", "Biofertiliser PGPR", "Fertiliser efficiency", "Soybean productivity", and "Acid soils". The Boolean search strategy and the resulting outcomes are summarised in Table 1.

Table 1
Search strategy used to gather applicable research articles

Search Strategy	Scopus	ScienceDirect
Bradyrhizobium AND Soybean	78	20
Nitrogen fixation AND PGPR	43	31
Soybean AND Acidic soils	22	50
PGPR AND fertiliser AND efficiency	22	53
Co-inoculation AND Soybean AND acidic soils	0	276
Co-inoculants AND fertiliser efficiency	13	57
Soybean Productivity AND fertiliser efficiency	48	750
Total Articles		1463

Data Retrieval for Bibliometric Analysis

Metadata was fetched exclusively from Scopus and ScienceDirect using the same combination of keywords in the bibliometric analysis. The retrieval was restricted to English-language articles with a year of publication between 2020 and 2024. Bibliographic data were exported in RIS format and analysed using VOSviewer version 1.6.19 to map keyword co- occurrences, thematic clusters, and temporal trends. The minimum benchmark of five keyword co-occurrences with a 60% relevance score was applied to highlight key research trends in relation to the enhancement of soybean productivity through microbial approaches under acidic soil stress conditions.

Systematic Literature Review Using PRISMA

This systematic literature review conforms to the PRISMA 2020 guidelines. Articles were retrieved from Scopus and ScienceDirect using the same combination of keywords; 1,463 articles were identified at the initial stage, and 12 articles were considered qualified for in-depth textual analysis. Mendeley Reference Manager was used to remove the duplicates, and screening based on titles and abstracts was used as well. The article selection and screening process is illustrated in Figure 1. If the articles addressed the role of *Bradyrhizobium* spp.

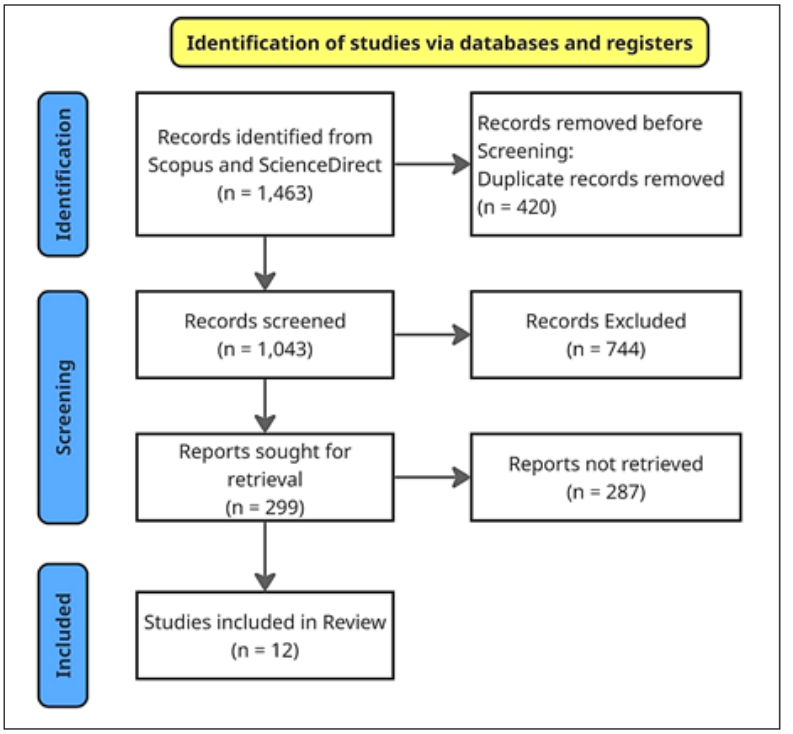

Figure 1. The PRISMA flow diagram outlining the stages of article selection for the systematic literature review

and co-inoculants in soybean growth in acidic soils and demonstrated measurable impacts on nutrient uptake, nodulation, or crop yield, they were included. The selection criteria are summarised in Table 2. These 12 articles are further summarised in Table 3 and form the ultimate evidence foundation, which presents the microbial agents, their functional roles, and the documented impacts under environmental adversity such as acidic soil stress.

Table 2
Approach used to gather applicable research articles

Criteria	Inclusion	Exclusion
Relevance topics	Journal focused on the application of *Bradyrhizobium* and co-inoculants in or relevant to soybean cultivation in acid soils	Journal without a core focus on the application of *Bradyrhizobium* and co-inoculants in or relevant to soybean cultivation in acid soils
Date of publication	2020-2024	< 2020
Type of publications	Research article	Book chapters, Encyclopedia, News, Conference abstracts
Language of publication	English	All other languages
Databases	Scopus and ScienceDirect	Articles that are not indexed by Scopus

RESULTS AND DISCUSSION

Bibliometric Analysis

Bibliometric analysis was undertaken using VOSviewer to uncover emerging themes and research trends from the past five years. Visual representations, including binary counting, were employed to create co- occurrence maps of document keywords. To identify 49 key keywords through diverse search methods, the minimum co-occurrence threshold for document keywords in the research articles was set at 5, with 60% relevance.

The network visualisation illustrates the connectivity among key concepts in soil microbiology, plant growth-promoting rhizobacteria (PGPR), and sustainable agriculture. The thematic groups are differentiated by colour: blue includes microbial agents linked with PGPR, green covers soybean plants' physiological responses, and red reflects agronomic management practices.

The blue colour (PGPR group) covers terms such as *Pseudomonas, Bacillus*, IAA production, and bioinoculant. The role of symbiotic microbes in stimulating plant growth under abiotic stress is represented by these terms; research by Ashwin et al. (2022) and Widodo et al. (2022) is in line with these findings, which substantiated that rhizobacterial inoculation enhances phosphorus solubilisation, root nodule formation, chlorophyll content, and seedling vigour. The green colour (soybean group) covers terms such as tolerance, abiotic stress, and seed germination. It emphasises that combining *Azospirillum brasilense* and *Bradyrhizobium* inoculation is important to enhance productivity under

Table 3
Microbial contributions to soybean cultivation under acid-stressed soil conditions

Microbial Agent	Functional Role	Benefit in Acid-Stressed Soils	Impact on Soybean Productivity (with Reference)
Bradyrhizobium japonicum, *Bradyrhizobium elkanii*, and *Sinorhizobium fredii*	Symbiotic nitrogen fixation; Host-specific Nod factor & T3SS signalling	Increase resistance to low pH, high temperature, salinity and high nitrate	Delay of nodule senescence & increased nitrogen fixation resulting in higher yields (Li et al., 2020)
Bradyrhizobium spp. and *Azospirillum brasilense*	Biological Nitrogen Fixation and Plant Growth Promotion (e.g., nutrient uptake, stress tolerance)	Improves resilience under tropical acidic conditions	Nodulation increased by up to 350%; yield rose on average by 8% and up to 80% in certain cases (Prando et al., 2024)
Pseudomonas sp. (PSB Lampung-2)	Phosphate solubilising	Increases P availability under low pH and Al toxicity	Increase yield by 45% (greenhouse) and 27% (field) with PSB + P fertiliser (Widodo et al., 2022)
Cupriavidus, *Klebsiella*, and *Proteobacteria*	Phosphorus mineralisation via acid phosphatase (AcP) and phoC gene	Enhances P availability and root-associated nutrient cycling	Improved adaptation and phosphorus acquisition under P-deficient acidic soil (Chen et al., 2024)
Rhizobium and Arbuscular Mycorrhizal Fungi (AMF)	Biological Nitrogen Fixation and boosts phosphorus uptake via mycorrhiza	Enhanced nodulation and nutrient uptake in acidic soils	Increase grain yield up to 356%, shoot biomass up to 140% and nodules up to 676% (Kamau et al., 2020)
Arbuscular Mycorrhizal Fungi (AMF), *Rhizobium, Talaromyces verruculosus,* and *Paraburkholderia soli*	N-fixation, P-uptake, and microbiome recruitment	Enhances Al stress tolerance, improves root and shoot biomass, especially in Al-sensitive genotypes; increases N uptake, synergistic with AMF in improving N cycling and enzyme activity	Increases shoot biomass by 112% and root biomass by 217% in Al-sensitive soybean (BD2); Promotes growth in both Al-tolerant and Al-sensitive soybean; Improves N and C accumulation; Enhances N content and biomass when combined with AMF (Wen et al., 2023)
Rhizobia (including *Bradyrhizobium*)	Symbiotic nitrogen fixation, root architecture modification, and acid adaptation	Root adaptation to phosphorus deficiency and aluminium toxicity	Potential to increase P and SNF efficiency in acid-tolerant varieties (Li et al., 2023)

Table 2 (*continued*)

Microbial Agent	Functional Role	Benefit in Acid-Stressed Soils	Impact on Soybean Productivity (with Reference)
Azospirillum brasilense, Arthrobacter crystallopoietes, Bacillus aryabhattai, and *Paenibacillus peoriae*	PGPR: P solubilisation, N fixation, hormone production	Biochar as a carrier increased pH and microbial stability in acidic sandy soils (pH 4.4); enhanced abundance and survival of PGPR	Maize biomass increased 2.6-3.2×, although not on soybean; mechanism and microbes are relevant (Kari et al., 2021)
Bradyrhizobium spp.	C-N transport in nodules, activation of β-1,3-glucanase enzyme	Regulation of nodule metabolic efficiency in acid soil via Mg	Increases nitrogen fixation symbiosis efficiency in soybeans (Cao et al., 2022)
Duddingtonia flagrans, Pochonia chlamydosporia, and *Bradyrhizobium japonicum*	Nematode biocontrol and increased nutrient uptake	Controlling *Meloidogyne javanica*, increasing nutrient intake in soil with nutrient decrease and high biotic stress	Increase root nutrients, nodulation, and soybean performance (Balbino et al., 2021)
Bradyrhizobium diazoefficiens (USDA110 & CB1809)	Nodule respiratory and SNF metabolic adaptations	Respiratory adaptation in conditions of P deficiency	Increases nitrogen efficiency even in P-deficient soils (Sulieman et al., 2024)
Bradyrhizobium japonicum, Bradyrhizobium diazoefficiens, Azospirillum brasilense, and *Bacillus subtilis*	Nitrogen fixation, growth hormone (IAA), antioxidants, and LCO metabolites	Increase drought resilience and efficiency in photosynthesis	Increase photosynthesis, nodulation and soybean yield up to 12.2% (Moretti et al., 2021)

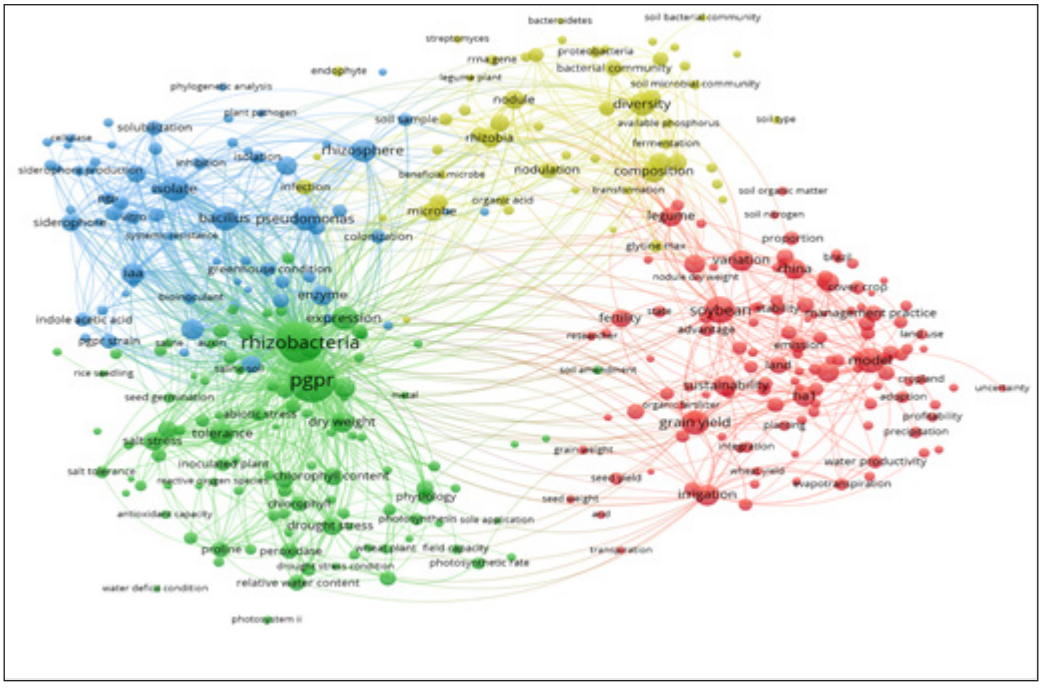

Figure 2. Network visualisation of the co-occurrence mapping of pertinent keywords related to research on the use of *Bradyrhizobium*, PGPR, and AMF to enhance soybean growth and fertiliser efficiency in acid soils

acidic soil stress (Prando et al., 2024). The red colour includes agronomic terms such as sustainability, irrigation, and land use, indicating the fusion of microbial inoculants with nutrient management and climate-resilient agricultural practices. Research by Ferdous et al. (2024) has further supported this statement; it reported *Rhizobium*'s survival improvement in conservation systems, and Zhang et al. (2023) identified precision agriculture as a primary driver in enhancing inoculant efficiency.

Generally, Figure 2 visualises the developing interconnection between microbial inputs, plant physiological responses, and environmental management strategies. Visualisation reinforces the relevance of co- inoculation technology for the sustainability of soybean production in tropical agroecosystems with acidic soil stress.

Figure 3 visualises the publication timeframe of the terms included in the analysis. The most recent publications are illustrated with keywords represented in yellow, with the colour changing from green to blue to illustrate older publication dates. Based on the visualisation, many articles were published in early to mid-2022, including the utility of *Bradyrhizobium* and co-inoculants to enhance soybean plant growth in acidic stress condition, which is aligned with this network visualisation, indicating that researchers studying this topic is still lacking.

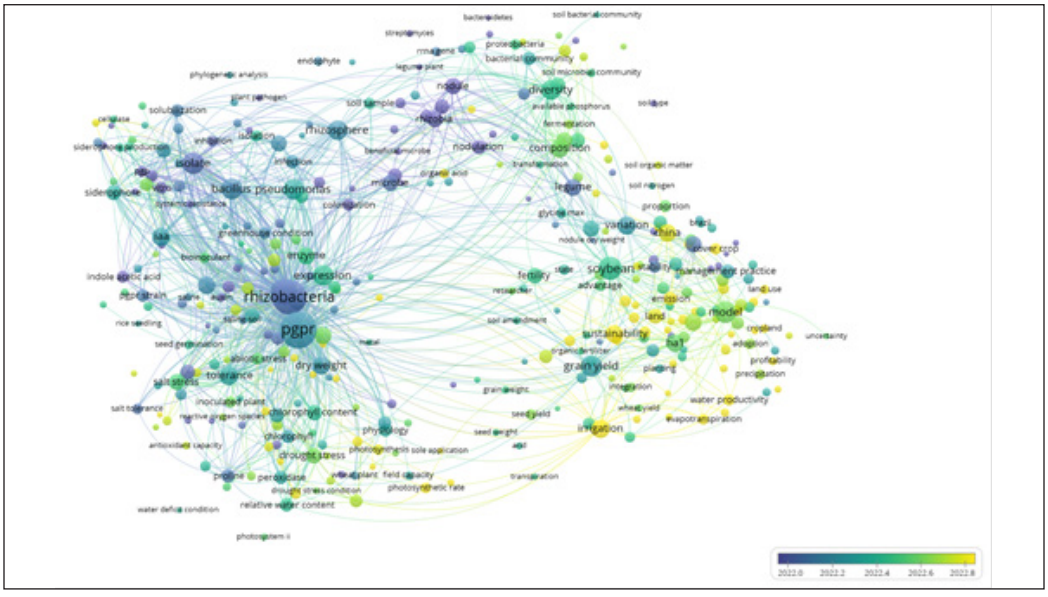

Figure 3. Mapping of co-occurrence of textual data provided in the titles and abstracts of the research articles used in this study

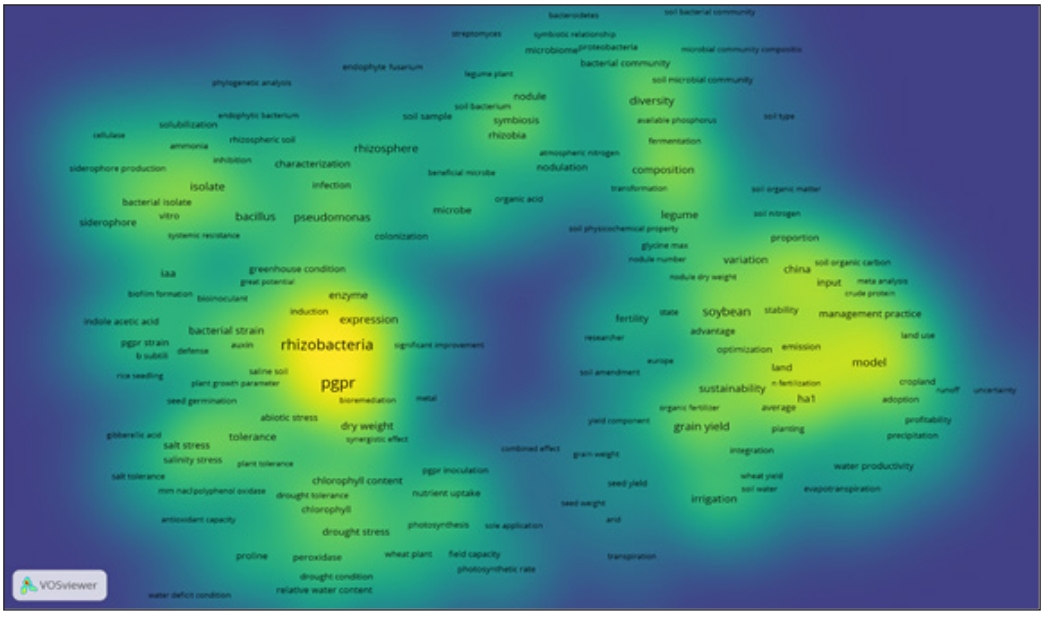

Figure 4. Overlay visualisation of publication year mapping related to research on soybean farming under acid soil stress

Keyword appearance by publication year overlaid in Figure 4, showing that most articles attentive to co-inoculation approaches and acidic stress adaptation were published

between 2022 and 2024, indicating a growing research trend and potential gap for deeper on-farm applications.

PRISMA Result

12 selected studies provide a comprehensive summary regarding the evidence reinforcing the synergistic effects of co-inoculation between *Bradyrhizobium* spp. and a wide variety of co-inoculants such as PGPR, AMF, PSB, and fungal biocontrol agents in boosting soybean growth and nutrient efficiency under acidic soil stress.

Field-scale experiments across diverse regions of Brazil have demonstrated an increase in root nodule formation and crop yields of up to 80% subsequent to inoculation with *Azospirillum brasilense* (Prando et al., 2024). Research in Kenya showed that the combined application of *Rhizobium* and arbuscular mycorrhizal fungi (AMF) promoted superior root nodule development, as well as enhanced phosphorus uptake and biomass accumulation in acidic soils (Kamau et al., 2020). The utility of *Bradyrhizobium liaoningense* combined with *Ambispora leptoticha* plays a role in higher drought stress tolerance, resulting in statistically meaningful gains in plant biomass and an 88% increase in grain yield (Ashwin et al., 2022). *Bacillus*, *Pseudomonas*, and *Paenibacillus* as phosphate-solubilising bacteria support phosphorus supply and crop productivity, thus decreasing dependency on chemical phosphate fertilisers (Chen et al., 2024; Widodo et al., 2022). Recent molecular studies have also explained that nutrient-poor acidic soils are a contributing factor in enhancing biological nitrogen fixation efficiency through respiration alterations and increased magnesium absorption into root nodules (Cao et al., 2022; Sulieman et al., 2024).

Research explains that the application of soil amendments and co-inoculation can enhance soybean crop response to acidic stress conditions through diverse mechanisms. Co-inoculation between *Bradyrhizobium* and plant growth-promoting rhizobacteria (PGPR) such as *Azospirillum* and *Bacillus* can enhance photosynthetic efficiency and soybean yields (Moretti et al., 2021). PGPR with biochar enhances microbial adaptiveness and root biomass in acidic sandy soils, thus boosting nitrogen utilisation (Kari et al., 2021). Advantageous microorganisms suppress nematodes and soil-borne pathogens, contributing to plant health. Fungal biocontrol agents such as *Duddingtonia flagrans* and *Purpureocillium* spp. have been presented to enhance root health and nutrient absorption, boosting soybean performance in acidic stress conditions (Balbino et al., 2021; Haarith et al., 2021).

Diverse studies have synthesised that microbial co-inoculation enhances soybean adaptation to acidic stress conditions through nutrient uptake, improved rhizosphere diversity, and stress resilience. Diverse rhizobial consortia, including *Bradyrhizobium*, *Rhizobium*, *Pararhizobium*, and *Sinorhizobium*, have been shown to foster microbial diversity and nodulation potential in acidic, no-till agricultural systems (Ferdous et al., 2024). Functional analyses of soybean rhizosphere microbiota further demonstrate that

beneficial bacteria possess traits associated with acid-stress mitigation, nutrient cycling, and enhanced nitrogen acquisition (Wen et al., 2023). These findings are supported by studies showing that PGPR improve stress tolerance, nitrogen uptake, chlorophyll content, root development, and nitrogen metabolism under acidic conditions, ultimately resulting in greater nutrient use efficiency and soybean productivity (Li et al., 2020; Shaffique et al., 2023; Sudarshna & Sharma, 2024).

The studies emphasised that integrating *Bradyrhizobium* spp. with co-inoculants (specifically PGPR, AMF, and PSB) can overcome agronomic-limiting factors in acidic stress conditions effectively. This combination improves biological nitrogen fixation (BNF), phosphorus solubilisation, abiotic stress resilience, and nutrient absorption, enhancing crop tolerance and efficiency in nutrient use. Consistently, results present increased soybean productivity throughout the studies, ranging from 8% to 88%, and boost long-term enhancements in soil health, rhizosphere microbial activity, and nutrient cycling as well.

In general, the findings firmly suggest that co-inoculation reduces dependency on chemical nitrogen fertilisers, especially in acidic stress conditions and low external input farming systems, even though the level of this reduction was not quantified explicitly in most of the 12 studies evaluated. This deduction is supported by other studies beyond the main dataset, which show that integration between *Bradyrhizobium* and PGPR can reduce nitrogen fertiliser use by 30-50% without sacrificing crop yields (de Souza et al., 2015; Zahran, 1999). These results emphasise that microbial-based solutions for soybean yield in tropical regions are ecologically efficient and sustainable. Regrettably, application at the field scale remains high-risk; to overcome this, key obstacles regarding stability in formulation, strain compatibility, and adaptability to various agro-ecological environments are addressed. This underscores the need for formulating local inoculants and integrated nutrient management systems.

Functional Role of *Bradyrhizobium* spp. and Co-Inoculants in Enhancing Soybean Productivity and Soil Fertility under Acid-Stressed Conditions

Synergistic interactions between *Bradyrhizobium* and other co-inoculants (such as *Bacillus, Azospirillum*, *Pseudomonas*, and arbuscular mycorrhizal fungi) play a key functional role in enhancing soybean growth and soil fertility, especially in acidic stress conditions, as presented in various studies. These microorganisms contribute to various fundamental biological processes, including symbiotic nitrogen fixation, phosphorus solubilisation, phytohormone production, and abiotic stress mitigation, all of which are highly relevant to plant activity under stressful soil conditions. The symbiotic relationship between *Bradyrhizobium* and soybean roots has made it widely recognised. *Bradyrhizobium* develops root nodules that provide plots for biological nitrogen fixation (BNF).

Nevertheless, acidic stress conditions result in low pH, aluminium (Al) toxicity, and phosphorus (P) deficiency, which deteriorate nitrogenase enzyme activity and root nodule development. These suppressive factors can be mitigated by co-inoculants—they provide functional support that enhances microbial efficacy and rhizosphere conditions.

Manganese and aluminium toxicity can be ameliorated by particular PGPR through diverse mechanisms. PGPR secrete organic acids, which can chelate Al^{3+} ions, thus reducing their toxicity levels and biological availability that accumulates in the rhizosphere. In addition, insoluble phosphorus compounds are dissolved by organic acids released by phosphate-solubilising bacteria, while suppressing the formation of Al-P chelates, thus increasing the presence of solubilised phosphate in soil under acidic stress conditions. Exopolysaccharides (EPS) are synthesised by some PGPR, which sequester toxic metal ions and shield root surfaces from direct aluminium contact. Moreover, indole-3-acetic acid (IAA) stimulates root growth, enabling plants to maintain water absorption and nutrients in spite of the presence of toxic metals, while siderophore synthesis enhances microbial activity and micronutrient uptake within the rhizosphere (Shaffique et al., 2023; Widodo et al., 2022). For example, using *Azospirillum brasilense* for co-inoculation was proven to enhance nodulation by up to 350% and soybean production by up to 80%, especially under tropical conditions that induce acidic stress (Prando et al., 2024). Likewise, nutrient solubilisation, siderophore, and IAA production are facilitated by *Pseudomonas* spp. and *Bacillus*, promoting root growth and nutrient absorption (Shaffique et al., 2023; Widodo et al., 2022).

AMF's function, especially *Ambispora leptoticha*, enhances nitrogen fixation through boosted phosphorus uptake and interactions between root and soil as well. Ashwin et al. (2022) presented that integration between rhizobia and AMF enhanced drought resilience significantly, seed production, and shoot dry matter in acid soils, confirming the ecological collaboration between these microbes. Additionally, studies by Wen et al. (2023) presented that inoculation with AMF and other fungi with stress resilience, such as *Talaromyces verruculosus,* is able to induce aluminium stress resilience, restructure root-interacting microbiomes, and enhance nitrogen and carbon accumulation in soybean tissue. Co-inoculants enhance sustainable soil fertility as well; they enhance enzymatic activity within soils, diversity in microbial communities, and nutrient cycling, especially nitrogen and phosphorus cycling, which is usually altered in acidic soils. For example, improved rhizobial survival and efficacy in acidic no-till soils are recorded in Ferdous et al. (2024), meaning that co-inoculation enhances soil microbial resilience and viability.

The functional characteristics explained above indicate that microbial co-inoculation is not only a long-term method for enhancing soybean performance in acidic stress conditions but also a highly effective approach to restoring degraded land and boosting agroecosystem health. Their biological mechanisms facilitate short-term yield increases as well as the sustainable improvement of soil microbial balance, fertility, and structure.

Challenge and Future Innovative Technology

Challenges remain in translating experimental efficacy into enhanced field adaptation, particularly in acidic stress conditions, in spite of the significant ecological and agronomic advantages of co-inoculation techniques. The main challenge is inconsistency in microbial performance under a wide variety of edaphic and climatic conditions. Acidic soils are commonly characterised by limited microbial activity, low pH, aluminium toxicity, and phosphorus deficiency. These factors inhibit the colonisation, survival, and symbiotic performance of the inoculated microbes. *Bradyrhizobium* and co-inoculants can become less effective under extreme conditions due to disrupted signalling pathways, limited nutrient mobility, and interference from indigenous soil microorganisms. For instance, a Rhizobium strain that performs well in laboratory analyses may exhibit low nitrogen fixation efficiency and poor nodulation when subjected to field stresses. Furthermore, most commercial inoculants are developed as generic products lacking specific adaptation to particular locations or crop varieties. Such mismatches often result in suboptimal microbial performance, particularly when not combined with appropriate agronomic practices, such as the addition of organic matter or pH adjustment.

In addition, challenges such as short shelf life, low carrier stability, and inefficient delivery systems hinder microbial performance in the field. Traditional application methods expose inoculants to desiccation and UV degradation, or result in inoculant death prior to root colonisation due to competition with antagonistic soil microbes. These limitations can be overcome through advanced technologies capable of maximising inoculant performance. Nanoencapsulation is one such technology, involving the loading of microbial cells into protective nanocarriers. This approach protects microbes from environmental stress, controls their release in the root zone, and enhances microbial survival and colonisation capabilities. Zhang et al. (2023) demonstrated that nano-formulated inoculants exhibit stronger adhesion and greater persistence on roots under acidic conditions. Other areas of research include the development of native strains selected or engineered for enhanced tolerance to acidity, aluminium toxicity, and nutrient stress. Genomic and functional metagenomic data can accelerate the identification of stress-tolerant microbial candidates. Sulieman et al. (2024) and Cao et al. (2022) have described how the regulation of nodulation efficiency and nodule respiration mechanisms can be managed to improve *Bradyrhizobium* performance in soils subject to phosphorus stress.

Integration between microbial inoculation and precision agriculture tools, such as automated seed coating, GIS-based soil mapping, and location-specific nutrient implementation can boost the targeting exactness of inoculants while reducing waste. Farmers are able to match specific microbial consortia to specific soil conditions with these technologies, thus increasing input use. Even though microbial co-inoculation has been shown to enhance soybean production and boost soil health, its extensive implementation

requires a breakthrough in formulation, strain resilience, and application precision. Bridging the gap between practice and research will be vital to realising the full potential of co-inoculants in sustainable agriculture, especially in tropical regions under acidic stress.

CONCLUSION

This result presents the functional synergism of *Bradyrhizobium* spp. and co-inoculants such as *Azospirillum*, *Bacillus*, *Pseudomonas*, and arbuscular mycorrhizal fungi (AMF) in soybean yield and soil fertility improvement against acid stress. Co-inoculation methods in different agroecosystems greatly improved nodulation efficiency, nutrient levels, drought stress, and biological nitrogen fixation with soybean yield increments ranging from 8% to 88%. These positive effects are elicited through microbial activities like indole-3-acetic acid (IAA) and siderophore production, phosphorus solubilisation, modulation of root architecture, and soil microbiome enrichment. Along with short-term agronomic effects, these microbiomes also confer long-term soil health through enzymatic activity, microbial community structure diversity, and nutrient cycling, further establishing their roles as soil-regenerative technologies.

IMPLICATION OF THE STUDY

Generally, co-inoculation with *Bradyrhizobium* was found to be climate-resilient, sustainable, and efficient in enhancing fertiliser use efficiency as well as soybean yield in acid-sensitive tropical soils. Advancing these technologies locally through local innovation will be paramount in realising their full capacity in facilitating agroecological restoration and food security.

LIMITATION AND RECOMMENDATION FOR FUTURE RESEARCH

Generally, co-inoculation with *Bradyrhizobium* was found to be climate-resilient, sustainable, and efficient in enhancing fertiliser use efficiency as well as soybean yield in acid-sensitive tropical soils. Advancing these technologies locally through local innovation will be paramount in realising their full capacity in facilitating agroecological restoration and food security.

ACKNOWLEDGEMENT

The authors thank the Academic Leadership Grant (ALG) from Padjadjaran University for their funding. Grateful thanks to reviewers and colleagues for helpful comments. The authors hold sole responsibility for the contents and inferences stated.

REFERENCES

Ahmad, M., Pataczek, L., Hilger, T. H., Zahir, Z. A., Hussain, A., Rasche, F., Schafleitner, R., & Solberg, S. Ø. (2018). Perspectives of microbial inoculation for sustainable development and environmental management. *Frontiers in Microbiology, 9*, Article 2992. https://doi.org/10.3389/fmicb.2018.02992

Ashwin, R., Bagyaraj, D. J., & Raju, B. M. (2022). Dual inoculation with rhizobia and arbuscular mycorrhizal fungus improves water stress tolerance and productivity in soybean. *Plant Stress*, *4*, Article 100084. https://doi.org/10.1016/j.stress.2022.100084

Balbino, H. M., Monteiro, T. S. A., Coutinho, R. R., Pacheco, P. V. M., & de Freitas, L. G. (2021). Association of *Duddingtonia flagrans* with microorganisms for management of *Meloidogyne javanica* and acquisition of nutrients in soybean. *Biological Control, 159*, Article 104626. https://doi.org/10.1016/j.biocontrol.2021.104626

Cao, H.-R., Peng, W.-T., Nie, M.-M., Bai, S., Chen, C.-Q., Liu, Q., Guo, Z.-L., Liao, H., & Chen, Z.-C. (2022). Carbon-nitrogen trading in symbiotic nodules depends on magnesium import. *Current Biology, 32*(20), 4337-4349.e5. https://doi.org/10.1016/j.cub.2022.08.019

Bedassa, T. A., Abebe, A. T., & Tolessa, A. R. (2022). Tolerance to soil acidity of soybean (*Glycine max* L.) genotypes under field conditions Southwestern Ethiopia. *PLOS ONE, 17*(9), Article e0272924. https://doi.org/10.1371/journal.pone.0272924

Chen, Q., Zhao Q, Xie, B., Lu, X., Guo, Q., Liu, G., Zhou, M., Tian, J., Lu, W., Chen, K., Tian, J., & Liang, C. (2024). Soybean (*Glycine max*) rhizosphere organic phosphorus recycling relies on acid phosphatase activity and specific phosphorus-mineralizing-related bacteria in phosphate deficient acidic soils. *Journal of Integrative Agriculture, 23*(5), 1685–1702. https://doi.org/10.1016/j.jia.2023.09.002

Ferdous, A. J., Wang, X., Lewis, K., & Zak, J. (2024). Comparative analysis of rhizobial and bacterial communities in experimental cotton fields: Impacts of conventional and conservation soil management in the Texas High Plains. *Soil and Tillage Research, 236*, Article 105920. https://doi.org/10.1016/j.still.2023.105920

Haarith, D., Kim, D.-G., Chen, S., & Bushley, K. E. (2021). Growth chamber and greenhouse screening of promising in vitro fungal biological control candidates for the soybean cyst nematode (*Heterodera glycines*). *Biological Control*, *160*, Article 104635. https://doi.org/10.1016/j.biocontrol.2021.104635

Jabborova, D., Kannepalli, A., Davranov, K., Narimanov, A., Enakiev, Y., Syed, A., Elgorban, A. M., Bahkali, A. H., Wirth, S., Sayyed, R. Z., & Gafur, A. (2021). Co-inoculation of rhizobacteria promotes growth, yield, and nutrient contents in soybean and improves soil enzymes and nutrients under drought conditions. *Scientific Reports, 11*(1), Article 22081. https://doi.org/10.1038/s41598-021-01337-9

Kamau, N. N., Kungu, J. B., & Mugendi, D. (2020). Effects of mycorrhizal and rhizobium inoculation on soybean growth in acidic soils of Gatanga, Kenya. *Cell Biology & Development*, *4*(1), 1-16. https://doi.org/10.13057/cellbioldev/v040101

Kari, A., Nagymáté, Z., Romsics, C., Vajna, B., Tóth, E., Lazanyi-Kovács, R., Rizó, B., Kutasi, J., Bernhardt, B., Farkas, É., & Ligeti, M. (2021). Evaluating the combined effect of biochar and PGPR inoculants on the bacterial community in acidic sandy soil. *Applied Soil Ecology, 160*, Article 103856. https://doi.org/10.1016/j.apsoil.2020.103856

Khan, R., Hussain, S., & Iqbal, M. (2023). Synergistic effects of *Bradyrhizobium* and PGPR on soybean growth under abiotic stress. *Agriculture, Ecosystems & Environment*, *348*, Article 108475. https://doi.org/10.1016/j.agee.2023.108475

Li, R., Chen, H., Yang, Z., Yuan, S., & Zhou, X. (2020). Research status of soybean symbiosis nitrogen fixation. *Oil Crop Science, 5*(1), 6–10. https://doi.org/10.1016/j.ocsci.2020.03.005

Li, X., Zhang, X., Zhao, Q., & Liao, H. (2023). Genetic improvement of legume roots for adaption to acid soils. *The Crop Journal, 11*(4), 1022–1033. https://doi.org/10.1016/j.cj.2023.04.002

Marinković, J., Miljaković, D., Đorđević, V., Vasiljević, M., Tamindžić, G., Miladinović, J., & Vasiljević, S. (2024). Perspectives of *Bradyrhizobium* and *Bacillus* inoculation for improvement of soybean tolerance to water deficit. *Agronomy, 14*(11), Article 2692. https://doi.org/10.3390/agronomy14112692

Moretti, L. G., Crusciol, C. A. C., Kuramae, E. E., Bossolani, J. W., Moreira, A., Costa, N. R., Alves, C. J., Pascoaloto, I. M., & Hungria, M. (2020). Yield gains in soybean-maize succession with inoculation and co-inoculation of *Bradyrhizobium* and *Azospirillum*. *Agronomy Journal, 112*(1), 587–599.

Moretti, L. G., Crusciol, C. A. C., Bossolani, J. W., Garcia, A., Calonego, J. C., Moreira, A., Garcia, A., Momesso, L., Kuramae, E. E., & Hungria, M. (2021). Beneficial microbial species and metabolites alleviate soybean oxidative damage and increase grain yield during short dry spells. *European Journal of Agronomy, 127,* Article 126293. https://doi.org/10.1016/j.eja.2021.126293

Prando, A. M., Barbosa, J. Z., Oliveira, A. B. de, Nogueira, M. A., Possamai, E. J., & Hungria, M. (2024). Benefits of soybean co-inoculation with *Bradyrhizobium* spp. and *Azospirillum brasilense*: Large-scale validation with farmers in Brazil. *European Journal of Agronomy*, *155*, Article 127112. https://doi.org/10.1016/j.eja.2024.127112

Santos, M. S., Nogueira, M. A., & Hungria, M. (2019). Microbial inoculants: Reviewing the past, discussing the present and previewing an outstanding future for the use of beneficial bacteria in agriculture. *AMB Express, 9*, Article 205. https://doi.org/10.1186/s13568-019-0932-0

Shaffique, S., Imran, M., Adhikari, A., Aaqil Khan, M., Rahim, W., Alomrani, S. O., Yun, B. -W., Kang, S. -M., & Lee, I. -J. (2023). A newly isolated *Bacillus pumilus* strain SH-9 modulates response to drought stress in soybean via endogenous phytohormones and gene expression (Daegu, South Korea). *Plant Stress, 10*, Article 100279. https://doi.org/10.1016/j.stress.2023.100279

de Souza, R., Ambrosini, A. M., & Passaglia, L. (2015). Plant growth-promoting bacteria as inoculants in agricultural soils. *Genetics and Molecular Biology, 38*(4), 401–419. https://doi.org/10.1590/S1415-475738420150053

Sudarshna, & Sharma, N. (2024). Endophytic bacteria associated with critically endangered medicinal plant *Trillium govanianum* (Wall ex. Royle) and their potential in soil nutrition alleviation. *Plant Stress*, *11*, Article 100349. https://doi.org/10.1016/j.stress.2024.100349

Sulieman, S., Van Ha, C., Le, D. T., Abdelrahman, M., Tran, C. D., Watanabe, Y., Tanaka, M., Ulhassan, Z., Sheteiwy, M. S., Gangurde, S. S., Mochida, K., Seki, M., & Tran, L.-S. P. (2024). Comparative transcriptome analysis of respiration-related genes in nodules of phosphate-deficient soybean (*Glycine max* cv. Williams 82). *Plant Stress, 11*, Article 100368. https://doi.org/10.1016/j.stress.2024.100368

Wei, W., Guan, D., Ma, M., Jiang, X., Fan, F., Meng, F., Li, L., Zhao, B., Zhao, Y., Cao, F., Chen, H., & Li, J. (2023). Long-term fertilization coupled with rhizobium inoculation promotes soybean yield and alters soil bacterial community composition. *Frontiers in Microbiology, 14*, Article 1161983. https://doi.org/10.3389/fmicb.2023.1161983

Wen, Z., Yang, M., Han, H., Fazal, A., Liao, Y., Ren, R., Yin, T., Qi, J., Sun, S., Lu, G., Hu, S., & Yang, Y. (2023). Mycorrhizae enhance soybean plant growth and aluminum stress tolerance in acidic soils. *Journal of Soil Science and Plant Nutrition, 11*(2), Article e0331022. https://doi.org/10.1128/spectrum.03310-22

Widodo, Y., Rozy, F., Rahmianna, A. A., Mejaya, M. J., & Indradewa, D. (2022). Effect of phosphate-solubilizing bacteria isolates in acid soil on soybean (Glycine max L.) seed yield. *Applied Ecology and Environmental Research*, 20(6), 4855–4863. https://doi.org/10.15666/aeer/2006_48554863

Zahran, H. H. (1999). Rhizobium-legume symbiosis and nitrogen fixation under severe conditions and in an unfavorable environment. *Microbiology and Molecular Biology Reviews*, *63*(4), 968-989. https://doi.org/10.1128/MMBR.63.4.968-989.1999

Zhang, M., Liu, Y., Wei, Q., Gou, J., Liu, L., Gu, X., & Wang, M. (2023). The co-application of PGPR and biochar enhances the production capacity of continuous cropping peppers in the karst yellow soil region of Southwest China. *Horticulturae, 9*(10), Article 1104. https://doi.org/10.3390/horticulturae9101104

Pertanika J. Trop. Agric. Sci. 49 (5): 2133 - 2153 (2026)

PERTANIKA JOURNALS

TROPICAL AGRICULTURAL SCIENCE

Journal homepage: http://www.pertanika.upm.edu.my/

Physiological and Metabolic Responses of Early Juvenile Blue Swimming Crab, *Portunus pelagicus,* to Dietary Deficiency

Jamali Muhammad-Firdaus[1], Ariffin Hidir[2], Donald Torsabo[1], Hon Jung Liew[2], Mhd Ikhwanuddin[2], and Noordiyana Mat Noordin[1]*

[1]Aquaculture Innovation and Empowerment RIG, Faculty of Fisheries and Food Science, Universiti Malaysia Terengganu, Kuala Nerus, 21030 Terengganu, Malaysia
[2]Higher Institution Centre of Excellence, Institute of Tropical Aquaculture and Fisheries, Universiti Malaysia Terengganu, Kuala Nerus, 21030 Terengganu, Malaysia

ABSTRACT

Crustaceans, especially early growth stage crabs, often face starvation in their natural environment due to their defensive behaviors to avoid predators and cannibalistic, prolonged hiding to avoid predators at the expense of foraging. Additionally, environmental influences, including seasonal changes and anthropogenic pollution, contribute to limited food availability, further increasing the challenges early juvenile crabs encounter in finding food. Therefore, this study examined the impact of temporary starvation on early juvenile crab by using *Portunus pelagicus* as a model, focusing on growth, respiration, and biochemical composition. The first experiment involving a 7-d period consisted of two treatments (0-d starved and 7-d starved). Results showed that 7-d starved crabs exhibited lower values across all measured parameters, including molting percentage (4.5%), respiration rate (71.5 mgO_2/g/h), glycogen content (0.24 mg/g), protein levels (2.92 mg/g), and lipid content (1.51 mg/g). The second experiment, involving a 14-d period, encompassed three treatments (0-d starved, 7-d starved followed by 7 days of re-feeding, and 14-d starved). A similar trend was observed in the starvation treatment groups (7-d and 14-d starved), resulting in reduced molting percentages and respiration rates compared to the Control. Starved crabs (14-d starved) exhibited reduced levels of glycogen (0.24 mg/g), protein (3.92 mg/g), and lipid (1.35 mg/g). Results from fatty acid analysis revealed decreased levels of ∑SAFA, ∑PUFA, ∑MUFA, ∑n-3, and ∑n-6 across all starved treatments. These findings suggest that glycogen, protein, and lipid stores in early juvenile crabs were utilised to sustain energy requirements during feed deficiency.

Keywords: P. pelagicus, starvation, respiration, biochemical composition

ARTICLE INFO

Article history:
Received: 16 June 2025
Accepted: 10 August 2026
Published: 30 October 2026

DOI: https://doi.org/10.47836/pjtas.49.5.02

E-mail addresses:
firfairus006@gmail.com (Muhammad Firdaus-Jamali)
hidirariffin@umt.edu.my (Hidir Ariffin)
dtorsabo@gmail.com (Donald Torsabo)
honjung@umt.edu.my (Liew Hon Jung)
ikhwanuddin@umt.edu.my (Mhd Ikhwanuddin)
diyananoordin@umt.edu.my (Noordiyana Mat Nordin)
* Corresponding author

© Universiti Putra Malaysia Press

INTRODUCTION

In a natural environment, crustaceans often experience starvation due to various factors, especially during the early growth stages of crabs. Adult crabs frequently have a competitive advantage over early juvenile crabs because of their higher predation skills and greater experience. Both adult and juvenile crabs tend to capture similar types of prey, but juveniles have a lower success rate due to their immaturity, leading to periods of starvation (Hines et al., 2026). During scavenging activities, adult crabs are typically the first to find dead prey because of their higher sensing capabilities and greater mobility. Juvenile crabs, on the other hand, have limited mobility, which restricts their access to scavenging prey (Bromilow & Lipcius, 2017). Additionally, cannibalism is common, with adult crabs often consuming smaller crabs of the same species, while early juvenile crabs are also more vulnerable to other predators such as fish and squid. This increased predation risk causes them to spend more time hiding and less time foraging, resulting in the need to tolerate food shortages or a complete absence of food for varying periods (Hines et al., 2026). Additionally,-reduced food availability occurs due to environmental influences, particularly seasonal changes that affect the availability of food. These changes impact early juvenile crabs more significantly due to their higher metabolic rates and lower food reserves (Dvoretsky & Dvoretsky, 2020). Seasonal changes have been more significant recently because of global climate change, which causes alterations in water temperature and ocean acidification. This phenomenon influences the distribution and abundance of plankton, the foundation of many aquatic food webs, leading to a reduction in upper trophic levels such as bivalves and gastropods. This indirectly reduces the availability of prey for early juvenile crabs (Dvoretsky & Dvoretsky, 2020). Furthermore, anthropogenic pollution and habitat degradation by humans affect coastal areas, which contain a wide variety of prey and serve as a main shelter for smaller crabs. Consequently, early juvenile crabs may experience starvation due to the decline in prey populations in these areas.

Commonly, crustaceans will experience frequent periodic molting during their lifetime for growth enhancement, particularly during their juvenile stages (Wang et al., 2019). In this growth stage, a high energy requirement is required to build a new exoskeleton (Josileen & Menon, 2005). However, there is still scarce information regarding how starvation could affect the growth performance of *early juvenile crabs* in terms of survival and molting. Perhaps prolonged starvation would prevent the molting process due to reduced energy expenditure on growth to benefit the crab's survival. Furthermore, crabs exhibit various metabolic responses under starvation conditions, involving crab respiration and biochemical composition such as glycogen, protein, and lipid (more specifically, fatty acids) (Ding et al., 2017). In response to starvation, the crabs will lower oxygen consumption, and this respiration cycle is interrelated with the breakdown process of storage reserves (glycogen, protein, lipid) for providing energy in the juvenile crab to prolong the survival of crabs

(Comoglio et al., 2005; Sánchez-Paz et al., 2006). At the beginning of the starvation process, the crabs metabolise glycogen reserve, followed by lipid reserve. When the accessible glycogen and lipid are depleted, the crabs then utilise protein as the final energy source just prior to death (Holme et al., 2009). However, little is known about these energy reserves in comparison to their use during starvation in early juvenile crabs. Most early growth stages of marine crabs have relatively limited nutrient reserves and are unable to molt to the next growth stage without an adequate food source (Wu et al., 2017). The utilisation of biochemical composition for energy expenses during starvation may differ regarding the growth stage, and the juvenile stage of crab has not been investigated previously (Sánchez-Paz et al., 2006). Previous studies only emphasised adult-stage crabs, which have been verified for their longer resilience in starvation. However, there is no information regarding the extent of early juvenile crabs' resistance against feed deficiency. A significant knowledge gap remains regarding how early juvenile crabs allocate their biochemical resources during feed deficiency and whether they have similar starvation tolerance as adults. Understanding the starvation response at the juvenile stage is crucial because this life stage is highly vulnerable and directly influences survival and subsequent aquaculture production performance. The present study provides a novel perspective by focusing on the early juvenile stage, which is an understudied phase with rapid growth, limited energy reserves, and high sensitivity to nutritional stress.

The blue swimming crab, *Portunus pelagicus*, can be found in vast areas of water throughout the Indo-West Pacific and is considered the most important crustacean species in fisheries and aquaculture. This crab has been suggested to be a good model to understand how starvation affects early juvenile crab (Potter & de Lestang, 2000). Therefore, to address this knowledge gap, the aim of the present study was to investigate the effects of temporary starvation on early juvenile *P. pelagicus* by evaluating changes in growth performance, respiration rate, and biochemical composition. We hypothesised that prolonged starvation would sequentially deplete glycogen, lipid, and protein reserves in early juvenile crabs, whereas re-feeding would partially restore these energy reserves and physiological performance. Understanding which energy reserves are used first during starvation is important for improving feeding and nursery management in aquaculture and predicting the survival of juvenile crabs in the wild during food shortages.

METHODS

Crab Sampling

Juveniles of *P. pelagicus* were obtained from the International Institute of Aquaculture & Aquatic Sciences (I-AQUAS), Port Dickson, Negeri Sembilan, Malaysia, and transported to the Faculty of Fisheries and Food Science (FPSM) hatchery, University of Malaysia Terengganu. Prior to the experiment, healthy and active crabs (weight: 11.19 ± 3.76 mg,

carapace width: 4.36 ± 0.71 mm) with all intact appendages were collected with a strainer and placed individually into a 750 ml circular plastic container to avoid cannibalism. The plastic container was modified with a netted hole at the bottom for water movement. The crabs were acclimatised for three days before the experiment began (Wang et al., 2021a).

Experimental Design

The present study was divided into two experimental periods (7-d and 14-d; d refers to day). For the 7-d experimental period, the crabs were subjected to two treatments (0-d starved and 7-d starved). For the 14-d experimental period, the crabs were subjected to three different treatments (0-d starved, 7-d starved, and 14-d starved), where the 7-d starved crabs were starved for the first seven days prior to being re-fed for the following seven days (Figure 1). These two independent starvation experiments (7-d and 14-d) were conducted to examine different phases of starvation response in early juvenile *P. pelagicus*. The 7-d period represented an initial starvation phase, whereas the 14-day period represented a prolonged starvation condition to evaluate juveniles' ability to adapt to extended feed deprivation.

In total, there were five treatments in the present study.

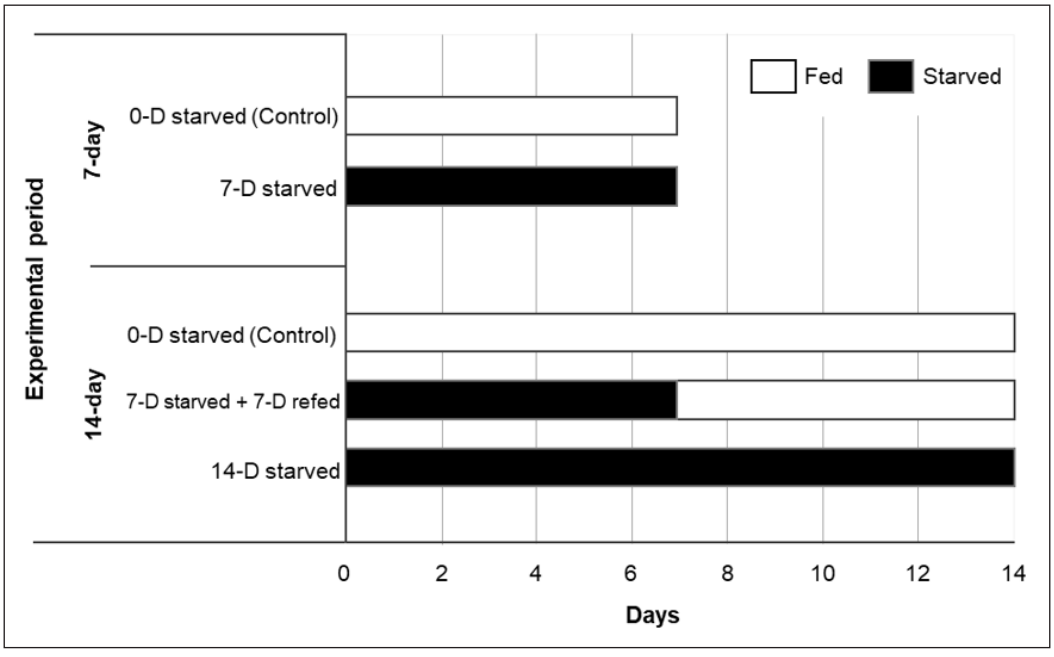

Figure 1. Three starvation treatments for juveniles of *P. pelagicus*

A total of 1,000 crabs were used in this study, with 200 crabs per treatment. For each treatment, there were five replicates (40 individuals per replicate). For growth performance analyses (survival, molting, and carapace measurement), all 1,000 crabs were included

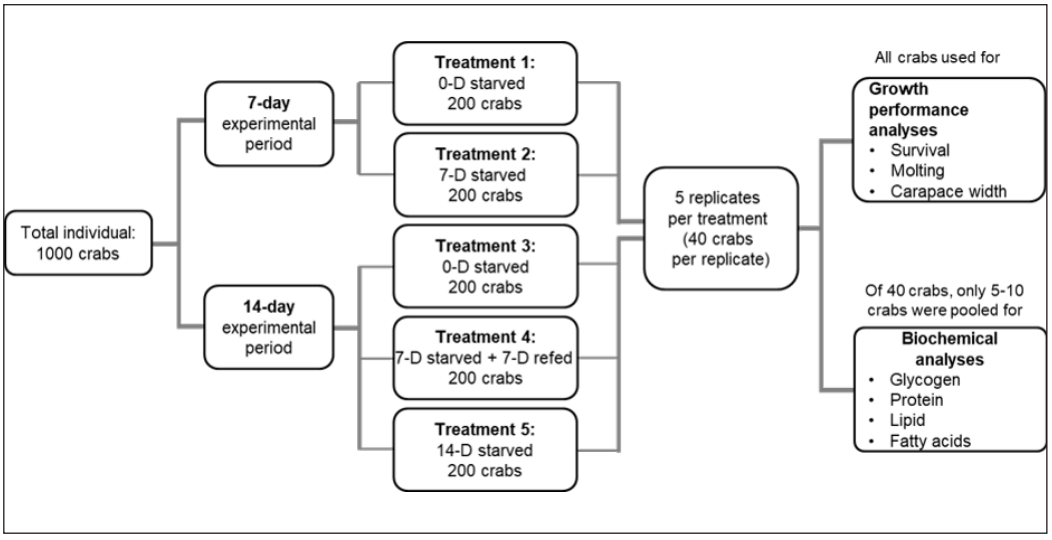

Figure 2. Number of treatments and replicates for growth performance and biochemical analyses

in these analyses (n = 5 replicate tanks). Meanwhile, for biochemical analyses of 1,000 crabs, a small portion of crabs from each replicate (five to ten individuals, pooled samples, and quantified in triplicate) were collected for glycogen, protein, lipid, and fatty acid analyses (Figure 2). Each pooled sample represented one biological replicate, with the experimental tank considered as the experimental unit (n = 5 replicate tanks). In collecting the sample, the crabs were immediately immersed in iced water to induce unconsciousness and death. They were then preserved in a refrigerator at -20 ℃ for further analysis, such as carapace measurement and biochemical constituent analyses. At the same time, for oxygen consumption analysis, from 1,000 crabs, 75 individuals (15 crabs representing five replicates per treatment with three crabs per replicate, n = 3 replicate crabs) were collected and subjected to respiration analysis for two hours (Figure 3).

Throughout the experiment, a feeding rate was provided to crabs with 3-5% body weight (Wang et al., 2021b) once per day (only for fed-crab treatment) with commercial prawn pellets designed for juvenile *Penaeus vannamei* (Brand: Gold Coin Post larval II Crumble, crude protein: 38%, crude fat: 5% and crude fiber: 3%). Any uneaten food was removed every morning before the pellet was provided; simultaneously, observation was conducted on survival and molting for all treatments. Any left carapace from molted crabs was removed. Exchanged 50% seawater was performed every three days. The salinity, temperature, pH, dissolved oxygen, and ammonia of the water were maintained at 30 ppt, 28 ± 2 °C, pH 7.0 - pH 7.9, 6 ppm -7 ppm, and lower than 0.05 ppm, respectively. Salinity was determined using a hand refractometer (HTC, calibrated with distilled water). Meanwhile, the temperature was controlled by submersible thermostat-controlled heaters (500-watt).

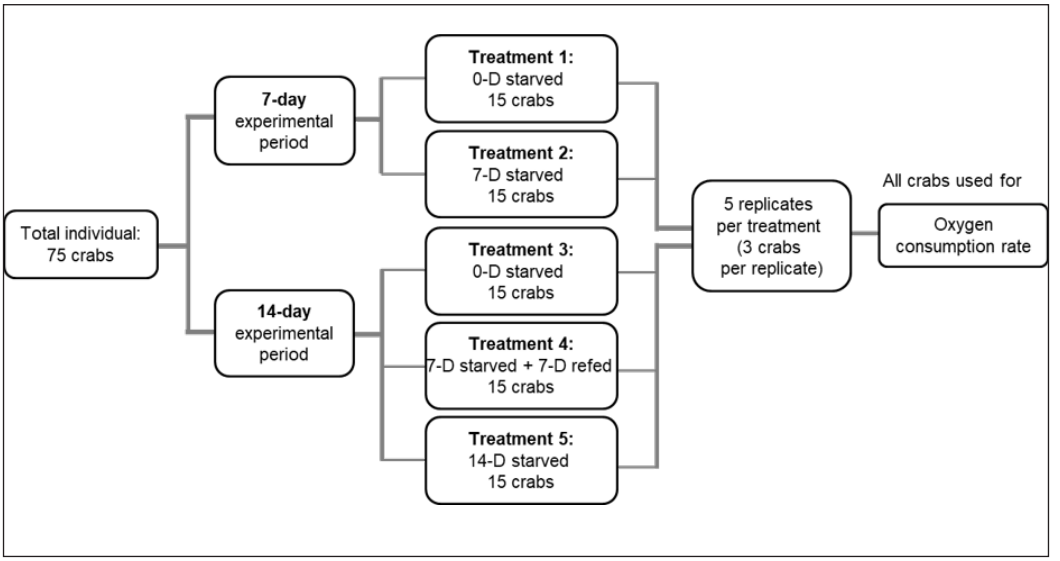

Figure 3. Number of treatments and replicates for respiration analyses

Survival, Molting Frequency and Growth Performance

Several data points were collected for growth performance, including survival, molting success, and carapace width. The carapace width was examined using a stereo zoom advanced research microscope (Nikon AZ100M) with a magnification of 0.5×. Values are presented as mean ± standard deviation. The formula was calculated according to Hidir et al. (2022) and Romano and Zeng (2006) as follows:

i. Survival rate (%) = (Final amount of crab) / (Initial amount of crab) × 100

ii. Molting success (%) = (Amount of successfully molted crab/Total amount ofcrab) × 100

iii. Carapace width = Distance between the tips of two lateral spines

Respiration

The individual crab was held in a sealed 3.9 L respiratory chamber equipped with calibrated oxygen electrodes (Wang et al., 2019). To minimise the potential impact from handling stress and feeding on recorded oxygen levels, the crabs were given a 2-hour settling period in respiratory chambers prior to initiating oxygen recording (Rodgers et al., 2016). To account for the potential influence of any unseen organisms that could affect respirometry readings, a blank respirometry control was conducted (Rodgers et al., 2016). The oxygen content in the respiratory chamber was recorded every five minutes for two hours. The dissolved oxygen concentration before beginning the readings ranged from 6.51 to 7.24 mg/l,

while at the end of the respiration experiment, the dissolved oxygen levels had dropped to a range of 4.57 to 5.43 mg/l. The oxygen consumption rate was calculated according to Wang et al. (2019), and the values are expressed as mean ± standard deviation (SD), as in Equation 1:

$$R = \frac{(DOi,\ crab - DOf, crab) - (DOi, blank - DOf, blank)\ \times V}{W\ \times T} \quad [1]$$

Where;
R = Oxygen consumption rate (mg O_2 g^{-1} h^{-1})
DOi and DOf = Initial and final dissolved oxygen concentrations (mg L^{-1})
V = Volume of the respiratory chamber (3.9 L)
W = Wet body weight of the individual crab (g)
T = Total duration of the logging window (h)

Biochemical Composition

A whole body of crab was analysed for total glycogen, protein, lipid, and fatty acids. For glycogen analysis, samples were homogenised in perchloric acid. The supernatant was collected, mixed with Anthron reagent, and incubated at 100 °C for 30 minutes before being read by a spectrophotometer at a wavelength of 630 nm (Roe & Dailey, 1966). Protein content was determined by Bradford's method, and bovine serum albumin was used as a standard (Bradford, 1976). Absorbance was quantified using a microplate reader at a wavelength of 600 nm. For lipid analysis, the crab's lipid was extracted using a mixture of chloroform-methanol, and then the extracted compound was examined using a spectrophotometer at a wavelength of 400 nm with tri-palmitine being used as a standard (Folch et al., 1957).

Fatty acid analysis was conducted using a one-step method by Abdulkadir and Tsuchiya (2008). Freeze-dried samples were mixed thoroughly with hexane, internal standard solution, 14% boron trifluoride (BF_3) in methanol, and nitrogen gas in a capped tube before being heated on a hot plate (100 °C for 120 min) with continuous stirring (700 rpm). After cooling to room temperature, hexane and distilled water were added, mixed, and centrifuged. The upper layer of supernatant that contained fatty acid methyl ester was collected and injected into gas chromatography (GC-2010 Shimadzu) using Zebron ZB-FAME (20 m length × 0.18 mm internal diameter, 0.15 µm thickness) and helium as column and carrier gas, respectively. The peaks of FAMEs were examined by comparing their retention times from the database of NIST08 Mass Spectral Library, and fatty acid concentration was quantified by comparing the peak area of fatty acid in the sample with the peak area of internal standard as in Equation 2 (Aaqillah-Amr et al., 2021):

$$\text{Fatty acid concentration (mg/g)} = (A_S/A_{IS}) \times (C_{IS}/W_S) \quad [2]$$

Where:
A_S = peak area of the fatty acid in the sample in the chromatogram
A_{IS} = peak area of internal standard in chromatogram
C_{IS} = concentration of internal standard (mg)
W_S = weight of sample (g)

Statistical Analysis

All statistical analyses were conducted using the Statistical Package for the Social Sciences (SPSS Version 26). The normal distribution assumption was assessed using the Shapiro-Wilk test, while the homogeneity of variances assumption was evaluated using Levene's test. Since all datasets met the assumptions of normality and homogeneity, for the 7-d experimental period, an unpaired t-test was used to analyse growth performance (survival, molting, and carapace width), oxygen consumption, and biochemical constituents (glycogen, lipid, protein, fatty acid). Meanwhile, for the 14-d experimental period, one-way Analysis of Variance (ANOVA) and Tukey's multiple comparison tests were used to analyse all the growth performance, oxygen consumption, and biochemical constituents. Differences at $p < 0.05$ were considered significant.

RESULTS

Survival, Molting Frequency and Growth Development

Figure 4 showed the effect of starvation on survival rate, molting success and carapace width of early juvenile crabs. Based on the result of the 7-d experimental period, high survival rate for crabs subjected to both 0-d starved and 7-d starved treatments were noted ($p = 1.000$). However, molting success was reduced significantly for 7-d starved crabs compared to 0-d starved crabs (t-test, $p < 0.001$). As molting success reduced, thus 7-d starved crabs) had a decline in carapace width compared to those crabs in the 0-d starved treatment (t-test, $p = 0.026$) (Figure 4). Regarding the result of the 14-d experimental period, 0-d starved crabs exhibited the highest survival rate, then followed by the 7-d starved crabs and 14-d starved crabs (ANOVA, $p < 0.001$). Similarly, molting success decreased for those crabs that reared either in 7-d starved or 14-d starved treatments compared to 0-d starved crabs (39.5%) ($p < 0.001$). Those crabs that starved for 7 days and 14 days indicated lower carapace width than 0-d starved crabs (ANOVA, $p < 0.001$) (Figure 4).

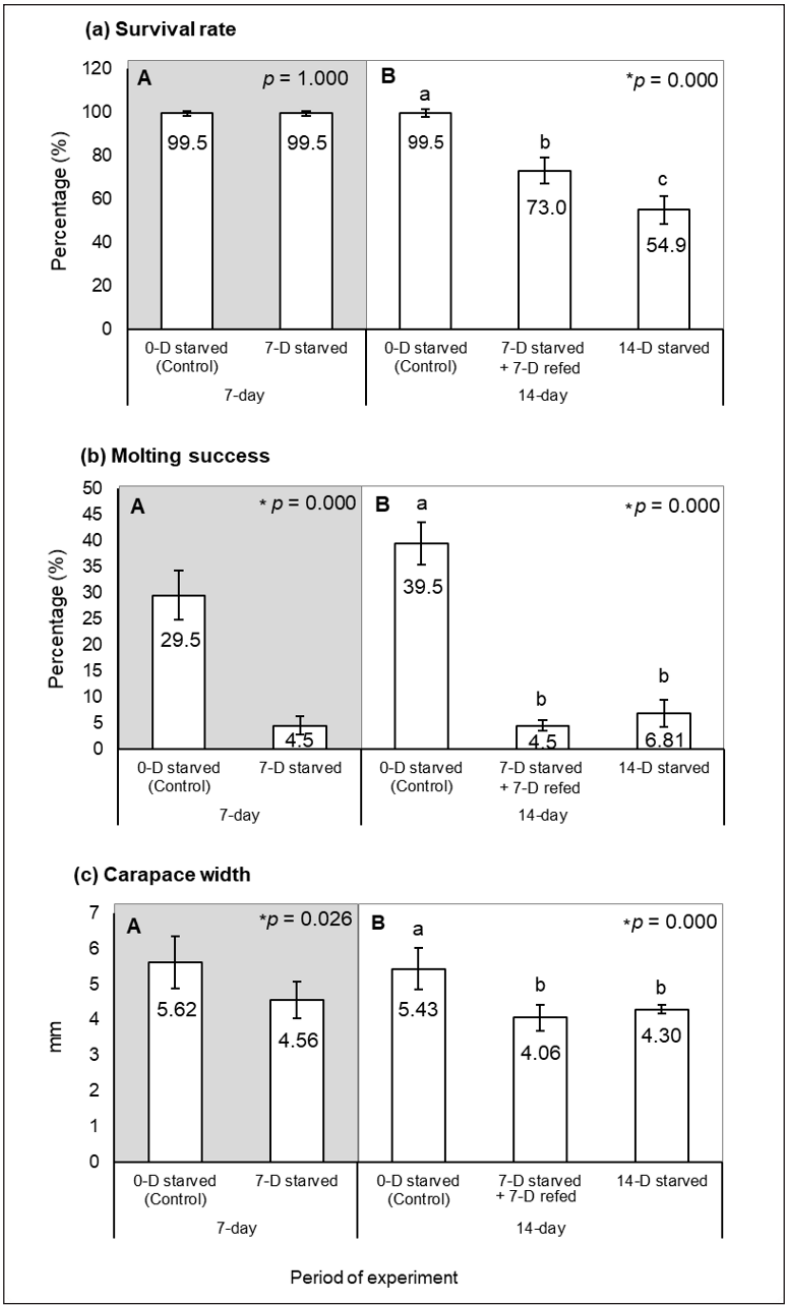

Figure 4. Starvation effect on juveniles of *P. pelagicus* during the (A) 7-day and (B) 14-day experimental periods. (a) Survival rate, (b) molting success, and (c) carapace width. Each treatment was divided into 5 replicates (40 individuals per replicate)

Note. Values are presented as mean ± standard error. [a,b,c] Means with different superscripts are significantly different ($p < 0.05$), and the comparisons were performed within each experimental period, with the 7-d experiment analysed using an unpaired t-test and the 14-d experiment analysed using one-way ANOVA followed by Tukey's post hoc test

Respiration Analysis

Figure 5 demonstrated starvation effect on crab's respiration of juvenile *P. pelagicus* based on the results from the 7-d experimental period, crabs demonstrated significantly higher oxygen consumption for 0-d starved treatments compared to the crabs in 7-d starved treatments (t-test, $p = 0$ .000). Regarding the results from the 14-d experimental period, 0-d starved crabs and 7-d starved crabs indicated higher oxygen consumption compared to the crabs subjected to 14-d starved treatment (ANOVA, $p < 0.001$).

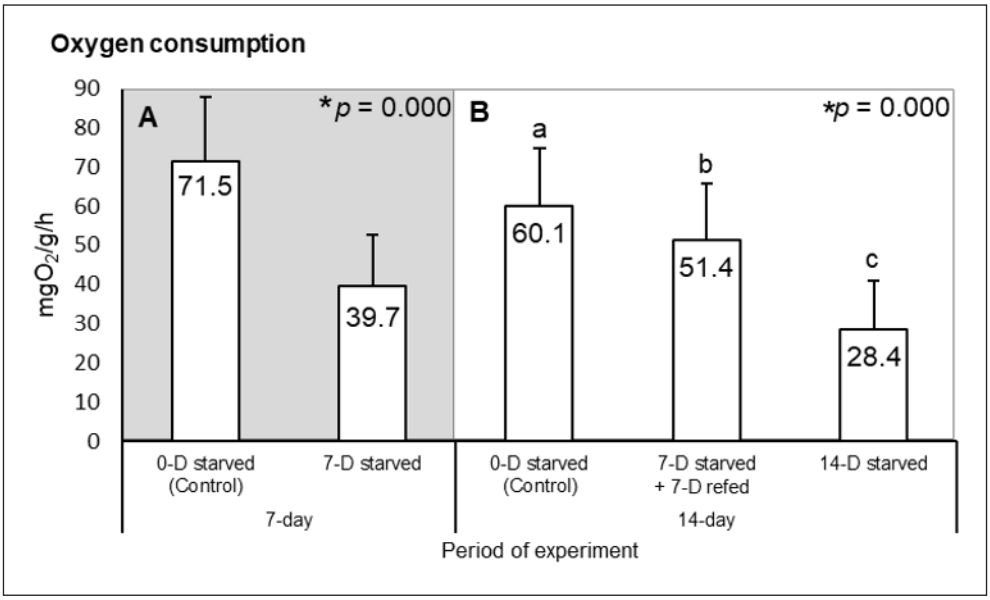

Figure 5. Effect of starvation on the respiration rate of *P. pelagicus* during the (A) 7-day and (B) 14-day experimental periods. Each treatment was divided into 5 replicates (3 individuals per replicate)
Note. Values are presented as mean ± standard error. [a,b,c] Means with different superscripts are significantly different ($p < 0.05$), and the comparisons were performed within each experimental period, with the 7-d experiment analysed using an unpaired t-test and the 14-d experiment analysed using one-way ANOVA followed by Tukey's post hoc test

Biochemical Analyses

Figure 6 shows the starvation effect on the biochemical constituents of juveniles of *P. pelagicus*. Based on the results from the 7-d experimental period, crabs subjected to 0-d starved treatment revealed significantly higher glycogen, protein, and lipid compared to the crabs subjected to 7-d starved (t-test, $p < 0.001$, $p < 0.001$, and $p = 0.026$ for glycogen, protein and lipid, respectively) (Figure 6). Regarding the 14-d experimental period, 7-d starved crabs had the highest glycogen, protein and lipid, followed by the 0-d starved crabs and 14-d starved crabs, with ANOVA, $p < 0.001$ (Figure 6).

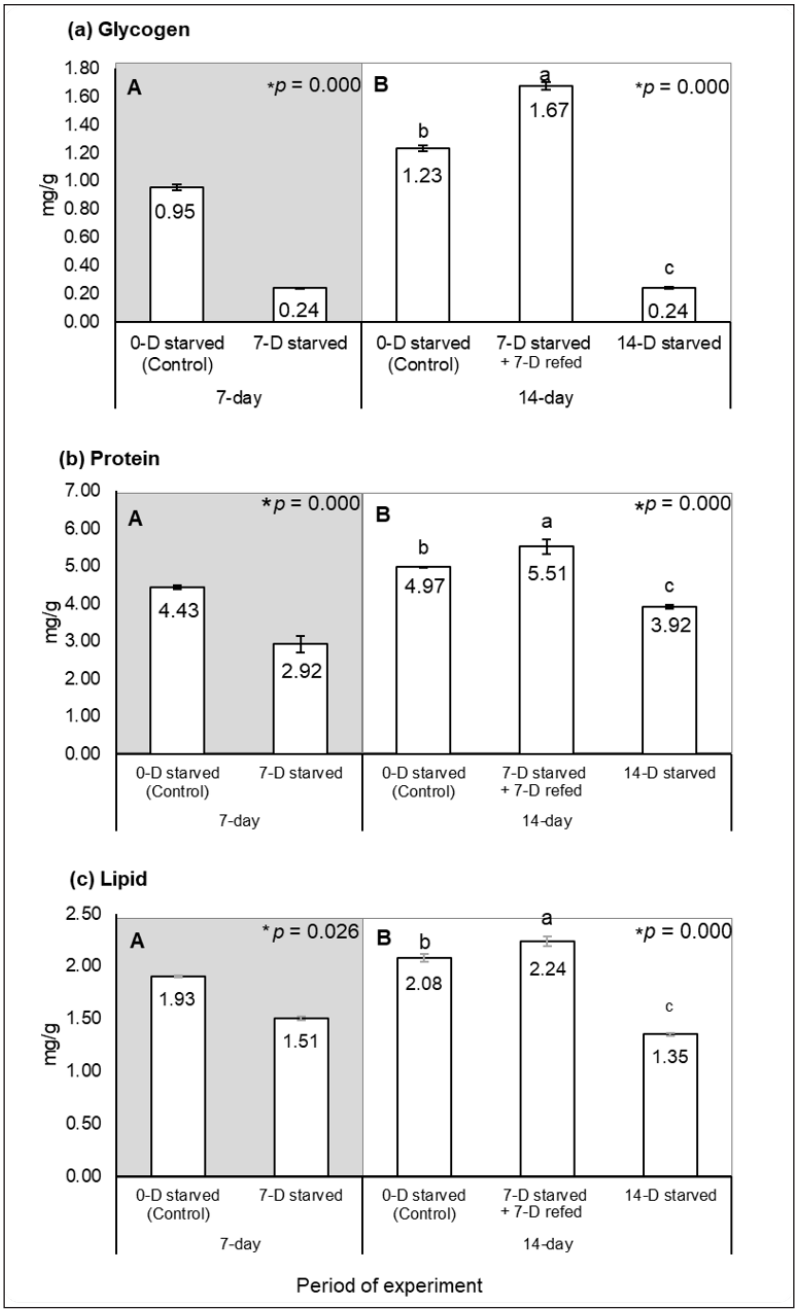

Figure 6. Starvation effect on juvenile's biochemical constituents of *P. pelagicus* during the (A) 7-day and (B) 14-day experimental periods. (a) Glycogen (b) protein and (c) lipid. Each treatment was divided into 5 replicates (5-10 individuals were pooled for per replicate)

Note. Values are presented as mean ± standard error. [a,b,c] Means with different superscripts are significantly different ($p < 0.05$), and the comparisons were performed within each experimental period, with the 7-day experiment analysed using an unpaired t-test and the 14-day experiment analysed using one-way ANOVA followed by Tukey's post hoc test

Fatty acid concentrations in early juvenile *P. pelagicus* were significantly impacted by both the duration of food deprivation and subsequent re-feeding (Table 1). Based on the results from the 7-d experimental period, the concentration of ∑SAFA, saturated fatty acid, ∑MUFA, monounsaturated fatty acid, ∑PUFA, polyunsaturated fatty acid was higher for 0-d starved crabs compared to 7-d starved crabs. This includes ∑n-3 and ∑n-6, which results demonstrated that 0-d starved crabs had higher concentration than 7-d starved crabs (t-test, ~~$p = 0.000$~~, $p < 0.001$ for ∑SAFA, ∑MUFA and ∑PUFA, respectively) (Table 1). Regarding results from the 14-d experimental period, 0-d starved crabs indicated the highest ∑SAFA, ∑MUFA, and ∑PUFA compared to 7-d starved crabs and 14-d starved crabs (ANOVA, $p < 0.001$ for ∑SAFA, ∑MUFA and ∑PUFA, respectively). No significant differences in ∑SAFA and ∑PUFA were observed between the 7-day and 14-day starved crabs, as indicated by the statistical analysis. For C20:5n-3 EPA, eicosapentaenoic acid, the 14-d starved crabs retain a high concentration of 1.13 ± 0.05 mg/g (marked with superscript ab), making them statistically identical to the fully fed control 1.21 ± 0.02 mg/g and significantly higher than the re-fed group 0.81 ± 0.03 mg/g. For C22:6n-3 DHA, docosahexaenoic acid, the 0-day starved crabs exhibited the highest concentration, with no significant difference observed between the 7-day and 14-day starved crabs. For ∑n-3 and ∑n-6, the 0-day starved crabs exhibited significantly higher concentrations than both the 7-day and 14-day starved crabs. But still, the 14-d completely starved crabs retain a substantially higher concentration (1.46 mg/g) of ∑n-3 than the 7-d starved + re-fed (1.05 mg/g).

Table 1
Starvation effect on fatty acid composition of P. pelagicus *juveniles. Each treatment was divided into 5 replicates (5-10 individuals were pooled for per replicate). Means with different superscripts indicate significant differences (p <0.05). ∑SAFA, total saturated fatty acids; ∑MUFA, total monounsaturated fatty acids; ∑PUFA, total polyunsaturated fatty acids; EPA, eicosapentaenoic acid (20:5n-3); DHA, docosahexaenoic acid (22:6n-3)*

Fatty Acids	Concentration of Fatty Acids (mg/g)				
	7-d Experimental Period		14-d Experimental Period		
	0-d Starved (Control)	7-d Starved	0-d Starved (Control)	7-d Starved + 7-d refed	14-d Starved
∑SAFA	5.65 ± 0.12^{a}	1.58 ± 0.05^{b}	3.62 ± 0.03^{a}	2.35 ± 0.05^{b}	2.53 ± 0.13^{b}
C11:0	0.28 ± 0.03^{a}	0.25 ± 0.05^{a}	0.23 ± 0.05^{a}	0.21 ± 0.04^{a}	0.26 ± 0.07^{a}
C14:0	0.24 ± 0.00^{a}	0.08 ± 0.00^{a}	0.13 ± 0.05^{a}	0.15 ± 0.03^{a}	0.16 ± 0.03^{a}
C16:0	4.90 ± 0.08^{a}	1.16 ± 0.04^{b}	3.09 ± 0.00^{a}	1.88 ± 0.05^{b}	1.98 ± 0.10^{b}
C17:0	0.24 ± 0.00^{a}	0.09 ± 0.00^{b}	0.16 ± 0.05^{a}	0.11 ± 0.07^{a}	0.13 ± 0.05^{a}
∑MUFA	3.03 ± 0.04^{a}	0.55 ± 0.02^{b}	2.25 ± 0.01^{a}	1.44 ± 0.07^{b}	0.95 ± 0.03^{c}
C16:1	0.18 ± 0.00^{a}	0.03 ± 0.00^{b}	0.12 ± 0.06^{a}	0.08 ± 0.07^{a}	0.06 ± 0.08^{a}

Table 1 (*continued*)

Fatty Acids	Concentration of Fatty Acids (mg/g)				
	7-d Experimental Period		14-d Experimental Period		
	0-d Starved (Control)	7-d Starved	0-d Starved (Control)	7-d Starved + 7-d refed	14-d Starved
C18:1	2.72 ± 0.05^{a}	0.47 ± 0.01^{b}	2.02 ± 0.03^{a}	1.28 ± 0.06^{b}	0.77 ± 0.03^{c}
C20:1	0.13 ± 0.02^{a}	0.05 ± 0.00^{b}	0.11 ± 0.05^{a}	0.08 ± 0.07^{a}	0.12 ± 0.04^{a}
∑PUFA	7.03 ± 0.18^{a}	1.48 ± 0.04^{b}	4.86 ± 0.05^{a}	2.72 ± 0.09^{b}	2.51 ± 0.11^{b}
C18:2n-6	3.32 ± 0.10^{a}	0.28 ± 0.01^{b}	2.36 ± 0.02^{a}	1.16 ± 0.05^{b}	0.46 ± 0.02^{c}
C18:3n-6	0.17 ± 0.01^{a}	0.04 ± 0.00^{b}	0.12 ± 0.05^{a}	0.08 ± 0.06^{a}	0.07 ± 0.05^{a}
C20:2n-6	0.27 ± 0.01^{a}	0.09 ± 0.00^{b}	0.27 ± 0.00^{a}	0.15 ± 0.01^{b}	0.18 ± 0.02^{b}
C20:4n-6	0.62 ± 0.02^{a}	0.21 ± 0.01^{b}	0.45 ± 0.01^{a}	0.29 ± 0.01^{b}	0.34 ± 0.01^{b}
C20:5n-3 EPA	1.92 ± 0.03^{a}	0.66 ± 0.02^{b}	1.21 ± 0.02^{a}	0.81 ± 0.03^{b}	1.13 ± 0.05^{ab}
C22:6n-3 DHA	0.73 ± 0.03^{a}	0.02 ± 0.01^{b}	0.45 ± 0.01^{a}	0.24 ± 0.01^{b}	0.33 ± 0.01^{b}
∑n-3	2.65	0.85	1.66	1.05	1.46
∑n-6	4.38	0.62	3.20	1.67	1.05
n-3: n-6	0.60	1.37	0.60	0.46	1.38

DISCUSSION

The shortage of food resources in nature causes the food deficiency period to become common in the lives of most wild crabs, particularly during the fragile stage (early juvenile). Following these emerging challenges, this study clarified how starvation could interfere with survival, growth, respiration process, and biochemical constituents of early juvenile *P. pelagicus*. The present study exhibited that survival remained high at 99.5% for early juvenile crabs subjected to both 0-d starved and 7-d starved treatments in a 7-d experimental period. Despite the survival being high, molting success reduced significantly for 7-d starved crabs compared to 0-d starved crabs, leading to a reduced carapace width of the 7-d starved crabs compared to 0-d starved crabs. Similarly, the result from the 14-d experimental period showed molting success, and carapace width decreased for those crabs that reared either in 7-d starved or 14-d starved treatments compared to 0-d starved crabs. The present finding is consistent with Souza et al. (2017), who observed that megalopa of mangrove crabs, such as *Sesarma curacaoense* and *Sesarma rectum*, exhibited significantly lower metamorphosis rates in crabs after going through a seven-day starvation period compared to the control treatment. Also, the megalopa of *Sesarma rectum* had prolonged days to metamorphosis to juvenile after being treated with a seven-day starvation period

(15.2 days) compared to the control crabs (11.8 days) (Souza et al., 2017). Gong et al. (2015) found that none of the C1 stage mud crab, *Scylla paramamosain*, subjected to starvation progressed to the C2 stage, while control crabs were able to molt normally after 4.8 days. The results of the present and previous studies emphasise d a delay in molting when attributed to a lack of food.

Additionally, present findings indicated lower oxygen consumption for any crabs exposed to fully-starved conditions, either for seven days or 14-d. Meanwhile, fully fed (0-d starved) and re-fed crabs (7-d starved in the 14-d experimental period) exhibited higher oxygen consumption. This result was in accordance with a past study, which discovered that the false southern king crab (*Paralomis granulosa* had reduced oxygen consumption as the crabs were subjected to six days and twelve days of starvation (23.8 µg O_2/h/g and 27.0 µg O_2/h/g, respectively) compared to the fully fed crabs (33.4 µg O_2/h/g) (Comoglio et al., 2005). Similarly, Jiang (2022) conducted a study on rock crab, *Cancer irroratus,* and found that the starved crabs had lower oxygen consumption (22.6 mgO_2/kg/h) than the fully fed crabs (60.6 mgO_2/kg/h). In response to starvation, crabs tend to lower their metabolic rate by reducing locomotor activity and heart rate to prevent unnecessary energy expenditure (Jiang, 2022).

In the context of biochemical constituents, fully starved juvenile crabs showed significantly lower glycogen, protein, and lipid compared to the control crabs, with glycogen reserve depleted rapidly (>74%), protein (<34%) and lipid (<35%). The result suggested that the energy demand for starved crabs was offset by utilising glycogen, protein, and lipid, which are necessary for prolonging the survival of the early juvenile crabs. This physiological trend has been clearly described in previous works. For example, Sacristán et al. (2019) demonstrated a reduction of glycogen content in the hepatopancreas of the southern king crab, *Lithodes Santolla*, after 60-d of starvation (0.48 mg/g) compared to the crabs being fed daily (0.64 mg/g). Similarly, a study by Vinagre and Chung (2016) indicated reduced glycogen content in the hepatopancreas and muscle of starved Atlantic ghost crab (*Ocypode quadrata),* by 40% and 50%, respectively. In terms of lipid, previous evidence demonstrated reduced lipid content in starved larvae of *P. pelagicus* after nine days (0.73 µg/larva) than the larvae on the initial day (1.19 µg/larva). Also, Comoglio et al. (2005) exhibited that the false southern king crab, *P. granulosa*, had reduced lipid content in 9-day starved crabs (4.3%) compared to control crabs (9.7%). The decrease in lipid in the present study is complemented by the result of fatty acids, which showed that starved crabs had reduced ∑SAFA, ∑MUFA, ∑PUFA, ∑n-3, and ∑n-6 (Table 2). Holme et al. (2009) reported that starved Zoea 5 and megalopa of mud crab, *S. serrata*, had decreased ∑SAFA, ∑MUFA, ∑PUFA, ∑n-3, and ∑n-6 than the fully fed group. Other previous studies also found Zoea 1 of blue swimming crab, *P. pelagicus,* indicated lower ∑SAFA, ∑MUFA, ∑PUFA, ∑n-3, and ∑n-6 than the fed group.

Table 2
The effect of starvation on fatty acid composition of different crab species. Comparison between the present study and the previous study

Species	Starvation Period	∑SAFA	∑MUFA	∑PUFA	EPA	DHA	Unit	Reference
Portunus pelagicus (Juvenile)	0-days	5.65	3.03	7.03	1.92	0.73	mg/g	Present study
	7-days	1.58	0.55	1.48	0.66	0.02		
P. pelagicus (Juvenile)	0-days	3.62	2.25	4.86	1.21	0.45	mg/g	Present study
	14-days	2.53	0.95	2.51	1.13	0.33		
P. pelagicus (Zoea 1)	0-days	0.13	0.10	0.26	0.10	0.10	%	Wu et al., 2017
	3-days	0.08	0.08	0.10	0.04	0.03		
P. trituberculatus (Adult)	0-days	29.7	37.4	32.7	8.08	12.3	%	Ding et al., 2017
	30-days	26.7	36.9	36.3	8.92	14.9		
P. trituberculatus (Adult)	0-days	36.6	52.3	10.3	1.1	1.9	%	Ding et al., 2017
	30-days	31.3	53.5	12.3	1.73	2.43		
Scylla serrata (Zoea 5)	0-days	11.0	11.4	10.3	4.4	1.47	µg/mg	Holme et al., 2009
	4-days	4.94	3.08	5.43	2.78	0.79		
S. serrata (Megalopa)	0-days	8.19	10.6	8.93	2.86	2.23	µg/mg	Holme et al., 2009
	6-days	4.20	4.20	3.90	1.55	0.77		

Note. The highlighted number indicated a higher fatty acid reading

However, looking at the fatty acid trend in adult blue crab, *Portunus trituberculatus* (Table 2), indicated no reduction of ∑PUFA, DHA and EPA in starved crabs, probably to ensure the functioning of the nervous system, membrane integrity, stress resistance, and immunity at an optimum state rather than utilising these fatty acids as a source of energy (Wu et al., 2017). This observation demonstrated differences in fatty acid utilisation between the early growth stage and the adult stage in crabs. Perhaps, owing to incomplete growth development, early-stage crabs would use all the fatty acids to prolong their survival as long as possible, regardless of the importance of specific fatty acids to carry out certain vital functions. Through this process, the larvae or early crabs expend considerable energy, which ultimately causes higher mortality among the early-stage crabs. Interestingly, regarding to 14-day experimental period, 7-d starved crablets stated higher glycogen, protein and lipid compared to the 0-d starved crablets. The result highlighted that the crablet subjected to 7-d of starvation, then re-fed for 7-d, had the highest glycogen, lipid, and protein content compared to the fully fed crablet. Perhaps, as the crablet experienced a 7-day starvation, it responded to this starvation stress by storing as much energy as possible during the re-fed state. The stored glycogen, lipids, and proteins could subsequently be utilised as energy reserves to support survival during prolonged starvation. This event is considered part of the acclimation process.

Additionally, the higher fatty acid concentrations observed in the 14-day starvation experiment compared with the 7-day starvation experiment should be interpreted with caution. Although prolonged starvation is generally expected to further deplete lipid reserves, the initial fatty acid composition of the control groups differed between the two independent experiments. Specifically, the 7-day experiment began with a higher total fatty acid content than the 14-day experiment, reflecting variation between experimental batches of crablets. This variation may be attributed to differences in the physiological condition, nutritional history, broodstock quality, or natural biological variability of juvenile *P. pelagicus* obtained from different spawning batches. Consequently, the fatty acid concentrations between the 7- and 14-day experiments are not directly comparable. Instead, each starvation period should be interpreted relative to its respective control, allowing the effects of starvation to be evaluated within each independent experimental batch. This batch-to-batch variation represents a limitation of the present study and should be considered when comparing the magnitude of lipid depletion between the two starvation durations.

Many crustaceans likely use glycogen reserves as a primary energy source rather than using lipids and proteins during starvation (Sacristán et al., 2019). The rapid depletion of glycogen observed during starvation is likely attributable to its role as the primary and readily accessible energy reserve in crustaceans. The hepatopancreas is the main site for crustacean energy reserves, which are stored as glycogen (Vinagre et al., 2020). As the

glucose level drops in the haemolymph due to starvation, the X-organ secretes CHH to stimulate glycogenolysis in the hepatopancreas, breaking down glycogen into sugar to maintain glucose levels in the haemolymph for sustaining muscular energy requirements (Sanchez-Paz et al., 2006). Glycogen also plays a role in crab moulting, which is imperative for chitin synthesis (Sugumar et al., 2013; Sanchez-Paz et al., 2006). Since the glycogen reserve is used to provide energy during the starvation period, it reduces the amount of glycogen available for crustacean molting, leading to molt delay for starved crabs, as shown in the present study. Additionally, lipids serve as an additional source of energy during prolonged periods of starvation. The hepatopancreas is also known as the main lipid storage tissue, and lipolysis occurs to break down lipids into glycerol and fatty acids (Sanchez-Paz et al., 2006). Glycerol is then converted into glucose through gluconeogenesis, whereas fatty acids proceed through the β-oxidation pathway, resulting in acetylCoA that can be oxidised by the tricarboxylic acid cycle, producing ATP or energy (Vinagre et al., 2020). The present study also found that while glycogen was rapidly utilised in starved crabs, protein concentration decreased slightly because some protein breakdown is necessary to support glycogenolysis (glycogen to glucose) during the initial state of starvation. When energy sources from glycogen and lipids are limited, then the gluconeogenesis (protein to glucose) process is initiated, whereby proteolysis in crab muscle is stimulated to degrade proteins into amino acids and mobilise them into tissues for glucose synthesis and ATP production (Pellegrino et al., 2013). However, prolonged starvation may cause harmful effects when proteins are used as an energy source due to insufficient nutrient availability.

CONCLUSION

Overall, this study provides insight into the starvation effect on survival, growth, respiration process, and biochemical constituents of early juvenile crabs by using *P. pelagicus as a model.* It was observed that starvation negatively affected survival, molting, and growth of early juvenile crabs after seven days of being subjected to starvation, while fully-fed crabs increased in growth and molting frequency. Likewise, respiration rate is reduced with the prolonged starvation period as one of the ways to lower crab metabolic rate in grappling with such adverse conditions. In the context of biochemical constituents, starved crabs demonstrated a reduction in glycogen, protein, and lipids, including all fatty acid elements such as ∑SAFA. ∑PUFA, ∑MUFA, DHA, and EPA in their body tissues. Therefore, we confirmed that the internal body of *P. pelagicus* lined up several strategies (such as delayed molting, reduced oxygen consumption, used reserve glycogen, lipid and protein) to overcome feed deprivation. This is until the crab's internal body mechanism exhausts all avenues to compensate for energy demand since all the storage energy is already being utilised, hence causing the mortality of the crabs. Overall, the present finding demonstrated the relation between the nutritional condition and starvation on *the early growth of crabs*.

Such knowledge should be valuable for a better understanding of early juveniles' resilience in enduring starvation. Likewise, studying the effects of starvation on crablets provides important insights for optimising feeding strategies and culture protocols in *P. pelagicus* aquaculture by identifying the species' tolerance to temporary feed deprivation and improving feed management practices.

ACKNOWLEDGEMENT

The authors are grateful to all the staff at the Faculty of Fisheries and Food Science and the Institute of Tropical Aquaculture and Fisheries, Universiti Malaysia Terengganu**.**

ETHICAL APPROVAL

The authors followed research ethics guidelines from the Office of Research Management (RMO), Universiti Malaysia Terengganu (UMT), Kuala Terengganu, for the care and use of animals in this whole experiment as outlined in the Research Ethics Guidelines for the Ethics of Research on Animals 2014 (UMT; https://studylib.net/doc/8738550/research-ethics-guidelines—pusat-pengurusan-penyelidikan).

DATA AVAILABILITY

This manuscript has no associated data.

COMPETING INTERESTS

The authors declare no conflict of interest. The funders had no role in the design of the study, in the collection, analyses, or interpretation of data, in the writing of the manuscript, or in the decision to publish the results.

FUNDING

The study was fully funded by the Fundamental Grant Research Scheme (FRGS), Universiti Malaysia Terengganu (Vot. No. 59460). The study is also part of the research program under the Higher Institution Center of Excellence (HICoE) Grant for the Development of Future Food Through Sustainable Shellfish Aquaculture (HICoE AKUATROP Trust Account No. 66955).

ABBREVIATION

D - day

SAFA - saturated fatty acid

MUFA - monounsaturated fatty acid

PUFA - polyunsaturated fatty acid

DHA - docosahexaenoic acid

EPA - eicosapentaenoic acid

REFERENCES

Aaqillah-Amr, M. A., Hidir, A., Ahmad-Ideris, A. R., Muhamad-Zulhilmi, R., Hong Peng, T., Abualreesh, M. H., Noordiyana, M. N., Ma, H., & Ikhwanuddin, M. (2021). The effect of lipid level on the growth and reproductive performance of female orange mud crab, *Scylla olivacea* (Herbst, 1796), during the fattening period. *Aquaculture Nutrition, 27*(6), 2497-2513. https://doi.org/10.1111/anu.13380

Abdulkadir, S., & Tsuchiya, M. (2008). One-step method for quantitative and qualitative analysis of fatty acids in marine animal samples. *Journal of Experimental Marine Biology and Ecology, 354*(1), 1-8. https://doi.org/10.1016/j.jembe.2007.08.024

Bradford, M. M. (1976). A rapid and sensitive method for the quantitation of microgram quantities of protein utilizing the principle of protein-dye binding. *Analytical Biochemistry, 72*(1-2), 248-254. https://doi.org/10.1016/0003-2697(76)90527-3

Bromilow, A. M., & Lipcius, R. N. (2017). Mechanisms governing ontogenetic habitat shifts: Role of trade-offs, predation, and cannibalism for the blue crab. *Marine Ecology Progress Series, 584*, 145-159. https://doi.org/10.3354/meps12405

Comoglio, L., Smolko, L., & Amin, O. (2005). Effects of starvation on oxygen consumption, ammonia excretion and biochemical composition of the hepatopancreas on adult males of the false southern king crab *Paralomis granulosa* (Crustacea, Decapoda). *Comparative Biochemistry and Physiology Part B: Biochemistry and Molecular Biology, 140*(3), 411-416. https://doi.org/10.1016/j.cbpc.2004.11.003

Ding, L., Fu, H., Hou, Y., Jin, M., Sun, P., & Zhou, Q. (2017). Effects of starvation and feeding on blood chemistry, fatty acid composition and expression of vitellogenin and fatty acid-binding protein genes in female swimming crab *Portunus trituberculatus* broodstock. *Fisheries Science, 83*(3), 455-464. https://doi.org/10.1007/s12562-017-1075-3

Dvoretsky, A. G., & Dvoretsky, V. G. (2020). Effects of environmental factors on the abundance, biomass, and individual weight of juvenile red king crabs in the Barents Sea. *Frontiers in Marine Science, 7*, Article 726. https://doi.org/10.3389/fmars.2020.00726

Folch, J., Lees, M., & Sloane Stanley, G. H. (1957). A simple method for the isolation and purification of total lipides from animal tissues. *Journal of Biological Chemistry, 226*(1), 497-509. https://doi.org/10.1016/S0021-9258(18)64849-5

Gong, J., Yu, K., Shu, L., Ye, H., Li, S., & Zeng, C. (2015). Evaluating the effects of temperature, salinity, starvation and autotomy on molting success, molting interval and expression of ecdysone receptor in early juvenile mud crabs, *Scylla paramamosain*. *Journal of Experimental Marine Biology and Ecology, 464*, 11-17. https://doi.org/10.1016/j.jembe.2014.12.008

Hidir, A., Aaqillah-Amr, M. A., Mohd-Sabri, M., Mohd-Zaidi, I., Shahreza, M. S., Abualreesh, M. H., Peng, T. H., Ma, H., Waiho, K., Fazhan, H., Mukti, A. T., & Ikhwanuddin, M. (2022). Thermal tolerance of purple

mud crab, *Scylla tranquebarica* (Fabricius, 1798), during egg incubation, larval rearing and juveniles' production. *Aquaculture Research, 53*(4), 1481-1491. https://doi.org/10.1111/are.15682

Hines, A. H., Kramer, M. A., Richie, K. D., Smith, L. D., Aguilar, R., Ogburn, M. B., Johnson, E. G., & Ruiz, G. M. (2026). Cannibalism, predation, and refuges of juvenile blue crabs from a 37-year experiment. *Proceedings of the National Academy of Sciences, 123*(12), Article e2533461123. https://doi.org/10.1073/pnas.2533461123

Holme, M., Brock, I., Southgate, P. C., & Zeng, C. (2009). Effects of starvation and feeding on lipid class and fatty acid profile of late stage mud crab, *Scylla serrata*, larvae. *Journal of the World Aquaculture Society, 40*(4), 493-504. https://doi.org/10.1111/j.1749-7345.2009.00278.x

Jiang, Q. (2022). *Effect of food deprivation states on behavioral and physiological responses to hypoxia in rock crabs (Cancer irroratus)* [Doctoral dissertation, Memorial University of Newfoundland]. Memorial University of Newfoundland Research Repository. https://research.library.mun.ca/15735/1/thesis.pdf

Josileen, J., & Menon, N. G. (2005). Growth of the blue swimmer crab, *Portunus pelagicus* (Linnaeus, 1758) (Decapoda, Brachyura) in captivity. *Crustaceana, 78*(1), 1-18. https://doi.org/10.1163/1568540054024556

Pellegrino, R., Martins, T. L., Pinto, C. B., Schein, V., Kucharski, L. C., & Da Silva, R. S. (2013). Effect of starvation and refeeding on amino acid metabolism in muscle of crab *Neohelice granulata* previously fed protein- or carbohydrate-rich diets. *Comparative Biochemistry and Physiology Part A: Molecular & Integrative Physiology, 164*(1), 29-35. https://doi.org/10.1016/j.cbpa.2012.08.004

Potter, I. C., & de Lestang, S. (2000). Biology of the blue swimmer crab *Portunus pelagicus* in Leschenault Estuary and Koombana Bay, south-western Australia. *Journal of the Royal Society of Western Australia, 83*(4), 443-458.

Rodgers, G. G., Tenzing, P., & Clark, T. D. (2016). Experimental methods in aquatic respirometry: The importance of mixing devices and accounting for background respiration. *Journal of Fish Biology, 88*(1), 65-80. https://doi.org/10.1111/jfb.12848

Roe, J. H., & Dailey, R. E. (1966). Determination of glycogen with the anthrone reagent. *Analytical Biochemistry, 15*(2), 245-250. https://doi.org/10.1016/0003-2697(66)90028-5

Romano, N., & Zeng, C. (2006). The effects of salinity on the survival, growth and haemolymph osmolality of early juvenile blue swimmer crabs, *Portunus pelagicus*. *Aquaculture, 260*(1-4), 151-162. https://doi.org/10.1016/j.aquaculture.2006.06.019

Sacristán, H. J., Di Salvatore, P., Fernández-Gimenez, A. V., & Lovrich, G. A. (2019). Effects of starvation and stocking density on the physiology of the male of the southern king crab *Lithodes santolla*. *Fisheries Research, 218*, 83-93. https://doi.org/10.1016/j.fishres.2019.05.006

Sánchez-Paz, A., García-Carreño, F., Muhlia-Almazán, A., Peregrino-Uriarte, A. B., Hernández-López, J., & Yepiz-Plascencia, G. (2006). Usage of energy reserves in crustaceans during starvation: Status and future directions. *Insect Biochemistry and Molecular Biology, 36*(4), 241-249. https://doi.org/10.1016/j.ibmb.2006.01.002

Souza, A. S., Paula, G. D., Simith, D. J. B., & Abrunhosa, F. A. (2017). Effects of temporary starvation and feeding on the survival and developmental time to metamorphosis in megalopa larvae of two Neotropical

mangrove crab species, genus *Sesarma* (Sesarmidae). *Journal of Experimental Marine Biology and Ecology, 497*, 134-142. https://doi.org/10.1016/j.jembe.2017.09.017

Sugumar, V., Vijayalakshmi, G., & Saranya, K. (2013). Molt cycle related changes and effect of short-term starvation on the biochemical constituents of the blue swimmer crab *Portunus pelagicus*. *Saudi Journal of Biological Sciences, 20*(1), 93-103. https://doi.org/10.1016/j.sjbs.2012.10.003

Vinagre, A. S., & Chung, J. S. (2016). Effects of starvation on energy metabolism and crustacean hyperglycemic hormone (CHH) of the Atlantic ghost crab *Ocypode quadrata* (Fabricius, 1787). *Marine Biology, 163*(1), Article 3. https://doi.org/10.1007/s00227-015-2797-3

Vinagre, A. S., Model, J. F. A., Vogt, E. L., Manara, L. M., Trapp, M., Silva, R. S. M., & Chung, J. S. (2020). Diet composition and long-term starvation do not affect crustacean hyperglycemic hormone (CHH) transcription in the burrowing crab *Neohelice granulata* (Dana, 1851). *Comparative Biochemistry and Physiology Part A: Molecular & Integrative Physiology, 247*, Article 110738. https://doi.org/10.1016/j.cbpa.2020.110738

Wang, S., Carter, C. G., Fitzgibbon, Q. P., & Smith, G. G. (2021a). The use of stoichiometric bioenergetics to elucidate metabolic energy substrate use and specific dynamic action in cultured juvenile spiny lobsters (*Sagmariasus verreauxi*) of different nutritional status. *Aquaculture, 532*, Article 736021. https://doi.org/10.1016/j.aquaculture.2020.736021

Wang, S., Carter, C. G., Fitzgibbon, Q. P., Codabaccus, B. M., & Smith, G. G. (2021b). Effect of dietary protein on energy metabolism including protein synthesis in the spiny lobster *Sagmariasus verreauxi*. *Scientific Reports, 11*, Article 11814. https://doi.org/10.1038/s41598-021-91304-1

Wang, S., Fitzgibbon, Q. P., Carter, C. G., & Smith, G. G. (2019). Effect of protein synthesis inhibitor cycloheximide on starvation, fasting and feeding oxygen consumption in juvenile spiny lobster *Sagmariasus verreauxi*. *Journal of Comparative Physiology B, 189*(3-4), 351-365. https://doi.org/10.1007/s00360-019-01221-z

Wu, X., Zeng, C., & Southgate, P. C. (2017). Effects of starvation on survival, biomass, and lipid composition of newly hatched larvae of the blue swimmer crab, *Portunus pelagicus* (Linnaeus, 1758). *Aquaculture International, 25*(1), 447-461. https://doi.org/10.1007/s10499-016-0042-9

Pertanika J. Trop. Agric. Sci. 49 (5): 2155 - 2169 (2026)

PERTANIKA JOURNALS

TROPICAL AGRICULTURAL SCIENCE

Journal homepage: http://www.pertanika.upm.edu.my/

Review Article

A Review on the Use of Spices in the Blending of Malaysian Curry Powder Matrix

Chon Lok Siaw, Nyuk Ling Chin* and Nor Amaiza Mohd Amin

Department of Process and Food Engineering, Faculty of Engineering, Universiti Putra Malaysia, 43400 UPM Serdang, Selangor, Malaysia

ABSTRACT

Malaysian curry powder is a complex spice matrix formulated to produce a characteristic balance of aroma, taste, pungency, heat and colour. This review aims to synthesise current knowledge on the principal spices used in Malaysian curry powder, their sensory and functional contributions, volatile flavour compounds, blending processes and quality requirements, thereby providing a scientific basis for formulation optimisation, consistent product quality and future industrial development. Common ingredients include coriander, cumin, fennel, chilli, turmeric, black or white pepper, cinnamon, star anise, cardamom, cloves, nutmeg, fenugreek and ginger, although their combinations vary according to culinary application and commercial formulation. The volatile compounds reported in Malaysian curry powder are consistent with the presence of several commonly used spices. For example, linalool is strongly associated with coriander, cuminaldehyde with cumin, *trans*-anethole with fennel or star anise, turmerones with turmeric and zingiberene with ginger. However, because several spices may contain the same volatile compounds, these associations should not be interpreted as definitive identification of their botanical sources. Processing operations, particularly cleaning, grinding and blending, influence flavour retention, homogeneity and product consistency. Commercial meat and fish curry powders also differ in their spice composition and sensory profiles, with meat curry powders generally exhibiting a stronger and more robust profile, while fish curry powders tend to be milder and more aromatic. Appropriate raw material selection, controlled processing, and compliance with chemical and microbiological quality requirements are therefore essential for producing consistent and acceptable curry powder. Further quantitative research on spice

ARTICLE INFO

Article history:
Received: 26 June 2026
Accepted: 17 September 2026
Published: 30 October 2026

DOI: https://doi.org/10.47836/pjtas.49.5.03

E-mail addresses:
currysiaw@gmail.com (Chon Lok Siaw)
chinnl@upm.edu.my (Nyuk Ling Chin)
myza@upm.edu.my (Nor Amaiza Mohd Amin)
* Corresponding author

© Universiti Putra Malaysia Press

proportions, flavour interactions and functional properties is needed to support formulation optimisation and industrial quality control.

Keywords: Aroma, flavour, functional, quality, spice

INTRODUCTION

Spices are edible plant products used to flavour foods and beverages due to their appealing fragrances and sensory attributes. Spices are among the oldest traded commodities, dating back to at least two millennia. For thousands of years, aromatic plant materials have been used in food preparation (Farrell, 185). Definitions of spices may vary according to their geographical origin and historical use. According to Hirasa and Takemasa (1998), spices are sometimes defined by where they are grown or when they started to be used as spices. They are derived from dried plant parts, such as flowers, leaves, bark, stems, seeds, and roots (Figure 1). These parts are usually dried and ground to a mesh size of 40-60, corresponding to a particle size range of approximately 250-425 µm. The American Spice Trade Association (ASTA) (2023) defines the term spice as any aromatic vegetable substance in the whole, broken or ground form, except for those substances which have been traditionally regarded as foods, such as onions, garlic and celery. Today, the United States is both the world's largest consumer and the major importer of spices (Furth & Cox, 2004).



Figure 1. Representative spices commonly used in Malaysian curry-powder formulations in the form of whole and ground spices
Source: Adapted from Killebrew (2025)

With the trend of moving towards using spices to compensate for less salt and fat in food and the heightened popularity of ethnic foods in the West, the demand for spices in the world is increasing to record levels. According to Chironi et al. (2021), the globalisation of markets and the migration phenomenon have contributed to the modification of food preferences of consumers who gradually introduce spices into their eating habits. The delicate aroma of spices also contributes to consumer acceptance (Karadbhajne & Saraf, 2017). In Malaysia, the blends of spices are commonly used as important ingredients in food formulations in industry, apart from individual households and also the caterers, restaurants, etc. The growth of ethnic food popularity, including curries, also fuels the increasing demand for spices and their blends, providing a flavourful, distinctive aroma and tasty food products. Spices and herbs are also known as excellent sources of phenolic and polyphenolic compounds with bioactive functions and phytochemicals (Embuscado, 2019). According to Chhetri et al. (2015) and Hirasa and Takemasa (1998), spices are also being used in medicine, pharmaceuticals, perfumery, cosmetics and several other industries. Al-Habsi et al. (2025) reviewed the therapeutic properties, antioxidant and antimicrobial activities of herbs and spices. Studies relating to curry powder are mostly scientific and experimentally based, such as Meher and Meher (2020), who investigated chemical, rheological and sensory properties of curry-spices blend and Siripongvutikorn et al. (2024), who investigated phytochemical profiling and antioxidant activities of Thai curries. This review is devoted specifically to Malaysian curry powder, outlining the integrated spice matrix, particularly the relationships among spice composition, volatile flavour compounds, sensory functions, processing operations and quality requirements.

KEY SPICES AND THEIR FUNCTIONAL ROLE

Spices are unique and play multiple roles in food systems because they add both flavour and colour even in small quantities. According to the Spices Board (2021), Raghavan Uhl (2000) and Reineccius (1999), the key spices used in basic curry blends such as curry powder are coriander, fennel, cumin, chilli, turmeric, cinnamon, star anise, black and white pepper, clove and cardamom. Occasionally, ginger, nutmeg and fenugreek are used depending on region, ethnicity and cultural practices. Each spice has a distinctive aroma and flavour profile and performs a specific role in flavour development. Spices, when added to foods, also contribute to pungency as Raghavan (2010) noted, curry powder is considered a food that contributes ‘heat’. These spices are the fundamental aroma and taste ingredients of the product. The appropriate use of spices based on their functional roles is direct and specific in cooking or blending. Hirasa and Takemasa (1998) identified four functional categories of spices, i.e. flavouring, masking, pungency and colouring, as listed in Table 1.

Table 1
Basic functions of spices used in food

Functions	Spices
Flavouring	Allspice, cinnamon, fennel, cumin, basil, star anise, marjoram, cardamom, dill, nutmeg, parsley, mace, tarragon
Masking	Garlic, clove, onion, coriander, bay leaf, thyme, caraway, sage, oregano
Pungency	Pepper, black and white pepper, ginger, mustard, Japanese pepper
Colourant	Turmeric, paprika, saffron

Spices are used in ground, broken or whole forms to impart specific aroma, flavour and taste to foods. They can also be blended to form spice mix preparations after the pre-cleaning and grinding process. Malaysia has many spice blends such as curry powder, Chinese 5-spice powder, tandoori, 'biryani' mix, chilli blends, 'rendang', 'masala', 'Sichuan mala', 'bakuteh' and other localised blends (Raghavan Uhl, 2000). The most famous spice blend is the Malaysian curry powder. According to Ganie et al. (2022), foods without spices are often rejected and not preferred by consumers. Thus, adding spices to food improves its taste and flavour. When different spices are combined, their collective effect produces a richer and more complex profile. Numerous studies have focused on the culinary uses of spices, but limited attention has been given to their roles in Malaysian curry powder formulations and their associated functional properties.

Each spice has a unique aroma, taste and mouthfeel, giving different sensorial attributes derived from the volatile and semi-volatile phytochemicals that are generally produced as secondary metabolites in plants. Table 2 summarises the associated spices that give specific sensory attributes in terms of taste, aroma (smell), chemesthetic (spiciness, hot/

Table 2
Grouping of spices following sensory attributes of taste, aroma, chemesthetic and appearance by associated spices

Sensory Attribute	Sub-Category	Reineccius (1999)	Raghavan Uhl (2000)	Spices Inc (2026)
Taste	Sour	--	--	tamarind, caper, kokum, pomegranate
	Bitter	fenugreek, clove	fenugreek, mace, thyme, bay leaf, oregano, celery, ajowan	fenugreek, clove, mace, nutmeg, thyme, bay leaf, oregano
Aroma	Sweet aromatic	fennel, star anise, onion, cinnamon	cardamom, anise, star anise, fennel, allspice, cinnamon	cardamom, anise, fennel, cinnamon, allspice
	Fruity	--	--	fennel, coriander, star anise, tamarind

Table 2 (*continued*)

Sensory Attribute	Sub-Category	Reineccius (1999)	Raghavan Uhl (2000)	Spices Inc (2026)
Chemesthetic	Spiciness	cumin, cardamom, clove, coriander, ginger, white pepper	clove, cumin, coriander, ginger, Thai basil, canela	clove, cumin, coriander, ginger, bay leaf
	Heat/Hot	chilli, black pepper, ginger	chilli pepper, mustard, white pepper, black pepper, wasabi, fenugreek, mace, clove, thyme, bay leaf, oregano	black and white peppers, ginger, mustard, red pepper
	Pungent	black pepper, ginger, chili, garlic, cumin	mustard, horseradish, wasabi, ginger, garlic, onion	peppers, ginger, onion, mustard, red pepper, galangal
Appearance	Colour-contributing	--	annatto, paprika, turmeric, parsley, saffron	--

heat and pungency) and colour (appearance) following the description of main references from Reineccius (1999), Raghavan Uhl (2000) and Spices Inc. (2026). These compounds evolve as chemicals in plants and function to protect them against herbivorous insects and vertebrates, fungi, pathogens and parasites (Fraenkel, 1959; Walker, 1994). The grouping of spices following sensory attributes has an important contribution, especially to the manufacturing and further processing of the spices.

FLAVOUR

Flavour is considered one of the most important factors influencing food choice (Glanz et al., 1998). Aroma refers to the odour detected by the nose, whereas flavour is the overall perception formed by integrating aroma, the basic tastes and oral sensations (Al-Khalili et al., 2025; Lamkey, 2022). Dozens or even hundreds of compounds may contribute to this perception, together with textural and chemesthetic responses such as the warmth produced by pepper or the cooling sensation of menthol (Reineccius, 1999). Aroma is therefore a major sensory attribute affecting food identification, choice and acceptance (Bortnowska, 2010).

In curry powder, flavour is determined by the types and proportions of spices used in the blend. Although spices may also provide antioxidant and preservative functions, their primary contribution to curry powder is the development of its characteristic aroma, taste, pungency and heat. A typical blend may contain roasted and ground coriander, turmeric, cumin, fennel, star anise and cinnamon, with fenugreek, clove, mustard, black pepper, nutmeg or ginger (Raghavan Uhl, 2000). Variations in their selection and proportions

produce profiles ranging from mild and aromatic to warm, robust and spicy. Colour also affects the perception and acceptance of Malaysian curry powder by providing visual cues about its composition and expected flavour intensity (Clydesdale, 1993). Turmeric contributes a yellow hue, whereas chilli increases redness and provides heat. Their relative proportions, therefore, influence both product appearance and consumers' expectations of pungency and flavour.

The flavour of curry powder can be assessed using both sensory and instrumental methods. A trained sensory panel may evaluate the intensity of aroma, taste, pungency, heat, aftertaste and overall balance using a structured scale. Consumer acceptance may be measured using a nine-point hedonic scale for aroma, taste and overall liking (Lawless & Heymann, 2010; Lim, 2011), while descriptive sensory analysis can compare different formulations (Murray et al., 2001; Marques et al., 2022). Headspace solid-phase microextraction coupled with gas chromatography-mass spectrometry (HS-SPME/GC-MS) can complement these assessments by identifying characteristic volatile compounds.

BLENDING OF SPICES

Spice blending involves combining different ground spices in specific proportions to create unique flavour profiles and aromas (Desai, 2022). According to the U.S. Department of Agriculture (USDA) (2010), a spice blend is a combination of two or more individual spices that may also be mixed with other ingredients, such as salt, herbs, or extracts. The main purpose is to enhance the flavour of the final product. These blends are created by mixing different spices in specific proportions to achieve a specific flavour profile. It is about achieving a blend that enhances the aroma and flavour of foods, creating a new, more balanced flavour (Rosenblatt, 2024). Blending techniques also help to reduce the specific flavour of one spice (Hirasa & Takemasa, 1998). In many culinary preparations, it will be about personalisation. In Malaysia, curry powder has its own unique spice blends, resulting in a diverse culture and vibrant array of flavours. Raghavan Uhl (2000) stressed that food practitioners must also understand the spices and flavourings used in all their varieties, as spices are the fundamental building blocks of these blends.

The process of blending begins with two steps: pre-cleaning and grinding. Spices for blending must first be free from physical contaminants through a pre-cleaning process or pre-dusting step. The process removes impurities and dust or leaf contamination in the dried spices. The pre-dusting step is important to keep food quality and prevent misuse of food additives and adulteration (Momin & Jamir, 2021). Mature, dried spices are often contaminated with dust, dirt, leaves and insects (ASTA, 2023). Pre-cleaning also ensures a more consistent, better quality and safer product for consumers. Subsequently, whole dried spices are ground to a particle size of 60-80 mesh before blending. Grinding is generally conducted at ambient temperature. The frictional heat generated during conventional

grinding can increase product temperature and promote loss of heat-sensitive compounds, thereby reducing aroma quality. Low-temperature or cryogenic grinding can improve volatile components and aroma retention and help preserve the overall quality of ground spices (Ghodki & Goswami, 2016; Sharma et al., 2016; Kharra et al., 2025). A good grinding method is a technique for better flavour retention and homogenisation during blending (Krejčová et al., 2008). According to Aradwad et al. (2021), grinding plays an important role and needs special attention, especially regarding the loss of flavour during grinding. The heat generated during the process may cause the loss of volatile compounds, thereby reducing the overall flavour and aroma of the curry blend.

MALAYSIAN CURRY POWDER

Curry powder is the most well-known spice blend (Hirasa & Takemasa,1998). According to Raghavan Uhl (2000), curry blends vary by country or culture of origin and by the applications in which they are used. Countries like Malaysia, Thailand, Indonesia, India and Sri Lanka have the most varied, intense and complex blends in the world. Regardless of variations, it is expected for any curry powder to have a uniform colour, to be powdery and must not be lumpy as shown in Figure 2. While the ingredient lists differ in several ways, the final colour is quite similar, with a pleasant aroma and a slightly bitter taste (Raghavan Uhl, 2000; Tayyem et al., 2006).



Figure 2. Blended curry powder illustrating flow behaviour

Raghavan Uhl (2000) noted that curry blends from Southeast Asia, including Malaysia, have the most aromatic, hot and pungent flavours. The Malaysian curry powder is a popular spice mix blend of Indian origin. It is widely accepted across Malaysia's major ethnic and

cultural communities. It is also famous worldwide for its great taste, exotic flavours, colours, and aromatic spices. Most recipes and producers of curry powder or blends usually include coriander, turmeric, cumin and fenugreek in their blends. Kevin (2022) described that the Malaysian curry powder is unique, such that it combines the cooking styles and flavours of the Malay, Chinese and Indian culinary traditions, unlike common curry powders, which are specifically labelled for meat or for fish, and each blend features different seasonings. The fusion of the different cooking styles and dishes of three major ethnic communities, mainly Malay, Chinese and Indian, was also adopted in the formulation of fermented curry paste in Malaysia (Abolhassani et al., 2009). The flavour of the curry powder is typically warm, spicy, fragrant and slightly sweet with a balance of aroma, heat and pungency (Raghavan Uhl, 2000). Depending on the recipe, additional ingredients such as coriander, cumin, fennel, cinnamon, clove, mustard, cardamom, nutmeg, white pepper and ginger can be added in the blending process. Malaysian consumers chose coriander, fennel, cumin, star anise, turmeric, clove, ginger and black pepper as their important spice ingredients. This is shown by the presence of linalool, trans-anethole, cuminaldehyde, pinene, curcumene, turmerone, zingiberene and limonene volatile components in chromatogram analysis listed in Table 3, showing the relationship between the volatile components associated with the major spices. While some volatile components, such as pinene, are associated with a few types of spices, including coriander, cumin, fennel and black pepper, there are also single spices, such as turmeric, that produces more than one volatile component, i.e. turmerone and curcumene. According to Hirasa and Takemasa (1998), the major characteristics of the spices used are derived from terpene compounds, i.e., monoterpenes (C_{10}) and sesquiterpenes (C_{15}). The monoterpenes generally have a strong aroma and are very volatile. Choi (2013) identified that curry powder contains forty-eight compounds, comprising 36 terpenes,

Table 3
Associations between major spices used in Malaysian curry powder, their characteristic volatile compounds and reported flavour attributes

Main Compounds	Classification	Spice	Flavour Character
Linalool	Monoterpene	coriander	spicy[1,2]
Cuminaldehyde	monoterpenoid aldehyde	cumin	pungent[1], spicy[1,2]
Estragole	Phenylpropanoid	cumin, star anise	spicy[1], bitterness[3]
Turmerone	Sesquiterpene	turmeric	pungent[3]
Trans-anethole	Phenylpropanoid	fennel, star anise	aroma[1,2], sweetness[2]
β-caryophyllene	Sesquiterpene	black pepper, clove	spicy[1]
Geranyl acetate	Monoterpene	coriander	aroma[1,2]
Zingiberene	Sesquiterpene	ginger	spicy[1,2], pungent[1,2]
Limonene	Monoterpene	fennel, black pepper	aroma[4]

Source: [1]Reineccius (1999), [2]Spices Inc. (2026), [3]Raghavan Uhl (2000), and [4]Ajayi et al. (2019)



Figure 3. The colour and design of popular Malaysian curry powders from major brands, Babas, Allagappa and Adabi, for cooking meat or fish

5 alcohols, 4 benzenes, 2 carbonyl compounds and 1 ester. Kim et al. (1989) stressed that the characteristic aroma is associated with nutmeg, cumin, cardamom, turmeric, coriander, clove, allspice, cassia, fennel, celery seed and black pepper. The redness comes from the chilli powder used in the formulation. It is not shown because it is non-volatile. It should be noted that although chilli is a major ingredient in curry powder blending, it does not appear in the chromatogram due to its non-volatile nature. The aromatic, spicy flavour comes from the essential volatile oils and other volatile components (Lamkey, 2022) of the various spices used in the blending process. Each spice contributes to the complexity of the flavour.

Malaysia generally has two main types of curry powders (Figure 3), meat and fish. These are commonly used in meat or fish curries. The top three most popular brands in Malaysia are Babas, Adabi, and Allagappa. The Malaysian curry powder design in the packaging shows the company's identity, using respective meat to show the intended use of curry. The photo for meat type is generally redder. These distinct blends of spices are designed to enhance the flavour of their respective dishes in Malaysia. The fish curry powder is often used for seafood dishes, while the meat curry powder is used for meats like chicken, beef and mutton. The difference lies in the specific spice blend. Typically, the meat curry powder is stronger, more robust, redder and spicier than the fish curry powder. The fish type is milder, more aromatic and a little more yellowish in colour. According to

the ingredient lists presented in Table 4, the common spices for meat types are coriander, cumin, fennel, chilli, turmeric, white pepper, cinnamon, cardamom and star anise, whereas the spices of the fish types are similar but fewer, with the presence of black pepper, fenugreek and ginger giving a different flavour profile affecting the taste. The fish type is more yellowish. The meat curry powder is more robust and spicier to suit the stronger flavour of red meat, whereas the fish curry powder is milder and more aromatic to suit the flavours of fish. The tangy taste of prepared fish curry is generally introduced during cooking through acidic ingredients such as tamarind, *asam gelugur*, tomato or lime. Table 4 shows that meat curry powders may possess a more complex aromatic profile from the ingredient lists, presenting the presence of cinnamon, cardamom, star anise and nutmeg spices. Black pepper generally contributes a more pronounced aroma and pungent flavour than white pepper, together with the characteristic of heat, primarily associated with piperine. Its distinctive sensory properties have helped maintain its position as one of the most widely used spices worldwide (Freedman, 2020; Spence, 2024; van Ruth et al., 2019).

Table 4
Contents listed on the label of meat and fish curry powder from two popular brands of Babas and Allagappa

List of Ingredients	Babas		Allagappa	
	Meat	Fish	Meat	Fish
Coriander	✓	✓	✓	✓
Cumin	✓	✓	✓	✓
Fennel	✓	✓	✓	✓
Chilli	✓	✓	✓	✓
Turmeric	✓	✓	✓	✓
White Pepper	✓	✓	✓	--
Cinnamon	✓	--	✓	--
Cardamom	✓	--	✓	--
Star Anise	✓	--	✓	--
Bay Leaf	✓	--	--	--
Clove	✓	--	--	--
Nutmeg	✓	--	--	--
Methi Seeds	✓	--	--	✓
Black Pepper	✓	✓	--	--
Fenugreek	--	✓	--	--
Ginger	--	✓	--	--
Rice Flour	✓	✓	--	--

Table 5
Chemical requirements of Malaysian curry powder

Parameter	Limit	Requirement
Moisture (%)	Maximum	9
Volatile oil (mL/100 g)	Minimum	0.3
Non-volatile ether extract (%)	Minimum	7.5
Acid insoluble ash (%)	Maximum	1
Crude fibre (%)	Maximum	18

Source: Adapted from Malaysian Food Regulations (1985)

QUALITY OF MALAYSIAN CURRY POWDER

The quality objective for Malaysian curry powder is to produce a safe, consistent and high-quality blend that meets specified sensory, chemical and microbiological requirements. Standard operating procedures should therefore include specifications for raw materials, control of grinding and blending processes, assessment of finished-product consistency and the use of suitable packaging that provides protection against light, oxygen and moisture. As spices are natural agricultural materials, variations in properties such as flavour, colour and volatile oil content should be managed through careful raw-material selection, formulation adjustment and process standardisation. Quality evaluation should begin with the individual spices and may include measurements of moisture content, total ash, acid-insoluble ash, volatile oil, non-volatile ether extract, crude fibre and extraneous matter. In Malaysia, curry powder must comply with the Malaysian Food Regulations 1985, as summarised in Table 5. It commonly consists of a blend of 10-15 spices ground to a particle size of 60-80 mesh (Raghavan Uhl, 2000). The Malaysian Food Regulations 1985 specify that curry powder may contain other permitted food ingredients but must comprise at least 85% spices and contain not less than 0.3 mL of volatile oil per 100 g. Quality, however, can extend beyond compliance with compositional standards. Shiba et al. (1993) described four progressive concepts of quality which is first, fitness to standard which is assurance in conformity with established specifications, second, fitness to use which assurance that the product satisfies consumers' practical and sensory requirements, third, fitness of cost, which is provision of the required quality at an acceptable cost and fourth, fitness to latent requirements which is anticipation of needs that consumers may not yet have explicitly expressed. For the Malaysian curry powder, these concepts indicate that quality involves not only regulatory compliance but also consistent flavour, suitability for its intended culinary application, affordability and responsiveness to changing consumer preferences.

CONCLUSION

Malaysian curry powder is a complex spice matrix in which the selection, proportion and processing of spices determine its characteristic aroma, taste, pungency, heat and colour.

Variations between meat and fish curry powders reflect formulations tailored to different culinary applications. Raw material quality, controlled grinding and blending, protective packaging, and regulatory compliance are essential for maintaining flavour and product consistency. However, current knowledge remains largely descriptive because quantitative information on spice proportions and flavour interactions is limited. Future studies integrating sensory evaluation, consumer testing and instrumental flavour analysis could support formulation optimisation, quality standardisation and the development of Malaysian curry powders with consistent sensory and functional properties. The limitation of this review is that it identifies the spices of the two most popular and recognised commercial brands of curry powder in Malaysia as representatives of the study and does not provide detailed quantitative proportions of each spice, which is proprietary to the manufacturers.

REFERENCES

Abolhassani, Y., Khan, M. A., Salam, A. B., & Ghasem, M. (2009). Some physico-chemical qualities and acceptability of fermented curry paste. *International Food Research Journal, 16*(4), 581-588.

Ajayi, G. O., Akinsanya, M. A., Agbabiaka, A. T., Oyebanjo, K. S., Hungbo, T. D., & Olagunju, J. A. (2019). D-limonene: A major bioactive constituent in *Allium fistulosum* identified by GC-MS analysis. *The Journal of Phytopharmacology, 8*(5), 257-259. https://doi.org/10.31254/phyto.2019.8509

Al-Habsi, N., Al-Khalili, M., Haque, S. A., Al Akhzami, N., Gonzalez-Gonzalez, C. R., Al Harthi, S., & Al Jufaili, M. (2025). Herbs and spices as functional food ingredients: A comprehensive review of their therapeutic properties, antioxidant and antimicrobial activities, and applications in food preservation. *Journal of Functional Foods, 129*, Article 106882. https://doi.org/10.1016/j.jff.2025.106882

Al-Khalili, M., Pathare, P. B., Rahman, S., & Al-Habsi, N. (2025). Aroma compounds in foods: Analysis, characterization and flavor perception. *Measurement: Food, 18*, Article 100220. https://doi.org/10.1016/j.meafoo.2025.100220

American Spice Trade Association (ASTA). (2023). *Good manufacturing practices (GMP) guide for spices.* https://astaspice.org/safe-view/28310

Aradwad, P. P., Arun Kumar, T. V., Sahoo, P. K., & Mani, I. (2021). Key issues and challenges in spice grinding. *Cleaner Engineering and Technology, 5*, Article 100347. https://doi.org/10.1016/j.clet.2021.100347

Bortnowska, Z. G. (2010). Influence of thermodynamic and kinetic factors on the retention and release of aroma compounds in liquid food systems: A review. *Polish Journal of Food and Nutrition Sciences, 60*(4), 301-307.

Chhetri, P., Vijayan, A. K., Bhat, S. K., Gudade, B. A., & Bora, S. S. (2015). An overview of grouping of spices. *Indian Botanists*. https://indianbotanists.blogspot.com/search?q=An+overview+of+grouping+of+spices

Chironi, S., Bacarella, S., Altamore, L., Columba, P., & Ingrassia, M. (2021). Consumption of spices and ethnic contamination in the daily diet of Italians: Consumers' preferences and modification of eating habits. *Journal of Ethnic Foods, 8*(1), Article 6. https://doi.org/10.1186/s42779-021-00082-8

Choi, J. B. (2013). Effect of packaging on aroma stability of curry powder during storage. *Korean Journal of Food and Cookery Science, 29*(2), 147-152. https://doi.org/10.9724/kfcs.2013.29.2.147

Clydesdale, F. (1993). Color as a factor in food choice. *Critical Reviews in Food Science and Nutrition, 33*(1), 83-101. https://doi.org/10.1080/10408399309527614

Desai, A. K. (2022). A study on global spice blends. *International Journal of Advanced Research in Science, Communication and Technology, 2*(4), 1-3.

Embuscado, M. E. (2019). Bioactives from culinary spices and herbs: A review. *Journal of Food Bioactives, 6*, 68-99. https://doi.org/10.31665/JFB.2019.6186

Farrell, K. T. (1985). *Spices, condiments and seasonings.* The AVI Publishing Company, Inc. https://archive.org/details/spicescondiments0000farr/page/n7/mode/2up

Freedman, P. (2020). History of spices. In H. L. Meiselman (Ed.), *Handbook of eating and drinking* (pp. 77-91). Springer. https://doi.org/10.1007/978-3-030-14504-0_9

Fraenkel, G. S. (1959). The raison d'être of secondary plant substances. *Science, 129*(3361), 1466-1470. https://doi.org/10.1126/science.129.3361.1466

Furth, P., & Cox, D. (2004). The spice market expands. *Food Technology, 58*(8), 30-34.

Ganie, N. A., Wani, S. A., Wagay, J. A., Farooq, U., Mir, W. Y., & Rather, A. M. (2022). Spices and their uses in foods. In S. A. Wani, A. Singh, & P. Kumar (Eds.), *Spice bioactive compounds: Properties, applications, and health benefits* (pp. 23-30). CRC Press. https://doi.org/10.1201/9781003215387-2

Ghodki, B. M., & Goswami, T. K. (2016). Effect of grinding temperatures on particle and physicochemical characteristics of black pepper powder. *Powder Technology, 299*, 168-177. https://doi.org/10.1016/j.powtec.2016.05.042

Glanz, K., Basil, M., Maiback, E., Goldberg, J., & Snyder, D. (1998). Why Americans eat what they do: Taste, nutrition, cost, convenience, and weight control concerns as influences on food consumption. *Journal of the American Dietetic Association, 98*(10), 1118-1126. https://doi.org/10.1016/S0002-8223(98)00260-0

Hirasa, K., & Takemasa, M. (1998). *Spice science and technology.* Marcel Dekker. https://doi.org/10.1201/9780367800451

Karadbhajne, S. V., & Saraf, N. A. (2017). Determination of physical, chemical and sensory characteristics of instant curry mix for vegetarian recipes. *International Journal of Food Science and Nutrition, 2*(6), 181-186.

Kevin. (2022, August 10). Malaysian curry powder. *Silk Road Recipes*. https://silkroadrecipes.com/malaysian-curry-powder/

Kharra, R., Thomas, M., Gupta, L., & Wadhawan, N. (2025). Key issues and challenges in spice grinding. *International Journal of Agro Nutrifood Practices, 5*(2), 1-10. https://doi.org/10.36647/IJANP/05.02.A001

Killebrew, K. (2025, March 24). Best curry powder. *The Daring Gourmet*. https://www.daringgourmet.com/curry-powder-recipe/

Kim, H.-W., Huh, K.-T., & Chooi, C.-U. (1989). Studies on the volatile flavour components of spices in curry. *Korean Journal of Food Science and Technology, 21*(1), 127-135.

Krejčová, A., Pouzar, M., Černohorský, T., & Pešková, K. (2008). The cryogenic grinding as the important homogenization step in analysis of inconsistent food samples. *Food Chemistry, 109*(4), 848-854. https://doi.org/10.1016/j.foodchem.2008.01.011

Lamkey, J. W. (2022). Spices, seasonings, and flavors—Achieving the desired result. *Meat and Muscle Biology, 5*(3), Article 13016, 1-4. https://doi.org/10.22175/mmb.13016

Lawless, H. T., & Heymann, H. (2010). *Sensory evaluation of food: Principles and practices* (2nd ed.). Springer. https://doi.org/10.1007/978-1-4419-6488-5

Lim, J. (2011). Hedonic scaling: A review of methods and theory. *Food Quality and Preference, 22*(8), 733-747. https://doi.org/10.1016/j.foodqual.2011.05.008

Malaysian Food Regulations. (1985). *Food Act 1983 and the Food Regulations 1985*. https://malaysianlaw.my/attachments/Malaysian-law-PUA-318-Food-Regulations-3-44557.pdf

Marques, C., Correia, E., Dinis, L.-T., & Vilela, A. (2022). An overview of sensory characterization techniques: From classical descriptive analysis to the emergence of novel profiling methods. *Foods, 11*(3), Article 255. https://doi.org/10.3390/foods11030255

Meher, J., & Meher, R. (2020). Investigation of chemical, rheological and sensory properties of curry-spices blend. *Journal of Agriculture and Food Research, 2*, Article 100093. https://doi.org/10.1016/j.jafr.2020.100093

Momin, M. Ch., & Jamir, A. R. (2021). Harvesting, handling, and processing of spices. In *Postharvest management of horticultural crops* (pp. 458-484). Jaya Publishing House.

Murray, J. M., Delahunty, C. M., & Baxter, I. A. (2001). Descriptive sensory analysis: Past, present and future. *Food Research International, 34*(6), 461-471. https://doi.org/10.1016/S0963-9969(01)00070-9

Raghavan Uhl, S. (2000). *Handbook of spices, seasonings, and flavorings* (1st ed.). CRC Press. https://doi.org/10.1201/9781420012552

Raghavan, S. (2010). *Flavors of Malaysia: A journey through time, tastes, and traditions.* Hippocrene Books.

Reineccius, G. (1999). *Source book of flavors* (2nd ed.). Aspen Publishers.

Rosenblatt, J. (2024, February 15). What is a spice blend. *RawSpiceBar*. https://rawspicebar.com/blogs/spices-101/what-are-spice-blends

Sharma, L. K., Agarwal, D., Rathore, S. S., Malhotra, S. K., & Saxena, S. N. (2016). Effect of cryogenic grinding on volatile and fatty oil constituents of cumin (*Cuminum cyminum* L.) genotypes. *Journal of Food Science and Technology, 53*(6), 2827-2834. https://doi.org/10.1007/s13197-016-2258-0

Shiba, S., Graham, A., & Walden, D. (1993). *A new American TQM: Four practical revolutions in management.* Productivity Press.

Siripongvutikorn, S., Pumethakul, K., Yupanqui, C. T., Seechamnanturakit, V., Detarun, P., Utaipan, T., Sirinupong, N., Chansuwan, W., Wittaya, T., & Samakradhamrongthai, R. S. (2024). Phytochemical profiling and antioxidant activities of the most favored ready-to-use Thai curries, Pad-Ka-Proa (spicy basil leaves) and Massaman. *Foods, 13*(4), Article 582. https://doi.org/10.3390/foods13040582

Spence, C. (2024). The king of spices: On pepper's pungent pleasure. *International Journal of Gastronomy and Food Science, 35*, Article 100900. https://doi.org/10.1016/j.ijgfs.2024.100900

Spices Board. (2021). Spices Board India. https://www.indianspices.com/sites/default/files/BSM%20

Spices Inc. (2026). Flavor characteristics of spices. https://spicesinc.com/blogs/flavor-characteristics-spices

Tayyem, R. F., Heath, D. D., Al-Delaimy, W. K., & Rock, C. L. (2006). Curcumin content of turmeric and curry powders. *Nutrition and Cancer, 55*(2), 126-131. https://doi.org/10.1207/s15327914nc5502_2

U.S. Department of Agriculture (USDA). (2010). *Spices and spice blends.* https://www.ams.usda.gov/sites/default/files/media/CID%20Spices%20and%20Spice%20Blends.pdf

van Ruth, S. M., Silvis, I. C. J., Ramos, M. E., Luning, P. A., Marc, J., Elliott, C. T., & Alweijn, M. (2019). A cool comparison of black and white pepper grades. *LWT, 106*, 122-127. https://doi.org/10.1016/j.lwt.2019.02.054

Walker, J. R. L. (1994). Antimicrobial compounds in food plants. In V. M. Dillon & R. G. Board (Eds.), *Natural antimicrobial systems and food preservation* (pp. 181-204). CAB International.

Pertanika J. Trop. Agric. Sci. 49 (5): 2171 - 2196 (2026)

PERTANIKA JOURNALS

TROPICAL AGRICULTURAL SCIENCE

Journal homepage: http://www.pertanika.upm.edu.my/

Biofertilisers and Micronutrients Enhance Productivity and Land-Use Efficiency of Cereal-Legume Intercropping Systems on Indonesian Drylands

Yanto Surdianto[1], Nana Sutrisna[1]*, Muhammad Iskandar Ishaq[1], Bambang Susanto[1], Yiyi Sulaeman[1], Eni Maftu'ah[1], Dwi Purnamawati Widiastuti[1], Jumakir[1], and Agus Nurawan[2]

[1]Research Center for Food Crops, Research Organization for Agriculture and Food, National Research and Innovation Agency, Cibinong Science Center, 16911 Bogor, West Java, Indonesia
[2]Research Center for Horticulture, Research Organization for Agriculture and Food, National Research and Innovation Agency, Cibinong Science Center, 16911 Bogor, West Java, Indonesia

ABSTRACT

Low soil fertility and limited availability of nutrients negatively affect the productivity and sustainability of tropical dryland agriculture. Cereal-legume intercropping can improve land use efficiency. However, the effectiveness of cereal-legume intercropping in nutrient-limited drylands is dependent on appropriate nutrient management. This study examined the effects of an integrated biofertiliser-micronutrient package on crop production, land use efficiency, cropping system productivity and economic performance of cereal-based intercropping systems in Indonesian drylands. The research was conducted in Garut, West Java, Indonesia, during October 2022-March 2023. The research used a split-plot randomised complete block design with four replications. Three intercropping systems, maize-upland rice, maize-soybean and upland rice-soybean, were the major plots. The subplots consisted of two nutrient management regimes: (P_0) locally advised fertilisation and (P_1) recommended fertilisation + biofertiliser at 5 L ha^{-1} + micronutrient fertiliser at 10 kg ha^{-1}. Organic manure (7.5 t ha^{-1}) and dolomite (1.5 t ha^{-1}) were uniformly applied to all plots. The integrated treatment improved crop growth and productivity, with responses varying among intercropping systems. Upland rice-soybean under integrated nutrient management achieved the highest Land Equivalent Ratio (LER; 1.56) and Cropping System Efficiency (CSE; 1.50), while farmers' income increased

ARTICLE INFO

Article history:
Received: 26 November 2025
Accepted: 15 September 2026
Published: 30 October 2026

DOI: https://doi.org/10.47836/pjtas.49.5.04

E-mail addresses:
yant014@brin.go.id (Yanto Surdianto)
ntrisna.ns@gmail.com (Nana Sutrisna)
muha319@brin.go.id (Muhammad Iskandar Ishaq)
bamsusanto40@gmail.com (Bambang Susanto)
yiyi.sulaeman@brin.go.id (Yiyi Sulaeman)
eni.maftuah@brin.go.id (Eni Maftu'ah)
dwwidiastuti@gmail.com (Dwi Purnamawati Widiastuti)
juma009@brin.go.id (Jumakir)
agus197@brin.go.id (Agus Nurawan)
* Corresponding author

e-ISSN: 2231-8542

© Universiti Putra Malaysia Press

by up to 81.72%. The novelty of this study lies in the field evaluation of an integrated biofertiliser-micronutrient package in different cereal-legume intercropping systems in the tropical dryland environments of Indonesia, correlating agronomic performance with land-use efficiency and economic returns. The findings demonstrate the potential of integrated biological and micronutrient management to support sustainable intensification of dryland farming.

Keywords: Agroecosystem, crop production, land equivalent ratio, mineral nutrition, plant growth-promoting microorganisms

INTRODUCTION

Dryland agriculture plays an important role in supporting food security and rural livelihoods in tropical regions, including Indonesia. The conversion of productive paddy fields to non-agricultural uses has reduced the area available for rice, maize, and soybean production, increasing the importance of drylands as an alternative resource for food-crop production (Mulyani, 2016). Indonesia has approximately 70 million ha of dryland resources (BPS, 2022; Pusat Data dan Sistem Informasi Pertanian [Pusdatin], 2021), providing considerable potential for agricultural intensification. However, the productivity of these lands remains constrained by low soil fertility, limited availability of macro- and micronutrients, low organic matter, erratic rainfall, and rapid nutrient depletion (Srinivasarao et al., 2023). In many dryland soils, low soil organic carbon and weak biological activity reduce nutrient retention and may limit the efficiency of conventional fertiliser inputs.

Cereal-legume intercropping is widely recognised as a sustainable intensification strategy for improving resource-use efficiency and land productivity in rainfed and dryland environments. Intercropping cereals such as maize and upland rice with legumes such as soybean or mungbean allows complementary use of light, water, space, and nutrients, while legumes may contribute biologically fixed nitrogen to the cropping system (Jensen et al., 2020; Omara et al., 2019; Peoples et al., 2022). The resulting complementarity can provide a land-use advantage over monocropping, commonly expressed by a Land Equivalent Ratio (LER) greater than one. However, the productivity advantage of cereal-legume intercropping is strongly influenced by soil fertility and nutrient management, particularly where soil nutrient availability and biological activity are low (Agsari et al., 2020; Kristiono et al., 2020). Thus, the biological complementarity between cereals and legumes does not necessarily translate into consistently high productivity under nutrient-constrained dryland conditions. Similar advantages of cereal-legume intercropping have been documented globally (Agbor et al., 2023; Latati et al., 2019; Pierre et al., 2022).

Inorganic fertilisers remain the major source of nutrients in many dryland production systems. However, inappropriate or imbalanced fertiliser use may contribute to declining soil quality, reduced nutrient-use efficiency, and deterioration of soil biological processes

(Krasilnikov et al., 2022; Titirmare et al., 2023; Wang et al., 2021). Excessive mineral fertiliser inputs may also negatively affect beneficial soil microorganisms, including mycorrhizal associations that contribute to nutrient acquisition and soil aggregation (Rillig et al., 2019). Complementary sources of nutrients are therefore increasingly important in sustainable agricultural intensification, especially when they can enhance nutrient availability and support biological activities in the soil.

Biofertilisers containing beneficial microorganisms such as *Azospirillum*, *Rhizobium*, and phosphate-solubilising bacteria can help make nutrients available to plants, stimulate root growth, and improve nutrient uptake (Mahanty et al., 2017; Soumare et al., 2020). Micronutrients such as zinc (Zn), boron (B) and iron (Fe) are also crucial for optimal plant growth and development as they participate in different physiological processes, including enzyme function, photosynthesis, reproductive development and grain formation. Therefore, combining biological nutrient inputs with micronutrients may provide a complementary nutrient-management strategy for crops grown under nutrient-constrained conditions. Nevertheless, previous studies have predominantly examined biofertilisers as individual inputs or in relation to particular cereal-legume combinations. For example, biofertiliser application has been shown to improve productivity and LER in maize-soybean intercropping systems (Ünay et al., 2021), while recent field research has further demonstrated positive effects of biofertilisers on land-use efficiency across cereal-legume mixtures (Pérez-Bernal et al., 2025). These findings establish the potential of biofertilisers but also indicate that the use of biofertiliser alone is not, in itself, a sufficient basis for claiming novelty.

The remaining knowledge gap concerns whether an integrated nutrient package combining biofertiliser and micronutrients with recommended mineral fertilisation can consistently improve cereal-legume intercropping performance under nutrient-constrained tropical dryland conditions. In particular, field-based evidence comparing the response of different cereal-legume combinations to such an integrated nutrient package in Indonesian drylands remains limited. Moreover, studies often focus on individual crop yield or LER, whereas a simultaneous evaluation of crop productivity, land-use efficiency, cropping-system efficiency, and economic returns can provide a more comprehensive assessment of the technology's practical value. This is important because an agronomically superior intercropping system is more likely to be adopted when its land-use advantage is accompanied by tangible economic benefits to farmers. Recent research has demonstrated that cereal-legume intercropping can provide economic advantages under variable rainfall conditions, highlighting the importance of integrating agronomic and economic assessments when evaluating dryland intensification strategies.

Therefore, the novelty of the present study is not the use of biofertiliser, micronutrients, or cereal-legume intercropping individually, all of which have been investigated

previously. Rather, the novelty lies in field-testing an integrated biofertiliser-micronutrient nutrient package, applied in addition to recommended fertilisation, across cereal-legume intercropping systems under Indonesian tropical dryland conditions and linking its effects on crop productivity with land-use efficiency and economic performance. This approach provides a system-level assessment of whether biological and micronutrient supplementation can strengthen the productivity advantage of cereal-legume intercropping in nutrient-constrained drylands.

Accordingly, this study aimed to evaluate the effects of supplementing recommended fertilisation with biofertiliser and micronutrients on crop growth, yield, land-use efficiency, cropping-system efficiency, and economic returns of cereal-legume intercropping systems in Indonesian drylands. The experiment compared two nutrient-management regimes: (1) recommended fertilisation and (2) recommended fertilisation supplemented with biofertiliser at 5 L ha^{-1} and micronutrients at 10 kg ha^{-1}, with organic manure at 7.5 t ha^{-1} and dolomite at 1.5 t ha^{-1} uniformly applied to all treatments. The study was designed to provide field-based evidence for an integrated nutrient management strategy that improves the productivity and resource-use efficiency of cereal-legume systems while enhancing their economic attractiveness to dryland farmers.

MATERIALS AND METHODS

Study Area and Experimental Materials

The field experiment was conducted in Pangeureunan Village, Balubur Limbangan District, Garut Regency, West Java Province, Indonesia (7°00′11″ S, 107°56′53″ E), during one cropping season from October 2022 to March 2023. The experimental site was located at approximately 600 m above sea level and had a tropical humid climate, with an average annual rainfall of approximately 2,075 mm and a mean annual temperature of approximately 20 °C. The soil was classified as Cambisols. The site had a medium-to-fine soil texture, good drainage, and hilly topography (Central Statistics Agency of Garut Regency. 2022). Before the experiment, the field had been used for a maize-tobacco rotation.

Before land preparation, composite soil samples were collected from the experimental area at a depth of 0-20 cm to characterise the initial soil condition. The initial soil analysis included [pH, organic C, total N, available P, exchangeable K, and other parameters actually measured in the study]. The results were used to characterise the nutrient status of the experimental site and to support the interpretation of the response to the nutrient-management treatments.

The evaluated crops were maize (*Zea mays* L.) cv. NASA 29, upland rice (*Oryza sativa* L.) cv. Inpago 11 and soybean (*Glycine max* L.) cv. Anjasmoro. Soil additions employed were organic fertiliser (manure) and dolomite. Inorganic fertilisers utilised were urea and NPK compound fertiliser; urea included 46% N, and NPK fertiliser contained 15% N,

10% P_2O_5 and 12% K_2O. The biofertiliser utilised in this experiment was *Bacillus* sp. (viable cell density > 1.0 × 10 6 CFU mL^{-1}), *Ochrobactrum sp*. (viable cell density > 1.0 × 10 5 CFU mL^{-1}) and *Alcaligenes* sp. (viable cell density > 1.0 × 10 5 CFU mL^{-1}). The micronutrient fertiliser was composed of 17% Zn, 3% Cu, 0.7% B, 0.6% Mn and 0.01% Mo.

Experimental Design and Treatments

The experiment employed a split-plot randomised complete block design (RCBD) with four replications. The experiment was established on approximately 1.5 ha of a farmer's field.

The main-plot factor was the cropping system, consisting of three cereal-legume or cereal-cereal intercropping systems:

a) **MR**: maize-upland rice;
b) **MS**: maize-soybean; and
c) **RS**: upland rice-soybean.

The subplot factor was nutrient management, consisting of two treatments:

a) **P_0:** locally recommended fertilisation (control); and
b) **P_1:** locally recommended fertilisation + biofertiliser + micronutrient fertiliser.

Thus, the experiment consisted of six treatment combinations (3 cropping systems × 2 nutrient-management treatments), with four replications, giving a total of 24 experimental units. Each experimental unit covered an area of 500 m².

The application rates for inorganic fertilisers (urea and compound NPK), biofertilisers, and micronutrient fertilisers were determined based on established recommendations for each crop and local farmers' production practices (Table 1).

Table 1
Intercropping arrangements and plant densities

Main Plot Treatments Code	Crop	Rows	Row Spacing (cm)	In-row Spacing (cm)	Population (plants ha-1)
MR	Maize	2	60	25	26,667
	Upland Rice	9	20	15	199,800
MS	Maize	2	60	25	24,000
	Soybean	7	30	15	142,222
RS	Upland Rice	9	20	15	183,333
	Soybean	5	30	15	100,000

Cropping System Arrangement

Planting appeared in the cropping patterns presented in Table 2. The population and spatial arrangement of plants were maintained consistent with the existing intercropping system to ensure the relative contribution of each crop component could be compared across systems.

Table 2
Fertiliser treatment details

Subplot Treatments Code	Crop	Inorganic Fertiliser	Biofertiliser (l ha-1)	Micronutrient (kg ha-1)
P0	Maize	Recommended Dosage	-	-
	Upland Rice	Recommended Dosage	-	-
	Soybean	Recommended Dosage	-	-
P1	Maize	Recommended Dosage	5	10
	Upland Rice	Recommended Dosage	5	10
	Soybean	Recommended Dosage	5	10

Note. Recommended inorganic fertilisers dosage (Maize = 150 kg/ha, upland rice = 100 kg/ha, and soybean = 50 kg/ha)

Monoculture crop yields used to calculate LER and CSE were obtained from farmers' fields near the experimental site, using management practices identical to those used in the experiment.

All treatments were uniformly managed using standard crop management procedures. Weeds were treated manually, and pests and diseases were controlled by locally recommended procedures. The crops were mainly rain-fed, with additional irrigation being used when necessary to prevent excessive water stress.

Application of Fertilisers and Biofertilisers

Soil amendments were organic fertiliser (manure) at 7.5 t ha^{-1} and dolomite at 1.5 t ha^{-1}. These components were evenly distributed to all experimental plots before planting. Inorganic fertilisers, Urea, compound NPK and micronutrients were treated in two doses at 10 days after planting (DAP) and 30 DAP. One-third of the dose was applied at 10 DAP and two-thirds at 30 DAP. The biofertiliser was applied 3 times at 7, 14, and 28 days after planting (DAP) by spraying the product onto the soil at a 1:60 ratio.

DATA COLLECTION

Data was collected through direct field observations and measurements at specific periods of crop growth.

Growth Parameters

Growth data were recorded at 2, 4, 6 and 8 weeks after planting (WAP). The variables measured were: (1) plant height (cm) of maize, upland rice and soybean; (2) stem diameter (mm) of maize; (3) number of tillers per $plant^{-1}$ of upland rice and (4) number of branches per $plant^{-1}$ of soybean.

Measurements were conducted on the representative plants within each plot, selected from the specified sampling area (excluding border plants). Repeated measurements were taken from the same plants if possible.

Crop Yield and Yield Components

Yield components and grain yield were measured at physiological maturity for each component crop. For maize, the measures were cob length, cob diameter, 100-grain weight, and grain yield. For upland rice, measurements included panicle length, number of filled grains per panicle^{-1}, 1,000-grain weight, and grain yield. For soybean, measurements included the number of filled pods per plant^{-1}, the number of unfilled pods per plant^{-1}, 100-grain weight, and grain yield.

Grain yield was determined from the harvested net plot area and converted to t ha^{-1} at the appropriate standard moisture content of 14% for upland rice and 12% for maize and soybean.

Land-Use Efficiency

Land-use efficiency is an important indicator for assessing the productivity advantage of intercropping relative to monocropping. In intercropping systems, land-use efficiency is commonly quantified using the Land Equivalent Ratio (LER), which represents the amount of land required under monocropping to produce the same yields obtained from one unit of land under intercropping (Khanal et al., 2021). LER is calculated using the formula as in Equation 1:

$$LER = \sum_{i=1}^{n} \frac{Xi}{Yi} \quad [1]$$

where:
X_i = yield of crop *i* (t ha^{-1}) in the intercropping system
Y_i = yield of crop *i* (t ha^{-1}) in monoculture

An LER > 1 indicates that intercropping uses land more efficiently than the corresponding monocropping systems, whereas LER = 1 indicates no land-use advantage and LER < 1 indicates a land-use disadvantage.

Cropping System Efficiency

Cropping System Efficiency (CSE) is an index used to evaluate the overall efficiency of an intercropping system by considering the combined yield of component crops relative to their corresponding monocultures and adjusting this productivity advantage according

to the duration of the cropping system (Dariush et al., 2006). Cropping System Efficiency (CSE) was calculated to assess the combined biological and temporal efficiency of the intercropping system as in Equation 2:

$$CSE = (Yia + Yib) / (Yma + Ymb) \times (ta + tb)/T \quad [2]$$

where:
Yia = yield of crop A in intercropping (t ha^{-1})
Yib = yield of crop B in intercropping (t ha^{-1})
Yma = yield of crop A in monocropping (t ha^{-1})
Ymb = yield of crop B in monocropping (t ha^{-1})
ta, tb = duration of monocropping for crop A and B (days)
T = total duration of intercropping (days)

A CSE value greater than 1 indicates an overall efficiency advantage of the intercropping system relative to the corresponding monocropping systems under the conditions of the experiment.

Economic Analysis

Economic performance was assessed using production costs, gross revenue, and the revenue-to-cost ratio (R/C ratio).

Production costs included seed, mineral fertilisers, biofertiliser, micronutrient fertiliser, organic manure, dolomite, labour, and other production inputs, which differed among treatments. The cost of each input was based on the prevailing local prices during the 2022-2023 cropping season. Gross revenue is calculated by multiplying crop yield (kg ha^{-1}) by the local farm-gate selling price (US$ kg^{-1}).

The revenue-to-cost ratio was calculated as (Beding, 2023) in Equation 3:

$$RC\ ratio = \frac{TR}{TC} \quad [3]$$

where:
TR = total revenue
TC = total production cost.

An R/C ratio > 1 indicates that the farming system generates revenue greater than its production cost.

For intercropping systems, total revenue was calculated from the combined value of all component crops harvested from the same land area.

Statistical Analysis

The experimental data were analysed according to the split-plot RCBD model, with cropping system as the main-plot factor and nutrient management as the subplot factor.

Analysis of variance (ANOVA) was conducted to test the main effects of cropping system and nutrient management and their interaction. The Least Significant Difference (LSD) test was used to differentiate significant differences at the 5% significance level. The statistical analysis was performed with SPSS version 25.

The interaction between cropping system and nutrient management was considered particularly important because it determined whether the response to the integrated biofertiliser-micronutrient treatment was consistent among maize-upland rice, maize-soybean, and upland rice-soybean intercropping systems.

RESULTS AND DISCUSSION

Site Description

A pre-experimental soil analysis was conducted to determine the soil's chemical and physical properties (Table 3).

The research site was characterised by acidic soils (pH < 4.5) with low available potassium (K_2O) and high phosphorus (P_2O_5) content that remains largely unavailable due to fixation. The soil texture was classified as silty clay. Acidic soils are prone to potassium leaching (Widowati et al., 2012) and aluminum (Al) saturation, which inhibits nutrient uptake. Furthermore, micronutrient deficiencies, particularly magnesium (Mg), are common under such conditions. Soil amendments, including lime and organic matter, are essential

Table 3
Physical and chemical properties of the experimental soil

Parameter	Unit	Value	Category
Chemical Properties			
pH (H_2O)	-	4.50	Acidic
pH (KCl)	-	3.90	Acidic
Organic carbon (C-organic)	%	2.01	Low
Total nitrogen (N-total)	%	0.15	Low
C/N ratio	-	13.00	-
P_2O_5	Mg 100g-1	58.00	High
K_2O	Mg 100g-1	25.90	Moderate
Available phosphorus (P)	Mg kg-1	11.58	High
Physical Properties			
Sand	%	23.00	-
Silt	%	30.00	-
Clay	%	47.00	Silty clay

for enhancing soil pH and organic carbon content, while micronutrient fertilisers restore trace-element availability.

Biofertilisers contribute to nutrient solubilisation, particularly phosphorus, by releasing P bound in the soil matrix. Their application improved plant height and growth parameters, particularly after eight weeks of planting, consistent with the time needed for microbial populations to establish under low-pH conditions. Rohmah et al. (2016) reported that nitrogen-fixing bacteria, such as Rhizobium, require a pH > 6 to proliferate and function effectively, as well as a carbon source derived from decomposed organic matter.

Crop Growth Response to Integrated Nutrient Management

Visual field observations indicated a good adaptation of all three crop species to closer spacing in the intercropping systems. Dryland conditions were characterised by vigorous vegetative development in upland rice (*Oryza sativa* var. Inpago 11), consistent with its tolerance to moderate shade. Maize (*Zea mays* var. NASA 29) produced robust stalks and, in many instances, two ear shoots per plant, showing early reproductive potential. The soybean (*Glycine max* var. Anjasmoro) showed uniform vegetative growth and was somewhat taller when intercropped with maize than with upland rice, indicating moderate etiolation due to partial light competition (Figure 1).

The ANOVA findings (Table 4) revealed no significant differences among the three intercropping combinations (maize-upland rice, maize-soybean, and upland rice-soybean) for most early vegetative attributes at 2-4 WAP. This means that the higher plant density did not generate crucial competition for light, as canopy light intensity was above 50%, and Padang et al. (2020) stated that this was sufficient for optimal upland rice growth. Only at lower light threshold values were substantial reductions in growth rate observed, confirming that evaluated planting configurations did not cause severe shading stress (Xu et al., 2024).



maize–upland rice intercropping (MR) | maize–soybean intercropping (MS) | Upland rice–soybean intercropping (MS)

Figure 1. Vegetative performance of maize-upland rice, maize-soybean, and upland rice-soybean intercropping under biofertiliser and micronutrient application

Table 4
ANOVA results for plant height and growth components of maize, upland rice, and soybean in intercropping systems with biofertiliser and micronutrient application

Parameter	Source of Variation	2 WAP		4 WAP		6 WAP		8 WAP	
		sig.	CV (%)	sig.	CV (%)	sig.	CV (%)	sig.	CV (%)
Plant height of maize	Intercropping system (T)	ns	4.95	ns	1.64	ns	1.45	ns	1.58
	Fertilisation (P)	ns	25.76	ns	2.38	ns	7.39	*	5.49
	Interaction (T×P)	ns		ns		ns		ns	
Plant height of upland rice	Intercropping system (T)	ns	5.63	ns	7.98	ns	3.65	ns	1.92
	Fertilisation (P)	ns	13.82	ns	20.51	ns	6.78	*	8.37
	Interaction (T×P)	ns		ns		ns		ns	
Plant height of soybean	Intercropping system (T)	ns	3.82	ns	5.61	*	2.31	*	2.25
	Fertilisation (P)	ns	7.69	ns	24.61	ns	10.61	**	3.13
	Interaction (T×P)	ns		ns		ns		ns	
Stem diameter maize	Intercropping system (T)	ns	24.73	ns	7.39	ns	5.95	ns	1.95
	Fertilisation (P)	ns	11.68	ns	1.15	ns	0.88	ns	9.79
	Interaction (T×P)	ns		ns		ns		ns	
Number of tillers of upland rice	Intercropping system (T)	ns	6.71	ns	6.38	ns	7.38	ns	4.91
	Fertilisation (P)	ns	5.45	ns	7.62	*	8.29	*	9.17
	Interaction (T×P)	ns		ns		ns		ns	
Number of branches soybean	Intercropping system (T)	ns	5.08	ns	2.81	ns	3.51	ns	7.46
	Fertilisation (P)	ns	6.15	ns	9.87	*	1.90	*	19.79
	Interaction (T×P)	ns		ns		ns		ns	

Note. * = significantly different at $p < 0.05$; ** = significantly different at $p < 0.01$; ns = not significant

The application of biofertiliser combined with micronutrients (P_1) significantly increased plant height in maize, upland rice, and soybean at 8 WAP, along with greater tiller production in upland rice and more branches in soybean from 6 WAP onwards (Tables 4 and 5). These responses can be explained by the enhancement of nutrient availability, particularly nitrogen (N), phosphorus (P), and potassium (K), mediated by biofertiliser components such as phosphate-solubilising bacteria (PSB), potassium-solubilising bacteria (KSB), and nitrogen-fixing microorganisms. The inclusion of phytohormone-producing microbes in biofertilisers that synthesise gibberellins, indole-3-acetic acid (IAA), and cytokinins likely promoted cell elongation, tiller initiation, and lateral branching (Asra & Samarlina, 2020).

The most significant plant reaction of soybean to P_1 may be connected to its ability to fix nitrogen from the air in symbiosis with *Bradyrhizobium japonicum* (Bhat et al., 2015). The symbiotic association may meet the nitrogen requirements of soybean and may also contribute to the nitrogen availability in the surrounding rhizosphere by root exudates and other rhizosphere processes (Yatsenko et al., 2023). The presence of micronutrients,

Table 5
LSD test results for the average plant height, corn stem diameter, number of upland rice tillers, and number of soybean branches influenced by the application of biofertiliser and micronutrients in intercropping systems

Fertilisers	Plant Type	Plant Height		Stem Diameter Maize	
Maize Crop		6 WAP	8 WAP	6 WAP	8 WAP
P_0	MR	175.40a	209.95a	3.15a	3.36a
	MS	172.93a	211.13a	3.37a	3.39a
P_1	MR	179.15a	220.80b	3.51a	3.60a
	MS	179.60a	225.07b	3.68a	3.69a
Fertilisers	**Plant Type**	**Plant Height**		**Number of Tillers Upland Rice**	
Upland Rice Crop		**6 WAP**	**8 WAP**	**6 WAP**	**8 WAP**
P_0	MR	77.67	102.73a	12.53a	14.30a
	RS	76.73	100.00a	11.00a	13.87a
P_1	MR	76.70	107.53b	14.03b	17.20b
	RS	75.40	106.87b	12.93a	16.83b
Fertilisers	**Plant Type**	**Plant Height**		**Number of Branches of Soybean**	
Soybean Crop		**6 WAP**	**8 WAP**	**6 WAP**	**8 WAP**
P_0	MS	73.90	98.62a	8.67a	13.28a
	RS	70.80	102.90a	8.13a	12.30a
P_1	MS	77.10	109.68b	10.97b	16.30a
	RS	74.45	114.48b	10.87b	17.85b

Note. Means followed by the same letter within a column are not significantly different according to the LSD test at $p < 0.05$

especially Zn and Cu, in P1 might have also played a role in promoting plant growth, as these elements participate in several physiological processes such as enzyme activity, chlorophyll synthesis and nucleic acid metabolism (Fauziah et al., 2018). Effects of P_1 on early vegetative development were less noticeable in maize and highland rice. However, an appropriate supply of micronutrients is necessary to maintain photosynthetic activity and to enable subsequent reproductive growth.

Vegetative increases under P_1 definitely extended into the reproductive period. Improved stem vigour and leaf area of maize resulted in more effective assimilate transport to the growing ear. Increased availability of P and K is known to promote cob initiation, kernel set and grain filling (Ndor et al., 2016). In upland rice, an increase in the tiller number at the end of the vegetative phase enhanced the productive panicles per plant, which is one of the primary components of grain output (Kalaitzidis et al., 2025).

In soybeans, better vegetative response (especially increased branching) resulted in increased reproductive nodes and hence increased pod set. Micronutrients like molybdenum (Mo) and Zn are of special importance for the reproductive performance of soybean as they promote nodulation efficiency, nitrogenase activity and seed filling processes (Fageria &

Oliveira, 2014). This explains the substantially increased seed weight of soybean under P_1 as compared to maize and upland rice, indicating its higher nutritional need and sensitivity.

Crop Yield Response to Integrated Nutrient Management

During the generative phase, all crop species developed vigorously in the generative phase throughout the treatments (Figure 2). Inpago 11 upland rice yielded grains that were well-filled, despite its characteristically short panicles. Approximately 80% of the maize (NASA 29) plants formed two large cobs, and Anjasmoro soybeans produced numerous, well-filled pods in all intercropping systems. Maize cobs were bigger, rice panicles were longer, and soybean pods were more abundant in biofertiliser-treated plots, showing more visual variations.

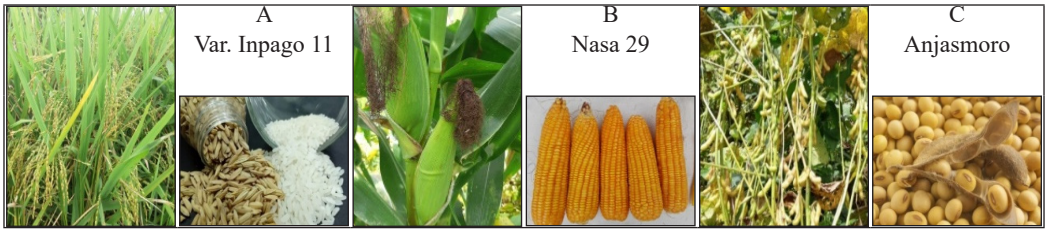

Figure 2. Plant performance during the generative phase of upland rice (A), maize (B), and soybean (C) in intercropping systems with biofertiliser and micronutrient application on dryland

ANOVA results (Table 6) indicated that biofertiliser and micronutrient application significantly improved cob diameter, cob length, 100-grain weight, and maize productivity, with the strongest effects observed in the maize-soybean (MS) intercropping system. In upland rice, both the intercropping system and fertilisation significantly influenced panicle length, number of grains per panicle, and productivity, with the rice-soybean (RS) combination under enhanced fertilisation showing the greatest gains. For soybeans, fertilisation significantly increased the number of filled pods in both MS and RS systems, while reducing the number of empty pods in the RS system. No significant interaction effects between the intercropping system and fertilisation were detected for any crop.

The LSD comparisons showed that the addition of biofertiliser and micronutrients (P_1) improved several yield components and crop productivity, although the magnitude of the response varied among crops and intercropping systems (Table 7). In maize, the clearest response occurred in the maize-soybean (MS) system. Compared with P_0, P_1 increased cob length from 18.17 to 20.55 cm (13.1%), cob diameter from 4.70 to 5.93 mm (26.2%), 100-grain weight from 26.89 to 29.75 g (10.6%), and grain productivity from 5.72 to 6.86 t ha^{-1} (19.9%). The different letters in the LSD test indicate that these values were significantly higher under P_1 in the MS system. In contrast, the maize-upland rice (MR) system showed smaller numerical increases, and the corresponding means shared the same

Table 6
ANOVA results for yield components and productivity of maize, upland rice, and soybean in intercropping systems with biofertiliser and micronutrient application

Crops	Source of Variation	Cob Diameter (Maize)		Cob Length		Weight 100 Grains		Productivity	
		sig.	CV (%)	sig.	CV (%)	sig.	CV (%)	sig.	CV (%)
Maize	Intercropping system (T)	ns	4.23	ns	9.71	ns	7.01	ns	3.08
	Fertilisation (P)	*	10.26	*	7.26	*	5.17	*	1.73
	Interaction (T×P)	ns		ns		ns		ns	
		Length Panicles		**Number of Grains per Panicle**		**Weight 1000 Grains**		**Productivity**	
Upland rice	Intercropping system (T)	*	4.41	*	1.13	ns	2.86	*	4.82
	Fertilisation (P)	*	10.37	*	13.83	ns	13.73	*	1.97
	Interaction (T×P)	ns		ns		ns		ns	
		Number of Filled Pods		**Number of Empty Pods**		**Weight 1000 Grains**		**Productivity**	
Soybean	Intercropping system (T)	ns	4.04	ns	6.08	ns	2.86	ns	4.82
	Fertilisation (P)	*	17.57	*	7.57	ns	13.73	*	1.97
	Interaction (T×P)	ns		ns		ns		ns	

Note. * = significantly different at $p < 0.05$; ns = not significant

Table 7
SD test results for yield components and productivity of maize, upland rice, and soybean in intercropping systems with biofertiliser and micronutrient application

Fertilisers	Plant Type	Maize			
		Cob Diameter (mm)	Cob Length (cm)	Weight 100 Grains (g)	Productivity (t ha-1)
P_0	MR	4.80a	17.50a	27.30a	5.80a
	MS	4.70a	18.17a	26.89a	5.72a
P_1	MR	5.57a	19.80a	27.70a	6.30a
	MS	5.93b	20.55b	29.75b	6.86b
Fertilisers	**Plant Type**	**Upland Rice**			
		Length Panicles (cm)	Number of Grains per Panicles	Weight 1000 Grains (g)	Productivity (t ha-1)
P_0	MR	21.10a	190.50a	23.50a	3.97a
	RS	23.40a	197.50a	24.60a	4.01a
P_1	MR	24.23a	200.00a	23.90a	4.23a
	RS	25.78b	205.00a	24.80a	5.20b
Fertilisers	**Plant Type**	**Soybean**			
		Number of Filled Pods	Number of Empty Pods	Weight 100 Grains (g)	Productivity (t ha-1)
P_0	MS	68.00a	11.70a	18.33a	1.94a
	RS	66.10a	11.20a	18.00a	1.70a
P_1	MS	75.20b	12.20a	19.30a	2.12b
	RS	73.40b	9.60b	19.33a	2.14b

Note. Means followed by the same letter within a column are not significantly different according to the LSD test at $p < 0.05$

statistical group. These results indicate that the integrated treatment improved maize yield formation, particularly under the maize-soybean system.

A similar response was observed in upland rice, particularly under the upland rice-soybean (RS) system. P_1 increased panicle length from 23.40 to 25.78 cm, representing a 10.2% increase relative to P_0. Grain productivity increased from 4.01 to 5.20 t ha^{-1}, equivalent to a 29.7% increase. The increase in panicle length and productivity was statistically significant according to the LSD test, whereas the number of grains per panicle and 1000-grain weight did not differ significantly between P_0 and P_1. This suggests that the higher productivity under P_1 was associated more strongly with improved panicle development and overall yield formation than with changes in individual grain weight.

Soybeans also responded positively to the integrated nutrient treatment. In the MS system, productivity increased from 1.94 to 2.12 t ha^{-1} (9.3%), while in the RS system it increased from 1.70 to 2.14 t ha^{-1} (25.9%). Both increases were statistically significant based on the LSD test. The number of filled pods increased from 68.00 to 75.20 pods

plant^{-1} (10.6%) in MS and from 66.10 to 73.40 pods plant^{-1} (11.0%) in RS. In the RS system, P_1 also reduced the number of empty pods from 11.20 to 9.60 pods plant^{-1} (14.3%), although the 100-grain weight increased only numerically from 18.00 to 19.33 g and was not statistically different. These results suggest that the soybean productivity response was primarily associated with improved pod formation and reproductive performance rather than a significant increase in individual seed weight.

Overall, the productivity response demonstrates that the integrated biofertiliser-micronutrient treatment increased the yield of the component crops without increasing the recommended rate of inorganic fertilisers. The largest productivity increases were observed in maize under MS (19.9%), upland rice under RS (29.7%), and soybean under RS (25.9%) (Table 8). The response was therefore not uniform across crops or cropping systems, reflecting differences in crop nutrient requirements and yield formation. Nevertheless, because the cropping system × nutrient-management interaction was not statistically significant for the measured agronomic parameters, these differences should be interpreted as variation in the magnitude of response rather than evidence that P_1 was statistically more effective in a particular intercropping system.

The stronger responsiveness of soybeans to microbial and micronutrient inputs under intercropping may be linked to their symbiotic nitrogen-fixing capacity, which enhances nutrient acquisition and indirectly benefits companion cereals. Micronutrients such as Mo, Zn, and B supplied via fertilisation can stimulate nodulation, enzyme activation, and seed filling. According to Thapa et al. (2021), the role of Mo in soybeans is crucial for nodule formation and biological N_2 fixation by *Bradyrhizobium japonicum*. When Mo is deficient, nitrogen fixation is disrupted, and chlorosis symptoms appear on both young and old leaves. In maize and rice, improved cob and panicle development under P_1 is likely associated with enhanced availability of phosphorus and potassium from biofertiliser application, thereby supporting reproductive organ growth and grain filling.

The combination of biofertilisers (such as *Azotobacter*, AMF, and *Bacillus circulans*) and organic fertilisers (e.g., humic acid) has been shown to improve growth, yield, seed quality, and microbial and enzymatic activities, including phosphatase and dehydrogenase (Gao et al., 2020). Phosphate- and potassium-solubilising microbes enhance the uptake of N, P, and K in maize, thereby supporting grain filling and cob development (Ghetiya

Table 8
Increased Yield in an intercropping system with biofertiliser and micronutrient fertiliser treatments

Crop	Intercropping System	P0 (t ha^{-1})	P1 (t ha^{-1})	Increase
Maize	MS	5.72	6.86	19.9%
Upland rice	RS	4.01	5.20	29.7%
Soybean	MS	1.94	2.12	9.3%
Soybean	RS	1.70	2.14	25.9%

et al., 2018). Mehata et al. (2023) found that certain biofertilisers can improve important attributes such as panicle length and weight, 1,000-grain weight, and number of grains per panicle, as well as SPAD values, indicating a positive effect on grain filling and grain yield. Additionally, complementary rooting patterns and distinct nutrient demands among maize, rice, and soybean likely reduced interspecific competition, enabling more efficient resource use and contributing to the observed yield improvements.

Land-Use Efficiency and Cropping System Performance

The production of maize, dryland rice, and soybeans is calculated as the product of productivity and the number of plants cultivated in each intercropping system, divided by the number of plants per hectare. Among the intercropping systems, the maize-soybean and upland rice-soybean intercropping systems had the most significant increase in production with the addition of Biofertiliser and micronutrients.

All intercropping systems had LER values more than one, indicating better land use and time efficiency than monoculture (Erythrina, 2022). The highest LER (1.56) was obtained from the upland rice-soybean combination, followed by maize-soybean and maize-upland rice (Figure 3). The maximum CSE value of 1.5 was likewise seen in upland rice-soybean intercropping (Figure 4).

The use of biofertiliser and micronutrients increased LER by 14.17% and CSE by 13.08%, indicating improved land productivity and cropping system efficiency. Farmers in the study area generally practice corn monoculture in a single planting season. However, market saturation at harvest means maize prices are depressed from the average US$ 0.33 kg^{-1} to as low as US$ 0.14-0.17 kg^{-1}. In this sense, intercropping offers a means of revenue stabilisation through crop diversity. The inclusion of legumes and upland rice provides yield resilience and price stability.

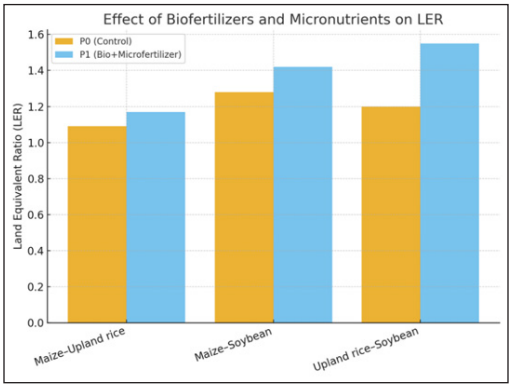

Figure 3. Effect of biofertilisers and micronutrients on Land Equivalent Ratio (LER)

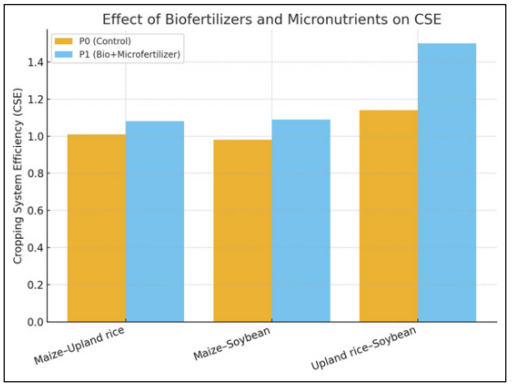

Figure 4. Effect of biofertilisers and micronutrients on Cropping System Efficiency (CSE)

The improved performance of the intercropping systems was attributed to increased productivity of the component crops. In instance, the RS system showed the strongest upland-rice productivity response and a significant soybean productivity improvement, matching its higher LER of 1.56 and CSE of 1.50. However, LER and CSE are system-level efficiencies and should be evaluated alongside the actual productivity of component crops, rather than as substitutes for crop yield measurements.

Economic Performance and Net Benefit

Financial analysis showed that all intercropping systems generated higher net benefits than the existing maize monoculture (US$742.40 ha^{-1}; R/C ratio = 1.68), although the magnitude varied among cropping systems (Table 9). Under P_1, net benefits reached US$840.70, US$1,230.40, and US$1,349.10 ha^{-1} in maize-upland rice, maize-soybean, and upland rice-soybean, respectively. Relative to maize monoculture, these values represented increases of 13.24%, 65.73%, and 81.72%, respectively (Table 10). Thus, the greatest economic advantage was achieved with the upland rice-soybean system under integrated biofertiliser-micronutrient management.

The addition of biofertiliser and micronutrients increased net benefit compared with P_0 in all intercropping systems, although the magnitude differed among systems. Net benefit increased from US$800.10 to US$840.70 ha^{-1} in maize-upland rice, from US$1,064.20 to US$1,230.40 ha^{-1} in maize-soybean, and from US$910.70 to US$1,349.10 ha^{-1} in upland rice-soybean. The corresponding R/C ratios were 1.63, 1.93, and 2.01 under P_1, respectively. The slightly lower R/C ratio in maize-upland rice under P_1 (1.63) than under P0 (1.65), despite the higher net benefit, indicates that the additional production costs were disproportionate to the increase in revenue. Therefore, net benefit and R/C ratio should be considered together when evaluating the economic performance of the integrated treatment.

The higher economic returns from intercropping resulted from the combined value of the component crops harvested from the same land area and the diversification of production. This diversification may reduce farmers' dependence on maize alone and provide greater flexibility under commodity price fluctuations. However, the superior economic performance of upland rice-soybean under P_1 should not be interpreted as evidence of a significant cropping system × nutrient-management interaction, because the interaction was not statistically significant for the measured agronomic variables. Rather, its higher economic return reflects the combined effects of crop productivity, crop composition, production costs, and prevailing crop prices during the experimental period.

Overall, all intercropping systems studied were economically feasible, with R/C ratios ranging from 1.63 to 2.01 under P_1. The upland rice-soybean system had the best net benefit and R/C ratio, indicating strong economic potential under current production and market conditions. Nevertheless, these results reflect the pricing and cost conditions

Table 9
Financial performance of intercropping systems under standard and enhanced fertilisation strategies

Intercropping Systems	Revenue (R) (US$)		Production Cost (C) (US$)		Benefit (B) (US$)		R/C	
	P_0	P_1	P_0	P_1	P_0	P_1	P_0	P_1
MR	2.026.4	2.175.4	1.226.3	1.334.7	800.1	840.7	1.65	1.63
MS	2.249.5	2.549.4	1.185.3	1.319.0	1.064.2	1.230.4	1.90	1.93
RS	2.127.6	2.684.5	1.216.9	1.335.4	910.7	1.349.1	1.75	2.01
Maize Monoculture (existing)	1.834.4		1.092.0		742.4		1.68	

Table 10
Increased benefit in an intercropping system with biofertiliser and micronutrient fertiliser treatments

Intercropping Systems	Benefit P_0	Benefit P_1	Increase vs. Monoculture P_0	Increase vs. Monoculture P_1	Mean
MR	800.10	840.70	7.77%	13.24%	10.51%
MS	1.064.20	1.230.40	43.35%	65.73%	54.54%
RS	910.70	1.349.10	22.67%	81.72%	52.20%
Maize Monoculture	742.40				

during the experiment and should not be taken as evidence that income will be stable over the long run. Additional sensitivity analysis incorporating changes in crop prices and production costs would be useful to determine the robustness of the economic advantage under unfavorable market conditions.

The results indicate that intercropping-based diversification is a risk-mitigation strategy against market volatility. Furthermore, the positive R/C ratios (>1) in all the treatments illustrate the economic viability and sustainability of the proposed systems for the farmers. This is consistent with previous studies showing that intercropping promotes income stability by spreading risk across different commodities (Hermawati, 2016).

The results encourage the adoption of intercropping systems in association with environmentally friendly fertilisation practices. Biofertilisers are microbiologically active, low-impact, environmentally safe, and improve soil structure, water infiltration, and aggregate stability (Martirosyan et al., 2023; Stehlík et al., 2019). Small amounts of inorganic fertilisers (Urea, NPK, and micronutrients) are used in regulated doses to augment organic inputs without causing soil degradation or contamination.

Therefore, the simultaneous use of biofertiliser, micronutrients, and site-specific inorganic fertilisers is a feasible approach to intensify drylands sustainably. These innovations are agronomically and commercially practicable, with R/C ratios>1 across all treatments (Ely & Darwanto, 2014; Msiska et al., 2024), and may serve as a paradigm for large-scale adoption in areas with similar agroecological limitations.

Mechanisms Underlying the Response to Integrated Biofertiliser and Micronutrient Management

The higher crop growth and production under the integrated biofertiliser-micronutrient treatment (P1) may be due to the combined effects of biological nutrient cycling and micronutrient application. The reaction was more pronounced at 6-8 weeks after planting (WAP), when the nutritional demand of the crops was higher, as evidenced by increased plant height in maize, upland rice, and soybean, and accelerated tiller development in upland rice and branch formation in soybean. This pattern is consistent with improved fertiliser supply through integrated treatment during the period of increasing crop demand. Nevertheless, as food consumption, microbial activity and nutrient fluxes were not clearly defined, these mechanisms should be treated as reasonable interpretations and not directly demonstrated processes.

Biofertilisers can improve the intake of plant nutrients by several microbial activities, including biological nitrogen transformation, phosphorus solubilisation, potassium mobilisation and generation of plant growth-stimulating chemicals. These microorganisms can change the availability of nutrients in the rhizosphere and support the roots of the plant in absorbing and using up nutrients (Mahanty et al., 2017; Soumare et al., 2020). For instance, phosphate-solubilising bacteria can render rarely accessible P mobile by

organic acid synthesis, proton release and enzymatic mineralisation. However, responses to microbial inoculants in the field can vary, as their efficiency depends on soil properties, native microbial populations, environmental conditions, and the establishment of the imported microorganisms (Raymond et al., 2021). Hence, the higher response at later growth stages could perhaps be explained by rising crop demand together with microbial-mediated nutrient cycling rather than an increase in the availability of nutrients in soil, as indicated in our experiment.

Micronutrient addition may have contributed to these biological processes, supporting important physiological and enzymatic functions. Small quantities of elements such as zinc, iron, manganese, boron and molybdenum are needed for enzyme activation, photosynthesis, reproductive development and food metabolism. Micronutrients play important roles in soybeans, and their deficiencies can impede growth, nodulation, and reproductive development (Bagale, 2021; Thapa et al., 2021). Therefore, the micronutrient component of P_1 may have improved the efficiency of physiological processes responsible for biomass synthesis and yield production, complementing the macronutrients supplied by the proposed fertilisation technique.

The soybean response is of particular interest since the symbiotic biological nitrogen fixation (BNF) may be a source of N nutrition. P and micronutrients, in particular, are important for nodule formation and nitrogenase activity, and their optimal availability is critical for effective BNF. Molybdenum is directly linked to nitrogenase activity, and other micronutrients also play roles in enzymatic and physiological processes that support the symbiotic relationship. Therefore, the increased branching, filled-pod development, and seed yield observed at P1 are consistent with more favourable nutritional conditions, which may improve soybean growth and symbiotic N acquisition. However, the present observations cannot be taken as a direct indication of increased biological nitrogen fixation by P1 because no data were obtained on nodulation, nitrogenase activity, or N_2 fixation.

The intercropping environment may have also contributed to the response through complementary utilisation of soil resources. Maize, upland rice and soybean have different rooting characteristics, nutritional requirements and crop development; therefore, they may compete less directly for light, water and nutrients. Therefore, the additional nutrients released by the integrated management may have been utilised by the component crops according to their distinct temporal and spatial demands. This interpretation is consistent with the higher land-use efficiency observed in intercropping systems, particularly in upland rice-soybean. However, the absence of a significant cropping system × nutrient-management interaction suggests that the positive response to P_1 was not statistically specific to a particular crop combination.

Overall, the results indicate that the benefit of combining biofertiliser and micronutrients with the recommended mineral fertilisation is likely due to complementary nutrient-

management functions: the biofertiliser may have improved biological nutrient cycling and mobilisation, while the micronutrients are involved in essential physiological and reproductive processes. These complementary effects could plausibly explain the higher growth, yield components and productivity under P_1 without raising the recommended rate of mineral fertilisers. Nonetheless, to verify these proposed mechanisms and to assess if treatment results in longer-term improvements in soil biological and chemical properties, direct measurements of microbial biomass and activity, soil nutrient availability, root traits, plant nutrient uptake, nodulation, and biological N fixation are needed.

CONCLUSION

Application of biofertilisers and micronutrients combined with the locally recommended inorganic fertilisation increased the crop growth, yield and overall productivity of the studied cereal-legume intercropping systems. In all intercropping systems, the Land Equivalent Ratio (LER) was greater than one, indicating that land was used more efficiently than in monocropping. Among the investigated systems, Upland rice-soybean had the highest LER (1.56) and Cropping System Efficiency (CSE) (1.50). The integrated nutrient treatment also yielded positive economic returns, with R/C ratios above unity across all intercropping systems. The upland rice-soybean system provided the highest economic return with an R/C ratio of 2.01.

The absence of a significant cropping system × nutrient-management interaction indicates that the positive agronomic response to biofertiliser and micronutrient supplementation was not statistically dependent on a particular intercropping combination. Therefore, the integrated nutrient-management approach can be considered a broadly applicable option for improving the productivity and economic performance of cereal-legume intercropping systems under the tested dryland conditions.

IMPLICATIONS OF THE STUDY

The findings support the use of biofertiliser and micronutrients as complementary inputs to locally recommended inorganic fertilisation for sustainable intensification of dryland agriculture.

LIMITATIONS AND RECOMMENDATIONS FOR FUTURE RESEARCH

However, the present study did not directly measure changes in soil microbial biomass, microbial activity, soil organic carbon, enzyme activity, aggregate stability, nutrient availability, or plant nutrient uptake after treatment. Therefore, improvements in soil health or soil fertility should not be considered a direct outcome of this experiment. The potential contribution of the integrated treatment to soil biological and chemical quality requires further verification.

For wider application, the recommended nutrient-management package should first be validated through multi-season and multi-location trials under dryland environments with similar agroecological conditions. Future studies should additionally quantify soil biological properties, soil organic carbon, nutrient availability, root characteristics, plant nutrient uptake, and biological nitrogen fixation to elucidate the mechanisms underlying the observed agronomic and economic responses and to determine the longer-term effects of integrated nutrient management on soil health.

ACKNOWLEDGEMENT

We are grateful for the labour support and participation from farmer groups in Pengeureunan Village, Limbangan District, Garut Regency, West Java Province, Indonesia.

REFERENCES

Agbor, D. T., Eboh, K. S., Sama, D. K., Teche, L. M., Tanyi, G. T., & Nkongho, R. N. (2023). Maize-legume intercropping and botanical Piper mitigating effect on pest populations while enhancing the yield of maize. *Journal of Natural Pesticide Research, 6*, Article 100060. https://doi.org/10.1016/j.napere.2023.100060

Agsari, D., Utomo, M., Hidayat, K. F., & Niswati, A. (2020). Response of macro- and micronutrient uptake and maize (*Zea mays* L.) production to nitrogen fertilisation and long-term tillage practices. *Journal of Tropical Upland Resources, 2*(1), 46-59. https://doi.org/10.23960/jtur.vol2no1.2020.78

Asra, R., & Samarlina, R. A. (2020). *Hormon Tumbuhan* [Plant hormones]. UKI Press.

Bagale, S. (2021). Nutrient management for soybean crops. *International Journal of Agronomy, 2021*, Article 3304634. https://doi.org/10.1155/2021/3304634

Beding, P. A., Lewaherilla, N. E., Lestari, R. H., Tirajoh, S., & Tiro, B. M. W. (2023). Analysis of the potential for development of maize commodities in the border area of the Unitary State of the Republic of Indonesia-Papua New Guinea, Keerom Regency, Papua. *SEPA: Jurnal Sosial Ekonomi Pertanian dan Agribisnis, 20*(2), 162-170. https://doi.org/10.20961/sepa.v20i2.52339

Bhat, T. A., Ahmad, L., Ganai, M. A., Shams-Ul-Haq, & Khan, O. A. (2015). Nitrogen fixing biofertilisers: Mechanism and growth promotion: A review. *Journal of Pure and Applied Microbiology, 9*(2), 1675-1690.

Central Statistics Agency of Garut Regency. (2022). *Garut Regency in figures 2021*. BPS Garut.

Dariush, M., Ahad, M., & Meysam, O. (2006). Assessing the land equivalent ratio (LER) of two corn (*Zea mays* L.) varieties intercropped at various nitrogen levels in Karaj, Iran. *Journal of Central European Agriculture, 7*(2), 359-364.

Ely, A., & Darwanto, D. D. (2014). Analisis kelayakan usaha dan strategi pengembangan budidaya rumput laut di kabupaten Seram Bagian Barat [Feasibility analysis and development strategy of seaweed cultivation business in Seram Bagian Barat Regency]. *Agro Ekonomi, 25*(2), 169-177. https://doi.org/10.22146/agroekonomi.17197

Erythrina, E., Susilawati, S., Slameto, S., Resiani, N. M. D., Arianti, F. D., Jumakir, J., Fahri, A., Bhermana, A., Jannah, A., & Sembiring, H. (2022). Yield advantage and economic performance of rice-maize, rice-

soybean, and maize-soybean intercropping in rainfed areas of Western Indonesia with a wet climate. *Agronomy, 12*(10), Article 2326. https://doi.org/10.3390/agronomy12102326

Fageria, N. K., & Oliveira, J. P. (2014). Nitrogen, phosphorus and potassium interactions in upland rice. *Journal of Plant Nutrition, 37*(10), 1586-1600. https://doi.org/10.1080/01904167.2014.920362

Fauziah, F., Wulansari, R., & Rezamela, E. (2018). Pengaruh pemberian pupuk mikro Zn dan Cu serta pupuk tanah terhadap perkembangan *Empoasca* sp. pada areal tanaman teh [The effect of Zn and Cu microfertilisers and soil fertiliser on the development of *Empoasca* sp. in the tea plantation area]. *Agrikultura, 29*(1), 26-34. https://doi.org/10.24198/agrikultura.v29i1.16923

Gao, C., El-Sawah, A. M., Ali, D. F. I., Hamoud, Y. A., Shaghaleh, H., & Sheteiwy, M. S. (2020). The integration of bio and organic fertilisers improve plant growth, grain yield, quality and metabolism of hybrid maize (*Zea mays* L.). *Agronomy, 10*(3), Article 319. https://doi.org/10.3390/agronomy10030319

Ghetiya, K. P., Bhalu, V. B., Mathukia, R. K., Hadavani, J. K., & Kamani, M. D. (2018). Effect of phosphate and potash solubilising bacteria on growth and yield of popcorn (*Zea mays* L. var. *everta*). *International Journal of Pure & Applied Biosciences, 6*(5), 167-174. https://doi.org/10.18782/2320-7051.6918

Hermawati, D. T. (2016). Economic study between monoculture cropping patterns and intercropping of corn, cabbage and spinach. *INOVASI, 18*(1), 66-71.

Jensen, E. S., Carlsson, G., & Hauggaard-Nielsen, H. (2020). Intercropping of grain legumes and cereals improves the use of soil N resources and reduces the requirement for synthetic fertiliser N: A global-scale analysis. *Agronomy for Sustainable Development, 40*, Article 5. https://doi.org/10.1007/s13593-020-0607-x

Kalaitzidis, A., Kadoglidou, K., Mylonas, I., Ghoghoberidze, S., Ninou, E., & Katsantonis, D. (2025). Investigating the impact of tillering on yield and yield-related traits in European rice cultivars. *Agriculture, 15*(6), Article 616. https://doi.org/10.3390/agriculture15060616

Khanal, U., Stott, K. J., Armstrong, R., Nuttall, J. G., Henry, F., Christy, B. P., Mitchell, M., Riffkin, P. A., Wallace, A. J., McCaskill, M., Thayalakumaran, T., & O'Leary, G. J. (2021). Intercropping—Evaluating the advantages to broadacre systems. *Agriculture, 11*(5), Article 453. https://doi.org/10.3390/agriculture11050453

Krasilnikov, P., Taboada, M. A., & Amanullah. (2022). Fertilizer use, soil health and agricultural sustainability. *Agriculture, 12*(4), Article 462. https://doi.org/10.3390/agriculture12040462

Kristiono, A., Muzaiyanah, S., Elisabeth, D. A. A., & Harsono, A. (2020). Productivity of soybean intercropping with maize at the end of rainy season in dry land with dry climate. *PANGAN, 29*(3), 197-210. https://doi.org/10.33964/jp.v29i3.495

Latati, M., Rebouh, N. Y., Aouiche, A., & Laouar, M. (2019). Modeling the functional role of the microorganisms in the daily exchanges of carbon and nitrogen in intercropping system under Mediterranean conditions. *Agronomy Research, 17*(2), 559-573. https://doi.org/10.15159/AR.19.050

Mahanty, T., Bhattacharjee, S., Goswami, M., Bhattacharyya, P., Das, B., Ghosh, A., & Tribedi, P. (2017). Biofertilisers: A potential approach for sustainable agriculture development. *Environmental Science and Pollution Research, 24*(4), 3315-3335. https://doi.org/10.1007/s11356-016-8104-0

Martirosyan, H. S., Mikaelyan, A. R., Asatryan, N. I., & Babayan, B. G. (2023). Assessment of 'Complex-Co' preparation efficiency for some cereal crops growth stimulation. *Agronomy Research, 21*(3), 1213-1220. https://doi.org/10.15159/AR.23.105

Mehata, D., Yadav, S., Ghimire, N., Oli, B., Mehata, R., & Acharya, R. (2023). Evaluating the impact of various biofertiliser sources on growth and yield attributes of spring rice (*Oryza sativa* L.) in Eastern Terai of Nepal. *Peruvian Journal of Agronomy, 7*(3), 200-219. https://doi.org/10.21704/pja.v7i3.1977

Mulyani, A., Kuncoro, D., Nursyamsi, D., & Agus, F. (2016). Analysis of paddy field conversion: The utilisation of high-resolution spatial data shows an alarming conversion rate. *Jurnal Tanah dan Iklim, 40*(2), 121-133.

Msiska, S. C., Padi, R. K., & Chimphango, A. (2024). Comparative techno-economic and life cycle assessments of single and intercropped-mixed feedstocks-based biorefineries for profitable and cleaner production of energy. *Journal of Cleaner Production, 450*, Article 141988. https://doi.org/10.1016/j.jclepro.2024.141988

Ndor, E., Jayeoba, J. O., Asadu, C. L. A., & Iheshiulo, E. M. A. (2016). Growth, nutrient uptake and dry matter yield of maize (*Zea mays* L.) grown in soil amended with rice husk and sawdust biochar. *International Journal of Scientific Research in Agricultural Sciences, 3*(3), 99-103. https://doi.org/10.12983/ijsras-2016-p0099-0103

Omara, P., Aula, L., Oyebiyi, F., & Raun, W. R. (2019). World cereal nitrogen use efficiency trends: Review and current knowledge. *Agrosystems, Geosciences & Environment, 2*, Article 180045, 1-8. https://doi.org/10.2134/age2018.10.0045

Padang, I. S., Tohari, & Widada, J. (2020). Response of upland rice (*Oryza sativa* L.) cultivars to different shade levels in sandy soil. *Ilmu Pertanian (Agricultural Science), 5*(3), 158-165. https://doi.org/10.22146/ipas.30643

Peoples, M. B., Ladha, J. K., Reddy, P. M., Biswas, J. C., Bennett, A., Jat, M. L., & Krupnik, T. J. (2022). Biological nitrogen fixation and prospects for ecological intensification in cereal-based cropping systems. *Field Crops Research, 283*, Article 108541. https://doi.org/10.1016/j.fcr.2022.108541

Pérez-Bernal, S., Sekar, J., Prabavathy, V. R., Mathimaran, N., Thimmegowda, M. N., Bagyaraj, D. J., & Kahmen, A. (2025). Biofertilisers enhance land-use efficiency in intercropping across crop mixtures and spatial arrangements. *Frontiers in Agronomy, 7*, Article 1562589. https://doi.org/10.3389/fagro.2025.1562589

Pierre, J. F., Latournerie-Moreno, L., Garruña, R., Jacobsen, K. L., Laboski, C. A. M., Us-Santamaría, R., & Ruiz-Sánchez, E. (2022). Effect of maize-legume intercropping on maize physio-agronomic parameters and beneficial insect abundance. *Sustainability, 14*(19), Article 12385. https://doi.org/10.3390/su141912385

Pusat Data dan Sistem Informasi Pertanian. (2021). *Agricultural statistics 2021*. Ministry of Agriculture. Republic of Indonesia.

Raymond, N. S., Gómez-Muñoz, B., van der Bom, F. J. T., Nybroe, O., Jensen, L. S., Müller-Stöver, D. S., Oberson, A., & Richardson, A. E. (2021). Phosphate-solubilising microorganisms for improved crop productivity: A critical assessment. *New Phytologist, 229*(3), 1268-1277. https://doi.org/10.1111/nph.16924

Rillig, M. C., Ryo, M., Lehmann, A., Aguilar-Trigueros, C. A., Buchert, S., Wulf, A., Iwasaki, A., Roy, J., & Yang, G. (2019). The role of multiple global change factors in driving soil functions and microbial biodiversity. *Science, 366*(6467), 886-890. https://doi.org/10.1126/science.aay2832

Rohmah, N., Muslihatin, W., & Nurhidayati, T. (2016). The effect of a combination of biological fertiliser carrier media with nitrogen-fixing bacteria on pH and nitrogen nutrients in soil. *Jurnal Sains dan Seni ITS, 4*(1).

Soumare, A., Diedhiou, A. G., Thuita, M., Hafidi, M., Ouhdouch, Y., Gopalakrishnan, S., & Kouisni, L. (2020). Exploiting biological nitrogen fixation: A route towards a sustainable agriculture. *Plants, 9*(8), Article 1011. https://doi.org/10.3390/plants9081011

Srinivasarao, C. G., Ranjith Kumar, G., Mansa, R., Pilli, K., Sahao, S., Rakesh, S., Kundu, S., Nataraj, K. C., Rao, K. V., Prasad, J. M. N. S., & Malleswari, S. (2023). Dryland farming: Technological and management options for sustainable agriculture and food systems. In M. Goss & M. Oliver (Eds.), *Encyclopedia of soils in the environment* (2nd ed., pp. 113-124). Elsevier. https://doi.org/10.1016/B978-0-12-822974-3.00219-6

Stehlík, M., Czako, A., Mayerová, M., & Madaras, M. (2019). Influence of organic and inorganic fertilisation on soil properties and water infiltration. *Agronomy Research, 17*(4), 1769-1778. https://doi.org/10.15159/AR.19.145

Thapa, S., Bhandari, A., Ghimire, R., Xue, Q., Kidwaro, F., Ghatrehsamani, S., Maharjan, B., & Goodwin, M. (2021). Managing micronutrients for improving soil fertility, health, and soybean yield. *Sustainability, 13*(21), Article 11766. https://doi.org/10.3390/su132111766

Titirmare, N. S., Ranshur, N. J., Patil, A. H., Patil, S. R., & Margal, P. B. (2023). Effect of inorganic fertilisers and organic manures on physical properties of soil: A review. *International Journal of Plant & Soil Science, 35*(19), 1015-1023. https://doi.org/10.9734/ijpss/2023/v35i193638

Ünay, A., Sabancı, İ., & Çınar, V. M. (2021). The effect of maize (*Zea mays* L.)/soybean (*Glycine max* (L.) Merr.) intercropping and biofertiliser (*Azotobacter*) on yield, leaf area index and land equivalent ratio. *Journal of Agricultural Sciences, 27*(1), 76-82. https://doi.org/10.15832/ankutbd.572495

Wang, J. L., Liu, K. L., Zhao, X. Q., Zhang, H. Q., Li, D., Li, J. J., & Shen, R. F. (2021). Balanced fertilization over four decades has sustained soil microbial communities and improved soil fertility and rice productivity in red paddy soil. *Science of the Total Environment, 793*, Article 148664. https://doi.org/10.1016/j.scitotenv.2021.148664

Widowati, Asnah, & Sutoyo. (2012). Pengaruh penggunaan biochar dan pupuk kalium terhadap pencucian dan serapan kalium pada tanaman jagung [Effect of using biochar and potassium fertiliser on leaching and uptake of potassium in maize plants]. *Buana Sains, 12*(1), 83-90.

Xu, T., Wang, D., Si, Y., Kong, Y., Shao, X., Geng, Y., Lv, Y., & Wang, Y. (2024). Plant growth regulators enhance maize (*Zea mays* L.) yield under high density by optimizing canopy structure and delaying leaf senescence. *Agronomy, 14*(6), Article 1262. https://doi.org/10.3390/agronomy14061262

Yatsenko, V., Yatsenko, N., Karpenko, V., Poltoretskyi, S., Lazariev, O., Kravchenko, V., Chynchyk, O., Vyshnevska, L., Tretiakova, S., & Kozyrsky, D. (2023). Agrobiological assessment of productivity and nitrogen fixation of vegetable soybean (edamame) in the conditions of Forest-Steppe of Ukraine. *Agronomy Research, 21*(2), 1006-1026. https://doi.org/10.15159/AR.23.097

Pertanika J. Trop. Agric. Sci. 49 (5): 2197 - 2215 (2026)

PERTANIKA JOURNALS

TROPICAL AGRICULTURAL SCIENCE

Journal homepage: http://www.pertanika.upm.edu.my/

Ameliorative Effects of dbcAMP and des (1-3) IGF-1 on Myogenic and Adipogenic mRNA Expression in Transdifferentiated C2C12 Myogenic Cells

Muhamad Faris Ab Aziz[1, 2]*, Zoe C.T.R. Daniel[2], Andrew Salter[2], and Tim Parr[2]

[1]Department of Animal Science, Faculty of Agriculture, Universiti Putra Malaysia, 43400 Selangor, Malaysia
[2]Division of Nutritional Sciences, School of Biosciences, Sutton Bonington Campus, University of Nottingham, LE12 5RD Leicestershire, United Kingdom

ABSTRACT

The metabolic modifiers, including beta agonist (BA) and growth hormone (GH), were extensively used in animal production as they increase protein synthesis and reduce lipid synthesis in animals, particularly in muscles. However, studies on their effects at the molecular level are limited. This study examined the effects of dibutyryl cyclic adenosine monophosphate (dbcAMP), a mimic of BA, and des (1-3) insulin-like growth factor-1 (des (1-3) IGF-1), an analogue for GH, on myogenic and adipogenic mRNA expression in transdifferentiated-myogenic C2C12 cell lines. Following treatment, lipid droplet formation was observed alongside the expression of myogenic and adipogenic mRNAs, indicating the coexistence of myotubes and adipocytes in the culture and reflecting a model resembling intramuscular fat deposition in vivo. Lipid droplet accumulation was significantly reduced ($P < 0.001$) by dbcAMP and des(1-3) IGF-1 treatments. Moreover, dbcAMP exerted a significant ($P < 0.05$) stimulatory effect on myogenesis-associated genes, while downregulating lipogenic and adipogenic mRNA expression ($P < 0.05$). Meanwhile, des (1-3) IGF-1 appeared to promote adipogenic differentiation, with no effect on lipogenic and lipolytic gene expression, suggesting different pathways of dbcAMP and IGF-1 induction on myogenesis and adipogenesis in vitro.

Keywords: Adipogenic, C2C12, dbcAMP, des (1-3) IGF-1, lipogenic, lipolytic, myogenic

ARTICLE INFO

Article history:
Received: 22 September 2025
Accepted: 27 August 2026
Published: 30 October 2026

DOI: https://doi.org/10.47836/pjtas.49.5.05

E-mail addresses:
mhd_faris@upm.edu.my (Muhamad Faris Ab Aziz)
zoe.daniel@nottingham.ac.uk (Zoe C.T.R. Daniel)
andrew.salter@nottingham.ac.uk (Andrew Salter)
tim.parr@nottingham.ac.uk (Tim Parr)
* Corresponding author

INTRODUCTION

Metabolic modifiers, including beta-agonist (BA) and growth hormone (GH), were utilised for feed efficiency enhancement

© Universiti Putra Malaysia Press

via improving animal growth performance and increasing lean tissue content, and thereby increasing profitability (Dunshea et al., 2016; Dikeman, 2007). Generally, their mode of action involves promoting protein accretion while reducing fat deposition (Chikani & Ho, 2013; Hostrup & Onslev, 2022; Pfau et al., 2024; 2023). These metabolic modifiers are often described as repartitioning agents, as they redirect nutrient utilisation away from adipose stores and the gastrointestinal tract towards skeletal muscle for hypertrophy and mammary glands for milk production (Brown et al., 2018; Bao et al., 2016; Scascia et al., 2015; Hemmings et al., 2015). Regarding lipid metabolism, BA are known to stimulate lipolysis while suppressing lipogenesis (Pfau et al., 2023; de Almeida et al., 2012; Dunshea et al., 2005; Mersmann, 2002). GH exerts similar observations, as it also reduced fat accretion (Dunshea et al., 2016). Thus, this may explain their role in modifying the composition of fat and subsequent impacts on meat tenderness and palatability (Dikeman, 2007; Ladeira et al., 2016; Warriss et al., 1990). As fat content in meat is considered unhealthy, the use of metabolic modifiers could benefit consumers by producing healthier products (Gebre et al., 2012). However, the improvement in lean meat production by these metabolic modifiers has been shown to negatively affect meat quality, likely through reduced intramuscular fat (IMF) (Dunshea et al., 2005).

Although the metabolic modifiers have been demonstrated to enhance performance and carcass characteristics, most in vitro studies have primarily focused on myogenesis, with far less attention given to how these agents modulate lipid metabolic processes at the molecular level. In muscle, BA appear to mediate activation of beta-adrenergic receptors and subsequently stimulate protein kinase A (PKA) activity (Johnson et al., 2014; Milioto et al., 2017). Meanwhile, the GH actions are exerted through insulin-like growth factor-1 (IGF-1), as indicated by the elevated levels of IGF-1 in the plasma after GH stimulation (Gahete et al., 2013; Yamamoto & Bando, 2023). Thus, the current study aimed to ascertain how BA and GH influence lipid-related processes, including adipogenesis, lipogenesis, and lipolysis, alongside their effects on myogenesis in cultured muscle cells.

The cyclic AMP analogue, dibutyryl cyclic adenosine monophosphate (dbcAMP), which mimics the effect of BA, and the analogue for IGF-1, des (1-3) IGF-1, which mimics the effect of GH, were used and their effects on several mRNA expression related to myogenesis, lipogenesis, lipolysis and adipogenesis were assessed on the transdifferentiated myogenic cells, that acquired 'adipocyte-like' characteristics in this study. The C2C12 cells were used as a skeletal muscle model and induced to undergo transdifferentiation in adipogenic medium, leading to the formation of adipocyte-like cells containing lipid droplets, representing an in vitro model of intramuscular fat, before the treatments with the agents. The response of these agents towards the expression of the key metabolic genes was assessed to explore the possible mechanisms underlying lipid metabolism in muscle tissue. We hypothesised that C2C12 incubated in adipogenic media would respond to dbcAMP

or des (1-3) IGF-1 by altering the transcription of myogenic, adipogenic, lipogenic, and lipolytic genes, which are associated with reduced fat deposition.

MATERIALS AND METHODS

C2C12 Culture Conditions and Treatment with dbcAMP and des (1-3) IGF-1

The mouse-derived C2C12 myoblast cell lines were grown in Dulbecco's modified Eagle's growth medium (DMEM) (Sigma-Aldrich, UK), and supplemented with 10% (v/v) heat-inactivated fetal bovine serum (hi-FBS) (Gibco, UK) and 1% (v/v) penicillin and streptomycin (P/S) (Sigma-Aldrich, UK), under maintenance at 5% CO_2 at 37°C. Once the cells reached approximately 70-80% confluence, the culture medium was replaced with adipogenic induction medium, consisting of DMEM with 10% (v/v) hi-FBS, 1% (v/v) P/S, 0.5 mM isobutylmethylxanthine (IBMX), 1 µM dexamethasone (DEX), 850 nM insulin, 10 nM triiodothyronine (T3) and 1 µM rosiglitazone (peroxisome proliferator activated receptor γ (PPARγ) agonist). This stage was designated as day 0 of differentiation. After two days, the induction medium was replaced with adipogenic differentiation medium, containing DMEM with 10% (v/v) hi-FBS, antibiotics, 850 nM insulin, 10 nM T3, and 1 mM rosiglitazone. The medium changes were performed every 48 hours for nutrient replenishment until the experiment was concluded. On day 6 of differentiation, the cells were exposed to either 100 ng/ml des (1-3) IGF-1 (DES) (Autogen Bioclea, Bioscience UK Ltd) or 1 mM dibutyryl cyclic adenosine monophosphate (dbcAMP) (DB) (Sigma-Aldrich, UK) that were added to the adipogenic differentiation media, while the control was unsupplemented. This point was marked as day 0 of treatment. The cells were scraped on days 1, 2, and 3 for the RNA extraction, whilst the lipid droplet quantification was performed on day 3 of treatment.

Lipid Droplets Quantification

Lipid droplet accumulation was assessed in C2C12 cells using Oil Red O staining and haematoxylin counterstaining, as described by Ryan et al. (2013). After staining, the cells were visualised and imaged using an Olympus SZH10 microscope (Olympus, Southend-on-Sea, UK). For each treatment replicate, ten random field-of-view images were taken and processed using ImageJ Software (version 1.50I, National Institutes of Health, USA). using the application of colour threshold on the stained regions, and the percentage of stained area for each image was quantified.

RNA Extraction, cDNA Synthesis, and Quantitative Real-Time PCR

The total RNA was extracted from cultured C2C12 cells using the High Pure RNA Isolation Kit (Roche, UK) according to the manufacturer’s guidelines. Subsequently, 500 ng RNA

was used to synthesise the complementary DNA (cDNA) using RevertAid First Strand cDNA Synthesis Kit (Thermo Scientific, UK) in accordance with the manufacturer's protocols. Quantitative real-time PCR (qPCR) was carried out using the SYBR-green method as outlined by Brown et al. (2012). Transcript abundances were quantified against a standard curve and normalised against a total cDNA content using the OliGreen® reagent (Life Technologies, Oregon, USA) as described by Rhinn et al. (2008) and established by Brown et al. (2012). The primer sequences were designed using the mouse reference genome (GRCm38), and their specificity was confirmed by melting curve analysis. The sequences are displayed in Table 1.

Analysis of Data

The data was analysed using Genstat for Windows 17th Edition (VSN International Ltd., UK). A one-way ANOVA was applied for lipid droplets quantification, and a two-way ANOVA for the effects of the duration of treatment and effects of the treatments (dbcAMP, des (1-3) IGF-1 or control) on the mRNA expressions. Where applicable, Bonferroni's post hoc was conducted. All data are displayed as mean ± standard error of mean (SEM), with $P < 0.05$ being considered significant.

RESULTS

Lipid Droplets Quantification

The exposure of C2C12 cells to the adipogenic conditions (incubation with adipogenic induction medium and adipogenic differentiation medium) appeared to induce adipogenic differentiation. During the treatment period, the cells were incubated in the adipogenic differentiation medium, supplemented with treatments: dbcAMP, and des (1-3) IGF-1, with an unsupplemented control. By the end of the treatment, noticeable lipid droplets were observed in all groups (Figure 1). However, the lipid droplet accumulation was significantly ($P < 0.001$) reduced in the dbcAMP- and des (1-3) IGF-1-treated cells, with higher accumulation in the control (Figure 2), suggesting that dbcAMP and des (1-3) IGF-1 significantly reduced lipid deposition in this model.

The Effects of dbcAMP and des (1-3) IGF-1 on the mRNA Expression Related to Myogenic Markers

Previously, it has been demonstrated that the C2C12 incubated in adipogenic conditions resulted in the formation of lipid droplets, while maintaining their capacity to differentiate into myotubes (Ryan et al., 2013). Likewise, the myogenic regulatory factors (MRFs) were expressed in the adipogenic condition and during the exposure to the treatments, as observed in this study. Across the 3-day treatment period, a significant ($P < 0.05$) reduction in Myf5 mRNA expression (Figure 3A, and a significant ($P < 0.01$) reduction of

Table 1
Quantitative PCR primers for mouse transcripts

Type	Target Gene	Sequence of the primer (5' to 3')
Myogenic Markers		
Myogenic Regulatory Factors	Myogenic Factor 5 (Myf5)	F: CAGCCCCACCTCCAACTG
		R: GCAGCACATGCATTTGATACATC
	Myogenic Differentiation 1 (MyoD)	F: CGTGGCAGCGAGCACTAC
		R: TGTAATCCATCATGCCATCAGA
	Myogenin	F: CCCATGGTGCCCAGTGAA
		R: GCAGATTGTGGGCGTCTGTA
Muscle Differentiation Marker	Creatine Kinase (CK)	F: GCACTGGCCGCAGCAT
		R: AGGGTAGTACTTGCCCTTGAACTC
Myofibrillar Protein Markers	Myosin Heavy Chain I (MyHCI)	F: CTCAAGCTGCTCAGCAATCTATTT
		R: GGAGCGCAAGTTTGTCATAAGT
	Myosin Heavy Chain IIa (MyHCIIa)	F: AGGCGGCTGAGGAGCACGTA
		R: GCGGCACAAGCAGCGTTGG
	Myosin Heavy Chain IIb (MyHCIIb)	F: CAATCAGGAACCTTCGGAACAC
		R: GTCCTGGCCTCTGAGAGCAT
	Myosin Heavy Chain IIx (MyHCIIx)	F: GAGGGACAGTTCATCGATAGCAA
		R: GGGCCAACTTGTCATCTCTCAT

Table 1 (*continued*)

Type	Target Gene	Sequence of the primer (5' to 3')
Lipid Turnover and Adipogenic Markers		
Lipogenic	Acetyl CoA-Carboxylase (ACC)	F: CCATTGGTATTGGGGCTTAC
		R: CCGACCAAGGACTTTGTTG
	Fatty Acid Synthase (FAS)	F: CGGAAACTTCAGGAAATGTCC
		R: TCAGAGACGTGTCACTCCTGG
Lipolytic	Adipose Triglyceride Lipase (ATGL)	F: CAACGCCACTCACATCTAC
		R GGACACCTCAATAATGTTG
	Hormone Sensitive Lipase (HSL)	F: GCGGCTGTCTAATGTCTTTGCA
		R: CCTTCATCACCCTCGAAGAAGA
Adipocyte Transcription Factors	Peroxisome Proliferator Activated Receptor γ (PPARγ)	F: GCATGGTGCCTTCGCTGA
		R: TGGCATCTCTGTGTCAACCATG
	Cluster Determinant 36 (CD/36)	F: AAACCCAGATGACGTGGC
		R: AAGATGGCTCCATTGGGC
	CCAAT/Enhancer Binding Protein Alpha (CEBPα)	F: GCCAAACTGAGACTCTTC
		R: GGAAGCCTAAGTCTTAGC
	Fatty Acid Binding Protein-4 (FABP4)	F: AAGTGGGAGTGGGCTTTGC
		R: TGGTGACCAAATCCCCATTT

Note. F, forward; R, reverse; all primers are listed 5' to 3'

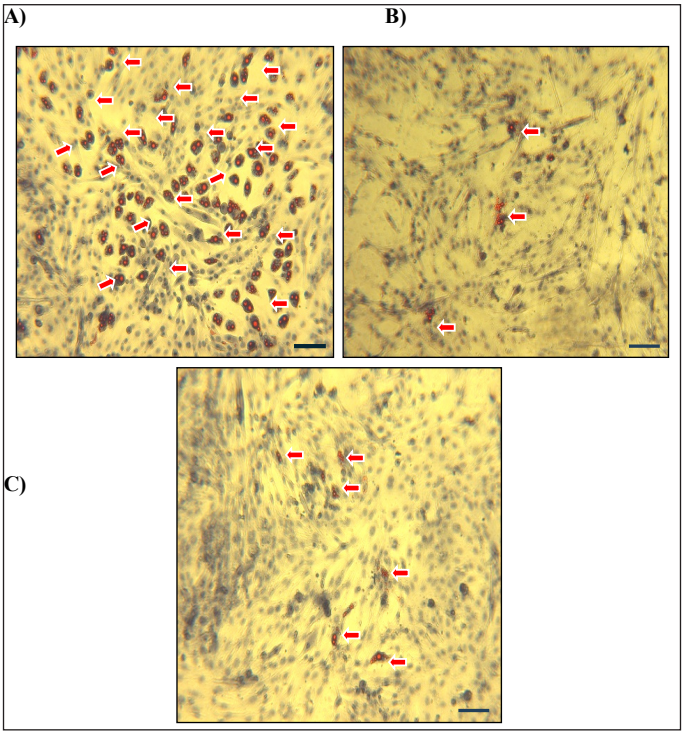

Figure 1. Effects of (A) control, (B) dbcAMP or (C) des (1-3) IGF-1 on lipid droplet accumulation (red arrows) in C2C12 muscle cells under adipogenic conditions. Scale bar = 100 µm

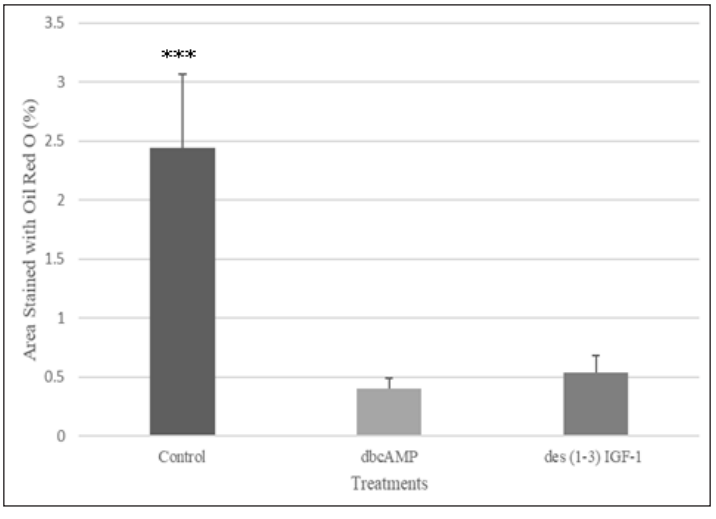

Figure 2. Effects of control, dbcAMP or des (1-3) IGF-1 on the percentage area stained with Oil Red O, with n = 3 per treatment group.
Note. Asterisks (***) indicate P <0.001 significant effect of treatment

both MyoD (Figure 3B) and Myogenin (Figure 3C) mRNA expressions were observed after 3 days of treatment, with no significant effect of treatment. In addition, no significant interaction was observed between the two factors on the mRNA expression of those MRFs.

In addition to the mRNA expression of myogenic transcription factors, C2C12 cells also showed significant creatine kinase (CK) mRNA expression, which is categorised as a myogenic differentiation marker. The cells treated with dbcAMP showed a significant ($P < 0.01$) increase in CK mRNA expression, as compared with other treatments (Figure 4). However, similar to the earlier observations on MRFs, there was no observation of any significant interaction between the two factors involved in the CK mRNA expression.

Meanwhile, the mRNA expression of all isoforms for the myosin heavy chain (MyHC), which are categorised as myofibrillar markers, was observed during treatments. The overall expression of MyHCI ($P < 0.001$) (Figure 5A), MyHCIIa ($P < 0.01$) (Figure 5B), and MyHCIIx mRNA ($P < 0.05$) (Figure 5D) were significantly reduced across the treatment

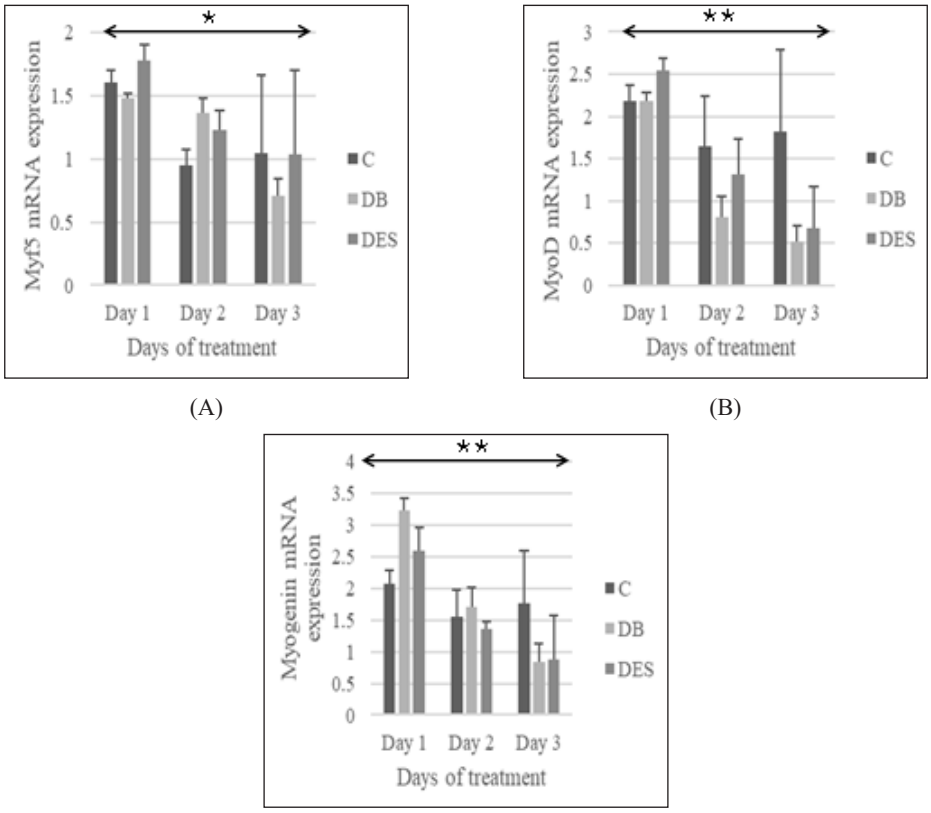

Figure 3. Effects of control (C), dbcAMP (DB) or des (1-3) IGF-1 (DES) on myogenic regulatory transcription factor mRNA expression in C2C12 muscle cells under adipogenic conditions. (A) Myf5, (B) MyoD, and (C) Myogenin mRNA, with n=3 per treatment group

Note. Asterisks (*) indicate a $P < 0.05$ or (**) indicate a $P < 0.01$ effect of days of treatment. The error bars are ± SEM

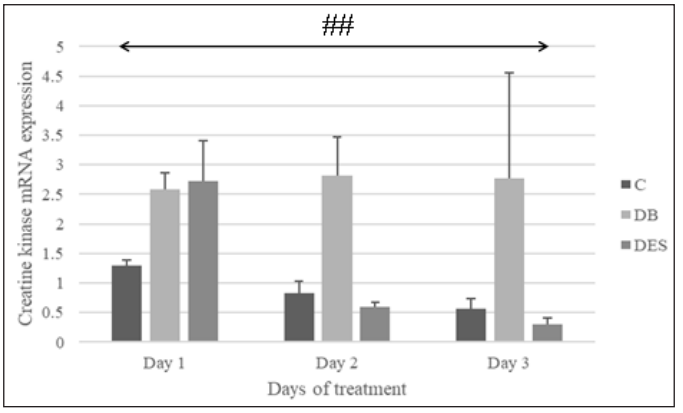

Figure 4. Effects of control (C), dbcAMP (DB) or des (1-3) IGF-1 (DES) on creatine kinase (CK) mRNA expression in C2C12 muscle cells under adipogenic conditions, with n=3 per treatment group
Note. Symbol (##) indicates a P <0.01 effect of treatment. The error bars are ± SEM

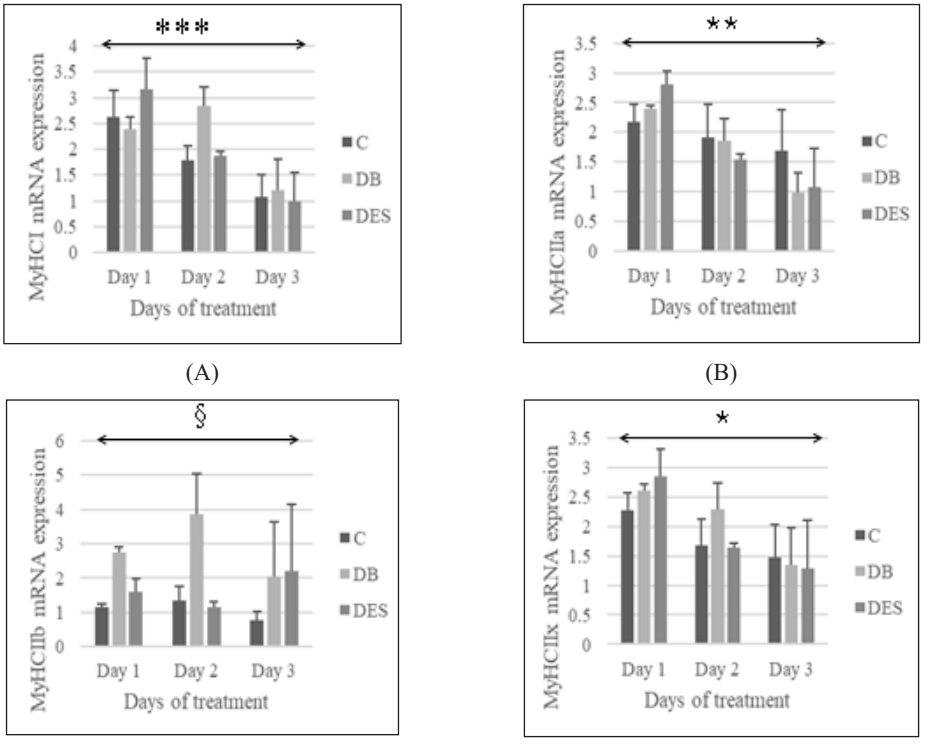

(A) (B)

(C) (D)

Figure 5. Effects of control (C), dbcAMP (DB) or des (1-3) IGF-1 (DES) on myosin heavy chain (MyHC) isoform mRNA expression in C2C12 muscle cells under adipogenic conditions. (A) MyHCI, (B) MyHCIIa, (C) MyHCIIb, and (D) MyHCIIx mRNA, with n=3 per treatment group
Note. Asterisks (*) indicate P <0.05, (**) indicate P <0.01, or (***) indicate P <0.001 for the effect of days of treatment, or (§) indicate a trend (P <0.10) for the effect of treatment. The error bars are ± SEM

period, while the expressions were not affected by the treatments. However, there was an observation of a trend toward the influence of treatment (P = 0.088), with dbcAMP tended to elevate the mRNA expression of MyHCIIb compared with other treatments (Figure 5C). Generally, neither factor signified any interaction in affecting all the mRNA expression of those myofibrillar markers.

The Effects of dbcAMP and des (1-3) IGF-1 on the mRNA Expression Related to Lipid Turnover and the Adipogenic Markers

ACC and FAS are two important lipogenic genes, while ATGL and HSL are lipolytic genes. For ACC mRNA expression, duration of treatment and the treatment had no effect on its expression (Figure 6A). In contrast, the prolonged duration of the treatment significantly (P <0.05) reduced the FAS mRNA expression, with the lowest levels being observed on day 3.

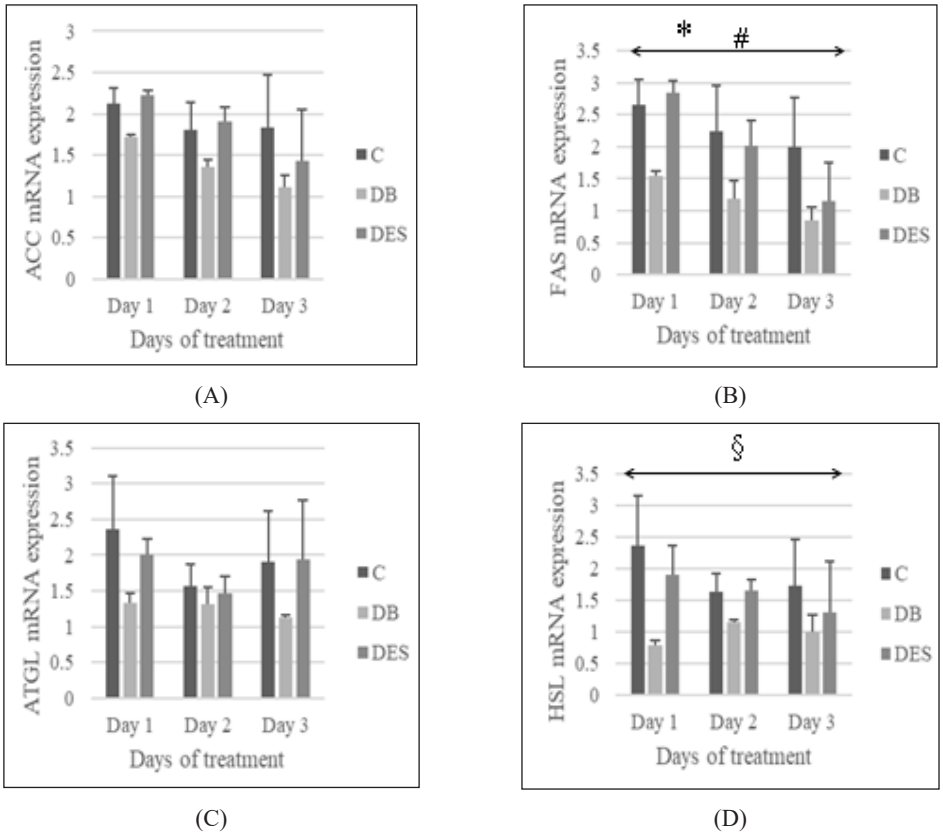

Figure 6. Effects of control (C), dbcAMP (DB) or des (1-3) IGF-1 (DES) on the lipid turnover-related mRNA expressions in C2C12 muscle cells under adipogenic conditions. (A) ACC, (B) FAS, (C) ATGL and (D) HSL mRNA, with n=3 per treatment group

Note. Symbol (§) indicate P <0.10 for the trend and (#) indicate P <0.05 for the effect of treatment, whilst (*) indicates P <0.05 for the effect of days of treatment. The error bars are ± SEM

In addition, the dbcAMP-treated cells displayed significantly lower FAS mRNA expression ($P < 0.05$) than other treatments (Figure 6B). Meanwhile, both factors had no effect on the ATGL mRNA expression (Figure 6C). However, for HSL mRNA expression, there was a trend ($P = 0.091$) for an effect of treatment, with dbcAMP-treated cells tending to have the lowest HSL mRNA expression (Figure 6D). For all lipid turnover markers, the significant interaction between both factors was not observed.

During adipogenesis, the differentiation of adipocytes is controlled by two regulators: PPARγ and CEBPα. Meanwhile, FABP4 is involved in the adipogenic activity inside the cells. The PPARγ also activates another target gene, including CD36, during preadipocyte differentiation into mature adipocytes. In the dbcAMP-treated cells, the FABP4 mRNA expression was significantly ($P < 0.05$) lower compared with other treatments (Figure 7A).

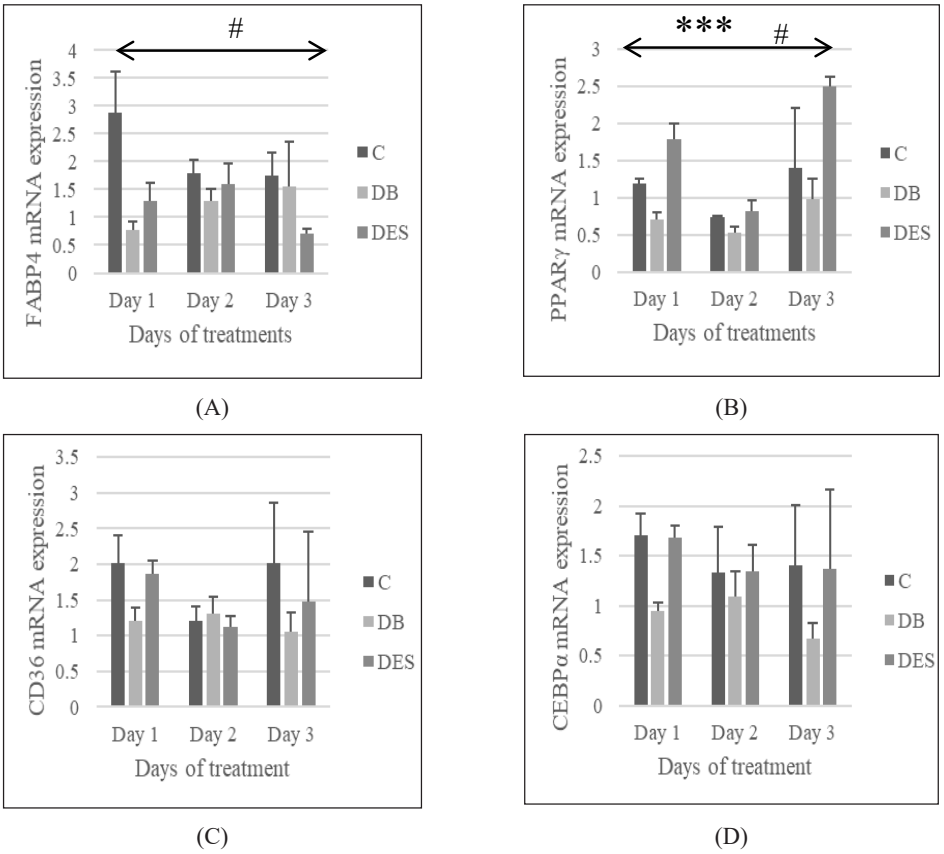

Figure 7. Effects of control (C), dbcAMP (DB) or des (1-3) IGF-1 (DES) on adipocyte differentiation transcription markers mRNA expression in C2C12 muscle cells under adipogenic conditions. (A) FABP4, (B) PPARγ, (C) CD36, and (D) CEBPα mRNA, with n = 3 per treatment group

Note. Symbol (#) indicate $P < 0.05$ for the effect of treatment, whilst (***) indicates $P < 0.001$ for the effect of days of treatment. The error bars are ± SEM

For PPARγ, the des (1-3) IGF-1 treatment led to a significantly ($P < 0.05$) higher expression compared with other treatments (Figure 7B). In addition, the PPARγ mRNA expression was significantly ($P < 0.001$) higher at day 3 (Figure 7B). Meanwhile, there were no effects of any factors, and any interactions were found for the CD36 and C/EBPα mRNA expression (Figure 7C and 7D). Moreover, no significant interaction between the duration of the treatment and the treatments in affecting the mRNA expression in all measured adipogenic markers.

DISCUSSION

This study demonstrated the influence of dbcAMP and des (1-3) IGF-1 on the expression of genes involving myogenesis and adipogenesis in C2C12 myoblast cells, with dbcAMP showing a stronger transcriptional response on both myogenic and adipogenic activities, while des (1-3) IGF-1 was mainly involved in adipogenic-associated gene expression, as summarised in Figure 8. In terms of myogenic development and regulations, dbcAMP

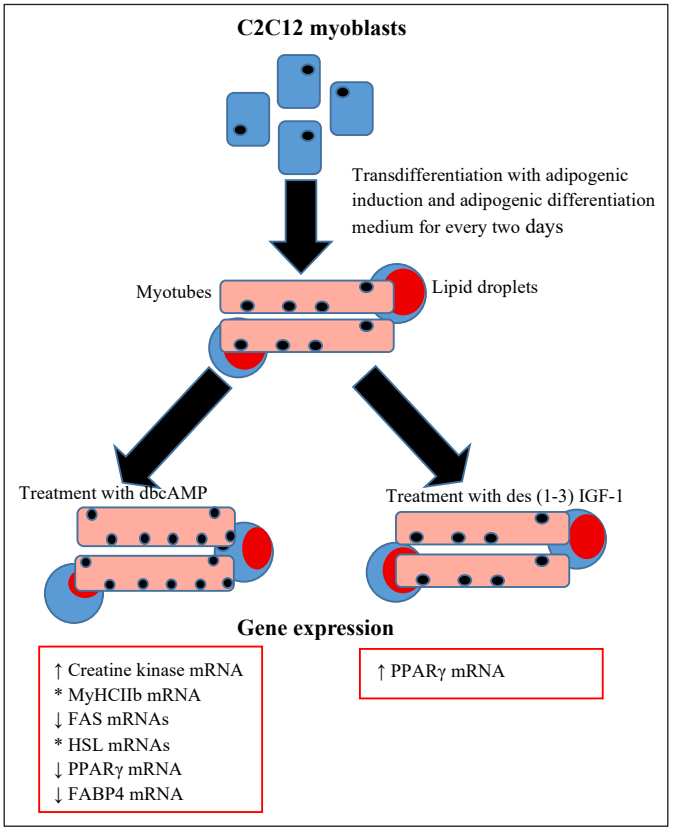

Figure 8. Schematic summary of the myogenic-related, lipogenic-related and adipogenic-related mRNA expressions upon treatment with dbcAMP and des (1-3) IGF-1 in the transdifferentiated C2C12 myoblasts
Note. The arrows adjacent to text indicate the changes in the mRNA expression; (↑) indicates an increase, (↓) indicates a decrease, and (*) indicates a trend. Other mRNA expressions were affected by a time-dependent effect

treatment increased CK mRNA expression, suggesting potential stimulation of the transcriptional pathway associated with cell differentiation. This effect was comparable to the BA treatment (clenbuterol) on neonatal rat muscle cell lines, which stimulated fusion and formation of myotubes, indicated by increased CK activity (McMillan et al., 1992). This observation implied that dbcAMP, along with other agents capable of stimulating cAMP production, such as BA, may contribute to the transcriptional regulation associated with myogenesis, supporting the role of cAMP-dependent signalling in mediating skeletal muscle hypertrophic response in vivo (Johnson et al., 2014; Lynch & Ryall, 2008).

Myf5, MyoD, Myogenin and MRF4 are several myogenic markers involved in controlling the myogenic development and regulation from progenitor cell commitment to myogenesis through to mononucleated myoblasts fusion into multinucleated myotubes, thus categorised as myogenic regulatory factors (MRFs) (Sabourin & Rudnicki, 2000; Yan et al., 2013). In this study, all MRFs mRNA expressions (except MRF4, which was not measured in this study) were increased at day 1, and reduced after 3 days of treatments, suggesting the early transcriptional response associated with myoblast differentiation to form myotubes, regardless the treatments, while adipogenic transcriptional pathway at later stage of the treatments, would supress the myogenic gene expression (Goffette et al., 2024), which are in line are with the observed creatine kinase mRNA expression which is consistent with the transcriptional changes associated with myotube differentiation as previously described.

Alterations in myofibrillar markers were also evident with dbcAMP treatment compared to other groups. Specifically, dbcAMP tended to increase MyHCIIb expression. This might be attributed to MyHCIIb being the predominant and widely distributed isoform in rodent skeletal muscle, which is also highly responsive towards experimental treatment (Harrison et al., 2011). This result also suggests that dbcAMP tended to induce the transcriptional response of fibre transition towards fast fibre characteristics, which is associated with myotube hypertrophy (Brearley et al., 2021; Brown et al., 2012; Hemmings et al., 2015). Meanwhile, MyHCI, MyHCIIa, and MyHCIIx mRNA expressions were reduced after 3 days of treatment, probably associated with the concurrent reduction in MRFs mRNA expressions, as well as the hypertrophic and contractility of the myotubes after prolonged treatment (Brown et al., 2012; Cerny & Bandman, 1986; Torgan & Daniels, 2001).

Meanwhile, in the aspect of lipid metabolism, the treatment with dbcAMP or des (1-3) IGF-1 led to a notable alteration in several lipogenic and lipolytic gene expressions, accompanied by the reduction in the lipid droplet deposition in all the treatment groups. The suppression of FAS by dbcAMP indicated reduced transcriptional activity associated with lipogenesis. In addition, the HSL expression showed a tendency to decline under dbcAMP treatment, suggesting a potential role of dbcAMP in reducing lipid turnover in the cells. Since BA action (mimics the action of dbcAMP) and mediated through cAMP-dependent protein kinase, has been reported to suppress lipogenesis of fat tissue in porcine (Peterla

& Scanes, 1990), suggesting the reduction of lipid turnover might also be associated with dbcAMP-mediated suppression of lipogenesis. This was also further supported by the marked decline of FAS mRNA expression after 3 days of treatment, whereas ATGL remained unaffected and HSL was only minimally affected, suggesting reduced lipogenic capacity after prolonged treatment.

Adipogenesis has been demonstrated to be regulated by des (1-3) IGF-1, which increased the expression of the key adipogenic gene, PPARγ. It has been reported that IGF-1 is the mediator in the GH response, thus suggesting that des (1-3) IGF-1 is one of its variants (Ballard et al., 1996). GH has been demonstrated to increase PPARγ expression in the 3T3-L1 preadipocytes via the JAK/STAT pathway (Kawai et al., 2007). In addition, the activation of PPARγ was induced by Akt signalling, which was apparently activated by IGF-1 during adipocyte differentiation as the activation was blocked by an Akt/PI3K inhibitor and knockdown of Akt1 (Kim et al., 2010). The induction of PPARγ would indicate a transcriptional response associated with adipogenic differentiation, which may be involved in the transdifferentiation of adipocyte-like cells from myoblasts and is associated with the adipocyte-like phenotype observed during C2C12 transdifferentiation. However, this effect did not align with the reduction in lipid droplets deposition, thus, it was unclear as PPARγ was reported to regulate the perilipin-1 gene (Plin1) expression, which is the essential in lipid droplets formation (Arimura et al., 2004; Dalen et al., 2004), suggesting the lipid droplets formation might be due to reduced post-translational activity of PPARγ, which was not measured in this study. This inconsistency between increased PPARγ mRNA expression and reduction in lipid droplets probably highlights the complexity of adipogenic regulation, as the mRNA abundance alone cannot reflect its protein abundance or post-translational activity PPARγ, which could be due to the altered post-transcriptional regulation, varying translational control efficiency, protein stability or degradation (Greenbaum et al., 2003). Meanwhile, according to Hu et al. (1995), ectopic expression of PPARγ did not induce the formation of lipid droplets, unless the effect was synergised with C/EBPα. The expression of C/EBPα mRNA was not significantly affected in this study, suggesting that increased PPARγ mRNA expression may not be accompanied by the transcription of C/EBPα, which may partly explain the limited accumulation of lipid droplets in the treated cells. The number of lipid droplets in des (1-3) IGF-1-treated cells was not as high as in the control cells. This may be due to deposition of lipid being more associated with the lipogenic gene, such as FAS and/or FABP4, whilst the effect of PPARγ is primarily associated with adipogenic differentiation, and these genes play slightly different roles in lipid metabolism.

In general, the adipogenic media induced the expression of FABP4 in all groups. Since FABP4 is categorised as a specific adipocyte marker due to its specific expression in adipose tissue, its downregulation following dbcAMP treatment suggested a reduction in the transcriptional program associated with adipogenesis. Jurie et al. (2007) reported

that FABP4 mRNA expression, in vivo, is closely linked to the intramuscular fat (IMF) formation, and this suggests the role of dbcAMP may influence molecular pathways associated with lipid accumulation, which was associated with a reduction in lipid droplet formation, and potentially in the mechanism of reduced IMF deposition. Another study by Okuda et al. (1989) demonstrated that p-aminophenol, a compound structurally similar to dbcAMP, promoted lipolysis in rat adipocytes, suggesting dbcAMP may modulate adipogenic and lipid metabolic pathways through cAMP-associated signalling. However, the present mRNA data in this study do not establish whether these transcriptional changes translate into increased lipolytic activity. As noted earlier, dbcAMP markedly reduced lipid turnover, and the suppression of FABP4 expression supports the hypothesis that dbcAMP, and by extension BA, enhance cAMP signalling, and may be involved in lipid accumulation and IMF deposition, although confirmation at the protein and functional levels is required.

CONCLUSION

The role of BA was demonstrated by the effect of dbcAMP in vitro, used as a cAMP analogue to modulate the mRNA expression related to myogenesis and adipogenesis in the transdifferentiated C2C12 model. The increase in myogenic mRNA expressions, including CK and MyHCIIb, suggests that cAMP-associated signalling contributes to the regulation of myogenic differentiation and fast-fibre characteristics. Meanwhile, des (1-3) IGF-1 was used to investigate the potential effects associated with GH involved in promoting the expression of genes associated with adipogenesis. Both agents appeared to modulate the expression of genes related to lipid metabolism by reducing lipogenesis and influencing lipid turnover by the changes in lipid droplet deposition, which suggested that both treatments may influence the balance between myogenic and adipogenic metabolic processes. Meanwhile, the transdifferentiation of a C2C12 mixed-cell-type (adipogenic and myogenic) culture model could be used as a tool to assess the potential effects of factors that alter muscle metabolism, thereby indicating their potential effects in muscles in vivo. However, the present study primarily determined mRNA expression, which does not establish corresponding changes in posttranslational regulation, protein abundance, and functional activity, which require further validation of those parameters. This could potentially apply in the identification of treatments that may allow the development of lean and healthy meat or understanding the mechanisms for reducing fat deposition in muscles in animals for healthy food production.

ACKNOWLEDGEMENT

The authors gratefully acknowledge the Ministry of Higher Education, Malaysia, for providing an international scholarship, and the University of Nottingham, United Kingdom, for research support and facilities to successfully conduct this study.

REFERENCES

Arimura, N., Horiba, T., Imagawa, M., Shimizu, M., & Sato, R. (2004). The peroxisome proliferator-activated receptor gamma regulates expression of the perilipin gene in adipocytes. *The Journal of Biological Chemistry, 279*(11), 10070-10076. https://doi.org/10.1074/jbc.M308522200

Ballard, F. J., Wallace, J. C., Francis, G. L., Read, L. C., & Tomas, F. M. (1996). Des(1-3)IGF-I: A truncated form of insulin-like growth factor-I. *The International Journal of Biochemistry & Cell Biology, 28*(10), 1085-1087. https://doi.org/10.1016/1357-2725(96)00056-8

Bao, Z., Lin, J., Ye, L., Zhang, Q., Chen, J., Yang, Q., & Yu, Q. (2016). Modulation of mammary gland development and milk production by growth hormone expression in GH transgenic goats. *Frontiers in Physiology, 7*, Article 278. https://doi.org/10.3389/fphys.2016.00278

Brearley, M. C., Loczenski-Brown, D. M., Loughna, P. T., Parr, T., & Brameld, J. M. (2021). Response of the porcine *MYH4*-promoter and *MYH4*-expressing myotubes to known anabolic and catabolic agents *in vitro*. *Biochemistry and Biophysics Reports, 25*, Article 100924. https://doi.org/10.1016/j.bbrep.2021.100924

Brown, D., Ryan, K., Daniel, Z., Mareko, M., Talbot, R., Moreton, J., Giles, T. C. B., Emes, R., Hodgman, C., Parr, T., & Brameld, J. M. (2018). The beta-adrenergic agonist, ractopamine, increases skeletal muscle expression of asparagine synthetase as part of an integrated stress response gene program. *Scientific Reports, 8*(1), Article 15915. https://doi.org/10.1038/s41598-018-34315-9

Brown, D. M., Parr, T., & Brameld, J. M. (2012). Myosin heavy chain mRNA isoforms are expressed in two distinct cohorts during C2C12 myogenesis. *Journal of Muscle Research and Cell Motility, 32*(6), 383-390. https://doi.org/10.1007/s10974-011-9267-4

Cerny, L. C., & Bandman, E. (1986). Contractile activity is required for the expression of neonatal myosin heavy chain in embryonic chick pectoral muscle cultures. *The Journal of Cell Biology, 103*(6 Pt 1), 2153-2161. https://doi.org/10.1083/jcb.103.6.2153

Chikani, V., & Ho, K. K. (2013). Action of GH on skeletal muscle function: Molecular and metabolic mechanisms. *Journal of Molecular Endocrinology, 52*(1), R107-R123. https://doi.org/10.1530/JME-13-0208

Dalen, K. T., Schoonjans, K., Ulven, S. M., Weedon-Fekjaer, M. S., Bentzen, T. G., Koutnikova, H., Auwerx, J., & Nebb, H. I. (2004). Adipose tissue expression of the lipid droplet-associating proteins S3-12 and perilipin is controlled by peroxisome proliferator-activated receptor-gamma. *Diabetes, 53*(5), 1243-1252. https://doi.org/10.2337/diabetes.53.5.1243

de Almeida, V. V., Nuñez, A. J. C., & Miyada, V. S. (2012). Ractopamine as a metabolic modifier feed additive for finishing pigs: A review. *Brazilian Archives of Biology and Technology, 55*(3), 445-456. https://doi.org/10.1590/S1516-89132012000300016

Dikeman, M. E. (2007). Effects of metabolic modifiers on carcass traits and meat quality. *Meat Science, 77*(1), 121-135. https://doi.org/10.1016/j.meatsci.2007.04.011

Dunshea, F. R., D'Souza, D. N., Pethick, D. W., Harper, G. S., & Warner, R. D. (2005). Effects of dietary factors and other metabolic modifiers on quality and nutritional value of meat. *Meat Science, 71*(1), 8-38. https://doi.org/10.1016/j.meatsci.2005.05.001

Dunshea, F. R., D'Souza, D. N., & Channon, H. A. (2016). Metabolic modifiers as performance-enhancing technologies for livestock production. *Animal Frontiers, 6*(4), 6-14. https://doi.org/10.2527/af.2016-0038

Gahete, M. D., Córdoba-Chacón, J., Lin, Q., Brüning, J. C., Kahn, C. R., Castaño, J. P., Christian, H., Luque, R. M., & Kineman, R. D. (2013). Insulin and IGF-I inhibit GH synthesis and release in vitro and in vivo by separate mechanisms. *Endocrinology, 154*(7), 2410-2420. https://doi.org/10.1210/en.2013-1261

Gebre, B. A., Gebretsadik, Z. T., & Anal, A. K. (2012). Effect of metabolic modifiers on meat quantity and quality. *African Journal of Food Science, 6*(11), 294-301. https://doi.org/10.5897/AJFS12.046

Goffette, V., Sabin, N., Bugeon, J., Jagot, S., Hue, I., & Gabillard, J. C. (2024). Mature adipocytes inhibit differentiation of myogenic cells but stimulate proliferation of fibro-adipogenic precursors derived from trout muscle in vitro. *Scientific Reports, 14*(1), Article 16422. https://doi.org/10.1038/s41598-024-67152-0

Greenbaum, D., Colangelo, C., Williams, K., & Gerstein, M. (2003). Comparing protein abundance and mRNA expression levels on a genomic scale. *Genome Biology, 4*(9), Article 117. https://doi.org/10.1186/gb-2003-4-9-117

Harrison, B. C., Allen, D. L., & Leinwand, L. A. (2011). IIb or not IIb? Regulation of myosin heavy chain gene expression in mice and men. *Skeletal Muscle, 1*(1), Article 5. https://doi.org/10.1186/2044-5040-1-5

Hemmings, K. M., Daniel, Z. C. T. R., Buttery, P. J., Parr, T., & Brameld, J. M. (2015). Differential effects of short-term β agonist and growth hormone treatments on expression of myosin heavy chain IIB and associated metabolic genes in sheep muscle. *Animal, 9*(2), 285-294. https://doi.org/10.1017/S175173111400233X

Hu, E., Tontonoz, P., & Spiegelman, B. M. (1995). Transdifferentiation of myoblasts by the adipogenic transcription factors PPAR gamma and C/EBP alpha. *Proceedings of the National Academy of Sciences of the United States of America, 92*(21), 9856-9860. https://doi.org/10.1073/pnas.92.21.9856

Hostrup, M., & Onslev, J. (2022). The beta2-adrenergic receptor—a re-emerging target to combat obesity and induce leanness? *The Journal of Physiology, 600*(5), 1209-1227. https://doi.org/10.1113/JP281819

Johnson, B. J., Smith, S. B., & Chung, K. Y. (2014). Historical overview of the effect of β-adrenergic agonists on beef cattle production. *Asian-Australasian Journal of Animal Sciences, 27*(5), 757-766. https://doi.org/10.5713/ajas.2012.12524

Jurie, C., Cassar-Malek, I., Bonnet, M., Leroux, C., Bauchart, D., Boulesteix, P., Pethick, D. W., & Hocquette, J. F. (2007). Adipocyte fatty acid-binding protein and mitochondrial enzyme activities in muscles as relevant indicators of marbling in cattle. *Journal of Animal Science, 85*(10), 2660-2669. https://doi.org/10.2527/jas.2006-837

Kawai, M., Namba, N., Mushiake, S., Etani, Y., Nishimura, R., Makishima, M., & Ozono, K. (2007). Growth hormone stimulates adipogenesis of 3T3-L1 cells through activation of the Stat5A/5B-PPARgamma pathway. *Journal of Molecular Endocrinology, 38*(1-2), 19-34. https://doi.org/10.1677/jme.1.02154

Kim, S. P., Ha, J. M., Yun, S. J., Kim, E. K., Chung, S. W., Hong, K. W., Kim, C. D., & Bae, S. S. (2010). Transcriptional activation of peroxisome proliferator-activated receptor-gamma requires activation of both protein kinase A and Akt during adipocyte differentiation. *Biochemical and Biophysical Research Communications, 399*(1), 55-59. https://doi.org/10.1016/j.bbrc.2010.07.038

Ladeira, M. M., Schoonmaker, J. P., Gionbelli, M. P., Dias, J. C., Gionbelli, T. R., Carvalho, J. R., & Teixeira, P. D. (2016). Nutrigenomics and beef quality: A review about lipogenesis. *International Journal of Molecular Sciences, 17*(6), Article 918. https://doi.org/10.3390/ijms17060918

Lynch, G. S., & Ryall, J. G. (2008). Role of beta-adrenoceptor signaling in skeletal muscle: Implications for muscle wasting and disease. *Physiological Reviews, 88*(2), 729-767. https://doi.org/10.1152/physrev.00028.2007

McMillan, D. N., Noble, B. S., & Maltin, C. A. (1992). The effect of the β-adrenergic agonist clenbuterol on growth and protein metabolism in rat muscle cell cultures. *Journal of Animal Science, 70*(10), 3014-3023. https://doi.org/10.2527/1992.70103014x

Milioto, C., Malena, A., Maino, E., Polanco, M. J., Marchioretti, C., Borgia, D., Pereira, M. G., Blaauw, B., Lieberman, A. P., Venturini, R., Plebani, M., Sambataro, F., Vergani, L., Pegoraro, E., Sorarù, G., & Pennuto, M. (2017). Beta-agonist stimulation ameliorates the phenotype of spinal and bulbar muscular atrophy mice and patient-derived myotubes. *Scientific Reports, 7*, Article 41046. https://doi.org/10.1038/srep41046

Mersmann, H. J. (2002). β-Adrenergic receptor modulation of adipocyte metabolism and growth. *Journal of Animal Science, 80*(Suppl. 1), E24-E29. https://doi.org/10.2527/animalsci2002.0021881200800ES10005x

Okuda, H., Sekiya, K., & Nakamura, H. (1989). Lipolytic activities of p-aminophenol and n-decylamine in endogenous lipid droplets from rat adipocytes. *Pharmacological Research, 21*(3), 255-262. https://doi.org/10.1016/S1043-6618(89)80003-9

Peterla, T. A., & Scanes, C. G. (1990). Effect of β-adrenergic agonists on lipolysis and lipogenesis by porcine adipose tissue in vitro. *Journal of Animal Science, 68*(4), 1024-1029. https://doi.org/10.2527/1990.6841024x

Pfau, A. P., Henniger, M. T., Samuelson, K. L., Hales, K. E., Löest, C. A., Hubbert, M. E., Lindholm-Perry, A. K., Egert-McLean, A. M., Mason, K. M., Shepherd, E. A., Voy, B. H., & Myer, P. R. (2024). Effects of protein concentration and beta-adrenergic agonists on ruminal bacterial communities in finishing beef heifers. *PLOS ONE, 19*(2), Article e0296407. https://doi.org/10.1371/journal.pone.0296407

Pfau, A. P., Shepherd, E. A., Martin, M. G., Ascolese, S., Mason, K. M., Egert-McLean, A. M., Voy, B. H., & Myer, P. R. (2023). Beta-adrenergic agonists, dietary protein, and rumen bacterial community interactions in beef cattle: A review. *Veterinary Sciences, 10*(9), Article 579. https://doi.org/10.3390/vetsci10090579

Rhinn, H., Scherman, D., & Escriou, V. (2008). One-step quantification of single-stranded DNA in the presence of RNA using Oligreen in a real-time polymerase chain reaction thermocycler. *Analytical Biochemistry, 372*(1), 116-118. https://doi.org/10.1016/j.ab.2007.08.023

Ryan, K. J., Daniel, Z. C., Craggs, L. J., Parr, T., & Brameld, J. M. (2013). Dose-dependent effects of vitamin D on transdifferentiation of skeletal muscle cells to adipose cells. *The Journal of Endocrinology, 217*(1), 45-58. https://doi.org/10.1530/JOE-12-0234

Sabourin, L. A., & Rudnicki, M. A. (2000). The molecular regulation of myogenesis. *Clinical Genetics, 57*(1), 16-25. https://doi.org/10.1034/j.1399-0004.2000.570103.x

Torgan, C. E., & Daniels, M. P. (2001). Regulation of myosin heavy chain expression during rat skeletal muscle development in vitro. *Molecular Biology of the Cell, 12*(5), 1499-1508. https://doi.org/10.1091/mbc.12.5.1499

Warriss, P. D., Kestin, S. C., Rolph, T. P., & Brown, S. N. (1990). The effects of the beta-adrenergic agonist salbutamol on meat quality in pigs. *Journal of Animal Science, 68*(1), 128-136. https://doi.org/10.2527/1990.681128x

Yan, X., Zhu, M. J., Dodson, M. V., & Du, M. (2013). Developmental programming of fetal skeletal muscle and adipose tissue development. *Journal of Genomics, 1*, 29-38. https://doi.org/10.7150/jgen.3930

Yamamoto, M., & Bando, H. (2023). A new insight into GH regulation and its disturbance from nutrition and autoimmune perspectives. *Endocrine Journal, 70*(9), 867-874. https://doi.org/10.1507/endocrj.EJ23-0264

Pertanika J. Trop. Agric. Sci. 49 (5): 2217 - 2236 (2026)

PERTANIKA JOURNALS

TROPICAL AGRICULTURAL SCIENCE

Journal homepage: http://www.pertanika.upm.edu.my/

Gallic Acid-Loaded Graphene Oxide (GAGO) Nanocomposite Attenuates Inflammatory Response in LPS-Stimulated RAW 264.7 Macrophages

Nur Hazwani Norjoshukrudin[1], Ida May Jen Ng[1], Seri Narti Edayu Sarchio[2], Masriana Hassan[3], Shafinaz Abd Gani[1], and Suhaili Shamsi[1,4]*

[1]Animal Biochemistry and Biotechnology Laboratory, Department of Biochemistry, Faculty of Biotechnology and Biomolecular Sciences, Universiti Putra Malaysia, 43400 Serdang, Selangor, Malaysia
[2]Department of Biomedical Science, Faculty of Medicine and Health Sciences, Universiti Putra Malaysia, 43400 Serdang, Selangor, Malaysia
[3]Department of Pathology, Faculty of Medicine and Health Sciences, Universiti Putra Malaysia, 43400 Serdang, Selangor, Malaysia
[4]Natural Medicine and Product Research Laboratory, Institute of Bioscience, Universiti Putra Malaysia, 43400 Serdang, Malaysia

ABSTRACT

Reckless use of non-steroidal anti-inflammatory drugs (NSAIDs) has contributed to adverse health effects. In the present study, a gallic acid-loaded graphene oxide (GAGO) nanocomposite was synthesised, and its cytotoxicity and anti-inflammatory properties were evaluated in vitro. GAGO was first synthesised and characterised using FTIR, FESEM, and zeta potential analyses. The gallic acid (GA) loading efficiency of GAGO was quantified, while stability was monitored following 90 days of storage at room temperature. NIH-3T3 fibroblast and RAW 264.7 macrophage cells were employed to evaluate the cytotoxicity of GAGO in vitro. Finally, the anti-inflammatory properties were assessed by measuring nitric oxide (NO) and pro-inflammatory cytokine levels, namely IL-6, TNF-α, and MCP-1, in LPS-induced RAW264.7 macrophages. GA was successfully loaded into GAGO at a loading efficiency of 51.07% ± 7.27% and remained stable upon storage for 90 days. GAGO exhibited a significantly improved in vitro cytotoxicity compared to GA, with LC50 values of 28.95 ± 6.674 µg/mL in NIH-3T3 cells, and 60.23 ± 0.168 µg/mL in RAW 264.7 cells at 72 h. GA significantly increased NO production at higher concentrations (≥30 µg/mL), indicating

ARTICLE INFO

Article history:
Received: 21 October 2025
Accepted: 25 September 2026
Published: 30 October 2026

DOI: https://doi.org/10.47836/pjtas.49.5.06

E-mail addresses:
nurhazwaninorjo@gmail.com (Nur Hazwani Norjoshukrudin)
idangmj@gmail.com (Ida May Jen Ng)
serinarti@upm.edu.my (Seri Narti Edayu Sarchio)
masriana@upm.edu.my (Masriana Hassan)
shafinaz_abgani@upm.edu.my (Shafinaz Abd Gani)
sh_suhaili@upm.edu.my (Suhaili Shamsi)
* Corresponding author

© Universiti Putra Malaysia Press

a potential pro-oxidant effect. In contrast, GAGO significantly suppressed the NO level at a low concentration (5 μg/mL), while no significant increase was observed at higher concentrations compared to the LPS-induced control. Furthermore, GAGO reduced IL-6 (45-60 μg/mL), TNF-α (≥15 μg/mL) and MCP-1 (≥10 μg/mL) levels, comparable to GA. The present study highlights the potential of GAGO nanocomposite to attenuate inflammation, but further mechanistic and in vivo investigations are warranted.

Keywords: GAGO, Gallic acid, graphene oxide, inflammation, nanoformulation

INTRODUCTION

Inflammation, the body's first initial response to injury or infection, is often mitigated by the administration of non-steroidal anti-inflammatory drugs (NSAIDs) (Gunaydin & Bilge, 2018). However, excessive and prolonged use of NSAIDs has contributed to serious adverse effects, which include gastrointestinal disorders like peptic ulcers (Tai & McAlindon, 2021), chronic kidney disease (CKD) (Drożdżal et al., 2021), and hepatotoxicity (Sriuttha et al., 2018). NSAIDs could also compromise the immune system, making it more susceptible to infection, which accelerates the emergence of antibiotic-resistant organisms (Chen et al., 2021; Li et al., 2023b).

In recent years, various studies have focused on identifying alternative treatments for inflammation, which is typically treated with NSAIDs. Phenolic compounds have garnered interest as potential alternatives to conventional NSAIDs due to their non-toxic nature and therapeutic potential in modulating various signalling pathways and stimulating various mechanisms of action (Arip et al., 2022; Sohrabi et al., 2021; Srivastava et al., 2014; Wang et al., 2020). A naturally derived phenolic compound, namely gallic acid (GA), has attracted the attention of many researchers for its ability to exhibit myriad pharmacological activities. This simple phenolic compound has demonstrated antioxidant (Jiang et al., 2024), anti-cancer (Ashrafizadeh et al., 2021), anti-microbial (Shamsi et al., 2018; Shamsi et al., 2022), and anti-inflammatory (Li et al., 2023a) activities in various in vitro and in vivo models (Reckziegel et al., 2016). Nevertheless, like many other naturally derived phenolic compounds, GA undergoes rapid degradation (Chikere et al., 2020) and is deemed unstable at pH above 7 and at high temperatures (Pasquet et al., 2024). GA is rapidly metabolised (Zhang et al., 2020), and, when combined with poor absorption, this results in low bioavailability and immediate clearance of GA following in vivo administration (Bai et al., 2021; Mao et al., 2016).

Numerous studies have then shifted their focus to improving the physicochemical properties of GA, including the use of nanoparticles as a delivery platform for GA. Nanoparticles have been shown to enhance bioavailability, improve stability, and enable targeted, controlled-release delivery (Díez-Pascual, 2021; Petrovic et al., 2024).

Nanoparticles have also been shown to possess prominent anti-inflammatory properties, through modulation of inflammatory mediators involved in inflammation, including nitric oxide (NO) and key pro-inflammatory cytokines, such as interleukin-6 (IL-6), tumour necrosis factor-α (TNF-α), and monocyte chemoattractant protein-1 (MCP-1) (Mi et al., 2022). One prominent example is curcumin-loaded nanoparticle systems that have been reported to suppress NO production and reduce the secretion of pro-inflammatory cytokines, including IL-6 and TNF-α, in activated macrophages through inhibition of nuclear factor-κB (NF-κB) signalling pathways (Chopra et al., 2021; Laurindo et al., 2023). Similarly, resveratrol-loaded nanocarriers have demonstrated significant inhibition of inflammatory mediators, including TNF-α and NO, by modulating inflammatory transcription factors (Grabarczyk et al., 2024; Siu et al., 2018). In addition, quercetin-encapsulated nanoparticles have been shown to attenuate inflammatory responses via sustained inhibition of the PI3K/Akt pathway (Lou et al., 2016). Collectively, these findings highlight the potential of nanoparticle-based delivery systems to enhance the therapeutic potential of bioactive compounds, including GA, for the management of inflammatory conditions, although their safety and efficacy require further investigation.

A nanocomposite formulation developed in our laboratory, GA-loaded graphene oxide (GAGO) nanocomposite, has previously demonstrated a significant anti-bacterial effect, as well as wound healing properties with an improved toxicity profile, making it a potential candidate for therapeutic applications (Azhari, 2023; Shamsi et al., 2018; 2020). GAGO exhibited improved toxicity profile compared to native GA and graphene oxide (GO) (Ghafor et al., 2020). Further research by Shamsi et al. (2022) investigated the antibacterial properties of GAGO against community and hospital-acquired methicillin-resistant Staphylococcus aureus (MRSA). They found that during the first two hours of bacterial exposure, the effectiveness of GAGO was comparable to that of GA and GO alone. At concentrations of ≥150 μg/mL, GAGO demonstrated antibacterial activity comparable to the conventional antibiotic, cefoxitin.

Bacterial infections and chronic wounds can lead to elevated inflammation; the next logical step in developing GAGO for clinical settings is to explore its anti-inflammatory potential. The present study endeavours to explore GAGO's potential to exert anti-inflammatory effects in an in vitro cell model using the established RAW 264.7 macrophage cell line induced with bacterial lipopolysaccharide (LPS). This study hopes to provide a potential alternative to NSAIDs with a view to developing GAGO nanocomposite as a multifunctional therapeutic with anti-inflammatory properties.

MATERIALS AND METHODS

Materials

All experiments performed in the present study utilised analytical grade chemicals and reagents. Graphite (Gr) powder procured from Fluka Chemical (Buchs, Switzerland)

was used as the starting material for GO synthesis. GA, sodium hydroxide (NaOH), hydrochloric acid (HCl), potassium permanganate ($KMnO_4$), phosphoric acid (H_3PO_4), sulphuric acid (H_2SO_4), diethyl ether, sodium dodecyl sulphate (SDS), sulphanilamide, N-1-naphthyl-ethylenediamine hydrochloride (NED), 3-[4,5-dimethylthiazol-2-yl]-2,5 diphenyl tetrazolium bromide (MTT) reagent, and phosphate buffered saline (PBS) were purchased from Sigma-Aldrich (Missouri, USA). Dulbecco's Modified Eagle's medium (DMEM) purchased from Nacalai Tesque (Kyoto, Japan) was supplemented with fetal bovine serum (FBS) from Tico Europe (South Holland, Netherlands) for cell culture maintenance. Penicillin, streptomycin, and trypsin-EDTA were obtained from Nacalai Tesque (Kyoto, Japan).

Synthesis and Characterisation of GAGO Nanocomposite

GO was accordingly synthesised using an Improved Hummer's method (Marcano, 2010). GAGO synthesis was conducted according to our previously developed method (Shamsi et al., 2018). GA and GO were mixed at a weight ratio of 5:1 in distilled water and stirred overnight. This was followed by centrifugation for 15 min at 4000 rpm. The mixture was washed three times successively with distilled water and subsequently dried at 40 °C (Memmert GmbH + Co.KG, Schwabach, Germany). For morphological observation of GO and GAGO, field-emission scanning electron microscopy (FESEM) equipped with energy-dispersive X-ray spectroscopy (EDX) for elemental analysis was employed. Presence of functional groups in GO and GAGO was monitored under Fourier-transform infrared spectroscopy (FTIR) (Shimadzu, Tokyo, Japan), alongside Gr and GA that served as controls. Dynamic light scattering (DLS) (Malvern Instruments, Worcestershire, United Kingdom) was utilised to measure the zeta potential of GO and GAGO nanocomposite. A previously developed method was used to quantify GA loading in the synthesised GAGO nanocomposite (Shamsi et al., 2022). Storage stability of the GAGO nanocomposite was monitored for 90 days at room temperature by evaluating the zeta potential and GA loading at specific time intervals (0, 7, 14, 21, 28, 60, and 90 days).

Cell Culture

NIH-3T3 fibroblast cells and RAW 264.7 macrophage cells obtained from the American Type Culture Collection (ATCC) were maintained in DMEM supplemented with 10% FBS and 1% penicillin-streptomycin. Cells were cultured at 37 °C in a humidified incubator (90% humidity) with a continuous supply of 5% CO2 (Nuaire, Minnesota, USA).

In Vitro Cytotoxicity Assay

A cytotoxicity study was conducted on both NIH-3T3 fibroblasts and RAW 264.7 macrophages using the MTT assay. Cells were seeded onto 96-well plates (NIH-3T3 cells

at 4×10^5 cells/mL and RAW 264.7 cells at 1.25×10^5 cells/mL) in 200 µL of supplemented DMEM. Upon confluency, cells were washed once with pre-warmed basal DMEM, followed by incubation with respective samples at concentrations of 0-1000 µg/mL (GO, GA and GAGO). Cells exposed to 0.1% w/v SDS served as the positive control, while cells exposed only to culture medium served as the negative control. Cells were treated with samples for 24 to 72 h, with fresh samples replenished at 24 h intervals. At the end of the incubation time, cells were then incubated with MTT reagent at 0.5 mg/mL for 4 h. The purple formazan crystal formed following incubation with MTT reagent was solubilised with DMSO (100 µL), and the absorbance values were recorded at 570 nm using a multiplate spectrophotometer (Multiskan FC, Thermo Fisher Scientific, Massachusetts, USA). The LC_{50} values for all samples were determined accordingly (Seisenbaeva et al., 2021).

LPS Stimulation in RAW 264.7 cells

Cells were seeded at a density of 1×10^5 cells/mL in phenol red-free DMEM containing only 2% FBS in a 24-well plate. Cells were induced with LPS from *Escherichia coli* 0111: B4 (ENZO Life Sciences, USA) at 1 µg/mL for 2 h (Zailan et al., 2020). The cells were then treated for 24 h with 0-60 µg/mL of the respective samples (GO, GA, or GAGO). Upon reaching 24 h of treatment, 500 µL of the cell supernatant was retrieved and stored in a -80 °C freezer until further use for Griess and cytometric beads array (CBA) assays.

Griess Assay

Cell supernatant (50 µL) was transferred into a 96-well plate, with the addition of 50 µL of Griess reagent containing 1% sulphanilamide and 0.1% N-1-naphthyl-ethylenediamine hydrochloride prepared with 2.5% of phosphoric acid. The absorbance value was recorded after 15 min incubation in the dark at 540 nm (Zailan et al., 2020). The level of NO in the cell supernatant was determined using a standard curve ($y = 0.0038x-0.0019$, $R^2 = 0.9986$) of sodium nitrate solution prepared at different concentrations (0-20 µM).

Determination of Cytokine Level using the Cytometric Beads Array (CBA) Assay

The levels of IL-6, TNF-α, and MCP-1 in LPS-induced RAW 264.7 cells were measured following treatment with GO, GA or GAGO (0-60 µg/mL) using the CBA assay. CBA assay was conducted according to the guidelines provided by the manufacturer (BD™ CBA Mouse Inflammation Kit from BD Biosciences, California, USA). Supernatant containing cells was added to 50 µL of mixed capture beads and phycoerythrin (PE) detection reagent and incubated in the dark for 2 h. Wash buffer was added, and the mixture was centrifuged for 5 min at 200 × g to obtain the pellet. Following this, cytokine levels were measured using

a flow cytometer (BD FACSCanto, BD Biosciences, USA). Results were generated and analysed using the FCAP Array™ Software (BD Biosciences, USA) (Zailan et al., 2020).

Statistical Analysis

All data ($n \geq 3$) are presented as mean ± standard deviation (SD). Data were statistically analysed by employing a One-Way or Two-Way Analysis of Variance (ANOVA) with Tukey's post hoc, unless otherwise stated (GraphPad Prism Version 9.0, GraphPad Software, California, USA). A p-value of ≤ 0.05 is considered statistically significant.

RESULTS

Synthesis and Characterisation of GAGO Nanocomposite

In Figure 1A, the black fine powder of GO was obtained, while the GAGO nanocomposite appears as a thin black film upon drying overnight at 40°C (Figure 1B). All samples were characterised by FTIR to determine the presence of functional groups (Figure 1C). Gr and GA analyses were also conducted as a control. According to Figure 1C, all black arrows represent new peaks that correspond to the characteristic peaks of GA, which are present in the GAGO nanocomposite. The first characteristic peak for GAGO was observed at 1375 cm^{-1}, which corresponds to the O-H plane bending functional group in GA. The second characteristic peak for GAGO occurs at 1444 cm^{-1}, which corresponds to the aromatic ring C=C stretching functional group in GA. The third characteristic peak for GAGO was at 3769 cm^{-1}, and this corresponds to the characteristic peak of the benzene ring O-H stretching of GA. Collectively, the FTIR spectrum of GAGO nanocomposite displays characteristic peaks of functional groups present in GO and GA, respectively, indicating successful loading of GA onto GO to form the GAGO nanocomposite. FESEM observations were conducted to assess differences in the morphology of GAGO compared with GO. Based on Figure 1D, it was revealed that GO appears as a wrinkled thin film, while GAGO appears thicker and denser, with an apparent crystalline structure, indicating the presence of GA (Figure 1E), which aligns with a previous study from our laboratory (Shamsi et al., 2022).

Figure 2A-2D presents the EDX spectra of all samples, including Gr and GA as controls, together with their corresponding FESEM micrographs. The EDX spectrum of Gr was dominated by carbon (C), with a minor oxygen (O) signal and low-intensity peaks corresponding to Fe, Mg, Si and Ca. These additional elemental signals may be attributed to trace mineral impurities associated with the Gr precursor. Previous studies have reported the presence of mineral inclusions containing Fe, Mg, Si and Ca in natural Gr, including silicate and carbonate minerals such as pyroxene, quartz, calcite and dolomite (Kumara et al., 2021). The low intensities of these signals suggest that these elements are minor constituents of the analysed Gr rather than its predominant components.

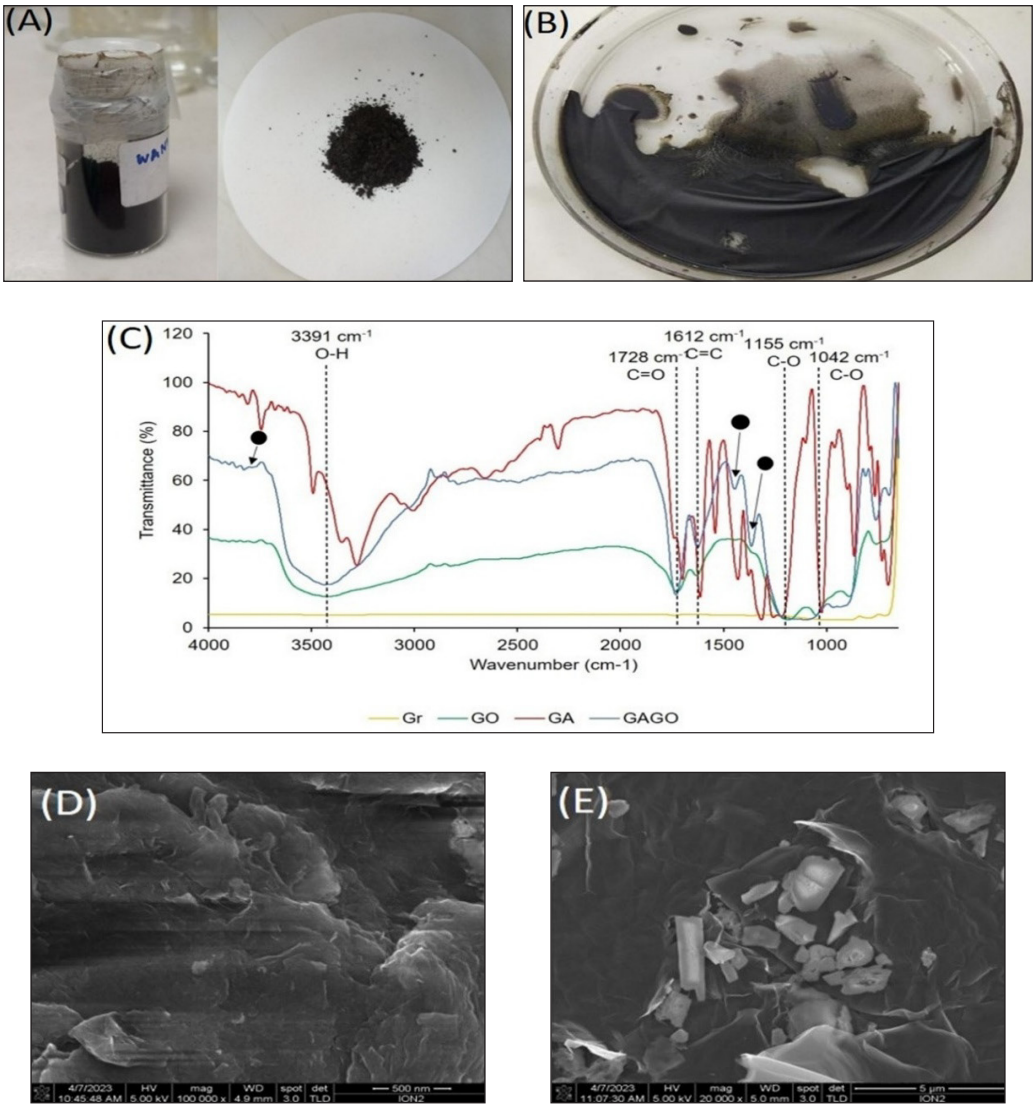

Figure 1. Characterisation of GO and GAGO nanocomposite. (A) GO powder obtained via a modified Hummer's method, (B) GAGO nanocomposite thin film prepared at a 1:5 w/w ratio of GA to GO, (C) FTIR spectra of GAGO, GO, GA, and Gr

Note. Black spots indicate characteristic peaks in the GAGO spectrum corresponding to GA. (D) FESEM micrograph of GO with a scale bar of 500 nm, and (E) FESEM micrograph of GAGO with a scale bar of 5 µm

As presented in Table 1, the C content of Gr was higher than that of GO (41.36%) and GAGO (49.90%), whereas the O content increased substantially from 6.51% in Gr to 47.09% in GO and 41.95% in GAGO. The reduction in the relative C content and the corresponding increase in O content following oxidation are consistent with the introduction of oxygen-containing functional groups during GO synthesis. These functional groups include hydroxyl, epoxy, carbonyl and carboxyl groups, which contribute to the oxygen-rich

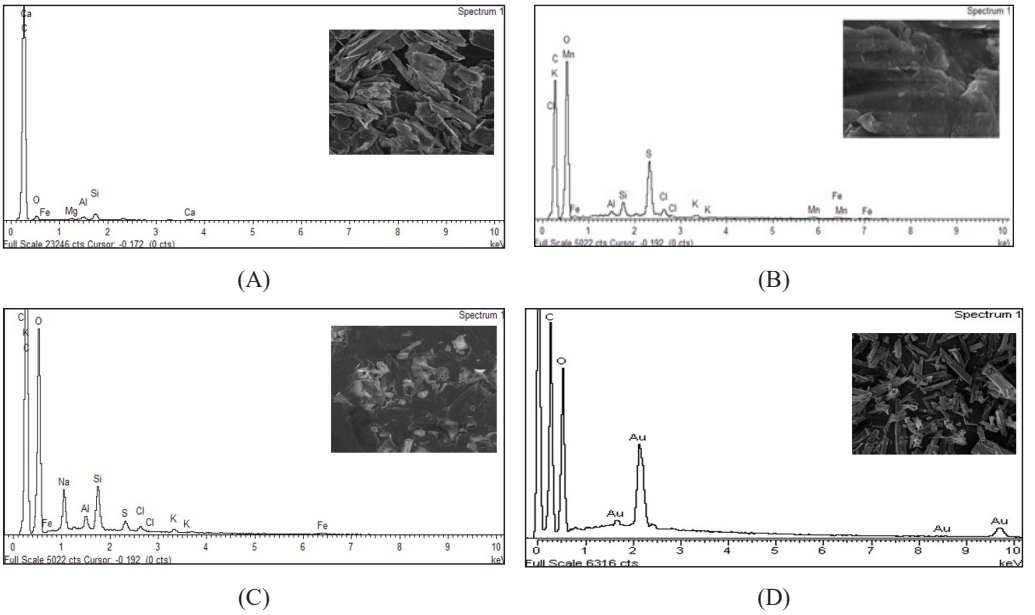

Figure 2. EDX spectra with corresponding FESEM micrographs (insets) of (A) Gr, (B) GO, (C) GAGO, and (D) GA. Prominent carbon (C) and oxygen (O) peaks are observed in GO and GAGO, confirming successful oxidation of Gr and the presence of oxygen-containing functional groups. GAGO exhibits higher C content than GO. Minor peaks corresponding to S, Cl, Mn, and other residual elements originate from the oxidation process during GO synthesis. The Au peaks observed in selected spectra are attributed to gold sputter coating during FESEM sample preparation

Table 1
Elemental analysis of Gr, GO, GAGO, and GA according to EDX

Element Weight (%)	Gr	GO	GAGO	GA
C	90.71	41.36	49.90	44.15
O	6.51	47.09	41.95	53.16
S	-	6.86	0.79	-
Cl	-	1.11	0.42	-
Al	0.50	0.36	0.71	-
Si	1.28	1.19	2.54	-
K	-	0.37	0.38	-
Mn	-	0.75	-	-
Fe	0.50	0.90	0.58	-
Ca	0.29	-	-	-
Mg	0.22	-	-	-
Na	-	-	2.73	-

Note. Trace elements detected in the samples, including S, Cl, Si, K, Mn, Fe, Ca, Mg, and Na, may have originated from the synthesis and sample preparation processes or from the reagents and materials used. These elements were not considered part of the intended elemental composition

composition of GO. Following GA loading, GAGO exhibited an increase in relative C content from 41.36% in GO to 49.90%, accompanied by a decrease in O content from 47.09% to 41.95%. These changes are consistent with the incorporation of GA, which contains both C and O, into the GO matrix. The higher relative C content of GAGO may be associated with the contribution of C from the loaded GA.

In addition to C and O, the EDX spectra of GO and GAGO revealed minor signals corresponding to Si, S, Cl and K. The presence of these elements may be associated with residual inorganic species originating from the Gr precursor, as well as the GO synthesis and purification processes. Specifically, S (6.86% in GO and 0.79% in GAGO) may be associated with residual sulphate-containing species from the use of H_2SO_4, while K may originate from $KMnO_4$, used as the oxidising agent during GO synthesis. Similarly, Cl (1.11% in GO and 0.42% in GAGO) may be associated with residual chloride-containing compounds when HCl was used during synthesis. The detection of Si may reflect mineral impurities inherited from the Gr precursor. The persistence of these elements in GAGO suggests that some of the minor elemental constituents detected in GO were retained following GA loading. In contrast, the EDX spectrum of GA exhibited only C and O signals, consistent with its expected elemental composition and supporting its high apparent elemental purity.

The additional Al and Au signals detected in the EDX spectra are attributed to the materials used during FESEM sample preparation. Specifically, the Al signal may originate from the aluminium stub used to mount the samples, particularly where the sample coating does not completely cover the underlying substrate. The Au signals observed in selected spectra are associated with the gold sputter coating applied to improve electrical conductivity and minimise charging during FESEM imaging. Therefore, these signals are considered preparation-related contributions rather than intrinsic elemental constituents of the analysed samples.

GA has been successfully loaded at 0.425 ± 0.06 g of GAGO, with a loading efficiency of 51.07% ± 7.27%. Additionally, the batch-to-batch consistency in terms of the yield and GA loading was confirmed in more than 3 batches ($n \geq 3$) of the synthesised GAGO nanocomposite. The stability of the GAGO nanocomposite during storage was monitored for GA loading and zeta potential under the following conditions: at room temperature in a sealed glass bottle, away from moisture and light. Figure 3A shows that no significant reduction in GA loading was observed until D90 ($p \leq 0.05$), despite a 68.50% ± 12.93% reduction. In addition to this, GAGO has also exhibited no significant reduction in the zeta potential after 90 days of storage ($p \leq 0.05$) (Figure 3B). Prolonged storage stability study, ideally up to 12 months, should be conducted to evaluate the suitable shelf life for the nanocomposite produced, prior to GAGO being introduced in the clinical settings.

Cytotoxicity of GA, GO, and GAGO in NIH-3T3 and RAW 264.7 cells

The LC_{50} values following treatment of NIH-3T3 and RAW 264.7 cells with samples of GO, GA, and GAGO were determined, as shown in Figure 4A and 4B, respectively. GA demonstrated lower LC_{50} values than GO and GAGO at all incubation times. GA displayed a higher toxicity in both cell lines, causing a 50% reduction in cell viability at 38.26 ± 8.549 µg/mL (Figure 4A) and 73.98 ± 0.146 µg/mL (Figure 4B) at 24 h. Based on Figure 4A, GAGO displayed higher LC_{50} values than GA at all incubation times, decreasing from 245.30 ± 9.867 µg/mL at 24 h, 78.91 ± 9.172 µg/mL at 48 h, and 28.95 ± 6.674 µg/mL at 72 h. Similarly, in RAW 264.7 macrophage cells (Figure 4B), GAGO demonstrated higher LC_{50} values compared to GA, reducing from 387.00 ± 0.189 µg/mL at 24 h, 71.75 ± 0.149 µg/mL at 48 h, and 60.23 ± 0.168 µg/mL at 72 h.

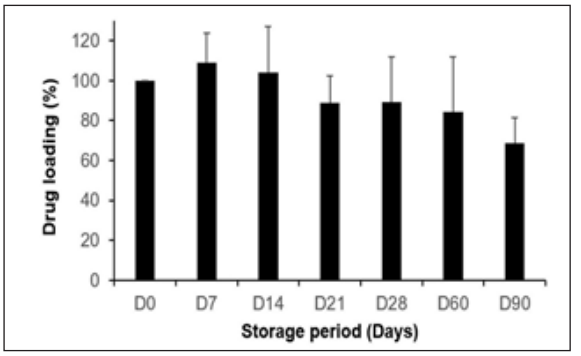

(A)

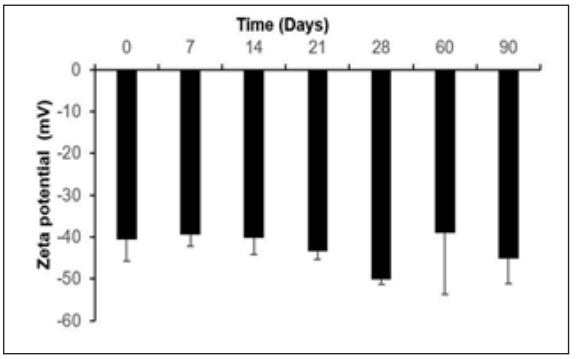

(B)

Figure 3. Storage stability of GAGO. (A) Drug loading (%) and (B) zeta potential values of GAGO after storage for 90 days ($n \geq 3$ different batches). No significant difference was observed in drug loading (GA) and zeta potential values at all storage periods compared to D0 ($p \leq 0.05$)

NO Level in LPS-induced RAW 264.7 Cells

Figure 5 illustrates the levels of NO produced in RAW 264.7 cells induced with 1 µg/mL of LPS, following treatment for 24 h with GA, GO, and GAGO samples at a concentration range of 0-60 µg/mL. The uninduced and untreated cells at 0 µg/mL served as controls. As shown in Figure 5, treatment with GA has increased the NO level in a concentration-independent manner, with a significant increase compared to control observed at higher concentrations (30, 45, and 60 µg/mL). In contrast, GO did not significantly increase the NO level. The NO levels remained relatively stable, indicating that GO did not promote inflammatory activation under these conditions. Conversely, in LPS-induced cells treated with GAGO, a significant reduction of NO level was observed at 5 µg/mL.

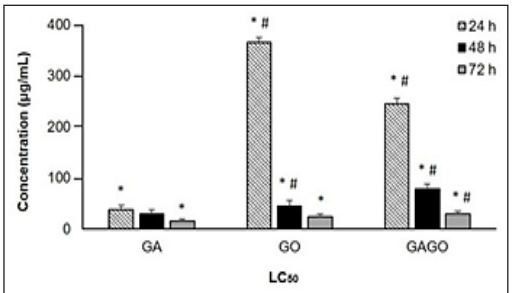

Exposure time (h)	LC50 (µg/mL)		
	GA	GO	GAGO
24	38.26 ± 8.549	364.10 ± 10.670	245.30 ± 9.867
48	29.62 ± 7.781	44.37 ± 11.190	78.91 ± 9.172
72	15.29 ± 4.424	24.52 ± 5.092	28.95 ± 6.674

(A)

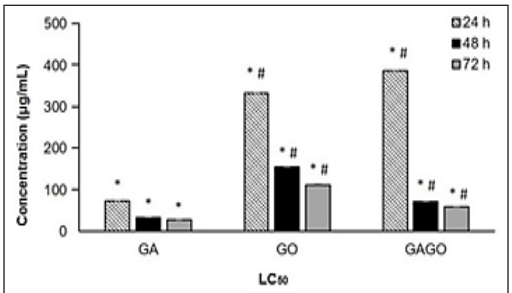

Exposure time (h)	LC50 (µg/mL)		
	GA	GO	GAGO
24	73.98 ± 0.146	334.10 ± 0.164	387.00 ± 0.189
48	33.89 ± 0.108	155.50 ± 0.168	71.75 ± 0.149
72	27.74 ± 0.094	112.90 ± 0.123	60.23 ± 0.168

(B)

Figure 4. LC_{50} values in (A) NIH-3T3 fibroblast cells and (B) RAW 264.7 macrophage cells following treatment with GA, GO and GAGO at 24, 48, and 72 hours

Note. The (*) symbol indicates a significant difference between 24 and 72 hours within the same sample, while the (#) symbol denotes a significant difference compared to GA at the same time point ($p \leq 0.05$). Data are presented as mean ± SD ($n \geq 3$)

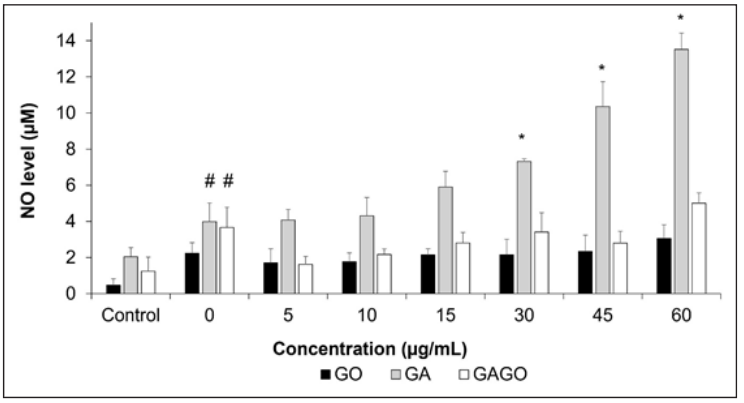

Figure 5. NO levels in LPS-induced RAW 264.7 macrophage cells following treatment with GO, GA and GAGO for 24 h. Cells were induced with 1 µg/mL of LPS for 2 h, followed by treatment of the cells with the respective samples at concentrations of 0-60 µg/mL for 24 h

Note. The (*) symbol denotes a significant difference compared to 0 µg/mL ($p \leq 0.05$), whereas the (#) symbol denotes a significant difference between control uninduced cells (Control) and 0 µg/mL ($p \leq 0.05$) ($n = 3$)

Inflammatory Cytokine Levels in RAW 264.7 Cells

Figure 6 shows the level of IL-6, TNF-α, and MCP-1 in LPS-induced RAW 264.7 macrophage cells after 24 h of treatment with GA, GO, and GAGO. IL-6, TNF-α, and

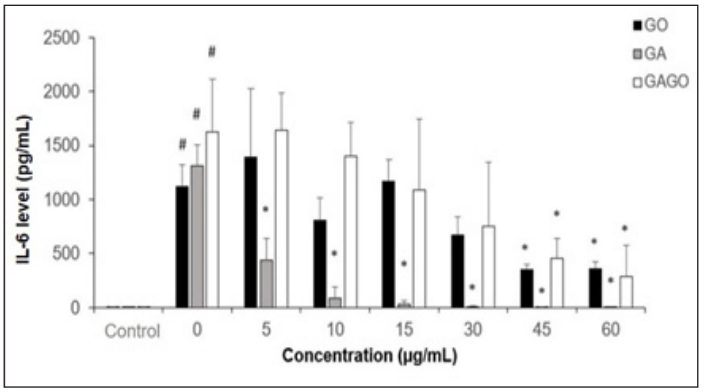

(A)

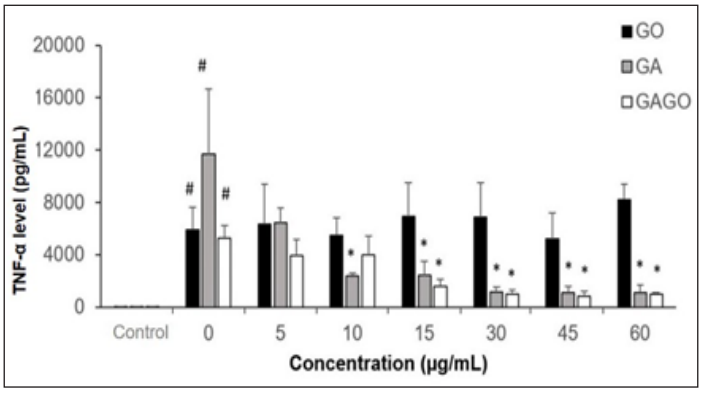

(B)

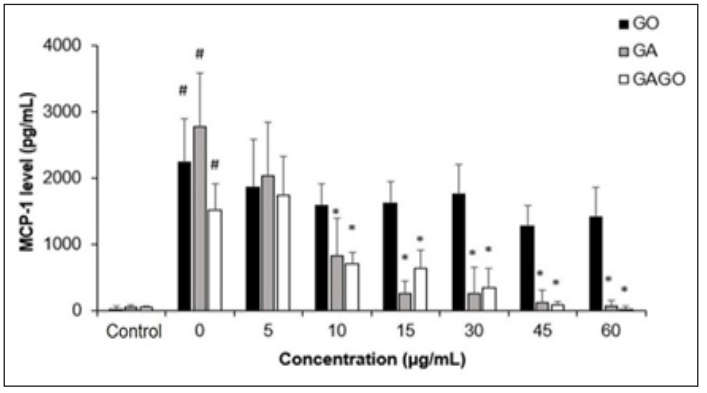

(C)

Figure 6. (A) IL-6, (B) TNF-α, and (C) MCP-1 (pg/mL) levels following treatment with GO, GA and GAGO in RAW 264.7 macrophage cells induced with LPS. RAW 264.7 cells were treated with samples at concentrations of 0-60 µg/mL for 24 h upon induction with 1 µg/mL of LPS, with non-induced cells serving as control. Significant difference of IL-6, TNF-α and MCP-1 levels to untreated cells (0 µg/mL) is denoted by (*), while (#) indicates a significant difference of control to untreated cells (0 µg/mL) ($p \leq 0.05$, $n \geq 3$)

MCP-1 levels were found to be negligible or undetectable in the uninduced cells (Control). In contrast, LPS stimulation significantly increased the levels of IL-6, TNF-α, and MCP-1 in untreated cells (0 μg/mL across all samples), indicating that LPS stimulation primarily accounted for the production of these pro-inflammatory cytokines. GA demonstrated a significant reduction of the IL-6 level in a concentration-dependent manner, as shown in Figure 6A. This reduction was significant when compared to 0 μg/mL at a concentration as low as 5 μg/mL. GAGO and GO, on the other hand, only exhibited a significantly reduced IL-6 level at 45 and 60 μg/mL. As depicted in Figure 6B, GO did not affect TNF-α levels, in contrast to the consistent decreases observed in GA- and GAGO-treated cells, with significant reductions at 10 μg/mL for GA and 15 μg/mL for GAGO. Similar to the observation of GO in TNF-α, GO did not affect the level of MCP-1, as illustrated in Figure 6C. Both GA and GAGO exhibited a significant decline in MCP-1 levels, with reductions observed starting at 10 μg/mL.

DISCUSSIONS

GAGO demonstrates reduced cytotoxicity compared to GA, indicating improved cellular compatibility up to 72 h of exposure period. One possible explanation is that interactions between GAGO and protein in the culture medium may alter the nanocomposite's surface properties and its interaction with the cells. In a previous study (Shamsi et al., 2022), the presence of protein corona on the surface of GAGO in DMEM with 10% FBS was apparent with small micellar particles (20-50 nm) observed under TEM. Protein adsorption could alter the physicochemical properties of GAGO, such as its surface charge and size, thereby modifying its "biological identity" and preventing recognition by immune cells. This influences the intracellular uptake of GAGO by macrophage cells (Cagliani et al., 2019). Protein corona formation on the surface of GAGO hinders the formation of aggregation, preventing recognition and phagocytosis by macrophage cells (Park et al., 2023).

A key finding of the present study was the ability of GA to elevate the level of NO at concentrations≥30 μg/mL, in contrast to GO and GAGO. This increase in NO could be attributed to rapid GA scavenging by cells and GA's pro-oxidant effects (Locatelli et al., 2013; Russell et al., 2012). This results in an exacerbated level of oxidative stress that activates the NF-κB signalling pathway, inducing iNOS expression and increasing NO production (Cheng et al., 2018; Wang et al., 2017), leading to cellular damage (Hassani et al., 2020). Supporting this mechanism, previous in vivo work from our laboratory demonstrated elevated ROS levels in GA-treated zebrafish embryos at higher concentrations (Ghafor et al., 2020). Li et al. (2023a) reported that GA reduced NO production through inhibition of the NF-κB signalling pathway in LPS-induced RAW 264.7 cells. At 100 μM GA (equivalent to 17.012 μg/mL), they observed NO levels of approximately 5-6 μM. This is comparable to the NO level of 5.89 μM observed in the present study at 15 μg/mL GA,

indicating agreement between the studies at similar concentrations. However, Li et al. (2023a) did not investigate the higher GA concentrations examined in the present study, where a significant increase in NO production was observed at concentrations above 30 μg/mL. Hence, it may suggest that the concentration of GA will crucially determine the extent of its anti-inflammatory effects. In contrast, GAGO has significantly suppressed NO production at 5 μg/mL, while no significant increase was observed at higher concentrations compared with the LPS-induced control (0 μg/mL). This indicates that nanocomposite formulation is able to modulate the release of GA, preventing rapid intracellular accumulation and limiting pro-oxidant activation. The controlled-release profile of GAGO may therefore prevent the sudden intracellular concentration spikes that are responsible for NF-κB overactivation (Shamsi et al., 2022).

As shown in Figure 6, GO reduced IL-6 levels but did not significantly affect TNF-α or MCP-1 levels under the conditions tested. Previous studies have shown that GO can produce different inflammatory responses depending on its physicochemical characteristics and the cell model used. For example, Feito et al. (2014) reported that six-arm PEG-functionalised GO increased TNF-α secretion in RAW 264.7 macrophages without significantly altering IL-6 or IL-1β levels. In the same study, reduced IL-6 levels were observed in stimulated primary splenocytes, highlighting that responses may differ between cell models and GO formulations. Hoyle et al. (2018) also reported reduced IL-6 without a corresponding reduction in TNF-α in a macrophage model, providing a relevant comparison with the selective IL-6 reduction observed here. In addition, Luo et al. (2020) found that GO size influenced inflammatory mediator responses in THP-1 macrophages, including effects on IL-6 and MCP-1. These findings provide broader evidence that GO can influence cytokine responses, although the differences in GO formulation and cell model mean that they do not directly explain the selective IL-6 response observed in the present study. The absence of a significant effect on MCP-1 should therefore be interpreted as an experimental finding rather than evidence of a specific pathway effect. Although TNF-α can participate in the regulation of MCP-1 production, the lack of a significant change in either mediator does not establish a shared mechanism in this study. Further studies are required to determine the mechanisms underlying the cytokine response to GO.

GA is a polyphenolic compound with reported antioxidant and anti-inflammatory activities (Badhani et al., 2015). Previous studies have shown that GA can reduce the production of inflammatory cytokines, including IL-6 and TNF-α, in experimental models of inflammation (Li et al., 2023a; Wu et al., 2022). Its anti-inflammatory activity has been proposed to involve attenuation of oxidative stress and modulation of inflammatory signalling pathways (Badhani et al., 2015). Li et al. (2023a) reported that GA at 100 μM (equivalent to 17.02 μg/mL) inhibited the secretion of IL-6 and TNF-α. In the present study, GA was evaluated over a broader concentration range of 5-60 μg/mL, and reductions in

both cytokines were observed at concentrations of 5 and 10 µg/mL and above, respectively. The reduction is also consistently exhibited at higher concentrations (Figure 6). This pattern agrees with the cytokine-reducing effects reported by Li et al. (2023a), who tested GA at 100 µM (equivalent to 17.02 µg/mL). Wu et al. (2022) also reported dose-dependent reductions in IL-6 and TNF-α in a rat model of acute inflammation, providing additional evidence that GA's effects may vary with concentration.

A critical finding of this study is the overlapping inhibition profiles of the GAGO nanocomposite, which mirror the selective behaviours of its individual components. Specifically, the IL-6 inhibition pattern under GAGO treatment closely resembles that of pristine GO, whereas the suppression patterns of TNF-α and MCP-1 align more closely with the behaviour of GA. This hybrid performance could be explained by a bifunctional, controlled-release mechanism inherent to the GAGO nanoarchitecture (Shamsi et al., 2022). At lower composite concentrations (10-30 µg/mL), the initial release of GA provides a localised concentration sufficient to canonically inhibit the upstream MAPK and NF-κB pathways. This is observed by the significant reduction in TNF-α and MCP-1 levels. Concurrently, the remaining signalling elements and post-transcriptional mRNA stabilisation machinery are robust enough to maintain IL-6 protein levels at these lower thresholds, rendering the early IL-6 response unaffected. As the concentration of GAGO increases to 45-60 µg/mL, this could cause a shift in the molecular mechanism. The internalisation of the GAGO nanocomposite (Dąbrowski et al., 2023), combined with an increased intracellular payload accumulation of released GA (Shamsi et al., 2022), triggers the activation of the Nrf2 pathway (Hoyle et al., 2018). In combination with the general shutdown of the NF-κB/MAPK engine, the synthesis of IL-6 was also completely inhibited. This dual-action, concentration-dependent kinetic framework explains why all three cytokines are suppressed at higher concentrations, establishing GAGO as a highly tunable, anti-inflammatory platform.

Despite promising findings, the present study is only limited to in vitro assessment. The molecular signalling pathways involved (e.g., NF-κB, MAPK, PI3K/Akt) were not directly investigated. Additionally, long-term stability beyond 90 days and in vivo pharmacokinetics remain to be evaluated. Future studies should focus on mechanistic pathway validation, controlled release kinetics, and in vivo efficacy models to further establish the translational potential of GAGO.

CONCLUSION

The findings from the present study collectively demonstrate improved biocompatibility of GAGO in NIH-3T3 fibroblasts and RAW 264.7 macrophages compared with native GA. GAGO also shows promising potential for anti-inflammatory effects, with significant modulation of NO levels and pro-inflammatory cytokines, namely IL-6, TNF-α, and

MCP-1. The present study provides a strong, fundamental basis for further development of GAGO in clinical settings. However, future study is warranted to assess the molecular mechanism, long-term stability and in vivo pharmacokinetics and pharmacodynamics of the GAGO nanocomposite.

ACKNOWLEDGEMENT

The authors would like to acknowledge the funding received from the Ministry of Higher Education, Malaysia, under the fundamental research grant scheme (FRGS/2018/SKK11/UPM/02/1 and FRGS/1/2023/WAB04/UPM/02/21) as well as from Universiti Putra Malaysia (GP-IPS/2023/9742000).

REFERENCES

Arip, M., Selvaraja, M., Mogana, R., Tan, L. F., Leong, M. Y., Tan, P. L., Yap, V. L., Chinnapan, S., Tat, N. C., Abdullah, M., Dharmendra, K., & Jubair, N. (2022). Review on plant-based management in combating antimicrobial resistance: Mechanistic perspective. *Frontiers in Pharmacology, 13*, Article 879495. https://doi.org/10.3389/fphar.2022.879495

Ashrafizadeh, M., Zarrabi, A., Mirzaei, S., Hashemi, F., Samarghandian, S., Zabolian, A., Hushmandi, K., Ang, H. L., Sethi, G., Kumar, A. P., Ahn, K. S., Nabavi, N., Khan, H., Makvandi, P., & Varma, R. S. (2021). Gallic acid for cancer therapy: Molecular mechanisms and boosting efficacy by nanoscopical delivery. *Food and Chemical Toxicology, 157*, Article 112576. https://doi.org/10.1016/j.fct.2021.112576

Azhari, A. (2023). *Gallic acid-loaded graphene oxide (GAGO) accelerates wound healing in in vitro and in vivo full-thickness excision wound models* [Unpublished master's thesis]. Universiti Putra Malaysia.

Bai, J., Zhang, Y., Tang, C., Hou, Y., Ai, X., Chen, X., Zhang, Y., Wang, X., & Meng, X. (2021). Gallic acid: Pharmacological activities and molecular mechanisms involved in inflammation-related diseases. *Biomedicine & Pharmacotherapy, 133*, Article 110985. https://doi.org/10.1016/j.biopha.2020.110985

Badhani, B., Sharma, N., & Kakkar, R. (2015). Gallic acid: A versatile antioxidant with promising therapeutic and industrial applications. *RSC Advances, 5*(35), 27540-27557. https://doi.org/10.1039/C5RA01911G

Cagliani, R., Gatto, F., & Bardi, G. (2019). Protein adsorption: A feasible method for nanoparticle functionalization? *Materials, 12*(12), Article 1991. https://doi.org/10.3390/ma12121991

Chen, J. S., Alfajaro, M. M., Chow, R. D., Wei, J., Filler, R. B., Eisenbarth, S. C., & Wilen, C. B. (2021). Nonsteroidal anti-inflammatory drugs dampen the cytokine and antibody response to SARS-CoV-2 infection. *Journal of Virology, 95*(7), Article e00014-21. https://doi.org/10.1128/JVI.00014-21

Cheng, Y., Li, X., Tse, H. F., & Rong, J. (2018). Gallic acid-L-leucine conjugate protects mice against LPS-induced inflammation and sepsis via correcting proinflammatory lipid mediator profiles and oxidative stress. *Oxidative Medicine and Cellular Longevity, 2018*, Article 1081287. https://doi.org/10.1155/2018/1081287

Chikere, C. O., Faisal, N. H., Kong-Thoo-Lin, P., & Fernandez, C. (2020). Interaction between amorphous zirconia nanoparticles and graphite: Electrochemical applications for gallic acid sensing using carbon paste electrodes in wine. *Nanomaterials, 10*(3), Article 537. https://doi.org/10.3390/nano10030537

Chopra, H., Dey, P. S., Das, D., Bhattacharya, T., Shah, M., Mubin, S., Maishu, S. P., Akter, R., Rahman, M. H., Karthika, C., Murad, W., Qusty, N., Qusti, S., Alshammari, E. M., Batiha, G. E.-S., Altalbawy, F. M. A., Albooq, M. I. M., & Alamri, B. M. (2021). Curcumin nanoparticles as promising therapeutic agents for drug targets. *Molecules, 26*(16), Article 4998. https://doi.org/10.3390/molecules26164998

Dąbrowski, B., Żuchowska, A., & Brzózka, Z. (2023). Graphene oxide internalization into mammalian cells: A review. *Colloids and Surfaces B: Biointerfaces, 221*, Article 112998. https://doi.org/10.1016/j.colsurfb.2022.112998

Díez-Pascual, A. M. (2021). Carbon-based nanomaterials. *International Journal of Molecular Sciences, 22*(14), Article 7726. https://doi.org/10.3390/ijms22147726

Drożdżal, S., Lechowicz, K., Szostak, B., Rosik, J., Kotfis, K., Machoy-Mokrzyńska, A., Białecka, M., Ciechanowski, K., & Gawrońska-Szklarz, B. (2021). Kidney damage from nonsteroidal anti-inflammatory drugs—Myth or truth? Review of selected literature. *Pharmacology Research & Perspectives, 9*(4), Article e00817. https://doi.org/10.1002/prp2.817

Feito, M. J., Vila, M., Matesanz, M. C., Linares, J., Gonçalves, G., Marques, P. A. A. P., Vallet-Regí, M., Rojo, J. M., & Portolés, M. T. (2014). *In vitro* evaluation of graphene oxide nanosheets on immune function. *Journal of Colloid and Interface Science, 432*, 221-228. https://doi.org/10.1016/j.jcis.2014.07.004

Grabarczyk, M., Justyńska, W., Czpakowska, J., Smolińska, E., Bielenin, A., Glabinski, A., & Szpakowski, P. (2024). Role of plant phytochemicals: Resveratrol, curcumin, luteolin and quercetin in demyelination, neurodegeneration, and epilepsy. *Antioxidants, 13*(11), Article 1364. https://doi.org/10.3390/antiox13111364

Ghafor, A. A. H. A., Elias, N., Shamsi, S., Yasin, F. M., & Sarchio, S. N. E. (2020). Toxicity assessment of gallic acid loaded graphene oxide (GAGO) nano-formulation in zebrafish (*Danio rerio*) embryos. *Pertanika Journal of Science and Technology, 28*(1), 311-326.

Gunaydin, C., & Bilge, S. S. (2018). Effects of nonsteroidal anti-inflammatory drugs at the molecular level. *Eurasian Journal of Medicine, 50*(2), 116-121. https://doi.org/10.5152/eurasianjmed.2018.0010

Hassani, A., Azarian, M. M. S., Ibrahim, W. N., & Hussain, S. A. (2020). Preparation, characterization and therapeutic properties of gum arabic-stabilized gallic acid nanoparticles. *Scientific Reports, 10*(1), Article 17808. https://doi.org/10.1038/s41598-020-71175-8

Hoyle, C., Rivers-Auty, J., Lemarchand, E., Vranic, S., Wang, E., Buggio, M., Rothwell, N. J., Allan, S. M., Kostarelos, K., & Brough, D. (2018). Small, thin graphene oxide is anti-inflammatory activating nuclear factor erythroid 2-related factor 2 via metabolic reprogramming. *ACS Nano, 12*(12), 11949-11962. https://doi.org/10.1021/acsnano.8b03642

Jiang, R., Lv, Y., Chen, B., Wu, X., Zou, Y., & Liang, L. (2024). Antioxidant effect of gallic acid on retinal ganglion cells in glaucoma model. *Scientific Reports, 14*(1), Article 14907. https://doi.org/10.1038/s41598-024-65965-7

Kumara, G. R. A., Pitawala, H. M. G. T. A., Karunarathne, B., Mantilaka, M. G. P. G. M., Rajapakse, G. R., Huang, H.-H., De Silva, K. K. H., & Yoshimura, M. (2021). Development of a chemical-free floatation technology for the purification of vein graphite and characterization of the products. *Scientific Reports, 11*(1), Article 22713. https://doi.org/10.1038/s41598-021-02101-9

Laurindo, L. F., de Carvalho, G. M., de Oliveira Zanuso, B., Figueira, M. E., Direito, R., de Alvares Goulart, R., Buglio, D. S., & Barbalho, S. M. (2023). Curcumin-based nanomedicines in the treatment of inflammatory and immunomodulated diseases: An evidence-based comprehensive review. *Pharmaceutics, 15*(1), Article 229. https://doi.org/10.3390/pharmaceutics15010229

Li, K., Gong, Q., Lu, B., Huang, K., Tong, Y., Mutsvene, T. E., Lin, M., Xu, Z., Lu, F., Li, X., & Hu, L. (2023a). Anti-inflammatory and antioxidative effects of gallic acid on experimental dry eye: *In vitro* and *in vivo* studies. *Eye and Vision, 10*(1), Article 17. https://doi.org/10.1186/s40662-023-00334-5

Li, X., Xue, X., Jia, J., Zou, X., Guan, Y., Zhu, L., & Wang, Z. (2023b). Non-steroidal anti-inflammatory drug diclofenac accelerates the emergence of antibiotic resistance via mutagenesis. *Environmental Pollution, 326*, Article 121457. https://doi.org/10.1016/j.envpol.2023.121457

Locatelli, C., Filippin-Monteiro, F. B., Centa, A., & Creczynski-Pasa, T. B. (2013). Antioxidant, antitumoral and anti-inflammatory activities of gallic acid. In M. A. Thompson & P. B. Collins (Eds.), *Handbook on gallic acid: Natural occurrences, antioxidant properties and health implications* (4th ed., pp. 1-23). Nova Science Publishers.

Lou, M., Zhang, L. N., Ji, P. G., Feng, F. Q., Liu, J. H., Yang, C., Li, B. F., & Wang, L. (2016). Quercetin nanoparticles induced autophagy and apoptosis through AKT/ERK/Caspase-3 signaling pathway in human neuroglioma cells: *In vitro* and *in vivo*. *Biomedicine & Pharmacotherapy, 84*, 1-9. https://doi.org/10.1016/j.biopha.2016.08.055

Luo, Y., Peng, J., Huang, C., & Cao, Y. (2020). Graphene oxide size-dependently altered lipid profiles in THP-1 macrophages. *Ecotoxicology and Environmental Safety, 199*, Article 110714. https://doi.org/10.1016/j.ecoenv.2020.110714

Mao, X., Wu, L. F., Zhao, H. J., Liang, W. Y., Chen, W. J., Han, S. X., Qi, Q., Cui, Y. P., Li, S., Yang, G. H., Shao, Y. Y., Zhu, D., Wang, R. F., You, Y., & Zhang, L. Z. (2016). Transport of corilagin, gallic acid, and ellagic acid from *Fructus Phyllanthi* tannin fraction in Caco-2 cell monolayers. *Evidence-Based Complementary and Alternative Medicine, 2016*, Article 9205379. https://doi.org/10.1155/2016/9205379

Marcano, D. C., Kosynkin, D. V., Berlin, J. M., Sinitskii, A., Sun, Z., Slesarev, A., Alemany, L. B., Lu, W., & Tour, J. M. (2010). Improved synthesis of graphene oxide. *ACS Nano, 4*(8), 4806-4814. https://doi.org/10.1021/nn1006368

Park, S., Ha, M. K., Lee, Y., Song, J., & Yoon, T. H. (2023). Effects of immune cell heterogeneity and protein corona on the cellular association and cytotoxicity of gold nanoparticles: A single-cell-based, high-dimensional mass cytometry study. *ACS Nanoscience Au, 3*(4), 323-334. https://doi.org/10.1021/acsnanoscienceau.3c00001

Parvin, M. S., Islam, M. S., Rahman, M. M., & Uddin, M. J. (2025). Quercetin-loaded polymeric nanoparticles inhibit PI3K/Akt signalling pathway in inflammatory cells. *International Journal of Biological Macromolecules, 260*, Article 123488.

Pasquet, P. L., Julien-David, D., Zhao, M., Villain-Gambier, M., & Trébouet, D. (2024). Stability and preservation of phenolic compounds and related antioxidant capacity from agro-food matrix: Effect of pH and atmosphere. *Food Bioscience, 57*, Article 103586. https://doi.org/10.1016/j.fbio.2024.103586

Petrovic, S., Bita, B., & Barbinta-Patrascu, M. E. (2024). Nanoformulations in pharmaceutical and biomedical applications: Green perspectives. *International Journal of Molecular Sciences, 25*(11), Article 5842. https://doi.org/10.3390/ijms25115842

Reckziegel, P., Dias, V. T., Benvegnú, D. M., Boufleur, N., Barcelos, R. C. S., Segat, H. J., Pase, C. S., dos Santos, C. M. M., Flores, E. M. M., & Bürger, M. E. (2016). Antioxidant protection of gallic acid against toxicity induced by Pb in blood, liver and kidney of rats. *Toxicology Reports, 3*, 351-356. https://doi.org/10.1016/j.toxrep.2016.02.005

Russell, L. H., Mazzio, E., Badisa, R. B., Zhu, Z. P., Agharahimi, M., Oriaku, E. T., & Goodman, C. B. (2012). Autoxidation of gallic acid induces ROS-dependent death in human prostate cancer LNCaP cells. *Anticancer Research, 32*(5), 1595-1602.

Samuelsson, I. P., & Pramling, N. (2016). Variation theory of learning and developmental pedagogy: Two context-related models of learning grounded in phenomenography. *Scandinavian Journal of Educational Research, 60*(3), 286-295. https://doi.org/10.1080/00313831.2015.1120232

Sabouripour, F., & Roslan, S. (2015). Resilience, optimism and social support among international students. *Asian Social Science, 11*(15), 159-170. https://doi.org/10.5539/ass.v11n15p159

Seisenbaeva, G. A., Ali, L. M. A., Vardanyan, A., Gary-Bobo, M., Budnyak, T. M., Kessler, V. G., & Durand, J. O. (2021). Mesoporous silica adsorbents modified with amino polycarboxylate ligands: Functional characteristics, health and environmental effects. *Journal of Hazardous Materials, 406*, Article 124698. https://doi.org/10.1016/j.jhazmat.2020.124698

Shamsi, S., Alagan, A. A., Sarchio, S. N. E., & Md Yasin, F. (2020). Synthesis, characterization, and toxicity assessment of Pluronic F127-functionalized graphene oxide on the embryonic development of zebrafish (*Danio rerio*). *International Journal of Nanomedicine, 15*, 8311-8329. https://doi.org/10.2147/IJN.S271159

Shamsi, S., Elias, N., Sarchio, S. N. E., & Md Yasin, F. (2018). Gallic acid loaded graphene oxide based nanoformulation (GAGO) as potential anti-bacterial agent against *Staphylococcus aureus*. *Materials Today: Proceedings, 5*, S160-S165. https://doi.org/10.1016/j.matpr.2018.08.059

Shamsi, S., Ghafor, A. A. H. A., Norjoshukrudin, N. H., Ng, I. M. J., Abdullah, S. N. S., Sarchio, S. N. E., Yasin, F. M., Gani, S. A., & Desa, M. N. M. (2022). Stability, toxicity, and antibacterial potential of gallic acid-loaded graphene oxide (GAGO) against methicillin-resistant *Staphylococcus aureus* (MRSA) strains. *International Journal of Nanomedicine, 17*, 5781-5807. https://doi.org/10.2147/IJN.S369373

Siu, F. Y., Ye, S., Lin, H., & Li, S. (2018). Galactosylated PLGA nanoparticles for the oral delivery of resveratrol: Enhanced bioavailability and *in vitro* anti-inflammatory activity. *International Journal of Nanomedicine, 13*, 4133-4144. https://doi.org/10.2147/IJN.S164235

Sohrabi, F., Dianat, M., Badavi, M., Radan, M., & Mard, S. A. (2021). Gallic acid suppresses inflammation and oxidative stress through modulating Nrf2-HO-1-NF-κB signaling pathways in elastase-induced emphysema in rats. *Environmental Science and Pollution Research, 28*(40), 56822-56834. https://doi.org/10.1007/s11356-021-14513-1

Sriuttha, P., Sirichanchuen, B., & Permsuwan, U. (2018). Hepatotoxicity of non-steroidal anti-inflammatory drugs: A systematic review of randomized controlled trials. *International Journal of Hepatology, 2018*, Article 5253623. https://doi.org/10.1155/2018/5253623

Srivastava, J., Chandra, H., Nautiyal, A. R., & Kalra, S. J. S. (2014). Antimicrobial resistance (AMR) and plant-derived antimicrobials (PDAms) as an alternative drug line to control infections. *3 Biotech, 4*(5), 451-460. https://doi.org/10.1007/s13205-013-0180-y

Wang, Q., de Oliveira, E. F., Alborzi, S., Bastarrachea, L. J., & Tikekar, R. V. (2017). On mechanism behind UV-A light enhanced antibacterial activity of gallic acid and propyl gallate against *Escherichia coli* O157. *Scientific Reports, 7*(1), Article 8325. https://doi.org/10.1038/s41598-017-08449-1

Wang, Z., Sun, W., Sun, X., Wang, Y., & Zhou, M. (2020). Kaempferol ameliorates cisplatin-induced nephrotoxicity by modulating oxidative stress, inflammation and apoptosis via ERK and NF-κB pathways. *AMB Express, 10*(1), Article 58. https://doi.org/10.1186/s13568-020-00993-w

Wu, Y., Li, K., Zeng, M., Qiao, B., & Zhou, B. (2022). Serum metabolomics analysis of the anti-inflammatory effects of gallic acid on rats with acute inflammation. *Frontiers in Pharmacology, 13*, Article 830439. https://doi.org/10.3389/fphar.2022.830439

Zailan, N. F. Z., Jaganathan, N., Sandramuti, T., Sarchio, S. N. E., & Hassan, M. (2020). Inhibition of GSK-3 by tideglusib suppresses activated macrophages and inflammatory responses in lipopolysaccharide-stimulated RAW 264.7 cell line. *Malaysian Journal of Medicine and Health Sciences, 16*(Suppl. 9), 2-8.

Zhang, L., McClements, D. J., Wei, Z., Wang, G., Liu, X., & Liu, F. (2020). Delivery of synergistic polyphenol combinations using biopolymer-based systems: Advances in physicochemical properties, stability and bioavailability. *Critical Reviews in Food Science and Nutrition, 60*(12), 2083-2097. https://doi.org/10.1080/10408398.2019.1630358

Pertanika J. Trop. Agric. Sci. 49 (5): 2237 - 2256 (2026)

PERTANIKA JOURNALS

TROPICAL AGRICULTURAL SCIENCE

Journal homepage: http://www.pertanika.upm.edu.my/

Integrating *Brassica* spp. Residues and Bioethanol to Mitigate Disease and Enhance Potato Seed Yield in Medium-Altitude Regions

Andi Muhibuddin[1]*, Zulkifli Maulana[1], Fatmawati[2], Haris Mahmud[3] and Andi Tenri Fada[4]

[1]Department of Agrotechnology, Faculty of Agriculture, Bosowa University, Makassar 90231, Indonesia
[2]Department of Food Technology, Faculty of Agriculture, Bosowa University, Makassar 90231, Indonesia
[3]Department of Agribusiness, Faculty of Agriculture, Khairun University, 97719 Ternate, Indonesia
[4]Department of Capture Fisheries, Faculty of Marine and Fisheries, Hasanuddin University, 90245 Makassar, Indonesia

ABSTRACT

This study evaluated the effectiveness of *Brassica spp*. residues in suppressing potato disease symptoms and investigated bioethanol as a CO_2 supplementation strategy for potato cultivation in medium-altitude areas. From June to September 2024, this study was conducted at approximately 500 masl in Bantaeng Regency, South Sulawesi, Indonesia. This study used a split-plot design, with bioethanol concentration as the main plot (0% (control), 15%, and 30%) and Brassica waste type as the subplot (treatments included cabbage, green mustard, Chinese cabbage, and radish residues). Analysis of variance (ANOVA) was applied, followed by Tukey's test ($p < 0.05$). The results showed that Chinese cabbage roots had the highest total glucosinolate content, at 144.16 ± 3.14 µmol g^{-1} dry weight, whereas cabbage roots had the lowest content, at 13.60 ± 1.57 µmol g^{-1} dry weight. At 60 days after planting (DAP), 30 % bioethanol reduced the intensity of leaf roll/leaf curl, leaf spot, and leaf blight symptoms compared with the control. In addition, 30 % bioethanol increased internal CO_2 concentration and photosynthetic rate, and increased plant height at 75 DAP from 69.91 to 79.91 cm, tuber number from 8.30 to 9.10 tubers per plant, and tuber weight from 302.63 to 318.88 g per plant, while reducing transpiration rate. The interaction between bioethanol concentration and Brassica residue type was not significant. These findings indicate that 30 % bioethanol and *Brassica spp*. Residues can reduce disease symptoms and improve potato growth and yield under medium-altitude conditions.

Keywords: *Brassica* spp., bioethanol, medium-altitude areas, potato seeds, photosynthesis

ARTICLE INFO

Article history:
Received: 26 June 2025
Accepted: 18 September 2026
Published: 30 October 2026

DOI: https://doi.org/10.47836/pjtas.49.5.07

E-mail addresses:
muhibuddin@universitasbosowa.ac.id (Andi Muhibuddin)
zulkifli.maulana@universitasbosowa.ac.id (Zulkifli Maulana)
fatmawati@universitasbosowa.ac.id (Fatmawati)
haris.mahmud@unkhair.ac.id (Haris Mahmud)
atenrifada@unhas.ac.id (Andi Tenri Fada)
* Corresponding author

e-ISSN: 2231-8542

© Universiti Putra Malaysia Press

INTRODUCTION

Potato seed production is generally carried out in highland areas with low temperatures, approximately 17-20 °C (Aklilu et al., 2024; Philiphos & Tafesse, 2024), at elevations above 1,000 m above sea level (masl) (Mamilianti et al., 2019; Molina et al., 2022). However, potato development in highland areas faces various constraints, including soil erosion, limited land availability, and high production costs (Ademe et al., 2024). These conditions have encouraged the expansion of potato seed production into medium-altitude areas at approximately ±500 masl, where larger areas of potentially suitable land remain available.

Although promising, potato cultivation in medium-altitude areas faces serious agronomic constraints. Relatively high temperatures, ranging from approximately 29 to 37 °C, can increase leaf photorespiration, reduce photosynthetic efficiency, and ultimately inhibit tuber initiation and bulking (Bernacchi et al., 2023; Opoku et al., 2024). In addition, environmental conditions in medium-altitude areas may increase disease intensity, thereby reducing potato seed productivity and quality (Diploid, 2019; Lal et al., 2022; Upadhaya, 2018). Therefore, cultivation technologies are needed that can not only suppress potato disease symptoms but also support plant physiological efficiency under high-temperature conditions.

One potential approach is using *Brassica* spp. plant residues as natural biofumigants. *Brassica* residues, such as cabbage, mustard, and other *Brassica* species, contain bioactive compounds, particularly glucosinolates, which can be hydrolysed into compounds that are toxic to several soil-borne pathogens (Eugui et al., 2023; Santos et al., 2021). Several studies have reported that *Brassica* spp. residues and their bioactive compounds have the potential to suppress soil-borne pathogens and plant diseases, including nematodes and diseases affecting potato (Charkowski et al., 2020; Iraboneye et al., 2021; Pacifico et al., 2021; Sagar et al., 2018). Therefore, *Brassica* spp. residues represent a promising alternative for environmentally friendly disease management, reducing dependence on synthetic chemical inputs.

Improving photosynthetic efficiency is also important for potato cultivation in medium-altitude areas. High temperatures can accelerate CO_2 loss from leaf mesophyll tissues by increasing photorespiration. It reduces the photosynthetic rate and ultimately decreases crop yield (Rykaczewska, 2015). Therefore, bioethanol may serve as a supportive treatment because it can be metabolised in plant tissues to CO_2 and H_2O. It has potential in increasing internal CO_2 availability (Costa et al., 2018). Increased CO_2 in the leaf intercellular spaces may enhance Rubisco-mediated carboxylation, improving photosynthetic rate and reducing the negative effects of photorespiration (McGiffen Jr. & Manthey, 1996).

Previous studies reported *Brassica* spp. residues as biofumigants for pathogen management, while other studies have evaluated improvements of photosynthetic efficiency under high-temperature stress using physiological approaches. Based on the available

literature, studies integrating *Brassica* spp. residues as biofumigants with bioethanol and CO_2 supplementation remain limited. This strategy within a single potato cultivation system in medium-altitude areas remains very limited. This research gap is important since potato seed production in medium-altitude areas faces two major constraints: disease and heat-induced photosynthetic disruption. Therefore, this study evaluates an integrated strategy that combines *Brassica* spp. residues and bioethanol to suppress disease symptoms, support plant physiological processes, and improve the growth and yield of potato seed under medium-altitude conditions.

MATERIALS AND METHODS

Experimental Design and Treatments

This study was conducted from June to September 2024 at the experimental field of the Horticultural Seed Center, Ulu Ere District, Bantaeng Regency, South Sulawesi, Indonesia. The land is at approximately 500 masl, with an average temperature ranging from 29 °C to 37 °C and relative humidity between 80 % and 90 % (Maulidiyah et al., 2024; Rusli et al., 2021). Glucosinolate content was analysed at the Agricultural Biotechnology Laboratory, Universitas Bosowa.

The experiment used a split-plot design with two factors. The main plot consisted of bioethanol at different concentrations: no bioethanol as the control (0%) (B0), 15% bioethanol (B1), and 30% bioethanol (B2). The subplot factor consisted of four types of *Brassica* residue: cabbage residue (*Brassica oleracea*) (C), green mustard residue (*Brassica juncea* Coss.) (G), Chinese cabbage residue (*Brassica chinensis*) (H), and radish residue (*Raphanus sativus*) (R).

There were 12 treatment combinations. Each treatment combination was replicated three times, making 36 experimental units. Each experimental unit had nine plants, giving a total of 324 plants used in this study. From each experimental unit, three sample plants were randomly selected for the observations.

Implementation Stage

Planting Material and Growing Medium

The planting material used in this study consisted of certified potato seed tubers of the Granola variety. They were of the same variety, weighed about 50-60 g, were healthy, free from visible symptoms of pest and disease infestation, mechanically undamaged, and relatively uniform in size.

The plants were moved to the pots containing 5 kg of sterilised soil. The soil used in this study was collected from the topsoil layer of agricultural land surrounding the experimental site. It was sterilised to reduce initial pathogen contamination and standardise growing

medium conditions. Each pot was planted with one potato seed tuber. The plants received standard maintenance: watering, weeding, and limited pest and disease management as needed. The pest management was carried out manually, without pesticides. All maintenance practices were applied uniformly to ensure that differences in plant responses were primarily attributable to the *Brassica* residue and bioethanol treatments.

Preparation of Brassica *spp. Residues and Biofumigation*

Residues of cabbage (*Brassica oleracea*), green mustard (*B. juncea* Coss.), Chinese cabbage (*B. chinensis*) and radish (*Raphanus sativus*) were obtained from post-harvest residues collected in Gowa, Jeneponto, and Enrekang, South Sulawesi Province, Indonesia. The plant parts used for the biofumigation treatment were a mixture of roots and stems, as they are abundantly available as post-harvest residues. They may also contain bioactive compounds, particularly glucosinolates, as natural biofumigants. In this study, roots and stems were not treated as separate experimental factors but were used together as residue materials, depending on *Brassica* species.

The *Brassica* residues were rinsed, then chopped into pieces approximately 1 cm in length. A total of 150 g of fresh residue was incorporated into each pot containing 5 kg of sterilised soil, thoroughly mixed, and watered to a moist consistency. The pots were then tightly covered for two weeks to support organic matter decomposition and the release of bioactive compounds through biofumigation. After biofumigation, the pots were uncovered and left for 3-5 days before planting the potato seed tubers to reduce the possibility of phytotoxic effects on the seedlings.

Analysis of Glucosinolate Content

Glucosinolate analysis was performed on *Brassica* spp. residue tissue samples to determine total glucosinolate content. The analysed samples included cabbage roots, cabbage stems, green mustard roots, green mustard stems, Chinese cabbage roots, Chinese cabbage stems, and radish roots. The plant samples were cleaned to remove adhering soil, cut into 2 × 2 × 1 cm pieces, placed in polyethylene bags, and stored at -20 °C. The samples were then freeze-dried and ground into a fine powder.

Glucosinolate extraction was carried out according to the method of Tian et al. (2005) with modifications. A total of 0.20 g of powdered sample was placed into an extraction tube, followed by the addition of 5 mL of 80 % methanol (v/v) as the extraction solvent. The sample was homogenised for 5 min, then incubated at 70°C for 15 min to inactivate myrosinase and facilitate glucosinolate extraction. The sample was subsequently centrifuged at 4,000 rpm for 10 min, and the supernatant was collected as the extract for glucosinolate analysis. When necessary, the extract was diluted with 80 % methanol at a 1:10 (v/v) ratio prior to measurement.

Glucosinolate detection was performed using a photometry-based method according to Fenwick et al. (1983). The absorbance of the extract was measured at 405 nm. Total glucosinolate concentration was calculated using the following formula: $x = (A_{405} - 0.13) \times 272$, where A_{405} represents the absorbance value at 405 nm and x indicates the total glucosinolate concentration expressed in μmol g^{-1}. In this study, the analysis was limited to determining total glucosinolate content and did not include identifying specific glucosinolate compounds.

Bioethanol Application

Water hyacinth was used as the bioethanol source, applied at 0%, 15%, and 30% treatment levels. The 0 % treatment served as the control (no bioethanol addition), while the 15 % and 30 % treatments were applied at the same volume to ensure uniform application. All treatments were applied simultaneously in the morning to minimise the influence of daily environmental variation. Two weeks after planting (WAP), bioethanol application was conducted and repeated every two weeks until the plants reached 10 WAP. Bioethanol was applied at 10 mL per plant/pot via foliar application. Foliar application provided direct contact with the leaf surface and enhanced CO_2 availability around photosynthetic tissues.

Assessment of Disease Symptoms

Disease observations were conducted based on visible symptoms, including leaf roll/leaf curl symptoms, yellowing, wilting, leaf spot symptoms, leaf blight symptoms, and other visible damage to the plant canopy. This assessment was not intended to identify causal pathogens, but to quantify disease symptom intensity or the level of visual plant damage.

Disease symptom intensity was assessed using a scale based on the percentage of leaves showing visible symptoms or damage (Equation 1):

$$I = \frac{\Sigma(\mathrm{ni} \times \mathrm{vi})}{\mathrm{Z} \times \mathrm{N}} \times 100\% \qquad [1]$$

Explanation: (I) represents disease intensity (%), (ni) is the number of plants assigned to the i-th score category, (Vi) is the symptom score value, (N) is the total number of observed plants, and (Z) is the highest score value. Table 1 presents the symptom scoring scale used in this study.

Physiological, Growth, and Yield Observations

Physiological observations were performed at 30, 45, and 60 days after planting (DAP) using a CID-320 Portable Photosynthesis System. Physiological parameters included

Table 1
Disease symptom scoring scale for potato plants

Score	Category	Description
0	No attack	No signs of disease or damage on the plant.
1	1 - ≤ 25 % leaves yellowing/wilting	Leaves affected cover 1 to 25 % of the total leaves of the plant.
2	> 25 - ≤ 50 % leaves yellowing/wilting	Leaves affected cover more than 25 % to 50 % of the total leaves of the plant.
3	> 50 - ≤ 75 % leaves yellowing/wilting	Leaves affected cover more than 50 % to 75 % of the total leaves of the plant.
4	> 75 - 100 % leaves yellowing/wilting	Leaves affected cover more than 75 % to 100 % of the total leaves of the plant.

internal CO_2 concentration (ppm), photosynthetic rate (μmol m^{-2} s^{-1}), and transpiration rate (mmol m^{-2} s^{-1}).

Yield parameters were observed at harvest, approximately 90 days after planting (DAP). The yield parameters included the number and weight of tubers per plant. The number of tubers was determined by counting all tubers formed on each plant, whereas tuber weight per plant was obtained by weighing all tubers harvested from each plant using a digital balance and was expressed in grams per plant.

Data Analysis

Data were analysed using analysis of variance (ANOVA) in a split-plot design to determine the effects of bioethanol concentration, *Brassica* residue type, and their interaction on disease symptom intensity, physiological parameters, growth, and potato yield. Data analysis was performed using IBM SPSS Statistics version 26. When ANOVA indicated a significant effect, mean comparisons were conducted using Tukey's test at the 5 % significance level ($p < 0.05$).

RESULTS

Total Glucosinolate Content in *Brassica* spp. Samples

The total glucosinolate content in *Brassica* spp. extracts was measured photometrically at 405 nm and subsequently calculated from the resulting absorbance values. The results showed that total glucosinolate content varied considerably among *Brassica* spp. tissues, ranging from 13.60 to 144.16 μmol g^{-1} (Table 2).

Based on the statistical analysis, the total glucosinolate content differed significantly among *Brassica* spp. tissue types. Chinese cabbage root (*Brassica chinensis*) exhibited the highest total glucosinolate content, at 144.16 ± 3.14 μmol g^{-1}, whereas cabbage root (*Brassica oleracea*) showed the lowest content, at 13.60 ± 1.57 μmol g^{-1}.

Table 2
Total glucosinolate content in root and stem tissues of selected Brassica spp. residues

No.	Type of Extract	Absorbance Value at 405 nm	Glucosinolate Concentration (µmol g-1)
1.	Root of Cabbage (Brassica oleracea)	0.18 ± 0.01	13.60 ± 1.57d
2.	Stem of Cabbage (Brassica oleracea)	0.41 ± 0.01	76.16 ± 1.57c
3.	Root of Mustard Greens (Brassica juncea Coss)	0.39 ± 0.01	70.72 ± 1.57c
4.	Green mustard Stem (Brassica juncea Coss)	0.48 ± 0.01	95.20 ± 1.57b
5.	Root of Chinese Cabbage (Brassica chinensis)	0.66 ± 0.01	144.16 ± 3.14a
6.	Stem of Chinese Cabbage (Brassica chinensis)	0.49 ± 0.01	97.92 ± 3.14b
7.	Root of Radish (Raphanus sativus)	0.40 ± 0.01	73.44 ± 1.57c

Note. Values are presented as mean ± standard error (SE), n = 3. Values followed by different letters within the same column indicate significant differences according to Tukey's test at $p < 0.05$

The total glucosinolate content in Chinese cabbage root was approximately 10.6-fold higher than that in cabbage root.

Disease Symptom Intensity

The ANOVA results showed that bioethanol and plant residue treatments had significant effects on disease symptom intensity, particularly at 60 days after planting (DAP), whereas the Bioethanol × Plant Residue interaction was not significant ($p > 0.05$; Table 3). For the bioethanol treatment, the application of 30 % bioethanol (B2) resulted in the lowest transformed disease symptom intensity values at 60 DAP, namely 0.491 for leaf roll/leaf curl symptoms, 0.567 for leaf spot symptoms, and 0.544 for leaf blight symptoms. These values were lower than those observed in the control treatment (B0), which were 0.544, 0.682, and 0.845, respectively. Based on the transformed values, these reductions were equivalent to 9.74 %, 16.86 %, and 35.62 %, respectively, compared with the control.

Plant residue treatment also had a significant effect on disease symptom intensity at 60 DAP. Chinese cabbage residue (H) produced the lowest transformed disease symptom intensity values, namely 0.690 for leaf roll/leaf curl symptoms, 0.505 for leaf spot symptoms, and 0.552 for leaf blight symptoms. These values were lower than those observed in several other plant residue treatments.

Physiological Activity

Internal CO_2 Concentration

The ANOVA results showed that bioethanol concentration significantly affected the internal CO_2 concentration of potato leaves at 30, 45, and 60 days after planting (DAP), whereas plant residue treatment and the Bioethanol × Plant Residue interaction did not.

Table 3
Intensity of leaf roll, leaf spot, and leaf blight symptoms in potato plants at 30, 45, and 60 days after planting (DAP) as affected by bioethanol and plant residue treatments[1]

Treatment	Leaf Roll/Leaf Curl Symptoms5			Leaf Spot Symptoms5			Leaf Blight Symptoms5		
	30 DAP4	45 DAP	60 DAP	30 DAP	45 DAP	60 DAP	30 DAP	45 DAP	60 DAP
Bioethanol:									
B0 2	0.301 a	0.301 a	0.544 a	0.301 a	0.301 a	0.682 a	0.301 a	0.477 a	0.845 a
B1	0.301 a	0.301 a	0.505 a	0.301 a	0.301 a	0.606 ab	0.301 a	0.505 a	0.690 ab
B2	0.301 a	0.301 a	0.491 b	0.301 a	0.301 a	0.567 b	0.301 a	0.505 a	0.544 b
Plant Residue:									
C[3]	0.301 a	0.301 a	0.753 a	0.301 a	0.301 a	0.748 a	0.301 a	0.301 a	0.653 a
H	0.301 a	0.301 a	0.690 b	0.301 a	0.301 a	0.505 b	0.301 a	0.301 a	0.552 b
G	0.301 a	0.301 a	0.740 a	0.301 a	0.301 a	0.753 a	0.301 a	0.301 a	0.758 ab
R	0.301 a	0.301 a	0.727 a	0.301 a	0.301 a	0.752 a	0.301 a	0.301 a	0.674 a

Note.
[1]Data has been transformed using the logarithmic transformation log(x),
[2]B0 = 0 % Bioetanol, B1= 15 % Bioetanol, B2 = 30 % Bioetanol,
[3]C = Cabbage Residue, H = Chinese cabbage Residue, G = Green Mustard Residue, R= Radish Residue,
[4]DAP = Days After Planting,
[5]Numbers in the same column followed by different letters indicate significant differences based on Tukey's post hoc test at $\alpha = 0.05$
[6]Values followed by different letters within the same column indicate significant differences according to Tukey's test at $p < 0.05$. The Bioethanol × Plant Residue interaction was not significant based on ANOVA; therefore, only the main effects are presented. Roots and stems were not included as treatment factors in the analysis of disease symptom intensity, but were analysed separately to support the characterization of total glucosinolate content

Tukey's test showed that 30 % bioethanol (E2) resulted in a higher internal CO_2 concentration than the control (E0), although it was not significantly different from 15 % bioethanol (E1) at some observation times (Figure 1A). Numerically, *Chinese cabbage* residue showed a relatively higher mean internal CO_2 concentration than several other plant residues; however, these differences were not statistically significant (Figure 1B).

Photosynthetic Rate

The ANOVA results showed that bioethanol concentration had a significant effect on the photosynthetic rate of potato plants, whereas plant residue treatment and the Bioethanol × Plant Residue interaction did not show significant effects. Based on Tukey's test, the 30 % bioethanol treatment (B2) resulted in a higher photosynthetic rate than the control (B0), although at some observation times its value was not significantly different from that of the 15 % bioethanol treatment (B1) (Figure 2A).

Plant residue treatment had no significant effect on the photosynthetic rate (Figure 2B). Numerically, Chinese cabbage residue showed a relatively higher mean photosynthetic

rate than several other residue treatments; however, these differences were not statistically significant.

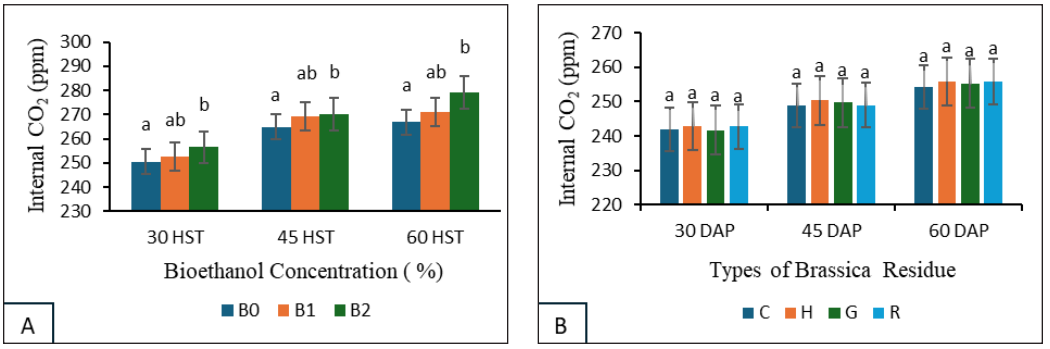

Figure 1. Internal CO_2 concentration (ppm) in potato leaves under different bioethanol concentrations (A) and plant residue treatments (B) at 30, 45, and 60 Days After Planting (DAP); B0 = 0 %, B1 = 15 %, B2 = 30 %; C = *Brassica oleracea*, H = *Brassica chinensis*, G = *Brassica juncea* Coss, R = *Raphanus sativus*

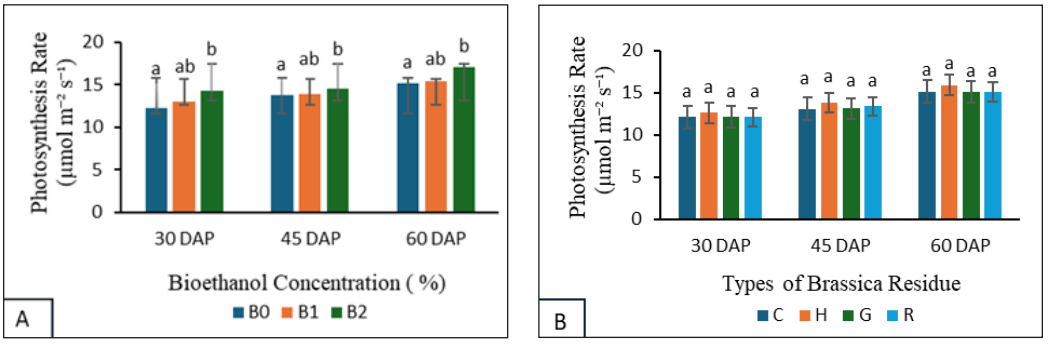

Figure 2. Photosynthesis rate (µmol m^{-2} s^{-1}) in potato plants under bioethanol treatments (A) and plant residue treatments (B) at 30, 45, and 60 Days After Planting (DAP); B0=0 %, B1 = 15 %, B2 = 30 %; C = *Brassica oleracea*, H = *Brassica chinensis*, G = *Brassica juncea* Coss, R = *Raphanus sativus*

Transpiration Rate

The ANOVA results showed that bioethanol concentration had a significant effect on the transpiration rate of potato plants, whereas plant residue treatment and the Bioethanol × Plant Residue interaction did not show significant effects. At 30, 45, and 60 DAP, the application of 30 % bioethanol (B2) resulted in a lower transpiration rate than the control without bioethanol (B0) (Figure 3A).

Plant residue treatment had no significant effect on the transpiration rate of potato plants at any observation time (Figure 3B). Numerically, Chinese cabbage residue showed a relatively lower mean transpiration rate than several other residue treatments; however, the differences among residues were not statistically significant.

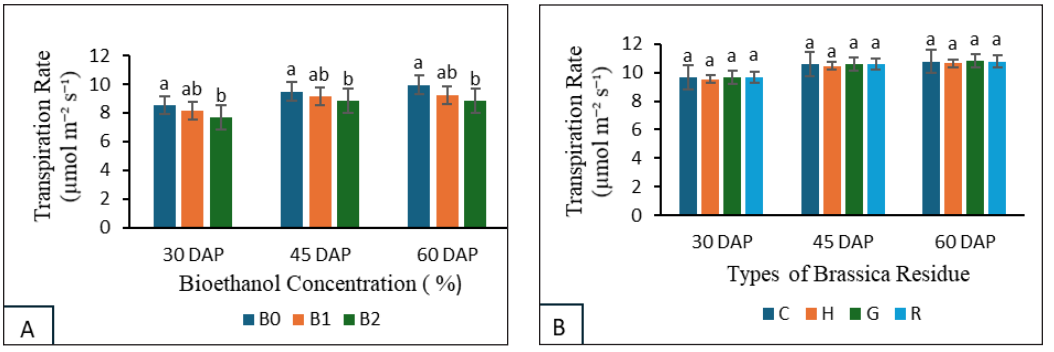

Figure 3. Transpiration rate of potato plants (mmol m^{-2} s^{-1}) at various bioethanol concentrations (A) and plant residue (B) at 30, 45, and 60 Days After Planting (DAP); B0=0 %, B1 = 15 %, B2 = 30 %; C = *Brassica oleracea*, H = *Brassica chinensis*, G = *Brassica juncea* Coss, R = *Raphanus sativus*

Growth and Production Aspects

Plant Height

ANOVA showed that bioethanol concentration and plant residue type significantly affected potato plant height, whereas the interaction between the two factors was not significant. Since the interaction was not significant, the data presented represent the main effects of each factor.

The 30 % bioethanol treatment (B2) resulted in greater plant height than the control treatment without bioethanol (B0), particularly at 45 and 60 days after planting (DAP) (Figure 4A). Plant height also differed among plant residue treatments. Numerically, Chinese cabbage residue showed the highest plant height compared with the other residue treatments (Figure 4B).

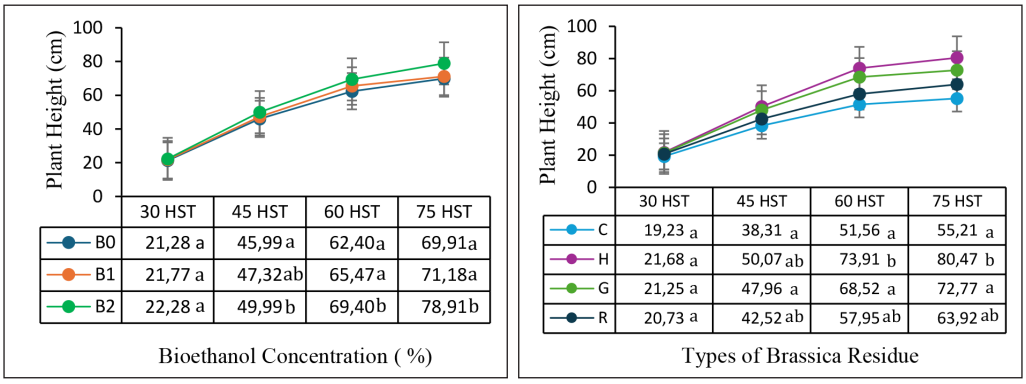

Figure 4. Effect of bioethanol concentration (A) and plant residue (B) on potato plant height (cm) at 30, 45, 60, and 75 Days After Planting (DAP); B0 = 0 %, B1 = 15 %, B2 = 30 %; C = *Brassica oleracea*, H = *Brassica chinensis*, G = *Brassica juncea* Coss, R = *Raphanus sativus*

Number of Tubers and Tuber Weight

The ANOVA results showed that bioethanol concentration and type of plant residue had significant effects on the number of tubers and tuber weight per plant, whereas the interaction between the two factors was not significant. Since the interaction was not significant, the data presented represent the main effects of each factor.

For the number of tubers, the 30 % bioethanol treatment (B2) produced a higher number of tubers per plant than the control (B0) and the 15 % bioethanol treatment (B1) (Figure 5A). Plant residue treatment also showed significant differences in the number of tubers per plant. Chinese cabbage and green mustard residues produced a higher number of tubers than cabbage and radish residues, with both treatments having the same statistical notation (Figure 5B).

For tuber weight, the 30 % bioethanol treatment (B2) also produced greater tuber weight per plant than the control (B0) and 15 % bioethanol (B1) treatments (Figure 6A). Meanwhile, based on plant residue type, Chinese cabbage and green mustard residues produced higher tuber weight per plant than cabbage and radish residues, with both

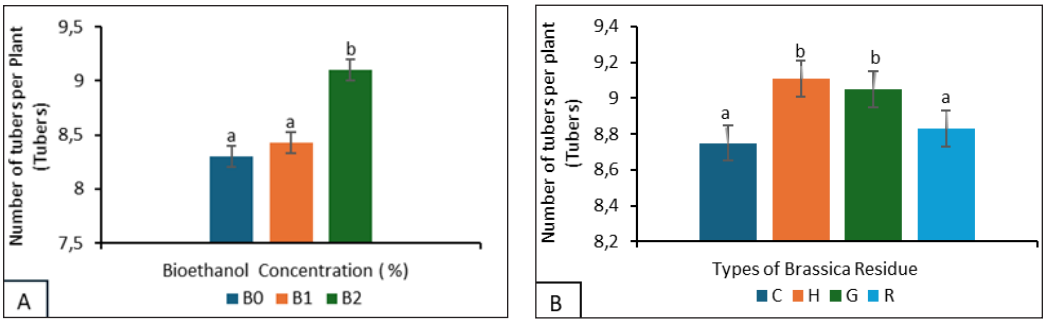

Figure 5. Effect of bioethanol concentration (A) and plant residue (B) on the number of potato tubers per plant (tubers) at the end of the study; B0 = 0 %, B1 = 15 %, B2 = 30 %; C = *Brassica oleracea*, H = *Brassica chinensis*, G = *Brassica juncea* Coss, R = *Raphanus sativus*

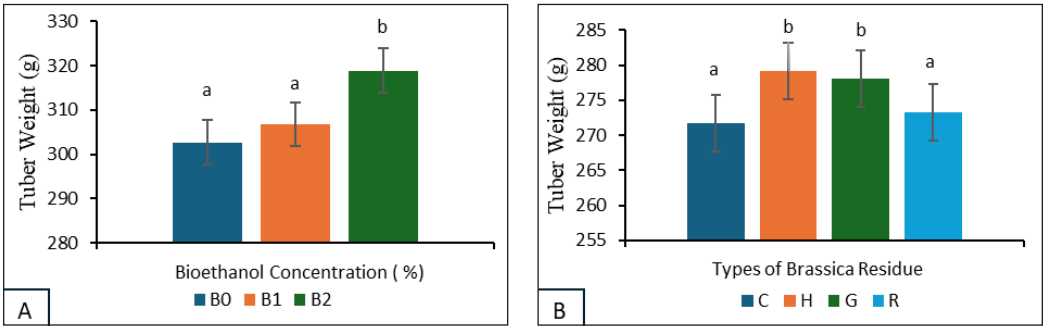

Figure 6. Effect of bioethanol concentration (A) and plant residue (B) on tuber weight per potato plant (g) at the end of the study; B0=0 %, B1=15 %, B2=30 %; C= *Brassica oleracea*, H= *Brassica chinensis*, G= *Brassica juncea* Coss, R= *Raphanus sativus*

treatments belonging to the same statistical notation group (Figure 6B). This pattern indicates that treatments producing a higher number of tubers also tended to produce greater tuber weight per plant.

DISCUSSIONS

Total Glucosinolate Content in *Brassica* spp. Samples

Differences in total glucosinolate content among plant species and tissues indicate that the biofumigation potential of *Brassica* spp. residues varies depending on the type of plant material used (Table 2). Chinese cabbage roots (*Brassica chinensis*), which had the highest total glucosinolate content, may contribute more substantially as a source of bioactive compounds in the biofumigation process. Conversely, the low total glucosinolate content in cabbage roots (*Brassica oleracea*) suggests that the effectiveness of residues as biofumigant materials may be influenced by plant species and tissue type.

Differences in total glucosinolate content are important because glucosinolates can be hydrolysed into various bioactive compounds, particularly isothiocyanates, which play a role in suppressing soil-borne pathogens. Therefore, *Brassica* spp. residues with higher total glucosinolate content may have greater biofumigation potential. However, because this study measured only total glucosinolate content and did not identify specific glucosinolate types, the results should be interpreted only in terms of biofumigation potential based on total glucosinolate content.

These results are consistent with Rhee et al. (2020), who stated that glucosinolate content can vary across plant species and tissue types. Dutta et al. (2019) also emphasised the relevance of glucosinolate profiles in distinguishing plant characteristics and their potential role in pathogen control. In addition, Ammar et al. (2023) and Ciska et al. (2021) reported that plant tissue type and processing methods can affect glucosinolate levels. Therefore, the selection of *Brassica* spp. residue type is an important aspect of developing biofumigation technology to support the management of disease symptoms in potato cultivation under medium-altitude conditions.

Disease Symptom Intensity

The reduction in disease symptom intensity under the 30 % bioethanol treatment indicates that bioethanol has the potential to suppress disease symptoms in potato plants. This response may be associated with improved plant physiological conditions following bioethanol application, enabling the plants to better withstand biotic stress. In addition, bioethanol or ethanol-based materials have also been reported to exhibit potential antimicrobial activity against certain microorganisms (Maulana et al., 2023; Pal & Srivastava, 2019; Suleiman et al., 2019). However, because this study did not directly test the antimicrobial activity of bioethanol, this explanation should be regarded as a possible mechanism.

For the plant residue treatment, the lower disease symptom intensity observed with Chinese cabbage residue was likely associated with its relatively high total glucosinolate content (Table 3). Glucosinolates in *Brassica* tissues can be hydrolysed into bioactive compounds. One of them is isothiocyanates, which are involved in biofumigation mechanisms and may suppress soil-borne pathogens. Since the Bioethanol and Plant Residue interaction was not significant, interpret the effects of these two factors as independent main effects rather than synergistic effects. In addition, because disease assessment was based only on visual symptoms, these results are more appropriately interpreted as reduced disease symptom severity rather than suppression of a specific pathogen.

Physiological Activity

Internal CO_2 Concentration

The increase in internal CO_2 concentration under bioethanol treatment was presumably associated with bioethanol's ability to enhance CO_2 availability around photosynthetic tissues, particularly at 30 % (Figure 1). This condition may improve the physiological environment of leaves, thereby supporting photosynthesis, especially in potato cultivation at medium altitudes where temperatures are relatively high. In C3 plants such as potato, improved internal CO_2 availability can support carboxylation by Rubisco and help reduce the negative effects of photorespiration (Muhibuddin et al., 2022; Taiz et al., 2018; Todaka et al., 2024).

In contrast, plant residue treatment had no significant effect on internal CO_2 concentration. This indicates that variation in internal CO_2 concentration was more closely associated with bioethanol concentration than with plant residue type. Therefore, the role of *Brassica* spp. residues in this study is more appropriately related to their biofumigation potential and the reduction of disease symptoms, rather than as a major factor affecting internal CO_2 concentration in leaves.

Photosynthetic Rate

The increase in photosynthetic rate under bioethanol treatment, particularly at the 30 % concentration, was more closely associated with bioethanol concentration than with the type of plant residue, because only the bioethanol factor had a significant effect on this parameter (Figure 2). This response was likely related to the increase in internal CO_2 concentration in the leaves, thereby improving CO_2 availability for photosynthesis. In C3 plants such as potato, increased internal CO_2 can support Rubisco carboxylation and improve photosynthetic efficiency, especially at medium altitudes where relatively high temperatures may enhance photorespiration (Muhibuddin et al., 2022).

In addition to supporting internal CO_2 availability, bioethanol was also presumed to improve leaf physiological conditions through stomatal regulation and enhanced

photosynthetic enzyme activity. This is consistent with Rahman et al. (2022) and Zhang et al. (2024), who reported that bioethanol application may be associated with stomatal regulation and increased photosynthetic enzyme activity. In contrast, plant residue treatment had no significant effect on photosynthetic rate; therefore, the role of *Brassica* spp. residues in this study is more appropriately associated with their potential to reduce disease symptoms through biofumigation mechanisms, rather than as a major factor affecting photosynthetic rate.

Transpiration Rate

The reduction in transpiration rate under the 30 % bioethanol treatment was likely associated with an increase in leaf internal CO_2 concentration. Increased internal CO_2 can contribute to partial stomatal closure, thereby reducing water loss through transpiration. This response indicates that bioethanol application has the potential to improve plant water-use efficiency, particularly in potato cultivation at medium altitudes, where plants are often exposed to relatively high temperatures. Thus, variation in transpiration rate in this study was more closely associated with bioethanol concentration than with plant residue type, as only bioethanol showed a significant effect on this parameter.

Transpiration is primarily regulated by stomatal conductance and plays an important role in nutrient transport, leaf cooling, and gas exchange (Abbas et al., 2021; Da Graça et al., 2010). The lower transpiration rate under bioethanol treatment may indicate that the plants were able to reduce water loss without fully inhibiting major physiological processes, particularly because photosynthetic rate still increased under the same treatment. This condition suggests a better balance among CO_2 uptake, photosynthesis, and water conservation.

Meanwhile, plant residue treatment had no significant effect on the transpiration rate (Figure 3). Therefore, the role of *Brassica* spp. residues in this study cannot be directly associated with stomatal regulation or reduced transpiration. Although Chinese cabbage residue showed a numerically lower transpiration value, this should be interpreted as a tendency that warrants further investigation rather than a significant effect.

Growth and Production Aspects

Plant Height

The increase in plant height under the 30 % bioethanol treatment was likely associated with increased internal leaf CO_2 availability, which may support CO_2 assimilation, enhance photosynthetic activity, and promote vegetative growth (Figure 4). Better CO_2 availability can increase carbon fixation and assimilate formation, thereby supporting plant growth, particularly under medium-altitude conditions characterised by relatively high temperatures

that may limit photosynthetic efficiency (Abbas et al., 2021; Lehretz et al., 2019; Rahman et al., 2022).

The tendency of Chinese cabbage residue to produce taller plants may be indirectly related to its relatively higher total glucosinolate content. Glucosinolates in Brassica residues can suppress disease symptoms through a biofumigation mechanism, thereby improving plant health and enabling vegetative growth to proceed more optimally. Thus, the relationship between total glucosinolate content and plant height should be interpreted as an indirect effect via improved plant health, rather than a direct effect on growth.

Number of Tubers and Tuber Weight

The increase in tuber number and tuber weight per plant under the 30 % bioethanol treatment was likely associated with increased internal leaf CO_2 availability. Improved CO_2 availability can support photosynthesis, increase assimilate production, and enhance carbon allocation to storage organs (Figure 5), including tubers (Rahman et al., 2022). In potato plants, assimilates produced through photosynthesis are subsequently translocated to the tubers to support tuber initiation, bulking, and dry matter accumulation (Chen & Setter, 2021; Darwesh et al., 2020; Naumann et al., 2020). In addition, increased CO_2 availability may suppress photorespiration, allowing more assimilates to be allocated to biomass formation and tuber yield (Saeed et al., 2022) (Figure 6).

This response is relevant to potato cultivation in medium-altitude areas, where relatively high temperatures can interfere with tuber formation and bulking. Therefore, bioethanol application has the potential to serve as an adaptive cultivation approach to support potato productivity under such environmental conditions, although its physiological mechanisms remain to be further investigated (Fang et al., 2024; Vijayakumar et al., 2024).

The higher tuber weight observed under Chinese cabbage and green mustard residue treatments was likely due to the role of Brassica residues in improving the growing environment, supporting root development, and suppressing disease symptoms through biofumigation (Abbas et al., 2021; Pacifico et al., 2021). However, because the interaction between bioethanol concentration and plant residue type had no significant effect, the effects of these two factors on tuber number and tuber weight should be interpreted as independent main effects rather than as a synergistic response.

This study was conducted under medium-altitude conditions and within a limited experimental scope. Therefore, further validation across different locations, seasons, soil conditions, and potato cultivars is still required. Future studies should also clarify the mechanisms linking bioethanol application, total glucosinolate content, disease symptom reduction, and tuber development.

The limitations of this study, relate to methodological and mechanistic aspects. Methodologically, the pot experiment using sterilised soil may not fully represent open-

field agroecosystem conditions, which are influenced by soil microbial dynamics, the presence of natural pathogens, moisture variation, and root-soil interactions. In addition, disease assessment based solely on visual symptoms, without identification of the causal pathogens, limits interpretation of the mechanisms underlying symptom reduction. The use of roots and stems as mixed residues, without separating them as treatment factors, also limits the understanding of the contribution of each plant tissue to disease suppression and improved plant growth.

CONCLUSION

The results showed that total glucosinolate content varied among Brassica spp. species and plant tissues, with the highest content observed in Chinese cabbage roots at 144.16 µmol g^{-1}, followed by Chinese cabbage stems at 97.92 µmol g^{-1} and green mustard stems at 95.20 µmol g^{-1}. These differences indicate that the potential of Brassica residues as a source of bioactive compounds for biofumigation is influenced by the plant species and tissue used. The application of 30 % bioethanol resulted in lower disease symptom intensity than the control and 15 % bioethanol treatments, particularly for leaf roll/leaf curl, leaf spot, and leaf blight symptoms at the final observation. The 30 % bioethanol treatment also produced better physiological responses, as indicated by increased internal CO_2 concentration and photosynthetic rate, along with reduced transpiration rate. In addition, 30 % bioethanol, as well as Chinese cabbage and green mustard residues, showed better responses in several growth and yield parameters, particularly plant height, number of tubers, and tuber weight per plant. No interaction was observed between bioethanol concentration and plant residue type for all observed parameters; therefore, the effects of these two factors are more appropriately interpreted as independent main effects. Because disease assessment was still based on visual symptoms, these results should be interpreted as a reduction in disease symptom intensity rather than suppression of specific pathogens.

ACKNOWLEDGEMENT

We express our gratitude for the research funding support through the Fundamental Basic Research Scheme from the Directorate of Research, Technology, and Community Service (DRTPM), Ministry of Education, Culture, Research, and Technology, under Contract Number: 111/ES/PG.02.00.PL/2024.

REFERENCES

Abbas, S., Amna, Javed, M. T., Ali, Q., Azeem, M., & Ali, S. (2021). Nutrient deficiency stress and relation with plant growth and development. In S. Fahad, O. Sönmez, S. Saud, D. Wang, C. Wu, M. Adnan, M. Arif, & Amanullah (Eds.), *Engineering tolerance in crop plants against abiotic stress* (1st ed., pp. 239-262). CRC Press. https://doi.org/10.1201/9781003160717-12

Ademe, D., Tesfaye, K., Simane, B., Zaitchik, B. F., Alemayehu, G., & Adgo, E. (2024). Optimizing agronomic practices to harness climate change impacts on potato production in tropical highland regions. *European Journal of Agronomy*, *152*, Article 127021. https://doi.org/10.1016/j.eja.2023.127021

Aklilu, Z., Berihun, T., Zena, S., & Alemu, A. (2024). Production efficiency of potato in south gondar zone, ethiopia. *Cogent Food & Agriculture*, *10*(1), Article 2378988. https://doi.org/10.1080/23311932.2024.2378988

Ammar, H. B., Arena, D., Treccarichi, S., Di Bella, M. C., Marghali, S., Ficcadenti, N., Lo Scalzo, R., & Branca, F. (2023). The effect of water stress on the glucosinolate content and profile: A comparative study on roots and leaves of *Brassica oleracea* L. Crops. *Agronomy*, *13*(2), Article 579. https://doi.org/10.3390/agronomy13020579

Bernacchi, C. J., Ruiz-Vera, U. M., Siebers, M. H., DeLucia, N. J., & Ort, D. R. (2023). Short- and long-term warming events on photosynthetic physiology, growth, and yields of field grown crops. *Biochemical Journal*, *480*(13), 999-1014. https://doi.org/10.1042/BCJ20220433

Charkowski, A., Sharma, K., Parker, M. L., Secor, G. A., & Elphinstone, J. (2020). Bacterial diseases of potato. In H. Campos & O. Ortiz (Eds.), *The potato crop* (pp. 351-388). Springer International Publishing. https://doi.org/10.1007/978-3-030-28683-5_10

Chen, C.-T., & Setter, T. L. (2021). Role of tuber developmental processes in response of potato to high temperature and elevated CO_2. *Plants*, *10*(5), Article 871. https://doi.org/10.3390/plants10050871

Ciska, E., Honke, J., & Drabińska, N. (2021). Changes in glucosinolates and their breakdown products during the fermentation of cabbage and prolonged storage of sauerkraut: Focus on sauerkraut juice. *Food Chemistry*, *365*, Article 130498. https://doi.org/10.1016/j.foodchem.2021.130498

Costa, D., Jesus, J., Virgínio E Silva, J., & Silveira, M. (2018). Life cycle assessment of bioethanol production from sweet potato (*Ipomoea batatas* L.) in an experimental plant. *BioEnergy Research*, *11*(3), 715-725. https://doi.org/10.1007/s12155-018-9932-1

Da Graça, J. P., Rodrigues, F. A., Farias, J. R. B., De Oliveira, M. C. N., Hoffmann-Campo, C. B., & Zingaretti, S. M. (2010). Physiological parameters in sugarcane cultivars submitted to water deficit. *Brazilian Journal of Plant Physiology*, *22*(3), 189-197. https://doi.org/10.1590/S1677-04202010000300006

Darwesh, O. M., El-Maraghy, S. H., Abdel-Rahman, H. M., & Zaghloul, R. A. (2020). Improvement of paper wastes conversion to bioethanol using novel cellulose degrading fungal isolate. *Fuel*, *262*, Article 116518. https://doi.org/10.1016/j.fuel.2019.116518

Diploid, D. S. C. (2019). Annual report of the potato association of America. *American Journal of Potato Research*, *96*(4), 317-378. https://doi.org/10.1007/s12230-019-09723-w

Dutta, T. K., Khan, M. R., & Phani, V. (2019). Plant-parasitic nematode management via biofumigation using brassica and non-Brassica plants: Current status and future prospects. *Current Plant Biology*, *17*, 17-32. https://doi.org/10.1016/j.cpb.2019.02.001

Eugui, D., Velasco, P., Abril-Urías, P., Escobar, C., Gómez-Torres, Ó., Caballero, S., & Poveda, J. (2023). Glucosinolate-extracts from residues of conventional and organic cultivated broccoli leaves (*Brassica oleracea* var. Italica) as potential industrially-scalable efficient biopesticides against fungi, oomycetes and plant parasitic nematodes. *Industrial Crops and Products*, *200*, Article 116841. https://doi.org/10.1016/j.indcrop.2023.116841

Fang, G., Yang, S., Ruan, B., Ye, G., He, M., Su, W., Zhou, Y., Wang, J., & Yang, S. (2024). Research progress on physiological, biochemical, and molecular mechanisms of potato in response to drought and high temperature. *Horticulturae*, *10*(8), Article 827. https://doi.org/10.3390/horticulturae10080827

Fenwick, G. R., Heaney, R. K., Mullin, W. J., & VanEtten, C. H. (1983). Glucosinolates and their breakdown products in food and food plants. *C R C Critical Reviews in Food Science and Nutrition*, *18*(2), 123-201. https://doi.org/10.1080/10408398209527361

Iraboneye, N., Charimbu, M. K., & Mungai, N. W. (2021). Effect of canola and compound fertilizer on potato (*Solanum tuberosum* L.) bacterial wilt management. *European Journal of Agriculture and Food Sciences*, *3*(1), 28-38. https://doi.org/10.24018/ejfood.2021.3.1.130

Lal, M., Kumar, A., Chaudhary, S., Singh, R. K., Sharma, S., & Kumar, M. (2022). Antagonistic and growth enhancement activities of native *Pseudomonas* spp. Against soil and tuber-borne diseases of potato (*Solanum tuberosum* L.). *Egyptian Journal of Biological Pest Control*, *32*(1), Article 22. https://doi.org/10.1186/s41938-022-00522-w

Lehretz, G. G., Sonnewald, S., Hornyik, C., Corral, J. M., & Sonnewald, U. (2019). Post-transcriptional regulation of flowering locus T modulates heat-dependent source-sink development in potato. *Current Biology*, *29*(10), 1614-1624.e1613. https://doi.org/10.1016/j.cub.2019.04.027

Mamilianti, W., Hanani, N., Mustadjab, M. M., & Asmara, R. (2019). Risk preference of farmers and production input allocation of potato farming in Tengger Highland, Indonesia. *EurAsian Journal of BioSciences*, *13*(2), 1777-1783.

Maulana, Z., Muhibuddin, A., Fitriyah, A. T., Rachmawaty, Saleh, H., & Karim, A. (2023). Methanol application and soil water content: Increased production and cultivation of soybean plants. *Nongye Jixie Xuebao/ Transactions of the Chinese Society of Agricultural Machinery*, *54*(10), 38-49.

Maulidiyah, R., Salam, M., Jamil, M. H., Tenriawaru, A. N., Rahmadanih, & Saadah. (2024). Examining the effects of input allocation on potato production, production efficiency, and technical inefficiency in potato farming: Evidence from the stochastic frontier model in search of sustainable farming practices. *Sustainable Futures*, *7*, Article 100218. https://doi.org/10.1016/j.sftr.2024.100218

McGiffen Jr., M. E., & Manthey, J. A. (1996). The role of methanol in promoting plant growth: A current evaluation. *HortScience*, *31*(7), 1092-1096. https://doi.org/10.21273/HORTSCI.31.7.1092

Molina, C. A., Dudenhoefer, D., Polar, V., Scurrah, M., Ccanto, R. C., & Heider, B. (2022). Gender roles and native potato diversity management in highland communities of Peru. *Sustainability*, *14*(6), Article 3455. https://doi.org/10.3390/su14063455

Muhibuddin, A., Maulana, Z., Salam, S., Syamsia, S., Reta, R., & Fattah, A. (2022). The effect of ethanol on potato growth and production at moderate elevation. *Research in Agricultural Engineering*, *68*(3), 113-119. https://doi.org/10.17221/45/2021-RAE

Naumann, M., Koch, M., Thiel, H., Gransee, A., & Pawelzik, E. (2020). The importance of nutrient management for potato production part II: Plant nutrition and tuber quality. *Potato Research*, *63*(1), 121-137. https://doi.org/10.1007/s11540-019-09430-3

Opoku, E., Sahu, P. P., Findurová, H., Holub, P., Urban, O., & Klem, K. (2024). Differential physiological and production responses of C3 and C4 crops to climate factor interactions. *Frontiers in Plant Science*, *15*, Article 1345462. https://doi.org/10.3389/fpls.2024.1345462

Pacifico, D., Lanzanova, C., Pagnotta, E., Bassolino, L., Mastrangelo, A. M., Marone, D., Matteo, R., Lo Scalzo, R., & Balconi, C. (2021). Sustainable use of bioactive compounds from solanum Tuberosum and Brassicaceae wastes and by-products for crop protection—A review. *Molecules*, *26*(8), Article 2174. https://doi.org/10.3390/molecules26082174

Pal, M., & Srivastava, J. (2019). Antifungal activity of the ethyl acetate extract of *Cyperus rotundus* rhizome against certain fungi responsible for food spoilage and plant diseases. *International Journal of Food Science and Nutrition*, *4*(3), 88-89.

Philiphos, F., & Tafesse, A. (2024). Analyzing the efficiency of potato production in Southern Ethiopia: A stochastic frontier analysis approach. *SN Business & Economics*, *5*(1), Article 10. https://doi.org/10.1007/s43546-024-00771-x

Rahman, M. M., Mostofa, M. G., Das, A. K., Anik, T. R., Keya, S. S., Ahsan, S. M., Khan, M. A. R., Ahmed, M., Rahman, M. A., Hossain, M. M., & Tran, L.-S. P. (2022). Ethanol positively modulates photosynthetic traits, antioxidant defense and osmoprotectant levels to enhance drought acclimatization in soybean. *Antioxidants*, *11*(3), Article 516. https://doi.org/10.3390/antiox11030516

Rhee, J.-H., Choi, S., Lee, J.-E., Hur, O.-S., Ro, N.-Y., Hwang, A.-J., Ko, H.-C., Chung, Y.-J., Noh, J.-J., & Assefa, A. D. (2020). Glucosinolate content in Brassica genetic resources and their distribution pattern within and between inner, middle, and outer leaves. *Plants*, *9*(11), Article 1421. https://doi.org/10.3390/plants9111421

Rusli, M., Chaerul, M., & Marzuki, I. (2021). Adaptation of climate change to vulnerability of raw water availability in Bantaeng, South Sulawesi. *Journal of Physics: Conference Series*, *1899*(1), Article 012062. https://doi.org/10.1088/1742-6596/1899/1/012062

Rykaczewska, K. (2015). The effect of high temperature occurring in subsequent stages of plant development on potato yield and tuber physiological defects. *American Journal of Potato Research*, *92*(3), 339-349. https://doi.org/10.1007/s12230-015-9436-x

Saeed, S., Samer, M., Mohamed, M. S. M., Abdelsalam, E., Mohamed, Y. M. A., Abdel-Hafez, S. H., & Attia, Y. A. (2022). Implementation of graphitic carbon nitride nanomaterials and laser irradiation for increasing bioethanol production from potato processing wastes. *Environmental Science and Pollution Research*, *29*(23), 34887-34897. https://doi.org/10.1007/s11356-021-18119-5

Sagar, N. A., Pareek, S., Sharma, S., Yahia, E. M., & Lobo, M. G. (2018). Fruit and vegetable waste: Bioactive compounds, their extraction, and possible utilization. *Comprehensive Reviews in Food Science and Food Safety*, *17*(3), 512-531. https://doi.org/10.1111/1541-4337.12330

Santos, C. A. D., Abboud, A. C. D. S., & Carmo, M. G. F. D. (2021). Biofumigation with species of the brassicaceae family: A review. *Ciência Rural*, *51*(1), Article e20200440. https://doi.org/10.1590/0103-8478cr2020040

Suleiman, W. B., El Bous, M. M., El Said, M., & El Baz, H. (2019). In vitro evaluation of *Syzygium aromaticum* L. Ethanol extract as biocontrol agent against postharvest tomato and potato diseases. *Egyptian Journal of Botany*, *59*(1), 81-94. https://doi.org/10.21608/ejbo.2018.3838.1180

Taiz, L., Zeiger, E., Mller, E. I. M., & Murphy, A. (2018). *Fundamentals of plant physiology*. Sinauer Associates.

Tian, Q., Rosselot, R. A., & Schwartz, S. J. (2005). Quantitative determination of intact glucosinolates in broccoli, broccoli sprouts, brussels sprouts, and cauliflower by high-performance liquid chromatography-electrospray ionization-tandem mass spectrometry. *Analytical Biochemistry*, *343*(1), 93-99. https://doi.org/10.1016/j.ab.2005.04.045

Todaka, D., Quynh, D. T. N., Tanaka, M., Utsumi, Y., Utsumi, C., Ezoe, A., Takahashi, S., Ishida, J., Kusano, M., Kobayashi, M., Saito, K., Nagano, A. J., Nakano, Y., Mitsuda, N., Fujiwara, S., & Seki, M. (2024). Application of ethanol alleviates heat damage to leaf growth and yield in tomato. *Frontiers in Plant Science*, *15*, Article 1325365. https://doi.org/10.3389/fpls.2024.1325365

Upadhaya, A. (2018). *Plant-parasitic nematodes in field pea and potato and their effect on plant growth and yield* [Master's thesis, North Dakota State University].

Vijayakumar, S., Wang, Y., Lehretz, G., Taylor, S., Carmo-Silva, E., & Long, S. (2024). Kinetic modeling identifies targets for engineering improved photosynthetic efficiency in potato (*Solanum tuberosum* cv. Solara). *The Plant Journal*, *117*(2), 561-572. https://doi.org/10.1111/tpj.16512

Zhang, K., Han, X., Fu, Y., Khan, Z., Zhang, B., Bi, J., Hu, L., & Luo, L. (2024). Biochar coating promoted rice growth under drought stress through modulating photosynthetic apparatus, chloroplast ultrastructure, stomatal traits and ROS homeostasis. *Plant Physiology and Biochemistry*, *216*, Article 109145. https://doi.org/10.1016/j.plaphy.2024.109145

Pertanika J. Trop. Agric. Sci. 49 (5): 2257 - 2274 (2026)

PERTANIKA JOURNALS

TROPICAL AGRICULTURAL SCIENCE

Journal homepage: http://www.pertanika.upm.edu.my/

Comparative Shelf-Life Predictions of Packaged Paddy Using Water Mass-Transfer Modelling and Quality-Deterioration Kinetics Under Different Controlled Relative Humidities

Astriella Awwali Maissy, Sri Rahayoe*, and Hanim Zuhrotul Amanah

Department of Agricultural and Biosystems Engineering, Faculty of Agricultural Technology, Universitas Gadjah Mada, Jl. Flora No. 1, Bulaksumur, Sleman, 55281 Yogyakarta, Indonesia

ABSTRACT

Even when paddy is sufficiently dry at the start of storage, its quality may deteriorate if humid storage air drives ongoing moisture exchange among the grain, the package, and the environment. This study evaluated the Inpari 32 paddy variety packed in woven polypropylene mini-sacks and stored for 90 days at 30 °C under relative humidity (RH) levels of 50%, 70%, and 90%. Shelf life was estimated from two endpoints: moisture change predicted with a water mass-transfer model and damaged-grain development predicted with first-order quality kinetics using Indonesian National Standard (SNI) 224:2023 limits (National Standardization Agency of Indonesia, 2023). After 90 days, moisture content was 12.7166% wb at RH 50%, 13.3864% wb at RH 70%, and 15.5008% wb at RH 90%, indicating net water loss under the driest condition and marked humidification at high RH. The fitted apparent transfer capacities (P) were 0.0880, 0.0062, and 0.0335, whereas the apparent water-transfer rate constant (Q) increased from 0.0020 to 0.0092 and 0.0212 day^{-1} as RH increased. Model fit was high (R^2 = 0.9913-0.9990; RMSE = 2.69×10^{-4}-8.64×10^{-4} g H_2O g^{-1} dry solid). Damaged-grain rate constants likewise increased with RH, from 0.0068 to 0.0127 and 0.0213 day^{-1}. Moisture-based shelf lives were 312, 176, and 105 days, whereas the Medium I damaged-grain endpoint gave 296, 159, and 95 days. Thus, physical-quality failure was predicted 5.1-9.7% earlier than the moisture endpoint. The results show that RH control, rather than initial moisture content alone, should guide paddy-storage decisions in humid tropical systems.

Keywords: Damaged grain, paddy, relative humidity, shelf life, storage, water mass transfer

ARTICLE INFO

Article history:
Received: 21 June 2025
Accepted: 19 August 2026
Published: 30 October 2026

DOI: https://doi.org/10.47836/pjtas.49.5.08

E-mail addresses:
astriella.awwali.m@ugm.ac.id (Astriella Awwali Maissy)
srahayoe@ugm.ac.id (Sri Rahayoe)
hanim_za@ugm.ac.id (Hanim Zuhrotul Amanah)
* Corresponding author

e-ISSN: 2231-8542

© Universiti Putra Malaysia Press

INTRODUCTION

Rice is the staple food for more than 90% of Indonesia's population and is central to the country's food and economic systems (Ansari et al., 2023; Santosa et al., 2024). Although rice supply is often discussed in terms of field yield, much of its final value is determined after harvest. Across the rice supply chain, postharvest management determines grain quality until milling and distribution (Atungulu et al., 2019; Tong et al., 2019). In Indonesia, paddy commonly enters storage near 13-14% moisture content (wet basis), below or close to the 14% maximum specified by SNI 224:2023 for Premium and Medium I paddy, while warehouse air may remain warm and humid for prolonged periods. Under these conditions, paddy continues to exchange water vapour with the surrounding air, and lot quality changes during storage, transport, and waiting time before milling (Atungulu et al., 2019; Müller et al., 2022; Tong et al., 2019). Shelf life should therefore be treated as condition-dependent rather than as a fixed calendar period.

Moisture exchange is a primary process governing storage stability. Paddy kernels and husks are hygroscopic: they release water when the surrounding air is dry and absorb water when it is humid. As moisture content rises, the risks of increased water activity, respiration, fungal activity, structural weakening, and visible grain defects also increase (El-Mesery et al., 2025; Garofalo et al., 2024; Wang et al., 2022). Consequently, two paddy lots with similar initial moisture contents can behave differently when exposed to different relative humidity (RH) levels. In humid equatorial regions, RH can determine whether an initially acceptable lot remains stable.

Moisture-based models quantify the environmental pressure on stored paddy. The P-Q water-transfer model proposed by Rahayoe et al. (2025), for example, represents storage behaviour through an apparent transfer capacity (P) and an apparent transfer-rate constant (Q). It is operationally simple because it does not require every input used in classical package shelf-life calculations, such as film permeability, exposed area, vapour-pressure difference, and a complete moisture-sorption isotherm. Moisture is nevertheless not the sole basis for market acceptance: a lot can exceed the permitted damaged-grain limit before reaching the selected moisture endpoint.

Classical packaged-food shelf-life models usually combine a moisture-sorption isotherm, often the Guggenheim-Anderson-de Boer (GAB) model, with package water-vapour permeability, exposed area, product mass, external vapour pressure, and a critical moisture content (Labuza & Altunakar, 2020; Robertson, 2005; Robertson & Lee, 2021; Lee & Robertson, 2022). These mechanistic approaches explicitly represent equilibrium sorption and package resistance, but predictions can be sensitive to isotherm selection and require material- and geometry-specific inputs; multidomain products may require additional transfer terms (Roca et al., 2008). In contrast, the empirical P-Q formulation estimates capacity and rate directly for the observed packaged paddy system. It was selected

here as a parsimonious method for comparing controlled RH treatments, not as a universal replacement for isotherm-based models. P and Q must be recalibrated when the variety, packaging, temperature, or humidity regime changes.

The present work, therefore, treated paddy storage life as a two-endpoint problem. The water-transfer endpoint described water gained or lost by the packaged grain, whereas the damaged-grain endpoint represented the visible quality limits in SNI 224:2023. The objectives were to (i) characterise moisture content and water mass transfer in the selected paddy variety at 30 °C and RH 50%, 70%, and 90%; (ii) estimate and validate P and Q in the water-transfer model and the damaged-grain deterioration-rate constant; and (iii) compare the two predicted endpoints and use the earlier one for a conservative storage recommendation.

MATERIALS AND METHODS

Material Packaging and Quality Endpoints

Inpari 32, an inbred paddy variety commonly cultivated in Indonesia, was obtained from Sekaran Village, Wonosari District, Klaten Regency, Central Java, Indonesia. Its initial moisture content was 13.0903 ± 0.1217% wet basis (wb). Samples were placed in woven polypropylene (PP) mini-sacks, a permeable package commonly used for paddy handling in Indonesia. Storage was conducted for 90 days at 30 °C under controlled RH levels of 50%, 70%, and 90%. The 30 °C subset was selected from the larger thesis dataset to isolate the effect of RH without adding temperature as a source of variation. Moisture content and physical-quality attributes were monitored during storage. Shelf life was defined as the predicted time required for a selected variable to reach a critical limit. The water-transfer calculation used a moisture-related limit, whereas the quality-kinetic calculation used the damaged-grain limit. Table 1 lists the SNI 224:2023 thresholds. The Medium I damaged-grain limit of 1.5% was the principal commercial endpoint; the Premium and Medium II limits were included for sensitivity analysis.

Three independent 52-L storage boxes were used per RH treatment (n = 3). Each box contained 15 mini-sacks, each holding 200 g of paddy. Three mini-sacks per box were weighed every 5 days for 90 days and averaged into a single box-level trajectory. One mini-

Table 1
Maximum SNI 224:2023 quality limits used as shelf-life endpoints for dry milled paddy

Quality component	Unit	Premium	Medium I	Medium II
Moisture content, maximum	% wb	14.0	14.0	15.0
Empty grains, maximum	%	1.0	2.0	3.0
Damaged grains, maximum	%	0.5	1.5	3.0
Foreign matter, maximum	%	0.01	0.05	0.10

sack per box was sampled every ten days for quality evaluation. The storage box, not the individual mini-sack, was the experimental unit. The mini-sacks were woven polypropylene (10 × 17 cm); thus, 45 mini-sacks were allocated to each RH treatment. Moisture content was measured thermogravimetrically on a single 5-g portion at day 0, day 90, and at 10-day intervals for quality classification. At each 10-day quality evaluation, a single 100-g portion from the sampled mini-sack was sorted visually into empty grains, damaged grains, and foreign matter. Mini-sacks within a box were therefore sampling units (subsamples), whereas the three storage boxes provided independent replicates for each RH treatment.

Moisture Content, Mass Balance, and Water-Transfer Model

Throughout this manuscript, moisture content denotes the mass fraction of water in paddy on a wet basis, whereas water mass transfer denotes the mass of water gained or lost by the packaged sample. For each RH treatment, the total sample mass, initial water mass, dry-solid mass, target water mass, and the transferred water target were calculated before fitting the P-Q model. Wet-basis moisture content was calculated as in Equation 1.

$$MC_{wb} = \left(\frac{M_w}{M_t} \times 100\right) \quad [1]$$

where MC_{wb} is moisture content on a wet basis (% wb), Mw is water mass (g), and M_t is total sample mass (g). Initial water mass and dry-solid mass were calculated as in Equations 2 and 3.

$$M_{w,0} = \left(M_t \times \frac{M_{C0}}{100}\right) \quad [2]$$

$$M_d = M_t - M_{w,0} \quad [3]$$

where $M_{w,0}$ is initial water mass (g), M_{C0} is initial moisture content (% wb), and M_d is dry-solid mass (g). For a selected target moisture content (M_{Ct}), the target water mass was calculated as Equation 4.

$$M_{w,t} = M_d \times \frac{M_{Ct}}{(100 - M_{Ct})} \quad [4]$$

The magnitude of water transferred per unit dry solid was then calculated as in Equation 5.

$$X_A, X_{A,t} = \frac{|M_{w,t} - M_{w,0}|}{M_d} \quad [5]$$

where $X_{A,t}$ is the target transferred-water magnitude (g H_2O g^{-1} dry solid). Its absolute value was used in the shelf-life equation, while the physical direction was determined from the measured moisture trajectory. Thus, RH 50% represented net desorption and RH 90% represented net adsorption.

Water mass transfer was modelled using the P-Q formulation of Rahayoe et al. (2025). The model describes cumulative transferred water per unit dry solid as an exponential approach to an apparent transfer capacity as in Equation 6.

$$X_A = P - P\,(\exp^{-Q.t}) \quad [6]$$

where $X_A(t)$ is the transferred water at storage time t (g H_2O g^{-1} dry solid), P is the apparent transfer capacity (g H_2O g^{-1} dry solid), and Q is the apparent transfer-rate constant (day^{-1}). P and Q were estimated by minimising the squared differences between observed and predicted X_A values.

Equation 7 was used to estimate moisture-based shelf life. Under net desorption, the calculated time represented the period required to reach the selected moisture-related endpoint through water loss; under net adsorption, it represented movement toward a moisture limit through water gain.

$$t_{water} = -\frac{1}{Q} ln\left[1 - \frac{X_{A,t}}{P}\right] \quad [7]$$

Damaged-Grain Deterioration Kinetics

Damaged grains were used as the physical-quality endpoint because this attribute is specified directly in SNI 224:2023 and is readily evaluated during postharvest inspection. The change in damaged-grain percentage during storage was fitted with a first-order expression as in Equation 8.

$$BR_{(t)} = BR_0 \times exp^{(kBR_t)} \quad [8]$$

where $BR_{(t)}$ is damaged-grain content at time t (%), BR0 is the initial damaged-grain content (%), and kBR is the deterioration-rate constant (day^{-1}). The time required to reach a selected damaged-grain limit was calculated as in Equation 9.

$$t_{quality} = \frac{ln\left(\frac{BR_{crit}}{BR_0}\right)}{k_{BR}} \quad [9]$$

where BR_{crit} is the SNI damaged-grain threshold for the selected class. The principal endpoint was BR_{crit} = 1.5% for Medium I; Premium (0.5%) and Medium II (3.0%) limits were sensitivity endpoints. The initial damaged-grain value was BR0 = 0.20%.

Model Validation, Cross-Validation and Decision Rule

Model performance was evaluated using the sum of squared errors (SSE), root mean square error (RMSE), and coefficient of determination (R^2). For observed values yi and predicted values ŷi, the indices were calculated as follows (Equations 10 to 12).

$$SSE = \sum(y_i - \hat{y}_i)^2 \quad [10]$$

$$RMSE = \sqrt{\frac{1}{n}\sum_{i=1}^{n}(y_i - \hat{y}_i)^2} \quad [11]$$

$$R^2 = 1 - \left[\frac{\sum(y_i - \hat{y}_i)^2}{\sum(y_i - \bar{y}_i)^2}\right] \quad [12]$$

where ȳ is the mean of the observed values and n is the number of observations in each model fit. The two shelf-life approaches were compared using absolute and relative differences. The final recommendation followed the conservative rule as in Equation 13:

$$t_{integrated} = min(t_{water}, t_{quality}) \quad [13]$$

Statistical Analysis

Descriptive results are reported as mean ± standard deviation. Differences among RH treatments were evaluated for final moisture content, P, Q, kBR, and validation indices. Analysis of variance (ANOVA) was applied at $\alpha = 0.05$, followed by Tukey's honestly significant difference (HSD) test when the RH effect was significant. Normality and homogeneity of variance were assessed before ANOVA. When assumptions were not satisfied, Welch's ANOVA or the Kruskal-Wallis test was used as a robustness check. Shelf-life values are model-derived predictions and were therefore compared descriptively rather than treated as independent experimental observations.

RESULTS AND DISCUSSION

Moisture Response and Direction of Water Transfer

The three RH environments produced distinct moisture responses (Figure 1). Paddy began at 13.0903 ± 0.1217% wb. After 90 days, moisture content decreased to 12.7166 ± 0.0076% wb at RH 50%, increased slightly to 13.3864 ± 0.0102% wb at RH 70%, and reached 15.5008 ± 0.0092% wb at RH 90%. Thus, the same initial paddy lot followed three storage trajectories: drying at RH 50%, near-equilibrium behaviour at RH 70%, and marked humidification at RH 90%.

The equilibrium moisture content (EMC) values at 30 °C explain these trajectories. EMC was 8.50%, 13.54%, and 15.74% wb at RH 50%, 70%, and 90%, respectively.

At RH 50%, final moisture remained above EMC, so desorption would probably continue during longer storage. At RH 70%, final moisture was close to EMC, indicating near-equilibrium conditions. At RH 90%, final moisture approached the high EMC and exceeded the 15% wb Medium II limit. Table 2 expresses these changes as transferred-water targets for the model. The target X_A values were 0.0408, 0.0050, and 0.0299 g H_2O g^{-1} dry solid at RH 50%, 70%, and 90%, respectively. Because $X_{A,t}$ was used as an absolute magnitude in Equation 7, its direction must be inferred from the measured moisture trajectory:

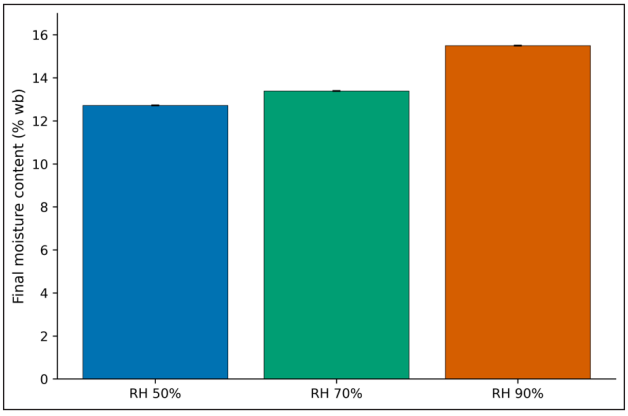

Figure 1. Final moisture content of packaged Inpari 32 paddy after 90 days at 30 °C under RH 50%, 70%, and 90%. Bars show means, and error bars show standard deviations

Table 2
Mass-balance inputs and moisture-transfer targets for packaged Inpari 32 paddy stored at 30 °C

Parameter	RH 50%	RH 70%	RH 90%
Final moisture after 90 days (% wb)	12.7166 ± 0.0076a	13.3864 ± 0.0102b	15.5008 ± 0.0092c
EMC at 30 °C (% wb)	8.50	13.54	15.74
Final moisture minus EMC (percentage points)	+4.2166	-0.1536	-0.2392
Moisture-rate constant, kM (day^{-1})	0.0038 ± 0.0001	0.0109 ± 0.0005	0.0176 ± 0.0002
Sample mass, M_t (g)	173.9836	174.2849	174.0705
Initial moisture, M_{C0} (% wb)	13.0903	13.0903	13.0903
Initial water mass, M_{w0} (g)	22.7749	22.8144	22.7863
Dry solid mass, M_d (g)	151.2087	151.4705	151.2842
Target moisture, M_{Ct} (% wb)	9.8954	13.4643	15.2896
Target water mass, M_{wt} (g)	16.6060	23.5676	27.3058
Water transfer magnitude, M_{wa} (g)	6.1690	0.7532	4.5195
Target X_A (g water g^{-1} dry solid)	0.0408	0.0050	0.0299

Note. Within the final-moisture row, means followed by different superscript letters differ significantly among RH treatments (Tukey HSD, $p < 0.05$). M_{wa} is the magnitude used in the shelf-life calculation; transfer direction is determined from the measured moisture trajectory

net water loss at RH 50%, only slight water gain at RH 70%, and marked water gain at RH 90%. This distinction is operationally important. Acceptable initial moisture content alone does not ensure safe storage when humid air continues to supply water vapour; RH control is therefore a primary barrier against increased water activity and subsequent physical deterioration (Carvalho et al., 2019; Garofalo et al., 2024; Müller et al., 2022).

Fitted P and Q Constants

The fitted constants describe the response of the tested paddy-package system to RH (Figure 2; Table 3). P was highest at RH 50% (0.0880 ± 0.0008), lowest at RH 70% (0.0062 ± 0.0002), and higher again at RH 90% (0.0335 ± 0.0001). P represents the apparent transfer capacity for the specific grain, package, temperature, RH, and model endpoint; it is not a universal material constant.

The Q parameter increased monotonically with RH, from 0.0020 ± 0.0000 day^{-1} at RH 50% to 0.0092 ± 0.0008 day^{-1} at RH 70% and 0.0212 ± 0.0004 day^{-1} at RH 90%. Thus, Q at RH 90% was approximately 10.6 times its value at RH 50%, indicating a much faster

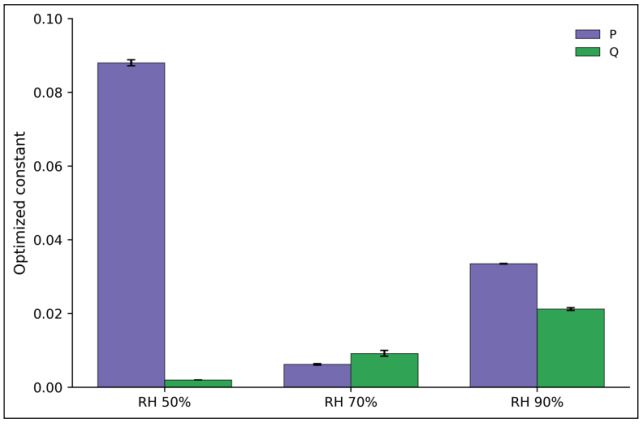

Figure 2. Optimised apparent transfer capacity (P) and transfer-rate constant (Q) for packaged Inpari 32 paddy stored at 30 °C under RH 50%, 70%, and 90%. Bars show means, and error bars show standard deviations

Table 3
Optimised P and Q constants and moisture-based shelf-life predictions for packaged Inpari 32 paddy at 30°C

RH (%)	P	Q (day^{-1})	Water-Transfer Shelf Life (days)
50	0.0880 ± 0.0008	0.0020 ± 0.0000	312
70	0.0062 ± 0.0002	0.0092 ± 0.0008	176
90	0.0335 ± 0.0001	0.0212 ± 0.0004	105

Note. P and Q were optimized from observed and predicted XA values and are specific to the tested variety, packaging, temperature, and RH

approach to the system-specific transfer asymptote. This pattern is physically consistent with a stronger water-vapour driving force under humidification. The broader temperature-RH dataset showed the same trend, with mean Q increasing from 0.0024 ± 0.0013 day^{-1} at RH 50% to 0.0242 ± 0.0110 day^{-1} at RH 90%. RH, therefore, affected both the apparent amount of water transferred and the rate of transfer.

Validation of the Water-Transfer Model

The water-transfer model closely fitted the observed X_A data during the 90-day experiment (Figure 3 and Table 4). R^2 was 0.9913 ± 0.0042 at RH 50%, 0.9928 ± 0.0016 at RH 70%, and 0.9990 ± 0.0003 at RH 90%. Together with the low error values, these results show that predicted transferred-water magnitudes tracked the observations within the calibration period. They support using Equation 7 for endpoint projection, while predictions beyond 90 days remain extrapolations.

RMSE ranged from 2.69×10^{-4} to 8.64×10^{-4} g H_2O g^{-1} dry solid, which was small relative to the transferred-water magnitudes used for shelf-life calculation. Goodness of fit does not represent storage safety. RH 90% yielded the highest R^2 because its strong,

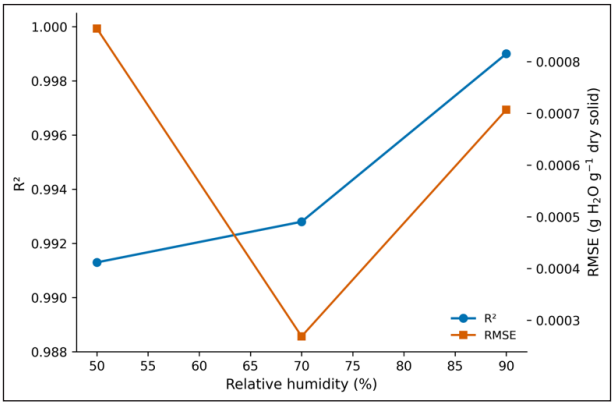

Figure 3. Goodness-of-fit statistics for the water mass-transfer model at 30 °C under RH 50%, 70%, and 90%. R^2 is the coefficient of determination, and RMSE is the root mean square error

Table 4
Validation statistics for the water mass-transfer model of packaged Inpari 32 paddy at 30 °C

RH (%)	R^2	SSE	RMSE (g H_2O g^{-1} dry solid)
50	0.9913 ± 0.0042	2.36×10^{-6}	8.64×10^{-4}
70	0.9928 ± 0.0016	2.22×10^{-8}	2.69×10^{-4}
90	0.9990 ± 0.0003	1.54×10^{-6}	7.07×10^{-4}

Note. RH = relative humidity; R^2 = coefficient of determination; SSE = sum of squared errors; RMSE = root mean square error. Statistics were calculated from observed and predicted X_A values

monotonic water-uptake signal was fitted consistently; nevertheless, the condition was hazardous because the moisture content exceeded the Medium II limit. The high fit quality at RH 90%, therefore, quantifies the hazardous trajectory rather than endorsing the storage condition.

Damaged-Grain Kinetics as a Quality Endpoint

Moisture transfer describes environmental pressure on the stored grain, whereas market decisions are often based on physical quality. Damaged grains were therefore modelled separately. The first-order rate constant kBR increased from 0.0068 ± 0.0001 day^{-1} at RH 50% to 0.0127 ± 0.0002 day^{-1} at RH 70% and 0.0213 ± 0.0002 day^{-1} at RH 90% (Figure 4A). The approximately threefold increase from RH 50% to RH 90% indicates much faster accumulation of visible defects and helps explain the reduction in Medium I quality-based shelf life from 296 to 95 days.

The selected SNI quality class strongly affected the predicted endpoint (Figure 4B). Under SNI 224:2023, Premium, Medium I, and Medium II paddy permit maximum damaged-grain contents of 0.5%, 1.5%, and 3.0%, respectively. The stricter Premium threshold was therefore reached much earlier than the Medium I and Medium II thresholds. Using the principal Medium I limit, predicted shelf life decreased from 296 days at RH 50% to 159 days at RH 70% and 95 days at RH 90%. Humid storage thus shortened shelf life by increasing both moisture content and the rate at which visible defects accumulated.

The RH effect on damaged grains is consistent with established storage behaviour. Moisture uptake can soften and stress the kernel structure, increase susceptibility to cracking, and create local wet zones within a bag. Such spatial variation may be obscured by a single mean moisture value but can appear as damaged grains during inspection.

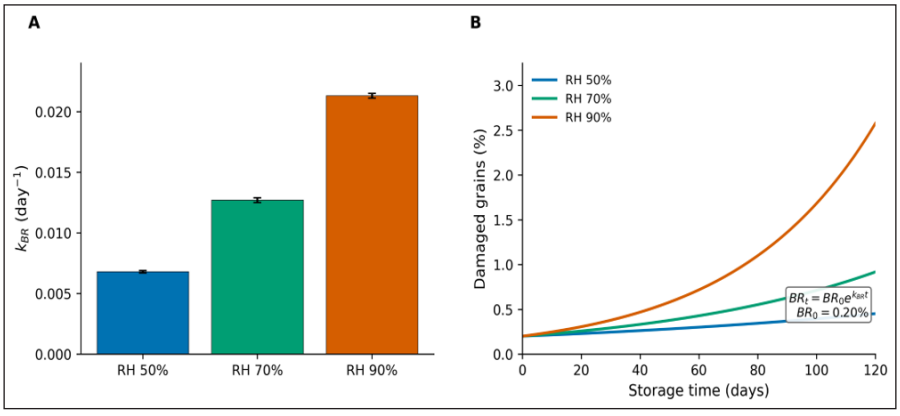

Figure 4. Damaged-grain deterioration of packaged Inpari 32 paddy at 30 °C. (A) First-order deterioration-rate constants (kBR), with error bars showing standard deviations; (B) model-predicted damaged-grain trajectories from BR0 = 0.20% under RH 50%, 70%, and 90%

Controlled-condition studies have likewise reported humidity-related physicochemical deterioration in stored rice (Garofalo et al., 2024), while work with polypropylene grain bags has shown that package and interstitial RH influence seed quality and pest risk (Rizwan et al., 2022). These studies support the direction of the present response, although numerical shelf lives are not directly comparable because commodities, packages, temperatures, and failure criteria differ.

The damaged-grain model also fitted acceptably, although less tightly at RH 90% than the water-transfer model. R^2 was 0.9913 ± 0.0065, 0.9872 ± 0.0066, and 0.9737 ± 0.0126 at RH 50%, 70%, and 90%, respectively. The larger error at RH 90% is plausible because physical defects vary among kernels depending on husk condition, local moisture exposure, and resistance to breakage, particularly during humid storage. Table 5 summarises the fitted damaged-grain kinetic constants, model-fit statistics, and predicted times to the Premium, Medium I, and Medium II quality endpoints for each RH treatment.

Comparison of Moisture and Quality-Based Endpoints

Both modelling routes ranked the RH treatments in the same order but yielded different endpoints. The water-transfer model predicted shelf lives of 312, 176, and 105 days at RH 50%, 70%, and 90%, respectively. The Medium I damaged-grain model yielded shorter predictions of 296, 159, and 95 days (Figure 5A). The differences were 16, 17, and 10 days, corresponding to reductions of 5.13%, 9.66%, and 9.52%, respectively, relative to the moisture-based predictions.

This difference is not contradictory because the models answer different questions. The P-Q model estimates when grain reaches a moisture-related endpoint, whereas the damaged-grain model estimates when a lot no longer meets a physical-quality limit. Their agreement in RH ranking strengthens the storage-risk interpretation, and the earlier damaged-grain

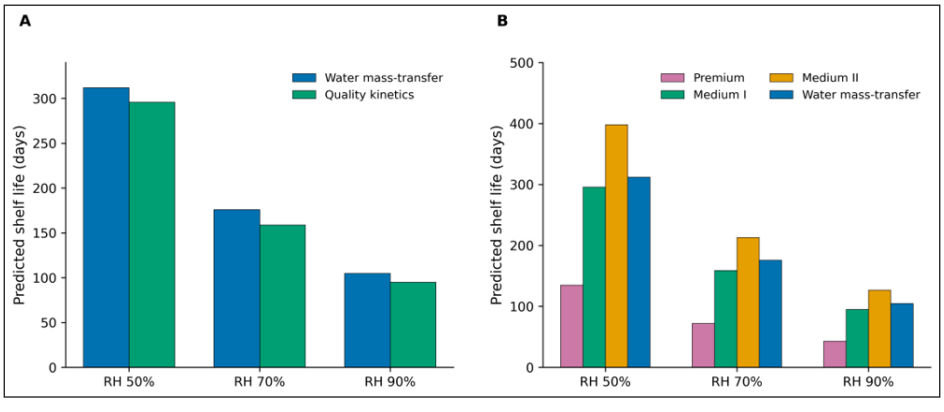

Figure 5. Shelf-life prediction and endpoint sensitivity for packaged Inpari 32 paddy at 30 °C. (A) Comparison of water mass-transfer and Medium I quality-kinetic shelf life; (B) sensitivity to the SNI 224:2023 Premium, Medium I, and Medium II damaged-grain endpoints

Table 5
Damaged-grain kinetic constants, validation statistics, and quality-based shelf-life predictions at 30 °C

RH (%)	kBR (day^{-1})	R^2	SSE	RMSE	Premium Endpoint (days)	Medium I Endpoint (days)	Medium II Endpoint (days)
50	0.0068 ± 0.0001	0.9913 ± 0.0065	0.0009 ± 0.0005	0.0077 ± 0.0059	135	296	398
70	0.0127 ± 0.0002	0.9872 ± 0.0066	0.0079 ± 0.0031	0.0217 ± 0.0181	72	159	213
90	0.0213 ± 0.0002	0.9737 ± 0.0126	0.1210 ± 0.0568	0.0686 ± 0.0875	43	95	127

Note. Shelf life was calculated from BR0 = 0.20% using SNI 224:2023 damaged-grain limits of 0.5%, 1.5%, and 3.0% for Premium, Medium I, and Medium II, respectively. RH = relative humidity; kBR = damaged-grain deterioration-rate constant; SSE = sum of squared errors; RMSE = root mean square error

endpoint provides a more conservative operational decision for Medium I paddy. Endpoint sensitivity reinforces this conclusion (Figure 5B): Premium quality required much shorter shelf lives, whereas the less restrictive Medium II limit permitted longer storage and made the water-transfer endpoint limiting in all three treatments. Shelf-life predictions should therefore always be reported with the intended market grade and failure criterion.

This dual-endpoint result also aligns with broader shelf-life research. Isotherm-based predictions for packaged dry foods vary with the selected sorption equation (Lee & Robertson, 2022; Robertson & Lee, 2021), while kinetic and time-to-failure approaches can yield different dates because they define failure differently (Kosegarten et al., 2022). The 5.13-9.66% differences observed here therefore quantify endpoint sensitivity for this paddy-package system rather than model disagreement.

Table 6 presents the absolute and relative differences between the water-transfer and Medium I damaged-grain endpoints and identifies the earlier endpoint used for the integrated storage decision

The integrated decision matrix in Figure 6 translates the model comparison into storage guidance. Damaged-grain kinetics was limiting for Premium and Medium I targets at every RH, whereas the water-transfer endpoint was limiting for Medium II because its

Table 6
Direct comparison of water-transfer and Medium I damaged-grain shelf-life predictions

RH (%)	Water-transfer Shelf Life (days)	Quality-kinetic Shelf Life (days)	Absolute Difference (days)	Quality Endpoint Earlier by (%)	Integrated Medium I Decision
50	312	296	16	5.13	296 days
70	176	159	17	9.66	159 days
90	105	95	10	9.52	95 days

Note. The integrated decision is the earlier predicted endpoint. Percentages are relative to the water-transfer prediction

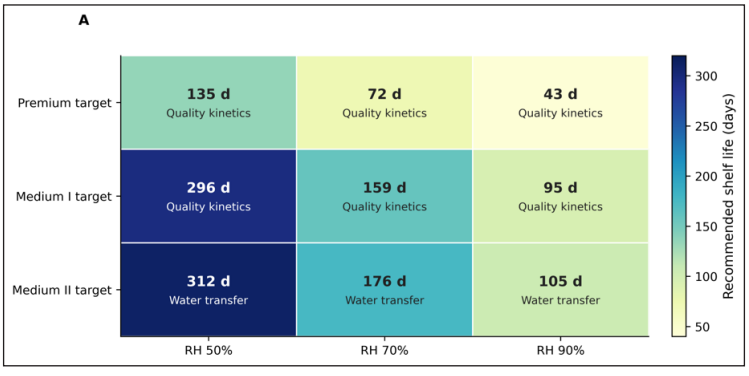

Figure 6. Integrated conservative shelf-life decision for packaged Inpari 32 paddy at 30 °C across RH levels and SNI quality targets. Each cell gives the earlier predicted shelf life and the limiting model

damaged-grain threshold was less restrictive. For Medium I paddy at 30 °C in woven PP sacks, recommended shelf lives were 296 days at RH 50%, 159 days at RH 70%, and 95 days at RH 90%. Lowering RH from 90% to 70% increased the predicted safe period by 64 days (67%), and lowering it from 70% to 50% added 137 days (86%); overall, RH 50% provided more than three times the predicted safe period at RH 90%. These differences directly affect inspection frequency, stock rotation, and decisions on drying, dehumidification, or improved barrier packaging.

RH-based P-Q Interpolation and Storage Decision Support

For decision support, P and Q were expressed as empirical RH interpolation equations over the tested range. These equations are scenario tools, not independently validated predictive models. They should not be applied outside RH 50-90% or to other varieties, packages, or temperatures without recalibration and validation, as in Equations 14 and 15.

$$P = 0.000136RH^2 - 0.020454RH + 0.769787 \quad [14]$$

$$Q = 5.982 \times 10^{-6}RH^2 - 0.000358RH + 0.004952 \quad [15]$$

where RH is expressed as a percentage. Figure 7 shows the interpolating curves. P reached a minimum near RH 70%, whereas Q increased over the tested range, indicating that RH affected both the apparent transfer capacity and the transfer rate. Because a quadratic curve was passed through only three RH levels, the reported $R^2 = 1.000$ reflects exact interpolation rather than independent evidence of predictive performance.

A simple example illustrates the interpolation. Paddy entering storage at 14% wb is already at the Premium and Medium I moisture limit and has only a small margin before the 15% wb

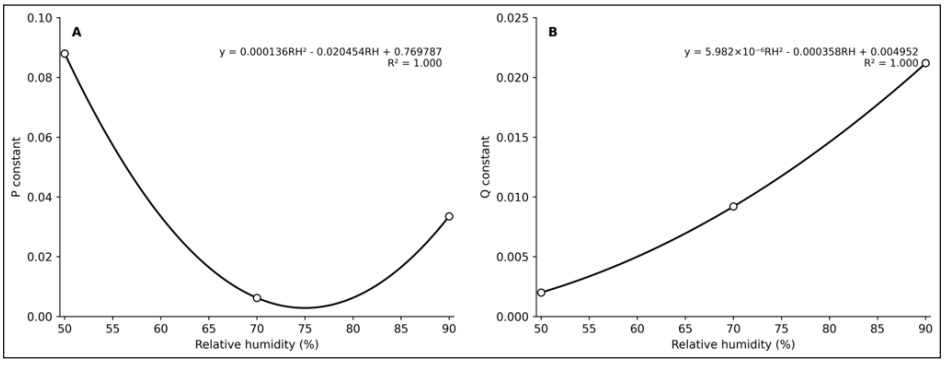

Figure 7. Empirical RH-dependent interpolation of water mass-transfer constants at 30 °C. (A) Apparent transfer capacity P; (B) apparent transfer-rate constant Q
Note. Open circles are fitted values at RH 50%, 70%, and 90%; solid curves are quadratic interpolations for scenario exploration only within the calibrated RH range

Medium II limit. Increasing from 14% to 15% wb requires approximately 0.0137 g H_2O g^{-1} dry solid. At RH 90%, Equation 7, with the fitted P and Q values, predicts this gain in approximately 25 days. At RH 70%, P is lower than the required increase, so the model does not predict that 15% wb will be reached within its calibrated asymptote; paddy beginning at 14% wb nevertheless requires close monitoring. At RH 50%, the observed direction was desorption, so movement toward a higher moisture limit was not applicable. Table 7 summarises the RH-specific moisture-transfer scenarios, predicted implications of the 15% wb endpoint, and corresponding storage-management actions for paddy entering storage at 14% wb.

Overall, RH 50% was the safest condition tested; RH 70% was a transition condition requiring routine inspection; and RH 90% was unsuitable for long-term storage. Paddy should preferably enter storage below 14% wb; lots near this value should be dried further or stored only under well-controlled humidity.

Assumptions, Scope, and Limitations

The models assume constant temperature and RH, time-invariant P, Q, and kBR values, a spatially averaged moisture state, first-order damaged-grain development from BR0 = 0.20%, and unchanged package properties. The experiment evaluated one paddy variety, one permeable mini-sack format, one temperature, and three fixed RH levels.

Table 7
Scenario-based interpretation for packaged paddy entering storage at 14% wb and 30 °C

Storage RH (%)	P	Q (day^{-1})	Moisture Endpoint Considered	Predicted Interpretation	Recommended Action
50	0.0880	0.0020	15% wb	Not applicable for moisture gain because the observed transfer direction was desorption.	Moisture risk is low, but damaged grains should still be monitored for long storage.
70	0.0062	0.0092	15% wb	The fitted P value is lower than the water increase required to reach 15% wb; the model therefore does not predict reaching 15% wb within the calibrated asymptote.	Acceptable only with monitoring because 14% wb is already the Premium/ Medium I moisture limit.
90	0.0335	0.0212	15% wb	Approximately 25 days from 14% to 15% wb.	Avoid prolonged storage; use rapid drying, RH control, stock rotation, or improved barrier packaging.

Note. The scenario uses Equation 7 and the P-Q interpolation equations at 30 °C. It addresses moisture transfer only and does not replace damaged-grain monitoring

It did not explicitly represent moisture gradients within sacks, fungi, insects, germination, sensory quality, mechanical handling, or interactions among these failure modes.

Model fit was evaluated within 90 days, but several shelf-life endpoints extend to 95-312 days and are therefore extrapolations. The RH interpolation is also based on only three levels, so its quadratic form is descriptive rather than independently validated. The numerical predictions should consequently be applied only to the tested Inpari 32-PP-sack-30 °C system and with an operational safety margin. Future work should use longer trials, independent validation data, commercial sack sizes, multiple cultivars and packaging barriers, and fluctuating warehouse temperature-RH profiles.

CONCLUSION

This study linked moisture- and quality-based shelf-life endpoints for Inpari 32 paddy in woven PP sacks at 30 °C. RH 50% produced net desorption, RH 70% produced a near-equilibrium response, and RH 90% increased moisture content to 15.5008% wb within 90 days. The P-Q model closely fitted the observed 90-day moisture data (R^2 = 0.9913-0.9990), and Q increased from 0.0020 to 0.0212 day^{-1} between RH 50% and RH 90%. Damaged-grain deterioration also accelerated, with kBR increasing from 0.0068 to 0.0213 day^{-1}. At the Medium I endpoint, quality kinetics predicted shelf lives of 296, 159, and 95 days, compared with 312, 176, and 105 days from the water-transfer model. Moisture-only prediction can therefore overestimate the commercially acceptable period. For paddy near 14% wb, RH 90% may reduce the margin to 15% wb to approximately 25 days. Operationally, paddy should be dried below 14% wb, prolonged exposure to RH 90% should be avoided, and RH and damaged grains should be monitored during stock rotation. Because several predicted endpoints extend beyond the 90-day experiment, commercial decisions should apply a safety margin until the model has been validated under longer, fluctuating warehouse conditions and across varieties and packaging systems.

ACKNOWLEDGEMENT

The authors thank the Department of Agricultural and Biosystems Engineering, Faculty of Agricultural Technology, Universitas Gadjah Mada, for laboratory support during the storage experiment.

DATA AVAILABILITY

The data used in this study are available from the corresponding author upon reasonable request.

DECLARATION

Ethics approval and consent to participate: Not applicable.

CONFLICTS OF INTEREST

The authors declare no competing interests.

FUNDING INFORMATION

This research was funded by Universitas Gadjah Mada through the Research Assistantship Programme, contract number 4588/UN1.P4/Dit-Lit/PT.01.03/2025. The authors gratefully acknowledge the financial support provided by the Research Assistance Program 2025 under Grant No. 4401/UN1.P1/Dit-Lit/PT.01.01/2025, dated 28 April 2025.

REFERENCES

Ansari, A., Pranesti, A., Telaumbanua, M., Alam, T., Taryono, Wulandari, R. A., Nugroho, B. D. A., & Supriyanta. (2023). Evaluating the effect of climate change on rice production in Indonesia using multimodelling approach. *Heliyon, 9*(9), Article e19639. https://doi.org/10.1016/j.heliyon.2023.e19639

Atungulu, G. G., Kolb, R. E., Karcher, J., & Shad, Z. M. (2019). Postharvest technology: Rice storage and cooling conservation. In *Rice: Chemistry and technology* (4th ed., pp. 517-555). AACC International Press. https://doi.org/10.1016/B978-0-12-811508-4.00016-2

Carvalho, M. O., Fradinho, P., Martins, M. J., Magro, A., Raymundo, A., & de Sousa, I. (2019). Paddy rice stored under hermetic conditions: The effect of relative humidity, temperature and storage time in suppressing *Sitophilus zeamais* and impact on rice quality. *Journal of Stored Products Research, 80*, 21-27. https://doi.org/10.1016/j.jspr.2018.11.002

El-Mesery, H. S., Omran, A. A., Adelusi, O. A., Kaveh, M., Okechukwu, V. O., Hu, Z., Salem, A., & Badawy, S. A. (2025). Evaluating and predicting the impact of storage conditions and packaging materials on the physical properties of paddy rice using machine learning approaches and artificial neural networks. *Journal of Stored Products Research, 112*, Article 102659. https://doi.org/10.1016/j.jspr.2025.102659

Garofalo, M. A., Salazar, R., Palacios-Ponce, A., Cornejo, F., & Corradini, M. G. (2024). Rice storage under controlled conditions: Changes in its physicochemical and functional properties. *Journal of Stored Products Research, 105*, Article 102236. https://doi.org/10.1016/j.jspr.2023.102236

Kosegarten, C. E., Ramírez-Corona, N., López-Malo, A., & Mani-López, E. (2022). Wheat-based fried snacks shelf-life prediction using kinetic, probabilistic, and time-to-fail models. *Journal of Food Processing and Preservation, 46*(5), Article e16548. https://doi.org/10.1111/jfpp.16548

Labuza, T. P., & Altunakar, B. (2020). Diffusion and sorption kinetics of water in foods. In *Water activity in foods: Fundamentals and applications* (pp. 287-309). https://doi.org/10.1002/9781118765982.ch12

Lee, D. S., & Robertson, G. L. (2022). Shelf-life estimation of packaged dried foods as affected by choice of moisture sorption isotherm models. *Journal of Food Processing and Preservation, 46*(3), Article e16335. https://doi.org/10.1111/jfpp.16335

Müller, A., Nunes, M. T., Maldaner, V., Coradi, P. C., de Moraes, R. S., Martens, S., Leal, A. F., Pereira, V. F., & Marin, C. K. (2022). Rice drying, storage and processing: Effects of post-harvest operations on grain quality. *Rice Science, 29*(1), 16-30. https://doi.org/10.1016/j.rsci.2021.12.002

Rahayoe, S., Diposari, R. P., Munawwaroh, F. D., Susanti, D. Y., & Bintoro, N. (2025). Prediction of the shelf life of porang chips and flour using a mathematical model of water mass transfer. *Discover Food, 5*(1). https://doi.org/10.1007/s44187-025-00435-1

Rizwan, M., Atta, B., Ali, M. Y., Ashraf, I., Arshad, M., Tahir, M., Rizwan, M., Sabir, A. M., Shehzadi, N., & Khalid, U. Bin. (2022). The comparison of interstitial relative humidity and temperatures of hermetic and polypropylene bag for wheat grain storage under different agro-climatic conditions of rice-wheat ecosystem of Pakistan: Effect on seed quality and protection against insect pests. *Journal of Stored Products Research, 96*, Article 101936. https://doi.org/10.1016/j.jspr.2022.101936

Robertson, G. L. (2005). *Food packaging: Principles and practice*. CRC Press. https://doi.org/10.1201/9781420056150

Robertson, G. L., & Lee, D. S. (2021). Comparison of linear and GAB isotherms for estimating the shelf life of low moisture foods packaged in plastic films. *Journal of Food Engineering, 291*, Article 110317. https://doi.org/10.1016/j.jfoodeng.2020.110317

Roca, E., Broyart, B., Guillard, V., Guilbert, S., & Gontard, N. (2008). Predicting moisture transfer and shelf-life of multidomain food products. *Journal of Food Engineering, 86*(1), 74-83. https://doi.org/10.1016/j.jfoodeng.2007.09.012

Santosa, Y. T., Kurniasih, B., Alam, T., Handayani, S., Supriyanta, Ansari, A., & Taryono. (2024). Investigating the dynamics of upland rice (*Oryza sativa* L.) in rainfed agroecosystems: An in-depth analysis of yield gap and strategic exploration for enhanced production. *Frontiers in Sustainable Food Systems, 8*, Article 1384530. https://doi.org/10.3389/fsufs.2024.1384530

National Standardization Agency of Indonesia. (2023). *SNI 224:2023* (Publication No. 38/KEP/BSN/3/2023). https://icert.id/wp-content/uploads/2025/11/SNI-224-2023-Gabah.pdf

Tong, C., Gao, H., Luo, S., Liu, L., & Bao, J. (2019). Impact of postharvest operations on rice grain quality: A review. *Comprehensive Reviews in Food Science and Food Safety, 18*(3), 626-640. https://doi.org/10.1111/1541-4337.12439

Wang, Q., Zhang, D., Zhao, L., Liu, J., Shang, B., Yang, W., Duan, X., & Sun, H. (2022). Metabolomic analysis reveals insights into deterioration of rice quality during storage. *Foods, 11*(12), Article 1729. https://doi.org/10.3390/foods11121729

Pertanika J. Trop. Agric. Sci. 49 (5): 2275 - 2302 (2026)

PERTANIKA JOURNALS

TROPICAL AGRICULTURAL SCIENCE

Journal homepage: http://www.pertanika.upm.edu.my/

Visible-Near Infrared Spectroscopy for Predicting Carotenoid and Antioxidant Composition in Healthy and Bronzed Jackfruit (*Artocarpus heterophyllus* Lam. cv. Tekam Yellow) at Different Maturity Stages

Kok Jeng Lim[1]*, Phebe Ding[1], Nazmi Mat Nawi[2,3], and Mashitah Jusoh[1]

[1]*Department of Crop Science, Faculty of Agriculture, Universiti Putra Malaysia, 43400 UPM Serdang, Selangor Malaysia*

[2]*Department of Biological and Agricultural Engineering, Faculty of Engineering, Universiti Putra Malaysia, 43400 UPM Serdang, Selangor, Malaysia*

[3]*Institute of Plantation Studies, Universiti Putra Malaysia, 43400 UPM Serdang, Selangor, Malaysia*

ABSTRACT

Jackfruit bronzing disease (JBD), associated with *Pantoea stewartii* subsp. *stewartii*, is a quality disorder in Malaysian jackfruit that causes internal discoloration without obvious changes to the rind. This study evaluated visible-near infrared spectroscopy (Vis-NIRS) for predicting selected carotenoid and antioxidant-related attributes in intact jackfruit cv. Tekam Yellow at 10, 12, and 14 weeks after anthesis (WAA). Reflectance spectra were collected at 30 rind locations per fruit within the 500–950 nm range. Partial least squares regression (PLSR) models were developed using alternative spectral preprocessing methods. Flesh β-carotene, lycopene, total flavonoid content (TFC), and total phenolic content (TPC) served as reference variables. Prediction performance varied according to maturity stage, fruit condition, target attribute, and spectral preprocessing. Among healthy fruit, the β-carotene model at 12 WAA achieved an Rp^2 of 0.88 and a residual predictive deviation (RPD) of 4.12, while the TFC model at 10 WAA yielded an Rp^2 of 0.98 and an RPD of 43.17. For bronzing-affected fruit at 14 WAA, the lycopene model achieved an Rp^2 of 0.94 and an RPD of 12.36, although this high RPD should be interpreted alongside prediction error and validation-data distribution. At 12 WAA, TPC models achieved Rp^2 values of 0.87 and 0.92 for healthy and bronzing-affected fruit, respectively, with corresponding RPD values of 3.57 and 2.54. Spectral regions near 760 and 945 nm contributed to several models. Overall, rind-based Vis-NIRS demonstrated potential

ARTICLE INFO

Article history:
Received: 26 June 2026
Accepted: 17 September 2026
Published: 30 October 2026

DOI: https://doi.org/10.47836/pjtas.49.5.09

E-mail addresses:
limkokjeng@gmail.com (Kok Jeng Lim)
phebe@upm.edu.my (Phebe Ding)
nazmimat@upm.edu.my (Nazmi Mat Nawi)
mashitahj@upm.edu.my (Mashitah Jusoh)
* Corresponding author

© Universiti Putra Malaysia Press

for predicting selected internal biochemical attributes under specific maturity and fruit-condition combinations, although performance varied among models.

Keywords: Carotenoids, flavonoid, jackfruit bronzing disease, partial least squares regression, phenolics, visible-near infrared spectroscopy

INTRODUCTION

Jackfruit (*Artocarpus heterophyllus* Lam.) is an important tropical fruit crop widely grown in South and Southeast Asia and a key source of income for smallholder growers. In Malaysia, cv. Tekam Yellow is commercially valued for its yellow flesh colour, characteristic aroma, relatively high soluble solids content, and firm aril texture, which make the fruit suitable for both fresh consumption and processing (Mijin & Ding, 2020). Production of this cultivar has increased with market demand, further highlighting its importance to the local jackfruit industry (Mijin et al., 2021; Lim et al., 2026a). Despite this, obtaining fruit with consistent maturity and internal quality remains difficult because the fruit's internal condition cannot always be accurately judged from its external appearance.

Jackfruit maturity is generally assessed using visible or sensory characteristics, including spine development and flattening, rind colour, leaf condition, and aroma. These characteristics are useful in practice, but their appearance can vary with orchard and environmental conditions, which may lead to differences in harvest maturity and eating quality (Jarman et al., 2023; Lim et al., 2026a). As the fruit develops, its chemical composition also changes. Pigments such as β-carotene and lycopene contribute to the characteristic colour of the edible tissues, while flavonoids and phenolic compounds form part of the antioxidant profile of the fruit. Changes in these compounds therefore provide useful information about the biochemical condition of the fruit during development.

Jackfruit bronzing disease (JBD) presents an additional quality problem in Malaysian production. The disease has been associated with *Pantoea stewartii* subsp. *stewartii* (Zulperi et al., 2017; Abidin et al., 2020) and is characterised by brownish to reddish discoloration within the edible tissues. In some affected fruits, the external rind shows little or no obvious indication of the internal disorder. This makes visual inspection alone unreliable for determining whether an apparently normal fruit is affected internally. Bronzing disease has also been reported in other jackfruit-producing regions, including China (Zhao et al., 2023; Abidin et al., 2021). A method that can provide information about internal fruit quality without cutting the fruit would therefore be useful for jackfruit quality assessment.

Visible-near infrared spectroscopy (Vis-NIRS) has been used to obtain information about fruit quality from spectral measurements taken without destructive sampling. The technique has been applied to intact and structurally complex fruits for estimating physicochemical properties and for studying physiological changes. For jackfruit, previous

work has shown that spectral information obtained from the fruit surface can be used to estimate attributes such as moisture and soluble solids content (Abdullah, 2019; Abdullah et al., 2018, 2021). Studies on other tropical and structurally complex fruits, including durian, kiwifruit, and mango, have also reported relationships between surface spectra and internal quality attributes (Clark et al., 2004, 2022; Li et al., 2023; Saechua et al., 2021).

However, using spectra collected from the rind to estimate biochemical properties measured inside a thick-skinned fruit such as jackfruit is not straightforward. The spectrum obtained from the rind should not be regarded as a direct measurement of the compounds present in the internal flesh. Instead, the relationship may arise from changes that occur together during fruit development or disease progression, including differences in tissue composition, water status, structural characteristics, and other physiological processes. Therefore, in this study, rind-based Vis-NIRS is treated as an indirect prediction method, where spectral information collected externally is related statistically to reference measurements of internal biochemical attributes.

Another consideration is the variation in rind structure across the surface of an intact jackfruit. A single scanning point may not adequately represent the spectral variability of the whole fruit. Collecting spectra from several locations can provide a broader representation of this surface variability and has been applied in studies involving heterogeneous fruit matrices (Li et al., 2023). Nevertheless, the use of multiple rind positions to relate surface spectral variation to internal biochemical attributes in healthy and bronzing-affected jackfruit has received limited attention.

The present study was designed to address this gap by examining both the biochemical variation associated with maturity and fruit condition and the usefulness of multi-position rind-based Vis-NIRS for prediction. β-Carotene, lycopene, total flavonoid content (TFC), and total phenolic content (TPC) were measured in healthy and bronzing-affected cv. Tekam Yellow fruit harvested at 10, 12, and 14 weeks after anthesis (WAA). Vis-NIR spectra collected from the rind were then used to develop partial least squares regression (PLSR) models. The effects of spectral preprocessing, maturity stage, and fruit condition on model performance were also examined.

The study was based on the expectation that biochemical changes occurring during fruit maturation and bronzing development may be accompanied by measurable changes in the rind spectral response. The specific objectives were to: (i) characterise maturity- and bronzing-associated changes in selected carotenoid and antioxidant-related attributes of Tekam Yellow jackfruit; (ii) evaluate multi-position rind-based Vis-NIRS for predicting these internal attributes using PLSR; and (iii) determine the spectral preprocessing and modelling conditions that provided useful prediction performance for healthy and bronzing-affected fruit. The results are intended to provide a basis for further work on non-destructive assessment of maturity- and bronzing-associated quality variation in jackfruit.

MATERIALS AND METHODS

Plant Material and Harvesting Stages

Jackfruit (*Artocarpus heterophyllus* Lam.) cv. Tekam Yellow was obtained from a commercial plantation operated by Agro BS Sdn. Bhd. in Jasin, Melaka, Malaysia (2°23′31.50″ N, 102°25′7.48″ E). Fruit sampling was carried out over three harvesting seasons, which were treated as three independent batches. A total of 54 syncarps were collected. Both healthy and bronzing-affected fruits were sampled at 10, 12, and 14 weeks after anthesis (WAA), with six fruits collected at each maturity stage in each batch.

The three harvesting stages were selected to represent different points of fruit development and to capture changes in biochemical composition associated with maturity and bronzing. The WAA of each fruit was determined from the anthesis records maintained at the plantation. After harvesting, the fruits were placed in plastic sacks and handled carefully to avoid unnecessary mechanical damage. The fruits were transported to the laboratory at Universiti Putra Malaysia within 2 hours of harvest for spectral measurements and subsequent chemical analysis.

Spectral Data Collection

Visible-near infrared (Vis-NIR) spectra were collected using an Ocean Optics HR4000 spectrometer (Ocean Optics Inc., Winter Park, FL, USA), which covers the 200-1100 nm wavelength range. For the multivariate analysis, the spectral region from 500 to 950 nm was used. Measurements were made in reflectance mode with a 1.5-cm scanning aperture.

Each intact fruit was measured at 30 locations on the rind. The measurement locations were distributed among five latitudinal zones: top (A), middle-top (B), middle (C), middle-bottom (D), and bottom (E). Six positions were measured within each zone (A1-A6, B1-B6, C1-C6, D1-D6, and E1-E6), giving 30 scanning positions per fruit. This arrangement was used to capture variation across the rind surface rather than relying on a single measurement location.

The HL-2000 halogen light source (Ocean Optics Inc., USA) was allowed to warm up for at least 30 min before measurements were started. A white reference standard, corresponding to approximately 100% reflectance, was recorded before each measurement session. Three spectra were collected at each position and averaged to obtain one representative spectrum for that location. Measurements were made inside a black chamber using a fibre-optic probe connected to the spectrometer and light source. The probe was placed directly against the rind surface during scanning. The measurements were carried out in a darkened room to minimise the effect of ambient light.

The decision to collect spectra from the rind was based partly on previous jackfruit studies showing that surface measurements can provide information related to physicochemical properties. Abdullah (2019) examined shortwave near-infrared

spectroscopy for jackfruit physicochemical properties, while Abdullah *et al*. (2018, 2021) reported the prediction of moisture content and soluble solids content using spectra collected from the peel surface. In the present study, spectra collected from the rind were paired with destructive measurements from the corresponding fruit tissues so that their statistical relationship with internal biochemical attributes could be examined.

Reference Methods

Determination of Flesh Carotenoids

Carotenoids were extracted following the procedure of Nagata and Yamashita (1992), with minor modifications. Approximately 5 g of fresh jackfruit flesh was homogenised with 50 mL of chilled acetone using a high-speed blender (Model MX V2N, National, Malaysia) for 1 min. The homogenate was then filtered through Whatman No. 1 filter paper. A 20-mL portion of the filtrate was transferred to a separate container and mixed with 20 mL of petroleum ether. Distilled water (5 mL) was then added to facilitate phase separation. The upper petroleum ether layer was collected, and its absorbance was measured at 663, 645, 505, and 453 nm using a UV-Visible spectrophotometer.

The concentrations of β-carotene and lycopene were calculated using the following Equations 1 and 2:

$$\textbf{β-carotene (mg/100 mL of extract)} = 0.216 \times A663 - 1.22 \times A645 - 0.304 \times A505 + 0.452 \times A453 \quad [1]$$

$$\textbf{Lycopene (mg/100 mL of extract)} = -0.0458 \times A663 + 0.204 \times A645 + 0.372 \times A505 - 0.0806 \times A453 \quad [2]$$

The carotenoid concentrations were expressed as milligrams per kilogram of fresh weight (mg/kg FW).

Assessment of Flesh Antioxidant Contents

Fresh jackfruit flesh was cut into approximately 1-cm³ pieces and homogenised using a food blender (Model MX V2N, National, Malaysia). A 1-g portion of the homogenised sample was extracted with 10 mL of 50% (v/v) methanol. The mixture was centrifuged at 4750 rpm for 10 min using a tabletop centrifuge (Model 1370R, Scanspeed, Denmark). The resulting supernatant was collected and used for the determination of total flavonoid content (TFC) and total phenolic content (TPC). The remaining extract was stored at -20°C until analysis.

Total Flavonoid Content. Total flavonoid content was measured using the colorimetric procedure adapted from Abu Bakar et al. (2009). An aliquot of 0.5 mL of extract was mixed with 2.25 mL of distilled water and 0.15 mL of 5% (w/v) sodium nitrite ($NaNO_3$). After 6 min, 0.3 mL of 10% (w/v) aluminium chloride ($AlCl_3$) was added and allowed to react for another 5 min. Then, 1.0 mL of 1 M sodium hydroxide (NaOH) was added. Absorbance was measured at 510 nm using a UV-Visible spectrophotometer (Multiskan Go, Thermo Fisher Scientific, UK). Quercetin was used as the calibration standard, and the results were expressed as milligrams of quercetin equivalents per gram of fresh weight (mg QE/g FW), as shown in Equation 3.

$$= \frac{\text{QE equivalent} \times \text{volume of fresh jackfruit extract} \times \text{dilution jackfruit extract}}{\text{weight of jackfruit flesh used}} \quad [3]$$

Total Phenolic Content. Total phenolic content was determined using the Folin-Ciocalteu procedure described by Musa et al. (2011), with slight modifications. A 0.5-mL aliquot of extract was mixed with 0.4 mL of distilled water and 0.1 mL of diluted Folin-Ciocalteu reagent. After 5 min, 1.0 mL of 7.5% (w/v) sodium carbonate (Na_2CO_3) was added. The mixture was kept at room temperature in the dark for 2 h. Absorbance was then measured at 765 nm using a UV-Visible spectrophotometer. Gallic acid was used as the calibration standard, and the results were expressed as milligrams of gallic acid equivalents per gram of fresh weight (mg GAE/g FW) in Equation 4.

$$= \frac{\text{GAE equivalent} \times \text{volume of fresh jackfruit extract} \times \text{dilution jackfruit extract}}{\text{weight of jackfruit flesh used}} \quad [4]$$

Multivariate and Statistical Analyses

Spectral data were analysed using Unscrambler X version 10.3 (CAMO AS, Oslo, Norway). The dataset was separated into calibration and external validation subsets using a 75:25 independent sample-level split. The calibration subset was used to build the models, while the validation subset was kept separate for evaluating external prediction performance. Leave-one-out cross-validation was carried out within the calibration subset to examine model stability (Ali et al., 2021; Sirisomboon & Nawayon, 2017).

Before the data were divided, the samples were arranged in ascending order according to their reference chemical values. The software was then used to make the random selection of calibration and validation samples. Importantly, the separation was made at the fruit level.

Thus, spectra obtained from the same fruit were not placed in both the calibration and external validation subsets, reducing the possibility of information leakage between the two datasets.

Several spectral preprocessing procedures were examined to reduce variation associated with the heterogeneous rind surface, including the effects of rind roughness and spine density. The evaluated procedures included Savitzky-Golay smoothing, baseline correction, median filtering, Gaussian filtering, standard normal variate (SNV), and multiplicative scatter correction (MSC), together with the combinations used in the analysis. Similar preprocessing approaches have been applied in Vis-NIR studies of intact fruit quality (Abdullah et al., 2021; Lim et al., 2026b, 2026d).

Partial least squares regression (PLSR) was used to relate the rind spectral data to the reference measurements obtained from the flesh. The models were developed using the 500-950 nm spectral interval. Approximately 5% of extreme spectral outliers were removed before modelling to minimise the influence of noise and anomalous measurements (Abdullah, 2019). After this screening step, 1,620 valid spectra remained, representing 30 scanning positions from each of the 54 fruits.

Model performance was examined using the coefficient of determination for calibration (R^2c), cross-validation (R^2cv), and external validation (Rp^2). The corresponding root means square errors for calibration (RMSEc), cross-validation (RMSEcv), and prediction (RMSEp), together with bias and residual predictive deviation (RPD), were also considered. These measures were evaluated together to describe the agreement between predicted and reference values and the stability of the models (Sirisomboon & Nawayon, 2017).

The performance indices were calculated using the following Equations 5 to 9:

$$R^2 = \frac{\sum_{i=1}^{n}(\hat{y}\mathrm{i} - \mathrm{yi})^2}{\sum_{i=1}^{n}(\hat{y}\mathrm{i} - \mathrm{ym})^2} \quad [5]$$

$$RMSEV = \sqrt{\frac{1}{\mathrm{nv} - 1}\sum_{i=1}^{nv}(\hat{y}\mathrm{i} - \mathrm{yi} - \mathrm{bias})^2} \quad [6]$$

$$RMSEC = \sqrt{\frac{1}{\mathrm{nc} - 1}\sum_{i=1}^{nc}(\hat{y}\mathrm{i} - \mathrm{yi})^2} \quad [7]$$

$$Bias = \frac{1}{\mathrm{nv}}\sum_{i=1}^{nv}(\hat{y}\mathrm{i} - \mathrm{yi}) \quad [8]$$

$$RPD = \frac{\text{SD}}{\text{RMSEP}} \quad [9]$$

Where n is the number of data samples, n_c is the number of data samples for calibration, n_v is the number of data samples for validation, $\hat{y}_i$ is the prediction value, y_i is the measured value and y_m is the mean value.

PLSR models were developed for β-carotene, lycopene, TFC, and TPC using the evaluated spectral preprocessing procedures. The number of latent variables (LVs) was tested sequentially from 1 to 7. This range was used to obtain suitable model complexity while limiting the possibility of overfitting, following Peirs et al. (2003) and Saechua et al. (2021).

The experiment followed a completely randomised design with three replications. Analysis of variance (ANOVA) was used to examine treatment effects, and mean comparisons were performed using Fisher's protected least significant difference (LSD) test at $p \leq 0.05$. Statistical analyses were conducted using R version 4.0.4.

RESULT

Distribution of Calibration and Prediction Reference Data

Carotenoid Dynamics Across Fruit Conditions and Maturity Stages

ß-Carotene. The β-carotene content of jackfruit flesh was significantly affected by the interaction between weeks after anthesis (WAA) and fruit condition (Table 1). The concentration changed across the three maturity stages and showed an overall decrease at

Table 1
Main and interaction effects of week after anthesis and fruit condition on the flesh ß-carotene and lycopene of jackfruit cv. Tekam Yellow.

Factor	ß-carotene (mg/kg FW)	Lycopene (mg/kg FW)
Harvest ae (WAA)		
W10	4.51b[x]	3.02b
W12	5.52a	3.79a
W14	3.91b	2.54b
Quality Condition (H)		
Asymptomatic (N)	5.36a	3.51a
Symptomatic (B)	4.02b	2.77b
Interaction		
WAA × H	**	-

Note. [x] For each factor, mean comparisons within the factors followed by different letters are significantly different by LSD at p≤0.05. NS, **, non-significant at p>0.05 or highly significant at p≤0.01, respectively

the later stage of fruit development (Figure 1). At 12 and 14 WAA, normal fruits contained significantly higher β-carotene concentrations than bronzing-affected fruits. The difference between the two fruit conditions became more apparent at the later maturity stages, indicating that the effect of fruit condition was dependent on the stage of fruit development.

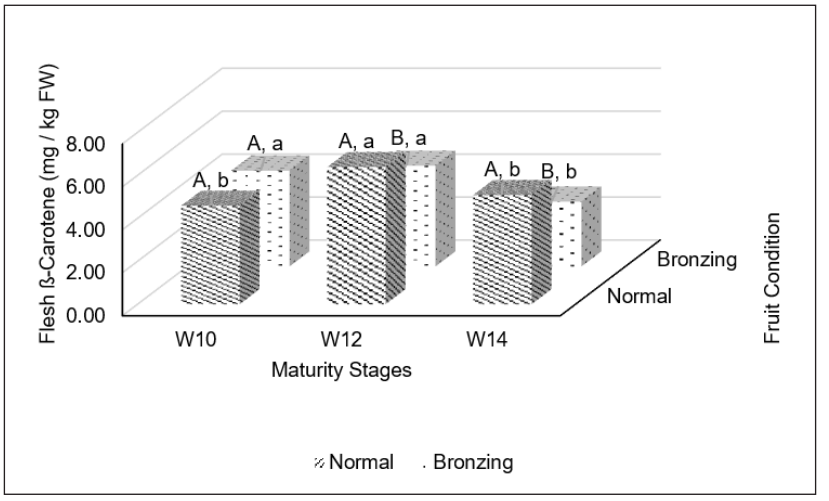

Figure 1. Effects of fruit condition and maturity stages (weeks after anthesis) on flesh ß-carotene of jackfruit cv. Tekam Yellow. Means separated by different capital and small letters are significantly different ($p \leq 0.05$) using LSD between fruit condition and maturity stages, respectively

Lycopene. The interaction between WAA and fruit condition did not significantly affect lycopene concentration (Table 1). Maturity stage, however, had a significant effect, with lycopene concentration decreasing at the later stages of development. Although the interaction was not significant, bronzing-affected fruits showed lower mean lycopene concentrations than normal fruits across the maturity stages. Thus, the difference between fruit conditions was observed in the measured means, but the magnitude of this difference did not change sufficiently across maturity stages to result in a significant interaction.

Antioxidant Contents across Fruit Conditions and Maturity Stages

Total Flavonoid Content. A significant interaction between WAA and fruit condition was found for total flavonoid content (TFC) (Table 2). The pattern changed with maturity. At 10 WAA, normal fruits had higher TFC than bronzing-affected fruits. At 12 and 14 WAA, this pattern was reversed, with bronzing-affected fruits showing higher mean TFC values (Figure 2). These results indicate that the relationship between fruit condition and TFC changed during fruit development.

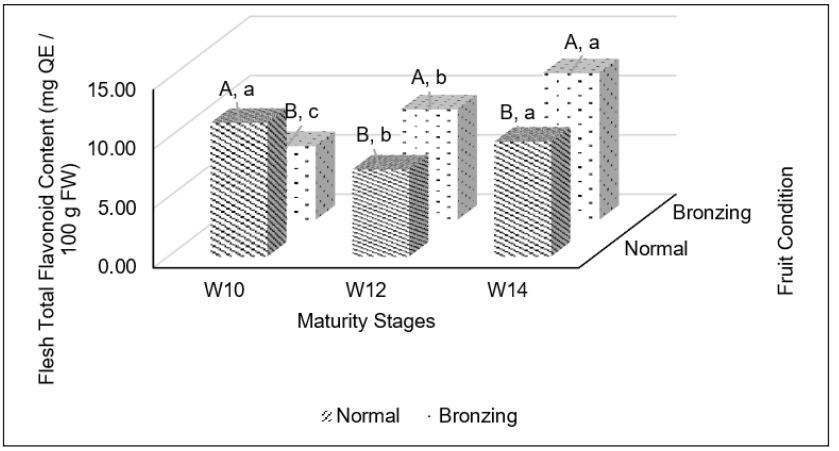

Figure 2. Effects of fruit condition and maturity stages (weeks after anthesis) on flesh total flavonoid content of jackfruit cv. Tekam Yellow. Means separated by different capital and small letters are significantly different ($p \leq 0.05$) using LSD between fruit condition and maturity stages, respectively

Table 2
Main and interaction effects of week after anthesis and fruit condition on the flesh total flavonoid content and total phenolic content of jackfruit cv. Tekam Yellow

Factor	Total Flavonoid Content (mg QE / 100 g FW)	Total Phenolic Content (mg GAE / 100 g FW)
Weeks after anthesis (WAA)		
10	8.39b[x]	3.52c
12	8.30b	6.14a
14	11.14a	4.51b
Fruit Condition (H)		
Normal (N)	9.37a	5.26a
Bronzing (B)	9.21a	4.19b
Interaction		
WAA × H	***	***

Note. [x] For each factor, mean comparisons within the factors followed by different letters are significantly different by LSD at $p \leq 0.05$. ***, highest significant at $p \leq 0.001$, respectively

Total Phenolic Content. Total phenolic content (TPC) was also significantly affected by the interaction between WAA and fruit condition (Table 2). In normal fruits, TPC decreased from 10 to 14 WAA, whereas the values for bronzing-affected fruits were comparatively less variable across the maturity stages. Normal fruits had lower TPC than bronzing-affected fruits at 10 WAA but higher values at 12 WAA (Figure 3). The results therefore show that the difference in TPC between the two fruit conditions was not consistent throughout fruit development.

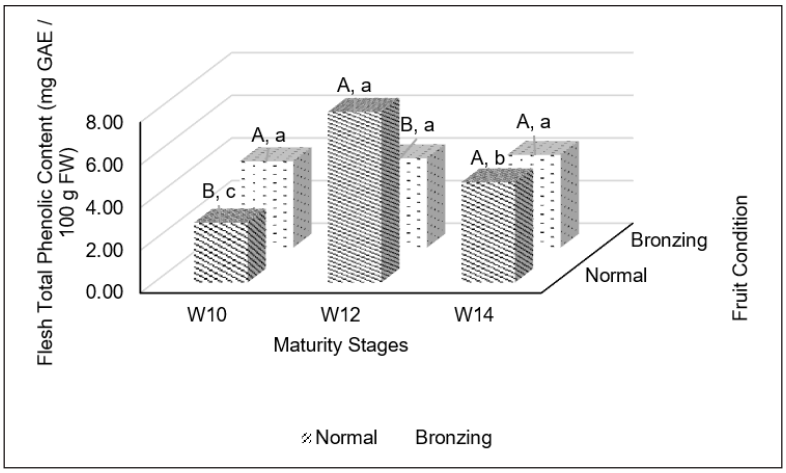

Figure 3. Effects of fruit condition and maturity stages (weeks after anthesis) on flesh total phenolic content of jackfruit cv. Tekam Yellow. Means separated by different capital and small letters are significantly different ($p \leq 0.05$) using LSD between fruit condition and maturity stages, respectively

Spectral Characteristics of Jackfruit Peel

Figures 4 and 5 present the raw Vis-NIR reflectance spectra of normal and bronzing-affected jackfruit rinds at 14 WAA, while Figures 6 and 7 show the corresponding preprocessed spectra. The spectra were obtained from 1,620 valid spectral observations. Broad and overlapping features were observed throughout the measured spectral range, which is expected for fruit tissues because the recorded response can contain contributions from several molecular vibration bands (Nicolaï et al., 2007).

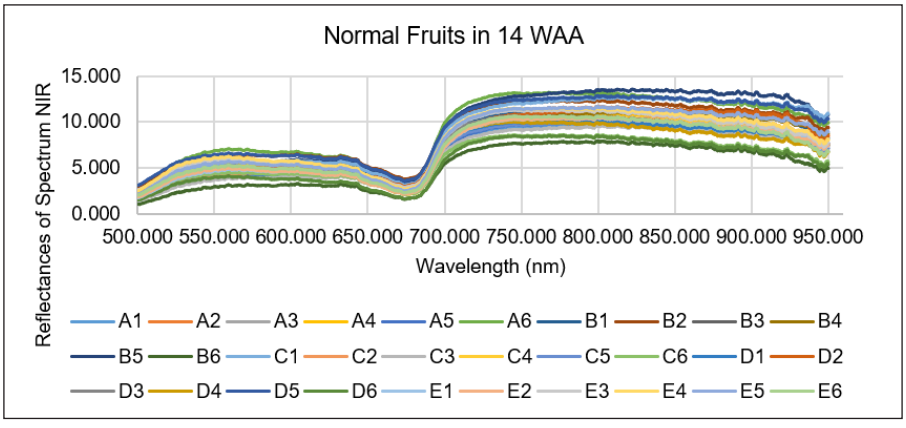

Figure 4. Mean spectral reflectance of raw material for healthy fruit of 30 portions at 14 WAA

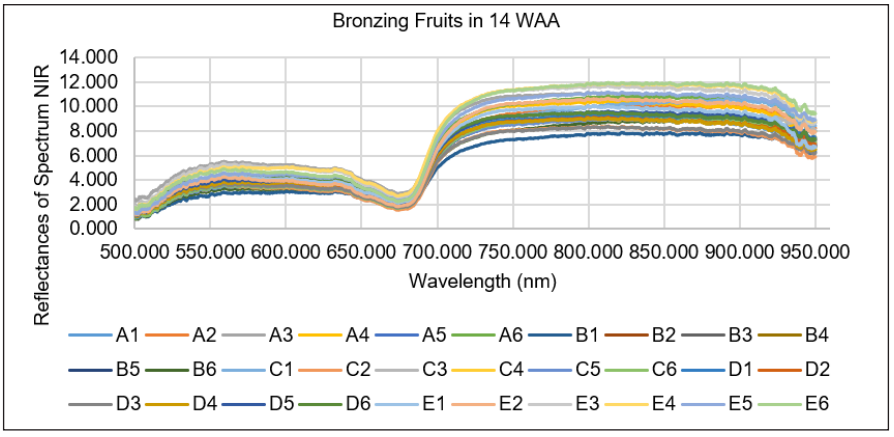

Figure 5. Mean spectral reflectance of raw material for bronzing-affected fruit of 30 portions at 14 WAA

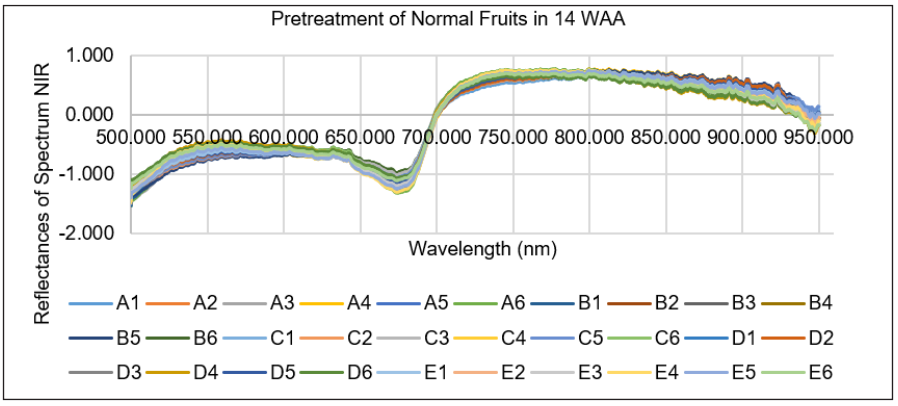

Figure 6. Preprocessed mean Vis-NIR reflectance spectra of healthy jackfruit rind at 14 WAA (30 portions) after Savitzky-Golay smoothing and SNV correction

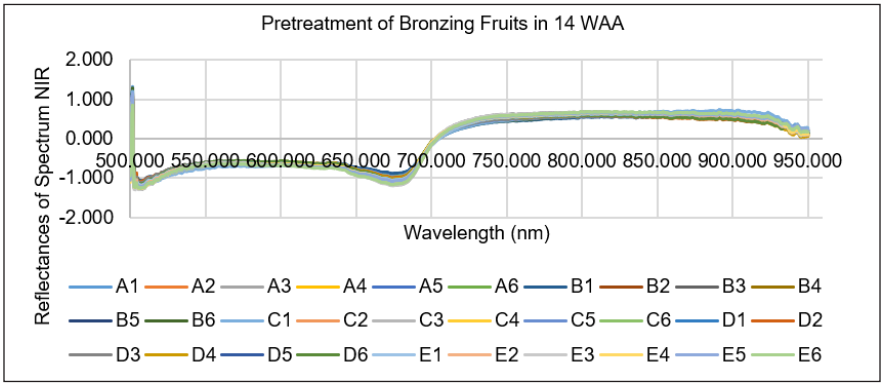

Figure 7. Preprocessed mean Vis-NIR reflectance spectra of bronzing-affected jackfruit rind at 14 WAA (30 portions) after Savitzky-Golay smoothing and SNV correction

The mean spectra obtained from the 30 scanning positions per fruit also showed variation among rind regions. The measurement positions covered five zones: top (A1-A6), middle-top (B1-B6), middle (C1-C6), middle-bottom (D1-D6), and bottom (E1-E6). Using all five zones allowed the spectral dataset to include variation across the heterogeneous rind surface.

Both normal and bronzing-affected rinds showed features around 675 and 945 nm, together with a broader response near 970 nm. The feature around 970 nm is associated mainly with O-H-related absorption and has been reported in fruit tissues (Nagy et al., 2016). The 940-970 nm region may also contain contributions from soluble constituents in fruit materials (Babu et al., 2020; Maniwara et al., 2014). Because the final modelling range was limited to 500-950 nm, the region around 970 nm was not included in the PLSR models.

Within the selected 500-950 nm range, responses around approximately 760 and 945 nm were visible. The raw spectra also showed baseline shifts and scattering effects. These features became less pronounced after spectral preprocessing, particularly after smoothing and SNV correction, resulting in more stable baseline profiles.

Regression coefficient plots for the selected models (Figures 8-15) showed influential regions around 754-760 nm and toward 945 nm. These wavelength regions should not be treated as specific spectral fingerprints of β-carotene, lycopene, TFC, TPC, or bronzing. Instead, they represent parts of the spectrum that contributed to the statistical relationships between the rind spectra and the biochemical measurements obtained from the flesh.

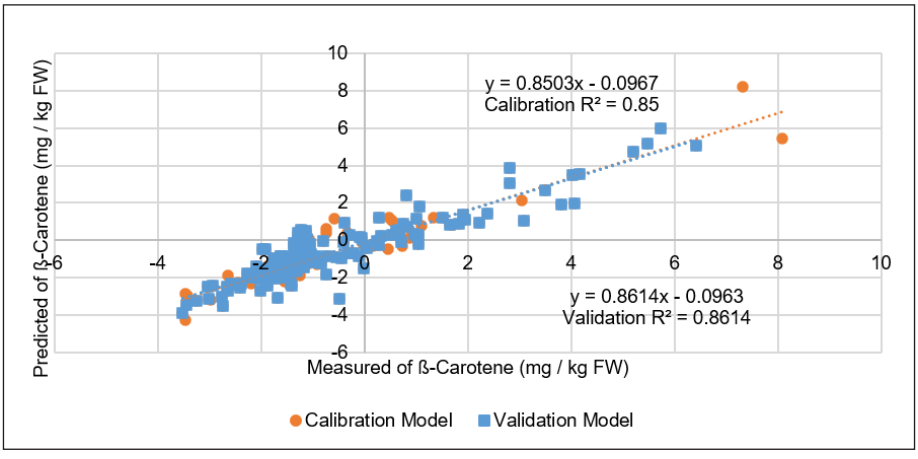

Figure 8. Scatter plots of measured versus predicted β-carotene concentrations in normal jackfruit flesh at 12 weeks after anthesis using Vis-NIR reflectance spectra

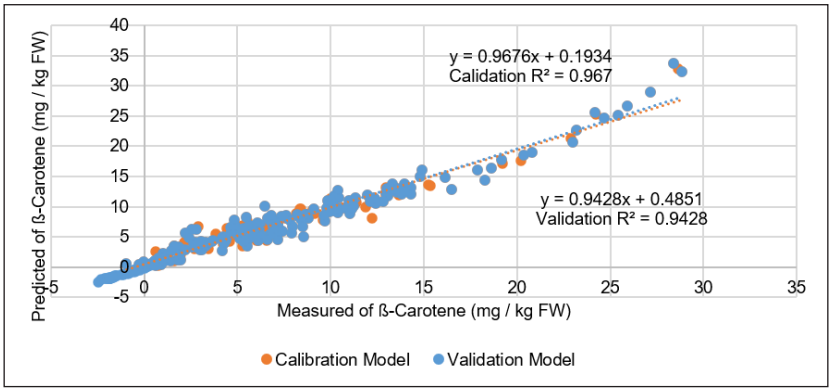

Figure 9. Scatter plots of measured versus predicted β-carotene concentrations in bronzed jackfruit flesh at 12 weeks after anthesis using Vis-NIR reflectance spectra

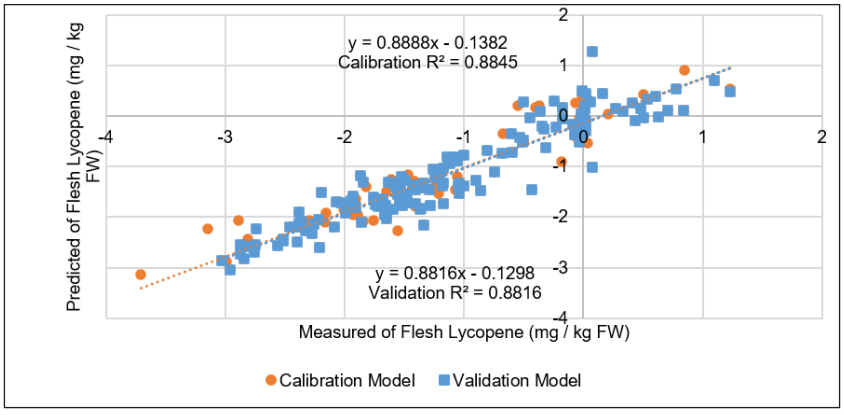

Figure 10. Scatter plots of measured versus predicted lycopene concentrations in normal jackfruit flesh at 14 WAA using Vis-NIR reflectance spectra

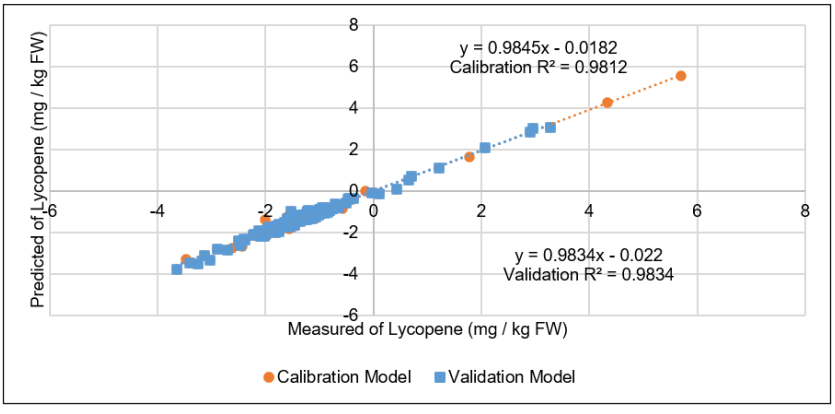

Figure 11. Scatter plots of measured versus predicted lycopene concentrations in bronzed jackfruit flesh at 14 WAA using Vis-NIR reflectance spectra

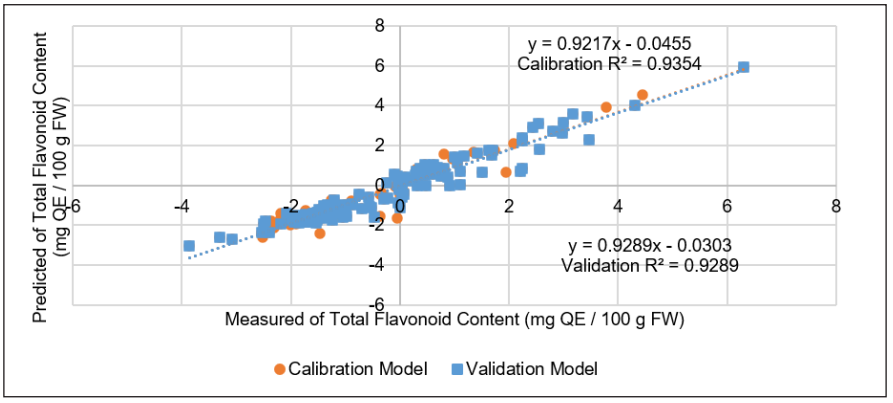

Figure 12. Scatter plots of measured versus predicted total flavonoid content in normal jackfruit flesh at 14 WAA using reflectance spectral data

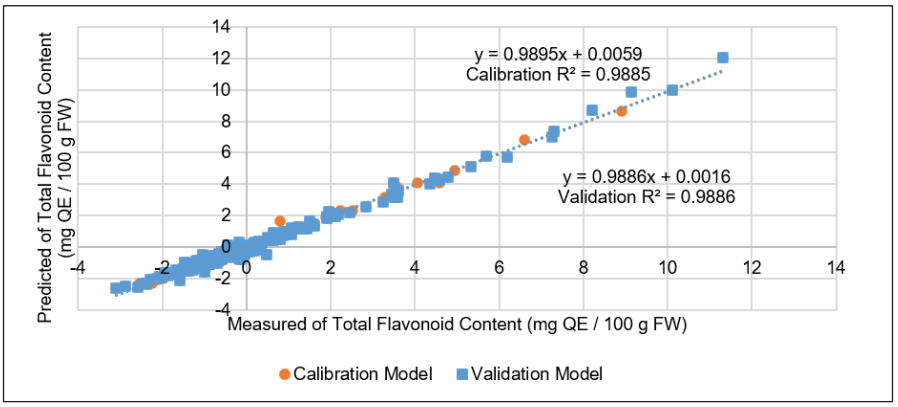

Figure 13. Scatter plots of measured versus predicted total flavonoid content in bronzed jackfruit flesh at 14 WAA using reflectance spectral data

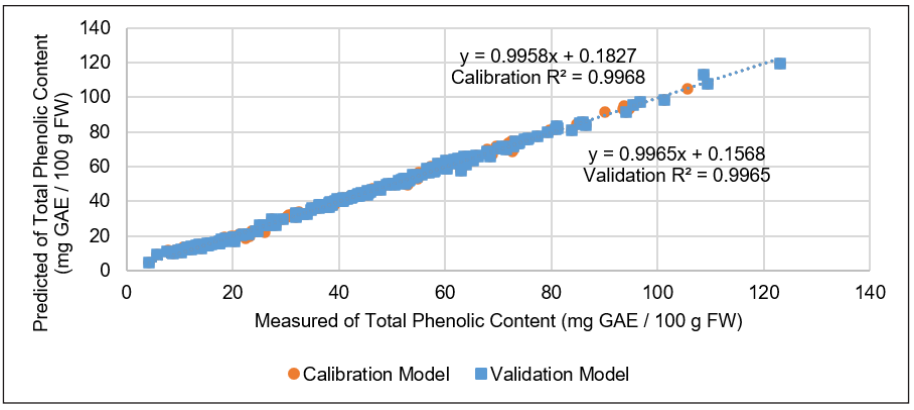

Figure 14. Scatter plots of measured versus predicted total phenolic content in normal jackfruit flesh at 12 WAA using reflectance spectral data

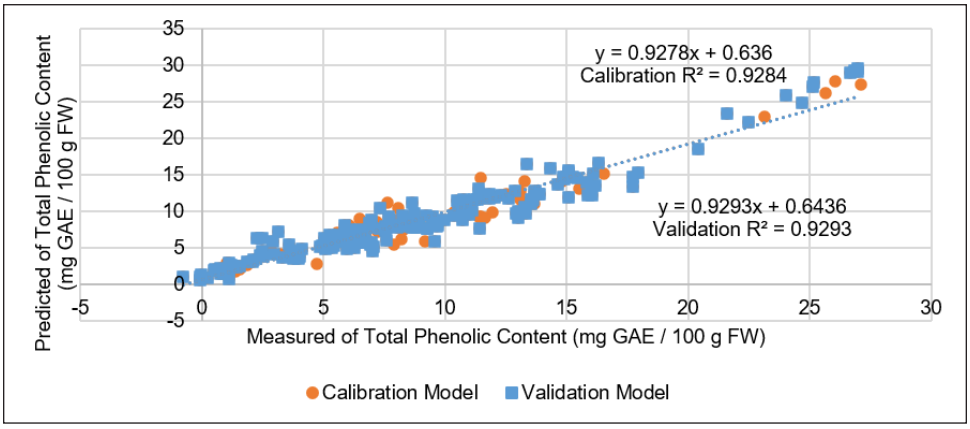

Figure 15. Scatter plots of measured versus predicted total phenolic content in bronzed jackfruit flesh at 12 WAA using reflectance spectral data

PLSR Prediction of Biochemical Attributes

β-Carotene Prediction at 12 and 14 WAA

The PLSR models for β-carotene showed different prediction performance across maturity stages and fruit conditions (Table 3). At 12 WAA, the selected model for normal fruit produced an Rc^2 of 0.95, Rp^2 of 0.88, RMSEP of 1.71, and RPD of 4.12. The corresponding model for bronzing-affected fruit produced Rc^2 of 0.89, Rp^2 of 0.90, RMSEP of 1.99, and RPD of 2.26. The correlation values were above 0.94, while the bias values ranged from -0.20 to 0.16.

At 14 WAA, the normal-fruit model produced Rc^2 of 0.98, Rp^2 of 0.98, RMSEP of 1.35, and RPD of 1.67. For bronzing-affected fruit, the model produced Rc^2 of 0.96, Rp^2 of 0.91, RMSEP of 0.89, and RPD of 4.12. Thus, the prediction results did not show a consistent change with increasing maturity or with fruit condition.

Lycopene Prediction at 14 WAA

Lycopene prediction was evaluated at 14 WAA for both normal and bronzing-affected fruit (Table 4). The selected model for normal fruit produced Rc^2 of 0.98, Rp^2 of 0.99, RMSEP of 1.17, and RPD of 1.47. For bronzing-affected fruit, the corresponding values were Rc^2 of 0.98, Rp^2 of 0.94, RMSEP of 0.22, and RPD of 12.36.

The RPD obtained for bronzing-affected fruit was considerably higher than that obtained for normal fruit. However, RPD is influenced by both prediction error and the spread of the reference values. Therefore, the high RPD should be considered together with Rp^2, RMSEP, bias, and the independent validation data rather than being interpreted on its own.

Table 3
Summary of PLSR results for β-carotene content prediction in jackfruit (cv. Tekam Yellow) at different fruit conditions and maturity stages (weeks after anthesis)

He	Wa	Means	SDe	Rc^2	RMSEc	Rp^2	RMSEp	Bi	Slo	Off	Corr	RPDe
No	12	6.39a	7.05	0.95	0.20	0.88	1.71	-0.20	0.92	0.40	0.94	4.12
Br	12	4.69b	4.49	0.89	1.99	0.90	1.99	0.16	0.91	0.95	0.95	2.26
No	14	5.09b	2.25	0.98	1.44	0.98	1.35	-0.19	0.99	-0.11	0.99	1.67
Br	14	3.02c	3.67	0.96	0.79	0.91	0.89	-0.08	0.91	0.20	0.95	4.12

Note. He = Fruit condition, No = Normal, Br = Bronzing, Wa = week after anthesis, SDe = standard deviation, Bi = bias, Slo = slope, Off = offset, Corr = correlation, RPDe = residual prediction deviation

Table 4
Summary of PLSR results for lycopene prediction in jackfruit (cv. Tekam Yellow) flesh at 14 weeks after anthesis under normal and bronzed conditions.

He	Wa	Means	SDe	Rc^2	RMSEc	Rp^2	RMSEp	Bi	Slo	Off	Corr	RPDe
No	14	2.98a	1.72	0.98	1.26	0.99	1.17	-0.15	0.99	-0.10	0.99	1.47
Br	14	2.21ab	2.72	0.98	0.19	0.94	0.22	0.01	0.89	-0.14	0.97	12.36

Note. He = Fruit condition, No = Normal, Br = Bronzing, Wa = week after anthesis, SDe = standard deviation, Bi =bias, Slo = slope, Off = offset, Corr = correlation, RPDe = residual prediction deviation

Total Flavonoid Content Prediction

The TFC models showed useful statistical relationships at several maturity stages, although the selected preprocessing treatment and number of latent variables differed between maturity stages and fruit conditions (Table 5).

At 10 WAA, the normal-fruit model produced Rp^2 of 0.98 and RPD of 43.17, while the bronzing-affected model produced Rp^2 of 0.87 and RPD of 14.49. At 12 WAA, Rp^2 values of 0.80 and 0.90 were obtained for normal and bronzing-affected fruit, respectively, with corresponding RPD values of 10.00 and 17.92. At 14 WAA, the normal-fruit model produced Rp^2 of 0.93 and RPD of 3.36, whereas the bronzing-affected model produced Rp^2 of 0.97 and RPD of 28.78.

The results indicate that TFC was statistically related to the rind spectral measurements under several of the conditions examined. Nevertheless, the large variation in RPD values means that the prediction results should be considered together with the other validation statistics and the distribution of the reference values.

Total Phenolic Content Prediction at 10 and 12 WAA

TPC prediction showed greater variation than TFC prediction (Table 6). At 10 WAA, the normal-fruit model produced Rp^2 of 0.99, RMSEP of 1.39, and RPD of 0.87. The bronzing-affected model produced Rp^2 of 0.87, RMSEP of 2.10, and RPD of 1.97

At 12 WAA, prediction performance improved for both fruit conditions. The normal-fruit model achieved Rc^2 of 0.94, Rp^2 of 0.87, RMSEP of 1.84, and RPD of 3.57. The bronzing-affected model produced Rc^2 of 0.94, Rp^2 of 0.92, RMSEP of 1.79, and RPD of 2.54. These results indicate that TPC prediction was affected by both maturity stage and fruit condition.

Comparative Interpretation of PLSR Performance

Prediction performance differed among biochemical attributes, maturity stages, fruit conditions, and spectral preprocessing treatments. Preprocessing combinations involving smoothing and scatter correction, particularly SG-SNV and related combinations, gave stable results for several of the models.

The effect of bronzing was not consistent across all attributes. Some models developed for bronzing-affected fruit produced higher Rp^2 or RPD values than the corresponding normal-fruit models, whereas other models showed lower performance. Therefore, the presence of bronzing did not result in a consistent increase or decrease in model performance.

Among the biochemical attributes examined, the stronger statistical relationships were obtained for selected β-carotene, lycopene, and TFC models, while TPC prediction

Table 5
Performance of PLSR models for predicting total flavonoid content in jackfruit (cv. Tekam Yellow) flesh at 10, 12, and 14 weeks after anthesis under normal and bronzed conditions

He	Wa	Means	SDe	Rc^2	RMSEc	Rp^2	RMSEp	Bi	Slo	Off	Corr	RPDe
No	10	11.28ab	10.36	0.99	0.23	0.98	0.24	0.07	0.98	0.07	0.99	43.17
Br	10	6,22d	6.52	0.95	0.38	0.87	0.45	0.00	0.86	-0.10	0.93	14.49
No	12	7.34cd	7.30	0.91	0.54	0.80	0.73	-0.06	0.81	-0.16	0.89	10.00
Br	12	9.31bc	6.81	0.75	0.62	0.90	0.38	0.11	0.98	0.10	0.96	17.92
No	14	9.69b	9.20	0.95	2.53	0.93	2.74	-0.04	0.94	0.37	0.96	3.36
Br	14	12.36a	10.65	0.98	0.30	0.97	0.37	-0.02	0.98	-0.02	0.99	28.78

Note. He = Fruit condition, No = Normal, Br = Bronzing, Wa = week after anthesis, SDe = standard deviation, Bi =bias, Slo = slope, Off = offset, Corr = correlation, RPDe = residual prediction deviation

Table 6
Performance of PLSR models for predicting total phenolic content in jackfruit (cv. Tekam Yellow) flesh at 10 and 12 weeks after anthesis under normal and bronzed conditions

He	Wa	Means	SDe	Rc^2	RMSEc	Rp^2	RMSEp	Bi	Slo	Off	Corr	RPDe
No	10	2.81c	1.21	0.99	1.48	0.99	1.39	0.10	0.99	0.65	1.00	0.87
Br	10	4.05b	4.14	0.92	1.71	0.87	2.10	0.13	0.78	2.15	0.94	1.97
No	12	8.00a	6.56	0.94	1.31	0.87	1.84	-0.16	0.88	0.72	0.94	3.57
Br	12	4.19b	4.55	0.94	1.53	0.92	1.79	-0.06	0.91	0.80	0.96	2.54

Note. He = Fruit condition, No = Normal, Br = Bronzing, Wa = week after anthesis, SDe = standard deviation, Bi =bias, Slo = slope, Off = offset, Corr = correlation, RPDe = residual prediction deviation

showed greater variation. The use of 30 scanning positions per fruit also provided a broader representation of spatial variation across the heterogeneous rind.

The results show that rind-acquired Vis-NIR spectra can be statistically related to biochemical attributes measured in the flesh. These models should be regarded as indirect predictions based on relationships between external spectral variation and internal biochemical variation, rather than as direct optical measurements of flesh constituents.

DISCUSSION

Maturity- and Bronzing-Associated Biochemical Changes

Maturity stage and fruit condition affected the biochemical composition of Tekam Yellow jackfruit, but the responses varied across the four attributes. The significant WAA × fruit condition interaction for β-carotene shows that the difference between normal and bronzing-affected fruit changed during fruit development. At the later maturity stages, normal fruit generally contained more β-carotene than bronzing-affected fruit. This pattern is consistent with changes in pigment composition that occur during jackfruit maturation and ripening (Kaur et al., 2024). The lower β-carotene content observed in bronzing-affected fruit may be related to changes in pigment stability under physiological stress. However, the present study did not investigate carotenoid biosynthesis, degradation, or related metabolic pathways, so this explanation remains tentative.

Lycopene followed a somewhat different pattern. Maturity stage significantly affected lycopene concentration, but the interaction between WAA and fruit condition was not significant. Bronzing-affected fruit nevertheless had lower mean lycopene values than normal fruit. This difference suggests that β-carotene and lycopene did not respond in exactly the same way during fruit development or under bronzing-associated physiological changes. Previous studies in other fruit systems have shown that visible/NIR spectroscopy can provide useful information related to carotenoid content (Clément et al., 2015; Tilahun et al., 2018a).

TFC and TPC were both affected by the interaction between maturity stage and fruit condition. The changes in these antioxidant-related attributes may be associated with changes in secondary metabolism during fruit development and physiological stress (Ding & Syazwani, 2016; Lin et al., 2016; Wulandari et al., 2020). Biotic stress can also alter cellular redox balance and antioxidant metabolism through the production and regulation of reactive oxygen species (Sahu et al., 2022). Nevertheless, the present measurements only describe differences in biochemical composition. They do not provide direct evidence for a particular metabolic pathway associated with bronzing.

The variation observed in the reference measurements was also important for the spectroscopic analysis. Differences among maturity stages and fruit conditions provided the range of biochemical values required to establish and test the PLSR relationships. Without

sufficient variation in the reference data, a regression model may show apparently good statistical fit without being useful across a wider population.

Spectral Characteristics and Preprocessing

The rind spectra contained broad, overlapping features, along with baseline variation and scattering effects. This type of spectral response is common in intact fruit because the measured signal is influenced not only by chemical composition but also by tissue structure and other physical properties (Lim et al., 2026c; Nicolaï et al., 2007). The rough and uneven surface of jackfruit rind can further increase variation between scanning positions.

The spectral regions around 760 and 970 nm were mainly associated with O-H-related responses, particularly those related to water. Similar water-related spectral behaviour has been reported in fruit and jackfruit studies (Babu et al., 2020; Maniwara et al., 2014; Saechua et al., 2021). These wavelengths should not be interpreted as unique markers for carotenoids, antioxidant compounds, or bronzing. The observed response may instead reflect combined effects of water status, tissue structure, and physiological changes occurring during fruit development.

The broader feature around 970 nm was visible in the measured spectra but was outside the final 500-950 nm modelling range. Within the selected range, regression coefficient profiles indicated contributions from regions around 754-760 nm and toward 945 nm. Because Vis-NIR absorption bands are broad and often overlap, these regions cannot be assigned to a single biochemical compound on the basis of the present data alone.

Spectral preprocessing helped reduce baseline variation, noise, and scattering effects in several of the models. Smoothing combined with SNV or MSC provided useful preprocessing for a number of attributes, which agrees with previous NIR studies of intact fruit (Guthrie et al., 1998; Golic & Walsh, 2006; Lim et al., 2026c; Saranwong et al., 2004). The use of multiple scanning positions was also relevant because jackfruit rind is not spectrally uniform. Measurements from 30 positions across five rind zones therefore gave a broader representation of the surface than would have been obtained from a single measurement location (Li et al., 2023).

Prediction of Carotenoids and Antioxidant Attributes

The PLSR results show that prediction performance depended on the biochemical attribute, maturity stage, and fruit condition. For β-carotene, the normal-fruit model at 12 WAA produced Rp^2 of 0.88 and RPD of 4.12, while the bronzing-affected model produced Rp^2 of 0.90 and RPD of 2.26. At 14 WAA, the normal-fruit model had Rp^2 of 0.98 but RPD of 1.67, whereas the bronzing-affected model had Rp^2 of 0.91 and RPD of 4.12. Thus, a higher Rp^2 did not necessarily correspond to a higher RPD. The differences also show that model behaviour changed with both maturity and fruit condition.

The lycopene results provide another example of why several validation statistics should be examined together. At 14 WAA, the normal-fruit model produced Rp^2 of 0.99 and RPD of 1.47, whereas the bronzing-affected model produced Rp^2 of 0.94 and RPD of 12.36. The high RPD for bronzing-affected fruit is associated with the low prediction error and the distribution of the validation reference values. It should therefore not be taken by itself as evidence that lycopene was directly measured through the rind. Similar visible/NIR approaches have been used to estimate carotenoid-related attributes in other fruit systems (Clément et al., 2015; Lim et al., 2026c; Tilahun et al., 2018a).

TFC showed relatively strong statistical relationships at several maturity stages, but the RPD values varied substantially. The normal-fruit model at 10 WAA, for example, produced Rp^2 of 0.98 and RPD of 43.17, whereas the corresponding bronzing-affected model produced Rp^2 of 0.87 and RPD of 14.49. At 14 WAA, RPD values of 3.36 and 28.78 were obtained for normal and bronzing-affected fruit, respectively. Such large RPD values should be treated carefully because RPD is calculated from the standard deviation of the validation reference values relative to prediction error. A narrow or unevenly distributed validation population can therefore influence the apparent magnitude of RPD.

TPC showed a different pattern. At 10 WAA, the normal-fruit model had Rp^2 of 0.99 but RPD of only 0.87, while the 12-WAA normal-fruit model had Rp^2 of 0.87 and RPD of 3.57. The bronzing-affected model at 12 WAA produced Rp^2 of 0.92 and RPD of 2.54. This difference between Rp^2 and RPD again shows why model performance should not be described using a single statistic. Similar variation in NIR prediction performance has been reported for biochemical attributes in agricultural products (Chaukhande et al., 2024; Clark et al., 2022).

Taken together, the results suggest that rind spectra contain information that can be used to establish statistical relationships with selected internal biochemical measurements. However, the strength of these relationships was condition-dependent. The models therefore should not be presented as universally applicable predictions for all maturity stages or fruit conditions.

Practical Relevance and Limitations

A key limitation of this study is the difference between the location of spectral measurement and the location of the reference measurement. Vis-NIR spectra were collected from the rind, whereas β-carotene, lycopene, TFC, and TPC were measured destructively from the flesh. The resulting models therefore describe relationships between external rind spectral characteristics and internal biochemical attributes. They should not be interpreted as direct optical measurements of the compounds present in the flesh.

Previous jackfruit studies have shown that skin-surface NIR measurements can provide information related to internal physicochemical properties. Abdullah (2019) investigated

shortwave NIR spectroscopy for jackfruit quality attributes, while Abdullah et al. (2018, 2021) reported prediction of moisture and soluble solids content using skin-surface spectra. These studies support the feasibility of indirect surface-based assessment, but they do not establish a specific optical penetration depth through the rind of Tekam Yellow under the conditions used in the present study.

Rind thickness may also affect the interaction between the incident radiation and the fruit tissue. However, rind thickness was not measured in this experiment. In the previous morphological and physical characterisation of Tekam Yellow, flesh thickness varied with maturity stage and fruit condition, whereas rind thickness was not reported (Lim et al., 2026a). Rind thickness should therefore be considered a possible source of spectral variation, although its contribution to the current models cannot be quantified from the available measurements.

The disease literature provides the biological context for jackfruit bronzing. Bronzing was reported as an emerging disease in Peninsular Malaysia in association with *Pantoea stewartii* subsp. *stewartii* (Zulperi et al., 2017), and subsequent molecular work supported this association (Ibrahim et al., 2020). Bronzing has also been reported in other jackfruit-producing regions, including China (Zhao et al., 2023). The present study, however, did not directly detect *P. stewartii* subsp. *stewartii* and did not develop a pathogen diagnostic test. The spectroscopic models were developed for biochemical prediction, so the observed spectral relationships should not be interpreted as direct pathogen detection or confirmation of bronzing disease.

The variation in model performance also points to the need for broader validation. NIR model robustness can be affected by biological variation, particularly when the calibration population is relatively limited (Bobelyn et al., 2010; Lim et al., 2026b; Peirs et al., 2003). Future work should include larger numbers of fruits from different seasons, orchards, cultivars, maturity stages, and levels of bronzing severity. Independent external validation would also be needed to determine whether the relationships observed in the present dataset can be transferred to other production conditions.

Measurements at different tissue depths or studies involving separate rind and internal tissue layers could further clarify the relationship between surface spectra and internal biochemical variation. For practical development, future calibration datasets should also contain sufficient representation of both healthy and bronzing-affected fruit across the relevant biochemical range. Recalibration may be necessary when the model is applied under different seasonal or production conditions.

Multi-position rind-based Vis-NIRS combined with PLSR provides a possible rapid screening approach for selected internal biochemical attributes of intact Tekam Yellow jackfruit. Its usefulness depends on the target attribute, maturity stage, fruit condition, preprocessing method, and reference-value distribution. The approach should therefore

be considered a potential indirect screening method rather than a direct measurement or diagnostic technique.

CONCLUSION

This study examined changes in selected carotenoid and antioxidant-related attributes of Tekam Yellow jackfruit at 10, 12, and 14 weeks after anthesis under normal and bronzing-affected conditions. β-Carotene, lycopene, TFC, and TPC showed different responses to maturity stage and fruit condition, providing a useful range of reference values for spectroscopic modelling.

Rind-acquired Vis-NIR spectra combined with PLSR were able to establish statistical relationships with selected biochemical attributes measured in the flesh. Prediction performance varied with the target attribute, maturity stage, fruit condition, and spectral preprocessing. The β-carotene model for normal fruit at 12 WAA produced Rp^2 of 0.88 and RPD of 4.12, while selected TFC and lycopene models also showed strong statistical relationships. For TPC at 12 WAA, Rp^2 values of 0.87 and 0.92 were obtained for normal and bronzing-affected fruit, respectively, with RPD values of 3.57 and 2.54.

The spectral responses around 760 and 945 nm contributed to several of the regression models, whereas the broader feature near 970 nm was mainly associated with water-related absorption and was outside the final modelling range. These wavelength regions should not be regarded as unique spectral signatures of individual biochemical compounds or bronzing.

The present findings support the use of multi-position rind-based Vis-NIRS as a potential non-destructive screening approach for selected internal biochemical attributes of intact Tekam Yellow jackfruit. However, the models represent indirect relationships between rind spectra and flesh measurements and should not be interpreted as direct measurement of internal compounds or as detection of *Pantoea stewartii* subsp. *stewartii*. The study was limited to one cultivar, three maturity stages, and the sampled production conditions. Larger datasets covering additional cultivars, seasons, orchards, maturity stages, and levels of bronzing severity, together with independent external validation, are needed before the models can be considered for wider practical application.

Data Availability Declaration

The datasets generated during and/or analyzed during the current study are available.

Funding Declaration

This research did not receive any specific grant from funding agencies in the public, commercial, or not-for-profit sectors.

Declaration of Competing Interest

The authors declare that there are no known financial conflicts of interest or personal relationships that could have influenced the research, analysis, or interpretation of the data presented in this manuscript.

ACKNOWLEDGEMENT

The authors sincerely express their gratitude to the Department of Crop Science, Faculty of Agriculture; the Department of Biological and Agricultural Engineering, Faculty of Engineering; and the Institute of Plantation Studies at Universiti Putra Malaysia for their invaluable technical assistance and logistical support throughout this research.

REFERENCES

Abdullah, N. (2019). *Application of shortwave near infrared spectroscopy in determining physicochemical properties of jackfruit* [Master's thesis, Universiti Putra Malaysia].

Abdullah, N., Nawi, N. M., Ding, P., Kassim, M. S. M., & Lazim, S. S. R. M. (2018). Preliminary study to predict moisture content of jackfruit skin using shortwave near infrared spectroscopy. *Food Research, 3*(2), 128-132. https://doi.org/10.26656/fr.2017.3(2).135

Abdullah, N., Nawi, N. M., Ding, P., Kassim, M. S. M., & Lazim, S. S. R. M. (2021). Prediction of soluble solids content of jackfruit from skin surface using spectroscopic method. *Agricultural Mechanization in Asia, Africa and Latin America, 52*(3), 4013-4021.

Abidin, N., Ismail, S. I., Vadamalai, G., Yusof, M. T., Hakiman, M., Karam, D. S., Ismail-Suhaimy, N. W., Ibrahim, R., & Zulperi, D. (2020). Genetic diversity of *Pantoea stewartii* subspecies *stewartii* causing jackfruit-bronzing disease in Malaysia. *PLOS ONE, 15*(6), Article e0234350. https://doi.org/10.1371/journal.pone.0234350

Abidin, N., Ismail, S. I., Vadamalai, G., Yusof, M. T., Hakiman, M., Karam, D. S., & Zulperi, D. (2021). Pathogenic variability of the jackfruit-bronzing bacterium *Pantoea stewartii* subspecies *stewartii* infection to jackfruit varieties and its pivotal plant hosts in Malaysia. *Agronomy, 11*(11), Article 2113. https://doi.org/10.3390/agronomy11112113

Abu Bakar, M. F., Mohamed, M., Rahmat, A., & Fry, J. (2009). Phytochemicals and antioxidant activity of different parts of bambangan (*Mangifera pajang*) and tarap (*Artocarpus odoratissimus*). *Food Chemistry, 113*, 479-483. https://doi.org/10.1016/j.foodchem.2008.07.081

Ali, M. M., Hashim, N., & Shahamshah, M. I. (2021). Durian (*Durio zibethinus*) ripeness detection using thermal imaging with multivariate analysis. *Postharvest Biology and Technology, 176*, Article 111517. https://doi.org/10.1016/j.postharvbio.2021.111517

Babu, P. S., Sudheer, K. P., Sarathjith, M. C., Mathew, S. M., & Gopinath, G. (2020). Quality evaluation of tender jackfruit using near-infrared reflectance spectroscopy. *Journal of Applied Horticulture, 22*(3), 171-175. https://doi.org/10.37855/jah.2020.v22i03.31

Bobelyn, E., Serban, A., Nicu, M., Lammertyn, J., Nicolaï, B. M., & Saeys, W. (2010). Postharvest quality of apple predicted by NIR spectroscopy: Study of the effect of biological variability on spectra and model performance. *Postharvest Biology and Technology, 55*(3), 133-143. https://doi.org/10.1016/j.postharvbio.2009.09.006

Chaukhande, P., Luthra, S. K., Patel, R. N., Padhi, S. R., Mankar, P., Mangal, M., & Riar, A. S. (2024). Development and validation of near-infrared reflectance spectroscopy prediction modeling for the rapid estimation of biochemical traits in potato. *Foods, 13*(11), Article 1655. https://doi.org/10.3390/foods13111655

Clark, C. J., McGlone, V. A., De Silva, H. N., Manning, M. A., Burdon, J., & Mowat, A. D. (2004). Prediction of storage disorders of kiwifruit (*Actinidia chinensis*) based on visible-NIR spectral characteristics at harvest. *Postharvest Biology and Technology, 32*(2), 147-158. https://doi.org/10.1016/j.postharvbio.2003.11.004

Clark, C. J., MacFall, J. S., & Rutherfurd, S. M. (2022). Application of near-infrared spectroscopy for rapid non-destructive assessment of tropical fruit quality. *Postharvest Biology and Technology, 188*, Article 111908. https://doi.org/10.1016/j.postharvbio.2022.111908

Clément, A., Bacon, R., Sirois, S., & Dorais, M. (2015). Mature-ripe tomato spectral classification according to lycopene content and fruit type by visible, NIR reflectance and intrinsic fluorescence. *Quality Assurance and Safety of Crops & Foods, 7*(5), 747-756. https://doi.org/10.3920/QAS2014.0521

Ding, P., & Syazwani, S. (2016). Physicochemical quality, antioxidant compounds and activity of MD-2 pineapple fruit at five ripening stages. *International Food Research Journal, 23*(2), 549-555. http://core.ac.uk/download/pdf/153810846.pdf

Golic, M., & Walsh, K. B. (2006). Robustness of calibration models based on near infrared spectroscopy for the in-line grading of stonefruit for total soluble solids content. *Analytica Chimica Acta, 555*(2), 286-291. https://doi.org/10.1016/j.aca.2005.09.014

Guthrie, J., Wedding, B., & Walsh, K. (1998). Robustness of NIR calibrations for soluble solids in intact melon and pineapple. *Journal of Near Infrared Spectroscopy, 6*(1), 259-265. https://doi.org/10.1255/jnirs.112

Ibrahim, R., Ismail-Suhaimy, N. W., Shu-Qing, T., Ismail, S. I., Abidin, N., Hakiman, M., Karam, D. S., Ahmad-Hamdani, M. S., Yusof, M. T., & Zulperi, D. (2020). Molecular characterization and phylogenetic analysis of *Pantoea stewartii* subspecies *stewartii* causing bronzing disease of jackfruit in Malaysia based on *cps* and *hrp* gene sequences. *Journal of Plant Pathology, 102*(1), 193-199. https://doi.org/10.1007/s42161-019-00383-7

Jarman, S., Carr, T., Hampel-Arias, Z., Flynn, E., & Moon, K. (2023). Ensemble segmentation for improved background estimation and gas plume identification in hyperspectral images. In *Applications of machine learning 2023* (Vol. 12675, pp. 41-58). SPIE. https://doi.org/10.1117/12.2677729

Kaur, J., Singh, Z., Mazhar, M. S., Shah, H. M. S., & Woodward, A. (2024). Changes in physical attributes, activities of fruit softening enzymes, cell wall polysaccharides and fruit quality of jackfruit (*Artocarpus heterophyllus* Lam.) as influenced by maturation and ripening. *Horticulturae, 10*(12), Article 1264. https://doi.org/10.3390/horticulturae10121264

Li, J., Zhang, Y., Zhang, Q., Duan, D., & Chen, L. (2023). Establishment of a multi-position general model for evaluation of water core and soluble solid content in 'Fuji' apples using on-line full-transmittance

visible and near infrared spectroscopy. *Journal of Food Composition and Analysis, 117*, Article 105150. https://doi.org/10.1016/j.jfca.2023.105150

Lim, K. J., Ding, P., Nawi, N. M., & Jusoh, M. (2026a). Morphological and physical characterization of bronzing-affected jackfruit (*Artocarpus heterophyllus* Lam. cv. Tekam Yellow) across maturity stages: Influence of rind and flesh attributes. *Journal of Food Science, 91*(4), Article e71075. https://doi.org/10.1111/1750-3841.71075

Lim, K. J., Ding, P., Nawi, N. M., Jusoh, M., Abdullah, N., & Lazim, S. S. R. M. (2026b). Predicting the soluble solid concentration and ascorbic acid of intact jackfruit var. Tekam Yellow using visible-near-infrared spectroscopy: Comparison of rind and flesh. *Food Analytical Methods, 19*(8), Article 218. https://doi.org/10.1007/s12161-026-03129-1

Lim, K. J., Ding, P., Nawi, N. M., Jusoh, M., & Khuzaimah, Z. (2026c). Comparative evaluation of hyperspectral, thermal, and near-infrared imaging systems for non-destructive prediction of fruit and vegetable quality: A review. *Journal of Nondestructive Evaluation, 45*, Article 79. https://doi.org/10.1007/s10921-026-01376-0

Lim, K. J., Ding, P., Nawi, N. M., & Jusoh, M. (2026d). Robust non-destructive prediction of color attributes associated with bronzing in jackfruit (*Artocarpus heterophyllus* cv. 'Tekam Yellow') using visible-near infrared spectroscopy. *Applied Fruit Science, 68*(4), Article 217. https://doi.org/10.1007/s10341-026-01925-x

Lin, D., Xiao, M., Zhao, J., Li, Z., Xing, B., Li, X., & Chen, S. (2016). An overview of plant phenolic compounds and their importance in human nutrition and management of type 2 diabetes. *Molecules, 21*(10), Article 1374. https://doi.org/10.3390/molecules21101374

Maniwara, P., Nakano, K., Boonyakiat, D., Ohashi, S., Hiroi, M., & Tohyama, T. (2014). The use of visible and near infrared spectroscopy for evaluating passion fruit postharvest quality. *Journal of Food Engineering, 143*, 33-43. https://doi.org/10.1016/j.jfoodeng.2014.06.028

Mijin, S., & Ding, P. (2020). Growth development and structural changes of Malaysian jackfruit cv. Tekam Yellow syncarp. *Scientia Horticulturae, 272*, Article 109594. https://doi.org/10.1016/j.scienta.2020.109594

Mijin, S., Ding, P., Saari, N., & Ramlee, S. I. (2021). Effects of pollination techniques and harvesting stage on the physico-chemical characteristics of jackfruit. *Scientia Horticulturae, 285*, Article 110199. https://doi.org/10.1016/j.scienta.2021.110199

Musa, K. H., Abdullah, A., Jusoh, K., & Subramaniam, V. (2011). Antioxidant activity of pink flesh guava (*Psidium guajava* L.): Effect of extraction techniques and solvents. *Food Analytical Methods, 4*(1), 100-107. https://doi.org/10.1007/s12161-010-9139-3

Nagata, M., & Yamashita, I. (1992). Simple method for simultaneous determination of chlorophyll and carotenoids in tomato fruit. *Journal of the Japanese Society for Food Science and Technology, 39*(10), 925-928. https://doi.org/10.3136/nskkk1962.39.925

Nagy, A., Riczu, P., & Tamas, J. (2016). Spectral evaluation of apple fruit ripening and pigment content alteration. *Scientia Horticulturae, 201*, 256-264. https://doi.org/10.1016/j.scienta.2016.02.016

Nicolaï, B. M., Beullens, K., Bobelyn, E., Peirs, A., Saeys, W., & Theron, K. I. (2007). Non-destructive measurement of fruit and vegetable quality by means of NIR spectroscopy: A review. *Postharvest Biology and Technology, 46*(2), 99-118. https://doi.org/10.1016/j.postharvbio.2007.06.024

Peirs, A., Tirry, J., Verlinden, B., Darius, P., & Nicolaï, B. M. (2003). Effect of biological variability on the robustness of NIR models for soluble solids content of apples. *Postharvest Biology and Technology, 28*(2), 269-280. https://doi.org/10.1016/S0925-5214(02)00196-5

Saechua, W., Sharma, S., Nakawajana, N., Leepaitoon, K., Chunsri, R., Posom, J., & Pornchaloempong, P. (2021). Integrating Vis-SWNIR spectrometer in a conveyor system for in-line measurement of dry matter content and soluble solids content of durian pulp. *Postharvest Biology and Technology, 181*, Article 111640. https://doi.org/10.1016/j.postharvbio.2021.111640

Sahu, P. K., Jayalakshmi, K., Tilgam, J., Gupta, A., Nagaraju, Y., Kumar, A., & Rajawat, M. V. S. (2022). ROS generated from biotic stress: Effects on plants and alleviation by endophytic microbes. *Frontiers in Plant Science, 13*, Article 1042936. https://doi.org/10.3389/fpls.2022.1042936

Saranwong, S., Sornsrivichai, J., & Kawano, S. (2004). Prediction of ripe-stage eating quality of mango fruit from its harvest quality measured nondestructively by near infrared spectroscopy. *Postharvest Biology and Technology, 31*(2), 137-145. https://doi.org/10.1016/j.postharvbio.2003.08.007

Sirisomboon, P., & Nawayon, J. (2017). Evaluation of soluble solids of curry soup containing coconut milk by near infrared spectroscopy. *Journal of Near Infrared Spectroscopy, 25*(3), 203-210. https://doi.org/10.1177/0967033517711472

Tilahun, S., Seo, M. H., Hwang, I. G., Kim, S. H., Choi, H. R., & Jeong, C. S. (2018a). Prediction of lycopene and β-carotene in tomatoes by portable chroma-meter and VIS/NIR spectra. *Postharvest Biology and Technology, 136*, 50-56. https://doi.org/10.1016/j.postharvbio.2017.10.007

Wulandari, L., Permana, B. D., & Kristiningrum, N. (2020). Determination of total flavonoid content in medicinal plant leaves powder using infrared spectroscopy and chemometrics. *Indonesian Journal of Chemistry, 20*(5), 1044-1051. https://doi.org/10.22146/ijc.47047

Zhao, Y., Xiao, M., Yan, C. B., Hu, F. C., Zhang, S. Q., Wang, X. H., & Fan, H. Y. (2023). First report of bronzing disease caused by *Pantoea stewartii* on jackfruit in China. *Plant Disease, 107*(8), 2514. https://doi.org/10.1094/PDIS-11-22-2740-PDN

Zulperi, D., Manaf, N., Ismail, S. I., Karam, D. S., & Yusof, M. T. (2017). First report of *Pantoea stewartii* subsp. *stewartii* causing fruit bronzing of jackfruit (*Artocarpus heterophyllus*), a new emerging disease in Peninsular Malaysia. *Plant Disease, 101*(5), 831. https://doi.org/10.1094/PDIS-11-16-1689-PDN

Pertanika J. Trop. Agric. Sci. 49 (5): 2303 - 2321 (2026)

PERTANIKA JOURNALS

TROPICAL AGRICULTURAL SCIENCE

Journal homepage: http://www.pertanika.upm.edu.my/

Review Article

An In-Depth Analysis of Cottonseed Oil and Its Composition, Digestibility, Health-Promoting Properties, Industrial Relevance, Animal Feed Value, and Green Technologies

Savanam Chandra Sekhar[1]*, Degala Pushpa Sri[2], Mohammed Irfan[3], Meeravali Shaik[4], B. Vasantha Lakshmi[5], Krishna Babu Sambaru[6], and Palagiri Tejovathi[7]

[1]KL Business School, Koneru Lakshmaiah Education Foundation, KL University, 522302 Vaddeswaram, Andhra Pradesh, India
[2]Department of MBA, PACE Institute of Technology and Sciences, 523272 Ongole, Andhra Pradesh, India
[3]Department of MBA, CMR Technical Campus, Kandlaloya, Medchal Road, 501401 Hyderabad, Telangana, India
[4]Department of Management, Rajiv Gandhi University of Knowledge Technologies-IIIT Ongole Campus, 523225 Ongole, Andhra Pradesh, India
[5]Department of MBA, Dhruva College of Management, 501401 Hyderabad, Telangana, India
[6]Department of MBA, Aditya Degree & PG College (A), 533003 Kakinada, Andhra Pradesh, India
[7]Department of Mathematics, St. Ann's College of Engineering & Technology, 523187 Chirala, Andhra Pradesh, India

ABSTRACT

Cottonseed oil is a versatile vegetable oil with diverse food, feed, and industrial applications. Its composition, processing characteristics, and safety profile have been examined extensively in the literature. Its physicochemical properties, including a high smoke point (232 °C) and oxidative stability due to natural tocopherols, make it highly suitable for cooking and frying. The rich fatty acid profile features prominent unsaturated fatty acids such as linoleic (50-58%) and oleic (13-25%). The relative proportions of unsaturated and saturated fatty acids vary among cultivars, growing conditions, and processing methods. Current American Heart Association guidance supports replacing saturated and trans fats with unsaturated plant oils; cottonseed oil is not specifically identified by the AHA as a "Heart Oil." Cottonseed oil has been reported to have an average digestibility of approximately 97% in humans in an earlier review, while animal

ARTICLE INFO

Article history:
Received: 05 September 2025
Accepted: 24 September 2026
Published: 30 October 2026

DOI: https://doi.org/10.47836/pjtas.49.5.10

E-mail addresses:
savanam.sekhar@gmail.com (Savanam Chandra Sekhar)
pushpasri.degala@gmail.com (Degala Pushpa Sri)
irfanmd2004@gmail.com (Mohammed Irfan)
meeravalimba@gmail.com (Meeravali Shaik)
vasanthalakshmibairu@gmail.com (B. Vasantha Lakshmi)
kbsambaru@gmail.com (Krishna Babu Sambaru)
tejovathipalagiri@gmail.com (Palagiri Tejovathi)
* Corresponding author

© Universiti Putra Malaysia Press

studies report high energy utilisation and digestibility under specific dietary conditions. Beyond its nutritional role, cottonseed oil has been investigated for effects on blood lipids and for antioxidant and other biological activities. Evidence for anti-inflammatory, anti-allergic, and anticancer effects is more appropriately described as experimental or preclinical rather than as established clinical benefits. Crucially, refining processes are indispensable for safety, reducing gossypol and other undesirable constituents and reducing or inactivating cyclopropenoid fatty acids. This supports the suitability of properly refined cottonseed oil for human consumption and its value as a byproduct of cotton production. The objective of this paper is to assess the digestibility and nutritive values of cottonseed oil for various applications.

Keywords: Fatty acids, gossypol, health benefits, oxidative stability, refining process

INTRODUCTION

Cotton (*Gossypium sp.*), particularly Upland cotton (*Gossypium hirsutum* L.), stands as a commercially vital annual fiber crop globally (Kumar et al., 2023). Beyond its primary role in textile production, it is considered one of the key oilseed crops worldwide, alongside peanut, soybean, sunflower, and rapeseed (Wu et al., 2022). Often referred to as "White gold" (Sekhar & Rao, 2010), cotton's significance is due to both its agricultural and industrial value, serving as the mainstay of India's textile industry and contributing significantly to fiber, food, and oil production (Sekhar et al., 2024). The production ratio of cotton fiber to cottonseed is approximately 1:1.65.

Cottonseed oil (CSO) is an important product obtained from the byproduct of cottonseeds, and it has considerable historical and contemporary global significance as an edible oil. Its use can be traced back more than a hundred years, and it held a leading position in the vegetable oil market in the USA until the introduction of soybean and canola oils in the 1950s (Zia et al., 2022). Globally, CSO ranks as the fifth-largest contributor to oilseed oil, representing about 4% of the overall vegetable oil output, with key production sectors situated in nations such as India, China, Pakistan, the United States, Brazil, and Turkey (Kalkan & Maskan, 2025b). Global consumption of CSO is projected to be approximately 5.2 million metric tons each year (Kumar et al., 2023).

Historically, CSO has been preferred for its versatility in cooking, often utilised as a cooking oil in both commercial and home kitchens because of its high smoke point (up to 232 °C). This feature renders it ideal for frying and for producing a range of food products, such as crackers, potato chips, biscuits, and mayonnaise (Kalkan & Maskan, 2025a). Refined CSO is valued for its soft flavor and golden hue, which makes it a popular component in shortening, margarine, and various processed foods (Zia et al., 2022).

The categorisation of cottonseed and its derivatives as byproducts of the more valuable cotton fiber production (accounting for only approximately 14-19% of the farm-gate value) underscores its intrinsic sustainability benefit compared to other oilseeds (Mirghani & Che Man, 2003). The status of this byproduct significantly improves its sustainability

metrics, since its economic utilisation is closely associated with the maximisation of cotton cultivation and minimisation of agricultural waste, all without the need for additional land use (Gutierrez & Komarnytsky, 2025). Additionally, CSO has attracted attention as a renewable feedstock for biodiesel and other bio-based fuels. However, the environmental benefit depends on feedstock sourcing, processing, transport, and the system boundaries used in life-cycle assessment.

The objectives of this paper are to provide a comprehensive overview of cottonseed oil, addressing its digestibility, nutritional composition, health benefits, safety concerns, and diverse applications. This encompasses the analysis of its physicochemical characteristics (including acid value, saponification value, iodine value, peroxide value, refractive index, specific gravity, and colour), assessing its bioactive constituents (such as antioxidants, flavonoids, gossypol, tocopherols, and sterols), and outlining its various applications in both food and non-food sectors. Special emphasis is placed on its health benefits, including its contribution to cardiovascular health, its effects on allergic reactions, its anticancer properties, and its antioxidant capabilities, along with its growing applications in cosmetics and personal care (Zia et al., 2022).

COMPOSITION AND PHYSICOCHEMICAL PROPERTIES

Fatty Acid Profile

Cottonseed oil has a unique fatty acid composition, which contributes to its nutritional balance. The key fatty acid is linoleic acid (polyunsaturated omega-6), typically found in concentrations between 40% and 58% (Andrade et al., 2025). Palmitic acid, the second most prevalent saturated fatty acid, constitutes about 16% to 28%. Additionally, oleic acid (a monounsaturated fatty acid) is present in quantities that range from 13% to 29.4% (Zhao et al., 2017). In addition to these major components, CSO contains minimal quantities of other fatty acids. This includes saturated fatty acids such as myristic (0.6-1.4%) and stearic (1-7%) acids, in addition to unsaturated fatty acids like palmitoleic (0.4-2%) and alpha-linolenic (trace to 2.41%) acids (Sekhar & Rao, 2011). This composition contributes to its enhanced oxidative stability, making it suitable for applications like frying without requiring additional processing that might form trans fatty acids. The composition of fatty acids in different edible oils is shown in Table 1.

Table 1
Fatty acid composition of various edible oils

Oil Source	Fatty Acids (%)						
	Myristic (14:0)	Palmitic (16:0)	Stearic (18:0)	Others	Oleic (18:1)	Linoleic (18:2)	Linolenic (18:3)
Cottonseed	0.79	24.70	2.20	-	20.87	50.76	-
Groundnut	-	13.69	1.96	3.28*	52.13	28.94	-
Sunflower	0.38	4.27	5.46	-	49.41	40.48	-

Table 1 (*continued*)

Oil Source	Fatty Acids (%)						
	Myristic (14:0)	**Palmitic (16:0)**	**Stearic (18:0)**	**Others**	**Oleic (18:1)**	**Linoleic (18:2)**	**Linolenic (18:3)**
Safflower	1.50	3.00	1.00	-	33.50	61.00	-
Til	-	10.02	5.85	-	40.11	44.02	-
Soybean	-	10.33	3.86	-	26.52	52.92	6.37
Corn	-	14.98	1.31	-	34.12	49.59	-
Mustard	-	2.10	0.39	3.010*	10.31	13.80	11.52
Coconut	18.76	8.38	2.18	62.17*	6.96	1.55	-
Palm	1.50	45.00	4.00	-	39.00	10.50	-

Note. *This includes caproic, caprylic, capric, lauric, arachidic, dehenic and lignoceric, either all or a few in different properties:
Palmitoleic (16:1) Cottonseed 0.68% Mustard 0.26%
Elcosenoic (20:1) Mustard 7.39%
Decosenoic (22:1) Mustard 51.2%
Source: AICOSCA Newsletter, Mumbai, June 2008

Minor Components

Cottonseed oil contains several important non-glyceride components that significantly influence its quality, stability, and safety profile.

Tocopherols, which are forms of Vitamin E, are abundant in CSO, with total content around 0.1% and high concentrations of γ-tocopherol (55%) and α-tocopherol (45%). These natural compounds act as potent antioxidants, effectively delaying primary oxidation and scavenging lipid peroxyl radicals, thereby enhancing the oxidative stability of CSO. Crude CSO may have approximately 1000 ppm (parts per million) of total tocopherols, which is 1.5 to 2 times greater than the levels found in many other vegetable oils.

Phytosterols, which make up about 1% of CSO, are primarily composed of β-sitosterol, campesterol, stigmasterol, and isofucosterol. Their levels are 2-3 times greater than those found in many other vegetable oils, and they play a significant role in enhancing the oil's oxidative stability, especially by inhibiting oxidative degradation during frying. Table 2

Table 2
Phytosterol profile of cottonseed oil (El-Mallah & El-Shami, 2011)

Phytosterols mg/L (ppm)	Cottonseed Oil			
	Crude	Neutralised	Bleached	Deodorised
β-Sitosterol	8,199	7,713	7,495	6,869
Campesterol	874	855	800	725
Stigmasterol	255	240	224	210
Isofucosterol	171	162	161	144
Avenasterol	58	50	46	38

presents the phytosterol content (β-sitosterol, campesterol, stigmasterol) at various stages of cottonseed oil refining.

Phospholipids, often referred to as "gums," are minor constituents in crude CSO, typically ranging from 0.7-0.9%. These substances, which can be hydratable or non-hydratable, act as emulsifiers and can negatively impact oil quality and refined yield if not properly removed. However, in crude form, phospholipids can also function as synergists for tocopherols, contributing to the oxidative firmness of CSO. Their removal through processes like degumming is crucial for purification (Zufarov & Serkayev, 2024).

Lastly, gossypol, a toxic polyphenolic compound, is naturally present in crude cottonseed oil, imparting a distinctive dark brown-red colour. While it provides natural defense against insects for the cotton plant and contributes some initial oxidative stability to crude oil, high concentrations are harmful to human health. Therefore, refining processes are essential to reduce gossypol content to low levels through refining; the applicable regulatory limit depends on the jurisdiction and product category (Kalkan & Maskan, 2025a).

Physicochemical Characteristics

Cottonseed oil exhibits a range of physicochemical characteristics that are critical for determining its suitability, stability, and quality for diverse uses. These characteristics can be influenced by the specific cotton variety, environmental conditions during growth, and various processing steps such as extraction, degumming, refining, bleaching, and deodorisation.

The iodine value, which reflects the level of unsaturation, typically ranges from 99.0 to 113.0 g I_2/100g, with specific values like 103-111 g/100g and 109-110 for crude and refined CSO, respectively. A value of 42.16 g I_2/100g has also been reported, highlighting potential variability. Higher iodine values generally correlate with lower oxidative stability.

The saponification value, which indicates the average molecular weight of fatty acids, generally ranges from 180.31 to 198 mg KOH/g (Ochida et al., 2024).

The peroxide value (PV) is an important measure of early oxidation and rancidity, where values under 10 meq O_2/kg of oil signify freshness. Reported PVs for CSO range from 1 to 6 meq/kg, with some studies noting values between 1.22 and 5.9 meq O_2/kg, and 3.43 meq/kg. For regulatory context, peroxide-value limits depend on the oil category and jurisdiction. Current Indian standards specify up to 10 milliequivalents of active oxygen/kg for refined oils, while other categories may have different limits (Food Safety and Standards Authority of India, 2025).

Acid value, which measures free fatty acid (FFA) content and indicates spoilage, has been reported from 5.75% to 6.82 mg/KOH/g. While acceptable limits for vegetable oils are generally ≤2 mg/KOH/g, crude oils can have higher values. Cottonseed oil generally has lower FFA content compared to soybean oil (Zhao et al., 2017).

Other important parameters include the refractive index, typically around 1.464 to 1.472 at 25°C; specific gravity ranging from 0.88 to 0.92 g/cc; and melting point, which can range from -12 °C for winterised oil to 0-16 °C for refined oil, and up to 53 °C for fully hydrogenated oil (Gutierrez & Komarnytsky, 2025). The smoke point of CSO is notably high, often around 230-232 °C, making it suitable for frying.

Finally, moisture content typically ranges from 0.09% to 0.35%, with low levels being crucial for extended shelf life (Ochida et al., 2024). The data pertaining to physicochemical properties of cottonseed oil are presented in Table 3.

Table 3
Physicochemical properties of cottonseed oil

Property	Typical Value/ Range	Unit	Notes
Specific gravity (25°C)	0.917 - 0.919	-	Indicates density relative to water
Refractive index (40°C)	1.465 - 1.467	-	Used for purity check
Viscosity (30°C)	48 - 54	cP	Flow property, important in processing
Iodine value	100 - 123	g I_2/100 g oil	Degree of unsaturation
Saponification value	189 - 198	mg KOH/g oil	Average molecular weight of fatty acids
Acid value	0.2 - 4.0	mg KOH/g oil	Indicates free fatty acids, quality indicator
Peroxide value	≤ 10	meq O_2/kg oil	Measures primary oxidation
Unsaponifiable matter	0.5 - 1.5	%	Includes sterols, tocopherols, hydrocarbons
Smoke point	216 - 232	°C	Temperature at which oil begins to smoke
Flash point	315 - 330	°C	Safety indicator
Fire point	350 - 370	°C	Safety indicator

DIGESTIBILITY AND BIOAVAILABILITY

General Digestibility

Cottonseed oil is practically completely digested in the normal individual, a key prerequisite for its utilisation in the human body. The degree of absorption, expressed as the coefficient of digestibility, is the usual index for evaluating how well a fat is utilised. For cottonseed oil, the average digestibility coefficient is approximately 97 percent in humans (Sekhar & Rao, 2011). This high digestibility applies to all natural fats, including cottonseed oil, that have melting points below about 38 °C. The nutritive value of a fat is directly proportional to its digestibility.

Digestibility in Ruminants (Sheep, Cattle)

In ruminant animals, lipid supplementation is a beneficial nutritional approach because of its high energy digestibility, which is 2.25 times that of carbohydrates. Studies on sheep involving cashew nutshell liquid (CNSL) blends revealed that feeding sheep with CNSL

mixed with canola oil led to increased intakes of saturated fatty acids (SFA), unsaturated fatty acids (UFA), and monounsaturated fatty acids (MUFA), while resulting in decreased intakes of polyunsaturated fatty acids (PUFA) (Andrade et al., 2025). Additionally, diets incorporating CNSL blended with cottonseed oil resulted in improved digestibility of dry matter (DM) and neutral detergent fiber (NDF) compared with other oil combinations. For fattening cattle, the inclusion of 1.5% cottonseed oil along with 0.5% tannins from tea by-products resulted in enhanced nutrient digestibility, a rise in crude protein (CP) intake, and a boost in daily weight gain, while also decreasing methane emission intensity by 4.8 to 12.1% (Thang & Hiep, 2020). This particular combination led to the lowest levels of enteric methane production in fattening cattle.

Digestibility in Monogastric Animals (Pigs)

In monogastric animals, particularly in growing pigs, CSO shows a high level of digestibility and energy value. Research has shown that the digestible energy (DE) and metabolisable energy (ME) levels, as well as the apparent total tract digestibility (ATTD) of cottonseed oil, were not significantly affected by the level of dietary inclusion, even when assessed across a range of 2% to 10%. The average DE and ME values for CSO were reported as 36.18 MJ/kg and 35.56 MJ/kg, respectively, with an ATTD of 90.66%. Moreover, the DE and ME values of CSO were found to be similar to those of soybean oil, despite soybean oil having a higher ratio of unsaturated to saturated fatty acids (5.11 for soybean oil vs. 2.79 for cottonseed oil). This indicates that the ratio of unsaturated to saturated fatty acids is not the only critical factor affecting the energy values and ATTD of oils. The true total tract digestibility (TTTD) of acid-hydrolysed ether extract (AEE) from cottonseed oil was found to be 92.40% in growing pigs, with an endogenous loss of AEE amounting to 13.83 g/kg of DM intake (Zhao et al., 2017).

NUTRITIONAL AND HEALTH BENEFITS

Essential Fatty Acids

Linoleic acid, which typically constitutes around 50% of CSO's fatty acid profile, with some sources reporting ranges from 40% to 57.1%, is vital for preventing the hardening of coronary arteries and generally supporting cardiovascular health. Historical reports indicate that diets deficient in linoleic acid, often due to high consumption of animal or hydrogenated fats, were considered a predisposing factor for conditions like atherosclerosis. Consequently, there has been a global emphasis on increasing the consumption of unsaturated fats, particularly those high in linoleic acid or polyunsaturated fatty acids (PUFA) (Sekhar & Rao, 2011).

Cardiovascular Health

Cottonseed oil contains predominantly unsaturated fatty acids, and substitution of saturated fats with unsaturated fats is consistent with current American Heart Association dietary guidance (Lichtenstein et al., 2026). The manuscript does not retain the earlier attribution of a "Heart Oil" designation or an "OK FOOD" listing to the American Heart Association. Studies have indicated that CSO-rich diets can lower total cholesterol and LDL cholesterol in normocholesterolemic subjects. For instance, an experiment involving 38 healthy adults showed that consuming a diet rich in CSO, a daily intake of 95 grams for one week, resulted in a decrease in total cholesterol and LDL levels. The lipid-lowering effects observed may be partially linked to the non-saponifiable component of CSO, which includes beneficial compounds like alpha-tocopherol and beta-sitosterol (Zia et al., 2022).

Antioxidant Properties

Cottonseed oil is particularly rich in natural antioxidants, especially tocopherols (Vitamin E), which are crucial for its oxidative stability and provide various health advantages. CSO contains high levels of tocopherols, such as α- and γ-tocopherol, often 1.5 to 2 times higher than many other vegetable oils. Besides tocopherols, other bioactive compounds like phytosterols and polyphenols contribute to improving the overall antioxidant capacity and stability of CSO. It is crucial to note that gossypol, a naturally occurring polyphenolic toxin, is found in crude cottonseed oil and must be substantially reduced during refining before human consumption; the applicable regulatory limit depends on the jurisdiction and product category.

Anti-Inflammatory Properties

Cottonseed oil contains anti-inflammatory properties, including omega-3 and omega-6 fatty acids, phytochemicals, and polyphenols (Ochida et al., 2024).

Anticancer Activity

Unsaturated fatty acids, including oleic acid, a primary fatty acid present in CSO, have been demonstrated to inhibit the proliferation of cancer cells. Additionally, gossypol exhibits antiradical and anti-proliferative properties against various human cancer cell lines, such as those originating from the breast, colon, ovary, and prostate (Zia et al., 2022).

Anti-Allergic Response

Research has studied cottonseed oil for its potential to affect allergic responses, indicating a crucial function in allergy defense. Investigations suggest that it may improve the humoral immune response as an adjuvant, enhancing secondary reactions, particularly a delayed-type

hypersensitivity response to ovalbumin. A notable advantage of using cottonseed oil in this context is its minimal occurrence of adverse side effects, attributed to its composition of biodegradable substances that the body can easily metabolise (Zia et al., 2022).

Skin Health and Personal Care

The cottonseed oil profile contributes to its notable moisturising, antioxidant, and anti-inflammatory effects. The beneficial linoleic-to-oleic acid ratio found in CSO is crucial for supporting and repairing the skin barrier function and regulating inflammatory responses. CSO also functions effectively as a carrier oil for other active ingredients due to its easy absorption, moderate-to-low comedogenic value, and excellent oxidative stability imparted by its unsaponifiable fraction. Additionally, its palmitic acid content serves as a natural precursor of human sebum components, helping maintain skin and hair hydration (Gutierrez & Komarnytsky, 2025).

SAFETY PROFILE AND REGULATORY CONSIDERATIONS

Gossypol

Crude cottonseed oil contains gossypol, a naturally occurring toxic polyphenolic pigment that imparts a strong brownish-red colour to the oil and acts as the plant's defense mechanism against insects (Candelaria et al., 2022). In high concentrations, gossypol is toxic to humans and monogastric animals, potentially causing adverse health effects such as reduced growth, various pathologies, and issues with the reproductive system. Consequently, refining processes, including alkali refining and bleaching, are crucial to lower gossypol levels to the approved low levels through refining; the applicable regulatory limit depends on the jurisdiction and product category, thereby making the oil suitable for human consumption. In parallel, efforts are being made to develop glandless cotton varieties that produce seeds with naturally very low gossypol content, offering a promising solution for the manufacturing of secure cottonseed oil (He et al., 2023).

Cyclopropenoid Fatty Acids (CPFAs)

Cottonseed oil is rich in distinctive CPFAs, namely malvalic and sterculic acids, which are defined by the inclusion of a cyclopropene group within their structure (Kumar et al., 2023). These naturally occurring compounds, including dihydrosterculic acid, can have adverse physiological effects in animals. In animal diets, the presence of CPFAs has been linked to issues such as diminished egg output, inadequate hatching rates, and pinkish egg whites in chickens, along with stunted growth and sexual maturation, and potentially carcinogenic effects in rats (Zia et al., 2022). Given their undesirable nutritional and health implications, refining processes are crucial for inactivating these acids. Conventional processing methods

like hydrogenation and deodorisation significantly reduce CPFA levels, for instance, from 0.53% to as low as 0.04% through deodorisation alone (Gutierrez & Komarnytsky, 2025).

Trans Fats

While cottonseed oil inherently offers a fatty acid profile that is stable for frying, precluding the need for further processing that forms trans fatty acids, its industrial application often involves hydrogenation. This process transforms unsaturated compounds and can generate trans fatty acids, which are widely regarded as unhealthy. Trans fats have a detrimental effect on health, as they raise LDL (bad) cholesterol levels while lowering HDL (good) cholesterol levels, elevating blood triglyceride levels, and fostering conditions like weight gain and excessive abdominal fat; all of these factors lead to a heightened risk of heart disease and diabetes. Cottonseed oil was notably one of the first oils to be hydrogenated for mass production, and its partially hydrogenated form contains nutritionally undesirable saturated and trans fatty acids. However, non-hydrogenated CSO acts as a substitute deep-frying medium to reduce trans fatty acid levels in fried foods. Notably, when CSO undergoes partial hydrogenation to achieve an Iodine Value of around 80, its fatty acid composition changes to consist of 50% monounsaturated, 21% polyunsaturated, and 29% saturated fats, a composition considered to be within current dietary guidelines (Sekhar & Rao, 2011).

Pesticide Residues

Concerns regarding pesticide residues in cottonseed oil have been raised, partly because regulations for non-food crops, such as cotton, may differ. However, insufficient testing has been conducted to conclusively demonstrate elevated contamination levels. Nevertheless, regular testing for pesticide residues is deemed crucial for detecting any contaminants that may arise from environmental pollution, agricultural practices, transportation, and processing. Crude vegetable oils naturally contain minor components like pesticides. Nevertheless, as a result of the thorough refining process, cottonseed oil has been investigated for cosmetic and personal-care applications; however, claims of being universally hypoallergenic should be avoided because individual sensitivity and product formulation can vary (Gutierrez & Komarnytsky, 2025).

Regulatory Status

Thanks to its thorough refining process, refined cottonseed oil offers a benefit compared to certain cold-pressed or virgin oils, which might have proteins that can provoke IgE-binding allergic reactions. Regulatory measures are in place to guarantee the oil's safety and effectiveness in cosmetic products, focusing on its agricultural origins, the removal of gossypol and cyclopropenoid acids during the refining process, and the need for rigorous

quality control. This rigorous processing contributes to its low contamination risk, minimal aroma, and extended shelf life, which are desirable features for personal care product development (Gutierrez & Komarnytsky, 2025).

PROCESSING METHODS AND IMPACT ON QUALITY

Extraction Methods

Cottonseed oil extraction employs various methods, encompassing both conventional and non-conventional techniques, with recent advancements focusing on green solvents to improve efficiency and environmental sustainability. Conventional methods include mechanical pressing, such as hydraulic and screw presses, which produce high-quality oil with natural characteristics but are less efficient, leaving up to 20% of the oil contained in the press cake. Solvent extraction, primarily using n-hexane, is a conventional method favored for its high oil recovery and affordability. However, hexane poses significant environmental and health risks, including air pollution, inhalation toxicity, flammability, and potential organ damage, leading to calls for its replacement (Kalkan & Maskan, 2025a).

A significant advancement in extraction involves integrating green solvents like Natural Deep Eutectic Solvents (NADES), which are biodegradable, non-flammable, and derived from plant metabolites. The Ultrasound-Homogenisation-Assisted (UHA) method incorporating NADES (specifically Choline Chloride: Oxalic acid) with ethyl acetate as a co-solvent has demonstrated superior oil recovery (90.68%) under milder operational conditions (30 °C, 60 min) compared to traditional UHA-Hexane methods (85.18%). This green approach is also significantly more energy-efficient, consuming about seven times less heating energy, and benefits from NADES reusability, leading to reduced environmental impact and operational costs (Kalkan & Maskan, 2025a).

Refining Process

The refining process for cottonseed oil is a multi-step procedure crucial for enhancing its quality, safety, and shelf life for edible and industrial applications. This process aims to remove undesirable substances present in crude oil, which include phospholipids, free fatty acids, pigments, gossypol, and volatile compounds.

The first step, degumming, involves removing hydrophilic substances, primarily phospholipids, which can interfere with processing and affect oil stability. Various degumming methods exist, including water, acid, total, soft, enzymatic, ultrafiltration, and ethanolamine degumming. Water degumming specifically removes hydratable phospholipids, such as phosphatidylcholine (which is 100% hydratable) and a significant portion of phosphatidylethanolamine and phosphatidylinositol, with removals up to 82.1% in solvent-extracted oil. Acid and total degumming further reduce non-hydratable

phospholipids, as well as levels of phosphorus, calcium, and magnesium, making the oil purer and more nutritionally valuable (Zufarov & Serkayev, 2024). Following this, alkaline neutralization removes free fatty acids through alkali refining.

Bleaching is then performed using activated clays to remove dark colours, pigments, and impurities, most notably the toxic polyphenolic compound gossypol (Mirghani & Che Man, 2003). Refining substantially reduces gossypol and other undesirable constituents. The previously stated universal 1-5 ppm limit has been removed because the cited FDA provision concerns modified cottonseed products rather than establishing a general gossypol limit for refined cottonseed oil. The final stage, deodorisation, removes volatile substances that contribute to unwanted odors and flavors, yielding a neutral-flavored and odorless oil. This step also significantly inactivates cyclopropenoid fatty acids (Zia et al., 2022).

Overall, refining dramatically impacts the final oil quality by improving its colour, flavor, and oxidative stability. It extends the shelf life of cottonseed oil by removing compounds that promote rancidity, making it a more robust cooking medium. However, the refining process also leads to a reduction in some beneficial nutritional components; for instance, phytosterol content can be reduced by about 15%, and tocopherol content, which acts as a natural antioxidant, can decrease by approximately 18% during refining, with significant losses (30-60%) occurring during deodorisation (Gutierrez & Komarnytsky, 2025). Despite these reductions, the comprehensive refining ensures the oil is safe, stable, and acceptable for diverse food and industrial applications (Kumar et al., 2023).

Further Modifications

Cottonseed oil undergoes further modifications, such as winterisation and hydrogenation, to tailor its physical and functional properties for specific applications.

Winterisation is a fractional crystallisation process that involves slowly cooling refined cottonseed oil to remove higher-melting stearin (palmitin) byproducts. This process is highly effective for cottonseed oil due to its negligible content of linolenic acid. The resulting winterised cottonseed oil remains clear and liquid at lower temperatures (with a melting point of approximately -12 °C), possesses a pleasant flavor, and exhibits increased stability. This modification is particularly advantageous for products requiring clarity and a liquid state in refrigerated conditions (Gutierrez & Komarnytsky, 2025).

Hydrogenation alters cottonseed oil by incorporating hydrogen atoms into its unsaturated fatty acids, thereby raising the levels of saturated and monounsaturated fatty acids. This process is used to harden the oil, raise its melting point, and provide solidity, making it suitable for applications such as shortening and margarine production. Fully hydrogenated cottonseed oil becomes solid at room temperature (with a melting point around 53 °C) and is primarily composed of stearic (76%) and palmitic (22%) acids, with virtually no polyunsaturated fatty acids, contributing to high oxidative stability. While

partial hydrogenation also increases monounsaturated and saturated fatty acid content and enhances stability, this can result in the creation of nutritionally harmful trans-fatty acids, which pose a considerable health risk (Zia et al., 2022). Hydrogenation also lightens the oil's colour and can produce a distinct, unpleasant odor that necessitates subsequent deodorisation.

APPLICATIONS

Edible Oil

Cottonseed oil is widely utilised as an edible oil in both commercial and home cooking, as well as in various food manufacturing applications. It is particularly valued for frying and cooking due to its high smoke point, which ranges from 230.52 to 232.2 °C. This characteristic allows it to withstand high temperatures without igniting, producing harmful fumes, or generating off-flavors, making it a robust cooking medium. Its desirable attributes, such as a mild, nut-like taste, clear colour, and flavor stability, further enhance its appeal (Sekhar & Rao, 2011). In food manufacturing, cottonseed oil is a key ingredient in products like crackers, biscuits, mayonnaise, shortening, and margarine. It is also used in salad dressings. Described as "naturally hydrogenated" and rich in natural antioxidants (tocopherols), it offers excellent oxidative stability, contributing to a longer fry life and extended shelf life for food products. Once refined to safe gossypol levels, it is suitable for human consumption.

Cosmetics and Personal Care

In the realm of cosmetics and personal care, cottonseed oil remains an underappreciated ingredient with a wide range of potential applications. It functions effectively as a carrier oil for other bioactive ingredients due to its easy absorption, moderately low comedogenic value, and superior oxidative and thermal stability provided by its unsaponifiable fraction, which is rich in phytosterols and tocopherols. For the repair of the skin barrier, its elevated linoleic acid content and advantageous linoleic-to-oleic acid ratio enable it to integrate seamlessly with the skin's natural lipid matrix, aiding in the reduction of transepidermal water loss and providing protection against external irritants. It has been incorporated into emollient lotions to improve skin barrier function and mitigate microbial dysbiosis. For hair conditioning, the oil is a popular ingredient in hair products, offering nourishing benefits and suitability for heat styling due to its high smoking point (230 °C). In cleansing soaps, its elevated levels of linoleic and palmitic acids render it ideal for producing both soft soap bars and liquid soaps, and its lack of strong aroma allows for versatile fragrance-free or scented formulations. Additionally, cottonseed oil is employed in drug delivery systems as a solubilising excipient in oral and injectable formulations, and serves as a long-term drug

delivery reservoir for lipophilic medications, demonstrating good permeation enhancer abilities. Its moisturising, anti-inflammatory properties and antioxidant activity further enhance its utility in personal care (Gutierrez & Komarnytsky, 2025).

Biofuels

Cottonseed oil is widely used in the production of biodiesel. Its potential environmental benefit depends on feedstock sourcing, processing, transport, and the life-cycle boundary used. Biodiesel derived from CSO, such as cottonseed oil methyl ester (CSOME), has shown better efficiency than commercial diesel and contributes to a cleaner environment (Mominou et al., 2025).

Industrial Applications

In the paint industry, cottonseed oil is a valuable raw material, notably in the production and modification of alkyd resins (polyesters) for industrial and household finishes (Zia et al., 2022). The composition of the oil renders it ideal for the production of detergents and soaps, as its high levels of palmitic and linoleic acids are beneficial for the formulation of liquid soaps and soft soap bars. Moreover, maleinised CSO acts as a plasticiser in poly(lactic acid) films, enhancing their flexibility (Kumar et al., 2023).

Animal Feed

Cottonseed oil provides essential energy supplements and protein sources for various livestock. In ruminants such as sheep and fattening cattle, the addition of cottonseed oil notably increases available energy, enhances nutrient digestibility, and improves overall performance (Thang & Hiep, 2020). It is included in diets to enhance energy density, improve palatability, and increase feed efficiency (Andrade et al., 2025). For growing pigs, cottonseed oil is a concentrated energy source. Dietary fat generally provides more energy per unit mass than carbohydrate, although the reported energy values should be interpreted using the specific experimental diet and analytical method (Zhao et al., 2017). Cottonseed products are essential in the diets of farm-raised fish, providing necessary protein (Candelaria et al., 2022). The consumption of nutrients and the digestibility of sheep on different diets are presented in Table 4.

Novel Food Products

Cottonseed oil is essential in creating innovative food products, particularly spreads that resemble plant-based butter. These spreads are typically produced from glandless cottonseed kernels to keep gossypol levels low, making them safe for consumption.

Table 4
Nutrient consumption and digestibility in sheep that were given diets comprising mixtures of CNSL at 0.5% of total DM along with various vegetable oils at 1.5% of total DM. (Andrade et al., 2025)

Variables	Vegetable Oils and CNSL[a] Blend					SEM[b]	P-value[c]
	MUFA	PUFA					
	Canola	Cottonseed	Sunflower	Corn	Soybean		
Intake (g/day)							
Dry matter	1376	1433	1460	1456	1388	60.6	0.440
Mineral matter	73.2	75.3	73.6	75.1	72.2	3.14	0.931
Crude protein	154	167	171	161	156	9.91	0.344
aNDF[d]	515	543	572	558	544	29.1	0.405
Ether extract	61.4	68.5	66.0	69.2	62.9	3.66	0.087
Non-fiber carbohydrates	572	579	577	592	552	19.5	0.581
Total digestible nutrients	788a	794a	755ab	723b	792a	11.3	0.0008
Metabolisable energy	4.14	4.17	4.35	4.43	4.35	0.27	0.816
Saturated FA	0.215c	0.346a	0.235bc	0.248b	0.057d	0.008	< .0001
Unsaturated FA	1.091bc	0.997c	1.165b	1.162b	1.307a	0.476	0.0012
Monounsaturated FA	0.406b	0.2453d	0.3735bc	0.299 cd	0.872a	0.024	< .0001
Polyunsaturated FA	0.685c	0.751bc	0.792ab	0.862a	0.435d	0.026	< .0001
Digestibility (g/100 g of intake)							
Dry matter	77.4a	77.3a	74.9b	73.6b	74.9b	3.72	0.001
Crude protein	77.0	75.1	73.9	73.7	75.6	5.43	0.209
aNDF[d]	77.5a	75.7a	69.6bc	71.7b	68.3c	5.94	0.002
Ether extract	83.9	86.4	81.7	83.8	87.1	5.53	0.239
Non-fiber carbohydrates	79.4	81.4	83.9	82.2	80.2	6.74	0.191

Note.[a]Cashew nut shell liquid; FA = Fatty acids; Canola = Source of monounsaturated fatty acids (MUFA); Cottonseed, Sunflower, Corn and Soybean = Source of monounsaturated fatty acids (MUFA);
[b]SEM = Standard error of the mean;
[c]Means followed by a different letter in the row are statistically different according to Tukey's test at 5% probability;
[d]Neutral detergent fiber assayed with a heat-stable amylase and expressed exclusively for residual ash;

The production process involves roasting the kernels and subsequently grinding them with certain additives such as additional cottonseed oil, cane sugar, and table salt.

The overall oil content is an essential factor that greatly influences the consistency, texture, and stability of these products. While glandless cottonseed kernels naturally contain about 35% oil, external cottonseed oil is added to achieve a desired total oil content, often ranging from 36% to 57%. Higher oil content generally improves textural properties, leading to softer, more spreadable products, but it can also reduce oxidative stability and increase oil separation during storage. In practical use, cottonseed butter products containing 47-50% total oil are noted for their firmness and smooth texture, along with adequate storage stability. In contrast, products with 53-57% oil content serve as creamier spreads but tend to have a reduced shelf life (He et al., 2023). These innovative plant-based butters provide essential nutrients and energy, enhancing the value and utility of cottonseed.

FUTURE PERSPECTIVES

Future research avenues for cottonseed oil are diverse, focusing on improving its sustainability, nutritional benefits, and market adaptability. A primary focus is on the further refinement of green extraction methods, particularly the ultrasound and Homogenisation-assisted natural deep eutectic solvent (UHA-NADES) technique, to enhance oil yield and quality while minimising environmental harm, energy use, and dependence on harmful solvents like hexane. Concurrently, genetic modification presents considerable opportunities for creating cottonseed varieties with superior nutritional characteristics. This encompasses boosting beneficial fatty acids such as oleic acid and reducing undesirable ones through innovative methods like gene silencing and CRISPR/Cas9 technology, thus producing high-oleic cottonseed oil and other tailored formulations. In addition to existing applications, there is a pressing need to investigate wider applications in functional foods and nutraceuticals, utilising the unique compounds found in cottonseed oil, including rare cyclic fatty acids, for potential health advantages such as enhancing liver metabolomic profiles, and broadening its use in various personal care products. Performing thorough life cycle assessments (LCA) is essential to comprehensively assess the environmental impact, including CO_2 emissions and energy consumption, throughout the entire production and usage process of cottonseed oil, ensuring its sustainability and beneficial effects in the long run.

CONCLUSION

Cottonseed oil is a highly digestible, nutritionally rich, and sustainable vegetable oil that is produced as a byproduct of cotton fiber manufacturing, providing both health and environmental advantages. With a digestibility rate of approximately 97%, it features a favorable fatty acid composition, approximately 65% unsaturated and 35% saturated,

predominantly consisting of linoleic, palmitic, and oleic acids, along with a relatively high proportion of polyunsaturated fatty acids. Abundant in tocopherols (Vitamin E), phytosterols (β-sitosterol, campesterol, stigmasterol), and vitamins A and K, CSO promotes cardiovascular health by reducing LDL and total cholesterol levels, while also demonstrating antioxidant, anti-inflammatory, anti-allergic, and anticancer effects. Current American Heart Association guidance supports replacing saturated fats with unsaturated plant oils; cottonseed oil is not specifically identified by the AHA as a "Heart Oil" (Lichtenstein et al., 2026). Cottonseed oil has also been investigated as a feedstock for biofuels. Proper refining reduces undesirable constituents and improves the quality and safety of the oil; environmental performance depends on the production and processing system.

ACKNOWLEDGEMENT

The authors express sincere thanks to the Functional Managers at Coromandel Agro Products and Oils Limited for their essential support in supplying data and facilitating the successful execution of this research project.

REFERENCES

Andrade, E. L. G., Perreira Filho, J. M., de Lucena, K. H. de O. S., Barros, L. S., Barbosa, A. M., Oliveira, R. L., Gonzaga Neto, S., de Oliveira, J. P. F., Fonseca, M. A., & Bezerra, L. R. (2025). Effects of dietary supplementation with vegetable oils of different unsaturated fatty acids composition on intake, digestibility, nitrogen balance performance, and carcass traits of sheep. *Tropical Animal Health and Production, 57*(3), 1- 11. https://doi.org/10.1007/s11250-025-04395-7

Candelaria, B., Yamamoto, F. Y., & Gatlin, D. M., III. (2022). The effects of dietary cottonseed oil on growth performance of juvenile red drum (*Sciaenops ocellatus* L.) and hybrid striped bass (*Morone chrysops* × *M. saxatilis* S.). *Aquaculture Nutrition, 2022*, Article 1077178. https://doi.org/10.1155/2022/1077178

El-Mallah, M., & El-Shami, S. (2011). Effect of chemical refining steps on the minor and major components of cottonseed oil. *Agriculture and Biology Journal of North America, 2*(2), 341- 349. https://doi.org/10.5251/abjna.2011.2.2.341.349

Food Safety and Standards Authority of India. (2025). *Food Safety and Standards (Food Products Standards and Food Additives) Regulations: Chapter 2.2—Fats, oils and fat emulsions* (Version 5, 1 August 2025). Government of India.

Gutierrez, J., & Komarnytsky, S. (2025). Cottonseed oil composition and its application to skin health and personal care. *Frontiers in Pharmacology, 16*, Article 1559139. https://doi.org/10.3389/fphar.2025.1559139

He, Z., Rogers, S. I., Nam, S., & Klasson, K. T. (2023). The effects of oil content on the structural and textural properties of cottonseed butter/spread products. *Foods, 12*(22), Article 4158. https://doi.org/10.3390/foods12224158

Kalkan, E., & Maskan, M. (2025a). A green approach: Optimization of ultrasound and homogenisation-assisted ethyl acetate extraction of cottonseed oil using natural deep eutectic solvent as a novel co-solvent. *Food and Bioprocess Technology, 18*(6), 5782- 5813. https://doi.org/10.1007/s11947-025-03801-0

Kalkan, E., & Maskan, M. (2025b). Optimization of sonication and homogenisation-assisted solvent extraction of cottonseed oil using RSM: Oil recovery, antioxidant properties, and oxidative stability. *Journal of Food Process Engineering, 48*(5), Article e70125. https://doi.org/10.1111/jfpe.70125

Kumar, M., Zhang, B., Potkule, J., Sharma, K., Radha, Hano, C., Sheri, V., Chandran, D., Dhumal, S., Dey, A., Rais, N., Senapathy, M., Natta, S., Viswanathan, S., Mohankumar, P., & Lorenzo, J. M. (2023). Cottonseed oil: Extraction, characterization, health benefits, safety profile, and application. *Food Analytical Methods, 16*(2), 266- 280. https://doi.org/10.1007/s12161-022-02410-3

Lichtenstein, A. H., Khera, A., Anderson, C. A. M., Appel, L. J., DeSilva, D. M., Gardner, C., Hu, F. B., Jones, D. W., & Petersen, K. S. (2026). 2026 dietary guidance to improve cardiovascular health: A scientific statement from the American Heart Association. *Circulation, 153*(18), e1285-e1295. https://doi.org/10.1161/CIR.0000000000001435

Mirghani, M. E. S., & Che Man, Y. B. (2003). A new method for determining gossypol in cottonseed oil by FTIR spectroscopy. *Journal of the American Oil Chemists' Society, 80*(7), 625- 628. https://doi.org/10.1007/s11746-003-0749-2

Mominou, N., Moctar, I., Mahlik, M., & Zisuh, A. (2025). Modelling gas and gasoline production from cottonseed oil on fixed-fluidized bed catalytic cracking over NbFeAPSO-5 molecular sieve. *International Journal of Environmental Chemistry, 9*(2), 28- 35. https://doi.org/10.11648/j.ijec.20250902.11

Ochida, C. O., Itodo, A. U., Anhwange, B. A., & Onoja, P. O. (2024). Physicochemical properties of mango, coconut and cotton seed oils and their ameliorating effect on renal toxicity in Wistar rats. *UMYU Journal of Microbiology Research, 9*(2), 159- 172. https://doi.org/10.47430/ujmr.2492.019

Sekhar, S. C., & Rao, V. K. B. (2010). White gold intricacies. *Emerging Science, 1*(12), 12- 14.

Sekhar, S. C., & Rao, V. K. B. (2011). Cottonseed oil as health oil. *Pertanika Journal of Tropical Agricultural Science, 34*(1), 17- 24.

Sekhar, S. C., Sai Dinesh, P., Ruthwik, A. S. S., Sandeep, M., & Yuva Vamsi, M. (2024). India's cotton balance sheet under two decadal scenarios: A review. *Agricultural Reviews, 45*(3), 456- 463. https://doi.org/10.18805/ag.R-2599

Thang, C. M., & Hiep, T. (2020). Combined effects of cottonseed oil and tannin from tea by-products (*Camellia sinensis*) supplementation on nutrient digestibility, performance and enteric methane production of fattening cattle. *Advances in Animal and Veterinary Sciences, 8*(6), 633- 638. https://doi.org/10.17582/journal.aavs/2020/8.6.633.638

Wu, M., Pei, W., Wedegaertner, T., Zhang, J., & Yu, J. (2022). Genetics, breeding and genetic engineering to improve cottonseed oil and protein: A review. *Frontiers in Plant Science, 13*, Article 864850. https://doi.org/10.3389/fpls.2022.864850

Zhao, J., Li, Z., Lyu, M., Liu, L., Piao, X., & Li, D. (2017). Evaluation of available energy and total tract digestibility of acid-hydrolyzed ether extract of cottonseed oil for growing pigs by the difference and regression methods. *Asian-Australasian Journal of Animal Sciences, 30*(5), 712- 719. https://doi.org/10.5713/ajas.16.0546

Zia, M. A., Shah, S. H., Shoukat, S., Hussain, Z., Khan, S. U., & Shafqat, N. (2022). Physicochemical features, functional characteristics, and health benefits of cottonseed oil: A review. *Brazilian Journal of Biology, 82*, Article e243511. https://doi.org/10.1590/1519-6984.243511

Zufarov, O., & Serkayev, K. (2024). Phospholipids in cottonseed oil and degumming methods. *Bulletin of the Transilvania University of Brasov. Series II: Forestry, Wood Industry, Agricultural Food Engineering, 17*(2), 171-184. https://doi.org/10.31926/but.fwiafe.2024.17.66.2.11

Pertanika J. Trop. Agric. Sci. 49 (5): 2323 - 2342 (2026)

PERTANIKA JOURNALS

TROPICAL AGRICULTURAL SCIENCE

Journal homepage: http://www.pertanika.upm.edu.my/

Comparative Phytochemical and Biological Properties of Unripe *Spondias pinnata* Fruit Extract

Rattana Meekrasae[1], Noppadon Somphol[2], Wuttisak Kunu[2], and Supawadee Patathananone[1]*

[1]*Department of Chemistry, Faculty of Science and Technology, Rajamangala University of Technology Thanyaburi, 12120 Pathum Thani, Thailand*
[2]*Program in Veterinary Technology and Veterinary Nursing, Faculty of Agricultural Technology, Rajabhat Maha Sarakham University, 44000 Maha Sarakham, Thailand*

ABSTRACT

Medicinal plants are recognised as valuable sources of phytochemicals with the potential to prevent biomolecular degeneration and promote human and animal health. This in vitro study investigated and compared the biological activities and phytochemical composition of raw *Spondias pinnata* fruit extracts prepared using three solvents: 70% acetone (WRA-1), 70% ethanol (WRA-2), and 70% methanol (WRA-3). All three extracts exhibited antityrosinase, antielastase, and antioxidant activities, as well as cytotoxic effects against cholangiocarcinoma (MO55) cells. The IC_{50} values on MO55 cells were 0.58, 1, and 2.1 mg/mL for WRA-1, WRA-2, and WRA-3, respectively. WRA-3 exhibited a significantly lower cytotoxic effect on MMNK1 cells. Comparable phytochemical profiles, including phenolic compounds, flavonoids, terpenoids, tannins, and cardiac glycosides, were observed in all three extracts. The total phenolic contents of WRA-1, WRA-2, and WRA-3 were 26.35 ± 4.89, 49.77 ± 3.81, 31.91 ± 1.52 mg GAE/g extract, respectively. 5-hydroxymethylfurfural, gallic acid, verbascoside, and isorhamnetin-3-rutinoside as the major bioactive constituents in WRA-1. As this study was limited to in vitro assays and did not include in vivo or clinical validation, the biological relevance of these findings to human and animal health remains to be established. Overall, the results suggest that unripe *S. pinnata* fruit represents a promising source of bioactive compounds and warrants further investigation for potential healthcare applications.

Keywords: Anticancer, antioxidant, anti-tyrosinase, anti-elastase, wild mango fruit

ARTICLE INFO

Article history:
Received: 20 July 2025
Accepted: 28 September 2026
Published: 30 October 2026

DOI: https://doi.org/10.47836/pjtas.49.5.11

E-mail addresses:
Rattana231139@gmail.com (Rattana Meekrasae)
Noppadon.so@rmu.ac.th (Noppadon Somphol)
Wuttisak.ku@lives.rmu.ac.th (Wuttisak Kunu)
Supawadee_P@rmutt.ac.th (Supawadee Patathananone)
* Corresponding author

e-ISSN: 2231-8542

© Universiti Putra Malaysia Press

INTRODUCTION

Currently, the rapidly increasing number of elderly people has led to a demographic shift. This issue has caused many countries around the world to face the challenges of an aging society, and they are moving towards becoming super-aged societies in the next few years.

In addition, one public health problem that arises alongside entering an aging society is illnesses, disabilities, and deaths from non-communicable diseases (NCDs). According to statistics collected by the World Health Organization (WHO), NCDs are the cause of death for humans, accounting for up to 79% (World Health Organization, 2024). The top four NCDs that affect health and cause a lot of human deaths are cardiovascular diseases (19 million people), cancer (10 million people), chronic respiratory diseases (4 million people), and diabetes (>2 million people). Similarly, in Thailand, Thai people die from NCDs at a rate of up to 74% of all causes of death. The continuous increase in the number of elderly people and patients with chronic non-communicable diseases is causing healthcare systems to spend more on patient care, impacting the economy and society in every country worldwide, especially in low- and middle-income countries (Thansa, 2025). Moreover, most developing countries rely on technology and imports of healthcare products from developed countries (Alfaouri et al., 2025; Sabogal et al., 2025). The fighting around the Strait of Hormuz has affected the transport of raw materials used in making medicines, treatment drugs, and medical supplies from the United States of America (USA), Europe, and the Middle East to the Asian region. Countries in the Asian region are affected by the risk factors mentioned above, leading to shortages of many types of medicines during conflict crises, as well as higher costs for importing key ingredients. Solving the problem of essential drug shortages caused by these factors in the public health system is therefore very important.

The progression of ageing and NCDs is associated with two major factors: (1) intrinsic factors (age, sex, hormones, genes, oxidative stress, etc.) and (2) extrinsic factors (environmental, food, lifestyle, etc.). Both factors have a mechanism of co-stimulation that causes biomolecular degeneration in many forms, leading to changes in their structure and malfunction, resulting in accelerated aging and NCDs (Guo et al., 2022). Therefore, studying ways to slow down the deterioration of biomolecules related to those factors might help reduce the number of people with NCDs.

Natural products are an exciting target source for human health prevention and therapy development. The safety of treatment substances and the reduction of side effects are two primary concerns that drive the interest in natural active ingredients, leading to a continuous increase in research studies. In addition, researching medicinal herbs with therapeutic properties for use within public health systems might help solve the problem of shortages of essential drugs for treating certain diseases. Phytochemical research can

create new opportunities and treatment options, which would positively impact the public health system and help reduce the economic burden (Wang et al., 2024).

Generally, the genus *Spondias*, which belongs to the family Anacardiaceae, comprises approximately 18 species. It is widely known as wild mango or hog plum (Laksemi et al., 2019; Nitheesh et al., 2024). In Thailand, most Thai people call trees in the genus Spondias 'Makok'. Leaves are used as vegetables, while fruits are used as ingredients in a variety of dishes, especially in papaya salad, a very popular dish. This widespread culinary use makes *Spondias* trees economically valuable.

The genus *Spondias* comprises nutritious plants that contain 16.3- 23.54% total carbohydrates, 12.23-12.54% crude fat, 3.13-4.03% crude fiber, 0.9-1.23% copper, 1.3- 1.5% iron, 0.96- 1.38% sodium, and 0.15-0.93% calcium. The edible part of *S. pinnata* fruit contained 90% moisture. Protein was detected at 0.7%, with several amino acids found, such as glycine, cystine, serine, alanine, and leucine, among others. In addition, *S. pinnata* fruit contains 4.5% carbohydrates, with sugars being made up of various types, such as sucrose, glucose, and fructose, etc. Moreover, *S. pinnata* fruit was also found to contain 3.0% fat, 1% dietary fiber, and 0.5% minerals and vitamins (calcium 36.0 mg/100g; phosphorus 11 mg/100 g; iron 3.9 mg/100 g; thiamine 0.02 mg/100 g; riboflavin 0.02 mg/100 g; niacin 0.3 mg/100 g; vitamin C 21 mg/100 g; and vitamin A up to 450 IU/100 g) (Nitheesh et al., 2024; Siegel et al., 2019).

Interestingly, the *Spondias* genus, especially *S. pinnata*, has been reported to contain groups of phytochemicals that show a variety of biological and pharmacological properties. Recent reports indicated that *S. pinnata* has important pharmacological effects, including hypoglycemic, anthelmintic, anti-cancer, ulcer-protective, cytotoxic, hepatoprotective, thrombolytic, anti-microbial, anti-diarrheal, antioxidant and anti-tyrosinase activities (Kunu et al., 2025; Nitheesh et al.,2024; Patathananone et al., 2019a). The extract of the leaves and stems of *S. mombin* with 80% ethanol contains various key compounds, including tannins and pseudotannins like geraniin, galloyl geraniin, and galloyl glucose. 3-O-[α-rhamnopyranosyl-(1→2)]-α-rhamnopyranosyl-(1→6)-β-glucopyranoside is a flavonoid found in the 80% MeOH leaf extract of *S. venulosa*. The extraction of key compounds from *S. purpurea* fruit using acetone revealed various flavonoids such as rhamnetin, isorhamnetin, kaempferol, kaempferide, astragalin, isoquercetin, and quercetin dihydrate, as well as phenolic acid derivatives like gallic acid and 3-caffeoylquinic acid. (Sameh et al., 2018). Ripe *S. pinnata* fruit extracts were found to contain phytochemicals, mainly phenolics, flavonoids, and terpenoids. These phytochemicals have shown biological properties such as inhibiting tyrosinase activity, acting as antioxidants, showing cytotoxicity toward certain cancer cells, and inhibiting antibiotic-resistant mastitis pathogens (Kunu et al., 2025; Patathananone et al., 2019a; Patathananone et al., 2019b). From the information above, plants in the *Spondias* genus are sources of bioactive and pharmacological compounds that can be developed as alternatives for use in human health.

However, comparative studies on the biological properties of phytochemicals from unripe *S. pinnata* fruits remain limited, particularly with respect to tyrosinase and elastase inhibition, antioxidant activity, and cytotoxic effects against cholangiocarcinoma and normal cells.

This research aims to extract bioactive compounds from unripe *S. pinnata* fruit using a mixed solvent system that includes an organic solvent and water. It also aims to compare the efficacy of the extracts in terms of antioxidant activity and the inhibition of tyrosinase and elastase — enzymes involved in key processes such as melanin synthesis, neurotransmitter production, and skin cell strength. Moreover, this research also aims to study and compare the cytotoxicity of key compounds from *S. pinnata* fruit extracts on cholangiocarcinoma cells and normal bile duct cells to assess their selective ability.

These findings are expected to contribute to improving the precision of drug delivery in the future, which might help reduce side effects from cancer treatments or lower the production costs of drugs used to treat cholangiocarcinoma, a disease with a high incidence in Thailand.

MATERIALS AND METHODS

Unripe wild mango (*S. pinnata*) fruit, a raw plant material, was collected in Kokyai village, Ban Fang district, Khon Kaen province, Thailand, from September to October. The characteristics of the plant material are exhibited in Figure 1. The plant material was taxonomically identified based on its morphological characteristics, following the taxonomic descriptions provided by Nitheesh et al. (2024). The organic solvents were purchased from LabScan. Mushroom tyrosinase and 2,2-diphenyl-1-picrylhydrazyl (DPPH) were bought from Sigma-Aldrich. L-Dopa and kojic acid were purchased from HiMedia company. Dulbecco's Modified Eagle Medium-high glucose (DMEM-Hg), fetal bovine serum (FBS), L-glutamine, penicillin-streptomycin, and trypsin- EDTA were ordered from Gibco B.R.L. (Grand Island, NY, USA). Additionally, 3- [4, 5-dimethylthiazol-2-yl]-2-5-diphenyltetrazolium bromide (MTT) and dimethyl sulfoxide were bought from Invitrogen (Carlsbad, CA).



(A) (B) (C)

Figure 1. *Spondias* genus plant used as the research material, located in Ban Fang District, Khon Kaen Province, Thailand. (A) *S. pinnata* tree; (B) leaves of *S. pinnata*; and (C) fruits of *S. pinnata*, exhibiting morphological characteristics consistent with the species identification

Unripe *S. pinnata* Fruit Extraction Process

Unripe *S. pinnata* fruits were washed three times using water. The fruits, including pericarp that are without seeds, were collected and placed in the ice-cold chamber at 4 °C. Approximately 300 g of unripe fruits and pericarp were homogenised using the blender for 5 min. Then, the homogenate was dried using a freeze-dryer. The lyophilised powder of unripe fruits and pericarp of *S. pinnata* fruit (10 g) was placed into the extraction chamber, and then 100 mL of 70% v/v acetone, 70% v/v ethanol, and 70% v/v methanol were added to each section. These extracted chambers were stirred using a magnetic stirrer at 750 rpm at room temperature for 72 h, and then incubated at 4 °C overnight. The extracts were filtered using Whatman® No. 1 and No. 5, respectively. The clear supernatant of each extract was evaporated at 50 °C using an evaporator to remove the organic solvent and concentrate. Evaporation was continued until the supernatant in the water part remained in a small volume (20 mL). Then, the hydrated part of the extracts was freeze-dried by lyophilisation. All extracts were kept at -20 °C until used. The ID names of these extracts were shown: WRA-1 (70% v/v acetone), WRA-2 (70% v/v ethanol), and WRA-3 (70% v/v methanol).

Anti-Tyrosinase Activity Assay

According to the modified procedure, the tyrosinase-inhibitory effect of the treated samples was determined using the Dopachrome method (Long et al., 2008). The reactions were conducted in a 96-well microplate. Kojic acid was used as a positive control. Firstly, the extracted powder was dissolved in 5% v/v DMSO (10 mg/mL). Then, different concentrations (0.13 - 3 mg/mL) of treatment samples (10 µL) were mixed with 100 µL of mushroom tyrosinase (10 µg/mL mushroom tyrosinase in 20 mM phosphate buffer, pH 6.8). The banked sample was tested together without being co-incubated with the enzyme. The reaction plates were incubated at 37 °C for 10 min. Next, 20 µL of L-Dopa (20 mM L-Dopa in DMSO) was added and mixed gently; after that, it was incubated at 37 °C for 30 min. The absorbance value was measured at a microplate reader's wavelength of 495 nm (Biochrom EZ Read 2000, USA). The percentage of tyrosinase inhibitory activity of tested substances was calculated using an equation previously reported by Patathananone et al. (2022).

Anti-Elastase Activity Assay

The treatment test observed the elastase inhibitory effect as previously described by Lee and Choi (1999). The experiment was briefly modified by decreasing the volume and setting the reaction system on a 96-well plate. In the pre-incubation step, 10 µL of the different concentrations of the extracts (0.25 - 2 mg/mL) were placed into 100 µL

of porcine elastase solution (Sigma-Aldrich) (approximately 0.06 Unit/mL elastase in 20 mM Tris-HCl buffer, pH 8), and then 70 µL of buffer was added, mixed gently, and incubated at 37 °C for 10 min. The absorbance value was measured at a wavelength of 410 nm using a microplate reader. In the next step, 20 µL of substrate solution (0.8 mM succ-(Ala)-3-nitroanilide in 20 mM Tris-HCl buffer, pH 8) was added to each pre-incubated reaction. The plate was mixed and incubated at the same temperature for 30 min. The absorbance value was analysed at 410 nm. The percentage of elastase inhibition was calculated according to the formula as in Equation 1.

$$\% \text{ Inhibition} = \frac{[\text{ Absorbance 410 nm of control} - \text{Absorbance 410 nm of sample }]}{[\text{ Absorbance 410 nm of control }]} \times 100 \quad [1]$$

Antioxidant Activity Assay

The antioxidant capability of the extracts was analysed using the briefly modified DPPH method according to the report by Pientaweeratch et al. (2022). The different concentrations (0 - 80 µg/mL) of the extracts (10 µL) were added to 190 µL of DPPH (0.101 mM DPPH in methanol) solution. After that, the reactions were incubated in the dark for 30 min at 37 °C. The absorbance was measured at 515 nm using a UV- vis spectrophotometer. The percentage of inhibition was calculated following the equation previously described by Chen et al. (2010).

Determination of Cell Viability Using MTT Assay

Cholangiocarcinoma (MO55 cells) and normal bile duct cells (MMNK1 cells) were cultured in DMEM high glucose supplemented with 10% v/v fetal bovine serum and 1% v/v penicillin-streptomycin in T-25 cell culture flasks as previously described by Patathananone et al. (2019a). The culture flasks were incubated in 5% CO_2 and 95% air at 37 °C until cells grew to approximately 90% of the flask area. Cells were trypsinised, collected, and washed with 1X phosphate-buffered saline (1X PBS) 3 times. The same culture medium was used to resuspend cells to prepare for cell viability tests. The initial numbers of both cell lines were set at approximately 9 x 105 cells/mL to place in a 96-well plate at 100 µL. MO55 and MMNK1 cells were seeded in a 96-well plate according to the experiment described by Patathananone et al. (2019a). Both cell lines were treated with different concentrations (0.05 - 3.2 mg/mL) of each extract for 24 and 48 h. Then, 100 µL of 0.5 mg/mL MTT solution (0.5 mg/mL MTT in 1X phosphate-buffered saline, pH 7.4) was added to each test well and mixed gently. The plate was incubated at 37 °C for 4 h, after which the MTT

solution was carefully removed from each well. Subsequently, 100 µL of dimethyl sulfoxide (DMSO) was added to dissolve the formazan crystals. The absorbance was measured at 570 nm using a microplate reader (Varioskan Flash). Cell viability (%) was calculated following the method described by Patathananone et al. (2019b). The IC_{50} value of each treatment sample was observed and compared between MO55 cells and MMNK1 cells.

Phytochemical Analysis

Phytochemical types of each extract (WRA-1, WRA-2, and WRA-3) were analysed following the report of Patathananone et al. (2019b). The extract was evaluated with specific reagents to observe the positive reaction. The extract results were compared according to each phytochemical type's positive or negative compound reaction.

Gas Chromatography-Mass Spectroscopy (GC-MS)

The terpenes and their derivatives in WRA-1 were determined using gas chromatography-mass spectrometry (GC-MS) on an Agilent 7890B system according to previous research by Kunu et al. (2025). The samples were separated on an HP-5MS column (25 m × 250 µm × 0.25 µm) with helium as the carrier gas at a flow rate of 1.2 mL/min. The initial inlet temperature was 250 °C in splitless mode for 0.75 min, and the MSD transfer line was maintained at 250 °C. The oven temperature program was as follows. The initial temperature was 60 °C, held for 3 min [and then run for 3 min: please clarify]. The temperature was then increased to 80 °C (Ramp 1) and held for 23 min. Next, the temperature was increased to 120 °C and held until 36.33 min. Finally, the temperature was increased to 240 °C, and the run was stopped at 66.33 min. The mass spectrometer (Agilent 5977B) was operated in electron ionisation (EI) mode at a fixed electron energy of 70 eV. Data were acquired in scan mode over a mass range of m/z 45-500, with the ion source temperature at 230 °C and the quadrupole temperature at 150 °C.

Liquid Chromatography-Mass Spectroscopy (LC-MS)

The different kinds of phenolic compounds in WRA-1 were examined using the LC-MS technique. The phytochemicals were purified using ultrahigh-performance liquid chromatography (UHPLC; Thermo Scientific model Accela) using a C18 column (C18 Agilent Eclipse Plus, 4.6 × 100 mM, 3.5 µm). A regulated temperature of 35 ºC was used for the column. The mobile phases A and B are 0.1% acetic acid in water and acetonitrile, respectively. The 500 µL/min is used as the flow rate of the separating. The purification time program was adjusted to the gradient of mobile phases A and B. Electrospray Ionisation (ESI) Mass Spectrometry (Thermo Scientific Surveyor MSQ Plus) was used to assess the mass of purified peaks. The MS condition was performed with the probe temperature at

450 ºC, the needle at 4.5 kV, and the negative ESI ionisation mode. The mass/charge was then scanned at 100 - 1000 m/z. The ion mass profile was examined in the database or library (Table 1).

Table 1
The gradient conditions of liquid chromatography

No.	Times	Mobile Phase		Flow Rate (µL/min)
		A%	B%	
0	0	15	85	500
1	5	25	75	500
2	10	35	65	500
3	28	60	40	500
4	28.01	15	85	500
5	35	15	85	500

Determination of Total Phenolic Contents

Phenolics are significant phytochemicals that are used for the survival of plants. Polyphenolic compounds represent various biological activities. The Folin-Ciocalteu test was utilised to examine the total phenolic contents in accordance with the previously mentioned methodology (Kozlowskal et al., 2021; Moolwong et al., 2023). The reaction was performed by subjecting 2% w/v Na_2CO_3 solution to approximately 3.50 mL in a test tube. The extracts at different concentrations (100 µL) were added and mixed gently. The mixture was subjected to a tenfold dilution of Folin reagent (400 µL). The reactions were incubated for 30 minutes in the dark at room temperature. After that, the absorbance value was measured at 750 nm by a spectrophotometer (Thermo Science, USA). In this experiment, gallic acid was used as the standard solution. The total phenolic contents of each extract were calculated.

Statistical Analysis

The proportion of the extracts' enzymatic inhibitory effect, antioxidant activity, and nitric oxide scavenging activities were computed and presented as the mean and standard deviation (mean ± SD). The ANOVA test (IBM SPSS Statistics ver. 29.0, IBM Corp., Armonk, NY, USA) was utilised in this study to analyse the cytotoxic data. The *P values* for all data points were below 0.05 (*), signifying statistically significant differences.

RESULTS AND DISCUSSIONS

In this report, *S. pinnata* fruit extracts were investigated for biological properties in line with the development aims, such as applications in functional foods/nutraceuticals, food

supplements, and as an ingredient to prevent biomolecule degradation in health care products. The data for each biological property, including phytochemical types and total phenolic contents, are represented below.

The Inhibitory Effect of Unripe *S. pinnata* Fruit Extracts on Tyrosinase Enzyme

The antityrosinase activity results of unripe *S. pinnata* fruit extracts are shown in Figure 2. According to the results, the three unripe *S. pinnata* fruit extracts can inhibit the tyrosinase enzyme activity in vitro. The effect of antityrosinase activity was expressed as dose-dependent. The IC_{50} value of WRA-1, WRA-2, and WRA-3 was exhibited at 0.55, 0.95, and 0.65 mg/mL, respectively. The data indicated that WRA-1 showed a more substantial tyrosinase inhibitory effect than WRA-2 and WRA-3.

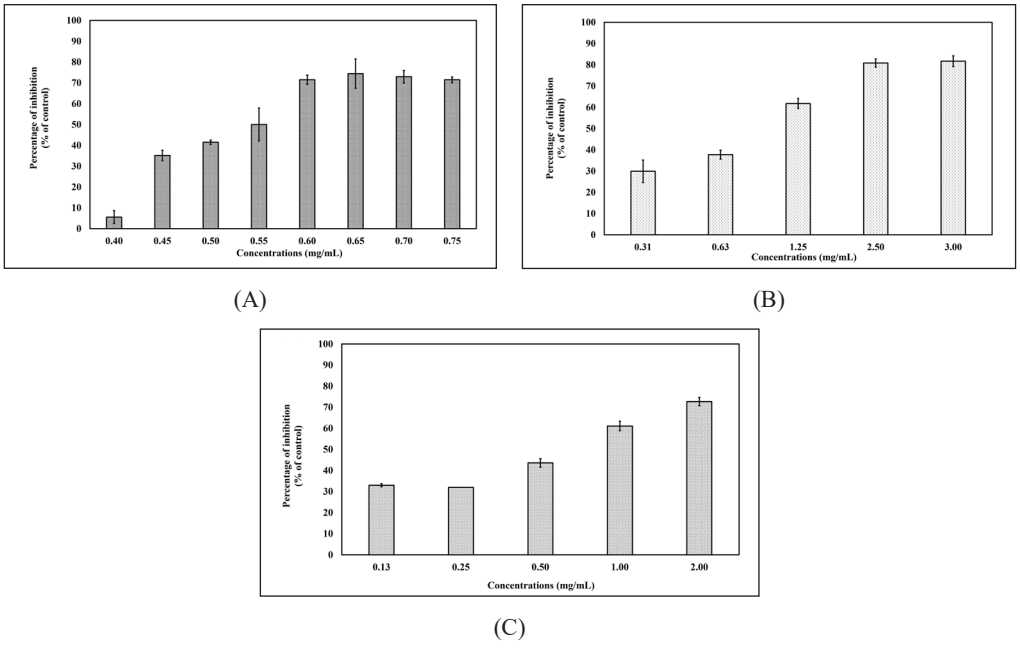

Figure 2. Antityrosinase activity of unripe *S. pinnata* fruit extracts. (A) WRA-1, (B) WRA-2, and (C) WRA-3. All samples were tested in triplicate (n = 3), and the results are presented as percentage inhibition (% inhibition) as the mean ± standard deviation (SD)

Anti-Elastase Activity

Elastase is an enzyme that can digest the protein in the extracellular matrix of cells, especially elastin protein. Therefore, elastase is the crucial enzyme associated with skin wrinkling. The elastase inhibitory effect of raw wild mango fruit extracts was expressed in Figure 3. The data indicated that the bioactive compounds of WRA-1

extract exhibited higher potential anti-elastase activity than WRA-2 and WRA-3. The IC_{50} value of WRA-1 was less than 0.25 mg/mL, while the IC_{50} dose of WRA-2 was approximately 2 mg/mL. However, WRA-3 showed lower elastase-inhibitory activity than WRA-2 and WRA-1. In addition, the results related to the tyrosinase inhibitory effect indicated that the WRA-1 extract exhibited an IC_{50} dose smaller than WRA-2 and WRA-3.

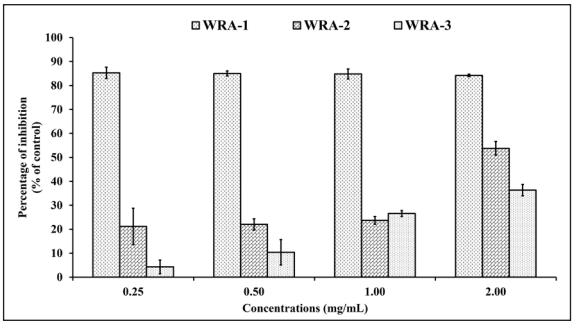

Figure 3. Elastase inhibitory activity of unripe *S. pinnata* fruit extracts. All samples were tested in triplicate (n = 3), and the results are presented as percentage inhibition (% inhibition) as the mean ± standard deviation (SD)

Antioxidant Activity of WRA-1, WRA-2, WRA-3 Extracts

The induction of oxidative stress by free radicals plays a significant role in aging. Many molecules are destroyed, which represents oxidative damage. Moreover, reactive oxygen species can activate the elastase, cellulase, and hyaluronidase activities. These enzymes can hydrolyze elastin, cellulose, and hyaluronic acid, promoting skin aging. Thus, the antioxidant activity and inhibition of these enzymes are the target goals for preventing cell aging. In this report, the antioxidant activity of extracts was analysed using a DPPH assay. Ascorbic acid and gallic acid served as reference antioxidant agents for comparison with the extracted samples. The results are expressed in Figure 4. The IC_{50} of each extract was calculated and compared with those of the standard antioxidants, namely ascorbic acid and gallic acid. WRA-1 ($y = 9.4372x + 33.55$, $R^2 = 0.9962$), WRA-2 ($y = 5.3494x + 5.822$, $R^2 = 0.9925$), and WRA-3 ($y = 10.993x + 2.447$, $R^2 = 0.9935$) exhibited IC_{50} values of 1.74, 8.26, and 4.43 µg/mL, respectively. By comparison, the IC_{50} of gallic acid ($y = 2.7307x + 4.439$, $R^2 = 0.9939$) and ascorbic acid ($y = 9.397x$, $R^2 = 0.9967$) were 16.68 and 5.32 µg/mL, respectively. These data indicate that the IC_{50} of WRA-1 was lower than that of WRA-2, WRA-3,

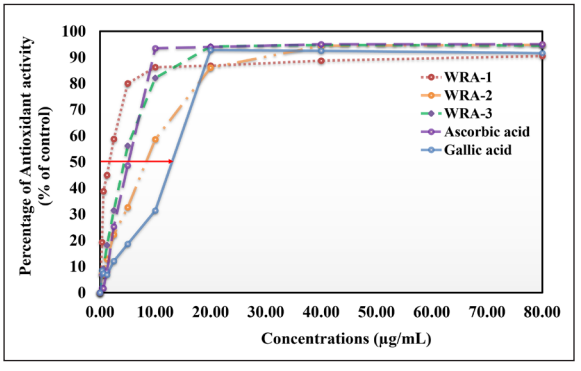

Figure 4. DPPH radical-scavenging activity of unripe *S. pinnata* fruit extracts. L-Ascorbic acid and gallic acid were used as positive controls for comparison with the extracts. All samples and positive controls were tested in triplicate (n = 3), and the results are presented as mean ± standard deviation (SD)

ascorbic acid, and gallic acid. This finding suggests that the compounds present in WRA-1 exhibited good efficacy in scavenging free radicals in vitro, with a higher capacity than the other extracts and standard antioxidant agents tested.

Cytotoxicity of Unripe *S. pinnata* Fruit Extracts

CCA is a specific localised carcinoma associated with prolonged and continuous parasite infection. Secretions and toxins produced by *O. viverrini* affect the biomolecules in the cells at the site of helminth infection. Individuals living in the freshwater basin and living an uncooked lifestyle are primary and secondary aquatic *O. viverrini* carriers. Their behavior and culture make them susceptible, and they have a higher rate of CCA detection than urban populations. CCA has few symptoms and occurs in specific locations, causing CCA to be detected in the invasion and migration stage. Reducing risk or preventing CCA is associated with various factors, especially food quality and appropriate public health systems among at-risk groups (Wasuworawong et al., 2015).

Functional foods/nutraceuticals are a factor in a relationship hypothesis that reduces risk and prevents human disease development, impacting the public health system. This report studied the *S. pinnata* fruit extracts from three solvent systems for their cytotoxic effect on cholangiocarcinoma (MO55 cells) and compared them with normal bile duct cells (MMNK1 cells). This experiment aims to analyse the feasibility of essential substances in the extracts that showed the role of selective ability between cancer cells and normal cells. The study results on the anticancer properties of raw *S. pinnata* fruit extracts on MO55 and MMNK1 cells are exhibited in Figures 5 and 6. The morphological changes of MO55 cells and the percentage of cell viability indicated the cytotoxic effect of *S. pinnata* fruit extracts. The MO55 cell density treated with unripe *S. pinnata* fruit extracts was lower than that of the control condition (untreated). This result is related to the percentage of MO55 cell viability that decreased after incubation with the tested extracts. These extracts have a cytotoxic impact that is dose- and time-dependent. The IC_{50} of WRA-1, WRA-2, and WRA-3 represented 0.58, 1, and 2.1 mg/mL, respectively. These data indicated that WRA-1 displayed a higher cytotoxic effect on MO55 cells than WRA-2 and WRA-3. In addition, the cytotoxic effect of unripe *S. pinnata* fruit extracts was compared between cholangiocarcinoma (MO55 cells) and normal bile duct cells (MMNK1 cells). The results showed that the percentage of MMNK1 cell viability similarily expressed with MO55 cells. However, the IC_{50} of WRA-2 and WRA-3 in MMNK1 is higher than what was found in MO55 cells (Table 2). The results suggest that the phytochemicals in WRA-2 and WRA-3 may be selectively cytotoxic, leading to lower cytotoxicity toward normal cells than cancer cells.

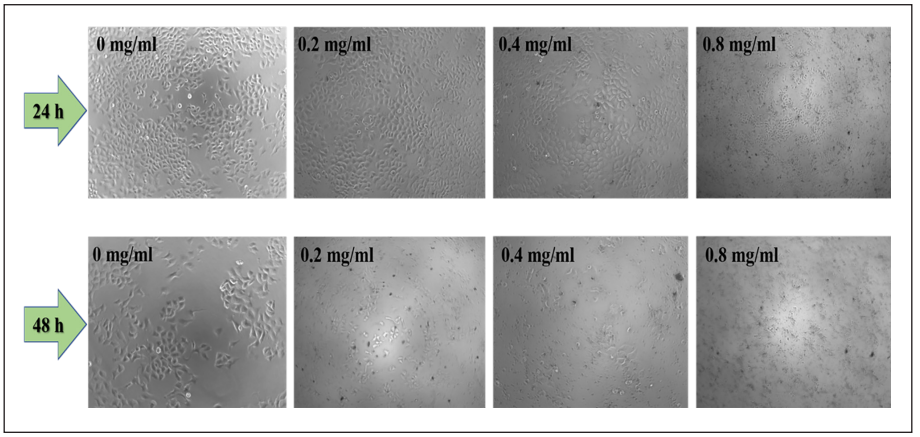

Figure 5. Morphological changes in MO55 cells following treatment with unripe *S. pinnata* fruit extract (WRA-1) for 24 and 48 h

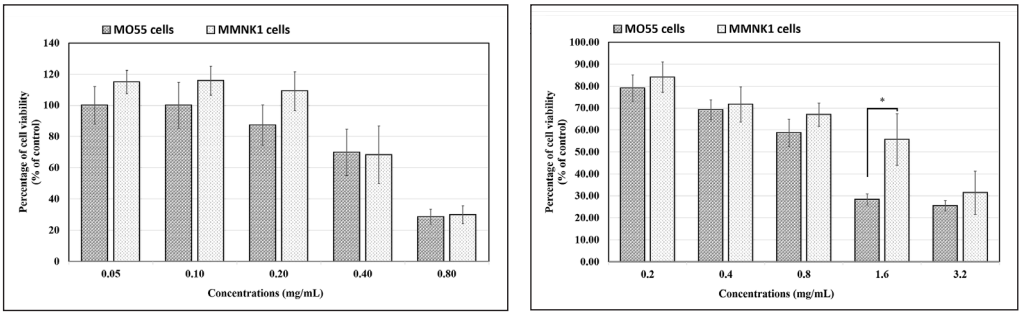

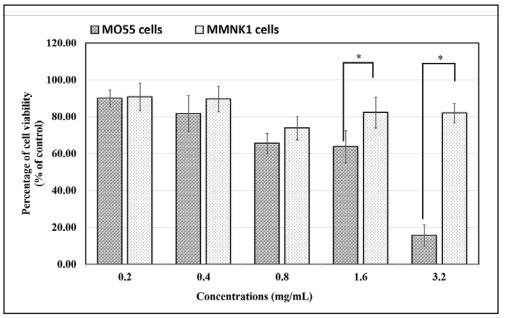

Figure 6. Comparison of cell viability (%) between MO55 and MMNK1 cells following treatment with unripe *S. pinnata* fruit extracts for 48 h. (A) WRA-1, (B) WRA-2, and (C) WRA-3. All samples were tested in triplicate (n = 3), and the results are presented as mean ± standard deviation (SD)

Table 2
The IC_{50} for cytotoxicity, antioxidant, and antityrosinase activities, including total phenolic content of all extracts (WRA-1, WRA-2, WRA-3)

Extracted ID	IC_{50} of Cytotoxicity (mg/mL)		IC_{50} of Antioxidant Activity (µg/mL)	IC_{50} of Antityrosinase Activity (mg/mL)	Total phenolic Contents (mg GAE/g extract)
	MO55 cells	MMNK1 cells			
WRA-1	0.58	0.57	1.74	0.55	26.35 ± 4.89
WRA-2	1.00	1.98	8.26	0.95	49.77 ± 3.81
WRA-3	2.10	> 3.20	4.43	0.65	31.91 ± 1.52

Total Phenolic Contents

The Folin reagent investigated the total phenolic contents of unripe *S. pinnata* fruit extract. The standard curve of gallic acid ($y = 11.202x$, $R^2 = 0.9954$) was used to calculate the total phenolic contents of the extracts. The results showed that the total phenolic contents of WRA-1, WRA-2, and WRA-3 were 26.35 ± 4.89, 49.77 ± 3.81, and 31.91 ± 1.52 mg GAE/g extract, respectively. The results indicated that the total phenolic contents of WRA-3 were higher than those of WRA-2 and WRA-1. These data showed that the high polarity of the extracted solvent can collect the phenolic compounds. Interestingly, the phenolic contents are not associated with the cytotoxicity level in MO55 cells. The potential biological activities in WRA-1 may be related to various bioactive agents. As a result, several kinds of bioactive substances in WRA-1 have been researched.

Phytochemicals in WRA-1, WRA-2, and WRA-3

The phytochemical screening results of WRA-1, WRA-2, and WRA-3 are shown in Table 3. Polyphenols/phenolic, flavonoids, flavones, terpenoids, tannins, and cardiac glycosides are phytochemical types found in these extracts. Only saponins were not detected in WRA-1. The detection of similar phytochemicals might be related to the solvent system used, which has a ratio of organic solvent mixed with water (70:30). The biological properties represented in unripe *S. pinnata* fruit extracts may be associated with these chemicals.

Table 3
Phytochemical screening data of unripe S. pinnata *fruit extracts*

Type of Phytochemical	WRA-1	WRA-2	WRA-3
Phenolic compounds	+	+	+
Flavonoids	+	+	+
Flavone	+	+	+
Leucoanthocyanidin	-	-	-
Terpenoid	+	+	+

Table 3 (*continued*)

Type of Phytochemical	WRA-1	WRA-2	WRA-3
Tannin	+	+	+
Saponin	-	+	+
Steroids	-	-	-
Cardiac glycoside	+	+	+

Moreover, WRA-1 represented a small concentration of IC_{50} in antioxidant and antityrosinase activities. Therefore, GC-MS and LC-MS were used to study the group of active compounds in WRA-1. 5-hydroxymethylfurfural (5-HMF) is represented in the GC-MS report. This compound has the molecular formula $C_6H_6O_3$. The match factor and Reverse Match Factor (RMF) presented in 891 indicate that the mass spectrum of the substance matches the database at a good to very good level. In addition, the program estimated the probability of identifying the substance at 94.9%, which supports that the identification of this substance is highly reliable. However, analysis with GC-MS and checking for similarities in these values is only a tentative identification. It's still necessary to have methods that help strengthen the data and make it more academically consistent.

LC-MS analysis of the sample revealed substance peaks at 0.4, 2.35, 2.98, 10.24, 10.43, 10.63, and 22.5 minutes. Of these, three peaks, at 2.35, 10.24, and 10.43 minutes, could be analysed further. LC-MS analysis in negative ion mode $[M-H]^-$ revealed the mass of each of these three peaks, as shown in Figure 7(B)-(D). Upon comparison with database records, the chromatographic profiles showed similarities to gallic acid, verbascoside, and isorhamnetin-3-rutinoside, respectively.

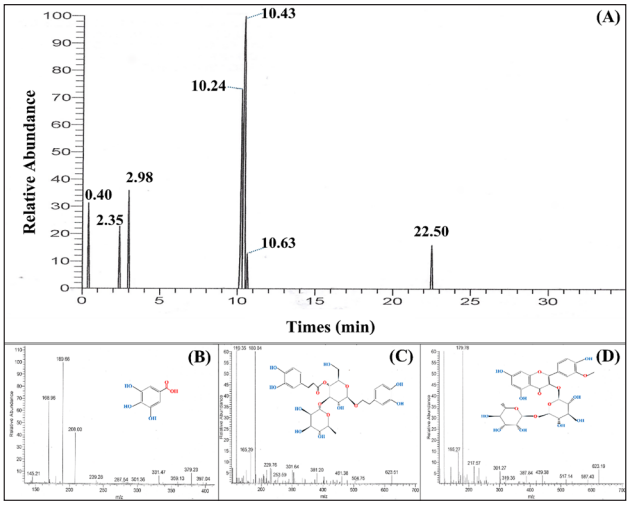

Figure 7. Purification chromatogram of WRA-1 obtained using C18-HPLC. (A) Chromatographic profile; (B- D) mass spectra of $[M-H]^{-1}$ corresponding to peaks with retention times of 2.35, 10.24, and 10.43 min, respectively

Drug discovery has long used natural products (NPs) as a source. Phytochemicals are being developed in various forms, including medicines, functional foods, and ingredients for topical products, with the primary goal of reducing human health problems (Nakadate et al., 2026).

In this study, phytochemicals were extracted using three solvent systems: (1) acetone-water, (2) ethanol-water, and (3) methanol-water, each at a 70:30 (v/v) ratio. The solvent systems (1) and (3) are similar to the study by Satpathy et al. (2011). However, this research added solvent system (2) to provide more comparative data on the efficiency of extracts from all three solvent systems. An important sample preparation technique is the combined use of mechanical and chemical extraction methods, which enhances the extraction of key compounds from raw materials. In addition, concentration involves a combination of two technologies. The first technology is evaporation, a method for removing organic solvents, followed by freeze-drying to remove the aqueous components from crude extracts. Using both technologies together helps reduce residual organic solvents in the extracts and preserves heat-sensitive compounds that cannot withstand high temperatures.

The results of this study show that the extracts WRA-1, WRA-2, and WRA-3 inhibit tyrosinase and elastase, act as antioxidants, and are cytotoxic to cancer cells. WRA-1 showed the highest overall bioactivity. Analysis of the compounds in WRA-1 identified 5-hydroxymethyl-2-furfural, gallic acid, verbascoside, and isorhamnetin-3-rutinoside.

Gallic acid and its derivatives are phenolic compounds. They are found in the extracts of various plants, including those of the genus *Spondias*. Previous research suggests that gallic acid exhibits antioxidant, antimicrobial, anti-inflammatory, and anticancer properties (Sameh et al., 2018), as well as antityrosinase activity (Patathananone et al., 2019a). The antioxidant mechanism of gallic acid involves transferring hydrogen atoms to free radicals (Hassanpour et al., 2023). Oxidative stress refers to the excessive production of free radicals within cells. These radicals damage biomolecules, causing them to degrade and lose their function. Therefore, reducing the quantity of free radicals is important for slowing the degeneration of biomolecules, thereby decreasing the risk of certain diseases, especially cancer (Kumpunya et al., 2014).

Verbascoside is a polyphenolic compound. It is a heterotrimer consisting of a catechol unit, glucose, and caffeic acid that is found in varieties of plant species. Several in vitro and in vivo studies have indicated that it exhibits neuroprotective, analgesic, antihypertensive, anti-inflammatory, and anti-tumor properties and inhibits protein kinase C (PKC) signaling pathways in the rat brain (Das et al., 2016).

Isorhamnetin and its derivatives (isorhamnetin-3-rutinoside) are secondary metabolites from various plants (Gómez-López et al., 2021). The flavonoid family, particularly the flavonol family, categorises these substances. Researchers have reported several biological activities of isorhamnetin, including antidiabetic, anti-inflammatory, antiproliferative, antioxidant, and antiobesity properties (Gong et al., 2020).

Tyrosinase (EC.1.14.18.1) is an enzyme found in many different living organisms. This enzyme is classified in class 1 of the oxidoreductases (monophenol, o-diphenol: oxygen oxidoreductase). In humans, the enzyme tyrosinase speeds up the oxidation of tyrosine to produce L-Dopa (3-(3',4'-dihydroxyphenyl)-L-alanine; L-Dopa), which then gets converted into dopaquinone. This dopaquinone goes through several reactions and eventually turns into melanin (Bae et al., 2013; Kim et al., 2016).

Although melanin helps protect DNA in skin cells from UV radiation and scavenges reactive oxygen species (ROS) generated by oxidative reactions, hyperpigmentation leading to melasma can negatively affect a person's appearance and self-confidence. Abnormal tyrosinase activity may be associated with several skin disorders, such as vitiligo, albinism, hyperpigmentation, and melanoma. Tyrosinase may also contribute to the toxicity of dopaminergic neurons and to neurodegeneration, which are implicated in Parkinson's disease (Chen, 2020). Therefore, inhibiting tyrosinase activity may be a strategy for preventing or slowing the progression of the conditions associated with excessive tyrosinase activity described above. This study shows that the phytochemicals in unripe *S. pinnata* fruit extracts (WRA-1, WRA-2, and WRA-3) inhibit tyrosinase in vitro, with WRA-1 having the lowest IC_{50} value of the three extracts and therefore the greatest inhibitory potency. However, in comparison with the positive control, kojic acid (IC_{50} = 0.03 mg/mL), all three crude extracts had significantly higher IC_{50} values, indicating lower tyrosinase-inhibitory potency. The tyrosinase inhibition activity of WRA-1 is related to the detected compounds 5-hydroxymethyl-2-furfural and gallic acid, which have been reported to have in vitro tyrosinase inhibitory properties (Patathananone et al., 2019a; Sameh et al., 2018). In addition, verbascoside and isorhamnetin-3-rutinoside may inhibit tyrosinase, and further studies will be conducted to test this hypothesis.

Elastases (EC 3.4.21.36) are a class of serine proteases with a broad range of substrate specificity that break down elastin (Famutimi et al., 2024). Abnormal expression of elastase is related to ROS free radicals (Patathananone et al., 2019a). Preventing elastin degradation may help slow skin aging (Garg, 2017). Moreover, elastase inhibition is associated with reduced cancer cell invasion and migration. Studying elastase inhibitors from plant sources may have applications in cosmetics and health care, as well as in strategies to reduce the risk of metastasis in certain cancers. Previous reports show that phenolic compounds such as catechin, epicatechin, procyanidin B2, and resveratrol, including flavonoid groups (for example, quercetin, kaempferol, and myricetin), have been reported to have high efficacy for anti-elastase activity (Pientaweeratch et al., 2016; Wasuworawong et al., 2015). The elastase inhibition results were consistent with those for tyrosinase, showing that WRA-1 has strong potential to inhibit elastase activity. The compounds detected in WRA-1 (5-hydroxymethyl-2-furfural, gallic acid, verbascoside, and isorhamnetin-3-rutinoside) may contribute to its in vitro inhibition of elastase activity. However, this study is preliminary.

Further research is needed to characterise the types and classes of compounds to elucidate the mechanism of elastase inhibition.

Free radical molecules contribute to the progression of cancer cells in the human body. Reactive oxygen species (ROS), particularly free radicals, trigger the oncogenic phenotype of cancer cells. Many factors, including an imbalance in the antioxidant system, contribute to the increasing number of free radicals. Therefore, antioxidants are important for reducing oxidative stress, which can help decrease the risk of developing various non-communicable chronic diseases, especially the risk of cancer (George et al., 2017). The results of this research indicated that phytochemicals in *Spondias* fruit exhibited good antioxidant potential. The IC_{50} of these extracts was detected at low concentrations, especially in WRA-1. The antioxidant potential present in WRA-1 may be related to the detected phytochemicals (5-hydroxymethyl-2-furfural, gallic acid, verbascoside, and isorhamnetin-3-rutinoside), which have previously been reported to show effective antioxidant properties in vitro (Das et al., 2016; Gong et al., 2020; Gómez-López et al., 2021; Hassanpour et al., 2023; Hazra et al., 2008; Sameh et al., 2018).

The cytotoxicity and selective properties of phytochemicals, which differ between cancer and normal cells, are targets for drug development research. Drugs with non-specific effects on cell groups can cause severe side effects for patients, so improving drug delivery efficiency is important for reducing these risks (Siegel et al., 2019). Interestingly, the data from this study showed that the group of phytochemicals in the WRA-3 sample displayed significantly less cytotoxicity in normal cells compared to cancer cells. This is different from WRA-1 and WRA-2, which were toxic to both cancer and normal cells at similar IC_{50} values. Based on these findings, the selective cytotoxicity of WRA-3 provides positive information for further research and development of drugs or drug delivery compounds that could be specifically targeted to certain cells in the future (Yolande et al., 2018).

CONCLUSION

Hog plum fruits in the *Spondias* genus are a source of bioactive compounds with important and diverse biological properties, like inhibiting tyrosinase and elastase enzymes, antioxidant effects, and cytotoxicity against cancer cells. Phytochemicals from *Spondias* fruits therefore have potential to be used as substitutes or alternatives in nutraceuticals and functional foods, and could also be used as ingredients in skincare products in the future.

ACKNOWLEDGEMENT

The authors would like to express their sincere gratitude to the National Research Council of Thailand (NRCT) for financial support under Grant No. 6575, which supported the initial stage of this research.

The authors also wish to thank all individuals and organisations who contributed to this study. Special appreciation is extended to the Faculty of Science and Technology, Rajamangala University of Technology Thanyaburi, Thailand, for providing the research facilities and technical support necessary to conduct this work.

The authors gratefully acknowledge the valuable assistance and constructive suggestions provided by colleagues and laboratory staff throughout the research process. Their expertise and support are sincerely appreciated.

The authors would like to express their sincere gratitude to Associate Professor Doctor Banchob Sripa (Khon Kaen University, Khon Kaen, Thailand). These cell lines were maintained and constructed as previously described by Wasuworawong et al. (2015).

Finally, the authors would like to thank the anonymous reviewers and the Editor for their insightful comments and constructive recommendations, which have significantly improved the quality of this manuscript.

REFERENCES

Alfaouri, M., Jaaron, A. A. M., & Igudia, E. (2025). Pharmaceutical supply chain management challenges in developing countries: A systematic literature review. *Journal of African Business, 26*(4), 798-841. https://doi.org/10.1080/15228916.2025.2532943

Bae, S. J., Ha, Y. M., Kim, J., Park, J. Y., Ha, T. K., Park, D., Chun, P., Park, N. H., Moon, H. R., & Chung, H. Y. (2013). A novel synthesized tyrosinase inhibitor: (*E*)-2-((2,4-dihydroxyphenyl)diazenyl)phenyl 4-methylbenzenesulfonate as an azo-resveratrol analog. *Bioscience, Biotechnology, and Biochemistry, 77*(1), 65-72. https://doi.org/10.1271/bbb.120547

Chen, Y. (2020). Advances in fluorescent probes for detection and imaging of endogenous tyrosinase activity. *Analytical Biochemistry, 594*, Article 113614. https://doi.org/10.1016/j.ab.2020.113614

Chen, Y., Lawless, C., Gillespie, C. S., Wu, J., Boys, R. J., & Wilkinson, D. J. (2010). CaliBayes and BASIS: Integrated tools for the calibration, simulation and storage of biological simulation models. *Briefings in Bioinformatics, 11*(3), 278-289. https://doi.org/10.1093/bib/bbp072

Das, J., Ramani, R., & Suraju, M. O. (2016). Polyphenol compounds and PKC signaling. *Biochimica et Biophysica Acta (BBA)—General Subjects, 1860*(10), 2107-2121. https://doi.org/10.1016/j.bbagen.2016.06.022

Famutimi, O. G., Adebiyi, V. G., Akinmolu, B. G., Dada, O. V., & Adewale, I. O. (2024). Trypsin, chymotrypsin and elastase in health and disease. *Future Journal of Pharmaceutical Sciences*, *10*, Article 126. https://doi.org/10.1186/s43094-024-00709-y

Garg, C. (2017). Molecular mechanisms of skin photoaging and plant inhibitors. *International Journal of Green Pharmacy, 11*(2), 217-232.

George, V. C., Dellaire, G., & Rupasinghe, H. V. (2017). Plant flavonoids in cancer chemoprevention: Role in genome stability. *The Journal of Nutritional Biochemistry, 45*, 1-14. https://doi.org/10.1016/j.jnutbio.2016.11.007

Gómez-López, I., Lobo-Rodrigo, G., Portillo, M. P., & Cano, M. P. (2021). Characterization, stability, and bioaccessibility of betalain and phenolic compounds from *Opuntia stricta* var. *dillenii* fruits and products of their industrialization. *Foods, 10*(7), Article 1593. https://doi.org/10.3390/foods10071593

Gong, G., Guan, Y.-Y., Zhang, Z.-L., Rahman, K., Wang, S.-J., Zhou, S., Luan, X., & Zhang, H. (2020). Isorhamnetin: A review of pharmacological effects. *Biomedicine & Pharmacotherapy, 128*, Article 110301. https://doi.org/10.1016/j.biopha.2020.110301

Guo, J., Huang, X., Dou, L., Yan, M., Shen, T., Tang, W., & Li, J. (2022). Aging and aging-related diseases: From molecular mechanisms to interventions and treatments. *Signal Transduction and Targeted Therapy, 7*, Article 391. https://doi.org/10.1038/s41392-022-01251-0

Hassanpour, S. H., & Doroudi, A. (2023). Review of the antioxidant potential of flavonoids as a subgroup of polyphenols and partial substitute for synthetic antioxidants. *Avicenna Journal of Phytomedicine, 13*(4), 354-376.

Hazra, B., Biswas, S., & Mandal, N. (2008). Antioxidant and free radical scavenging activity of *Spondias pinnata*. *BMC Complementary and Alternative Medicine, 8,* 1-10, Article 63. https://doi.org/10.1186/1472-6882-8-63

Kim, D. W., Woo, H. S., Kim, J. Y., Ryuk, J. A., Park, K. H., & Ko, B. S. (2016). Phenols displaying tyrosinase inhibition from *Humulus lupulus*. *Journal of Enzyme Inhibition and Medicinal Chemistry, 31*(5), 742-747. https://doi.org/10.3109/14756366.2015.1063621

Kozlowskal, M., Ścibisz, I., Przybył, J. L., Ziarno, M., Żbikowska, A., & Majewska, E. (2021). Phenolic contents and antioxidant activity of extracts of selected fresh and dried herbal materials. *Polish Journal of Food and Nutrition Sciences, 71*(3), 269-278. https://doi.org/10.31883/pjfns/139035

Kumpunya, S., & Praputbut, S. (2014). Antioxidant activities of *Vernonia cinerea* L. extract in endotoxin- and cytokine-stimulated macrophages. *Thai Journal of Pharmacology, 36*(2), 29-43.

Kunu, W., Meekrasae, R., Peethong, O., Khanma, S., Insamran, Y., & Patathananone, S. (2025). Phytochemical analysis and effectiveness of ripened *Spondias pinnata* fruit extracts against antibiotic-resistant mastitis-causing bacteria. *International Journal of Veterinary Science, 14*(1), 196-203.

Laksemi, D. A. (2019). Biological activity of *Spondias pinnata*: A review. *Indonesian Journal of Biomedical Science, 13*(2), 88-93. https://doi.org/10.15562/ijbs.v13i2.218

Lee, K. K., & Choi, J. D. (1999). The effects of *Areca catechu* L. extract on antiaging. *International Journal of Cosmetic Science, 21*(4), 285-295. https://doi.org/10.1046/j.1467-2494.1999.196590.x

Long, H. H., Schmidt, D. D., & Baldwin, I. T. (2008). Native bacterial endophytes promote host growth in a species-specific manner; phytohormone manipulations do not result in common growth responses. *PLoS ONE, 3*(7), Article e2702. https://doi.org/10.1371/journal.pone.0002702

Moolwong, J., Klinthong, W., & Chuacharoen, T. (2023). Physicochemical properties, antioxidant capacity, and consumer acceptability of ice cream incorporated with avocado (*Persea americana* Mill.) pulp. *Polish Journal of Food and Nutrition Sciences, 73*(3), 289-296. https://doi.org/10.31883/pjfns/170938

Nakadate, K., Ito, N., & Kawakami, K. (2026). Repositioning natural products in modern drug discovery: Technological innovation, systems pharmacology, and pathological validation. *International Journal of Molecular Sciences, 27*(10), Article 4330. https://doi.org/10.3390/ijms27104330

Nitheesh, S., Devanathan, K., & Balaji, R. (2024). A review of *Spondias pinnata* (L.f.) Kurz's phytochemical constituents, traditional uses, and pharmacological activities: An important medicinal plant in Ayurveda. *Texila International Journal of Public Health, 24*(5), Special Issue. https://doi.org/10.21522/TIJPH.2013.SE.24.05.Art022

Patathananone, S., Daduang, J., Koraneekij, A., & Chia-Ying, L. (2019a). Tyrosinase inhibitory effect, antioxidant and anticancer activities of bioactive compounds in ripe hog plum (*Spondias pinnata*) fruit extracts. *Oriental Journal of Chemistry, 35*(3), 916-926. https://doi.org/10.13005/ojc/350302

Patathananone, S., Daduang, J., & Koraneekij, A. (2019b). Anti-cholangiocarcinoma cell growth and selective ability of bioactive components of ripe wild mango (*Spondias pinnata*) fruit extract. *Malaysian Applied Biology, 48*(4), 107-114.

Pientaweeratch, S., Panapisal, V., & Tansirikongkol, A. (2016). Antioxidant, anti-collagenase and anti-elastase activities of *Phyllanthus emblica*, *Manilkara zapota* and silymarin: An in vitro comparative study for antiaging applications. *Pharmaceutical Biology, 54*(9), 1865-1872. https://doi.org/10.3109/13880209.2015.1133658

Sabogal De La Pava, M. L., & Tucker, E. L. (2025). Effects of geopolitical strain on global pharmaceutical supply chain design and drug shortages. *European Journal of Operational Research, 327*, 641-654. https://doi.org/10.1016/j.ejor.2025.05.002

Sameh, S., Al-Sayed, E., Labib, R. M., & Singab, A. N. (2018). Genus *Spondias*: A phytochemical and pharmacological review. *Evidence-Based Complementary and Alternative Medicine, 2018*(1), Article 5382904. https://doi.org/10.1155/2018/5382904

Satpathy, G., Tyagi, Y. K., & Gupta, R. K. (2011). Preliminary evaluation of nutraceutical and therapeutic potential of raw *Spondias pinnata* K., an exotic fruit of India. *Food Research International, 44*(7), 2076-2087. https://doi.org/10.1016/j.foodres.2011.01.040

Siegel, R. L., Miller, K. D., & Jemal, A. (2019). Cancer statistics, 2019. *CA: A Cancer Journal for Clinicians, 69*(1), 7-34. https://doi.org/10.3322/caac.21551

Thansa, W. (2025). Trends and disparities in non-communicable diseases among Thai older adults: Analysis of national health examination surveys, 2008-2020. *Interprofessional Journal of Health Sciences, 23*(2), Article IJHS-0813. https://li05.tci-thaijo.org/index.php/IJHS/article/view/813

Wang, Y., Wang, F., Liu, W., Geng, Y., Shi, Y., Tian, Y., Zhang, B., Luo, Y., & Sun, X. (2024). New drug discovery and development from natural products: Advances and strategies. *Pharmacology & Therapeutics, 264*, Article 108752. https://doi.org/10.1016/j.pharmthera.2024.108752

Wasuworawong, K., Roytrakul, S., Paemanee, A., Jindapornprasert, K., & Komyod, W. (2015). Comparative proteomic analysis of human cholangiocarcinoma cell lines: S100A2 as a potential candidate protein inducer of invasion. *Disease Markers, 2015*(1), Article 629367. https://doi.org/10.1155/2015/629367

World Health Organization. (2025, September 25). *Noncommunicable diseases*. https://www.who.int/en/news-room/fact-sheets/detail/noncommunicable-diseases

Yolande, F. N., Sayantan, B., Paramita, G., Deblina, S., Simplice, M. R., Christopher, T. B., & Murmu, N. (2018). Cytotoxic effect of *Spondias cytherea* fruit extract in murine melanoma model in vivo and in vitro. *Journal of Environmental Pathology, Toxicology and Oncology, 37*(3), 231-240. https://doi.org/10.1615/JEnvironPatholToxicolOncol.2018026697

Pertanika J. Trop. Agric. Sci. 49 (5): 2343 - 2359 (2026)

PERTANIKA JOURNALS

TROPICAL AGRICULTURAL SCIENCE

Journal homepage: http://www.pertanika.upm.edu.my/

Antioxidant Film Packaging from Red Tilapia Fish Scale Gelatin with Kesum (*Persicaria Odorata*) Powder

Nur Syazwani Yusri, Roseliza Kadir Basha*, Siti Nurnajihah Salahuddin, Nazatul Shima Azmi, Farah Saleena Taip, Noor Zafira Noor Hasnan, and Nor Amaiza Mohd Amin

Department of Process and Food Engineering, Faculty of Engineering, Universiti Putra Malaysia, 43400 Serdang, Selangor, Malaysia

ABSTRACT

This study examines the feasibility of using scale, an organic waste product from processing red tilapia, as a source of gelatin for packaging materials. The antioxidant activity of gelatin-based films is increased by adding kesum leaf powder, thereby enhancing the films' functionality as active packaging materials. However, the particular effect of kesum leaf powder on these films hasn't been fully investigated. The study aims to close this gap by methodically examining a number of factors, such as moisture content, optical characteristics, mechanical strength, scanning electron microscopy (SEM), Fourier-transform infrared spectroscopy (FTIR), and antioxidant activity in gelatin-glycerol films combined with kesum leaf powder (Gel/Gly/Kes). The analysis findings show that the Gel/Gly/Kes films retain their transparency while adding a deeper colour with green and yellow undertones. Additionally, adding the kesum powder lowers the moisture content and modifies mechanical characteristics, most notably by increasing elongation at break (28.2%). Furthermore, the Gel/Gly/Kes films show a significant increase in antioxidant activity, with 73.5% inhibition, indicating potential use in active food-preservation packaging. The successful incorporation of kesum leaf powder results in an uneven surface with white areas visible under scanning electron microscopy (SEM). In conclusion, the Gel/Gly/Kes films exhibit favourable characteristics, establishing them as a successful active packaging material with the potential to preserve the quality and prolong food products' shelf lives.

Keywords: Antioxidant packaging, gelatin-based film, kesum leaf powder, red tilapia fish scale

ARTICLE INFO

Article history:
Received: 21 August 2025
Accepted: 25 September 2026
Published: 30 October 2026

DOI: https://doi.org/10.47836/pjtas.49.5.12

E-mail addresses:
roseliza@upm.edu.my (Roseliza Kadir Basha)
work.syazwaniyusri@gmail.com (Nur Syazwani Yusri)
203705@student.upm.edu.my (Siti Nurnajihah Salahuddin)
nazatuls@uthm.edu.my (Nazatul Shima Azmi)
farahsaleena@upm.edu.my (Farah Saleena Taip)
noorzafira@upm.edu.my (Noor Zafira Noor Hasnan)
myza@upm.edu.my (Nor Amaiza Mohd Amin)
* Corresponding author

e-ISSN: 2231-8542

© Universiti Putra Malaysia Press

INTRODUCTION

Malaysia has established aquaculture facilities supporting the cultivation of at least 49 freshwater and marine fish species. The most commonly farmed marine fish species include asian seabass, snapper, and grouper. In freshwater aquaculture, catfish, tilapia, and riverine catfish dominate, with a combined production of 121,553.75 metric tons in 2020 (Ridzuan et al., 2022). The Department of Fisheries (n.d.) data showed that up to 20,000 tonnes of red tilapia were produced, making it the second-largest cultured species in 2025. However, as fish production increases in Malaysia, so does the generation of fish waste, including bones, scales, skin, and shells. Additional waste also arises from aquaculture-related activities such as canning, filleting, salting, and smoking. An estimated 7.2 to 12 million metric tons of fish waste are thrown away globally each year (Qin et al., 2022). The dumping of fish waste, especially fish scales, in landfills can seriously damage the environment and waste resources (Qin et al., 2022). As a result, transforming fish scales into useful products like gelatin might generate additional revenue streams and contribute to a more sustainable and environmentally friendly aquaculture industry. Red tilapia fish scales have a high protein content of up to 47%, showing their suitability as a gelatin source (Pertiwi et al., 2025). According to Luo et al. (2022), the food industry uses gelatin extensively because of its many useful properties.

Moreover, gelatin has garnered significant attention as a promising material for edible films and food packaging (Hanani et al., 2014; Hoque et al., 2011; Nagarajan et al., 2012; Prodpran et al., 2017; Tongnuanchan et al., 2016). It has been fascinating due to its ability to form films and its potential to produce active packaging with practical applications in the food industry (Kumnerdsiri et al., 2024). Polymer films, which are thin and continuous structures, are commonly used in packaging to protect products from the external environment. The addition of plasticisers to gelatin films enhances their viscoelasticity, workability, elongation, and uniformity. Azmi et al. (2020) demonstrated that different types and concentrations of plasticisers used in gelatin films significantly affect the functionality of tilapia fish-scale gelatin films. Furthermore, gelatin-based films function not only as barriers against oxygen, carbon dioxide, and volatile compounds but also as platforms for integrating diverse additives. These additives include antimicrobials, antioxidants, antifungal agents, colorants, and other nutrients, as demonstrated by previous studies (Ahmad et al., 2012; Rhim & Ng, 2007). This feature allows for the design of active bio-based packaging materials with antioxidant capabilities.

Research into active packaging has seen recent growth due to its potential to prevent food degradation and extend shelf life. Previously, gelatin-based packaging films have been approved for their ability to protect, preserve, and demonstrate strong film-forming capabilities (Said & Sarbon, 2022). The use of gelatin-based packaging film with antioxidants has been shown to prolong shelf life, as antioxidants inhibit the growth of microorganisms

(Ratna et al., 2023). This is supported by a study by Sinlapapanya et al. (2024), which concluded that antioxidant activities can significantly inhibit lipid oxidation and microbial growth, thereby extending the shelf life of the product. The incorporation of antioxidant capabilities from natural extracts, as highlighted by Najwa et al. (2020), is a key aspect in the development of active packaging solutions. According to Christapher et al. (2015), kesum powder has shown promising antibacterial, antifungal, anti-inflammatory, and antioxidant properties. As stated by Ahmad et al. (2014) and Salbiah et al. (2015), kesum has created an inhibitory zone against a variety of foodborne pathogens. To prolong the shelf life of food by reducing oxidation rates, antioxidant-active food packaging has been proposed as a solution. Although the bioactive qualities of kesum-derived extracts have been investigated, there is still a lack of research on the use of kesum leaf powder in fish scale gelatin films. The effects of kesum leaf powder towards the physicochemical, structural, and functional characteristics of fish scale gelatin film remain insufficiently explored. Therefore, the purpose of this study was to investigate the effects of incorporating kesum leaf powder into gelatin-based films, especially on their antioxidant packaging properties.

MATERIALS AND METHODS

Extraction and Proximate Analysis of Gelatin from Red Tilapia Fish Scale

The procedure adhered to the methods outlined by Limpisophon et al. (2009) and Weng & Wu (2015), with a minor adjustment. The red tilapia scales were collected from a wet market in Pahang and washed thoroughly to remove dirt and blood. Subsequently, the scales went through alkaline treatment by soaking in a solution of 0.05 M sodium hydroxide (NaOH) and 25% methanol with a scale-to-solution ratio of 1:4 at 10 °C for 24 hours to remove the lipids, pigments, and non-collagenous proteins. Following the alkaline treatment, the scales were soaked for 2 hours in 0.05 M hydrochloric acid (HCl) at room temperature. The scales were thoroughly cleaned and rinsed before the gelatin was extracted. The gelatin was then heated in distilled water to 80 °C for an hour. Then, the mixture was centrifuged (Universal 320, Hettich GmbH & Co., Canada) at 9000 rpm for 33 minutes. The gelatin extract supernatant was freeze-dried using a freeze-dryer (Scanvac, Labogene, Denmark) and stored at -20 °C until further use.

The Association of Official Analytical Chemists (AOAC) International (2016) methodologies were used to determine the protein, fat, ash, and moisture contents of fish scales and gelatin powder.

Preparation and Proximate Analysis of Kesum Leaf Powder

Polygonum minus (kesum) was obtained from a nearby wet market located in Kajang, Selangor. The botanical sample was cleaned with flowing tap water and then rinsed with

distilled water to eliminate dirt and impurities. The procedure for preparing kesum powder followed Abu Samah et al. (2019), with a minor modification. The prepared plant material was subsequently placed in an oven at 50 °C and dried for 3 days until a stable weight was reached. The dried plant sample was then weighed, blended with a high-speed mixer, and kept at room temperature for additional analysis.

The proximate analysis of the powdered leaves was conducted to determine the protein, fat, ash, and moisture content following the standard procedures outlined by the Association of Official Analytical Chemists (AOAC) (AOAC International, 2016).

Preparation and Characterisation of Kesum/Gelatin-Based Film

The gelatin films were developed using the same method for solution casting method as in González et al. (2016), with some modifications. The film-forming solution was created by dissolving 2% (w/v) of freeze-dried gelatin, along with 30% (w/w of the gelatin) of plasticisers, in distilled water at 60 °C for 30 minutes with continuous stirring. Glycerol served as the plasticiser. Kesum powder was incorporated at varying concentrations of 0.05%, 0.1%, and 0.2% to produce Kesum-incorporated films of Gel/Gly/Kes (C0.5), Gel/Gly/Kes (C1.0) and Gel/Gly/Kes (C2.0), respectively. The concentrations was chosen based on a study by Sabbah et al. (2023) for the incorporation of olive and guava leaves with pectin films.

The solution underwent sonication for 10 minutes (Chang et al., 2010) to eliminate air bubbles. Then, the film-forming solution was cast into 14-cm-diameter Petri dishes placed on a levelled surface and allowed to dry at room temperature for 48 hours. Upon complete drying, the film was carefully peeled off and stored in sealed plastic film at 57% humidity (Xu et al., 2005).

Optical Properties of Films

The colour was determined using a colourimeter (ColourFlex EZ, HunterLab, Virginia, USA). The colour profile was described using the colour parameters L* (lightness component), a* (green-red), and b* (blue-yellow). An average of at least three replications is shown by the colour values. The formula, where ΔL*, Δa*, and Δb* represent the differences between the standard white tile and film samples, respectively, was used to get the total colour difference (ΔE). Furthermore, film opacity was calculated using the formula opacity = A600/L, where L is the film thickness (mM), and A600 is the absorbance value at 600 nm (Nordin et al., 2020).

Moisture Content

The weight loss of the films during drying was used to assess their moisture content. The film was dried in a ventilated oven C (UF110, Memmert, Germany) at 105 °C for 24 hours.

The film's weight was recorded at the beginning and end, and the moisture content was assessed by calculating the weight change.

Fourier-Transform Infrared Spectroscopy (FTIR)

A Thermonicolet (Model Nicolet 6700, United States) spectrometer was used to record FTIR spectra, and thin, transparent potassium bromide (KBr) pellets were used to acquire transmission spectra (Saikia et al., 2010).

Scanning Electron Microscopy (SEM)

This analysis will result in an image taken at 15 kV as the accelerating voltage. The Scanning Electron Microscope (SEM), specifically a JEOL Model JSM-6400 from the USA, was used to assess the film's morphology. To eliminate charging effects, a thin layer of gold was applied to coat the specimens.

Film Mechanical Performance Analysis

The measurements of tensile strength (TS) and percentage elongation at break (EAB) are crucial for linking the mechanical characteristics of films to their chemical composition. The Texture Analyser (TA.XT2, Stable Micro Systems, UK) was used to determine these properties following the guidelines outlined in ASTM D882-02 (ASTM, 2002). Sample strips measuring 100 × 15 mM from each film type were cut for testing. Prior to testing, the film thickness was measured using a Digital Vernier Caliper (MIT-500-196-20, Japan). The averages of these data were used to calculate the cross-sectional area of each film.

Antioxidant Activity

The antioxidant activity was assessed using the 1,1-diphenyl-2-picrylhydrazyl (DPPH) assay method (Hsu et al., 2008, 2011). In particular, 20 mL of a 55 mM DPPH solution in methanol was applied to the 20 film sections (1 × 1 cm^2). Following a 24-hour incubation period in the incubator, the absorbance of the supernatant was measured at 516 nm using a UV-Vis Spectrophotometer (Ultrospec 3100, Amersham Biosciences, Germany). A control was established using a blank DPPH solution without any sample. The free radical scavenging effect of all kesum powders on DPPH radical was evaluated to assess their antioxidant activities, using a method by Akowuah et al. (2005) with minor adjustments. Two milliliters of 0.1 mM DPPH methanolic solution were combined with 200 microliters of sample extracts and 0.8 millilitres of methanol. The blend was completely stirred and stored in the dark for one hour. The control was made by blending 2 mL of DPPH with 1 mL of methanol. Absorbance was recorded at 517 nm using a UV-Vis spectrophotometer, and the samples were assessed in triplicate.

Statistical Analysis

The statistical analysis of the data obtained from the physicochemical, morphological and antioxidant properties of the films was performed by ANOVA using SPSS to determine significant differences among treatment means at a significance level of $p < 0.05$. In film properties analysis, Gel/Gly film was used as a control. Triplicates of each of the films were used in the analysis, and the values were presented as means ± standard deviation.

RESULTS AND DISCUSSIONS

Gelatin Extraction



Figure 1. The gelatin extracted from red tilapia's fish scales

The successful extraction of gelatin from raw red tilapia fish scales was achieved, with approximately 6.8 wt% of gelatin obtained from a dry weight of 100 g of fish scales. Based on the visual appearance represented in Figure 1, the gelatin extracted from the red tilapia fish scales displayed a snowy white, crystal-like appearance and a light texture after freeze-drying. Additionally, the extracted gelatin exhibits a nearly unnoticeable fishy odour.

The freeze-dried gelatin exhibited a porous structure. The flank of the freeze-dried gelatin was bright white and shiny. On the wall side, the sample gelatin had a rough, porous surface. The scaffold's bottom surface is smooth and features a radial design. The gelatin scaffold is white, while gelatin film, capsules, or foam are typically light yellow (Wu et al., 2010).

The approximate composition of the fish scales and the extracted gelatin is presented in Table 1, which include the amounts of protein, fat, ash, and moisture content. The red tilapia fish scales contained approximately 24.6% protein, 0.6% total fat, 15.8% ash, and 59% moisture. Protein and moisture comprised the majority of the scales, with smaller amounts of ash and fat. The protein content figures are generally consistent with the findings of Sockalingam ane Abdullah (2015), but there are differences in the moisture and ash contents, possibly due to variations in tilapia species.

Table 1
Percentage of proximate composition of red tilapia's fish scale and extracted gelatin

Composition	Yield (%)	
	Fish Scale	Extracted Gelatin
Protein	24.6	85.8
Total fat	0.6	0.4
Ash	15.8	2.5
Moisture	59.0	11.0

Kesum Leaf Powder

Proximate analysis involves the identification and quantification of the primary components present in feed and other raw plant materials. Its primary purpose is to evaluate whether the feed adheres to its typical compositional parameters or if any adulteration has occurred. In the present study, proximate parameters were assessed for the kesum leaf powder. Based on the results in Table 2 showed that kesum leaf powder has total ash (23.0%), moisture content (7.5%), total fat (0.6%), carbohydrate (57.2%), and protein (11.7%).

Table 2
Proximate analysis of the kesum leaves powder

Parameters	%
Total ash	23.0
Moisture content	7.5
Total fat	0.6
Carbohydrate	57.2
Protein	11.7
Energy	281 kcal/100g

Film Properties

Optical Properties of Film

The colour of films is an important attribute that consequently affects their appearances, marketability, and suitability for various applications. According to Table 3, the L* value of gelatin-based film decreases significantly ($p < 0.05$) from 86.78 to 64.74 with increasing incorporated concentration of kesum leaf powder. This is due to the kesum powder, which is opaque in nature, directly affecting the overall luminosity of the film. Hence, decreased the film's lightness.

Table 3
Optical properties of different concentrations of kesum incorporated into the kesum/gelatin-based films

Sample	L*	a*	b*	Opacity	ΔE
Gel	85.83 ± 0.26	0.73 ± 0.02	0.43 ± 0.29	3.80 ± 2.04	11.24 ± 0.25
Gel/Gly	86.78 ± 0.56	-1.38 ± 0.12	3.22 ± 0.51	7.02 ± 1.45	10.33 ± 0.30
Gel/Gly/Kes(C0.5)	80.79 ± 0.44	-0.57 ± 0.16	-12.76 ± 1.38	5.19 ± 2.42	21.97 ± 1.05
Gel/Gly/Kes(C1.0)	68.90 ± 2.66	-1.38 ± 0.60	-37.45 ± 2.96	4.17 ± 1.24	48.53 ± 3.61
Gel/Gly/Kes(C2.0)	64.74 ± 4.62	-3.25 ± 0.97	-37.39 ± 2.88	3.78 ± 2.61	74.82 ± 5.30

Note. ΔE: Total colour different; Gel: Gelatin; Gly: Glycerol; Kes: Kesum powder; C: Concentration of kesum powder incorporated into the film

Colour analysis revealed that the Gel/Gly film exhibited a light yellowish tint. However, the values of a* and b* significantly increased ($p < 0.05$) as the concentration

of kesum powder in the film increased. This can be attributed to the dark green colour of the kesum powder, which dominated the film's overall colour, resulting in stronger green (a-) and blue (b-) hues. The total colour difference (ΔE) showed that the inclusion of kesum powder in gelatin film can affect the overall colour, with an increase as the kesum powder concentration increases. According to Kuan et al. (2020), the edible film produced becomes darker, greener, and yellower as the amount of mulberry leaf extract increases. In accordance with the findings of Kuan et al. (2020), the result demonstrates that the kesum powder colour gives a greener colour to the gelatin-based film, as shown in Figure 2. The increase in the yellowish and greenish colour of the film was attributed to the natural colour of the kesum leaf. In the Gel/Gly film, the film appeared to be nearly transparent, with no visible green or yellow colouration due to the absence of kesum powder. The Gel/Gly/Kes (0.5) film exhibited a slight yellowish-green tint, while the Gel/Gly/Kes (1.0) film showed a more noticeable yellowish-green colouration. Meanwhile, the Gel/Gly/Kes (2.0) film exhibited the strongest yellowish-green coloration, giving the film a distinctly darker yellow-green appearance due to higher kesum powder content.

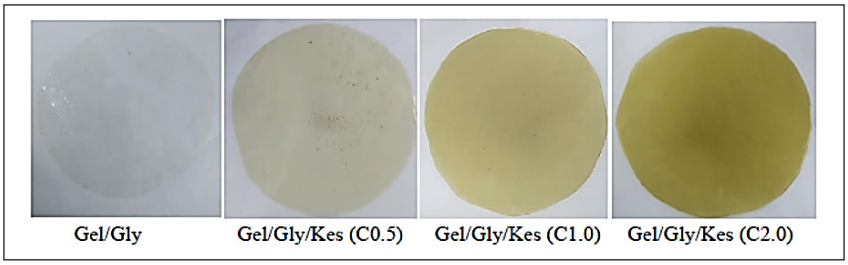

Figure 2. Gelatin-based film with and without incorporation of kesum powder

Moisture Content Analysis

The gelatin film without plasticiser had the greatest moisture content, at 27.05%. The incorporation of kesum leaf powder, as shown in Table 4, significantly ($p < 0.05$) decreased the moisture content of the gelatin composite films from 15.48% to 6.77%. The reduced moisture level of the film with kesum leaf powder may suggest the establishment of an inclusion complex between the gelatin matrix and the polyphenolic compounds via hydrogen

Table 4
Moisture content of different concentrations of kesum powder incorporated into the kesum/gelatin-based films and moisture content of kesum powder

Sample	Moisture Content (%)
Gel	27.05 ± 5.84
Gel/Gly	17.29 ± 5.63
Gel/Gly/Kes (C0.5)	15.48 ± 2.89
Gel/Gly/Kes (C1.0)	12.39 ± 6.43
Gel/Gly/Kes (C2.0)	6.77 ± 0.85
Kesum Powder	8.83 ± 0.61

Note. Gel: Gelatin; Gly: Glycerol; Kes: Kesum powder; C: Concentration of kesum powder incorporated into the film

bonds. Weak intermolecular interactions between the gelatin matrix and polyphenols competed with water molecules, reducing the matrix's capacity to interact with water and leading to a decrease in the moisture content of the developed film. The results align with findings by Rambabu and Bharath (2019), who explain that moisture content decreased as the concentration of mango leaf extract increased due to the hydrophobic nature of moisture, which reduces the capacity for water absorption in films.

The moisture content of kesum powder was measured at 8.83 ± 0.61%. Typically, during the drying process, fresh kesum leaves are dehydrated to reduce their moisture content and increase their shelf stability. It is important to note that the moisture content of kesum powder can be influenced by storage conditions. If stored improperly in a humid environment, the powder can absorb moisture from the surroundings, increasing its moisture content over time.

Fourier Transform Infrared Spectroscopy (FTIR)

Data for Fourier transform infrared spectroscopy of the film were based on Figure 3 and Table 5. The Amide A band in the Gel/Gly/Kes films were mainly attributed to the presence of N-H stretching vibrations, which were observed in the range of 3307.48 cm^{-1} - 3312.64 cm^{-1}. As shown in Table 5, N-H bond stretching is detected across all kesum concentration loadings in the films, indicating the presence of the amide group.

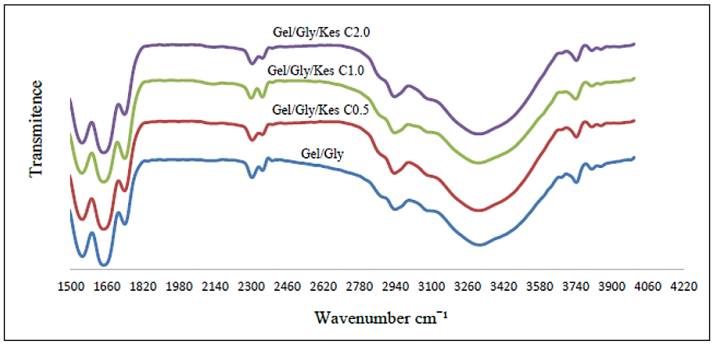

Figure 3. FTIR result for the gelatin-based film incorporation with kesum powder

Next, the Amide I band was mainly associated with the stretching vibrations of the carbonyl group along the polypeptide backbone of the gelatin-based films, which is the major structure of gelatin. With the addition of kesum powder, the peaks in the amide A-III region showed no obvious shift, indicating no conformational changes in the higher structure of gelatin. The absorption bands in the film with a concentration of 1.0% kesum powder, amide band III at 1226.58 cm^{-1}, are slightly different from those in films with 0.5% and 2.0% kesum powder, with bands at 1236.34 cm^{-1} and 1231.33 cm^{-1}, respectively.

This showed that the kesum-gelatin films correspond to C—O—C stretching vibrations and a composite of C—O—C stretching vibrations and C—C skeleton vibrations, which are typical functional groups of gelatin (Wang et al., 2017). For kesum powder, common functional groups found in plant materials, including kesum, include hydroxyl (OH), carbonyl (C=O), carboxyl (COOH), aromatic (C=C), and alkyl (C-H) groups (Xiao et al., 2021). The presence of amide bands, particularly the amide I (C=O stretching) and amide II (N-H bending) bands, can provide information about the proteinaceous components in the sample. Kesum powder, like many plant materials, may contain cellulosic components. Peaks in the 1600 - 1800 cm^{-1} range often indicate the presence of cellulose and hemicellulose, while peaks in the 1500-1600 cm^{-1} range may be associated with lignin.

Table 5
Amide band wavenumber for different concentrations of kesum powder incorporated with gelatin-based film and kesum powder

Amide Band	Wavenumber (cm^{-1})				
	Gel/Gly	Gel/Gly/Kes (C0.5)	Gel/Gly/Kes (C1.0)	Gel/Gly/Kes (C2.0)	Kesum Powder
A	33742.48	3312.64	3307.48	3310.20	3371.12
I	1739.51	1739.04	1739.01	1738.40	1737.16
II	1646.12	1646.06	1645.23	1645.79	1632.59
III	1233.95	1236.34	1226.58	1231.33	1221.34

Note. Gel: Gelatin; Gly: Glycerol; Kes: Kesum powder; C: Concentration of kesum powder incorporated into the film

Morphological Analysis of the Film

As shown in Figure 4, the surface structures were observed in SEM at 100 μm. Based on the SEM micrograph, the surface was not smooth; white patches were observed, likely due to kesum powder. White patches in both samples seemed uneven. This indicated that supplementation of kesum powder might affect the active ingredients. Kesum powder contains polar organic compounds, which are only soluble in polar solvents. The extraction effectiveness of a particular compound depends on its solubility in the solvent, which in turn reduces the film matrix density and affects the film porosity. Smaller particles have a higher surface area, which facilitates their dispersion and interaction with the solvent or polymer matrix. This can lead to better uniformity and homogeneity of the powder distribution within the film.

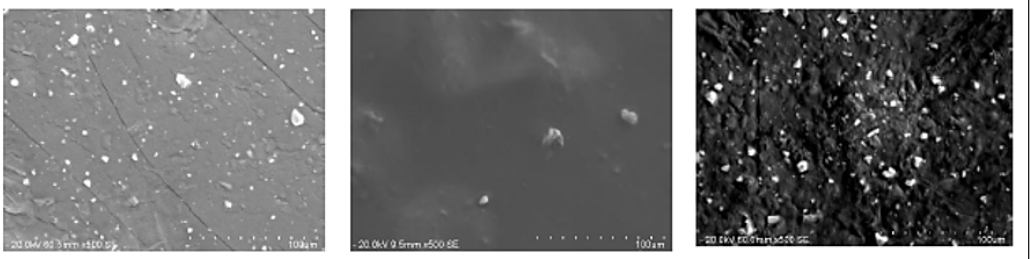

(a) Gel/Gly/Kes (C0.5) (b) Gel/Gly/Kes (C1.0) (c) Gel/Gly/Kes (C2.0)

Figure 4. SEM micrograph of the kesum/gelatin-based film with different concentrations

Mechanical Properties of Kesum/Gelatin-Based Film

In finding stretchability and flexibility, elongation plays a vital role. The tensile strength required for the versatility of packaging films depends on their intended use and the subsequent transportation, handling, and storage of packaged foods. Table 6 clearly showed the effect of kesum concentration at 0.5%, 1.0%. and 2.0% had an inverse relationship between the elongation and the corresponding tensile strength. As expected, the increase in kesum concentration significantly enhanced film elongation from 14.67 ± 3.42% to 28.23%. On the other hand, the elongation of the control film without plasticiser and of the gelatin with plasticiser showed values of 1.57% and 8.37%, respectively. This is because active ingredients such as polyphenols can alter the membrane's physicochemical characteristics, causing the polymeric network to break. (Nguyen et al., 2022).

Table 6
Mechanical properties of different concentrations of kesum powder incorporated into the film

Sample	TS (MPa)	EAB (%)
Gel	26.32 ± 14.96	1.57 ± 0.94
Gel/Gly	21.09 ± 0.95	8.37 ± 4.37
Gel/Gly/Kes (C0.5)	23.65 ± 8.44	14.67 ± 3.42
Gel/Gly/Kes (C1.0)	15.89 ± 4.86	17.06 ± 1.36
Gel/Gly/Kes (C2.0)	9.47 ± 1.16	28.23 ± 2.68

Note. TS: Tensile strength; EAB: Elongation at break; Gel: Gelatin; Gly: Glycerol; Kes: Kesum powder; C: Concentration of kesum powder incorporated into the film

Generally, incorporating kesum powder into a gelatin film can reduced tensile strength. The reduction in tensile strength observed in the films can be attributed to the intrinsic properties of the gelatin matrix and the overall structural composition of the film. Similar results were reported by Kuan et al. (2020), who found that adding 4% mulberry leaf

extract decreased the tensile strength of alginate films. Nguyen et al. (2022) explained that incorporating leaf extracts potentially filled the spaces between the film matrix, thereby reducing biopolymer interactions and increasing the free volume and mobility of polymer chains within the matrix. In contrast, films with a more open or flexible structure typically exhibit increased elongation at break, albeit with reduced tensile strength. Arfat et al. (2014) reported similar findings, as tensile strength decreases while elongation at break increases in films incorporated with basil essential oils. This suggested that incorporating essential oil promotes a heterogeneous film structure that disrupts the continuity of the film network, thereby reducing the rigidity and mechanical strength of the film matrix.

Antioxidant Activity

Similar to other plant-based antioxidants, kesum leaf powder can scavenge the DPPH radical, thereby reducing oxidative activity due to the presence of active compounds such as phenolics and flavonoids. Compared with ginger and turmeric, kesum exhibited antioxidant activity and contained total phenolic compounds (Maizura et al., 2011). The antioxidant activity of kesum leaf powder is influenced by several factors, including the herb's quality, cultivation conditions, processing techniques and storage conditions.

Figure 5 illustrates the percentage of antioxidant inhibition in the films. The results revealed a significant ($p < 0.05$) increase in the antioxidant activity of the gelatin-based film after incorporating kesum leaf powder. Even a low loading of kesum is sufficient for the radical-scavenging performance of the film, as kesum has reversible redox properties and can be readily oxidised and reduced by species in contact with the film. This efficiency in scavenging the free radical DPPH can be attributed to kesum's redox-active property, which enhances the antioxidant activity of the material. The concentration-dependent increase in antioxidant activity corresponds to the increasing active compounds in the films. This observation aligns with other research by Nurdiani et al. (2022) that showed gelatin-based films incorporated with *B. gymnorhiza* and *S. alba* leaves exhibited higher antioxidant

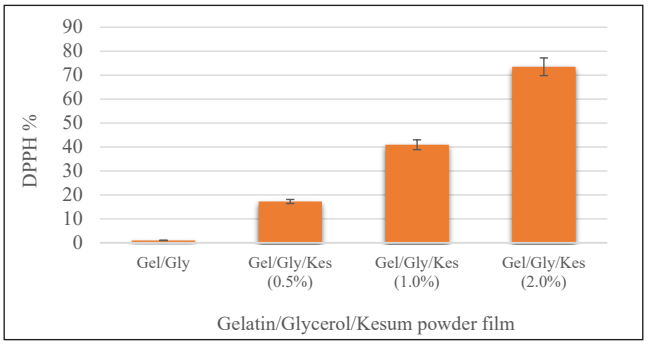

Figure 5. Antioxidant activity of gelatin-based film with and without incorporation of kesum powder

activity with the increase in plant material extracts, demonstrating the enhanced antioxidant activity in active packaging. This shows that the antioxidant agents in kesum leaf powder enhanced the antioxidant functionality of the developed Gel/Gly/Kes films.

CONCLUSION

Gelatin with good film-forming properties has been extracted successfully from red tilapia's fish scales and further developed as a film incorporated with kesum leaf powder. The incorporation of kesum leaf powder into gelatin-based films modified their physicochemical and functional properties, including visual appearance, mechanical properties, moisture content, and antioxidant activity. The gelatin-based film incorporated with the highest kesum leaf powder concentration exhibited a yellowish-green colouration with lower moisture content (6.77%) and increased elongation at break (28.2%). The functional properties of antioxidant activity of the gelatin-based film increased with the addition of kesum leaf powder, as the Gel/Gly/Kes (2.0) exhibited 73.5% antioxidant inhibition. This demonstrated that incorporating kesum leaf powder enhanced the antioxidant functionality of the gelatin-based film. Overall, this study implemented sustainable approaches through the valorisation of fish by-products and the incorporation of natural plant-derived bioactive compounds. The demonstration showed of the potential of kesum leaf powder to be incorporated into fish scale gelatin-based films as active packaging materials with antioxidant functionality, thus providing a foundation for their application in food packaging systems. Future research on food applications and storage analysis can be conducted to establish the functionality of these films in preserving food quality and extending shelf life.

IMPLICATION OF STUDY

This study demonstrated the potential of biological resources as the raw materials for the development of value-added functional packaging materials. The incorporation of kesum leaf powder into red tilapia fish scale gelatin films demonstrates the potential to valorise fish by-products as biopolymers and to combine them with natural, plant-based bioactive materials to impart additional functionality to gelatin packaging materials. In particular, this research revealed enhanced antioxidant activity in gelatin films as kesum leaf powder concentration increased. This indicated that kesum leaf powder provides bioactive components that reduce the oxidation processes in the films. Overall, this study provides a foundation for the green development of sustainable antioxidant packaging materials by valorising fish scale gelatin and incorporating plant-derived bioactive compounds from kesum leaves.

LIMITATION AND RECOMMENDATION FOR FUTURE RESEARCH

Future research on the performance of the antioxidant films on actual food products under controlled storage conditions should be done to determine the functionality of the developed films. Physicochemical, microbial, and antioxidant analyses of the food products can be conducted to evaluate the effectiveness of the antioxidant films in maintaining quality and extending shelf life. These analyses would provide a comprehensive assessment to determine the suitability of the films as antioxidant film materials for food packaging applications.

ACKNOWLEDGEMENT

This work was supported by Universiti Putra Malaysia under grant GP/2024/979100.

REFERENCES

Abu Samah, N., Mahamudin, M., Muhamad, S., & Ibrahim, A. L. (2019). Green synthesis of silver nanoparticles from *Polygonum minus* extract and its antimicrobial properties. *Journal of Academia, 7*(2), 46-55.

Ahmad, M., Benjakul, S., Prodpran, T., & Agustini, T. W. (2012). Physico-mechanical and antimicrobial properties of gelatin film from the skin of unicorn leatherjacket incorporated with essential oils. *Food Hydrocolloids, 28*, 189-199. https://doi.org/10.1016/j.foodhyd.2011.12.003

Ahmad, R., Baharum, S. N., Bunawan, H., Lee, M., Noor, N. M., Rohani, E. R., Ilias, N., & Zin, N. M. (2014). Volatile profiling of aromatic traditional medicinal plant, *Polygonum minus*, in different tissues and its biological activities. *Molecules, 19*(11), 19220-19242. https://doi.org/10.3390/molecules191119220

Arfat, Y. A., Benjakul, S., Prodpran, T., Sumpavapol, P., & Songtipya, P. (2014). Properties and antimicrobial activity of fish protein isolate/fish skin gelatin film containing basil leaf essential oil and zinc oxide nanoparticles. *Food Hydrocolloids, 41*, 265-273. https://doi.org/10.1016/j.foodhyd.2014.04.023

Azmi, N. S., Basha, R. K., Arifin, N. N. T., Othman, S. H., & Mohammed, M. A. P. (2020). Functional properties of tilapia's fish scale gelatin film: Effects of different types of plasticizers. *Sains Malaysiana, 49*(9), 2221-2229. https://doi.org/10.17576/jsm-2020-4909-19

Christapher, P. V., Parasuraman, S., Christina, J. M. A., Asmawi, M. Z., & Vikneswaran, M. (2015). Review on *Polygonum minus* Huds., a commonly used food additive in Southeast Asia. *Pharmacognosy Research, 7*(1), 1-6. https://doi.org/10.4103/0974-8490.147125

Department of Fisheries Malaysia. (n.d.). *Fisheries statistics I*. https://www.dof.gov.my/en/resources/fisheries-statistics-i/

Hanani, Z. A. N., Roos, Y. H., & Kerry, J. P. (2014). Use and application of gelatin as potential biodegradable packaging materials for food products. *International Journal of Biological Macromolecules, 71*, 94-102. https://doi.org/10.1016/j.ijbiomac.2014.04.027

Hoque, M. S., Benjakul, S., & Prodpran, T. (2011). Properties of film from cuttlefish (*Sepia pharaonis*) skin gelatin incorporated with cinnamon, clove and star anise extracts. *Food Hydrocolloids, 25*(5), 1085-1097. https://doi.org/10.1016/j.foodhyd.2010.10.005

Hsu, C. F., Zhang, L., Peng, H., Travas-Sejdic, J., & Kilmartin, P. A. (2008). Scavenging of DPPH free radicals by polypyrrole powders of varying levels of overoxidation and/or reduction. *Synthetic Metals, 158*(21-24), 946-952. https://doi.org/10.1016/j.synthmet.2008.06.017

Hsu, C. F., Peng, H., Basle, C., Travas-Sejdic, J., & Kilmartin, P. A. (2011). ABTS•+ scavenging activity of polypyrrole, polyaniline and poly(3,4-ethylenedioxythiophene). *Polymer International, 60*(1), 69-77. https://doi.org/10.1002/pi.2912

Kuan, Y. L., Sivanasvaran, S. N., Pui, L. P., Yusof, Y. A., & Senphan, T. (2020). Physicochemical properties of sodium alginate edible film incorporated with mulberry (*Morus australis*) leaf extract. *Pertanika Journal of Tropical Agricultural Science, 43*(3), 359-376.

Kumnerdsiri, P., Sanprasert, S., Praiboon, J., Seubsai, A., Sirisarn, W., Pongsetkul, J., Harnkarnsujarit, N., Rawdkuen, S., Karnjanapratum, S., Sai-Ut, S., & Kingwascharapong, P. (2024). Characterization of Cha-Kram leaf extract powder using ultrasound-assisted extraction and its application in gelatin-based film as biodegradable active film. *Future Foods, 10*, Article 100419. https://doi.org/10.1016/j.fufo.2024.100419

Limpisophon, K., Tanaka, M., Weng, W. Y., Abe, S., & Osako, K. (2009). Characterization of gelatin films prepared from under-utilized blue shark (*Prionace glauca*) skin. *Food Hydrocolloids, 23*(7), 1993-2000. https://doi.org/10.1016/j.foodhyd.2009.03.014

Luo, Q., Hossen, M. A., Zeng, Y., Dai, J., Li, S., Qin, W., & Liu, Y. (2022). Gelatin-based composite films and their application in food packaging: A review. *Journal of Food Engineering, 313*, Article 110762. https://doi.org/10.1016/j.jfoodeng.2021.110762

Maizura, M., Aminah, A., & Wan Aida, W. M. (2011). Total phenolic content and antioxidant activity of kesum (*Polygonum minus*), ginger (*Zingiber officinale*) and turmeric (*Curcuma longa*) extract. *International Food Research Journal, 18*, 529-531.

Nagarajan, M., Benjakul, S., Prodpran, T., & Songtipya, P. (2012). Properties of film from splendid squid (*Loligo formosana*) skin gelatin with various extraction temperatures. *International Journal of Biological Macromolecules, 51*(4), 489-496. https://doi.org/10.1016/j.ijbiomac.2012.06.017

Najwa, N. A. I. S., Guerrero, P., Caba, K. D. L., & Nur Hanani, Z. A. (2020). Physical and antioxidant properties of starch/gelatin films incorporated with *Garcinia atroviridis* leaves. *Food Packaging and Shelf Life, 26*, Article 100583. https://doi.org/10.1016/j.fpsl.2020.100583

Nguyen, T. T. T., Le, T. Q., Nguyen, T. T. A., Nguyen, L. T. M., Nguyen, D. T. C., & Van Tran, T. (2022). Characterizations and antibacterial activities of passion fruit peel pectin/chitosan composite films incorporated with *Piper betle* L. leaf extract for preservation of purple eggplants. *Heliyon, 8*(8), Article e10096. https://doi.org/10.1016/j.heliyon.2022.e10096

Nurdiani, R., Ma'rifah, R. D. A., Busyro, I. K., Jaziri, A. A., Prihanto, A. A., Firdaus, M., Talib, R. A., & Huda, N. (2022). Physical and functional properties of fish gelatin-based film incorporated with mangrove extracts. *PeerJ, 10*, Article e13062. https://doi.org/10.7717/peerj.13062

Pertiwi, R. M., Nurilmala, M., Nurjanah, & Nurhayati, T. (2025). Karakteristik sisik ikan nila merah sebagai bahan baku kolagen [Characteristics of red tilapia scales as a raw material for collagen]. *Jurnal Pengolahan Hasil Perikanan Indonesia, 28*(6), 546-558. https://doi.org/10.17844/jphpi.v28i6.50129

Prodpran, T., Chuaynukul, K., Nagarajan, M., Benjakul, S., & Prasarpran, S. (2017). Impacts of plasticizer and pre-heating conditions on properties of bovine and fish gelatin films fabricated by thermo-compression molding technique. *Italian Journal of Food Science, 29*(3), 487-504. https://doi.org/10.14674/IJFS-611

Qin, D., Bi, S., You, X., Wang, M., Cong, X., Yuan, C., Yu, Mu., Cheng, X., & Chen, X. (2022). Development and application of fish scale wastes as versatile natural biomaterials. *Chemical Engineering Journal, 428*, Article 131102. https://doi.org/10.1016/j.cej.2021.131102

Rambabu, K., & Bharath, G. (2019). Mango leaf extract incorporated chitosan antioxidant film for active food packaging. *International Journal of Biological Macromolecules, 126*, 1234-1243. https://doi.org/10.1016/j.ijbiomac.2018.12.196

Ratna, R., Aprilia, S., Arahman, N., & Munawar, A. A. (2023). Effect of edible film gelatin nanobiocomposite packaging and storage temperature on the store quality of strawberry (*Fragaria* × *ananassa* var. *Duchesne*). *Future Foods, 8*, Article 100276. https://doi.org/10.1016/j.fufo.2023.100276

Rhim, J. W., & Ng, P. K. W. (2007). Natural biopolymer-based nanocomposite films for packaging applications. *Critical Reviews in Food Science and Nutrition, 47*(4), 411-433. https://doi.org/10.1080/10408390600846366

Ridzuan, M. S. M., Abdullah, A., Ramly, R., Mansor, N. N., Ramli, N., & Firdaus-Nawi, M. (2022). Current status and advances of fish vaccines in Malaysia. *Veterinary World, 15*(2), 465-482. https://doi.org/10.14202/vetworld.2022.465-482

Sabbah, M., Al-Asmar, A., Younis, D., Al-Rimawi, F., Famiglietti, M., & Mariniello, L. (2023). Production and characterisation of active pectin films with olive or guava leaf extract used as soluble sachets for chicken stock powder. *Coatings, 13*(7), Article 1253. https://doi.org/10.3390/coatings13071253

Said, N. S., & Sarbon, N. M. (2022). Physical and mechanical characteristics of gelatin-based films as a potential food packaging material: A review. *Membranes, 12*(5), Article 442. https://doi.org/10.3390/membranes12050442

Salbiah, S., Abdul, S., Talip, M. A., Wong, C. F., Alimon, H., Bakar, N. A., Rusmawati, W., & Mahamod, W. (2015). Determination of Malaysian herbs and spices as biopreservative agents in food products. *American Journal of Plant Sciences, 6*, 718-724. https://doi.org/10.4236/ajps.2015.65077

Sinlapapanya, P., Sumpavapol, P., Buatong, J., & Benjakul, S. (2024). Ethanolic cashew leaf extract: Antioxidant potential and impact on quality changes of dried fermented catfish during storage. *Future Foods, 9*, Article 100296. https://doi.org/10.1016/j.fufo.2024.100296

Sockalingam, K., & Abdullah, H. Z. (2015). Extraction and characterization of gelatin biopolymer from black tilapia (*Oreochromis mossambicus*) scales. *AIP Conference Proceedings, 1669*(1), Article 020053. https://doi.org/10.1063/1.4919191

Tongnuanchan, T., Benjakul, S., Prodpran, T., Pisuchpen, S., & Osako, K. (2016). Mechanical, thermal and heat sealing properties of fish skin gelatin film containing palm oil and basil essential oil with different surfactants. *Food Hydrocolloids, 56*, 93-107. https://doi.org/10.1016/j.foodhyd.2015.12.005

Weng, W., & Wu, F. (2015). Water resistance and mechanical property improvement of tilapia (*Tilapia zillii*) scale gelatin films by dehydrated thermal treatment. *Journal of Food Science and Technology, 52*(6), 3358-3366. https://doi.org/10.1007/s13197-014-1401-z

Wu, X., Liu, Y., Li, X., Wen, P., Zhang, Y., Long, Y., Wang, X., Guo, Y., Xing, F., & Gao, J. (2010). Preparation of aligned porous gelatin scaffolds by unidirectional freeze-drying method. *Acta Biomaterialia, 6*(3), 1167-1177. https://doi.org/10.1016/j.actbio.2009.08.041

Pertanika J. Trop. Agric. Sci. 49 (5): 2361 - 2385 (2026)

PERTANIKA JOURNALS

TROPICAL AGRICULTURAL SCIENCE

Journal homepage: http://www.pertanika.upm.edu.my/

Comparison of Plant Nutrient Requirements During the Annual Phenological Development of Young Rubber Trees (*Hevea brasiliensis* Mull. Arg.) Prior to the Rubber Tapping Process in Upland and Lowland Areas

Surachart Pechkeo* and Sayan Sdoodee

Agricultural Innovation and Management Division, Faculty of Natural Resources, Prince of Songkla University, 90110 Hat Yai, Thailand

ABSTRACT

The expansion of rubber plantations in Thailand has led to the conversion of lowland rice fields into rubber cultivation areas. However, the unsuitability of these areas for rubber cultivation has led to slow tree growth and low latex yields. This research investigated the accumulation patterns and interrelationships of plant nutrients in soil and young rubber trees grown in upland and lowland areas prior to tapping throughout the annual phenological development cycle. Four experimental plots were established in Phatthalung Province, Thailand. Soil samples were collected at 0-15 cm depth beneath tree canopies, and leaf samples were collected every 2 months from the 2nd to 10th month after leaf flushing (ALF). Physical and chemical properties of soil and plant nutrient concentrations were analysed. Results indicated distinct nutrient demand patterns between locations. In upland areas, rubber trees showed high demand for Na during the 2nd month ALF; K during the 4th month ALF; N and S during the 6th month ALF; K and Cu during the 8th month ALF; and P, K, Mg, Cu and Zn during the 10th month ALF. In lowland areas, high demand was observed for Ca during the 2nd month ALF; Fe during the 4th month ALF; N and Fe during the 6th month ALF; P, K and Cu during the 8th month ALF; and K and Mg during the 10th month ALF. These findings provide valuable information for developing site-specific nutrient management strategies to enhance tree growth, latex yield and quality.

ARTICLE INFO

Article history:
Received: 28 October 2025
Accepted: 25 September 2026
Published: 30 October 2026

DOI: https://doi.org/10.47836/pjtas.49.5.13

E-mail addresses:
Surachart.p@psu.ac.th (Surachart Pechkeo)
Sayan.sdoodee103@gmail.com (Sayan Sdoodee)
* Corresponding author

Keywords: Nutrient accumulation, nutrient dynamics, rubber, pre-tapping rubber trees, soil and plant management

INTRODUCTION

In 2021, Thailand produced approximately one-third of the world's natural rubber

© Universiti Putra Malaysia Press

output (33.81%), totaling 4.75 million tons year^{-1}, out of a global production of 14.05 million tons (Bureau of Agricultural Economic Research, 2023). Thailand's rubber (*Hevea brasiliensis* Mull. Arg.) plantation areas expanded from approximately 30,000 km^2 in 1990 to 39,000 km^2 in 2021, representing a 30% increase. Southern Thailand accounted for approximately 23,000 km^2, or 59% of the country's total rubber plantation areas (Rubber Research Institute, 2010; Office of Agricultural Economics, 2023b). However, many plantations occupy unsuitable areas, particularly lowland sites previously used as paddy fields. These areas experience flooding during the rainy season, adversely affecting tree growth and latex quality. Studies by the Agricultural Extension and Development Region 5 (2004) and the Office of Agricultural Economics (2023a) revealed that paddy field area in southern Thailand decreased from approximately 4,400 km^2 in 2000 to 1,700 km^2 in 2019, representing a reduction of 2,800 km^2 (average 142 km^2 year^{-1}) or 63.63%. This decline resulted primarily from farmers converting rice fields to rubber plantations, which offer higher income and require less intensive management.

Recent climate change has intensified the challenges of rubber cultivation in lowland areas of southern Thailand. The increasing frequency of flash floods and prolonged dry spells (Meteorological Department of Thailand, 2023) creates extreme oscillations between waterlogged and drought conditions. These fluctuations disrupt nutrient availability through alternating oxidation-reduction cycles in soils, accelerate nutrient leaching during heavy rainfall events, and impair root function through repeated stress (Carr, 2012; Kunjet et al., 2013). The synchronisation of nutrient uptake during critical phenological periods becomes increasingly unpredictable, making traditional fertilisation schedules inadequate.

Therefore, investigating the relationship between soil properties and plant nutrient accumulation in upland and lowland rubber plantations (formerly paddy fields) is essential. This research aims to develop appropriate soil and fertiliser management strategies for rubber cultivation that will benefit farmers economically. Implementing proper nutrient management practices can increase rubber farmers' income while reducing unnecessary costs associated with soil management and fertiliser applications in rubber plantations.

Upland and lowland areas are defined as follows: (1) Upland areas have flat to undulating topography without waterlogging, well-drained soil with moderate to rapid permeability, and groundwater levels exceeding 50 cm below the surface. (2) Lowland areas possess low-lying or floodplain topography prone to flooding during the rainy season, poorly drained soil with slow water permeability, and groundwater levels less than 50 cm below the surface, resulting in prolonged soil moisture or flooding.

Two research hypotheses are (1) when soil nutrient levels are lowest, rubber trees have the highest demand for those nutrients during that period, and (2) when leaf nutrient concentrations are lowest, rubber trees have the highest demand for those nutrients during that period. This research aimed to (1) investigate nutrient accumulation and relationships

in soil prior to rubber tapping during annual phenological development (APD) in upland and lowland plantations, and (2) develop appropriate pre-tapping nutrient management guidelines.

MATERIALS AND METHODS

The Experimental Site

The upland rubber plantation was located in Ban Phrao Subdistrict, Pa Phayom District, Phatthalung Province, southern Thailand (experimental site no.1 at 7°49'34.6"N, 99°55'2.0"E, and site no.2 at 7°49'43.4"N, 99°55'4.5"E). Experimental sites no. 1 and no. 2 covered 0.0048 and 0.0128 km², with 6 and 5 year old rubber trees, respectively. The soil is classified as fine-silty, kaolinitic, isohyperthermic, Aquic Kandiudults (in soil taxonomy). This upland area features undulating to rolling topography with 2-5% slope, elevated approximately 20 m above mean sea level, without flooding. The soil formed from riverine sediment deposits with poor drainage, slow surface runoff and moderate permeability. Soil fertility is low but suitable for perennial trees, fruit trees, rubber, oil palms and field crops (Division of Soil Survey and Classification, Department of Land Development, 1987). Surrounding land uses included fruit orchards, rubber plantations, paddy fields and residential communities (Figure 1).

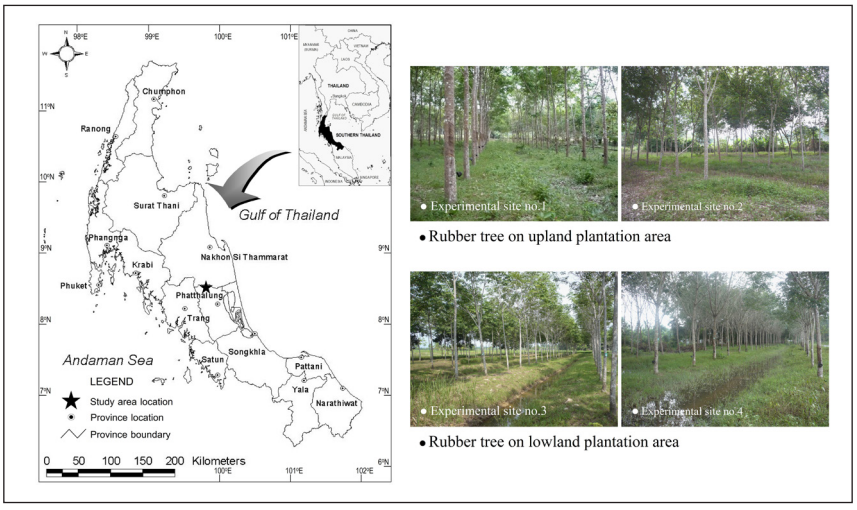

Figure 1. The experimental sites in Pa Phayom District, Phatthalung Province, southern Thailand

The lowland rubber plantation was located in Pa Phayom Subdistrict, Pa Phayom District, Phatthalung Province, southern Thailand (experimental site no.3 at 7°51'44.8"N, 99°57'41.3"E, and site no.4 at 7°51'40.2"N, 99°57'43.2"E). Experimental sites no.3 and no.4 covered 0.0064 and 0.0032 km², with 7 and 6 year old rubber trees, respectively. The soil is

classified as very-fine, kaolinitic, isohyperthermic, Typic Plinthaquults (in soil taxonomy). This lowland area features smooth to nearly flat topography with 0-2% slope, elevated approximately 10 m above mean sea level, experiencing seasonal or year-round flooding. The soil formed from river deposited sediments with poor drainage, slow surface runoff and slow permeability. Soil fertility is low, suitable for rice but unsuitable for perennial trees, rubber, oil palms and field crops due to prolonged waterlogging (Division of Soil Survey and Classification, Department of Land Development, 1987). Surrounding land uses included rubber plantations, paddy fields and residential communities (Figure 1).

Experiments were conducted in 4 plots with young RRIM 600 rubber trees (5-7 years old) prior to tapping: 2 upland and 2 lowland plots with 3×6 m spacing and 10 replicate trees $plot^{-1}$ (Figure 1).

Soil Management in Field

Composite soil samples (4 cores $tree^{-1}$) were collected at 0-15 cm depth around tree canopies (1.00-1.25 m from the trunk) every 2 months during APD from the 2nd to the 10th month of ALF (5 sampling times). Soil samples at depths of 0 and 30 cm were collected bi-monthly for moisture analysis.

Soil Analysis in Laboratory

Air-dried soils were sieved (2 mm) and analysed for: soil texture by hydrometer (Gee & Bauder, 1986), pH (1:1 soil: water) (McLean, 1982), electrical conductivity (1:1 soil: water) (Rhoades, 1982), organic matter by Walkley-Black method (Nelson & Sommers, 1982), total N by Kjeldahl (Dennis, 1982), exchangeable Ca, Mg, K by 1M ammonium acetate pH 7.0 (Thomas, 1982), available P by Bray 2 (Olsen & Sommers, 1982), available S by 0.01 M $Ca(H_2PO_4)_2$ (Tabatabai, 1982), and extractable Fe, Mn, Cu, Zn by DTPA (Baker & Amacher, 1982; Olson & Roscoe, 1982; Gambrell & William, 1982).

Plant Management in Field

The 1st and 2nd lower leaf pairs (intermediate-aged leaves) were randomly collected from 4 sides (North, South, East and West) of tree canopies (4 leaves $side^{-1}$), combined into composite samples (16 leaves $tree^{-1}$) representing each tree across 4 experimental sites. Leaf sampling occurred bi-monthly during APD from the 2nd to the 10th month of ALF (5 sampling times), excluding the 10th-12th month of ALF when leaves had completely abscised.

Plant Nutrient Analysis in Laboratory

Leaves were cleaned with deionised water, oven-dried (68-80°C, 24-48 hours), ground, and sieved (1 mm). Analyses included total N (Kjeldahl), P, S, Fe, Mn, Cu, Zn ($HNO_3/HClO_4$),

K, Ca, Mg, Na (wet digestion) and B (azomethine-H) (Kerven, 1980; Maneepong, 1994; Onthong, 2002; Oweczkin & Kerven, 1980).

Physiological Characteristics of Rubber Trees

Physiological characteristics measured during APD included trunk circumference, trunk diameter (at 1.50 m height), and canopy width.

Statistical Analysis

Analysis of variance (ANOVA) was performed to test differences in soil and plant properties. Means were separated using Duncan's Multiple Range Test (DMRT) at $P \leq 0.05$ using SPSS software.

RESULTS AND DISCUSSION

Rubber Tree Growth and Management

Throughout the APD, upland rubber trees (sites no.1 and no.2) exhibited average trunk circumferences of 54.19 and 23.73 cm, with monthly increases of 0.92 and 1.18 cm (11.04 and 14.20 cm $year^{-1}$), respectively. Average trunk diameters were 34.48 and 15.10 cm, increasing 0.59 and 0.75 cm $month^{-1}$ (7.03 and 9.03 cm $year^{-1}$), respectively. Average canopy diameters measured 8.39 and 2.69 m, respectively. Lowland rubber trees (sites no.3 and no.4) showed average trunk circumferences of 43.42 and 36.45 cm, with monthly increases of 0.49 and 0.61 cm (5.90 and 7.37 cm $year^{-1}$), respectively. Average trunk diameters were 27.63 and 23.20 cm, increasing 0.31 and 0.39 cm $month^{-1}$ (3.75 and 4.69 cm $year^{-1}$), respectively. Average canopy diameters measured 6.02 and 5.56 m, respectively.

Annual physiological assessments clearly demonstrated superior growth of upland rubber trees compared to lowland counterparts. The primary factor was prolonged flooding in lowland areas from seasonal rainfall. Despite farmers' mitigation efforts through raised planting beds and drainage channels, waterlogging remained problematic in lowland plantations while absent in upland areas.

Rubber Tree Characteristics During APD

Rubber trees enter the period of leaf shedding (falling leaves) around the beginning of February. Then the rubber leaves will gradually fall off until the old set of rubber leaves (10th month ALF) completely falls off around the end of March (takes about 2 months). At the same time, when April begins, the rubber trees will enter the leaf flushing period and then enter the stage of rubber leaf development (from the 1st, 2nd, …, 10th month ALF, respectively) until January. (The leaf development period is 10 months, April to January (next year). Then the rubber leaves will begin to shed again. Rubber trees will enter the

period of leaf shedding (falling leaves) again around the beginning of February. The rubber phenological development on the eastern side of southern Thailand (experimental sites) will be delayed by about 1 month compared to that of the western side of southern Thailand.

Soil Physical Properties of Rubber Plantation

Upland soils were dark brown to yellowish brown and gray to dark gray. Soil texture (0 - 15 cm depth) in sites no.1 and no.2 was loamy to sandy clay loam (clay: 23.03-30.21%, silt: 21.14-30.23%, sand: 45.73-48.65%). Soil texture (0-15 cm depth) in sites no.3 and no.4 was clay loam to clay texture (clay: 35.03-38.87%, silt: 36.33-56.67% and sand: 4.58-26.69%).

In upland sites (no.1 and no.2), topsoil (0 cm) moisture ranged 9.90-24.46% and 15.85-17.57%, while subsoil (30 cm) moisture ranged 8.06-20.57% and 11.96-17.01%, respectively (Figures 2A and 2B). In lowland sites (no.3 and no.4), topsoil moisture ranged 18.45-23.88% and 18.12-28.47%, while subsoil moisture ranged 19.56-23.90% and 17.83-22.43%, respectively (Figures 2C and 2D).

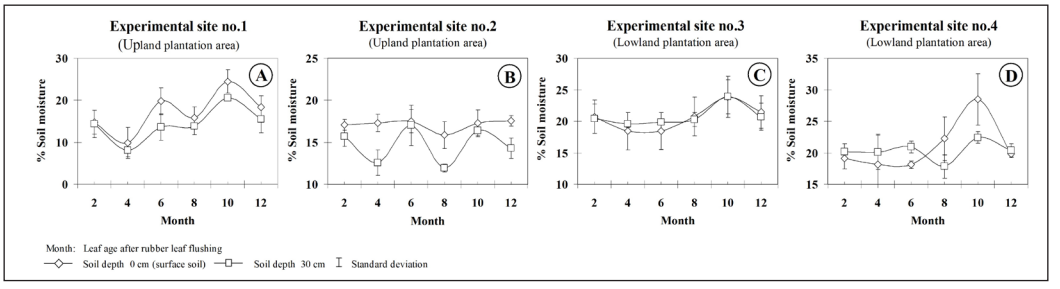

Figure 2. Soil moisture content under rubber tree shade during ADP in upland and lowland areas, (A) Experimental site no.1: Pre-tapping upland area; (B) Experimental site no.2: Pre-tapping upland area; (C) Experimental site no.3: Pre-tapping lowland area; and (D) Experimental site no.4: Pre-tapping lowland area

Lowland clay loam to clay soils with poor drainage and groundwater levels above 50 cm (Division of Soil Survey and Classification, Department of Land Development, 1987) experienced persistent waterlogging at tree bases where roots concentrate, particularly during rainy seasons and tropical storm events. Waterlogging reduced soil aeration, decreasing O_2 availability and impairing active water uptake by roots. Simultaneously, increased soil CO_2 levels reduced root permeability, consequently limiting nutrient absorption. Kungpisadan (2009) surveyed rubber plantations in Pa Bon District, Phatthalung Province, finding that upland trees (groundwater >50 cm depth) exhibited shoot dieback at 7-10 years, while lowland trees (groundwater <50 cm depth) showed dieback symptoms at 2-5 years, depending on plantation drainage conditions.

Soil Chemical Properties of Pre-Tapping Rubber Trees in the Upland Area (Site no.1)

The results of the study found that the amounts of plant nutrients in soils showed no significant difference ($p < .05$), except that avai.S was significantly different ($p < .05$), and exch. Na and ext.Cu were significantly different ($p < .01$) (Figure 3). Soil pH was 5.04-5.60 (Figure 3A). Soil EC was 0.07-0.13 mS cm^{-1} (Figure 3B) and soil OM was 14.48-20.17 g kg^{-1} (Figure 3C). During the 2nd month of ALF, the highest plant nutrients were total N = 1.15 g kg-1, ext.Cu = 3.14 mg kg-1, and ext.Zn = 2.68 mg kg-1 (Figure 3D, 3M and 3N), whereas the lowest plant nutrient was observed. During the 4th month ALF: The highest plant nutrient was exch.K = 0.25 $cmol_c kg^{-1}$ (Figure 3G), while the lowest plant nutrient was total N = 1.02 g kg^{-1} (Figure 3D). During the 6th month ALF: The highest plant nutrients were exch.Ca, Mg and Na = 5.39, 1.24 and 0.090 $cmol_c kg^{-1}$, respectively (Figure 3H, 3I and 3J), whereas the lowest plant nutrient was ext.Mn = 25.04 mg kg^{-1} (Figure 3L). During the 8th month ALF: The highest plant nutrients were avai.P = 220.31 mg kg^{-1}, ext.Mn = 48.76 mg kg^{-1} (Figure 3E and 3L) whereas the lowest plant nutrients were avai.S = 18.06 mg kg^{-1}, exch.K = 0.16 $cmol_c kg^{-1}$ and ext.Fe = 99.24 mg kg^{-1} (Figure 3F, 3G and 3K). During 10th month ALF: The highest plant nutrient was avai.S = 68.12 mg kg^{-1} (Figure 3F) while the lowest plant nutrients were avai.P = 37.69 mg kg^{-1}, Exch.Ca, Mg and Na = 0.31, 0.23 and 0.012 $cmol_c kg^{-1}$, respectively and ext.Fe, Cu and Zn = 141.28, 0.57 and 0.63 mg kg^{-1}, respectively (Figure 3E, 3H, 3I, 3J, 3K, 3M and 3N).

Soil Chemical Properties of Pre-Tapping Rubber Trees in the Upland Area (Site no.2)

The study found that the amounts of plant nutrients in soils showed no significant differences ($p<.01$), except for exchangeable Mg, which showed a significant difference ($p<.05$) (Figure 3). Soil pH was 4.47-5.73 (Figure 3A). Soil EC was 0.05-0.18 mS cm^{-1} (Figure 3B), and soil OM was 9.26-20.92 g kg^{-1} (Figure 3C). During the 2nd month ALF: The highest plant nutrients were avai.P = 128.42 mg kg^{-1}, exch.K and Mg = 0.20 and 1.21 $cmol_c kg^{-1}$, respectively and ext.Zn = 2.03 g kg^{-1} (Figure 3E, 3G, 3I and 3N). The lowest plant nutrients were total N = 0.91 g kg^{-1} and exch.Na = 0.026 $cmol_c kg^{-1}$ (Figure 3D and 3J). During the 4th month ALF: The highest plant nutrient was absent, whereas the lowest plant nutrient was exch.K = 0.13 $cmol_c$ kg^{-1} (Figure 3G). During the 6th month ALF: The highest plant nutrients were avai.S = 30.19 mg kg^{-1}, exch.Ca = 2.94 $cmol_c kg^{-1}$ and ext.Cu = 3.02 mg kg^{-1} (Figure 3F, 3H and 3M), whereas the lowest plant nutrient was ext.Mn = 23.90 mg kg^{-1} (Figure 3L). During the 8th month ALF: The highest plant nutrient was ext.Mn = 139.05 mg kg^{1} (Figure 3L), while the lowest plant nutrients were total N = 0.91 g kg^{-1}, avai.P = 90.08 mg kg^{-1} and ext.Fe and Cu = 58.41 and 1.78 mg kg^{-1}, respectively (Figure 3D, 3E, 3K and 3M). During the 10th month ALF: The highest plant nutrients were total N = 1.68 g kg^{-1}, avai.S = 30.19 mg kg^{-1}, exch.Na = 0.061 $cmol_c kg^{-1}$ and ext.Fe = 100.71 mg kg^{-1} (Figure 3D, 3F, 3J and 3K), whereas

the lowest plant nutrients were exch.Ca and Mg = 1.65 and 0.76 $cmol_c kg^{-1}$, respectively and ext.Zn = 1.39 g kg^{-1} (Figure 3H, 3I and 3N).

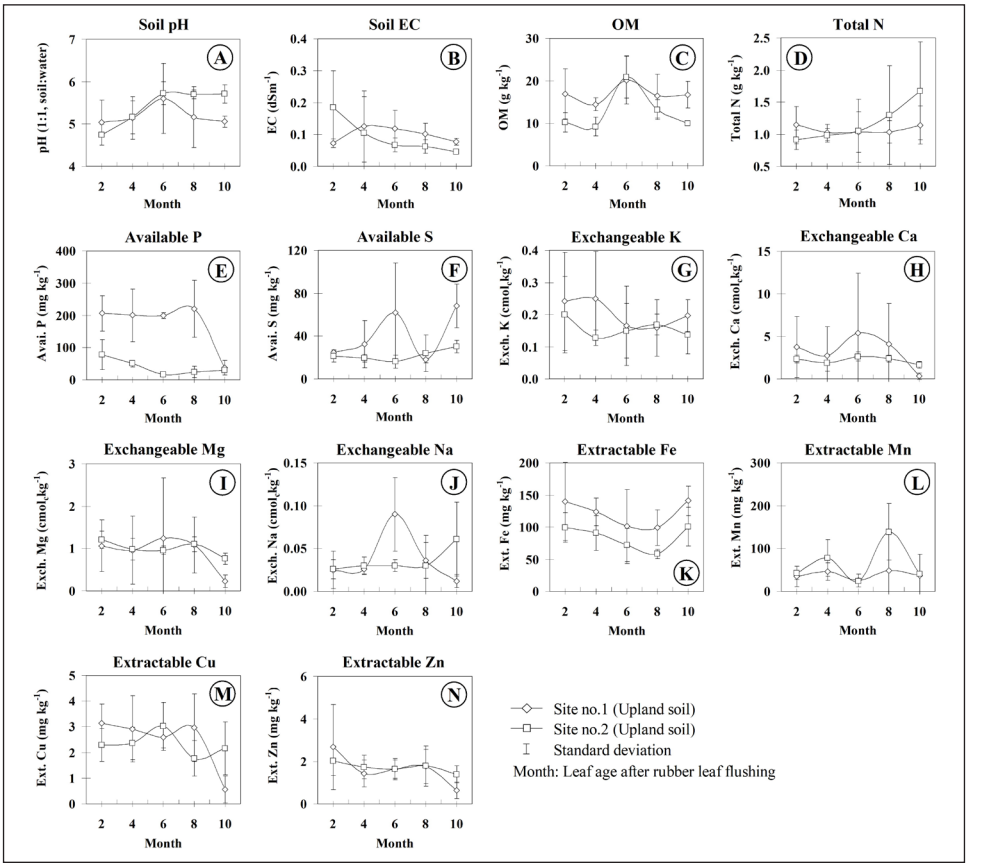

Figure 3. Some soil properties under the shade of rubber trees during APD of rubber trees grown in upland areas: (A) = Soil pH, (B) = Soil EC, (C) = Soil OM, (D) = Total N, (E) = Exchangeable Ca, (F) = Exchangeable Mg, (G) = Exchangeable K, (H) = Exchangeable Na, (I) = Available P, (J) = Available S, (K) = Extractable Fe, (L) = Extractable Mn, (M) = Extractable Cu and (N) = Extractable Zn

Soil Chemical Properties of Pre-Tapping Rubber Trees in the Lowland Area (Site no.3)

The results of the study found that the amounts of plant nutrients in soils showed no significant difference ($p < .05$), except that ext.Mn showed a significant difference ($p < .05$) and avai.P, exch.K and ext.Fe showed significant differences ($p < .01$) (Figure 4). Soil pH was 5.09-5.46 (Figure 4A). Soil EC was 0.10-0.05 mS cm^{-1} (Figure 4B) and soil OM was 20.35-15.94 g kg^{-1} (Figure 4C). (1) During the 2nd month ALF: The highest plant nutrient was ext.Cu (1.51 mg kg^{-1}) (Figure 4M), while the lowest plant nutrients were total N = 1.13 g kg^{-1}, avai.P = 3.69 mg kg^{-1} and exch.Ca = 2.17 $cmol_c kg^{-1}$ (Figure 4D, 4E and 4F). (2) During 4th month ALF: The highest plant nutrients were

avai.S = 40.25 mg kg^{-1} and exch.K and Mg = 0.18 and 1.01 $cmol_c kg^{-1}$ respectively (Figure 4F, 4G and 4I), whereas the lowest plant nutrients were ext.Fe, Cu and Zn = 64.92, 1.31 and 0.53 mg kg^{-1}, respectively (Figure 4K, 4M and 4N). (3) During 6th month ALF: The highest plant nutrient was ext.Zn = 0.72 mg kg^{-1} (Figure 4N) while the lowest plant nutrients were avai.S = 26.32 mg kg^{-1} and ext.Mn = 218.38 mg kg^{-1} (Figure 4F and 4L). (4) During the 8th month ALF: The highest plant nutrients were total N = 2.08 g kg^{-1}, avai.P = 6.45 mg kg^{-1} and exch.Ca and Mg = (3.88 and 1.01 $cmol_c kg^{-1}$, respectively and ext.Mn = 218.38 mg kg^{-1} (Figure 4D, 4E, 4H, 4I and 4L), whereas the lowest plant nutrient was exch.Na = 0.040 $cmol_c kg^{-1}$ (Figure 5J). (5) During the 10th month ALF: The highest plant nutrients were exch.Na = 0.096 $cmol_c kg^{-1}$ and ext.Fe = 115.02 mg kg^{-1} (Figure 4J and 4K), whereas the lowest plant nutrients were exch.K and Mg = 0.09 and 0.64 $cmol_c kg^{-1}$, respectively (Figure 4G and 4I).

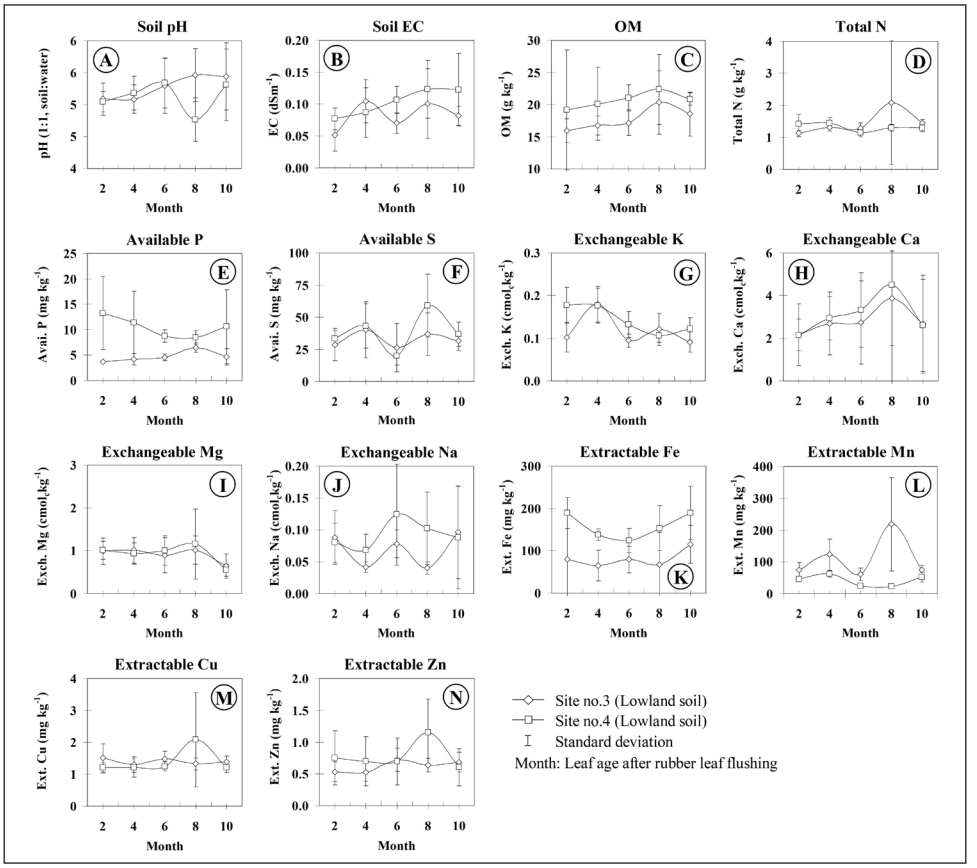

Figure 4. Some soil properties under the shade of rubber trees during APD of rubber trees grown in lowland areas: (A) = Soil pH, (B) = Soil EC, (C) = Soil OM, (D) = Total N, (E) = Exchangeable Ca, (F) = Exchangeable Mg, (G) = Exchangeable K, (H) = Exchangeable Na, (I) = Available P, (J) = Available S, (K) = Extractable Fe, (L) = Extractable Mn, (M) = Extractable Cu and (N) = Extractable Zn

Soil Chemical Properties of Pre-Tapping Rubber Trees in the Lowland Area (Site no.4)

The results of the study found that the amounts of plant nutrients in soils showed no significant difference ($p < .05$), except that avai.S, exch.K and ext.Mn showed significant differences ($p < .01$) (Figure 4). Soil pH was 5.05-5.34 (Figure 4A). Soil EC was 0.12-0.12 mS cm^{-1} (Figure 4B), and soil OM was 19.19-22.38 g kg^{-1} (Figure 4C). During the 2nd month ALF: The highest plant nutrients were avai.P = 13.25 mg kg^{-1}, exch.K = 0.18 $cmol_c kg^{-1}$, ext.Fe = 189.60 mg kg^{-1} (Figure 4E, 4G and 4K) whereas the lowest plant nutrients were exch.Ca = 2.16 $cmol_c kg^{-1}$ and ext.Cu = 1.21 mg kg^{-1} (Figure 4H and 4M). During the 4th month ALF: The highest plant nutrients were total N = 3.73 g kg^{-1}, exch.K = 0.18 $cmol_c kg^{-1}$, and ext.Mn = 62.04 mg kg^{-1} (Figure 4D, 4G and 4L), whereas the lowest plant nutrients were exch.Na = 0.068 $cmol_c kg^{-1}$ and ext.Cu = 1.21 mg kg^{-1} (Figure 4J and 4M). During the 6th month ALF: The highest plant nutrients were exch.Na = 0.124 $cmol_c kg^{-1}$ (Figure 4J, while the lowest plant nutrients were total N = 1.14 g kg^{-1}, avai.S = 19.83 mg kg^{-1}) and ext.Fe = 124.39 mg kg^{-1} (Figure 4D, 4F and 4K). During 8th month ALF: The highest plant nutrients were exch.Ca and Mg = 4.50 and 1.16 $cmol_c kg^{-1}$, respectively and ext.Cu and Zn = 2.09 and 1.16 mg kg^{-1}, respectively (Figure 4H, 4I, 4M and 4N), while the lowest plant nutrients were avai.P and S = 8.47 and 59.03 mg kg^{-1}, respectively, exch.K = 0.11 $cmol_c kg^{-1}$ and ext.Mn = 22.68 mg kg^{-1} (Figure 4E, 4F, 4G and 4L). During the 10th month ALF: There were no highest plant nutrients, whereas the lowest plant nutrients were exch.Mg = 0.55 $cmol_c kg^{-1}$ and ext.Cu and Zn = 1.21 and 0.61 mg kg^{-1} (Figure 4I, 4M and 4N).

Rubber soils in both upland and lowland areas exhibited moderate to low nutrient levels necessary for rubber growth (Table 1). High rainfall (seasonal and off-seasonal) maintained elevated soil moisture beneath tree canopies. While promoting microbial decomposition of OM, OM levels remained sufficient for rubber growth. However, OM was susceptible to leaching by rainfall (Sutthipradit, 1993), evidenced by lower OM in upland versus lowland soils (Figures 3C and 4C; Table 1). Additionally, nutrients were readily leached by rainfall, and extremely acidic conditions limited nutrient solubility for plant uptake (Department of Soil Science, 2001). Conversely, phosphorus, resistant to loss, accumulated more than other nutrients. Available P exceeding 45 mg kg^{-1} indicates excessive amounts for plant growth (Kheoruenromn, 1990; Im-Erb, 1991), particularly in upland rubber soils. Nutrient levels in experimental sites aligned with Suchartkul's (2011) findings for RRIM 600 rubber soils in southern Thailand (Chumphon, Surat Thani, Nakhon Si Thammarat): OM = 6.0-23.0 g kg^{-1}, avai.P and S = 0.3-28.0 and 17.0-38.0 mg kg^{-1}, exch.K, Ca, Mg, Na = 18.0-113.0, 18.0-576.0, 3.0-144.0, 3.9-40.0 mg kg^{-1}, ext.Fe, Mn, Cu, Zn, B = 13.5-97.5, 0.5-110.2, 0.03-1.48, 0.14-1.40, 0.14-0.61 mg kg^{-1}, respectively. Values also corresponded with mangosteen soil analyses by Nilnond et al. (1995) and Pechkeo (1999, 2007), reporting N, P, K, Ca, Mg, S, B concentrations of 0.76-1.25 g kg^{-1}, 2.45-61.69 mg kg^{-1}, 0.10-0.26, 0.09-2.43, 0.05-0.50 $cmol_c$ kg^{-1}, 1.85-15.32, 0.16-0.84 mg kg^{-1}, respectively.

Table 1
The results of soil fertility assessment for rubber growth in experimental sites (upland and lowland areas)

Soil Properties	Soil Fertility Level															
	Experimental Site No.1 (Upland Areas)				Experimental Site No.2 (Upland Areas)				Experimental Site No.3 (Lowland Areas)				Experimental Site No.4 (Lowland Areas)			
	Soil Analysis Result[1/]	Low	Medium	High	Soil Analysis Result[1/]	Low	Medium	High	Soil Analysis Result[1/]	Low	Medium	High	Soil Analysis Result[1/]	Low	Medium	High
Soil texture (0 - 15 cm)	Loam	-	-	-	Sandy clay loam	-	-	-	Clay	-	-	-	Clay loam	-	-	-
Soil pH (1:1, soil:water)	5.02 - 5.86	-	-	-	4.74 - 5.73	-	-	-	4.98 - 5.46	-	-	-	4.76 - 5.34	-	-	-
Soil EC ($mScm^{-1}$, 1:1, soil:water)	0.05 - 0.13	-	-	-	0.04 - 0.18	-	-	-	0.04 - 0.10	-	-	-	0.05 - 0.12	-	-	-
Soil OM ($g\ kg^{-1}$)	11.73 - 20.17	-	●	-	7.12 - 20.92	●	●	-	12.25 - 20.35	-	●	-	13.29 - 22.38	-	●	-
Total N ($g\ kg^{-1}$)	0.64 - 1.15	●	●	-	0.67 - 1.68	●	-	-	0.92 - 2.08	●	●	-	0.82 - 3.73	●	●	●
Available P ($mg\ kg^{-1}$)	10.29 - 220.31	●	●	●	23.86 - 128.42	-	●	●	2.78 - 6.45	●	●	-	4.24 - 13.25	●	●	-
Available S ($mg\ kg^{-1}$)	14.99 - 68.12	-	-	-	11.63 - 30.19	-	-	-	11.64 - 40.25	-	-	-	15.45 - 59.03	-	-	-
Exchangeable Ca ($cmol_C kg^{-1}$)	0.09 - 0.25	●	-	-	0.08 - 0.20	●	-	-	0.06 - 0.18	●	-	-	0.06 - 0.18	●	-	-

Table 1 (*continued*)

Soil Properties	Soil Fertility Level															
	Experimental Site No.1 (Upland Areas)				Experimental Site No.2 (Upland Areas)				Experimental Site No.3 (Lowland Areas)				Experimental Site No.4 (Lowland Areas)			
	Soil Analysis Result[1/]	Low	Medium	High	Soil Analysis Result[1/]	Low	Medium	High	Soil Analysis Result[1/]	Low	Medium	High	Soil Analysis Result[1/]	Low	Medium	High
Exchangeable Mg ($cmol_c kg^{-1}$)	0.10 - 5.39	●	●	-	1.37 - 2.64	-	●	-	1.61 - 3.88	-	●	-	1.17 - 4.50	-	●	-
Exchangeable K ($cmol_c kg^{-1}$)	0.13 - 1.24	-	●	●	0.62 - 1.21	-	-	●	0.42 - 1.01	-	-	●	0.30 - 1.16	-	-	●
Exchangeable Na ($cmol_c kg^{-1}$)	0.008 - 0.09	-	-	-	0.01 - 0.06	-	-	-	0.03 - 0.10	-	-	-	0.04 - 0.12	-	-	-
Extractable Fe (mg kg^{-1})	59.74 - 141.28	-	-	●	44.92 - 100.71	-	-	●	55.74 - 115.02	-	-	●	64.78 - 189.60	-	-	●
Extractable Mn (mg kg^{-1})	15.30 - 48.76	-	-	●	17.93 - 139.05	-	-	●	54.28 - 218.38	-	-	●	19.38 - 62.04	-	-	
Extractable Cu (mg kg^{-1})	0.34 - 3.14	●	●	●	1.11 - 3.02	-	-	●	1.02 - 1.51	-	●	●	1.00 - 2.09	-	-	●
Extractable Zn (mg kg^{-1})	0.36 - 2.68	●	●	●	0.69 - 2.03	-	-	●	0.39 - 0.72	-	●	●	0.47 - 1.16	-	●	●
Soil fertility level (overview)		●	●	-		●	●	-		●	●	-		●	●	-

Note. [1/] Average values of soil physical and chemical properties (0 - 15 cm in depth) under the rubber tree shade during the APD

Changes in Plant Nutrient Content in Soils During APD

Upland rubber plantations: N demand increased from the 2nd through the 4th-6th month ALF, then decreased during the 8th-10th month ALF. Phosphorus, K, S and Fe demand was low during the 2nd-4th month ALF, increased during the 6th-8th month ALF, then decreased at the 10th month ALF. Calcium, Mg and Zn demand was low at the 2nd month ALF, increased at the 4th month ALF, decreased during the 6th-8th month ALF, then increased at the 10th month ALF. Sodium demand was high during the 2nd-4th month ALF, decreased at the 6th month ALF, then increased during the 8th-10th month ALF. Manganese demand was high at the 2nd month ALF, decreased at the 4th month ALF, increased at the 6th month ALF, decreased at the 8th month ALF, then increased at the 10th month ALF. Copper demand remained low during the 2nd-8th months of ALF, increasing at the 10th month of ALF (Figure 3 and Table 2).

Lowland rubber plantations: N demand was low during the 2nd-4th month of ALF, increased at the 6th month of ALF, then decreased during the 8th-10th month of ALF. Phosphorus, K, Mg and Mn demand was low during the 2nd-4th month of ALF, increased during the 6th-8th month of ALF, then decreased at the 10th month of ALF. Calcium demand was high at the 2nd month of ALF, continued increasing through the 4th-8th month of ALF, then decreased at the 10th month of ALF. Sodium demand was low at the 2nd month of ALF, increased at the 4th month of ALF, decreased at the 6th month of ALF, then increased during the 8th-10th month of ALF. Sulfur demand was high at the 2nd month of ALF, decreased at the 4th month of ALF, increased at the 6th month of ALF, then decreased during the 8th-10th month of ALF. Copper and Zn demand was high during the 2nd-6th months ALF, decreased in the 8th month ALF, then increased at the 10th month ALF. Iron demand was low at the 2nd month ALF, increased during the 4th-6th month ALF, then decreased during the 8th-10th month ALF (Figure 4 and Table 2).

Acidic soil conditions (pH <5.5) in experimental sites may inhibit microbial OM decomposition while promoting dissolution of Al and Mn to potentially toxic levels (Department of Soil Science, 2001). In highly acidic conditions, Fe^{3+}, Al^{3+} and hydrous oxides of Fe, Al and Mn form insoluble compounds with soluble P, reducing P absorption and translocation (Moncharoen, 2002). Similarly, Poowarodom (2001) reported low K in durian orchards in eastern Thailand due to acidic conditions, coarse texture, and heavy rainfall causing K leaching, applicable to other nutrients. This explains reduced nutrient accumulation in rubber leaves, particularly in upland plantations. Adjusting soil pH to ≥5.5 with lime or dolomite enhances nutrient solubility and availability (Department of Soil Science, 2001) and promotes microbial decomposition of OM, thereby increasing soil nutrient content for rubber cultivation.

Table 2
The overview of plant nutrient requirements from soils and leaves for rubber growth during ADP

Time[1/]	Plant Nutrient Requirement from Soils[2/]		Plant Nutrient Requirement from Leaves[2/]		Plant Nutrient Requirement from Soils and Leaves[2/]	
Month	**Upland Areas**	**Lowland Areas**	**Upland Areas**	**Lowland Areas**	**Upland Areas**	**Lowland Areas**
2	N Na	Ca N P Cu Zn	Ca Na B S Mn	Ca Na B S Mn	Na	Ca
4	N K	Cu Na Fe Zn	P S Fe	P S Fe	K	Fe
6	Mn N K S	K S Mn N Fe	N Cu Fe Zn	N Cu Fe Zn	N S	N Fe
8	Fe N K S P Cu	Na P K Mn Cu	P K Cu Zn	P K Cu Zn	K Cu	P K Cu
10	Ca Mg Zn P K Na Cu	Mg K Cu Zn	Mg K P Mn	Mg K P Mn	P K Mg Cu Zn	K Mg

Note. When the amount of plant nutrients in the soil is lowest, rubber trees require more plant nutrients from the soil for growth than at other times
[1/] = Age of rubber leaves ALF (months)
[2/] = Overview of nutrient requirements in both experimental sites

Seasonal flooding in lowland rubber plantations creates physiological constraints that severely limit nutrient uptake despite adequate or elevated soil nutrient levels. Brief periods of waterlogging (2-5 days) induce root hypoxia, shifting metabolism to anaerobic respiration, which produces toxic metabolites and impairs energy-dependent cation transport (Ezin et al., 2010; Pezeshki, 2001). Recovery requires 7-14 days, but recurring flooding every 2-3 weeks creates continuous stress. Root architecture differs fundamentally between locations: upland trees develop deep tap roots (>150 cm) while lowland trees face subsurface compaction from former paddy plow pans at 20-35 cm depth, restricting roots to shallow zones and reducing biomass by 30-40% (Division of Soil Survey and Classification, 1987; Carr, 2012). Nutrient deficiencies were evident-Ca (<10 g kg^{-1}), Mg (<2.5 g kg^{-1}), and P fixation by Fe/Al oxides at pH 4.5-5.5. Elevated Fe (37-82 mg kg^{-1}) and Mn (465-1,091 mg kg^{-1}) remained within sufficiency ranges, indicating physiological requirement rather than toxicity (Foy, 1984; Sahrawat, 2005). However, high Mn:Fe ratios (6.8:1) suggest subclinical metabolic inefficiencies and the induction of Zn/Cu deficiencies. Temporal patterns reveal critical Ca/Mg deficiency windows during early-season flooding when trees require these nutrients for cell wall synthesis, necessitating synchronised fertilisation strategies.

Plant Nutrients in Leaves of Pre-Tapping Rubber Trees in the Upland Area (Site no.1)

The study found that the amounts of plant nutrients in rubber leaves differed significantly ($p < .01$), except for B and Fe, which showed no significant difference ($p < .05$) (Figure 5). During the 2nd month ALF: The highest plant nutrients were total K, Na and Zn = 26.43, 0.0833 and 0.0556 g kg^{-1}, respectively) (Figure 5C, 5F and 5L) whereas the lowest plant nutrients were total Ca and S = 10.09 and 3.30 g kg^{-1}, respectively) Figure 5D and 5G). During the 4th month ALF, the highest plant nutrient was absent, whereas the lowest plant nutrient was total B (32.06 mg kg^{-1}) (Figure 5H). During the 6th month of ALF. The highest plant nutrient was total Mn = 0.0718 g kg^{-1} (Figure 5J), while the lowest plant nutrients were total N and Fe = 2.51 and 0.0653 g kg^{-1}, respectively (Figure 5A and 5I). During 8th month ALF: The highest plant nutrients were total N, P, Ca, Mg, S and Fe = 37.41, 3.67, 18.15, 4.04, 5.03, 67.51 and 0.0841 g kg^{-1}, respectively and total B = 67.51 mg kg^{-1} (Figure 5A, 5B, 5D, 5E, 5G, 5H and 5I) whereas the lowest plant nutrient was total Cu = 0.0072 g kg^{-1} (Figure 5K). During 10th month ALF: The highest plant nutrient was total Cu = 0.0109 g kg^{-1} (Figure 5K) while the lowest plant nutrients were total P, K, Mg, Na, Mn and Zn = 2.51, 0.39, 1.36, 0.0195, 0.2366 and 0.0240 g kg^{-1}, respectively (Figure 5B, 5C, 5E, 5F, 5J and 5L).

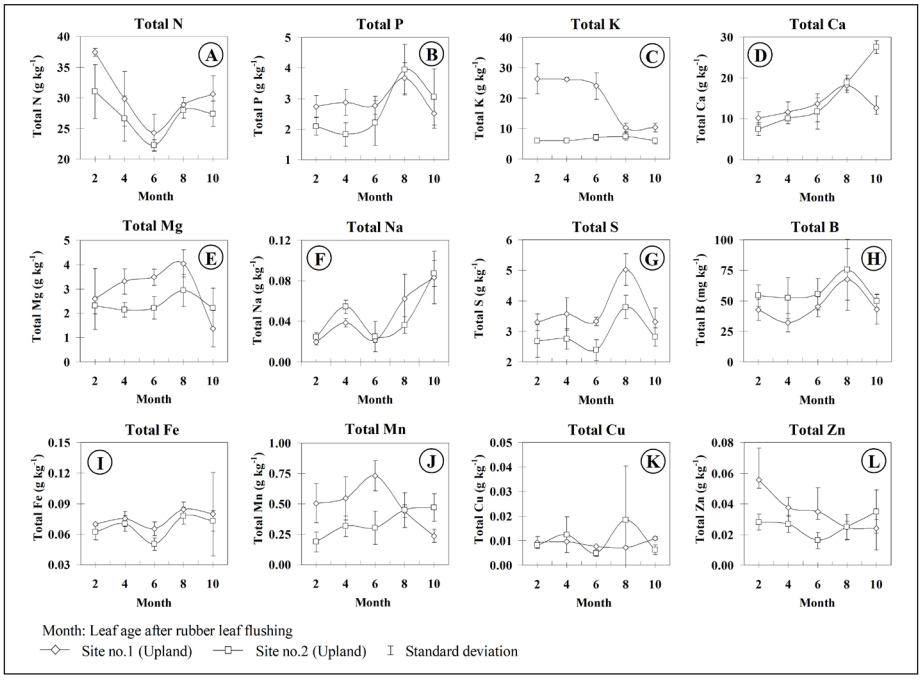

Figure 5. Plant nutrients accumulated in rubber leaves during APD in upland areas: (A) = Total N, (B) = Total P, (C) = Total K, (D) = Total Ca, (E) = Total Mg, (F) = Total Na, (G) = Total S, (H) = Total B, (I) = Total Fe, (J) = Total Mn, (K) = Total Cu and (L) = Total Zn

Plant Nutrients in Leaves of Pre-Tapping Rubber Trees in the Upland Area (Site no.2)

The results of the study found that the amounts of plant nutrients in rubber leaves showed significant differences ($p<.01$), except for total K, Mg, B and Cu, which showed no significant difference ($p<.05$), and total Zn showed no significant difference ($p<.05$) (Figure 5). During the 2nd month of ALF, the highest plant nutrient was total N = 31.04 g kg^{-1} (Figure 5A), whereas the lowest plant nutrients were total Ca, Na and Mn = 7.46, 0.0245 and 0.1880 g kg^{-1}, respectively) (Figure 5D, 5F and 5J). During the 4th month ALF: No plant nutrient was the highest, whereas the lowest plant nutrient was total P = 1.83 g kg^{-1} (Figure 5B). During the 6th month ALF: The highest plant nutrient was absent, while the lowest plant nutrients were total N, S, Fe, Cu and Zn = 22.27, 2.39, 0.0502, 0.0049, and 0.0611 g kg^{-1}, respectively (Figure 5A, 5G, 5I, 5K and 5L). During the 8th month ALF: The highest plant nutrients were total P, K, S, Fe and Cu = 3.94, 7.50, 3.80, 0.0781 and 0.0183 g kg^{-1} and total B = 75.38 mg kg^{-1} (Figure 5B, 5C, 5G, 5H, 5I and 5K), while the lowest plant nutrient was absent. During the 10th month ALF: The highest plant nutrients were total Ca, Na, Mn and Zn = 27.52, 0.0872, 0.4472 and 0.0349 g kg^{-1}, respectively (Figure 5D, 5F, 5J and 5L), whereas the lowest plant nutrients were total K = 5.99 g kg^{-1} and total B = 49.99 mg kg^{-1} (Figure 5C and 5H).

Plant Nutrients in Leaves of Pre-Tapping Rubber Trees in the Lowland Area (Site no.3)

The results of the study found that the amounts of plant nutrients in rubber leaves showed significant differences ($p<.01$ and $p<.05$), except for total N, Mg, B, Fe and Mn, which showed no significant differences ($p<.05$) (Figure 6). During the 2nd month ALF: The highest plant nutrient was total Fe = 0.0823 g kg^{-1} (Figure 6I), while the lowest plant nutrients were total Ca, Na and S = 8.76, 0.0245 and 3.32 g $kg^{-1,}$ respectively, with total B = 27.50 g kg^{-1} (Figure 6D, 6F, 6G and 6H). During the 4th month ALF: The highest plant nutrients were total P, K and Cu = 2.29, 25.83 and 0.0250 g kg^{-1}, respectively (Figure 6B, 6C and 6K). The lowest plant nutrient was total Fe = 0.0660 g kg^{-1} (Figure 6I). During the 6th month ALF: The highest plant nutrients were total B = 54.53 mg kg^{-1}, total Mn and Zn = 0.8067 and 0.0461 g kg^{-1}, respectively (Figure 6H, 6J and 6L). The lowest plant nutrients were total N and Cu (22.31 and 0.0080 g kg^{-1}, respectively) (Figure 6A and 6K). During the 8th month of ALF, the highest plant nutrients were total N, Mg and S = 27.17, 3.12 and 4.31 g kg^{-1}, respectively (Figure 6A, 6E, and 6G), whereas the lowest plant nutrients were total K and Zn = 7.89 and 0.0461 g kg^{-1}, respectively) (Figure 6C and 6L). During the 10th month ALF: The highest plant nutrients were total Ca and Na = 20.85 and 0.1833 g kg^{-1}, respectively) (Figure 6D and 6F) while the lowest plant nutrients were total P, Mg and Mn = 1.86, 2.30 and 0.4928 g kg^{-1}, respectively) (Figure 6B, 6E and 6J).

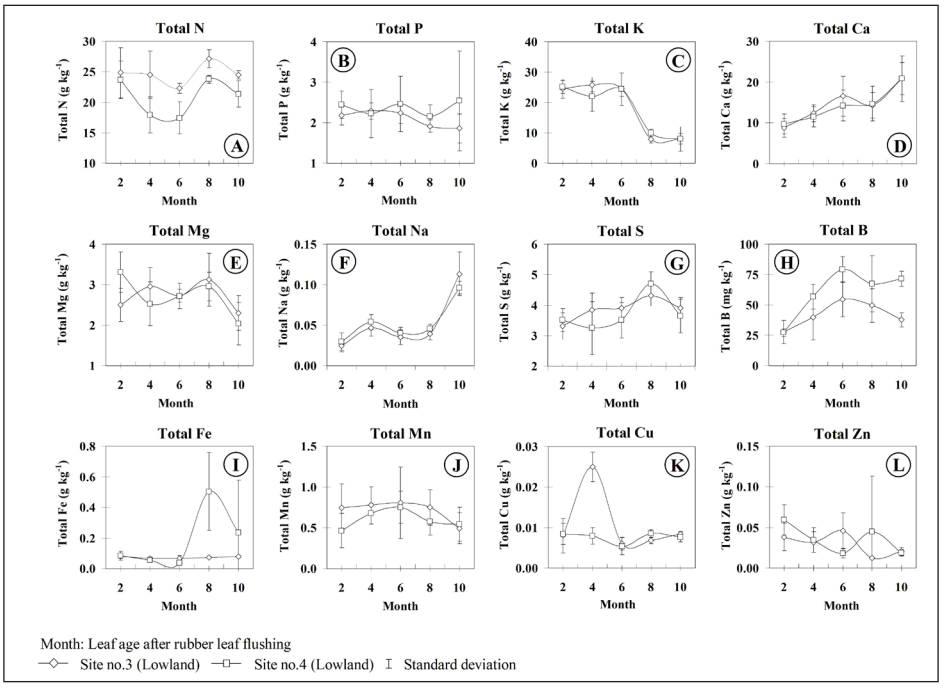

Figure 6. Plant nutrients accumulated in rubber leaves during APD in lowland areas: (A) = Total N, (B) = Total P, (C) = Total K, (D) = Total Ca, (E) = Total Mg, (F) = Total Na, (G) = Total S, (H) = Total B, (I) = Total Fe, (J) = Total Mn, (K) = Total Cu and (L) = Total Zn

Plant Nutrients in Leaves of Pre-Tapping Rubber Trees in the Lowland Area (Site no.4)

The results of the study found that the amounts of plant nutrients in rubber leaves showed significant differences ($p<.01$), except for total P, Mn, Cu and Zn, which showed no significant differences ($p<.05$) (Figure 6). During the 2nd month ALF: The highest plant nutrients were total K, Mg and Zn = 25.18, 3.31 and 0.0595 g kg^{-1}, respectively (Figure 6C, 6E and 6L) whereas the lowest plant nutrients were total Ca, Na and Mn = 4.74, 0.0290 and 0.4645 g kg^{-1}, respectively and total B = 27.17 mg kg^{-1} (Figure 6D, 6F, 6H and 6J). During the 4th month of ALF, no highest plant nutrient was observed, while the lowest plant nutrient was total S = 3.25 g kg^{-1} (Figure 6G). During the 6th month ALF: The highest plant nutrients were total B = 79.26 mg kg^{-1}, total Mn = 0.7495 g kg^{-1} (Figure 6H and 6J) while the lowest plant nutrients were total N, Fe, Cu, and Zn = 17.41, 0.0374, 0.0054 and 0.0183 g kg^{-1}, respectively (Figure 6A, 6I, 6K and 6L). During the 8th month ALF: The highest plant nutrients were total N, S, Fe and Cu = 23.79, 4.70, 0.5030, and 0.0085 g kg^{-1}, respectively (Figure 6A, 6G, 6I and 6K), whereas the lowest plant nutrient was total P = 2.16 g kg^{-1} (Figure 6B). During the 10th month ALF: The highest plant nutrients were total P, Ca and Na = 2.54, 20.84 and 0.0962 g kg^{-1}, respectively (Figure 6B, 6D and 6F) while the lowest plant nutrients were total K and Mg = 8.11 and 2.03 g kg^{-1}, respectively (Figure 6C and 6E).

The Status of Plant Nutrients in Rubber Leaves Affecting Rubber Tree Growth

Plant nutrients accumulated in rubber leaves from both upland and lowland areas were classified as medium to low (Table 3). Nutrient concentrations aligned with Suchartkul's (2011) findings for RRIM 600 rubber in southern Thailand (Chumphon, Surat Thani, Nakhon Si Thammarat): N, P, K, Ca, Mg, S = 22.00-35.10, 1.60-2.90, 7.20-14.60, 5.60-19.40, 1.80-4.00, 1.10-3.70 g kg^{-1}; Fe, Mn, Cu, Zn, B = 64.00-151.00, 142.00-574.00, 8.00-14.00, 19.00-61.00, 11.00-85.00 mg kg^{-1}, respectively. Values also corresponded with Yingjajaval and Bangjan's (2006) analysis of 4-month-old RRIM 600 leaves: N, P, K, Ca, Mg = 28.69, 1.91, 8.47, 8.81, 3.70 g kg^{-1}, respectively.

Changes in Plant Nutrient Content in Leaves During APD

Upland rubber plantations: Nitrogen and Zn demand were low during the 2nd-4th month ALF, increased at the 6th month ALF, then decreased during the 8th-10th months ALF. Phosphorus, Ca and Mg demand were high at the 2nd month ALF, decreased during the 4th-6th month ALF, then increased during the 8th-10th month ALF. Potassium demand was low during the 2nd-6th month ALF, then increased during the 8th-10th month ALF. Sodium demand was high at the 2nd month ALF, decreased at the 4th month ALF, increased at the 6th month ALF, then decreased during the 8th-10th month ALF. Sulfur, Fe and Cu demand

was high at the 2nd month ALF, decreased at the 4th month ALF, increased at the 6th month ALF, decreased at the 8th month ALF, then increased at the 10th month ALF. Boron demand was low at the 2nd month ALF, increased at the 4th month ALF, decreased during the 6th-8th month ALF, then increased at the 10th month ALF. Manganese demand was high at the 2nd month ALF, decreased during the 4th-6th month ALF, then increased during the 8th-10th month ALF (Figure 5 and Table 2).

Lowland rubber plantations: Nitrogen, P, K, Mg and Zn demand was low during the 2nd-4th month ALF, increased at the 6th month ALF, decreased at the 8th month ALF, then increased at the 10th month ALF. Calcium demand was high at the 2nd month ALF, decreased during the 4th-6th month ALF, increased at the 8th month ALF, then decreased at the 10th month ALF. Sulfur demand was high during the 2nd-4th month ALF, decreased during the 6th-8th month ALF, then increased at the 10th month ALF. Boron and Mn demand was high at the 2nd month ALF, decreased during the 4th-6th month ALF, then increased during the 8th-10th month ALF. Iron demand was high during the 2nd-6th month ALF, decreased at the 8th month ALF, then increased at the 10th month ALF. Sodium and Cu demand were high at the 2nd month ALF, decreased at the 4th month ALF, increased at the 6th month ALF, then decreased during the 8th-10th month ALF (Figure 6 and Table 2).

Relationship between Plant Nutrients in the Soil and Leaf During APD

Upland areas: Rubber trees demonstrated high Na demand from soil and leaves at the 2nd month ALF; K at the 4th month ALF; N and S at the 6th month ALF; K and Cu at the 8th month ALF; P, K, Mg, Cu and Zn at the 10th month ALF (Figure 3, 4, 5 and 6 and Table 2). Lowland areas: High Ca demand occurred at the 2nd month ALF; Fe at the 4th month ALF; N and Fe at the 6th month ALF; P, K and Cu at the 8th month ALF; K and Mg at the 10th month ALF (Figures 3, 4, 5 and 6 and Table 2).

Nutrient demand patterns differed fundamentally between locations due to distinct soil-plant-environment interactions. Upland sites showed high K demand during the 4th, 8th, and 10th months of ALF, coinciding with rapid canopy expansion, which requires K for stomatal regulation, enzyme activation, and osmotic adjustment (Marschner, 2012; Priyadarshan, 2017). Conversely, lowland sites exhibited sustained Ca demand from the 2nd-8th month ALF, reflecting dual roles in cell wall synthesis and root membrane stability under periodic anaerobic stress. Low exch.Ca (2.16-4.50 $cmol_c kg^{-1}$) created supply-demand imbalances, maintaining deficient leaf concentrations (4.74-20.85 g kg^{-1}) throughout the season. Acidic conditions (pH = 4.47-5.86) influenced nutrient availability location-specifically: uplands maintained active microbial cycling, while lowlands experienced oscillating redox conditions that alternately mobilised Fe^{2+}/Mn^{2+} during waterlogging and precipitated oxides upon reoxidation, creating temporal fluctuations in availability.

Table 3
Shows the results of evaluating the status of plant nutrients accumulated in rubber leaves that are appropriate for the growth of rubber trees

Plant Nutrients	Plant Nutrient Levels in Leaves															
	Experimental Site No.1 (Upland Areas)				Experimental Site No.2 (Upland Areas)				Experimental Site No.3 (Lowland Areas)				Experimental Site No.4 (Lowland Areas)			
	Leaves Analysis Result[1/]	Low	Medium	High	Leaves analysis result[1/]	Low	Medium	High	Leaves analysis result[1/]	Low	Medium	High	Leaves analysis result[1/]	Low	Medium	High
Total N (g kg^{-1})	25.25 - 35.67	●	●	-	23.04 - 32.65	●	●	-	19.47 - 29.17	●	-	-	14.67 - 21.38	●	-	-
Total P (g kg^{-1})	2.47 - 3.55	-	●	●	1.48 - 2.46	●	●	-	2.05 - 2.55	-	●	●	1.63 - 3.05	●	●	●
Total K (g kg^{-1})	25.77 - 26.75	-	-	●	5.95 - 6.54	●	-	-	22.37 - 28.35	-	-	●	14.87 - 26.85	-	●	●
Total Ca (g kg^{-1})	9.24 - 15.45	-	-	●	8.34 - 11.17		-	●	10.67 - 15.67	-	-		9.23 - 15.33	-	-	●
Total Mg (g kg^{-1})	2.47 - 3.85	-	●	●	1.75 - 2.27	●	●	-	2.16 - 3.43	-	●	●	1.57 - 2.86	●	●	●
Total Na (g kg^{-1})	0.0327 - 0.0427	-	-	-	0.0455 - 0.0604	-	-	-	0.0375 - 0.0577	-	-	-	0.0428 - 0.0677	-	-	-
Total S (g kg^{-1})	3.08 - 4.32	-	-	●	2.54 - 3.25	-	-	●	3.27 - 4.65	-	-	●	2.06 - 4.73	-	●	●
Total B (mg kg^{-1})	24.86 - 39.72	-	-	●	38.15 - 70.79	-	-	●	26.47 - 60.79	-	-		47.70 - 67.89	-	-	●
Total Fe (g kg^{-1})	0.0655 - 0.0863	-	●	●	0.0598 - 0.0798	-	●	-	0.0525 - 0.0713	●	●	-	0.0444 - 0.0743	●	●	-

Table 3 (*continued*)

Plant Nutrients	Plant Nutrient Levels in Leaves															
	Experimental Site No.1 (Upland Areas)				Experimental Site No.2 (Upland Areas)				Experimental Site No.3 (Lowland Areas)				Experimental Site No.4 (Lowland Areas)			
	Leaves Analysis Result[1/]	Low	Medium	High	Leaves analysis result[1/]	Low	Medium	High	Leaves analysis result[1/]	Low	Medium	High	Leaves analysis result[1/]	Low	Medium	High
Total Mn (g kg^{-1})	0.3636 - 0.7718	-	-	●	0.2285 - 0.4406	-	-	●	0.4783 - 1.0913	-	-		0.5226 - 0.8176	-	-	●
Total Cu (g kg^{-1})	0.0091 - 0.0100	●	●	-	0.0084 - 0.0255	●	●	●	0.0215 - 0.0300	-	-	●	0.0053 - 0.0103	●	●	-
Total Zn (g kg^{-1})	0.0283 - 0.0444	-	-	●	0.0198 - 0.0347	-	●	●	0.0155 - 0.0512	●	●	●	0.0233 - 0.0612	-	-	●
Plant nutrient status in leaves (overview)		-	●	●		●	●	-		-	-	●		-	-	●

Note. [1/] Range of average plant nutrient levels in rubber leaves aged 4 months, ALF, which was an appropriate time for collecting rubber leaf samples to analyse general plant nutrient content

Guidelines for Increasing Plant Nutrient Content for Rubber Trees

Results (Table 2) establish nutrient management guidelines throughout APD: (1) Upland plantations: Increase Na at 2nd month ALF; K at 4th month ALF; N and S at 6th month ALF; K and Cu during 8th-10th month ALF; P, Mg and Zn at 10th month ALF. (2) Lowland plantations: Increase Ca at 2nd month ALF; Fe during 4th-6th month ALF; N at 6th month ALF; P and Cu at 8th month ALF; K during 8th-10th month ALF; Mg at 10th month ALF.

Site-specific fertilisation must address physiological constraints beyond soil test values. Upland plantations require elevated K applications (118 g K_2O tree^{-1}) split across growth flushes and supplemental S (20 g tree^{-1}) for weathered Ultisols (Havlin et al., 2014). Lowland strategies necessitate pre-season liming (500-1,000 g $CaMg(CO_3)_2$ tree^{-1}) to raise pH ≥5.5, improving Ca/Mg availability (Brady & Weil, 2016), with early $Ca(NO_3)_2$ (300 g tree^{-1}) addressing hypoxia-induced deficiency and chelated Fe (20 g tree^{-1}) overcoming oxide fixation (Marschner, 2012). Elevated K rates (130 g K_2O tree^{-1}, 30% above upland) compensate for leaching losses under saturated conditions (Dobermann & Fairhurst, 2000).

CONCLUSION

Pre-tapping upland rubber plantations require higher Na from soil and leaves at 2nd month ALF; K at 4th month ALF; N and S at 6th month ALF; K and Cu at 8th month ALF; P, K, Mg, Cu and Zn at 10th month ALF compared to other periods. Pre-tapping lowland plantations require higher Ca at the 2nd month ALF; Fe at the 4th month ALF; N and Fe at the 6th month ALF; P, K and Cu at the 8th month ALF; K and Mg at the 10th month ALF compared to other periods. Characterising nutrient accumulation and relationships in soil and leaves throughout APD provides fundamental information for determining appropriate nutrient management strategies. This enables rubber trees to receive sufficient nutrients, in both type and quantity, for optimal growth and production.

ACKNOWLEDGEMENT

The authors wish to acknowledge the financial support provided by Prince of Songkla University, Research Project No. AGR540591S.

REFERENCES

Agricultural Extension and Development Region 5. (2004). *Report on rice growing areas in the southern region for the crop years 1999–2004*. Department of Agricultural Extension, Ministry of Agriculture and Cooperatives. http://sdoae.doae.go.th/work.php

Baker, D. E., & Amacher, M. C. (1982). Nickel, copper, zinc, and cadmium. In A. L. Page (Ed.), *Methods of soil analysis: Part 2. Chemical and microbiological properties* (2nd ed., pp. 323–336). American Society of Agronomy; Soil Science Society of America.

Brady, N. C., & Weil, R. R. (2016). *The nature and properties of soils* (15th ed.). Pearson.

Bureau of Agricultural Economic Research. (2023). *Situation of important agricultural products and trends in 2023*. Office of Agricultural Economics, Ministry of Agriculture and Cooperatives.

Carr, M. K. V. (2012). The water relations of rubber (*Hevea brasiliensis*): A review. *Experimental Agriculture, 48*(2), 176–193. https://doi.org/10.1017/S0014479711000901

Department of Soil Science. (2001). *Principles of soil science* (9th ed.). Kasetsart University.

Division of Soil Survey and Classification, Department of Land Development. (1987). *Soil survey report of Phatthalung province* (Issue 436). Soil Survey Region 12, Department of Land Development, Ministry of Agriculture and Cooperatives.

Dobermann, A., & Fairhurst, T. (2000). *Rice: Nutrient disorders and nutrient management*. International Rice Research Institute.

Ezin, V., De La Peña, R., & Ahanchede, A. (2010). Flooding tolerance of tomato genotypes during vegetative and reproductive stages. *Brazilian Journal of Plant Physiology, 22*(2), 131–142. https://doi.org/10.1590/S1677-04202010000200006

Foy, C. D. (1984). Physiological effects of hydrogen, aluminum, and manganese toxicities in acid soil. In F. Adams (Ed.), *Soil acidity and liming* (2nd ed., pp. 57–97). American Society of Agronomy. https://doi.org/10.2134/agronmonogr12.2ed.c2

Gambrell, R. P., & Patrick, W. H., Jr. (1982). Manganese. In A. L. Page (Ed.), *Methods of soil analysis: Part 2. Chemical and microbiological properties* (2nd ed., pp. 313–322). American Society of Agronomy; Soil Science Society of America.

Gee, G. W., & Bauder, J. W. (1986). Particle-size analysis. In A. Klute (Ed.), *Methods of soil analysis: Part 1. Physical and mineralogical methods* (2nd ed., pp. 383–412). American Society of Agronomy; Soil Science Society of America. https://doi.org/10.2136/sssabookser5.1.2ed.c15

Havlin, J. L., Tisdale, S. L., Nelson, W. L., & Beaton, J. D. (2014). *Soil fertility and fertilizers: An introduction to nutrient management* (8th ed.). Pearson.

Im-Erb, A. (1991). Soil test. *Journal of Soil and Water Conservation, 7*(4), 5–27.

Keeney, D. R. (1982). Nitrogen-availability indices. In A. L. Page (Ed.), *Methods of soil analysis: Part 2. Chemical and microbiological properties* (2nd ed., pp. 711–733). American Society of Agronomy; Soil Science Society of America. https://doi.org/10.2134/agronmonogr9.2.2ed.c35

Kerven, G. (1980). *Applications of atomic absorption spectroscopy to the analysis of biological materials*. Department of Agriculture, University of Queensland.

Kheoruenromn, I. (1990). *Soil of Thailand*. Department of Soil Science, Kasetsart University.

Kungpisadan, N. (2009). *Sustainable rubber management: Soil, water and plant nutrient*. Rubber Research Institute, Department of Agriculture.

Kunjet, S., Thaler, P., Gay, F., Thevathasan, N. V., Gordon, A., Dufour, L., Jirawat, A., Sdoodee, S., & Chantuma, P. (2013). Consequences of drought on rubber tree (*Hevea brasiliensis*) growth and latex yield. *Rubber Science, 26*(1), 73–82.

Maneepong, S. (1994). *Soil and plant analysis*. Department of Earth Science, Faculty of Natural Resources, Prince of Songkla University.

Marschner, P. (Ed.). (2012). *Marschner's mineral nutrition of higher plants* (3rd ed.). Academic Press.

McLean, E. O. (1982). Soil pH and lime requirement. In A. L. Page (Ed.), *Methods of soil analysis: Part 2. Chemical and microbiological properties* (2nd ed., pp. 199–224). American Society of Agronomy; Soil Science Society of America. https://doi.org/10.2134/agronmonogr9.2.2ed.c12

Meteorological Department of Thailand. (2023). *Climate change patterns in Southern Thailand*. Ministry of Digital Economy and Society.

Moncharoen, P. (2002). *Soil analysis interpretation for soil improvement and fertilizer recommendation*. Department of Land Development, Ministry of Agriculture and Cooperatives.

Nelson, D. W., & Sommers, L. E. (1982). Total carbon, organic carbon and organic matter. In A. L. Page (Ed.), *Methods of soil analysis: Part 2. Chemical and microbiological properties* (2nd ed., pp. 539–579). American Society of Agronomy; Soil Science Society of America. https://doi.org/10.2134/agronmonogr9.2.2ed.c29

Nilnond, C., Jatupote, W., Leowarin, W., & Yong, S. (1995). Chemical fertility status of some growing mangosteen soils in southern Thailand. *Songklanakarin Journal of Science and Technology, 17*(4), 381–393.

Office of Agricultural Economics. (2023a). *Agricultural economic information: Landuse*. Ministry of Agriculture and Cooperatives. https://www.oae.go.th/view/1/Landuse/TH-TH

Office of Agricultural Economics. (2023b). *Agricultural economic information: Para rubber*. Ministry of Agriculture and Cooperatives. https://www.oae.go.th/view/1/Pararubber/TH-TH

Olsen, S. R., & Sommers, L. E. (1982). Phosphorus. In A. L. Page, R. H. Miller, & D. R. Keeney (Eds.), *Methods of soil analysis: Part 2. Chemical and microbiological properties* (2nd ed., pp. 403–430). American Society of Agronomy; Soil Science Society of America. https://doi.org/10.2134/agronmonogr9.2.2ed.c17

Olson, R. V., & Ellis, R., Jr. (1982). Iron. In A. L. Page (Ed.), *Methods of soil analysis: Part 2. Chemical and microbiological properties* (2nd ed., pp. 301–312). American Society of Agronomy; Soil Science Society of America. https://doi.org/10.2134/agronmonogr9.2.2ed.c17

Onthong, J. (2002). *Soil and plant analysis*. Faculty of Natural Resources, Prince of Songkla University.

Oweczkin, J., & Kerven, G. (1980). *Methods of analysis for nitrogen, phosphorus, sulphur and potassium in plant tissue*. Department of Agriculture, University of Queensland.

Pechkeo, S. (1999). *Research report: Land potential for mangosteen cultivation in southern Thailand; Some soil properties of mangosteen soil in southern Thailand; Some soil properties of mangosteen soil in Namom District, Songkhla Province*. Department of Earth Science, Faculty of Natural Resources, Prince of Songkla University.

Pechkeo, S. (2007). *Changes of plant nutrients concentration in mangosteen (Garcinia mangostana L.) during phenological development and effects of calcium on the incidence of translucent flesh disorder and gamboge of mangosteen fruits* [Doctoral dissertation, Prince of Songkla University].

Pezeshki, S. R. (2001). Wetland plant responses to soil flooding. *Environmental and Experimental Botany, 46*(3), 299–312. https://doi.org/10.1016/S0098-8472(01)00107-1

Poowarodom, S. (2001). Nutrient management for durian. In *Training documents on the seminar on plant nutrient management strategies for sustainable income* (pp. 43–49). Kasetsart University.

Priyadarshan, P. M. (2017). *Biology of Hevea rubber*. Springer International Publishing. https://doi.org/10.1007/978-3-319-54506-6

Rhoades, J. D. (1982). Soluble salts. In A. L. Page (Ed.), *Methods of soil analysis: Part 2. Chemical and microbiological properties* (2nd ed., pp. 167–179). American Society of Agronomy; Soil Science Society of America. https://doi.org/10.2134/agronmonogr9.2.2ed.c10

Sahrawat, K. L. (2005). Iron toxicity in wetland rice and the role of other nutrients. *Journal of Plant Nutrition, 27*(8), 1471–1504. https://doi.org/10.1081/PLN-200025869

Suchartkul, S. (2011). *Establishment of standard values for nutritional diagnosis in soil and leaves of immature rubber tree* [Master's thesis, Walailak University].

Sutthipradit, S. (1993). *Soil fertility*. Department of Earth Science, Faculty of Natural Resources, Prince of Songkla University.

Tabatabai, M. A. (1982). Sulfur. In A. L. Page, R. H. Miller, & D. R. Keeney (Eds.), *Methods of soil analysis: Part 2. Chemical and microbiological properties* (2nd ed., pp. 501–538). American Society of Agronomy; Soil Science Society of America.

Thomas, G. W. (1982). Exchangeable cations. In A. L. (Ed.), *Methods of soil analysis: Part 2. Chemical and microbiological properties* (2nd ed., pp. 159–165). American Society of Agronomy; Soil Science Society of America. https://doi.org/10.2134/agronmonogr9.2.2ed.c9

Yingjajaval, S., & Bangjan, J. (2006). Major plant nutrient contents in para rubber (RRIM 600). *Agricultural Science Journal, 37*(4), 353–364.

Pertanika J. Trop. Agric. Sci. 49 (5): 2387 - 2412 (2026)

PERTANIKA JOURNALS

TROPICAL AGRICULTURAL SCIENCE

Journal homepage: http://www.pertanika.upm.edu.my/

Integrated Effects of DAP Fertiliser, Soil Amendments, and Nano-Biostimulant Foliar Application on Growth and Yield of Wheat

Maher Adhafa Drai'am Al-Aboudi, Hayyawi W. A. Al-Juthery*, and Luma Abdalalah Sagban Alabadi

Department of Soil Sciences and Water Resources, College of Agriculture, University of Al-Qadisiyah, 58002 Al Diwaniyah, Iraq

ABSTRACT

This study evaluated the effects of DAP fertiliser rates, soil amendments, and foliar applications of biostimulants and chelated micronutrient nano-fertiliser on the growth and yield of wheat. A field trial was conducted over a single growing season in a randomised complete block design with a split-split plot arrangement and three replications. Treatments comprised three DAP rates (0, 150, and 300 kg ha^{-1}), three soil amendment levels (none, agricultural gypsum at 800 kg ha^{-1}, and EM Bokashi bio-organic fertiliser at 5 t ha^{-1}), and four foliar treatments (water, EM liquid biofertiliser, the biostimulant Fertigrain, and chelated nano-fertiliser). DAP at 300 kg ha^{-1} increased biological yield (BIY) by 24.8% (from 16.347 to 20.403 Mg ha^{-1}) and grain yield (GRY) by 17.1% (from 4.857 to 5.690 Mg ha^{-1}) compared with the control. Bokashi had a greater effect, increasing GRY by 26.6% and BIY by 30.2%, whereas chelated nano-fertiliser increased GRY by 17.0% compared with water spray. Two- and three-way combinations were clearly superior: 300 kg ha^{-1} DAP + Bokashi + nano-fertiliser produced the highest GRY (7.287 Mg ha^{-1}; 72.7% above the control, 4.220 Mg ha^{-1}) and BIY (26.260 Mg ha^{-1}; 94.9% increase). The harvest index was highest without DAP (29.73%) and declined to 27.94% at 300 kg ha^{-1}. Post-harvest soil properties were not assessed, which is the main limitation of this study. Combining mineral, organic, and nano-based inputs is a practical strategy for improving wheat productivity on nutrient-poor, salt-affected soils in dryland and semi-arid regions.

Keywords: Bokashi, DAP Fertiliser, Fertigrain, grain yield, nano-fertiliser

ARTICLE INFO

Article history:
Received: 04 July 2026
Accepted: 23 September 2026
Published: 30 October 2026

DOI: https://doi.org/10.47836/pjtas.49.5.14

E-mail addresses:
agr23.ph04@qu.edu.iq (Maher Adhafa Drai'am Al-Aboudi)
hayyawi.aljutheri@qu.edu.iq (Hayyawi W. A. Al-Juthery)
luma.al-abadi@qu.edu.iq (Luma Abdalalah Sagban Alabadi)
* Corresponding author

INTRODUCTION

Wheat can be said to be the most consumed cereal crop in the world based on its

© Universiti Putra Malaysia Press

nutritional value, its usage in bread, and its products. Wheat and barley are the oldest domesticated cereal crops by humans. The domestication of wheat is said to have begun more than ten thousand years ago. The earliest domesticated wheat species was Emmer. Emmer crops originated in the Fertile Crescent in the Middle East, comprising countries such as Iraq, Syria, Jordan, Palestine, and Turkey (Erenstein et al., 2022; Gąsiorowski, 2004). Wheat is important for food security; thus, grain production and quality depend on the physical characteristics of the soils in which wheat is grown. The nutrient content in soils favours the development of plants and grains, whereas the presence of heavy metals such as Cd and Pb reduces the accumulation of metals in grains (Rizwan et al., 2016; Shahad et al., 2026). The accumulation negatively impacts grain quality and poses health hazards for humans and animals. Therefore, there is a need to enhance soil quality and use the best fertilisers, including bio-fertilisers and nano-fertilisers, to promote sustainable production and safe grain for human consumption (Al-Juthery et al., 2025; Bhardwaj et al., 2014).

Genaidy (2011), Qadir et al. (2014), and Zoca and Penn (2017) indicated that agricultural gypsum, $CaSO_4 \cdot H_2O$, is one of the most important reclamation materials for saline and alkaline soils. It improves the soil's physical, chemical, and biological properties. It also helps reduce the harmful accumulation of sodium in the soil. It improves soil permeability and helps leach salts. It also improves the availability of essential nutrients in the soil, which are important for wheat growth, thereby increasing its productivity. Apart from gypsum applications, the use of nano-fertilisers is beneficial for efficiently increasing nutrient uptake by the plant. This is due to the small size of the particles, which enables efficient nutrient absorption by minimising nutrient loss and increasing the reactive sites of the roots. Moreover, it is advantageous for reducing heavy metal levels in grains, improving crop quality, and protecting the environment by reducing chemical residues in water and soil (Al-Juthery et al., 2026; Parra-Torrejón et al., 2023; Zulfiqar et al., 2019). The application of nano-fertilisers is also beneficial in increasing plant nutrient uptake due to their small particle size, which enables the plant to absorb nutrients more efficiently by increasing the number of reaction sites in the roots and reducing nutrient loss (Alzreejawi & Al-Juthery, 2020). Furthermore, nano-fertilisers help reduce heavy metals in grains and improve crop quality and the environment by reducing chemical residues in water and soil (Al-Juthery et al., 2018; Dimkpa & Bindraban, 2018; Parra-Torrejón et al., 2023).

In addition to the above factors that play a vital role in increasing soil fertility and promoting plant growth, the use of biofertiliser s such as EM (Effective Microorganisms) provides specific nutrients, including nitrogen, phosphorus, potassium, and micronutrients. The microorganisms also increase plants' resistance to environmental stresses such as drought and heavy-metal contamination in soil, as well as improve crop quality (Adesemoye & Kloepper, 2009; Al-Silmawy et al., 2025; Bhardwaj et al., 2014; Itelima et al., 2018). Liquid biofertiliser also plays an important role in reducing cultivation costs, as it does not require processing or sterilisation, which are often required for other products.

Liquid biofertiliser s also requires less labour, materials, and storage space, unlike other biofertilisers that use a carrier medium to maintain bacteria (Velineni & Brahmaprakash, 2011). Based on the above, this research aims to investigate the effect of various rates of DAP Fertiliser, soil conditioners such as gypsum and organic biofertiliser Bokashi, foliar spray of chelated nano-fertilisers such as Zn, Cu, Fe, and Mn, liquid biofertiliser AM, and biostimulant Fertigrain on some of the key growth and yield-contributing characters of wheat. While the individual effects of mineral fertilisers, organic amendments, and nano-based biostimulants on wheat have each been documented separately, few field studies have evaluated their combined, three-way interaction within a single factorial trial. Salinity and nutrient-poor soils constrain wheat productivity across many dryland and semi-arid regions worldwide, not only in Mesopotamia, so evidence on integrated mineral-organic-nano fertilisation strategies of this kind is relevant to wheat production systems facing similar constraints internationally.

MATERIALS AND METHODS

Experiment Site

The field experiment was conducted in District 7, Umm Al-Hatr area, Al-Nasr District, Dhi Qar Governorate, Nasiriyah City, Iraq, at the geographical coordinates of latitude (31°55′28.7″ N) and longitude (46°12′57.4″ E). The experimental field at establishment and at the flowering stage is shown in Figure 1 and Figure 2, respectively.

Experiment Design

The experiment was conducted according to a factorial arrangement within a Randomised Complete Block Design (RCBD) with three replications using a split-split plot system.



Figure 1. Field experiment layout at establishment, showing randomised treatment plots marked with numbered flags



Figure 2. Wheat plots at the flowering stage, showing the same treatment plot layout under crop cover

The main plots consisted of three levels of DAP Fertiliser application (0, 150, and 300 kg ha^{-1}). The sub-plots included soil amendments represented by agricultural gypsum (800 kg ha^{-1}) and EM Bokashi bio-organic Fertiliser (5 t ha^{-1}). Sodicity indicators for the experimental soil were measured and are reported in Table 1: SAR = 6.35, exchangeable Na^+ = 2.00 cmolc kg^{-1}, and ESP = 7.38%, which is below the classic sodic-soil threshold (ESP > 15%; Richards, 1954). The 800 kg ha^{-1} gypsum rate was therefore not calculated from a sodicity-reclamation equation, since the soil was not classified as sodic; rather, it was selected as a moderate, practical rate intended primarily to supply soluble Ca^{2+} and improve the soil's chemical and physical conditions, while avoiding an excessive addition that could unnecessarily raise the soluble salt concentration of the soil. This rate is consistent with its use as a general conditioning amendment in previous studies conducted under similar agricultural conditions in Iraq. The sub-sub plots involved foliar applications, including water spray (control), liquid biofertiliser EM at 5 ml L^{-1}, Fertigrain biostimulant at 2.5 ml L^{-1}, and nano-chelated fertiliser at 2.5 g L^{-1}. All foliar treatments were applied sequentially in three sprays during the growing season.

Preparation of the Experimental Field

The field was ploughed twice crosswise, then leveled and smoothed to ensure uniform soil conditions. Soil samples were randomly collected from representative locations at a depth of 0-30 cm before planting for physical and chemical analyses as presented in Table 1. The total experimental area was 450 m^2 and was divided into three replications, each containing 36 experimental units. The area of each experimental unit was 3 m^2 (1.5 m × 2 m). Irrigation channels were established between the experimental units to facilitate irrigation.

Fertilisation

After ploughing, levelling, and dividing the experimental field, the experimental units were fertilised according to the treatments: DAP Fertiliser (Nippon Jordan Fertiliser Company, NJFC, Jordan) at three levels (0, 150, and 300 kg ha^{-1}), agricultural gypsum (Advanced Village Co., Iraq) at a level of (800 kg ha^{-1}), and the organic biofertiliser EM Bokashi (EM Research Organisation, EMRO, Japan) (5 tons ha^{-1}) mixed with the soil. Foliar spray treatments included a chelated nano-Fertiliser compound of micronutrients (Zn, Cu, Fe, and Mn) (Nano Chelated Complete Micro Fertiliser; Khazra Nanochelating Technology, Sodour Ahrar Shargh Co., Tehran, Iran) at a concentration of (2.5 g L^{-1}), liquid biofertiliser EM (EMRO / EM-1 system, Japan) at a concentration of (5 ml L^{-1}), and the biostimulant Fertigrain (Fertigrain Foliar; AgriTecno Fertilizantes, S.L., Valencia, Spain) at a concentration of (2.5 ml L^{-1}), as per Table 2. Three sprays were applied at the branching, budding, and 50% flowering stages, starting on February 17, 2025.

Table 1
Physical and chemical properties of the field soil before planting

Property		Value	Unit
Soil reaction (pH)		7.6	---
Electrical conductivity (EC)		3.0	dS m^{-1}
Cation exchange capacity (CEC)		27.1	cmolc kg^{-1} soil
Soil organic matter		1.4	%
Carbonate minerals		219	g kg^{-1} soil
Bulk density		1.3	Mg m^{-3}
Available nitrogen		21.1	mg N kg^{-1} soil
Available phosphorus		11.3	mg P kg^{-1} soil
Available potassium		260.2	mg K kg^{-1} soil
Available sulfur		20.4	mg S kg^{-1} soil
Soluble calcium (Ca^{2+})		10.2	mmolc L^{-1}
Soluble magnesium (Mg^{2+})		6.8	mmolc L^{-1}
Soluble sodium (Na^{+})		18.5	mmolc L^{-1}
Sodium adsorption ratio (SAR)		6.4	(mmolc L^{-1})½
Exchangeable sodium (Na^{+} exch)		2.0	cmolc kg^{-1} soil
Exchangeable sodium percentage (ESP)		7.4	%
Soil separates	Sand	132	132 g kg^{-1} soil
	Silt	560	560 g kg^{-1} soil
	Clay	308	308 g kg^{-1} soil
Soil texture		Silty clay loam	

Note. Sodicity indicators were calculated as: $SAR = Na^{+} / \sqrt{[(Ca^{2+} + Mg^{2+}) / 2]}$, using soluble cation concentrations (mmolc L^{-1}) in the saturation extract; and ESP (%) = (exchangeable Na / CEC) × 100, using exchangeable sodium and CEC (cmolc kg^{-1} soil) (Richards, 1954)

Plantation and Crop Management

The Wafiya wheat variety, of Italian origin and approved by the Iraqi Ministry of Agriculture, was used. The seeds were planted on November 18, 2024, at a rate of 90 kg ha-1 using a tractor-mounted seeder.

Harvest

The wheat crop was harvested on May 9, 2025, when all treated plants were fully mature. Each experimental unit was packed in a plastic bag and transported to its designated location for laboratory analysis.

Table 2
Fertilisers used in the experiment and their components

Fertiliser Name	Fertiliser Type	Components
DAP	Granular	Nitrogen (N) 18-21%, Phosphorus (P_2O_5) 46-48%
Agricultural gypsum	Granular	Calcium (Ca) 23-24%, Sulfur (S) 18-19%
EM.Bokashi	Bio-organic Fertiliser	Nocardia [45.45%], Streptomyces [36.36%], Terrabacter [9.1%], Micromonospora [4.54%], Mycobacterium [4.54%], Lactobacillus spp. [30-50%], Aspergillus spp., Dactylium spp., Rhizopus spp.; $CaCO_3$ [2-3%], $Ca_3(PO_4)_2$ [1-2%], (Mn, Fe, Zn) [0.5-1%], OM [82.5%], pH [4.9], NaCl [0.25%], Na [0.10%], EC [7.30 mhos/cm], Moisture [7.74%], CFU [1.45×10^6]
Nano-chelated micronutrient Fertiliser	Granular nanomaterial	Fe 8%, Mg 2%, Zn 1.5%, Cu 0.5%, Mn 1.5%, B 0.5%, Mo 0.5%
Fertigrain (biostimulant)	Liquid Fertiliser	Plant-derived organic matter 40%, Free amino acids 10%, Total N 5.50% + Zn 0.75% + Mn 0.50% + B 0.10% + Fe 0.10% + Cu 0.10% + Mo 0.02% + Co 0.01%
Liquid biofertiliser EM	Liquid biofertiliser	Photosynthetic bacteria (Rhodospirillum, Rhodopseudomonas palustris, Rhodobacter sphaeroides), lactic acid bacteria (Lactobacillus casei, Lactobacillus delbrueckii, Lactobacillus fermentum), actinomycetes (Streptococcus spp.), yeasts (Saccharomyces cerevisiae), phosphate-solubilizers (Aerobacter, Candida, Penicillium, Xanthomonas), N-fixing bacteria (Azotobacter, Azospirillum, Pseudomonas), fungi (Aspergillus, Penicillium)

Studied Indicators before Harvest

Chlorophyll Index (SPAD)

The chlorophyll index in leaves was measured at 50% flowering using a portable SPAD-502 device. Readings were taken randomly from ten plants in each experimental unit, and the average was calculated by dividing the sum of the readings by the number of leaves (Markwell et al., 1995)

Plant Height

When plants reached full maturity (100%), plant height was measured from the soil surface to the top of the plant using a measuring tape. Ten plants were randomly selected from each experimental unit, and the average height was calculated by dividing the sum of the measurements by the number of plants (Singh & Stoskopf, 1971)

Post-Harvest Indices

Biological Yield

The total dry weight of aboveground plant material per square meter of the experimental unit was calculated after 10 days of air drying and then converted to (Mg ha^{-1}) (Sharma & Smith, 1986).

Grain Yield

The grain yield for each experimental unit was determined after drying the plants. The grains were separated from the biomass and weighed in kilograms per square meter, then converted to Mg ha-1 after confirming that the moisture content was approximately 14% using a moisture meter (Sharma & Smith, 1986).

Harvest Index

The harvest index for wheat was calculated using Equation 1 (Sharma & Smith, 1986).

$$Harvest\ Index = \frac{Grain\ yield\ Mg\ ha^{-1}}{Biological\ yield\ Mg\ ha^{-1}} \times 100 \text{ for each treatment} \quad [1]$$

Thousand Grain Weight

The weight of 1,000 grains was estimated. 1,000 grains were counted per treatment with a grain counter, then weighed on a sensitive electronic scale (Dhi Qar Agriculture Directorate Research Station).

Percentage Yield Increase over Control (PYI) for Production

Percentage Yield Increase over Control (PYI) for production was calculated as: Grain yield in the fertilised treatment (Mg ha-1) - Grain yield in the control treatment (Mg ha-1) / Grain yield in the control treatment (Mg ha-1) × 100 (Fixen et al., 2014). This index expresses the relative yield gain over the control and is therefore distinct from conventional fertiliser-use efficiency metrics, which normalise the yield gain by the quantity of nutrient applied (e.g., agronomic efficiency, kg yield per kg nutrient)

Statistical Analysis

The data obtained were statistically analysed using GenStat software according to the Randomised Complete Block Design (RCBD) with a split-split-plot arrangement. Analysis of variance (ANOVA) was performed to evaluate the effects of the experimental treatments on the studied traits. Mean comparisons were conducted using the Least Significant

Difference (LSD) test at the 0.05 probability level to determine significant differences among treatment means.

RESULTS

Plant Height (PLH): The results in Table 3 indicated that the average height of wheat plants with no application of DAP Fertiliser was 68.065 cm, which increased to 69.778 cm at 150 kg ha^{-1} of DAP Fertiliser, and then reached the highest average of 72.833 cm at 300 kg ha^{-1}.It also showed that the application of soil amendments significantly affected PLH. The highest average PLH of 72.306 cm was recorded when Bokashi Fertiliser was applied, followed by agricultural gypsum with an average PLH of 69.833 cm, and the lowest average PLH of 68.528 cm when no amendment was applied. As shown in Table 3, spraying with

Table 3
Effect of DAP fertiliser levels, soil amendments, foliar applications of biostimulants and chelated nano-fertiliser, and their interactions on wheat height (cm)

DAP Level	Soil Amendment	Spraying Transactions				DAP Levels × Amendments
		Water	Fertigrain	Nano-Fertiliser	Biofertiliser	
No addition	No treatment	65.333	66.333	67.667	67.000	66.583
	gypsum	67.667	68.333	68.667	68.667	68.334
	Bokashi	68.000	69.000	70.333	69.667	69.250
150 kg ha^{-1}	No treatment	68.333	68.667	69.333	69.000	68.833
	gypsum	69.000	69.333	70.333	69.333	69.500
	Bokashi	69.000	70.667	73.000	71.333	71.000
300 kg ha^{-1}	No treatment	67.333	70.667	71.667	71.000	70.167
	gypsum	71.000	71.333	72.333	72.000	71.667
	Bokashi	72.667	74.667	83.333	76.000	76.667
LSD 0.05			1.348			0.775
Effect of DAP Levels						
DAP Fertiliser × Spraying	No addition	67.000	67.889	68.889	68.445	68.065
	150 kg ha^{-1}	68.778	69.556	70.889	69.889	69.778
	300 kg ha^{-1}	70.333	72.222	75.778	73.000	72.833
LSD 0.05			0.844			0.678
Effect of Enhancers						
Enhancers × sprays	No treatment	67.000	68.556	69.556	69.000	68.528
	gypsum	69.222	69.666	70.444	70.000	69.833
	Bokashi	69.889	71.445	75.555	72.333	72.306
LSD (0.05)			0.756			0.404
Effect of spraying		68.704	69.889	71.852	70.444	
LSD (0.05)				0.441		

water alone resulted in the lowest average height of 68.704 cm, which increased to 69.889 cm with the biostimulant Fertigrain and to 70.444 cm with the liquid biofertiliser EM. The chelated nano-Fertiliser for micronutrients achieved the highest average height of 71.852 cm. The interaction effect of DAP Fertiliser and soil amendments was significant, with wheat PLH increasing as DAP Fertiliser increased. The highest PLH of 76.667 cm was recorded with 300 kg ha^{-1} of DAP Fertiliser and Bokashi Fertiliser, compared with the lowest PLH of 66.583 cm recorded without DAP Fertiliser and amendments. Similarly, the interaction between DAP Fertiliser and foliar treatments indicated a progressive response. The average height increased from 67.000 cm without DAP and water spray only to 75.778 cm with 300 kg/ha DAP and chelated nano-Fertiliser.

The interaction of soil amendments and foliar treatments showed the lowest average height of 67.000 cm with no amendment and water spray, and the highest value of 75.555 cm was obtained with Bokashi Fertiliser combined with nano-fertiliser spray. Finally, the three-way interaction between DAP levels, soil amendments, and foliar treatments produced the highest response. PLH ranged from 65.333 cm without any treatments applied to a maximum of 83.333 cm when 300 kg ha^{-1} DAP was applied in combination with Bokashi Fertiliser and chelated nano-Fertiliser spray for micronutrient supply.

Chlorophyll Index (SPAD)

The results in Table 4 indicate that the SPAD increased with increasing rates of DAP Fertiliser. On average, it rose from 47.353 SPAD in the no-fertiliser treatment to 49.764 SPAD in the 150 kg ha^{-1} treatment, and it reached its peak in the 300 kg ha^{-1} treatment, which recorded 50.097 SPAD. In terms of soil amendment, Bokashi Fertiliser had the highest SPAD among the treatments. Its average was 52.803 SPAD, compared to 48.336 SPAD in the gypsum treatment and 46.075 SPAD in the control.

Foliar treatments also resulted in a significant increase in SPAD compared with the control (water spray). The average SPAD for nano-chelate Fertiliser spraying was 51.711 SPAD units, whereas for water spray, it was only 46.955 SPAD units. The SPAD for all foliar treatments increased gradually with increasing DAP concentration, and the highest SPAD of 52.389 units was recorded for the 300 kg ha^{-1} DAP and nano-chelate Fertiliser spray. Moreover, the interaction between DAP levels and soil amendments contributed to bokashi, with 55.109 SPAD units at all DAP levels. Furthermore, the interaction between soil amendments and foliar application showed that bokashi with nano-chelated Fertiliser spray had the highest SPAD value of 58.145. The triple interaction effect of DAP levels, soil amendment, and foliar spray was significant for SPAD, with the highest value of 62.867 SPAD recorded at 150 kg ha^{-1} DAP with bokashi + nano-chelated fertiliser spray, whereas the lowest value was 46.004 SPAD in the control treatment.

Table 4
Effect of DAP fertiliser levels, soil amendments, and foliar applications of bio-stimulants, chelated nano-fertilisers, and their interactions on chlorophyll index SPAD

DAP Level	Soil Amendment	Spraying Transactions				DAP Levels × Amendments
		Water	Fertigrain	Nano-Fertiliser	Biofertiliser	
No addition	No treatment	41.600	45.033	46.267	45.267	44.542
	Gypsum	46.400	47.467	47.733	47.700	47.325
	Bokashi	47.733	48.467	54.667	49.900	50.192
150 kg ha^{-1}	No treatment	43.133	46.633	48.000	47.000	46.192
	Gypsum	47.100	47.467	48.700	48.700	47.992
	Bokashi	51.533	51.867	62.867	54.167	55.109
300 kg ha^{-1}	No treatment	46.000	46.767	48.933	48.267	47.492
	Gypsum	49.067	49.167	51.333	49.200	49.692
	Bokashi	50.033	51.333	56.900	54.167	53.108
LSD 0.05		0.945				0.661
Effect of DAP Levels						
DAP Fertiliser × spraying	No addition	45.244	46.989	49.556	47.622	47.353
	150 kg ha^{-1}	47.255	48.656	53.189	49.956	49.764
	300 kg ha^{-1}	48.367	49.089	52.389	50.545	50.097
LSD (0.05)		0.450				0.248
Effect of Enhancers						
Enhancers × sprays	No treatment	43.578	46.144	47.733	46.845	46.075
	Gypsum	47.522	48.034	49.255	48.533	48.336
	Bokashi	49.766	50.556	58.145	52.745	52.803
LSD 0.05		0.756				0.404
Effect of Spraying		46.955	48.245	51.711	49.374	
LSD 0.05		0.275				

Biological Yield (BIY)

From the results presented in Table 5, it is clear that as DAP Fertiliser levels increased, BIY increased significantly. The average yield was 16.347 Mg ha^{-1} without Fertiliser application, increasing to 18.360 Mg ha^{-1} at 150 kg ha^{-1} and then to 20.403 Mg ha^{-1} at 300 kg ha^{-1}. However, it is observed that as levels increased from 150 kg ha^{-1} to 300 kg ha^{-1}, the increase in BIY is not as significant as that from 0 to 150 kg ha^{-1}. This is due to the fact that the plant had almost reached sufficiency. Regarding the effect of the soil amendments on BIY, Bokashi Fertiliser recorded the highest mean value of 20.988 Mg ha^{-1}, whereas agricultural gypsum recorded the second-highest value of 18.000 Mg ha^{-1}. The lowest value of 16.122 Mg ha^{-1} was recorded without the application of any amendment. It is noticed that chelated nano-Fertiliser ranked first in foliar treatments with the highest mean of BIY (19.394 Mg ha^{-1}), followed by liquid biofertiliser EM and biostimulant Fertigrain, while water spray only ranked last with the lowest mean (17.360 Mg ha^{-1}). The two-way

interaction between DAP Fertiliser and soil amendments revealed that the interaction of 300 kg ha^{-1} of DAP Fertiliser with Bokashi Fertiliser produced the highest BIY of 24.043 Mg ha^{-1}, compared to 14.875 Mg ha^{-1} when both factors were absent.

In addition, the interaction of 300 kg ha^{-1} DAP with chelated nano-Fertiliser recorded the highest BIY of 21.409 Mg ha^{-1}, while Bokashi with nano-Fertiliser spray recorded a high BIY of 22.911 Mg ha^{-1}. The highest value of BIY (26.260 Mg ha^{-1}) was recorded when 300 kg ha^{-1} of DAP, Bokashi Fertiliser, and chelated nano-Fertiliser spray were used, while the lowest value (13.477 Mg ha^{-1}) was recorded when all factors were absent.

Table 5
Effect of DAP fertiliser levels, soil amendments, foliar applications of biostimulants, chelated nano-fertiliser, and their interactions on biological yield (Mg ha^{-1})

DAP Level	Soil Amendment	Spraying Transactions				DAP Levels × Amendments
		Water	Fertigrain	Nano-Fertiliser	Biofertiliser	
No addition	No treatment	13.477	14.057	16.033	15.933	14.875
	Gypsum	16.050	16.117	16.147	16.310	16.156
	Bokashi	16.590	16.607	20.907	17.933	18.009
150 kg ha^{-1}	No treatment	14.697	16.227	16.873	16.253	16.013
	Gypsum	16.883	18.253	18.797	18.693	18.157
	Bokashi	20.123	20.770	21.567	21.180	20.910
300 kg ha^{-1}	No treatment	17.120	17.183	17.933	17.673	17.477
	Gypsum	19.053	19.820	20.033	19.847	19.688
	Bokashi	22.243	22.507	26.260	25.163	24.043
LSD 0.05			0.953			0.486
Effect of DAP Levels						
DAP Fertiliser × Spraying	No addition	15.372	15.594	17.696	16.725	16.347
	150 kg ha^{-1}	17.234	18.417	19.079	18.709	18.360
	300 kg ha^{-1}	19.472	19.837	21.409	20.894	20.403
LSD 0.05			0.550			0.340
Effect of Enhancers						
Enhancers × sprays	No treatment	15.098	15.822	16.946	16.620	16.122
	Gypsum	17.329	18.063	18.326	18.283	18.000
	Bokashi	19.652	19.961	22.911	21.425	20.988
LSD 0.05			0.550			0.281
Effect of Spraying		17.360	17.949	19.394	18.776	
LSD 0.05			0.318			

Grain Yield (GRY)

The results in Table 6 show that the average GRY improved from 4.857 Mg ha^{-1} without Fertiliser application to 5.410 Mg ha^{-1} when DAP Fertiliser level was 150 kg ha^{-1}, and

Table 6
Effect of DAP fertiliser levels, soil amendments, foliar applications of biostimulants, chelated nano-fertiliser, and their interactions on grain yield (Mg ha⁻¹)

DAP Level	Soil Amendment	Spraying Transactions				DAP Levels × Amendments
		Water	Fertigrain	Nano-Fertiliser	Biofertiliser	
No addition	No treatment	4.220	4.387	4.670	4.357	4.409
	Gypsum	4.473	4.903	5.033	4.930	4.835
	Bokashi	4.457	5.263	5.933	5.660	5.328
150 kg ha⁻¹	No treatment	4.423	4.943	4.977	4.830	4.793
	Gypsum	4.943	5.577	5.627	5.237	5.346
	Bokashi	5.713	6.317	6.460	5.867	6.089
300 kg ha⁻¹	No treatment	4.457	4.930	5.340	5.137	4.966
	Gypsum	5.273	5.523	5.963	5.597	5.589
	Bokashi	5.867	6.460	7.287	6.450	6.516
LSD (0.05)		0.227				0.244
Effect of DAP Levels						
DAP Fertiliser × Spraying	No addition	4.383	4.851	5.212	4.982	4.857
	150 kg ha⁻¹	5.026	5.612	5.688	5.311	5.410
	300 kg ha⁻¹	5.199	5.638	6.197	5.728	5.690
LSD (0.05)		0.131				0.119
Effect of Enhancers						
Enhancers × sprays	No treatment	4.367	4.753	4.996	4.775	4.723
	Gypsum	4.896	5.334	5.541	5.255	5.257
	Bokashi	5.346	6.013	6.560	5.992	5.978
LSD 0.05		0.131				0.141
Effect of Spraying		4.870	5.367	5.699	5.341	
LSD 0.05		0.076				

finally to 5.690 Mg ha⁻¹ when DAP Fertiliser level was 300 kg ha⁻¹. Bokashi Fertiliser produced the highest average GRY (5.978 Mg ha⁻¹), while agricultural gypsum produced the second highest average GRY (5.257 Mg ha⁻¹), and the lowest average GRY (4.723 Mg ha⁻¹) was recorded without applying any Fertiliser to the soil. Among the foliar treatments, chelated nano-Fertiliser for micronutrients was found to be superior, with a value of 5.699 Mg ha⁻¹ compared to other treatments, while water spraying alone gave the lowest value. The two-way interaction of DAP Fertiliser and soil amendments showed that the highest GRY was obtained by using 300 kg ha⁻¹ of DAP Fertiliser with Bokashi Fertiliser, giving 6.516 Mg ha⁻¹, compared to the lowest value of 4.409 Mg ha⁻¹ when both factors were absent. Among the interactions of DAP Fertiliser and foliar application, the highest mean value was recorded from the combination of 300 kg ha⁻¹ DAP and nano-Fertiliser spray, i.e., 6.197 Mg ha⁻¹, and the lowest value, i.e., 4.383 Mg ha⁻¹, was recorded from no DAP

and water spray only. Likewise, the blend of Bokashi Fertiliser with nano-fertiliser spray produced the highest GRY of 6.560 Mg ha^{-1}, whereas the control treatment, which received no amendment and used water spray, produced only 4.367 Mg ha^{-1}. Finally, the three-way interaction revealed that the highest GRY of 7.287 Mg ha^{-1} was obtained by using 300 kg ha^{-1} of DAP Fertiliser in combination with Bokashi Fertiliser and chelated nano-Fertiliser, whereas the lowest GRY of 4.220 Mg ha^{-1} was obtained in the absence of all three factors.

Harvest Index (HI)

The results in Table 7 indicated that the average HI was highest without DAP Fertiliser application (29.73%), decreased slightly to 29.47% at 150 kg ha^{-1}, and declined further to 27.94% at 300 kg ha^{-1}. The decrease in the HI was around 6%. The results also indicated that

Table 7
Effect of DAP fertiliser levels, soil amendments, foliar applications of biostimulants, chelated nano-fertiliser, and their interactions on HI (%)

DAP Level	Soil Amendment	Spraying Transactions				DAP Levels × Amendments
		Water	Fertigrain	Nano-Fertiliser	Biofertiliser	
No addition	No treatment	31.260	31.161	29.089	27.306	29.704
	Gypsum	27.831	30.384	31.134	30.191	29.885
	Bokashi	26.829	31.657	28.356	31.533	29.594
150 kg ha^{-1}	No treatment	30.050	30.425	29.463	29.681	29.905
	Gypsum	29.244	30.525	29.908	27.988	29.416
	Bokashi	28.366	30.392	29.933	27.679	29.092
300 kg ha^{-1}	No treatment	25.999	28.658	29.747	29.036	28.360
	Gypsum	27.648	27.841	29.742	28.176	28.352
	Bokashi	26.356	28.683	27.735	25.617	27.098
LSD 0.05		0.466				0.446
Effect of DAP Levels						
DAP Fertiliser × Spraying	No addition	28.640	31.067	29.526	29.677	29.728
	150 kg ha^{-1}	29.220	30.447	29.768	28.449	29.471
	300 kg ha^{-1}	26.668	28.394	29.075	27.609	27.936
LSD (0.05)		0.388				0.396
Effect of Enhancers						
Enhancers × Sprays	No treatment	29.103	30.081	29.433	28.674	29.323
	Gypsum	28.241	29.583	30.261	28.785	29.218
	Bokashi	27.184	30.244	28.674	28.276	28.595
LSD 0.05		0.241				0.228
Effect of Spraying		28.176	29.970	29.456	28.578	
LSD 0.05		0.060				

the soil amendments affected the HI. The average HI was around 29.218% for agricultural gypsum and 28.595% for Bokashi Fertiliser, whereas it was around 29.323% without any amendment. Foliar applications of biostimulants and nano-fertilisers clearly outperformed water spray only, as the HI increased from 28.176% to 29.97% with Fertigrain spray, achieving an increase of approximately 6.3%. The two-way interaction of DAP Fertiliser with soil amendment revealed that 150 kg ha^{-1} DAP + water spray only recorded the highest value of HI (29.905%), whereas 300 kg ha^{-1} DAP + Bokashi recorded only 27.098%. Likewise, 150 kg ha^{-1} DAP + Fertigrain spray recorded the highest value of HI (30.447%), whereas 300 kg ha^{-1} DAP + Fertigrain recorded only 28.394%. The interaction of soil amendment with foliar spray revealed that Bokashi Fertiliser + Fertigrain spray recorded the highest value of HI (30.244%), whereas Bokashi + EM liquid biofertiliser recorded only 28.276%. The three-way interaction showed that the highest HI value (31.657%) was obtained when no DAP Fertiliser was applied and Bokashi Fertiliser and Fertigrain spray were used, whereas the lowest value was recorded when 300 kg ha^{-1} DAP Fertiliser was applied without any soil amendments and foliar spray.

Weight of 1,000 grains (g)

It is clearly shown in Table 8 that the average thousand-grain weight increases from 34.389 g without DAP to 37.018 g with 150 kg ha^{-1} of DAP and then decreases to 35.611 g with 300 kg ha^{-1} of DAP. Therefore, it can be concluded that the average thousand-grain weight is best promoted with the medium level of DAP Fertiliser. On the other hand, Table 8 also shows that the highest average thousand-grain weight is with Bokashi Fertiliser, at 38.083 g, compared to 34.991 g with agricultural gypsum and 33.945 g without any amendment. In addition, Table 8 shows that the highest average thousand-grain weight was with the chelated nano-fertiliser, at 36.954 g, compared to other foliar treatments. The interaction of DAP Fertiliser and soil amendments showed that the highest thousand-grain weight was obtained when the plants were subjected to the application of 150 kg ha^{-1} of DAP Fertiliser and Bokashi, at 41.083 g. The interaction between DAP Fertiliser and foliar application showed that the highest average was obtained when the plants were subjected to 150 kg ha^{-1} of DAP Fertiliser and chelated nano-fertiliser, with the highest weight of 38 g. As for the interaction between the soil amendments and the foliar, the addition of Bokashi along with EM bio-fertiliser resulted in the highest average thousand-grain weight of 40g, whereas the lowest average of 32.889 g was recorded in the absence of all factors, where only water was sprayed. Finally, the three-way interaction resulted in the highest thousand-grain weight of 45g for the combination of 150 kg ha^{-1} DAP, Bokashi, and chelated nano-Fertiliser, whereas the lowest value of 33.000 g was recorded in the absence of all factors.

Table 8
Effect of DAP fertiliser levels, soil amendments, and foliar applications of bio-stimulants, chelated nano-fertilisers, and their interactions on thousand-grain weight (g)

DAP Level	Soil Amendment	Spraying Transactions				DAP × Amendments
		Water	Fertigrain	Nano-Fertiliser	Biofertiliser	
No addition	No treatment	33.000	33.667	33.667	33.667	33.500
	Gypsum	33.667	34.000	35.000	34.333	34.250
	Bokashi	35.333	35.333	35.667	35.333	35.417
150 kg ha^{-1}	No treatment	34.000	35.000	35.000	35.000	34.750
	Gypsum	34.667	35.333	35.555	35.333	35.222
	Bokashi	34.667	40.333	45.000	44.333	41.083
300 kg ha^{-1}	No treatment	31.667	33.667	34.667	34.333	33.584
	Gypsum	35.000	35.333	36.000	35.667	35.500
	Bokashi	35.667	37.000	39.333	39.000	37.750
LSD 0.05	1.959					0.498
Effect of DAP Levels						
DAP × Spraying	No addition	34.000	34.333	34.778	34.444	34.389
	150 kg ha^{-1}	34.445	36.889	38.518	38.222	37.018
	300 kg ha^{-1}	34.111	35.333	36.667	36.333	35.611
LSD 0.05	1.131					0.629
Effect of Enhancers						
Enhancers × Sprays	No	32.889	34.111	34.445	34.333	33.945
	Gypsum	34.445	34.889	35.518	35.111	34.991
	Bokashi	35.222	37.555	40.000	39.555	38.083
LSD 0.05		1.131				0.288
Spraying Nano-Bio		34.185	35.518	36.954	36.333	
LSD 0.05		0.653				

Percentage Yield Increase over Control (PYI)

As depicted in Table 9, significant differences were exhibited in the results obtained for PYI (%). The PYI value ranged from 0.00% in the control treatment (with no addition + no treatment + water spray), up to the value of 72.68% in the treatment involving addition of 300kg ha^{-1} of DAP Fertiliser + Bokashi + spraying with chelated nano-Fertiliser (Zn, Cu, Fe, Mn). The results demonstrated that Bokashi soil amendment treatments attained high PYI values across different DAP Fertiliser and spraying treatments, ranging from 5.62% to 72.68%. The highest PYI value was observed when the Bokashi treatment was applied in combination with high quantities of DAP Fertiliser and nanoelement spraying. It was further found that increasing the DAP Fertiliser rate led to a gradual increase in PYI. Treatment with 300kg ha^{-1} DAP Fertiliser attained higher PYI than those with 150 kg ha^{-1} or with no treatment at all, in conjunction with soil amendment and spray treatments.

Table 9
Effect of DAP fertiliser levels, soil amendments, foliar spray treatments with biostimulants, chelated nano-fertiliser, and their interactions on PYI for production (%)

No.	DAP Level	Soil Amendment	Foliar Treatment	GRY (Mg ha^{-1})	PYI (%)
1	No addition	None	Water spray only	4.220	0.00
2	No addition	None	Fertigrain	4.387	3.96
3	No addition	None	Nano-chelated	4.670	10.66
4	No addition	None	EM	4.357	3.25
5	No addition	Gypsum	Water spray only	4.473	6.00
6	No addition	Gypsum	Fertigrain	4.903	16.18
7	No addition	Gypsum	Nano-chelated	5.033	19.27
8	No addition	Gypsum	EM	4.930	16.82
9	No addition	Bokashi	Water spray only	4.457	5.62
10	No addition	Bokashi	Fertigrain	5.263	24.72
11	No addition	Bokashi	Nano-chelated	5.933	40.59
12	No addition	Bokashi	EM	5.660	34.12
13	150 kg ha^{-1}	None	Water spray only	4.423	4.81
14	150 kg ha^{-1}	None	Fertigrain	4.943	17.13
15	150 kg ha^{-1}	None	Nano-chelated	4.977	17.94
16	150 kg ha^{-1}	None	EM	4.830	14.45
17	150 kg ha^{-1}	Gypsum	Water spray only	4.943	17.13
18	150 kg ha^{-1}	Gypsum	Fertigrain	5.577	32.16
19	150 kg ha^{-1}	Gypsum	Nano-chelated	5.627	33.34
20	150 kg ha^{-1}	Gypsum	EM	5.237	24.10
21	150 kg ha^{-1}	Bokashi	Water spray only	5.713	35.38
22	150 kg ha^{-1}	Bokashi	Fertigrain	6.317	49.69
23	150 kg ha^{-1}	Bokashi	Nano-chelated	6.460	53.08
24	150 kg ha^{-1}	Bokashi	EM	5.867	39.03
25	300 kg ha^{-1}	None	Water spray only	4.457	5.62
26	300 kg ha^{-1}	None	Fertigrain	4.930	16.82
27	300 kg ha^{-1}	None	Nano-chelated	5.340	26.54
28	300 kg ha^{-1}	None	EM	5.137	21.73
29	300 kg ha^{-1}	Gypsum	Water spray only	5.273	24.95
30	300 kg ha^{-1}	Gypsum	Fertigrain	5.523	30.88
31	300 kg ha^{-1}	Gypsum	Nano-chelated	5.963	41.30
32	300 kg ha^{-1}	Gypsum	EM	5.597	32.63
33	300 kg ha^{-1}	Bokashi	Water spray only	5.867	39.03
34	300 kg ha^{-1}	Bokashi	Fertigrain	6.460	53.08
35	300 kg ha^{-1}	Bokashi	Nano-chelated	7.287	72.68
36	300 kg ha^{-1}	Bokashi	EM	6.450	52.84

The results further illustrated that treatments with chelated nano-Fertiliser produced the highest PYI values in comparison with other treatments, ranging from 10.66% to 72.68% according to the different interactions, while treatment with water spray recorded low PYI values.

DISCUSSION

The results show that the three-dip treatment (DAP × soil amendments × spraying) is superior to both the individual and dual treatments, as these interactions yielded the highest PYI values for production under experimental conditions. This increase in SPAD levels in response to DAP Fertilisers resulted from the fertilisers' ability to act as sources of both nitrogen and phosphorus. The former is an element that constitutes chlorophyll and Rubisco proteins involved in carbon fixation, whereas the latter is a key element involved in energy transport processes in chloroplasts through ATP, hence increasing photosynthetic efficiency and chlorophyll content in leaves (Arzu et al., 2024; Marschner, 2012). However, the superiority of Bokashi treatment was attributed to its role in enhancing soil conditions and stimulating microbial growth around plant roots. The influence of agricultural gypsum on crops is related to improved soil characteristics due to soluble calcium and reduced exchangeable sodium. Thus, such factors can positively influence soil structure and water permeability, increase nutrient uptake efficiency, and stabilise chlorophyll levels in leaves (Qadir et al., 2014; Zoca & Penn, 2017). Treatment with a nano-formula of micronutrients and biostimulants increases chlorophyll levels by activating the enzymatic system responsible for photosynthesis. For instance, iron contributes to electron transport in plants, manganese to the second photosynthetic system, and zinc helps to regulate the process of chlorophyll synthesis. Moreover, the application of nano-formulations positively influences the efficiency of absorption and transport in plants (Ali et al., 2023; Raliya et al., 2018; Zulfiqar et al., 2019).

The notable increase in height of wheat plants with the application of DAP Fertiliser is associated with its contribution to increasing soil fertilisation with nitrogen and phosphorus. The role of nitrogen includes protein synthesis, chlorophyll synthesis, and enzyme production for growth purposes, whereas the role of phosphorus lies in energy exchange reactions and stimulation of root growth. As a consequence, cell division, photosynthesis, and internode elongation occur, resulting in increased plant height (Arzu et al., 2024; Marschner, 2012). An explanation of improved productivity with the use of Bokashi Fertiliser can be provided by its contribution to improved rhizosphere conditions. Organic materials improve soil structure and increase porosity, and stimulate phosphate-solubilising microbes that produce growth hormones (Almashhadani et al., 2026; Diacono & Montemurro, 2010; Quiroz & Céspedes, 2019). Agricultural gypsum influences the effect via the enhancement of cationic balance within the soil due to the

replacement of exchangeable sodium with soluble calcium, enhancing the soil structure and water permeability and minimising osmotic pressure in the root zone (Alsalami et al., 2025a; Qadir et al., 2014; Zoca & Penn, 2017). This results in improved uptake capacity of plants, in addition to promoting cell and vegetation growth (Qadir et al., 2014; Zoca & Penn, 2017). The leaf spraying of nano-fertilisers containing both micronutrients and biostimulants triggers physiological activities related to growth. These include the control of auxin synthesis through zinc and copper, resulting in cell elongation. Manganese is involved in enzyme activation for metabolic processes (Ali et al., 2023; Raliya et al., 2018; Zulfiqar et al., 2019). The use of nano-fertilisers increases the absorption efficiency by the plants, resulting in vegetative growth (Al-Juthery et al., 2018; Raliya et al., 2018; Zulfiqar et al., 2019). The advantage in the interaction of the three is evident from the combination of mineral fertilisation, soil improvement, and physiological activation of plants, leading to meristem and internode elongation (Khalaf & Al-Juthery, 2025; Wu & Ma, 2015).

An impressive increase in the number of wheat grains is associated with higher efficiency of photosynthesis-driven conversion of source tissues into grains during the flowering and grain-filling stages. DAP Fertiliser is an easily obtainable source of nitrogen and phosphorus. The former stimulates cell division and protein production and increases the effectiveness of carbohydrate-producing surfaces, whereas phosphorus plays an important role in energy transfer and regulation of carbohydrate flow to the grains, thus contributing to effective grain formation and filling (Arzu et al., 2024; Marschner, 2012). Better performance of the Bokashi treatment is caused by better conditions in terms of soil fertility and nutrient availability. Organic matter helps increase the capacity for ketones exchange and activate phosphorus solubilisers and growth regulators, thus ensuring nutrient supply at the crucial grain formation stage (Diacono & Montemurro, 2010; Quiroz & Céspedes, 2019). The effect of agricultural gypsum is due to several reasons, such as improving the root environment through balancing ions, repairing soil structure and improving its ability to transport water. Such changes reduce osmotic pressure and facilitate water and nutrient absorption, as well as the transport of carbohydrates to grains, thereby increasing production levels (Alsalami et al., 2025b; Qadir et al., 2014; Zoca & Penn, 2017). As for the impact of micro- and nano-fertilisers used as sprays, their effect on yield components is mainly related to activating enzymes involved in photosynthesis and the synthesis of carbohydrates and proteins. Furthermore, using nano-fertilisers increases plant nutrient and carbohydrate absorption and transport, thereby enhancing grain filling (Ali et al., 2023; Raliya et al., 2018; Zulfiqar et al., 2019).

The two-way and three-way interactions indicate a combination of mineral fertilisation, increased soil fertility, and physiological activation of plants, thereby making efficient use of nutrients and improving dry matter conversion into grain. It is therefore understandable why the three-way interaction outperforms other treatments in the context of integrated plant nutrition management (Khalaf & Al-Juthery, 2025; Wu & Ma, 2015).

The considerable increase in wheat biomass yield is due to enhanced photosynthetic efficiency and increased dry mass accumulation during the growth period. The DAP Fertiliser is an easily accessible source of nitrogen and phosphorus, which leads to greater leaf area and enzyme activation for carbon assimilation and energy transmission processes, thereby contributing to biomass formation (Arzu et al., 2024; Marschner, 2012). The better performance of bokashi composting lies in its contributions to soil fertility and food security. Organic matter increases the capacity for ketone exchange and stimulates the activity of phosphate solubilising microbes and growth regulators, hence leading to higher nutrient uptake and dry matter accumulation (Diacono & Montemurro, 2010; Quiroz & Céspedes, 2019). Gypsum used in agriculture increases biomass by improving soil quality, ketone metabolism, and water permeability, thereby decreasing salt stress and promoting plant development (Qadir et al., 2014; Zoca & Penn, 2017). On the other hand, micronutrient and nanonutrient sprays stimulate enzymes involved in photosynthesis and respiration. Such nutrients include iron, zinc, manganese, and copper. The metabolism of micronutrients affects biological processes in plants. In addition, nanonutrients enhance nutrient uptake and transport within the plant, thereby increasing biomass productivity (Ali et al., 2023; Dimkpa & Bindraban, 2018; Zulfiqar et al., 2019). The binary and tertiary use cases involve a combination of mineral and organic Fertilisers with foliar sprays. The effect is enhanced nutrient availability, absorption, and physiological functions in plants, which increases dry weight production and yield (Khalaf & Al-Juthery, 2025; Wu & Ma, 2015).

Regarding the harvest index, it is more concerned with the efficiency of dry matter partitioning between vegetative biomass and grain than with the total yield produced. The heavy application of DAP results in a higher biological yield than grain yield, leading to a lower amount of dry matter partitioned into grains due to excessive vegetative growth (Marschner, 2012; Sharma & Smith, 1986). Conversely, the moderate amount of DAP ensures better balance between vegetative and reproductive growth, leading to efficient dry matter partitioning into grains (Wu & Ma, 2015). Amendments such as bokashi encourage biomass production rather than economic yield by improving root conditions and microbial metabolism, whereas gypsum helps maintain harvest index stability by altering cation composition and alleviating salt stress (Quiroz & Céspedes, 2019; Zoca & Penn, 2017). In addition, the application of biostimulants enhances carbohydrate transport into seeds and promotes efficient distribution, and micronutrients may enhance vegetative development in certain instances, thereby minimising their influence on harvest index (Ali et al., 2023; Dimkpa & Bindraban, 2018; Zulfiqar et al., 2019).

The interaction between fertilisation and biostimulation at two and three levels is related to the harvest index's sensitivity to nutrition balance. Balanced fertilisation and biostimulation improve dry matter allocation and the conversion of energy into grain (Khalaf & Al-Juthery, 2025; Wu & Ma, 2015). Additionally, the findings also showed that

the effects of wheat depend on the combination of mineral Fertilisers, soil management, and physiological stimulation. The DAP Fertiliser stimulates vegetative growth and photosynthetic activity, soil management improves nutrient supply, and foliar sprays boost metabolism (Ali et al., 2023; Marschner, 2012). Therefore, the harvest index reflects the balance between vegetative and reproductive growth stages and highlights the importance of integrating plant nutrition to ensure high productivity and effective dry matter distribution (Khalaf & Al-Juthery, 2025; Wu & Ma, 2015).

The predominance of the 150 kg ha-1 DAP Fertiliser dose for increasing grain weight is due to balanced phosphorus nutrition, which promotes grain development and filling and makes nutrient transfer more effective. A relative reduction in this trait may be due to reduced physiological efficiency from over-fertilisation or a relative nutritional imbalance. The predominance of Bokashi Fertiliser is due to improved root conditions, enhanced microbial activity, and more efficient nutrient use. The predominance of secondary material spraying indicates increased enzyme activity and grain filling efficiency during the late development stage (Rossini et al., 2025; Tan et al., 2026). The reason behind the superiority of two-way and three-way interactions is that using 150 kg ha^{-1} DAP, bokashi fertilisation, and secondary sources resulted in an optimal balance between soil nutrition, soil management, and leaf nutrition. This optimal balance enhanced grain filling, increased dry matter content, and gave the best thousand-grain weight among combined treatments, single treatments, and the control group (Rossini et al., 2025; Tan et al., 2026).

Furthermore, the findings from the percentage yield increase (PYI) evaluation indicate a definite increase in yield across all experimental treatments. Treatments involving mineral fertilisation, soil amendment, and nano-spraying had the highest success rate. This was because of the combined effects of these factors in improving nutrient utilisation efficiency and yielding higher crop yields. The soil amendment Bokashi appears to have contributed to this higher percentage yield increase (PYI). Soil physical, chemical, and biological properties were not directly measured in this study (see Limitations); however, Bokashi application has been reported in the literature to increase soil organic matter and microbial activity, thereby enhancing nutrient availability and reducing nutrient losses (Diacono & Montemurro, 2010; Quiroz & Céspedes, 2019). Moreover, the findings indicated that applying higher doses of mineral fertiliser (DAP) enhances the fertilisation process, particularly when applied together with organic amendments. Mineral Fertilisers deliver nutrients rapidly, whereas organic Fertilisers ensure high nutrient retention in the soil and minimise nutrient losses, hence increasing nutrient use efficiency. According to research, the practice of integrated fertilisation (application of mineral and organic Fertilisers) enhances nutrient use efficiency and productivity compared to single Fertiliser application (Ali et al., 2023; Khalaf & Al-Juthery, 2025). In spray applications, the use of chelated nano-fertilisers was more effective at enhancing the percentage yield increase (PYI). This was due to certain features of nanoparticles, including small size, large surface

area, and enhanced ability to penetrate plant tissues (Al-Shahmani & Al-Juthery, 2021). Nano-fertilisers also help minimise nutrient losses and improve utilisation efficiency. According to recent findings, agricultural nanotechnology helps in improving nutrient utilisation efficiency and productivity (Dimkpa & Bindraban, 2018; Shoukat et al., 2025).

Another reason for the effectiveness of the three-dip technique (DAP×Bokashi×nano-spray) may be attributed to the synergy among these variables. Specifically, Bokashi enhances soil conditions and boosts microbial activity; the mineral Fertiliser supplies plant nutrients, whereas the nano-spray facilitates their absorption (Al-Juthery & Al-Shami, 2019; Al-Shahmani & Al-Juthery, 2021). Research findings have confirmed that the use of organic and mineral fertilisers, alongside nanotechnology, is a promising approach to optimising fertilisation techniques and maintaining agricultural sustainability (Khalaf & Al-Juthery, 2025; Quiroz & Céspedes, 2019).

CONCLUSION

Results revealed a positive effect of increased DAP Fertiliser application on growth and productivity parameters. The highest fertiliser amount applied (300 kg ha^{-1}) yielded the highest values for plant height, biomass production, and grain production compared with no Fertiliser application. This indicates the essential contributions of nitrogen and phosphorus to plant photosynthesis and the formation of dry matter, due to their physiological roles. Moreover, Bokashi organic biofertiliser proved more effective than agricultural gypsum fertiliser and the control group in promoting biomass and grain yields, likely through improved nutrient supply (soil properties were not directly measured in this study). Spraying treatments were also significantly better than the rest, with the chelated nano-fertiliser having the best values for all studied parameters. It is also evident from the findings that two-way and three-way interactions among DAP Fertilisers, soil amendments, and sprays resulted in maximum productivity. The three-way treatment (300 kg ha-1 DAP Fertiliser + Bokashi + spraying nano-fertiliser) produced the best grain yield (7.287 Mg ha-1), bioyield (26.260 Mg ha-1), and percentage yield increase over the control (72.68%). This underscores the need for integrated application of mineral and organic Fertilisers with nanotechnology to boost nutrient utilisation efficiency. On the other hand, medium doses of DAP (150 kg ha-1) exhibited the maximum thousand-grain weight, while the harvest index was highest without DAP Fertiliser application and declined progressively with increasing DAP rate, emphasising the need for nutrient balance in optimising quality parameters. Thus, integrated fertilisation management that combines mineral, organic, and nano-based inputs may be recommended to achieve high productivity and sustainability in agriculture. Because nutrient-poor and salt-affected soils constrain wheat production well beyond Iraq, these findings offer a transferable framework for improving wheat productivity in other dryland and semi-arid wheat-growing regions internationally.

IMPLICATIONS OF THE STUDY

It draws out the practical takeaway: the three-way DAP × Bokashi × nano-fertiliser interaction supports shifting Fertiliser recommendations toward integrated mineral-organic-nano strategies, with direct relevance to sustainable wheat intensification on salt-affected Mesopotamian soils and national food security, and broader relevance to wheat production on nutrient-poor and salt-affected soils in other dryland and semi-arid regions internationally.

LIMITATIONS AND RECOMMENDATIONS FOR FUTURE RESEARCH

This study was conducted over a single growing season at a single experimental location under the environmental conditions of southern Iraq. Therefore, the results may vary under different climatic conditions, soil types, and management practices (Hassan et al., 2021). In addition, the experiment focused primarily on growth and yield parameters without evaluating changes in soil biological activity, nutrient use efficiency, root characteristics, or grain quality traits. The long-term residual effects of DAP Fertiliser, Bokashi, agricultural gypsum, and nano-biostimulant applications on soil health and sustainability were also beyond the scope of this study.

Future studies should evaluate these integrated fertilisation strategies across multiple growing seasons and diverse agroecological regions to validate their stability and applicability (Arshad et al., 2025; Al-Salihi et al., 2026). Long-term experiments are recommended to assess their effects on soil fertility, microbial diversity, carbon sequestration, and nutrient cycling. Further research should also investigate the physiological and molecular mechanisms responsible for the observed improvements in wheat performance, including nutrient uptake efficiency, antioxidant responses, and photosynthetic activity. In addition, economic feasibility analyses and environmental impact assessments should be incorporated to determine the practicality and sustainability of integrated applications of DAP Fertiliser, soil amendments, and nano-biostimulants for large-scale wheat production.

ACKNOWLEDGEMENT

The authors would like to express their sincere gratitude to the Department of Soil Sciences and Water Resources at the University of Al-Qadisiyah and the Dhi Qar Agriculture Directorate Research Station for their valuable support and assistance in conducting this research.

REFERENCES

Adesemoye, A. O., & Kloepper, J. W. (2009). Plant-microbes interactions in enhanced fertilizer-use efficiency. *Applied Microbiology and Biotechnology, 85*, 1-12. https://doi.org/10.1007/s00253-009-2196-0

Ali, M. M., Ghazal, R. A., & Al-Juthery, H. W. A. (2023). Effect of Rhizobacterein biofertiliser, nano-NPK and nano-micro complete on some parameters of growth and yield of bean and number of bacteria in the rhizosphere. *IOP Conference Series: Earth and Environmental Science, 1213*, 1-11, Article 012096. https://doi.org/10.1088/1755-1315/1213/1/012096

Al-Juthery, H. W. A., & Al-Shami, Q. M. N. (2019). Impact of fertigation of nano-NPK fertilisers on nutrient-use efficiency and nutrient distribution in soil of potato (*Solanum tuberosum* L.). *Plant Archives, 19*(Supplement 1), 1087-1096.

Al-Juthery, H. W. A., Al-Taee, R. A. H. G., Alhasan, A. S., Hassan, D. F., Al-Jassani, N. A. A., & Jarallah, R. S. (2025). Nano-biofertilizers: A promising technology for sustainable soil fertility, soil health, and environmental protection. *Asian Journal of Water, Environment and Pollution, 22*(3), 15-31. https://doi.org/10.36922/AJWEP025160123

Al-Juthery, H. W. A., Hassan, A. K. H., Musa, R. F., & Sahan, A. H. (2018). Maximize growth and yield of wheat by foliar application of complete nano-fertiliser and some biostimulators. *Research on Crops, 19*(3), 387-393. https://doi.org/10.31830/2348-7542.2018.0001.4

Al-Juthery, H. W. A., Lahmoud, N. R., Al-Juthery, H. H., Hassan, D. F., Hamid, M. Q., & Al-Taee, R. A. H. G. (2026). Smart targeting of nanopesticides: Advancing environmental protection and sustainable agriculture. *Plant Science Today, 13*(2). https://doi.org/10.14719/pst.11630

Almashhadani, B. M. K., Hamid, M. Q., Al-Silmawy, N., & Hassan, D. F. (2026). Combined effect of nano-silica and plant growth-promoting rhizobacteria (PGPR) on the physical and mechanical properties of soil. *Pakistan Journal of Agricultural Research, 39*(1), 119-126. https://doi.org/10.17582/journal.pjar/2026/39.1.119.126

Alsalami, J. J., Al-Murshedi, K. R., & Hassan, D. F. (2025a). Environmental modelling of drip irrigation system using HYDRUS-2D program by studying the moisture distribution of surface and subsurface. *Applied Chemical Engineering, 8*(1). https://doi.org/10.59429/ace.v8i1.5574

Alsalami, J. J., Almershidy, K. R., & Hassan, D. F. (2025b). Hydraulic performance analysis for drip irrigation systems efficiency and water productivity. *International Journal of Computational and Experimental Science and Engineering, 11*(1), 1567-1577. https://doi.org/10.22399/ijcesen.1200

Al-Salihi, Z. K., Hassan, D. F., Hamid, M. Q., & Hussain, S. (2026). Satellite-based monitoring of soil moisture and land degradation in Iraq's major river systems. In *Proceedings of the 8th International Symposium on Water Resource and Environmental Management* (pp. 77-95). Springer. https://doi.org/10.1007/978-3-032-19088-8_8

Al-Shahmani, A. M. K., & Al-Juthery, H. W. A. (2021). Response of rice (*Oryza sativa* L.) to silica fertilisation and spraying with nano-potassium and calcium. *IOP Conference Series: Earth and Environmental Science, 735*, Article 012068. https://doi.org/10.1088/1755-1315/735/1/012068

Al-Silmawy, N. A., Abd, E. H., Shahad, R. F., & Mohammed, R. J. (2025). Effect of using *Pseudomonas fluorescens* bacteria, *Glomus mosseae* fungus and liquid organic fertilizer on soil available nitrogen and phosphorus and some characteristics of fenugreek (*Trigonella foenum-graecum* L.) and choline seed content. *Agronomy Research, 23*(1), 266-279. https://doi.org/10.15159/AR.25.012

Alzreejawi, S. A. M., & Al-Juthery, H. W. A. (2020). Effect of spraying with nano-NPK, complete micro fertilisers and nano amino acids on some growth and yield indicators of maize (*Zea mays* L.). *IOP Conference Series: Earth and Environmental Science, 553*, Article 012010. https://doi.org/10.1088/1755-1315/553/1/012010

Arshad, M. Z., Hussain, S., Qaisrani, S. A., Iqbal, Z., Saeed, M., Mubeen, M., Javeed, H. M. R., Tahir, M., Hassan, D. F., Raza, A., Mostafazadeh, R., & Karuppannan, S. (2025). Using Google Earth Engine to detect the land use changes, climate change and vegetation dynamics. *Geoscience Letters, 12*, Article 54. https://doi.org/10.1186/s40562-025-00424-3

Arzu, Vikrant, Kumar, S., Singh, S. K., Maurya, D. K., & Kumar, M. (2024). Effect of nitrogen and phosphorus fertilisation on the growth and yield of wheat (*Triticum aestivum* L.). *International Journal of Environment and Climate Change, 14*(1), 552-557. https://doi.org/10.9734/ijecc/2024/v14i13869

Bhardwaj, D., Ansari, M. W., Sahoo, R. K., & Tuteja, N. (2014). Biofertilizers function as key player in sustainable agriculture by improving soil fertility, plant tolerance and crop productivity. *Microbial Cell Factories, 13*, Article 66. https://doi.org/10.1186/1475-2859-13-66

Diacono, M., & Montemurro, F. (2010). Long-term effects of organic amendments on soil fertility. A review. *Agronomy for Sustainable Development, 30*(2), 401-422. https://doi.org/10.1051/agro/2009040

Dimkpa, C. O., & Bindraban, P. S. (2018). Nanofertilizers: New products for the industry? *Journal of Agricultural and Food Chemistry, 66*(26), 6462-6473. https://doi.org/10.1021/acs.jafc.7b02150

Erenstein, O., Jaleta, M., Mottaleb, K. A., Sonder, K., Donovan, J., & Braun, H.-J. (2022). Global trends in wheat production, consumption and trade. In M. P. Reynolds & H.-J. Braun (Eds.), *Wheat improvement: Food security in a changing climate* (pp. 47-66). Springer. https://doi.org/10.1007/978-3-030-90673-3_4

Fixen, P., Brentrup, F., Bruulsema, T., Garcia, F., Norton, R., & Zingore, S. (2014). *Nutrient/fertiliser use efficiency: Measurement, current situation and trends*. International Fertiliser Industry Association.

Gąsiorowski, H. (2004). *Wheat: Chemistry and technology*. Wiley-Interscience.

Genaidy, S. A. M. (2011). *Research and application bases in soil chemistry and fertility* [Book in Arabic]. Al-Dar Al-Arabia Lil Nashr Wa Al-Tawzeia.

Hassan, D. F., Ati, A. S., & Neima, A. S. (2021). Calibration and evaluation of AquaCrop for maize (*Zea mays* L.) under different irrigation and cultivation methods. *Journal of Ecological Engineering, 22*(10), 192-204. https://doi.org/10.12911/22998993/142123

Itelima, J. U., Bang, W. J., Sila, M. D., Onyimba, I. A., & Egbere, O. J. (2018). A review: Biofertiliser: A key player in enhancing soil fertility and crop productivity. *Journal of Microbiology and Biotechnology, 2*(1), 22-28. https://www.pulsus.com/abstract/a-review-biofertilizer--a-key-player-in-enhancing-soil-fertility-and-crop-productivity-4328.html

Khalaf, M. H., & Al-Juthery, H. W. A. (2025). Influence of bokashi organic fertiliser, balanced mineral fertiliser, and foliar application of selenium and silicon nanoparticles on soil sustainability and the growth and yield of cabbage (*Brassica oleracea*). *Applied Chemical Engineering, 8*(4), 1-13. https://doi.org/10.59429/ace.v8i4.5732

Markwell, J., Osterman, J. C., & Mitchell, J. L. (1995). Calibration of the Minolta SPAD-502 leaf chlorophyll meter. *Photosynthesis Research, 46*(3), 467-472. https://doi.org/10.1007/BF00032301

Marschner, P. (Ed.). (2012). *Marschner's mineral nutrition of higher plants* (3rd ed.). Academic Press.

Parra-Torrejón, B., Cáceres, A., Sánchez, M., Sainz, L., Guzmán, M., Bermúdez-Perez, F. J., Ramírez-Rodríguez, G. B., & Delgado-López, J. M. (2023). Multifunctional nanomaterials for biofortification and protection of tomato plants. *Environmental Science & Technology, 57*(40), 14950-14960. https://doi.org/10.1021/acs.est.3c02559

-Qadir, M., Quillérou, E., Nangia, V., Murtaza, G., Singh, M., Thomas, R. J., Drechsel, P., & Noble, A. D. (2014). Economics of salt-induced land degradation and restoration. *Natural Resources Forum, 38*(4), 282-295. https://doi.org/10.1111/1477-8947.12054

Quiroz, M., & Céspedes, C. (2019). Bokashi as an amendment and source of nitrogen in sustainable agricultural systems: A review. *Journal of Soil Science and Plant Nutrition, 19*(1), 237-248. https://doi.org/10.1007/s42729-019-0009-9

-Raliya, R., Saharan, V., Dimkpa, C., & Biswas, P. (2018). Nanofertilizer for precision and sustainable agriculture: Current state and future perspectives. *Journal of Agricultural and Food Chemistry, 66*(26), 6487-6503. https://doi.org/10.1021/acs.jafc.7b02178

Richards, L. A. (1954). *Diagnosis and improvement of saline and alkali soils* (USDA Agriculture Handbook No. 60). *Soil Science, 78*(2), U.S. Department of Agriculture. https://doi.org/10.1097/00010694-195408000-00012

Rizwan, M., Ali, S., Abbas, T., Zia-ur-Rehman, M., Hannan, F., Keller, C., Al-Wabel, M. I., & Ok, Y. S. (2016). Cadmium minimization in wheat: A critical review. *Ecotoxicology and Environmental Safety, 130*, 43-53. https://doi.org/10.1016/j.ecoenv.2016.04.001

Rossini, A., Ruggeri, R., & Rossini, F. (2025). Use of foliar biostimulants in durum wheat: understanding its potential in improving agronomic and quality responses under Mediterranean field conditions. *Plants*, *14*(15), Article 2276. https://doi.org/10.3390/plants14152276

Shahad, R. F., Mohammed, R. J., Abdalkadhum, A. J., Hussain, S., Khallouf, A., & Almayahi, A. T. (2026). Assessment of soil composition, vegetation, and geochemical properties using GIS tools in Iraq. *Innovative Infrastructure Solutions, 11*(8), Article 459. https://doi.org/10.1007/s41062-026-02856-y

-Sharma, R. C., & Smith, E. L. (1986). Selection for high and low harvest index in three winter wheat populations. *Crop Science, 26*(6), 1147-1150. https://doi.org/10.2135/cropsci1986.0011183X002600060013x

Shoukat, A., Maryam, U., Pitann, B., Zafar, M. M., Nawaz, A., Hassan, W., Seleiman, M. F., Saqib, Z. A., & Mühling, K. H. (2025). Efficacy of nano and conventional zinc and silicon fertilizers for nutrient use efficiency and yield benefits in maize under saline field conditions. *Plants, 14*(5), Article 673. https://doi.org/10.3390/plants14050673

Singh, I. D., & Stoskopf, N. C. (1971). Harvest index in cereals. Agronomy Journal, 63(2), 224-226. https://doi.org/10.2134/agronj1971.00021962006300020008x

Tan, S., Fu, S., Liu, Y., Tian, W., & Xu, J. (2026). Foliar application of amino acids enhances grain yield and bread-making quality in wheat (*Triticum aestivum* L.). *Journal of Cereal Science, 127*, Article 104319. https://doi.org/10.1016/j.jcs.2025.104319

Velineni, S., & Brahmaprakash, G. P. (2011). Liquid biofertilisers: An overview of production and application. *Journal of Biofertilisers, 2*, 1-5.

Wu, W., & Ma, B. (2015). Integrated nutrient management (INM) for sustaining crop productivity and reducing environmental impact: A review. *Science of the Total Environment, 512-513*, 415-427. https://doi.org/10.1016/j.scitotenv.2014.12.101

Zoca, S. M., & Penn, C. (2017). An important tool with no instruction manual: A review of gypsum use in agriculture. *Advances in Agronomy, 144*, 1-44. https://doi.org/10.1016/bs.agron.2017.03.001

Zulfiqar, F., Navarro, M., Ashraf, M., Akram, N. A., & Munné-Bosch, S. (2019). Nanofertilizer use for sustainable agriculture: Advantages and limitations. *Plant Science, 289*, Article 110270. https://doi.org/10.1016/j.plantsci.2019.110270

Pertanika J. Trop. Agric. Sci. 49 (5): 2413 - 2438 (2026)

PERTANIKA JOURNALS

TROPICAL AGRICULTURAL SCIENCE

Journal homepage: http://www.pertanika.upm.edu.my/

Microalgae for Anti-Aging Cosmeceuticals: Synergistic Bioactivities and Physicochemical Potential

Felicia Stella Indarto[1], Sook Chin Chew[1,2], Fatimah Md Yusoff[3], Malinna Jusoh[4], and Norazira Abdu Rahman[1,2]*

[1]China-ASEAN College of Marine Sciences, Xiamen University Malaysia, 43900 Sepang, Selangor, Malaysia
[2]Centre of Excellence for Sustainable Technologies for Agricultural Advancement and a Zero-Waste Economy, Xiamen University Malaysia, 43900 Sepang, Selangor, Malaysia
[3]Department of Aquaculture, Faculty of Agriculture, Universiti Putra Malaysia, 43400 Serdang, Selangor, Malaysia
[4]Faculty of Science and Marine Environment, Universiti Malaysia Terengganu, 21030 Gong Badak, Terengganu, Malaysia

ABSTRACT

Microalgae are promising biofactories for cosmeceuticals owing to their ability to produce high-value metabolites with antioxidant and anti-aging potential. Yet, comparative studies across strains, extraction methods, and their application in skincare remain scarce. This study evaluated ethanol-water extracts (20%, 50%, 90%, 100% v/v) from *Thalassiosira weissflogii* TRG10-P105 (Tw), *Arthrospira platensis* (Sp), *Chlorella vulgaris* (Cv), and a 1:1 Sp-Cv mixture (SC). Extracts were initially screened for carotenoids and total phenolics, while selected Tw and SC extracts were further analysed for total flavonoids, phenolic profiles, antioxidant activity (DPPH), and collagenase inhibition as anti-ageing-related bioactivities. 90% ethanol was the most efficient for extracting both hydrophilic and lipophilic compounds. Tw had the highest carotenoid (2.97-8.63 mg g^{-1}) and flavonoid content (8.83 mg g^{-1}), whereas SC showed the highest phenolics (6.57-19.12 mg g^{-1}) with diverse compounds including catechin, quercetin, ferulic acid, and caffeic acid. SC also exhibited the highest radical-scavenging activity (23.96 mg TE g^{-1} DW) and collagenase inhibition (31.4-100%), supporting its anti-ageing-related potential. Based on these results, 90% ethanol extracts of Tw and SC were formulated into anti-aging creams, which showed acceptable pH, spreadability, stability,

ARTICLE INFO

Article history:
Received: 19 September 2025
Accepted: 07 October 2026
Published: 30 October 2026

DOI: https://doi.org/10.47836/pjtas.49.5.15

E-mail addresses:
mbt2109900@xmu.edu.my (Felicia Stella Indarto)
sookchin.chew@xmu.edu.my (Sook Chin Chew)
fatimahyus@gmail.com (Fatimah Md Yusoff)
malinna@umt.edu.my (Malinna Jusoh)
norazira.abdurahman@xmu.edu.my (Norazira Abdu Rahman)
* Corresponding author

e-ISSN: 2231-8542

© Universiti Putra Malaysia Press

and rheology. These findings highlight Tw and SC as potential microalgal ingredients for further development in anti-ageing cosmeceutical formulations.

Keywords: Anti-aging, antioxidant, carotenoid, microalgae, phenolic

INTRODUCTION

The global cosmeceutical industry is shifting toward natural, sustainable, bioactive-rich ingredients, driven by consumer demand for multifunctional products that enhance appearance while providing therapeutic benefits (Ragusa et al., 2021). The global market for natural and organic cosmetics and personal care products was valued at USD 37 billion in 2022 and is projected to reach USD 58.6 billion by 2031 (Ruf et al., 2024). Cosmeceuticals, which combine the properties of cosmetics and pharmaceuticals, are widely used to manage photoaging, hyperpigmentation, oxidative stress, and inflammation. Growing concerns about the health and environmental risks of synthetic ingredients have further intensified the search for safe, eco-friendly alternatives. Algae have emerged as a promising bioresource for cosmeceutical applications (Table 1) because of their rich metabolic diversity, high biomass productivity, and low ecological footprint. The microalgae market in cosmetics is projected to exceed USD 1.3 billion by 2030, driven by growing interest in naturally derived bioactive ingredients (Chinjoo & Golzary, 2025). This interest is largely due to

Table 1
Various algae strains and their concentration in some formulation types. w/w: weight-to-weight ratio

Algae Species	Concentration	Purpose	Formulation Type	Citation
Laminaria japonica	10% (w/w)	Moisturizing	Cream	Choi et al. (2013)
Rhizoclonium hieroglyphicum	0.5%	Moisturizing	Cream	Leelapornpisid et al. (2014)
Sargassum muticum	0.15% (w/w)	Antioxidant	Cream	Balboa et al. (2017)
Fucus vesiculosus	0.1% (w/w)	Antioxidant	Cream	Hermund et al. (2018)
Spirulina sp.	5% (w/w)	Anti-aging and anti-acne	Cream	Józsa et al. (2020)
Chlorella vulgaris	5%	Anti-aging, antioxidant, and anti-wrinkles	Gel	Amrutkar et al. (2020)
Gracilaria sp.	3%	Psoriasis treatment	Cream	Shatalebi et al. (2020)
Gelidium spinosum	0.75%	Anti-aging	Cream	Poulose et al. (2020)
Sargassum spp.	0.5 g	Brightening and anti-aging	Cream	Al-Momani et al. (2022)
Fucus vesiculosus	28% (w/w)	UV protection and antioxidant	Lotion	Hermund et al. (2022)

their production of carotenoids, phenolics, flavonoids, polysaccharides, and polyunsaturated fatty acids (PUFAs), which exhibit antioxidant, anti-inflammatory, UV-protective, and antimicrobial activities. Their ability to thrive under extreme conditions also enables the synthesis of structurally unique and stable bioactives (Yarkent et al., 2020). Compared with terrestrial plants, microalgae grow year-round, do not compete with food crops for land, and can be cultivated using seawater or wastewater, aligning with the principles of the circular bioeconomy.

Oxidative stress is a major driver of skin aging, causing collagen degradation, reduced elasticity, wrinkles, and impaired skin barrier function. Microalgal bioactives may counter these processes through several mechanisms, including scavenging reactive oxygen species (ROS), limiting lipid peroxidation, modulating endogenous antioxidant defenses, and inhibiting collagen-degrading enzymes (Nascimento et al., 2019). In cellular systems, some microalgal compounds may also attenuate ROS-mediated matrix metalloproteinase expression, thereby helping to limit extracellular matrix degradation. For instance, *Dunaliella salina* is rich in β-carotene and vitamin F, protecting skin from oxidative damage (Tsai et al., 2012); *Haematococcus pluvialis* produces astaxanthin, which reduces blemishes, fine lines, and sagging (Budzianowska et al., 2025); and *Tetraselmis chuii* supports detoxification pathways, delaying aging (Cokdinleyen et al., 2024). Among the studied species, *Thalassiosira weissflogii* TRG10-P105 is notable for its fucoxanthin and eicosapentaenoic acid (EPA), both of which are linked to antioxidant and anti-aging effects (Katayama et al., 2022; Rahman et al., 2020). *Arthrospira platensis* (commonly known as *Spirulina*) is rich in carotenoids and phenolic acids (Uzlaşır et al., 2024), while *Chlorella vulgaris* contains β-carotene, lutein, and zeaxanthin, supporting oxidative stress protection (Serra et al., 2021). Other diatoms, including *Phaeodactylum tricornutum* and *Chaetoceros calcitrans*, also possess omega-3 fatty acids, fucoxanthin, and phenolics, which reduce inflammation and repair barrier function (Mourelle et al., 2024). Since diatoms are inherently rich in fucoxanthin, they may offer greater anti-aging potential compared to phenolic-rich species such as *Spirulina* and *Chlorella*.

Although individual microalgae have been widely investigated for skin-related bioactivities, the effects of combining different microalgal species remain poorly understood. The cosmeceutical potential of individual microalgal ingredients is supported by studies extending beyond chemical assays; for example, a fucoxanthin concentrate from *Phaeodactylum tricornutum* showed collagen-related effects in human fibroblasts and was subsequently evaluated in a topical cream, while a *Dunaliella salina* extract demonstrated antiglycation and anti-inflammatory activities in ex vivo skin models and improvements in selected skin-ageing parameters in a clinical study (Havas et al., 2022). However, comparable evidence for formulations combining multiple microalgal species remains scarce. Studies involving other biological combinations provide some rationale for

examining complementary extract mixtures. Hejna et al. (2024) reported complementary or synergistic antioxidant interactions in selected 1:1 mixtures of the seaweeds *Ascophyllum nodosum*, *Palmaria palmata*, and *Ulva lactuca*, whereas Abu-Serie et al. (2018) observed synergistic antioxidant activity when *C. vulgaris* extract was combined with the mushroom *Ganoderma lucidum*. Although neither study represents a multi-microalgal combination, both indicate that combining extracts with different biochemical profiles can alter antioxidant activity.

Extraction conditions can substantially alter the chemical profile of a microalgal extract because pigments, phenolics, flavonoids, lipids, and other metabolites differ in polarity and solubility. In *Spirulina*, water favoured phycocyanin recovery, whereas ethanol was more effective for chlorophylls and carotenoids, and 70% ethanol yielded the highest polyphenol content (Tavakoli et al., 2021). Ethanol concentration likewise influenced the recovery of carotenoids and lipids from *Heterochlorella luteoviridis* (Jaeschke et al., 2016). In *C. vulgaris*, 90% aqueous ethanol was effective for extracting carotenoids and chlorophylls, while changes in extraction conditions also affected phenolic content and antioxidant activity (Georgiopoulou et al., 2022). Hence, solvent composition influences not only extraction yield but also the relative abundance of bioactive constituents and, consequently, the activity measured in the resulting extract. Nevertheless, the suitability of an extract for cosmeceutical use cannot, however, be inferred from bioactivity alone. Once incorporated into a topical formulation, the extract is exposed to a different physicochemical environment that may influence its dispersion, release, stability, and overall product performance. In *Spirulina*-containing creams, the emulsifying system affected the release of the incorporated material and its antioxidant activity (Józsa et al., 2020). Similarly, creams containing *Spirulina*, *Tetraselmis* sp., or *Dunaliella* sp. showed species-dependent differences in texture and colour stability during storage, despite maintaining acceptable overall physicochemical stability (Dammak et al., 2022). These highlight the importance of evaluating microalgal extracts not only for chemical composition and bioactivity but also for their behavior after incorporation into a topical formulation.

This study therefore compared *T. weissflogii*, *Spirulina*, *C. vulgaris*, and a 1:1 *Spirulina* - *C. vulgaris* mixture extracted with different ethanol concentrations (20-100%). *T. weissflogii* TRG10-P105 was included as a previously identified high-performing strain with strong antioxidant capacity and a metabolite profile rich in carotenoids and n-3 PUFAs (Katayama et al., 2022; Rahman et al., 2020). *Spirulina* and *C. vulgaris*, by contrast, are well-characterised sources of antioxidant and cosmeceutically relevant metabolites and were examined both individually and as a 1:1 mixture to determine whether their combination could improve bioactivity compared with the corresponding single-species extracts. This targeted design allowed *T. weissflogii* to serve as a previously screened reference candidate while specifically testing the effect of combining two established microalgal sources. The

extracts were characterised for carotenoid, total phenolic and flavonoid contents, selected phenolic compounds, radical-scavenging activity, and collagenase inhibition as an anti-aging-related endpoint. Selected extracts were subsequently incorporated into cream formulations and evaluated for appearance, pH, spreadability, physical stability, particle size, and rheological behaviour. By integrating solvent-dependent extraction, individual and mixed-species comparison, bioactivity screening, and formulation characterisation, this study provides a comparative basis for selecting potential microalgal ingredients for further development in anti-aging cosmeceuticals.

MATERIALS AND METHODS

Microalgae and Growth Conditions

Microalgae species including *Thalassiosira weissflogii* TRG10-P105 (Rahman et al., 2020), *Arthrospira platensis* (*Spirulina*), and *Chlorella vulgaris* (Natrah et al., 2007) were maintained in the exponential growth phase using 250 mL Conway medium prepared with 30 ppt sterile seawater, following Tompkins et al. (1995). Cultures were grown under continuous aeration at 24 ± 1 °C, illuminated at 100 µmol photons m^{-2} s^{-1} with a 12:12 h light-dark cycle until sufficient biomass was obtained. On day 7 of cultivation, cells were harvested by centrifugation at 4500 rpm for 10 min, freeze-dried, and stored at -80 °C until analysis.

Extraction of Microalgae with Different Solvents

Prior to analysis, freeze-dried microalgal powders (0.25 mg mL^{-1}) were sonicated (Devey KQ-250DE, China) at 100% amplitude for 10 min in 20%, 50%, 90%, or 100% ethanol to disrupt the biomass and enhance solvent penetration. The suspensions were then incubated at 4 °C for 12-16 h to allow further diffusion and extraction of soluble metabolites before filtration. Alongside the individual preparations of *T. weissflogii* (Tw), *Spirulina* (Sp), and *C. vulgaris* (Cv), a *Spirulina* - *C. vulgaris* mixture (SC) was prepared at a 1:1 ratio by dry biomass weight. Equal amounts of Sp and Cv were combined before extraction and processed under the same conditions as the individual samples. All mixtures were filtered through 0.22 µm PTFE syringe filters to obtain clear supernatants, which were stored at -20 °C until further analysis.

For subsequent analyses, Tw, Sp, Cv, and SC were first screened across four ethanol concentrations for total carotenoid and phenolic contents. Tw and SC were then selected for further characterisation, representing the highest carotenoid and TPC responses, respectively, with SC also serving as the mixed-microalgal preparation of interest. Both were subsequently evaluated for phenolic composition, total flavonoid content, radical-scavenging activity, collagenase inhibition, and cream formulation.

Total Carotenoid Content

Total carotenoid content was determined following the method described by Lichtenthaler (1987). Algal extracts (0.25 mg mL^{-1}) were prepared in triplicate and analysed using a double-beam UV-Vis spectrophotometer (Jasco V-770, Japan). Absorbance readings were taken at 470 nm, 652.4 nm, 665.2 nm, and 750 nm. The absorbance at 750 nm was subtracted from the other readings to correct for turbidity.

Total Phenolic Content (TPC)

TPC was measured using the Folin-Ciocalteu method (Farahin et al., 2019). Extracts (25 µL, 0.25 mg mL^{-1}) were mixed with Folin-Ciocalteu reagent and sodium carbonate, incubated for 2 h in the dark, and measured at 765 nm. Gallic acid (0-100 µg mL^{-1}) was used as the standard, and results were expressed as mg GAE g^{-1} DW (mean ± SD).

Determination of Phenolic Compounds via Ultra-High Performance Liquid Chromatography (UHPLC)

Phenolic compounds in extracts of *Thalassiosira weissflogii* (Tw) and the *Spirulina-Chlorella vulgaris* (SC) mixture (10 mg mL^{-1}) were analysed using UHPLC (Waters Acquity Arc UPLC, USA) with an InfinityLab Poroshell 120-EC-C18 column (4.6 × 250 mm, 4 µm). Detection was performed at 280, 290, 310, 330, and 360 nm. Separation used gradient elution with methanol (phase A) and 1% acetic acid in water (phase B) as described in Table 2. Each run lasted 45 min, consuming ~12.2 mL A and 34 mL B. Compounds were identified by retention times and UV spectra against standards (Table 3).

Table 2
Composition of two different mobile phases for a 45-minute UHPLC

Time (min)	Composition (%)	
	Mobile Phase A	Mobile Phase B
0	4	96
4	4	96
24	22	78
30	60	40
34	90	10
40	20	80
45	4	96

Total Flavonoid Content (TFC)

TFC was measured spectrophotometrically following Srisuksomwong et al. (2023) with minor modifications. A quercetin stock (1 mg mL^{-1}) was used to prepare the calibration curve (0.2-2.0 mL). For each assay, 250 µL of sample (13.3 mg mL^{-1}) or blank was mixed with 50 µL of 10% $AlCl_3$, 750 µL methanol, 50 µL of 1 M potassium acetate, and 1400 µL water. After 30 min incubation in the dark at room temperature, absorbance was read at 415 nm (Jasco V-770, Japan). Results were expressed as mg quercetin equivalents (QE) per g dry weight.

Table 3
Absorbance and retention time of phenolic compounds (45-Minute UHPLC)

Compounds	Absorbance (nm)	Retention Time (min)
Gallic acid	280	7.4
4-hydroxybenzoic acid	280	20.4
Catechin	280	23.0
Protocatechuic acid	290	13.5
Vanillic acid	290	25.9
p-coumaric acid	310	30.9
Caffeine acid	320	27.2
Ferulic acid	320	31.6
Chlorogenic acid	330	25.2
Quercetin	360	34.6
Kaempferol	360	35.4

DPPH (2,2-Diphenyl-1-picrylhydrazyl) Assay

Antioxidant activity was assessed with a DPPH Assay Kit (D678, Dojindo). Trolox (0-80 μg mL^{-1}) served as the standard. Samples (20 μL, 13.3 mg mL^{-1}), standards, or blanks were mixed with 80 μL assay buffer and 100 μL DPPH solution in 96-well plates, incubated at 25 °C in the dark for 30 min, and read at 517 nm (Tecan Spark). Results were expressed as mg Trolox equivalents (TE) g^{-1} DW.

Collagenase Inhibition Assay

Collagenase inhibition was measured with a fluorometric Collagenase Inhibitor Screening Kit (Abcam, ab211108). Algal extracts (0.01-0.10 mg mL^{-1}) or control (1,10-phenanthroline) were added to wells with diluted collagenase (5 μL) and fluorogenic substrate (50 μL). After 15 min incubation, fluorescence was recorded at 490/520 nm (Tecan Spark).

Formulation of Anti-Aging Creams

Cream formulation followed a modified protocol from Mawazi et al. (2022). Ingredients (Table 4) were grouped into oil, water, active, antimicrobial, and pH adjuster phases. The oil and water phases were separately heated to 75 °C, combined under stirring to form a stable emulsion, and then cooled to ~30 °C. Algal extracts were incorporated during cooling and mixed thoroughly. The final cream was stabilised at 25 °C for 24 h before physicochemical and biological evaluation.

Table 4
Composition and function of ingredients of the formulated anti-aging creams

Ingredient	Function	% w/w
Oil Phase		
Stearic Acid	Thickening agent and stabiliser	2%
Glyceryl Stearate SE	Emulsifier and improves spreadability	3%
Cetearyl Alcohol	Emulsifier, stabiliser, and enhances texture	2%
Squalane (Plant-derived)	Lightweight emollient and skin barrier repair	6%
Caprylic/Capric Triglyceride (MCT Oil)	Non-greasy moisturiser and enhances penetration	12%
Water Phase		
Distilled Water	Solvent	Q.S. to 100%
Glycerin	Humectant and prevents dehydration	4%
Active Phase		
Microalgae Extract	Anti-aging, antioxidant, and collagen booster	1% or 2.5%
Antimicrobial System		
Liquid Germall Plus	Antimicrobial	1%
Stabilisers & pH Adjusters		
Xanthan Gum	Natural stabiliser and improves consistency	0.3%
Citric Acid	Adjusts pH (4.5-5.5)	0.2%

Note. Change 1% to 0.5% and 2.5% to 1.25% of each microalgae extract for the combination cream. Q.S. (quantum satis or quantity sufficient): Replace microalgae with distilled water for the control formulation

Physicochemical Properties of the Formulated Creams

Appearance, Odour, and Homogeneity Test

The formulated cream was assessed for organoleptic properties, including colour, odour, and homogeneity. Colour was visually inspected under consistent lighting (Dąbrowska et al., 2015), while odour and homogeneity were evaluated as described by Chen et al. (2016). For homogeneity, a small amount of cream was pressed between two fingers to check texture uniformity.

pH, Stability and Spreadability

To determine the pH of the formulation, 0.5 g of the cream was dispersed in 50 mL of distilled water and left to equilibrate at room temperature for approximately two hours. The pH was then measured using a calibrated digital pH meter, following the procedure described by Miettinen et al. (2006). Meanwhile, the spreadability of the formulated cream was evaluated following the method of Chen et al. (2016), with minor modifications. Briefly, 0.5 g of the cream was placed between two glass slides, and a 57 g weight was applied to the upper slide to facilitate spreading. After one minute, the diameter of the resulting spread was measured to assess spreadability.

To determine stability, the creams were stored in 50 mL centrifuge tubes and subjected to six freeze-thaw cycles (-18 ± 2 °C for 24 h, then 40 ± 2 °C for 24 h), following Daudt et al. (2015). After each cycle, stability was checked by centrifuging 1 g of sample at 3,000 rpm for 30 min (Papaioanou et al., 2018; Tafuro et al., 2022). Samples were deemed stable if no creaming, phase separation, or sedimentation occurred (Chu & Nyam, 2020). Colour and odour were also recorded to monitor sensory stability.

Particle Size Test

Particle size distribution was measured using a dynamic image analyser (Litesizer DIA 500, Anton Paar, Austria). Cream samples were dispersed in distilled water, vortexed to avoid agglomeration, and transferred into a water-filled cuvette for analysis.

Rheological Characterisation

Rheological properties were analysed using a rheometer (MCR 320e, Anton Paar, Austria) with a 50 mm CP50-1 plate. Cream samples were carefully loaded to avoid air entrapment, and flow ramp tests were performed by increasing shear rate from 0.1 to 100 s^{-1} at 37 ± 0.1 °C. Viscosity-shear rate plots were generated to evaluate flow behaviour.

Statistical Analysis

Statistical analyses were performed in SPSS v30.0 (IBM, Armonk, NY, USA). Data are presented as mean ± SD from triplicate measurements. Total carotenoid and phenolic contents were analysed by two-way ANOVA using microalgal preparation and ethanol concentration as factors, including their interaction. Collagenase inhibition was analysed similarly, using extract type and concentration as factors. Cream physicochemical properties were compared by one-way ANOVA. Tukey's HSD test was used for post hoc comparisons, and homogeneity of variance was assessed using Levene's test. Statistical significance was set at $p < 0.05$.

RESULTS AND DISCUSSION

Total Carotenoids

Figure 1 shows the total carotenoids of microalgae extracted with varying ethanol concentrations (20-100%). Among these, 100% EtOH consistently yielded the highest ($p < 0.05$) carotenoid levels across all strains (Tw, Sp, SC, Cv), while 20% EtOH produced no detectable carotenoids, confirming its ineffectiveness. Moderate yields were obtained with 50% and 90% EtOH, though significantly lower ($p < 0.05$) than with 100% EtOH. Tw exhibited the highest carotenoid content, reaching 8.63 mg g^{-1} in 100% EtOH, followed

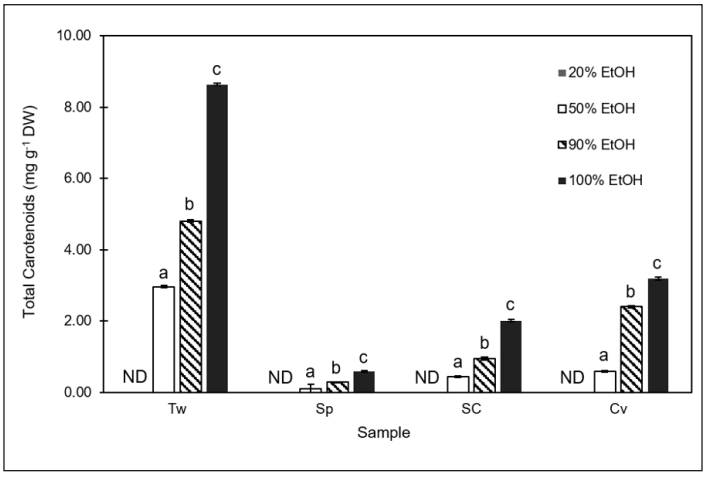

Figure 1. Total carotenoid content. Tw: *Thalassiosira weisslflogii*; Sp: *Spirulina platensis*; SC: combination of *Spirulina platensis* and *Chlorella vulgaris*; Cv: *Chlorella vulgaris*. ND: Not detected. Significant differences ($p < 0.05$) are indicated by different letters

by 4.81 and 2.97 mg g^{-1} in 90% and 50% EtOH, respectively. Cv and SC produced moderate yields, whereas Sp consistently had the lowest yield, at only 0.59 mg g^{-1} in 100% EtOH. Interestingly, the mixed extract SC showed higher carotenoid levels than Sp alone, suggesting a possible synergistic or complementary effect. Previous studies support these trends. *Thalassiosira weissflogii* TRG10-p105 contains high fucoxanthin (11.5 mg g^{-1} DW) and total carotenoids of 20.2 mg g^{-1} DW (Katayama et al., 2022), explaining the higher yields observed in Tw compared to *Spirulina* and *Chlorella*. While *Spirulina* is rich in β-carotene and zeaxanthin (7393 ± 2.76 and 6652 ± 3.69 μg mL^{-1}) (Maoka, 2011), *Chlorella* contains diverse carotenoids, including astaxanthin, lutein, β-cryptoxanthin, and canthaxanthin (Pantami et al., 2020).

Extraction efficiency depends on solvent polarity, solute-solvent interactions, and cell wall properties. Carotenoids are lipophilic; thus, less polar solvents enhance recovery. In this study, 100% ethanol was most effective, consistent with Jaeschke et al. (2016), who reported the highest carotenoid yield in *C. vulgaris* with 75% ethanol (1.21 ± 0.08 mg g^{-1}), compared to much lower yields with 50% and 20%. By contrast, Sp yielded less here than in acetone extraction (1.69 ± 0.07 mg g^{-1}) (Rahim et al., 2021), likely because acetone penetrates *Spirulina*'s protein-polysaccharide cell wall more effectively. Similarly, Katayama et al. (2022) reported higher carotenoids from Tw in 95% methanol (20.2 mg g^{-1} DW) compared to ethanol (8.63 mg g^{-1} DW), reflecting methanol's higher polarity and stronger disruption of pigment-protein complexes. Although methanol can provide efficient pigment extraction, its toxicity limits its suitability for cosmeceutical applications (Mojica et al., 2020). Ethanol therefore represents a more appropriate food- and cosmetic-grade alternative while maintaining effective carotenoid recovery.

Total Phenolic Content (TPC)

Figure 2 presents the total phenolic content (TPC) of microalgae strains extracted with ethanol at concentrations ranging from 20% to 100%. No significant differences ($p > 0.05$) were observed between 50% and 100% ethanol, both of which yielded lower TPC than 20% and 90% ethanol ($p < 0.05$). SC showed the highest TPC with 20% ethanol (19.12 mg g^{-1}), followed by 90% ethanol (12.74 mg g^{-1}), 100% ethanol (7.62 mg g^{-1}), and 50% ethanol (6.57 mg g^{-1}). Sp similarly produced its maximum in 20% ethanol (15.75 mg g^{-1}), whereas Cv and Tw showed higher values with 90% ethanol (15.48 mg g^{-1} and 7.38 mg g^{-1}, respectively).

Solvent polarity plays a key role in phenolic extraction, as the moderate polarity of ethanol dissolves both hydrophilic and lipophilic phenolics while maintaining safety for food and cosmetic use. In *Thalassiosira rotula*, 70% ethanol yielded nearly double the TPC of 50% ethanol (Matas et al., 2023), aligning with the present findings where Tw performed better at higher ethanol concentrations. Similarly, *Chlorella vulgaris* showed higher TPC in 96% ethanol than in water (Garcia et al., 2024), consistent with the elevated values for Cv and Tw in 90% ethanol. By contrast, Sp yielded significantly higher TPC in 20% ethanol, in line with Kumar et al. (2022a), who reported greater phenolic recovery from aqueous extracts. This reflects the hydrophilic nature of many cyanobacterial phenolics, such as simple phenolic acids and water-soluble flavonoids. Notably, the TPC obtained here (15.75 ± 1.30 mg g^{-1}) was higher than previous aqueous reports, suggesting 20% ethanol enhances solubilisation beyond water alone.

The observed patterns also correspond with known phenolic diversity: Sp contains flavonoids such as acacetin, pinocembrin, and sakuranetin, while Cv contains ferulic,

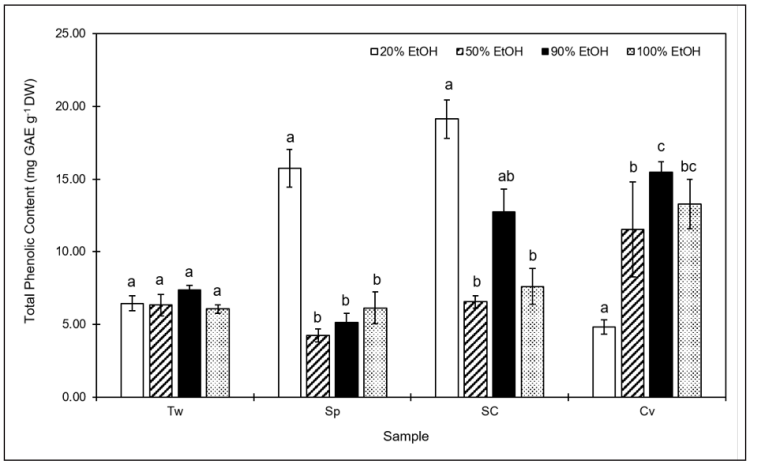

Figure 2. Total phenolic content of *Thalassiosira weissflogii* (Tw), *Spirulina* (Sp), *Chlorella vulgaris* (Cv), and the 1:1 *Spirulina* - *C. vulgaris* mixture (SC) extracted with different ethanol concentrations. Different letters indicate significant differences among treatments ($p < 0.05$)

caffeic, and p-coumaric acids (Guldas et al., 2020; Zakaria et al., 2020). Ferulic acid has limited water solubility but dissolves readily in ethanol, while caffeic and p-coumaric acids are ethanol-soluble (Tuzen & Ozdemir, 2003). These solubility characteristics explain why Sp was optimal at 20% ethanol, whereas Cv and Tw peaked at 90% ethanol. The high TPC in SC at both 20% and 90% ethanol further suggests synergistic effects from combining Sp and Cv. Overall, 90% ethanol emerged as the most versatile solvent, providing strong extraction for both phenolics and carotenoids, especially in Tw and SC. Its intermediate polarity enables recovery of hydrophilic and lipophilic compounds, making it well-suited for multiphase formulations such as emulsions (Cubero-Cardoso et al., 2024). Notably, 90% ethanol extracts from Tw yielded the highest levels of carotenoids, while SC extracts yielded the highest levels of phenolics. This dual enrichment highlights their potential as bioactive-rich candidates for anti-aging cosmeceutical development.

UHPLC Determination of Phenolic Compounds

The phenolic profiles of *Thalassiosira weissflogii* (Tw) and the *Spirulina-Chlorella* combination (SC) were analysed by UHPLC (Table 5). SC exhibited a significantly higher total phenolic content (1156.02 µg g^{-1} DW) than Tw (519.10 µg g^{-1} DW), indicating its richer polyphenolic composition. Both extracts contained gallic acid, 4-hydroxybenzoic acid, vanillic acid, and kaempferol at comparable levels ($p > 0.05$). However, SC demonstrated a broader spectrum, with additional phenolics detected exclusively in this extract: catechin (390.72 µg g^{-1}), quercetin (103.43 µg g^{-1}), chlorogenic acid (58.03 µg g^{-1}),

Table 5
List of major phenolic composition via UHPLC

Phenolic Composition	TW (µg g-1 DW)	SC (µg g-1 DW)
Gallic acid	169.05 ± 0.27a	174.37 ± 2.56a
4-Hydroxybenzoic acid	68.69 ± 2.42a	75.57 ± 5.45a
Catechin	ND	390.72 ± 2.81
Protocatechuic acid	ND	ND
Vanillic acid	208.29 ± 0.42a	208.89 ± 0.77a
p-Coumaric acid	ND	53.85 ± 0.01
Caffeic acid	ND	ND
Ferulic acid	ND	19.69 ± 0.10
Chlorogenic acid	ND	58.03 ± 0.12
Quercetin	ND	103.43 ± 0.26
Kaempferol	73.07 ± 0.15a	72.47 ± 0.27a
Total	519.10 ± 2.47a	1156.02 ± 6.70b

Note. Tw: *Thalassiosira weisslflogii*; SC: combination of *Spirulina platensis* and *Chlorella vulgaris*. Significant differences ($p < 0.05$) are indicated by different letters

p-coumaric acid (53.85 μg g^{-1}), and ferulic acid (19.69 μg g^{-1}). In contrast, Tw was limited to only four detectable compounds, all shared with SC. The broader profile of SC suggests stronger antioxidant potential, as many of these compounds are known to be bioactive. Ferulic and caffeic acids exhibit potent radical scavenging capacity and protect against oxidative stress (Tutun & Yipel, 2024), while quercetin inhibits free radical propagation. These phenolics are also widely used in cosmeceuticals; ferulic acid, quercetin, and gallic acid are common in skincare formulations at 0.1-0.5%, while ferulic and caffeic acids provide photoprotection in sunscreen and after-sun products (Jesus et al., 2025). The high levels of catechin and quercetin in SC thus support its stronger antioxidant and anti-aging potential compared to Tw.

Although studies on Tw remain limited, related diatoms such as *Phaeodactylum tricornutum* contain diverse phenolics including gallic acid, protocatechuic acid, catechin, and vanillic acid, with catechin and sinapic acid as major constituents (Rico et al., 2012). However, catechin was absent in Tw here, suggesting species-specific variation among diatoms. In contrast, previous reports on Sp and Cv align with the present findings. Sp has been shown to contain chlorogenic acid, caffeic acid, quercetin, gallic acid, and kaempferol (Guldas et al., 2020), though at much lower levels than those observed in this study. Arrari et al. (2023) also identified catechin as the predominant phenolic in Sp, consistent with the high catechin content of SC. Similarly, Cv extracts have been reported to contain gallic, chlorogenic, caffeic, p-coumaric, and ferulic acids (Zakaria et al., 2020). The detected phenolics further support the cosmeceutical potential of both extracts. Gallic acid, present in Tw and SC, has been shown to suppress UVB-induced ROS and MMP-1 while increasing type I procollagen in human dermal fibroblasts (Hwang et al., 2014). SC additionally contains chlorogenic acid, which increased collagen I and reduced MMP-1 and MMP-3 in UVA-exposed human dermal fibroblasts (Xue et al., 2022). Ferulic acid has demonstrated topical photoprotective activity in an experimental skin model, while quercetin reduced UV-induced inflammatory signalling in primary human keratinocytes (Lin et al., 2005). These compound-specific activities provide a stronger biological basis for the anti-aging potential of Tw and, in particular, the more phenolics-diverse SC extract.

Total Flavonoid Content (TFC)

As shown in Figure 3, the total flavonoid content (TFC) of *Thalassiosira weissflogii* (Tw) was significantly higher ($p < 0.05$) than that of the *Spirulina-Chlorella* combination (SC), with values of 8.83 and 7.28 mg g^{-1} DW, respectively. This suggests that Tw contributes a relatively flavonoid-rich antioxidant potential. Flavonoids are well recognised for their roles in mitigating oxidative stress, scavenging reactive oxygen species (ROS), inhibiting lipid peroxidation, and modulating signalling pathways associated with inflammation and aging (Matin et al., 2024). Their relevance to skincare is particularly significant, as

oxidative damage from UV exposure and environmental pollutants is a primary driver of skin aging. While data on the TFC of Tw remain limited, Ashashalini et al. (2019) reported a TFC of 2.06 mg g-1 DW using methanolic extraction, significantly lower than the value observed in this study (8.83 ± 0.34 mg g-1 DW using ethanol). This finding suggests that ethanol is more efficient for extracting flavonoids from Tw, likely due to its ability to solubilise both hydrophilic and moderately lipophilic compounds. For SC, the moderately high TFC (7.28 mg g^{-1} DW) may reflect the synergistic contribution of *Spirulina* and *Chlorella*, which together broaden the flavonoid spectrum and enhance the overall antioxidant potential.

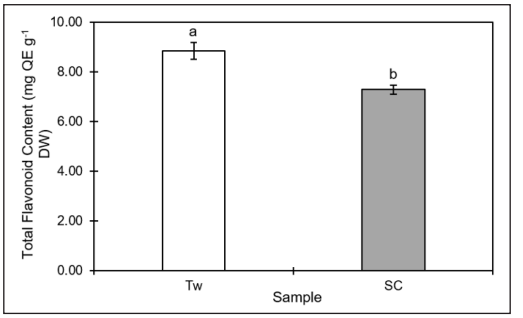

Figure 3. Total flavonoid content of *Thalassiosira weisslflogii* (Tw) and the combination of *Spirulina platensis* and *Chlorella vulgaris* (SC). Significant differences ($p < 0.05$) are indicated by different letters

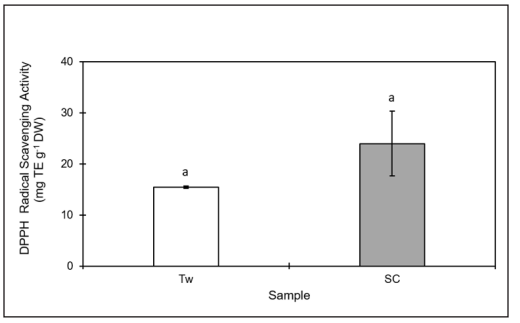

Figure 4. DPPH radical scavenging activity of the samples via a microplate reader. Tw: *Thalassiosira weisslflogii*; SC: combination of *Spirulina platensis* and *Chlorella vulgaris*. A significant difference ($p < 0.05$) is indicated by different letters

DPPH Radical Scavenging Activity

As shown in Figure 4, the DPPH radical scavenging activity of SC (23.96 mg TE g^{-1}) was higher than that of Tw (15.43 mg TE g^{-1}), although the difference was not statistically significant ($p > 0.05$). This trend suggests that SC may have comparatively stronger antioxidant potential. This activity is relevant to anti-aging cosmeceutical applications because mitigating oxidative stress may help limit processes associated with collagen degradation, inflammation, and wrinkle formation.

Tw also exhibited substantial radical-scavenging activity, likely linked to its carotenoid and phenolic contents. Previous studies have reported that Tw contains fucoxanthin and phenolic compounds with antioxidant, anti-inflammatory, and photoprotective properties (Katayama et al., 2022; Rahman et al., 2020), supporting its potential as a cosmeceutical ingredient for skin protection. In contrast, the higher activity observed in SC may reflect its richer, more diverse phenolic profile identified by UHPLC, consistent with previous findings showing stronger antioxidant activity in *Spirulina* than in *C. vulgaris,* which is associated with its higher polyphenolic content (Agregán et al., 2018). *C. vulgaris* may nevertheless contribute complementary phenolics, including ferulic acid, caffeic acid, and

quercetin, which can participate in radical scavenging, metal-ion chelation, and modulation of oxidative processes (Tutun & Yipel, 2024). Thus, combining Sp and Cv may broaden the antioxidant compound profile of SC and contribute to the higher antioxidant trend observed here. Although from a cosmetic-development perspective, no established minimum DPPH activity or bioactive-compound concentration currently defines the suitability of a microalgal extract as a cosmetic ingredient. Accordingly, the measurable antioxidant activity of Tw and SC, together with their quantified carotenoid and phenolic contents, provides functional evidence supporting their further evaluation as cosmeceutical active ingredients.

Collagenase Inhibition Activity

As shown in Table 6, both Tw and SC extracts exhibited a dose-dependent increase in collagenase inhibition. At all tested concentrations, SC demonstrated significantly higher activity than Tw. At 1 µg mL^{-1}, inhibition was 31.4% for SC versus 11.1% for Tw; at 3 µg mL^{-1}, 40.4% versus 23.1%; and at 5 µg mL^{-1}, 67.7% versus 43.7%. At the highest concentration (10 µg mL^{-1}), SC achieved complete inhibition (100%), while Tw reached 86.7%. This was reflected in the IC_{50} values, with SC (3.552 µg mL^{-1}) exhibiting stronger potency than Tw (5.728 µg mL^{-1}).

Table 6
Collagenase inhibition (%) of Tw and SC

Concentration (µg mL-1)	Inhibition Percentage (%)	
	Tw	SC
1	11.1 ± 0.23a	31.4 ± 0.29a
3	23.1 ± 0.91b	40.4 ± 0.01b
5	43.7 ± 0.14c	67.7 ± 0.23c
10	86.7 ± 0.24d	100.0 ± 0.08d
IC50 value (µg mL-1)	5.728a	3.552b

Note. Tw: *Thalassiosira weisslflogii*; SC: combination of *Spirulina platensis* and *Chlorella vulgaris*. Significant differences ($p < 0.05$) are indicated by different letters

Collagenase, a matrix metalloproteinase (MMP), is a key enzyme that degrades dermal collagen and accelerates skin aging (Pittayapruek et al., 2016). Inhibiting its activity is therefore an important strategy in anti-aging skincare. According to Findrianny et al. (2015), IC_{50} values below 50 µg mL^{-1} indicate extremely strong activity, while 50-100 µg mL^{-1} represent strong activity. Based on this classification, SC demonstrated strong-to-extremely strong activity, whereas Tw showed strong activity. Compared with earlier studies, SC displayed higher inhibitory efficiency at lower concentrations. For example, Masoumifeshani et al. (2025) reported 86.21% and 90.52% inhibition for *Spirulina* and *Chlorella vulgaris*, respectively, but only at 80 µg mL^{-1}. Similarly, peptide-rich fractions from *Arthrospira maxima* achieved 92.5% inhibition at 75 µg mL^{-1} (Montalvo et al., 2019), while *Chlamydomonas reinhardtii* reached 83% inhibition at 1 mg mL^{-1} (Falcao et al., 2020). By contrast, brown macroalgae such as *Sargassum plagyophyllum* and *Carpomitra costata* exhibited substantially lower inhibition rates, even at much higher concentrations (Susano et al., 2021). The enhanced inhibition observed in SC may be attributed to the

synergistic contribution of its abundant phenolics, particularly catechin, caffeic acid, and quercetin. These compounds are recognised as MMP inhibitors, acting through zinc chelation at the catalytic site of collagenase, as well as by modulating signalling pathways such as NF-κB and MAPKs that regulate MMP expression (Staniforth et al., 2012). This mechanistic explanation is consistent with the strong radical scavenging capacity observed in the DPPH assay, suggesting overlapping antioxidant and anti-collagenase mechanisms.

In contrast, Tw showed comparatively lower inhibition, which may reflect its bioactivity being driven mainly by carotenoids rather than phenolics. Although carotenoids such as fucoxanthin have demonstrated antioxidant and potential anti-MMP effects (Lee et al., 2024), their inhibitory efficiency against collagenase may be weaker, mechanistically distinct from that of phenolics and flavonoids, or require higher concentrations to achieve comparable effects. Overall, both extracts exhibited strong anti-collagenase activity, but SC consistently outperformed Tw due to its higher phenolic diversity and content. These highlight the value of combining microalgal extracts with complementary phytochemical profiles, as in SC, to achieve enhanced antioxidant and anti-collagenase activity. Such properties reinforce the potential of both extracts, particularly SC, as functional ingredients in dermocosmetic formulations targeting oxidative stress, collagen degradation, and photoaging.

Physicochemical Properties of the Formulated Creams

Five creams were formulated using different microalgal strains and concentrations: a control without microalgae; 1% Tw (Tw1); 2.5% Tw (Tw2); 1% SC (SC1); and 2.5% SC (SC2). Distinct visual differences were observed among formulations (Figure 5). The control cream remained white, while Tw1 appeared yellow and SC1 pale green. At higher concentrations, Tw2 and SC2 developed a darker green colouration, reflecting the higher pigment load. After 24 h incubation at 4 °C, all creams exhibited uniform odour and homogeneity, with smooth textures and pleasant, acceptable scents (Table 7).

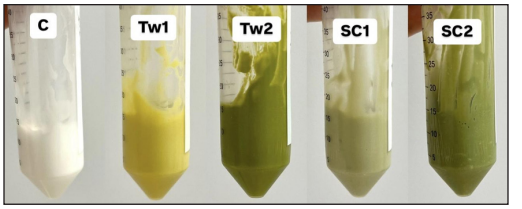

Figure 5. Colour differences of the formulated creams after 24-hour incubation. C: control cream (without algae); Tw1: 1% *Thalassiosira weisslflogii*; Tw2: 2.5% *Thalassiosira weisslflogii*; SC1: 1% combination of *Spirulina platensis* and *Chlorella vulgaris*; SC2: 2.5% combination of *Spirulina platensis* and *Chlorella vulgaris*

The physicochemical properties were strongly influenced by both algal type and concentration. Pigmentation was consistent with the known profiles of the respective species: *T. weissflogii* contains fucoxanthin and chlorophyll, producing yellow-brown hues, while *Spirulina* and *Chlorella vulgaris* are rich in phycocyanin and chlorophyll, respectively.

Table 7
Various physicochemical properties of the formulated creams after 24-hour incubation

Parameter	C	Tw1	Tw2	SC1	SC2
Colour	White	Yellow	Dark green	Pale green	Dark green
Odour	Acceptable	Acceptable	Acceptable	Acceptable	Acceptable
Homogeneity	Homogeneous	Homogeneous	Homogeneous	Homogeneous	Homogeneous
pH	6.47 ± 0.03a	6.53 ± 0.03a	6.03 ± 0.07b	6.47 ± 0.03a	6.07 ± 0.09b
Spreadability (cm)	3.63 ± 0.15a	3.07 ± 0.15b	2.43 ± 0.12c	3.47 ± 0.03 ab	3.03 ± 0.03b
Stability	No colour and odour changes; stable and no phase separation	No colour and odour changes; stable and no phase separation	No colour and odour changes; stable and no phase separation	No colour and odour changes; stable and no phase separation	No colour and odour changes; stable and no phase separation
Particle size (µm)	36.66 ± 0.89a	22.64 ± 1.01b	15.47 ± 0.39c	9.36 ± 0.02d	50.36 ± 1.46e

Note. C: control cream (without microalgae); Tw1: 1% *Thalassiosira weisslflogii*; Tw2: 2.5% *Thalassiosira weisslflogii*; SC1: 1% combination of *Spirulina platensis* and *Chlorella vulgaris*; SC2: 2.5% combination of *Spirulina platensis* and *Chlorella vulgaris*. Significant differences ($p < 0.05$) are indicated by different letters

Consequently, Tw-based creams (Tw1, Tw2) ranged from yellow to dark green, whereas SC-based creams (SC1, SC2) displayed pale to deep green shades. Increased extract concentration further intensified colouration, whereas the control cream remained pigment-free. Beyond colour, the formulations retained smooth and homogeneous textures, facilitating even distribution during application. The mild, naturally derived aroma from microalgae extracts, achieved without added fragrances, offers an advantage for users sensitive to synthetic scents, thereby supporting the broad acceptability of these formulations (Biswas et al., 2016).

As shown in Table 7, Tw2 (6.03) and SC2 (6.07) exhibited significantly lower pH values ($p < 0.05$) compared to other samples. In contrast, Control (6.47), Tw1 (6.53), and SC1 (6.47) did not differ significantly ($p > 0.05$) and showed higher pH values. A concentration-dependent trend was evident, with higher microalgal content lowering pH. Importantly, all formulations remained within the reported skin-compatible range (4.5-5.75), which is critical for maintaining barrier function, hydration, and microbial balance (Paramanya et al., 2024). Spreadability also declined with higher extract concentrations. Tw2 showed the lowest value (2.43 ± 0.12 cm), while the control exhibited the highest (3.63 ± 0.15 cm). This reduction is likely attributed to increased viscosity from the extracts. Nonetheless, all formulations remained within the acceptable cosmetic range of 18.33-32.33 mm (Fatima et al., 2017), ensuring ease of application. Physical stability was further confirmed by freeze-thaw and centrifugation tests. None of the formulations showed changes in colour, odour, or phase separation after stress cycles. This stability under thermal and mechanical stress highlights the structural robustness and suitability of the creams for topical application.

Based on Table 7, different microalgae strains and concentrations show no direct correlation with the resulting particle size. The higher concentration of Tw resulted in a reduced particle size, while the higher concentration of SC resulted in an increased particle size. Subsequently, SC1 exhibited the lowest ($p < 0.05$) particle size (9.36 μm) among the other samples, suggesting it can be most easily absorbed by the skin. In contrast, SC2 showed the highest ($p < 0.05$) particle size (50.36 μm), indicating that more time is required for absorption by the skin. Moreover, Tw2, Tw1, and Control exhibited moderate ($p < 0.05$) particle sizes, which were 15.47, 22.64, and 36.66 μm, respectively, suggesting they are less effective at being absorbed by the skin than SC1, even though they are more optimal than SC2. Although optimal transdermal penetration is often associated with nanoscale particle sizes (~100 nm), which facilitate absorption through hair follicles (Adib et al., 2016), the creams formulated in this study exceeded that threshold. Larger particle sizes may reduce penetration efficiency and slow down active delivery; however, they can still provide significant topical benefits. These include forming an occlusive layer that reduces transepidermal water loss and releasing bioactive compounds at the stratum corneum, where antioxidant and anti-aging effects remain highly relevant (Hoang et al., 2021). Thus, even without deep skin penetration, the formulations may effectively deliver surface-level efficacy. Nonetheless, future optimisation using advanced technologies such as high-pressure homogenisation, spray drying, or supercritical anti-solvent processing (Kumar et al., 2022b) could further reduce particle size and improve skin absorption.

At low shear rates (~0.1 s^{-1}), Control exhibited the highest viscosity (~240,000 cP; $p < 0.05$), followed by Tw2 (~180,000-200,000 cP). Tw1, SC1, and SC2 showed slightly lower values (~120,000-150,000 cP; $p > 0.05$). At moderate shear rates (1-10 s^{-1}), viscosities narrowed, but Control and Tw2 remained higher, while Tw1, SC1, and SC2 were consistently lower. Under high shear (≈100 s^{-1}), all formulations converged within 500-2,000 cP, indicating comparable performance during application (Figure 6). The lower viscosity values suggest higher water content, contributing to faster skin absorption, though no direct correlation between microalgal strain/concentration and viscosity was observed. Nonetheless, all formulations demonstrated pseudoplastic (shear-thinning) behaviour, with viscosity decreasing as shear rate increased. This flow profile is advantageous for topical products: high viscosity at rest ensures storage stability, while reduced viscosity under stress (e.g., spreading) enhances spreadability and even skin distribution (Deuschle et al., 2015). Differences in viscosity likely reflect extract composition. The higher values in TW may be linked to polysaccharide and protein content, which strengthen emulsion structure via water-binding and thickening effects. In contrast, SC1 and SC2 (Sp-Cv combination) maintained more balanced viscosities, possibly due to phycobiliproteins and chlorophyll derivatives that stabilise emulsions without excessive thickening (Morone et al., 2022). Importantly, all creams maintained high-shear viscosities within the acceptable cosmetic

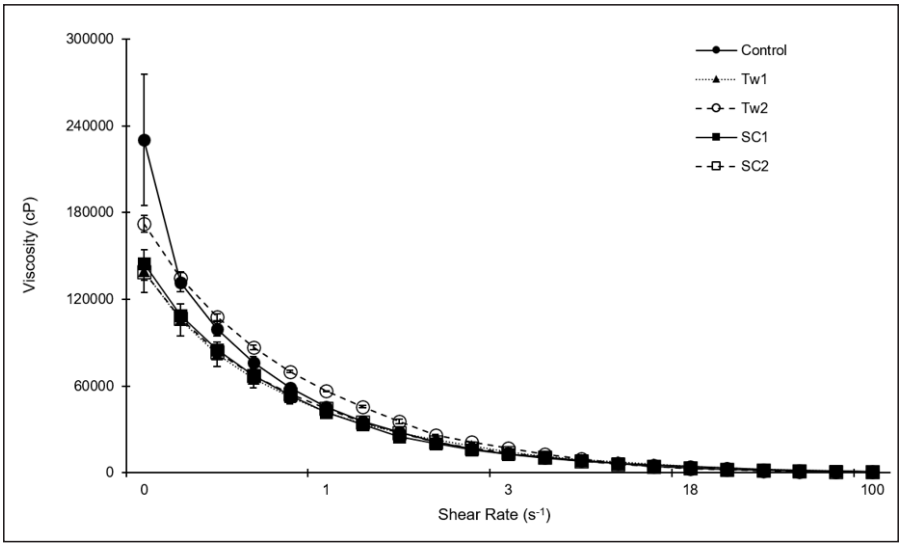

Figure 6. Viscosity of the formulated creams. Control cream (without algae); Tw1: 1% *Thalassiosira weisslflogii*; Tw2: 2.5% *Thalassiosira weisslflogii*; SC1: 1% combination of *Spirulina platensis* and *Chlorella vulgaris*; SC2: 2.5% combination of *Spirulina platensis* and *Chlorella vulgaris*

range (500-5,000 cP), ensuring consumer-friendly flow and effective skin adherence (Stabrauskiene et al., 2025). Overall, the rheological profiles confirm the creams' suitability for cosmeceutical use, balancing structural integrity with ease of application.

CONCLUSION

This study demonstrated the antioxidant and anti-aging potential of the diatom *Thalassiosira weissflogii* (Tw) and a mixed extract *of Spirulina* and *Chlorella vulgaris* (SC) through detailed phytochemical and bioactivity analyses. Tw was particularly rich in carotenoids, whereas SC contained higher levels of phenolics, with strong radical-scavenging and collagenase-inhibiting activities, indicating considerable potential for anti-aging efficacy. Notably, the SC extract exhibited a distinct, enriched bioactive profile, highlighting the potential of mixed-species approaches to enhance the functional properties of microalgal cosmeceutical ingredients. Both extracts were successfully incorporated into stable cream formulations with acceptable physicochemical properties, demonstrating their feasibility for topical use. Overall, these findings position Tw and SC as promising bioactive sources for developing natural cosmeceutical formulations targeting skin aging-related processes.

ACKNOWLEDGEMENT

The study was supported by Xiamen University Malaysia Research Fund (XMUMRF) Grant numbers: XMUMRF/2025-C16/ICAM/0021 and XMUMRF/2022-C10/ICAM/0010.

CONFLICT OF INTEREST

The authors declare that they have no known competing financial interests or personal relationships that could have appeared to influence the work reported in this paper.

REFERENCES

Abu-Serie, M. M., Habashy, N. H., & Attia, W. E. (2018). In vitro evaluation of the synergistic antioxidant and anti-inflammatory activities of the combined extracts from Malaysian *Ganoderma lucidum* and Egyptian *Chlorella vulgaris*. *BMC Complementary and Alternative Medicine, 18*(1), Article 154. https://doi.org/10.1186/s12906-018-2218-5

Adib, Z. M., Ghanbarzadeh, S., Kouhsoltani, M., Khosroshahi, A. Y., & Hamishehkar, H. (2016). The effect of particle size on the deposition of solid lipid nanoparticles in different skin layers: A histological study. *Advanced Pharmaceutical Bulletin, 6*(1), 31-36. https://doi.org/10.15171/apb.2016.06

Agregán, R., Munekata, P. E. S., Franco, D., Carballo, J., Barba, F. J., & Lorenzo, J. M. (2018). Antioxidant potential of extracts obtained from macro- (*Ascophyllum nodosum*, *Fucus vesiculosus*, and *Bifurcaria bifurcata*) and micro-algae (*Chlorella vulgaris* and *Spirulina platensis*) assisted by ultrasound. *Medicines, 5*(2), Article 33. https://doi.org/10.3390/medicines5020033

Al-Momani, R. M., Arabeyyat, Z. H., Malkawi, E. E., & Al-Zibdah, M. K. (2022). Formulation and evaluation of herbal antioxidant face cream using extract of the marine seaweed *Sargassum* spp. (Phaeophyceae). *Journal of Research in Pharmacy, 26*(4), 828-833. https://dergipark.org.tr/tr/download/article-file/4826778

Amrutkar, P. R., Borikar, S. P., Chaudhari, V. A., Badgujar, N. D., & Bhamre, R. D. (2020). Formulation and evaluation of photo-aging face gel by using algae powder extract (*Chlorella vulgaris*). *International Journal of Current Innovation Research and Advanced Studies, 2*(12), 17-24. http://ijciras.com/PublishedPaper/IJCIRAS1573.pdf

Arrari, F., Jabri, M.-A., Ayari, A., Dakhli, N., Ben Fayala, C., Boubaker, S., & Sebai, H. (2023). Chromatographic analyses of *Spirulina* (*Arthrospira platensis*) and mechanism of its protective effects against experimental obesity and hepatic steatosis in rats. *Medicina, 59*(10), Article 1823. https://doi.org/10.3390/medicina59101823

Ashashalini, Ali, M. S., Anuradha, V., Suganya, V., & Bhuvana, P. (2019). Estimation of total phenolic, flavonoid and antioxidant of methanolic extract of *Thalassiosira weissflogii*. *World Journal of Pharmaceutical Research, 8*(7), 1463-1481. https://www.wjpr.net/abstract_file/12497

Balboa, E., Conde, E., Constenla, A., Falqué, E., & Domínguez, H. (2017). Sensory evaluation and oxidative stability of a suncream formulated with thermal spring waters from Ourense (NW Spain) and *Sargassum muticum* extracts. *Cosmetics, 4*(2), Article 19. https://doi.org/10.3390/cosmetics4020019

Biswas, R., Mukherjee, P. K., Kar, A., Bahadur, S., Harwansh, R. K., Biswas, S., Al-Dhabi, N. A., & Duraipandiyan, V. (2016). Evaluation of Ubtan - A traditional Indian skin care formulation. *Journal of Ethnopharmacology, 192*, 283-291. https://doi.org/10.1016/j.jep.2016.07.034

Budzianowska, A., Banaś, K., Budzianowski, J., & Kikowska, M. (2025). Antioxidants to defend healthy and youthful skin—Current trends and future directions in cosmetology. *Applied Sciences, 15*(5), Article 2571. https://doi.org/10.3390/app15052571

Chen, M. X., Alexander, K. S., & Baki, G. (2016). Formulation and evaluation of antibacterial creams and gels containing metal ions for topical application. *Journal of Pharmaceutics, 2016*(1), Article 5754349. https://doi.org/10.1155/2016/5754349

Chinjoo, N., & Golzary, A. (2025). Microalgae: Revolutionizing skin repair and enhancement. *Biotechnology Reports, 47*, Article e00911. https://doi.org/10.1016/j.btre.2025.e00911

Choi, J. -S., Moon, W. S., Choi, J. N., Do, K. H., Moon, S. H., Cho, K. K., Han, C. -J., & Choi, I. S. (2013). Effects of seaweed *Laminaria japonica* extracts on skin moisturizing activity in vivo. *Journal of Cosmetic Science, 64*(3), 193-205. https://pubmed.ncbi.nlm.nih.gov/23752034/

Chu, C. C., & Nyam, K. L. (2020). Kenaf (*Hibiscus cannabinus* L.) seed oil: Application as cosmetic product ingredients. *Industrial Crops and Products, 156*, Article 112871. https://doi.org/10.1016/j.indcrop.2020.112871

Cokdinleyen, M., Alvarez-Rivera, G., Tejera, J. L. G., Mendiola, J. A., Valdés, A., Kara, H., Ibáñez, E., & Cifuentes, A. (2024). *Tetraselmis chuii* edible microalga as a new source of neuroprotective compounds obtained using fast biosolvent extraction. *International Journal of Molecular Sciences, 25*(7), Article 3897. https://doi.org/10.3390/ijms25073897

Cubero-Cardoso, J., Eibes, G., & Carballa, M. (2024). Exploring macroalgae biorefinery: Extraction of bioactive compounds and production of volatile fatty acids. *Environmental Research, 263*(Part 1), Article 120008. https://doi.org/10.1016/j.envres.2024.120008

Dąbrowska, A. K., Rotaru, G. -M., Derler, S., Spano, F., Camenzind, M., Annaheim, S., Stämpfli, R., Schmid, M., & Rossi, R. M. (2015). Materials used to simulate physical properties of human skin. *Skin Research and Technology, 22*(1), 3-14. https://doi.org/10.1111/srt.12235

Dammak, M., Ben Hlima, H., Smaoui, S., Fendri, I., Michaud, P., Ayadi, M. A., & Abdelkafi, S. (2022). Conception of an environmentally friendly O/W cosmetic emulsion from microalgae. *Environmental Science and Pollution Research, 29*(49), 73896-73909. https://doi.org/10.1007/s11356-022-20824-8

Daudt, R. M., Back, P. I., Cardozo, N. S. M., Marczak, L. D. F., & Külkamp-Guerreiro, I. C. (2015). *Pinhão* starch and coat extract as new natural cosmetic ingredients: Topical formulation stability and sensory analysis. *Carbohydrate Polymers, 134*, 573-580. https://doi.org/10.1016/j.carbpol.2015.08.038

Deuschle, V. C. K. N., Deuschle, R. A. N., Bortoluzzi, M. R., & Athayde, M. L. (2015). Physical chemistry evaluation of stability, spreadability, in vitro antioxidant, and photo-protective capacities of topical formulations containing *Calendula officinalis* L. leaf extract. *Brazilian Journal of Pharmaceutical Sciences, 51*(1), 63-75. https://doi.org/10.1590/S1984-82502015000100007

Falcao, B., Vishwakarma, J., Jadav, H., & Vavilala, S. L. (2020). In vitro evaluation of the antioxidant and anti-skin aging properties of green algal sulfated polysaccharides. *Archives of Microbiology & Immunology, 4*(2), 75-90. https://doi.org/10.26502/ami.93650047

Farahin, A. W., Yusoff, F. M., Basri, M., Nagao, N., & Shariff, M. (2019). Use of microalgae: *Tetraselmis tetrathele* extract in formulation of nanoemulsions for cosmeceutical application. *Journal of Applied Phycology, 31*, 1743-1752. https://doi.org/10.1007/s10811-018-1694-9

Fatima, S., Zaman, R., Haider, N., Shamsi, S., & Alam, A. (2017). Design and development of Unani anti-inflammatory cream. *Journal of Ayurveda and Integrative Medicine, 8*(3), 140-144. https://doi.org/10.1016/j.jaim.2017.03.002

Garcia, M. P., Regueiras, A., Lopes, G., Matos, G., da Silva, L. P., Cerqueira, M. T., Cardoso, H., Correia, N., Saraiva, J. A., Silva, J. L., Martins, R., & Marques, A. P. (2024). Nonthermal high-pressure microalgae extracts: A new source of natural ingredients for cosmetics. *Algal Research, 81*, Article 103591. https://doi.org/10.1016/j.algal.2024.103591

Georgiopoulou, I., Tzima, S., Pappa, G. D., Louli, V., Voutsas, E., & Magoulas, K. (2022). Experimental design and optimisation of recovering bioactive compounds from *Chlorella vulgaris* through conventional extraction. *Molecules, 27*(1), Article 29. https://doi.org/10.3390/molecules27010029

Guldas, M., Ziyanok-Demirtas, S., Sahan, Y., Yildiz, E., & Gurbuz, O. (2020). Antioxidant and anti-diabetic properties of *Spirulina platensis* produced in Turkey. *Food Science and Technology, 41*(3), 615-625. https://doi.org/10.1590/fst.23920

Havas, F., Krispin, S., Cohen, M., Loing, E., Farge, M., Suere, T., & Attia-Vigneau, J. (2022). A *Dunaliella salina* extract counteracts skin aging under intense solar irradiation thanks to its antiglycation and anti-inflammatory properties. *Marine Drugs, 20*(2), Article 104. https://doi.org/10.3390/md20020104

Hejna, M., Dell'Anno, M., Liu, Y., Rossi, L., Aksmann, A., Pogorzelski, G., & Jóźwik, A. (2024). Assessment of the antibacterial and antioxidant activities of seaweed-derived extracts. *Scientific Reports, 14*, Article 21044. https://doi.org/10.1038/s41598-024-71961-8

Hermund, D. B., Heung, S. Y., Thomsen, B. R., Akoh, C. C., & Jacobsen, C. (2018). Improving oxidative stability of skin care emulsions with antioxidant extracts from brown alga *Fucus vesiculosus*. *Journal of the American Oil Chemists' Society, 95*(12), 1509-1520. https://doi.org/10.1002/aocs.12156

Hermund, D. B., Torsteinsen, H., Vega, J., Figueroa, F. L., & Jacobsen, C. (2022). Screening for new cosmeceuticals from brown algae *Fucus vesiculosus* with antioxidant and photo-protecting properties. *Marine Drugs, 20*(11), Article 687. https://doi.org/10.3390/md20110687

Hoang, H. T., Moon, J. -Y., & Lee, Y. -C. (2021). Natural antioxidants from plant extracts in skincare cosmetics: Recent applications, challenges and perspectives. *Cosmetics, 8*(4), Article 106. https://doi.org/10.3390/cosmetics8040106

Hwang, E., Park, S. -Y., Lee, H. J., Lee, T. Y., Sun, Z. -w., & Yi, T. H. (2014). Gallic acid regulates skin photoaging in UVB-exposed fibroblasts and hairless mice. *Phytotherapy Research, 28*(12), 1778-1788. https://doi.org/10.1002/ptr.5198

Jaeschke, D. P., Menegol, T., Rech, R., Mercali, G. D., & Marczak, L. D. F. (2016). Carotenoid and lipid extraction from *Heterochlorella luteoviridis* using moderate electric field and ethanol. *Process Biochemistry, 51*(10), 1636-1643. https://doi.org/10.1016/j.procbio.2016.07.016

Jesus, A., Ratanji, S., Cidade, H., Sousa, E., Cruz, M. T., Oliveira, R., & Almeida, I. F. (2025). Phenolics as active ingredients in skincare products: A myth or reality? *Molecules, 30*(7), Article 1423. https://doi.org/10.3390/molecules30071423

Józsa, L., Ujhelyi, Z., Vasvári, G., Sinka, D., Nemes, D., Fenyvesi, F., Váradi, J., Vecsernyés, M., Szabó, J., Kalló, G., Vasas, G., Bácskay, I., & Fehér, P. (2020). Formulation of creams containing *Spirulina platensis* powder with different nonionic surfactants for treatment of acne vulgaris. *Molecules, 25*(20), Article 4856. https://doi.org/10.3390/molecules25204856

Katayama, T., Rahman, N. A., Khatoon, H., Kasan, N. A., Nagao, N., Yamada, Y., Takahashi, K., Furuya, K., Wahid, M. E. A., Yusoff, F. M., & Jusoh, M. (2022). Bioprospecting of tropical microalgae for high-

value products: n-3 polyunsaturated fatty acids and carotenoids. *Aquaculture Reports, 27*, Article 101406. https://doi.org/10.1016/j.aqrep.2022.101406

Kumar, A., Ramamoorthy, D., Verma, D. K., Kumar, A., Kumar, N., Kanak, K. R., Marwein, B. M., & Mohan, K. (2022a). Antioxidant and phytonutrient activities of *Spirulina platensis*. *Energy Nexus, 6*, Article 100070. https://doi.org/10.1016/j.nexus.2022.100070

Kumar, R., Thakur, A. K., Chaudhari, P., & Banerjee, N. (2022b). Particle size reduction techniques of pharmaceutical compounds for enhancement of dissolution rate and bioavailability. *Journal of Pharmaceutical Innovation, 17*(2), 333-352. https://doi.org/10.1007/s12247-020-09530-5

Lee, H., Jang, H., Heo, D., Eom, J.-I., Han, C.-H., Kim, S.-M., Shin, Y.-S., Pan, C.-H., & Yang, S. (2024). *Tisochrysis lutea* fucoxanthin suppresses NF-κB, JNK, and p38-associated MMP expression in arthritis pathogenesis via antioxidant activity. *Antioxidants, 13*(8), Article 941. https://doi.org/10.3390/antiox13080941

Leelapornpisid, P., Mungmai, L., Sirithunyalug, B., Jiranusornkul, S., & Peerapornpisal, Y. (2014). A novel moisturiser extracted from freshwater macroalga [*Rhizoclonium hieroglyphicum* (C. Agardh) *Kützing*] for skincare cosmetic. *Chiang Mai Journal of Science, 41*(5/2), 1195-1207. https://epg.science.cmu.ac.th/ejournal/journal-detail.php?id=5274

Lichtenthaler, H. K. (1987). Chlorophyll and carotenoid determination (after Lichtenthaler 1987): A practical instruction. *Methods in Enzymology, 148*, 350-382. https://doi.org/10.1016/0076-6879(87)48036-1

Lin, F.-H., Lin, J.-Y., Gupta, R. D., Tournas, J. A., Burch, J. A., Selim, M. A., Monteiro-Riviere, N. A., Grichnik, J. M., Zielinski, J., & Pinnell, S. R. (2005). Ferulic acid stabilises a solution of vitamins C and E and doubles its photoprotection of skin. *Journal of Investigative Dermatology, 125*(4), 826-832. https://doi.org/10.1111/j.0022-202X.2005.23768.x

Maoka, T. (2011). Carotenoids in marine animals. *Marine Drugs, 9*(2), 278-293. https://doi.org/10.3390/md9020278

Masoumifeshani, B., Abedian Kenari, A., Sottorff, I., Crüsemann, M., & Amiri Moghaddam, J. (2025). Identification and evaluation of antioxidant and anti-aging peptide fractions from enzymatically hydrolyzed proteins of *Spirulina platensis* and *Chlorella vulgaris*. *Marine Drugs, 23*(4), Article 162. https://doi.org/10.3390/md23040162

Matas, R. F., Popović, M., Čagalj, M., & Šimat, V. (2023). The marine diatom *Thalassiosira rotula*: Chemical profile and antioxidant activity of hydroalcoholic extracts. *Frontiers in Marine Science, 10*, Article 1221417. https://doi.org/10.3389/fmars.2023.1221417

Matin, M., M., Koszarska, M., Atanasov, A. G., Król-Szmajda, K., Jóźwik, A., Stelmasiak, A., & Hejna, M. (2024). Bioactive potential of algae and algae-derived compounds: Focus on anti-inflammatory, antimicrobial, and antioxidant effects. *Molecules, 29*(19), Article 4695. https://doi.org/10.3390/molecules29194695

Mawazi, S. M., Ann, J., Othman, N., Khan, J., Alolayan, S. O., Al Thagfan, S. S., & Kaleemullah, M. (2022). A review of moisturisers: History, preparation, characterization and applications. *Cosmetics, 9*(3), Article 61. https://doi.org/10.3390/cosmetics9030061

Miettinen, M., Mönkkönen, J., Lahtinen, M. -R., Nuutinen, J., & Lahtinen, T. (2006). Measurement of oedema in irritant-exposed skin by a dielectric technique. *Skin Research and Technology, 12*(4), 235-240. https://doi.org/10.1111/j.0909-752X.2006.00162.x

Mojica, C. V., Pasol, E. A., Dizon, M. L., Kiat Jr., W. A., Lim, T. R. U., Dominguez, J. C., Valencia, V. V., & Tuaño, B. J. P. (2020). Chronic methanol toxicity through topical and inhalational routes presenting as vision loss and restricted diffusion of optic nerves on MRI: A case report and literature review. *eNeurologicalSci, 20*, Article 100258. https://doi.org/10.1016/j.ensci.2020.100258

Montalvo, G. E. B., Thomaz-Soccol, V., Vandenberghe, L. P. S., Carvalho, J. C., Faulds, C. B., Bertrand, E., Prado, M. R. M., Bonatto, S. J. R., & Soccol, C. R. (2019). *Arthrospira maxima* OF15 biomass cultivation at laboratory and pilot scale from sugarcane vinasse for new peptide production. *Bioresource Technology, 273*, 103-113. https://doi.org/10.1016/j.biortech.2018.10.081

Morone, J., Lopes, G., Morais, J., Neves, J., Vasconcelos, V., & Martins, R. (2022). Cosmetic application of cyanobacteria extracts with a sustainable vision to skincare: Role in the antioxidant and antiaging process. *Marine Drugs, 20*(12), Article 761. https://doi.org/10.3390/md20120761

Mourelle, M. L., Segura de Yebra, J., Ayats, J., Vitale, M., & López Sánchez, A. (2024). Potential benefits of a cosmetic ingredient combining thermal spring water and diatom algae extract. *Cosmetics, 11*(2), Article 62. https://doi.org/10.3390/cosmetics11020062

Nascimento, T. C. d., Cazarin, C. B. B., Maróstica Jr., M. R., Mercadante, A. Z., Jacob-Lopes, E., & Zepka, L. Q. (2019). Microalgae carotenoids intake: Influence on cholesterol levels, lipid peroxidation and antioxidant enzymes. *Food Research International, 128*, Article 108770. https://doi.org/10.1016/j.foodres.2019.108770

Natrah, F. M. I., Yusoff, F. M., Shariff, M., Abas, F., & Mariana, N. S. (2007). Screening of Malaysian indigenous microalgae for antioxidant properties and nutritional value. *Journal of Applied Phycology, 19*, 711-718. https://doi.org/10.1007/s10811-007-9192-5

Pantami, H. A., Ahamad Bustamam, M. S., Lee, S. Y., Ismail, I. S., Mohd Faudzi, S. M., Nakakuni, M., & Shaari, K. (2020). Comprehensive GCMS and LC-MS/MS Metabolite Profiling of Chlorella vulgaris. *Marine Drugs, 1*8(7), Article 367. https://doi.org/10.3390/md18070367

Papaioanou, M., Chronopoulou, E. G., Ciobotari, G., Efrose, R. C., Sfichi-Duke, L., Chatzikonstantinou, M., Pappa, E., Ganopoulos, I., Madesis, P., Nianiou-Obeidat, I., Zeng, T., & Labrou, N. E. (2018). Cosmeceutical properties of two cultivars of red raspberry grown under different conditions. *Cosmetics, 5*(1), Article 20. https://doi.org/10.3390/cosmetics5010020

Paramanya, A., Abdoul Latif, F. M., & Ali, A. (2024). Analysis of antioxidant, antityrosinase and antiglycating properties of a blue-green algae-based skin cream. *Annals of Phytomedicine, 13*(1), 621-630.

Pittayapruek, P., Meephansan, J., Prapapan, O., Komine, M., & Ohtsuki, M. (2016). Role of matrix metalloproteinases in photoaging and photocarcinogenesis. *International Journal of Molecular Sciences, 17*(6), Article 868. https://doi.org/10.3390/ijms17060868

Poulose, N., Sajayan, A., Ravindran, A., Sreechithra, T. V., Vardhan, V., Selvin, J., & Kiran, G. S. (2020). Photoprotective effect of nanomelanin-seaweed concentrate in formulated cosmetic cream: With improved antioxidant and wound healing properties. *Journal of Photochemistry and Photobiology B: Biology, 205*, Article 111816. https://doi.org/10.1016/j.jphotobiol.2020.111816

Ragusa, I., Nardone, G. N., Zanatta, S., Bertin, W., & Amadio, E. (2021). *Spirulina* for skin care: A bright blue future. *Cosmetics, 8*(1), Article 7. https://doi.org/10.3390/cosmetics8010007

Rahim, A., Çakir, C., Ozturk, M., Şahin, B., Soulaimani, A., Sibaoueih, M., Nasser, B., Eddoha, R., Essamadi, A., & El Amiri, B. (2021). Chemical characterization and nutritional value of *Spirulina platensis* cultivated in natural conditions of Chichaoua region (Morocco). *South African Journal of Botany, 141*, 235-242. https://doi.org/10.1016/j.sajb.2021.05.006

Rahman, N. A., Katayama, T., Wahid, M. E. A., Kasan, N. A., Khatoon, H., Yamada, Y., & Takahashi, K. (2020). Taxon- and growth-phase-specific antioxidant production by chlorophyte, bacillariophyte, and haptophyte strains isolated from tropical waters. *Frontiers in Bioengineering and Biotechnology, 8*, Article 581628. https://doi.org/10.3389/fbioe.2020.581628

Rico, M., López, A., Santana-Casiano, J. M., González, A. G., & González-Dávila, M. (2012). Variability of the phenolic profile in the diatom *Phaeodactylum tricornutum* under copper and iron stress. *Limnology and Oceanography, 58*(1), 144-152. https://doi.org/10.4319/lo.2013.58.1.0144

Ruf, J., Menrad, K., & Emberger-Klein, A. (2024). The local range of natural cosmetics: Consumer perceptions and assessments in Germany. *Business Strategy and the Environment, 33*(7), 7462-7478. https://doi.org/10.1002/bse.3862

Serra, A. T., Silva, S. D., Pleno de Gouveia, L., Alexandre, A. M. R. C., Pereira, C. V., Pereira, A. B., Partidário, A. C., Silva, N. E., Bohn, T., Gonçalves, V. S. S., Real, G., Escudero, P., Fernández, N., Matias, A. A., & Bronze, M. R. (2021). A single dose of marine *Chlorella vulgaris* increases plasma concentrations of lutein, β-carotene, and zeaxanthin in healthy male volunteers. *Antioxidants, 10*(8), Article 1164. https://doi.org/10.3390/antiox10081164

Shatalebi, M. A., Jazi, S. B., Yegdaneh, A., Iraji, F., Siadat, A. H., & Noorshargh, P. (2020). Comparative evaluation of *Gracilaria* algae 3% cream vs. clobetasol 0.05% cream in plaque-type psoriasis: A randomized, split-body, triple-blinded clinical trial. *Dermatologic Therapy, 33*(6), Article e14317. https://doi.org/10.1111/dth.14317

Srisuksomwong, P., Kaenhin, L., & Mungmai, L. (2023). Collagenase and tyrosinase inhibitory activities and stability of facial cream formulation containing cashew leaf extract. *Cosmetics, 10*(1), Article 17. https://doi.org/10.3390/cosmetics10010017

Stabrauskiene, J., Mazurkevičiūtė, A., Majiene, D., Balanaskiene, R., & Bernatoniene, J. (2025). Development and evaluation of an anti-inflammatory emulsion: Skin penetration, physicochemical properties, and fibroblast viability assessment. *Pharmaceutics, 17*(7), Article 933. https://doi.org/10.3390/pharmaceutics17070933

Staniforth, V., Huang, W. -C., Aravindaram, K., & Yang, N. -S. (2012). Ferulic acid, a phenolic phytochemical, inhibits UVB-induced matrix metalloproteinases in mouse skin via post-translational mechanisms. *Journal of Nutritional Biochemistry, 23*(5), 443-451. https://doi.org/10.1016/j.jnutbio.2011.01.009

Susano, P., Silva, J., Alves, C., Martins, A., Gaspar, H., Pinteus, S., Mouga, T., Goettert, M. I., Petrovski, Ž., Branco, L. B., & Pedrosa, R. (2021). Unravelling the dermatological potential of the brown seaweed *Carpomitra costata*. *Marine Drugs, 19*(3), Article 135. https://doi.org/10.3390/md19030135

Tafuro, G., Di Domenico, E., Costantini, A., Francescato, S., Busata, L., Baratto, G., & Semenzato, A. (2022). Stability and application properties of surfactant-free cosmetic emulsions: An instrumental approach to evaluate their potential. *Cosmetics, 9*(6), Article 123. https://doi.org/10.3390/cosmetics9060123

Tavakoli, S., Hong, H., Wang, K., Yang, Q., Gahruie, H. H., Zhuang, S., Li, Y., Liang, Y., Tan, Y., & Luo, Y. (2021). Ultrasonic-assisted food-grade solvent extraction of high-value added compounds from microalgae *Spirulina platensis* and evaluation of their antioxidant and antibacterial properties. *Algal Research, 60*, Article 102493. https://doi.org/10.1016/j.algal.2021.102493

Tompkins, J., De Ville, M., Day, J. G., & Turner, M. F. (1995). *Culture collection of algae & protozoa: Catalogue of strains*. Titus Wilson and Son Ltd.

Tsai, C. -F., Lu, F. -J., & Hsu, Y. -W. (2012). Protective effects of *Dunaliella salina*—a carotenoid-rich alga—against ultraviolet B-induced corneal oxidative damage in mice. *Molecular Vision, 18*, 1540-1547. https://pmc.ncbi.nlm.nih.gov/articles/PMC3380915/

Tutun, H., & Yipel, M. (2024). Phenolic acids as potent antioxidant agents. In *Advancement of Phenolic Acids in Drug Discovery* (pp. 145-175). Elsevier. https://doi.org/10.1016/B978-0-443-18538-0.00003-2

Tuzen, M., & Ozdemir, M. (2003). Chromatographic determination of phenolic acids in the snowdrop by HPLC. *Turkish Journal of Chemistry, 27*(1), 49-54. https://journals.tubitak.gov.tr/chem/vol27/iss1/8/

Uzlaşır, T., Selli, S., & Kelebek, H. (2024). *Spirulina platensis* and *Phaeodactylum tricornutum* as sustainable sources of bioactive compounds: Health implications and applications in the food industry. *Future Postharvest Food, 1*(1), 34-46. https://doi.org/10.1002/fpf2.12008

Xue, N., Liu, Y., Jin, J., Ji, M., & Chen, X. (2022). Chlorogenic acid prevents UVA-induced skin photoaging through regulating collagen metabolism and apoptosis in human dermal fibroblasts. *International Journal of Molecular Sciences, 23*(13), Article 6941. https://doi.org/10.3390/ijms23136941

Yarkent, Ç., Gürlek, C., & Oncel, S. S. (2020). Potential of microalgal compounds in trending natural cosmetics: A review. *Sustainable Chemistry and Pharmacy, 17*, Article 100304. https://doi.org/10.1016/j.scp.2020.100304

Zakaria, S. M., Kamal, S. M. M., Harun, R., Omar, R., & Siajam, S. I. (2020). Characterization of phenolic acids and antioxidant activity of microalgae *Chlorella* sp. using subcritical water extraction. *Sains Malaysiana, 49*(4), 765-774. https://doi.org/10.17576/jsm-2020-4904-05

Pertanika J. Trop. Agric. Sci. 49 (5): 2439 - 2460 (2026)

PERTANIKA JOURNALS

TROPICAL AGRICULTURAL SCIENCE

Journal homepage: http://www.pertanika.upm.edu.my/

Combination Effects of Cocopeat and Chicken Manure on the Vegetative Growth and Yield Performance of Eggplant

Kahar*, Rian Christian Sondakh, and Irmawati

Department of Agrotechnology, Faculty of Agriculture, Madako Tolitoli University, 94516 Tolitoli, Indonesia

ABSTRACT

Eggplant (*Solanum melongena* L.) growth and productivity are influenced by growing-medium composition and nutrient availability. This study evaluated the effects of cocopeat and chicken manure combinations on purple eggplant growth and yield. The experiment was conducted from May to July 2022 at Madako University, Tolitoli, Indonesia, using a randomised block design with five treatments and three replications: C0 (control), C1 (25 g cocopeat + 150 g chicken manure), C2 (50 g + 200 g), C3 (75 g + 250 g), and C4 (100 g + 300 g), comprising 45 experimental units. Parameters included plant height, leaf number, flowering time, productive branches, fruit number, fruit length, diameter, and weight. At six weeks after planting, C4 recorded the highest numerical plant height (48.40 cm), compared with 33.39 cm in the control. C4 also produced the earliest flowering (38 days after planting) and five productive branches, compared with 47 days and two branches in the control, respectively. Fruit length in amended treatments ranged from 19.7 to 21.0 cm, while fruit weight generally exceeded that of the control. Treatment responses varied across parameters and harvesting periods. Although C4 showed favorable results for several characteristics, it was not consistently superior. Further research is needed to confirm statistical differences and evaluate economic feasibility before practical recommendations can be established.

Keywords: Coconut fiber, coconut waste, horticulture, kohe

ARTICLE INFO

Article history:
Received: 24 November 2025
Accepted: 16 October 2026
Published: 30 October 2026

DOI: https://doi.org/10.47836/pjtas.49.5.16

E-mail addresses:
kahar@umada.ac.id (Kahar)
riansondakh@umada.ac.id (Rian Christian Sondakh)
irmawati_agrotek@umada.ac.id (Irmawati)
* Corresponding author

INTRODUCTION

Eggplant (*Solanum melongena* L.) is an important horticultural crop grown for its agricultural and economic value. Its growth and productivity are influenced by genetic characters, environmental conditions, properties of the growing medium and nutrient management. Availability of

© Universiti Putra Malaysia Press

adequate nutrients and root zone conditions are essential to support vegetative growth, flowering, fruit formation and fruit development (Putra et al., 2025). Hence, suitable growing-medium amendments and proper nutrient management strategies are essential for boosting eggplant growth and productivity, while also protecting soil quality and fostering sustainable crop production (Mansurat et al., 2023).

Interest in using organic amendments to improve crop production and promote more sustainable nutrient management is increasing. Cocopeat is a fine material derived from coconut husk. It can be used as a component of the growing medium because of its water-holding capacity and its influence on the substrate's physical properties. Meanwhile, chicken manure provides organic matter and plant nutrients that support crop growth. Meanwhile, chicken manure provides organic matter and plant nutrients that can promote crop growth. Cocopeat and organic manure have been investigated for horticultural production. For example, Sanyang et al. (2025) how different organic fertilisers affect the growth and yield potential of eggplant and other vegetable crops. The use of cocopeat and manure for chili pepper planting was studied by Nasution & Tammin T. (2022). These studies give relevant information for the study of organic amendments, but results from other crops and growing conditions cannot be directly extrapolated to purple eggplant.

Recent research further demonstrated the importance of evaluating organic fertilisation strategies, particularly for eggplant. Ramadhan et al. (2024) studied the compost and digestate in combination with plant-based and microbial biostimulants. The results indicated that the fertilisation strategies affected the productivity of eggplant and the biostimulant treatments affected some selected characteristics of fruit quality. The study underscores the need to evaluate organic nutrient management practices in terms of specific agronomic outcomes. However, its emphasis on compost, digestate and biostimulants is different from the cocopeat and chicken manure combination evaluated in the present study.

Although the use of organic amendments in eggplant production is increasingly being considered, the response to a specific combination of cocopeat and chicken manure needs further assessment under specific growing conditions. Particularly, the performance of different combinations of applications should be compared based on vegetative growth and fruit-related parameters rather than a single growth parameter. However, the interpretation of these responses should also be based on the experimental conditions and the possibility of different plant characteristics responding differently to the same combination of amendments (Mostfa et al., 2025).

Therefore, the present study was conducted to evaluate five combinations of cocopeat and chicken manure, including an unamended control, on vegetative growth and yield-related characteristics of purple eggplant. The treatments were C0 (control), C1 (25 g cocopeat + 150 g chicken manure), C2 (50 g cocopeat + 200 g chicken manure), C3 (75 g cocopeat + 250 g chicken manure), and C4 (100 g cocopeat + 300 g chicken manure). We

measured plant height, number of leaves, flowering age, number of productive branches, number of fruits, fruit length, diameter, and fruit weight.

The contribution of this study is the evaluation of specific cocopeat - chicken manure combination treatments on multiple vegetative and reproductive parameters under the experimental conditions in Tolitoli, Indonesia. The study provides site-specific experimental evidence on the possible use of these organic materials in purple eggplant cultivation by comparing the responses among the five treatments. The combined treatments were analysed rather than the independent effects of each material because cocopeat and chicken manure rates were increased simultaneously. The results are intended to inform further research on organic growing-medium formulations and provide a basis for more comprehensive experiments involving separate amendment treatments, additional controls and evaluation across different growing environments.

Literature Review

Eggplant (*Solanum melongena* L.) is a widely cultivated vegetable crop of high nutritional value and economic importance. It has vital nutrients like dietary fiber, vitamins and minerals, which are beneficial for human health. Although eggplant has great potential for economic development and food security, its production is constrained by low soil fertility, traditional farming practices and overdependence on synthetic fertilisers. Park et al. (2024) extensive studies have found that prolonged use of chemical fertilisers affects the soil structure, drastically reduces microbial diversity, contaminates the groundwater and poses serious challenges to long-term environmental sustainability and crop production.

Cocopeat has been reported to improve root development, water-holding capacity and provide a good environment for plant growth, especially in dryland areas (Wu et al., 2025). Besides, cocopeat is an economical and eco-friendly option that can be a sustainable alternative to the traditional media for growing.

Knowledge of the interaction of these two materials is a prerequisite for the development of efficient and sustainable fertilisation strategies. The present study is therefore aimed at filling this gap by evaluating the combined effects of cocopeat and chicken manure on eggplant growth and yield to advance environmentally friendly agricultural methods. Previously, it has been shown that the use of chicken manure improves vegetative growth, flowering and yield of different crops, as in eggplant (Soares & Gomes, 2024). Too much can cause toxicity or nutrient imbalance. So the dose and the mixing with other ingredients are important.

The synergistic effect of combining organic compounds in plant growth promotion has been studied in recent years. It has been proven that cocopeat + chicken manure improves soil structure, nutrient availability and water retention capacity. This combination gives a healthy root-zone environment for efficient nutrient uptake and vegetative and reproductive

growth. Moreover, the interaction of organic matter and soil microorganisms has a significant effect on enhancing nutrient mineralisation and plant performance (Setiawan & Sudradjat, 2025).

Though the individual effects of cocopeat and organic fertilisers have been studied by a few researchers, little work has been done on the combined application of these materials, particularly when growing eggplants. It is necessary to understand the interaction between these two materials to be able to develop efficient and sustainable fertilisation strategies. Hence, the objective of this study was to fill this gap by assessing the combined effects of cocopeat and chicken manure on the growth and yield of eggplant, contributing to the progress of environmentally friendly agricultural methods.

MATERIALS AND METHODS

The experiment was conducted from May to July 2022 at the Experimental Land of the Faculty of Agriculture, Madako University, Tolitoli, Indonesia. This study was conducted to evaluate the effects of combinations of cocopeat and chicken manure on the vegetative growth and yield performance of purple eggplant (*Solanum melongena* L.).

The experiment was laid out in a Randomised Block design (RBD) with five treatments and three blocks, giving a total of 15 treatment-by-block experimental units. The treatments were C0 (control), C1 (25 g cocopeat + 150 g chicken manure), C2 (50 g cocopeat + 200 g chicken manure), C3 (75 g cocopeat + 250 g chicken manure), and C4 (100 g cocopeat + 300 g chicken manure). Each experimental unit was made up of three polybags, making a total of 45 polybags.

For statistical purposes, the experimental unit was defined as the smallest unit to which an independent assignment of a treatment could be made. If the three polybags within each treatment by block unit received the same treatment and had not been independently randomised, the three polybags were treated as subsamples, not independent experimental replicates. In this case, the observations in the three polybags must be averaged within each experimental unit before comparing treatments. This gives three independent replicates per treatment. This method avoids pseudoreplication and ensures that the statistical analysis reflects the true experimental design. Therefore, the number of independent replicates was three per treatment, as the three blocks were independently set up and treatments were randomised within each block. Experimental workflow can be seen at Figure 1.

Research Procedures

The research procedure started with the preparation of coconut fiber powder (cocopeat). The dried coconut fiber was cut into smaller pieces and brushed with a one- or two-directional wire brush to separate the fibers into a mixture of coarse fiber and fine powder. The mixture was then filtered to separate the fine powder from the coconut fiber. The cocopeat obtained was washed with clean water until the foam disappeared and then soaked in clean water

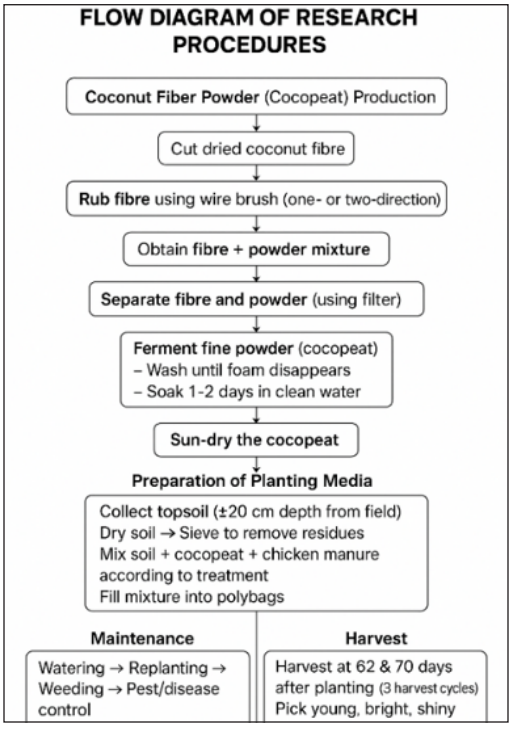

Figure 1. Experimental workflow for cocopeat preparation, growing-medium formulation, eggplant cultivation, and data collection under a randomised block design (RBD). The experiment consisted of five treatments and three blocks, with three polybags per treatment-by-block unit, for a total of 45 polybags

for 1-2 days. The cocopeat was soaked and then dried under the sun for use as part of the planting medium.

Topsoil was collected from approximately 20 cm depth, air-dried, and sieved to remove coarse materials. The prepared soil was used as the base growing medium in the polybags. The amount of topsoil in each polybag was 1.3 kg. The specified amount of soil was thoroughly mixed with the corresponding amount of cocopeat and chicken manure according to the assigned treatment. The control treatment (C0) was the base soil only without the supplement of cocopeat or chicken manure.

The growing media were prepared before the eggplant seedlings were transplanted. The mixture was packed in polybags, and the seedlings were transplanted and maintained under the same cultivation conditions. As required, watering, weeding and pest and disease control were carried out during the experimental period.

During the maintenance period, the plants were watered regularly as per their requirements. Where plants did not establish well, replanting was done as necessary. Weed control and pest and disease management were also carried out to maintain suitable growing conditions throughout the experiment.

Harvest was taken at 62 and 70 days after sowing as per the experimental procedure. The fruits selected were ripe and had physical characteristics such as a bright appearance and shiny skin. Thereafter, the harvested fruits were subjected to assessment of relevant yield parameters in accordance with the study protocol.

Observation Variables

Plant height and number of leaves were measured on the same plants at 2, 3, 4, 5, and 6 WAP. Plant height was measured in cm from the soil surface to the growing point, and the number of leaves was determined by counting the fully expanded leaves. Flowering age was recorded as the number of days after planting until the first flower was observed.

Yield-related parameters included the number of productive branches, number of fruits, fruit length, fruit diameter, and fruit weight. Fruit length was measured with a ruler and diameter with digital calipers, and fruit weight was measured with an analytical balance. Fruit observations were made at the relevant time for each parameter at 67, 72 and 76 days after planting (DAP). Repeated observations from the same plant were considered as correlated measurements instead of independent observations.

Statistical Analysis

Statistical analysis was conducted in a randomised complete block design. For responses measured once per experimental unit.

Plant height and leaf number, repeatedly measured at 2-6 WAP, were analysed using a repeated-measures linear mixed-effects model with treatment, observation time, and their interaction as fixed effects, and block and experimental unit as appropriate random effects. The model also accounted for the covariance between repeated measurements on the same experimental unit. When the same experimental units were observed across multiple harvest dates, yield parameters collected at those dates were analysed using a corresponding repeated-measures model. If measurements represented different independent experimental units at each harvest, date-specific analyses were performed instead.

Residual distributions were inspected for approximate normality before conducting inferential analysis, and residuals versus fitted plots were examined for homogeneity of variance. Further diagnostic tests were used where appropriate to assess model assumptions. Data transformations or alternative models were considered when the assumptions were not met adequately.

Where there was a significant treatment effect, treatment means were separated by Duncan's Multiple Range Test (DMRT) at $P \leq 0.05$, if the model and comparison procedure were appropriate for the response variable being analysed. Results are reported as treatment means, measures of variability, effect sizes, and 95% confidence intervals where appropriate. Exact p-values were given for the statistical tests of interest. Separate repeated-measures analyses were conducted for the treatment effect, the observation-time effect, and the treatment-by-time interaction. Statistical Duncan's multiple range test (DMRT) at $P \leq 0.05$ was calculated.

All analyses were performed using the statistical software and version as described in the original analysis. Degrees of freedom and IBM SPSS Statistics version 29 software were recorded for reproducibility.

RESULTS AND DISCUSSION

The chemical properties of the soil used as a growing medium were revisited to ensure that the reported values, units of analysis and interpretations were consistent with the original

laboratory data. Special attention was given to soil pH measured in water and potassium chloride (H2O and KCl pH) and to the reported concentrations of calcium, phosphorus and potassium. These are shown in Table 1.

Reported pH values were 6.96 (pH H2O) and 4.77 (pH KCl). These measurements correspond to different analytical conditions and therefore should be reported separately, specifying the extraction methods. The calcium, P2O5 and K2O values must also be checked against the original laboratory report for units, analytical basis and accuracy. Any interpretation of soil fertility will be changed only when these values have been confirmed. More is shown in Table 2.

Table 1
Soil chemical properties and texture before experiment

Parameter	Value	Unit	Measurement Method
C-Organic	2.92%	%	Walkley and Black
N-Total	0.24%	%	Kjeldahl
Calcium (Ca)	13.63*	%*	Titrimetri
Potassium (K)	0.23*	%*	Flamephotometer
Sodium (Na)	0.02*	%*	Flamephotometer
P_2O_5	25.42*	%*	Spektrophotometer UV-Vis
K_2O	31.31*	%*	Spektrophotometer UV-Vis
pH (H_2O)	6.96	-	Potensiometer
pH (KCl)	4.77	-	Potensiometer
Soil Texture	Dusty Clay	-	-

*Source: Soil Science Unit Laboratory, Faculty of Agriculture, Tadulako University (2021)

Table 2
Chemical properties of chicken manure + cocopeat

Parameter	Value	Unit	Measurement Method
Nitrogen (N)	2.10%	%	Kjeldahl
Phosphorus (P)	0.219%	%	Spektrophotometer UV-Vis
Potassium (K)	0.803%	%	Spektrophotometer UV-Vis
C-Organic	42.29%	%	Walkley and Black
C/N Ratio	20.13		-

*Source: Soil Science Unit Laboratory, Faculty of Agriculture, Tadulako University

Plant Height

Based on the results of the ANOVA and 5% DMRT test, the average height of purple eggplant plants shows that the combination treatment of cocopeat with chicken manure has a significant effect at ages 4 and 6 (WAP) and no significant effect at ages 2, 3, and 5 (WAP) (Figure 2).

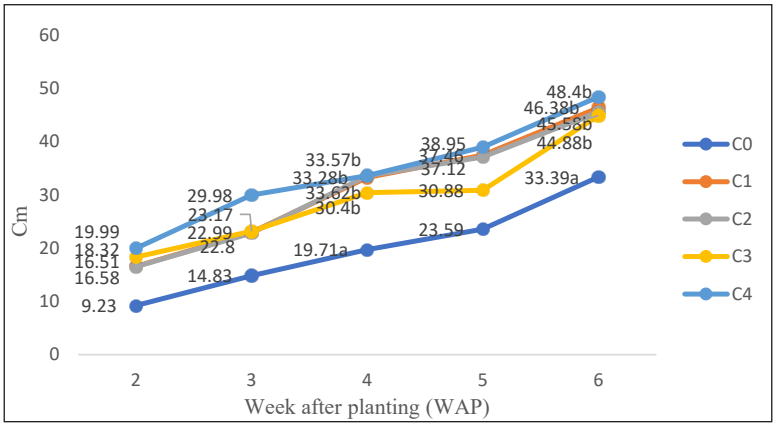

Figure 2. Illustrates the effect of cocopeat and chicken manure on Plant Height. Numbers marked with different letters in the same graphic show (DMRT) at $P \leq 0.05$

In all five treatments, plant height increased over the observation period from 2 to 6 weeks after planting (WAP). But the size of the increase differed between treatments. The plant height was 9.23 cm in the control treatment (C0) and 19.99 cm in C4 at 2 WAP. At 3 WAP, C4 was the tallest treatment at 29.98 cm, while C0 was 14.83 cm.

C4 had a plant height of 33.57 cm at 4 WAP, followed by C2 with a height of 33.28 cm. The lowest height was recorded in the C0 treatment (19.71cm). Maximum plant height at 5 WAP was observed in C4 (38.95cm), followed by C2 (37.12cm), C1 (36.45cm), C3 (30.88cm) and C0 (23.59cm).

At 6 WAP, C4 was still the tallest treatment (48.4 cm), followed by C1 (46.38 cm), C2 (45.5 cm) and C3 (44.88 cm). The plant height was lowest in the control treatment (33.39 cm). In general, the graph indicates that the treatments with cocopeat and chicken manure were associated with higher plant height than the control, with C4 showing the highest final value.

The increase in eggplant plant height from 2 to 6 WAP indicated that the plants were still growing across all treatments during the observation period. However, the differences in plant height among treatments suggest that the growing medium formulations may have influenced vegetative development. The application of cocopeat and chicken manure was associated with higher plant height compared to the control, but the magnitude of the response varied across observation times (Fernanda et al., 2025).

The highest plant height was recorded in treatment C4, containing 100g cocopeat and 300g chicken manure. The plant height reached 48.4 cm at 6 WAP. The control treatment (C0) reached 33.39 cm, in comparison. The difference was 15.01 cm, indicating about 45.0% higher plant height in C4 than in C0. This comparison is a description of the numerical difference between the treatments and is not to be taken as statistically significant unless backed up by the appropriate statistical test.

The relatively taller plants under C4 may be due to the combined effects of cocopeat and chicken manure on the growing medium. Cocopeat improves water retention and modifies the growing medium's physical properties, while chicken manure provides organic matter and nutrients for plants. Adequate water and nutrient availability can favor cell division, cell elongation, leaf development, and stem growth. However, these mechanisms are still plausible explanations since the experiment did not directly measure changes in substrate water retention, nutrient availability, or nutrient uptake (Poliquit, 2025).

The response was not perfectly consistent across observation periods. The heights recorded at 4 WAP for C4 (33.57 cm) and C2 (33.28 cm) were relatively similar. At 5 WAP, C4 was 38.95 cm, compared with 30.88 cm for C3. By 6 WAP, the height of C1, C2, C3, and C4 ranged from 44.88- 48.4 cm, showing that differences among the amended treatments were relatively small compared with the difference between these treatments and the control. This pattern indicates that the highest amendment rate did not necessarily yield a proportionally greater response at each observation time.

The relatively low plant height in C0 could be due to the absence of additional cocopeat and chicken manure in the growing medium. This interpretation must be approached with caution, however, as the initial soil conditions, the availability of nutrients during the growth of the plants and other environmental factors could also have influenced the development of the plants.

Number of Leaves

The results of ANOVA and 5% DMRT test are shown in Figure 3. The average number of leaves of purple eggplant plants showed that the combination treatment of cocopeat and chicken manure significantly impacted the number of leaves.

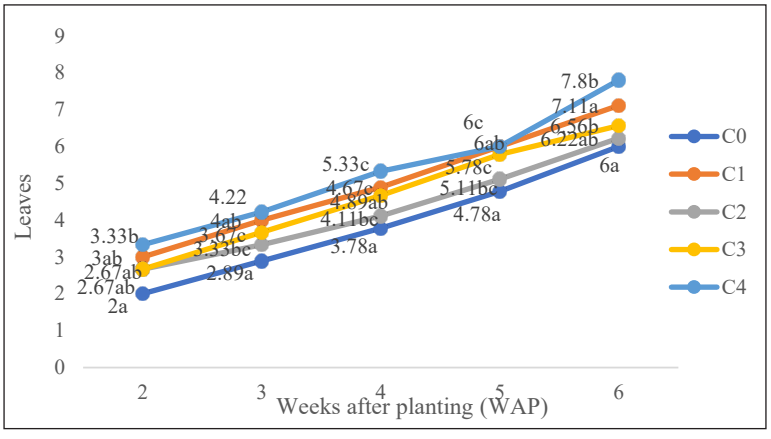

Figure 3. Influence of cocopeat and chicken manure on the number of Leaves. Numbers followed by different letters in the same graphic are (DMRT) at $P \leq 0.05$

The number of leaves increased gradually from 2 to 6 weeks after planting (WAP) in all the treatments, though the magnitude of the increase varied among the cocopeat and manure combinations. At 2 WAP, leaves were maximum in treatment C4 (100 g cocopeat + 300 g manure) i.e. 3.33 followed by C1 (25 g cocopeat + 150 g manure) i.e. 3.00, C2 (50 g cocopeat + 200 g manure) i.e. 2.67, C3 (75 g cocopeat + 250 g manure) i.e. 2.67 and C0 (control) i.e. 2.00. At 3 WAP, C4 was still highest with 4.22, followed by C1 with 4.00, C3 with 3.67, C2 with 3.33 and C0 with 2.89. The number of leaves at 4 WAP for C4 was 5.33, while it was 4.89, 4.67, 4.11 and 3.78 for C1, C3, C2 and C0, respectively (Figure 3). Similarly, at 5 WAP, the same general trend continued, with C4 and C1 having about 6.00 and 5.78 leaves, respectively, followed by C3 at 5.38, C2 at 5.11 and C0 at 4.78. At 6 WAP, C4 had the highest value (7.80 leaves), followed by C1 (7.11), C3 (6.56), C2 (6.22) and C0 (6.00). C4 produced the highest number of leaves in general during the observation period, while the control treatment generally recorded the lowest values.

The increased number of leaves in treatment C4 could be due to the synergistic effects of cocopeat and manure on the growing-medium conditions and nutrient supply. Cocopeat helps in retaining water and moisture around the root zone, whereas manure helps in providing organic matter and vital nutrients for vegetative growth. Adequate water and nutrient availability are important for leaf initiation and expansion and the development of new shoots (Liu et al., 2021). The progressive increase in leaf number from 2 to 6 WAP in all the treatments indicates that the plants were still developing vegetative tissues during the period of observation. However, the higher response under C4 suggests that the mixture of 100 g cocopeat and 300 g manure could have provided better growing conditions than the other treatments. These explanations are potential mechanisms and would require supporting measurements of nutrient availability, growing-medium properties, or other growth parameters to be confirmed (Kamaluddin et al., 2022).

The treatment C4 at 6 WAP produced 7.80 leaves and the control treatment produced 6.00 leaves, which is an increase of about 30%. The difference showed that the highest combination of cocopeat and manure was associated with greater leaf production under the experimental conditions. More leaves may cause more light interception and photosynthetic capacity, which may support more plant growth and development (Lukman & Kusrianty, 2021). However, based on the differences observed in the graph, these should not be considered statistically significant until analysis of variance (ANOVA) and a suitable post hoc test are performed. The results showed that the combination of 100 g cocopeat and 300 g manure was the most promising treatment to increase the number of leaves during the six-week observation period. Further statistical analysis and evaluation of other parameters of growth and yield are needed to determine if this treatment is a consistent agronomic benefit. Reduced water stress also supports early leaf formation in cocopeat-based media (Shintiavira et al., 2023).

Flowering Age

The combined effect of cocopeat with chicken manure significantly affects the mean Flowering Age of purple eggplant plants. More in Figure 4.

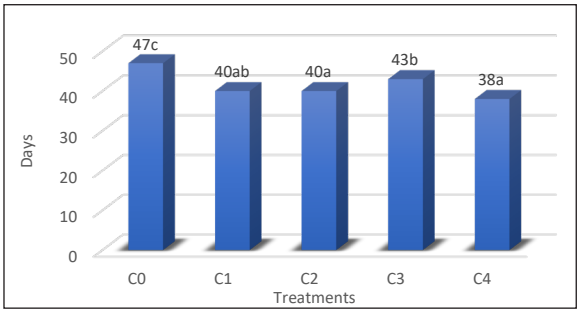

Figure 4. Illustrates the effect of cocopeat and chicken manure on Flowering Age. Numbers marked with different letters in the same graphic show (DMRT) at $P \leq 0.05$

The results of the study show that the application of different treatments (C1- C4) had a remarkable influence on the flowering age of plants compared with the control (C0). The control treatment had the latest flowering age (47 days), suggesting a slower physiological transition from vegetative to reproductive growth. By comparison, all treatments resulted in earlier flowering, with flowering ages ranging from 38 to 43 days. C1 and C2 treatments resulted in similar flowering ages (40 days). Statistical grouping of C1 and C2 treatments (ab and a) indicates that both treatments were effective in promoting earlier floral initiation compared to the control. Treatment C3 had a moderate effect (43 days) and was classified in group b, while treatment C4 had the earliest flowering (38 days) and was classified as a, indicating the most potent effect among all treatments.

Fitrianti et al. (2023) emphasise the importance of nutrient management and organic amendments in regulating flowering physiology. Recent research has highlighted that improved nutrient availability, especially nitrogen and phosphorus, boosts metabolic and hormonal processes driving reproductive development (Adnan et al., 2023). Improved nutrient status has been reported to result in increased growth regulators (auxins, gibberellins and cytokinins) and is closely associated with floral induction pathways. Early flowering in treatments C1-C4 suggests that these treatments probably improved nutrient uptake efficiency or supplied bioactive compounds which stimulated the shift to reproductive growth, in agreement with the hormonal and metabolic mechanisms.

Moreover, studies during this period Panjaitan et al. (2023) indicate that suitable fertilisation strategies or organic amendments can shorten flowering time by 10- 20% in several crop species. The results obtained for treatment C4, which was the earliest flowering treatment, support these findings and suggest that the composition of this treatment may have provided a more balanced nutrient profile or better bioavailability. Overall, the outcomes validate that the implementation of enhanced nutrient-based treatments can substantially control and optimise flowering time, strengthening the wider scientific consensus set in recent literature.

Number of Production Branches

Based on the ANOVA and 5% DMRT results, Figure 5 presents the average number of production branches in purple eggplant plants. The combination of cocopeat and chicken manure significantly affected the number of production branches.

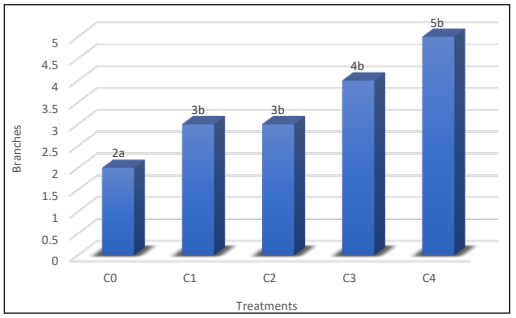

Figure 5. The average number of production branches of purple eggplant plants shows that the combination treatment of cocopeat with chicken manure has (DMRT) at $P \leq 0.05$

Results indicate that the number of production branches differed significantly among treatments (C0-C4). The control (C0) showed the least number of branches, with 2 branches, indicating less vegetative development in the untreated condition. In contrast, the number of production branches was considerably increased by all treatments applied (C1-C4). Treatments C1 and C2 had three branches each and were statistically classified as b, showing a significant increase over the control. Treatment C3 showed four branches and was still in the same statistical group, suggesting a more intense but similar stimulatory effect. The response was most prominent in treatment C4, which resulted in five branches and was in group b, indicating that this treatment produced the highest degree of vegetative branching of all treatments.

Kartika et al. (2025) emphasised that nutrient management, organic amendments and growth-promoting substances are important in the development of branches in horticultural crops. During this period, it has been found that enhancement of nutrient supply, particularly nitrogen and phosphorus, increases axillary bud activation through modulation of auxin-cytokinin balance, an important regulatory mechanism of lateral shoot initiation. Cytokinins stimulate the development and growth of lateral buds, and sufficient nitrogen availability supports strong vegetative growth, which supports the formation of branches.

Moreover, Wasis & Fitriani (2022) stated that the use of organic fertilisers and bioactive soil amendments improves photosynthetic efficiency, carbon allocation, and soil biological activity, which later increases vegetative branching. The enhanced responses in treatments C3 and C4 suggest that these treatments might have had higher nutrient concentrations or more available forms of nutrients, which provided better physiological support for branch development.

In general, the increase in the number of production branches from C1 to C4 indicates the effectiveness of these treatments on vegetative growth. Specifically, the superior performance of treatment C4 aligns with recent literature suggesting that optimised nutrient formulations can improve branching by 20-40%, depending on plant species and treatment characteristics. These results are consistent with general scientific knowledge

that enhanced nutrient management is part of maintaining vegetative structure and yield formation in cultivated plants.

Number of Fruits

The results of ANOVA and DMRT at 5% are presented. The combined cocopeat and chicken manure treatment significantly affects the average number of fruits of purple eggplant plants. See more in Figure 6.

Based on Figure 6, the combination of cocopeat and manure showed different responses to the observed parameter at 67, 72, and 76 days after planting (DAP). At 67 DAP, treatment C4 (100 g cocopeat + 300 g manure) had the highest value of 1.78 units followed by C3 (75 g cocopeat + 250 g manure) 1.33 units, C2 (50 g cocopeat + 200 g manure) 1.22 units, C1 (25 g cocopeat + 150 g manure) 1.11 units and C0 (control) 1.00 unit. C4 had the highest value (2.56 units) at 72 DAP, followed by C3 (2.00 units), C1 (1.33 units) and C0 and C2 (1.22 units each). The maximum value was 4.11 units at 76 DAP for C4, followed by C3 (2.56 units), C2 (2.11 units), C1 (1.78 units), and C0 (1.11 units). These results indicate that C4 always produced the highest observed values during the period of observation, with the greatest increase between 72 and 76 DAP.

The increased values in treatment C4 could be due to the synergistic effects of cocopeat and manure on the growing medium. Cocopeat has water-retention properties, which can help keep moisture available around plant roots, and manure can add organic matter and vital nutrients that support plant growth and development. Also, the breakdown of manure can provide a slow release of nutrients, and the cocopeat can help to keep the physical conditions of the growing medium favorable. Thus, the combination of these materials may support water and nutrient availability during the observation period.

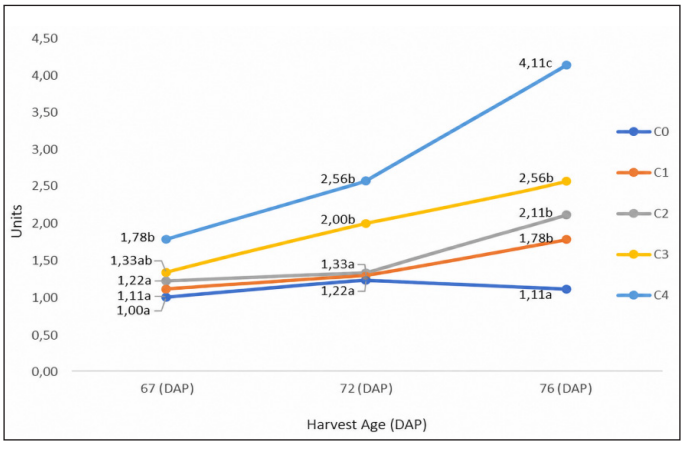

Figure 6. Effect of cocopeat and chicken manure on the number of Fruits. Numbers in the same chart with different letters are (DMRT) at $P \leq 0.05$

However, these explanations are possible mechanisms based on the observed trends and need to be supported by additional measurements of properties of the growing medium and other relevant parameters of plant growth (Yanti et al., 2025).

The observed values of C4 were more and more different from the control treatment with increasing harvest age. At 76 DAP, C4 was 4.11 units, which is about 3.70 times the control value (1.11 units). The result revealed that among the treatments tested, a mixture of 100g cocopeat and 300g manure gave the best result. However, without confirmation by analysis of variance (ANOVA) and an appropriate post hoc test, the differences observed cannot be statistically significant. Overall, the results showed that the blend of cocopeat and manure might result in better plant responses at the time of harvest, with C4 consistently yielding the highest values (Shafira et al., 2021). Further assessment of statistical significance, cost of application and growing conditions is required before this combination can be recommended as the optimum treatment. At 76 DAP, the highest production was still in C1 with 2.56 fruits, followed by C3 (2.11) and C2 (1.78). There was little effect of C4, indicating that adding too much manure does not enhance fruiting. Interestingly, the control sharply increased to 4.11 fruits, likely in a delayed reproductive response under nutrient stress, a pattern noted previously in crops experiencing nutrient-limited conditions (Ardi & Nuraeni, 2023).

Fruit Length

The results of the ANOVA and 5% DMRT test were presented in Figure 7. The average Fruit Length of purple eggplant plants shows that the treatment combination of cocopeat with chicken manure has a significant effect on Fruit Length of purple eggplant plants.

Results show that the combination of cocopeat and chicken manure consistently influenced fruit length of eggplant at the three harvest ages (67, 72 and 76 DAP).

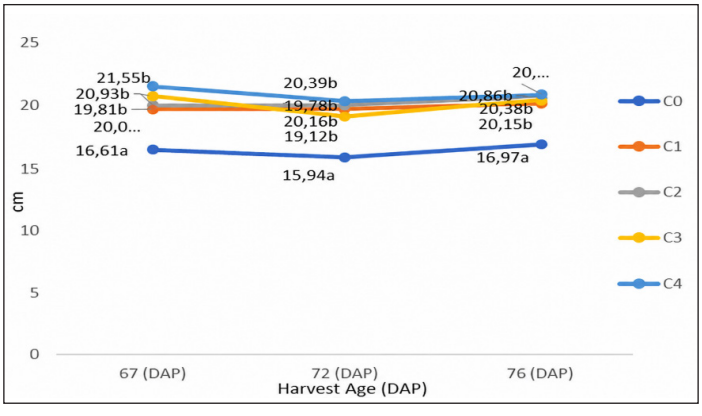

Figure 7. Shows the effect of cocopeat and chicken manure on Fruit Length. Numbers followed by different letters in the same chart are (DMRT) at $P \leq 0.05$

All amended treatments (C1-C4) resulted in longer fruits compared to the control (C0), which had the least fruit length at each observation. This pattern indicated that the plants without amendment had limited nutrient availability and less than optimal physical conditions for growth, resulting in a decrease in fruit elongation. (Sinaga et al., 2021), also reported similar findings where the size of eggplant fruits decreased when the substrates were nutrient deficient.

The longest fruits (19.7- 21.0 cm) were always produced by the highest doses of cocopeat- manure (especially C3 (75 g + 250 g manure) and C4 (100 g + 300 g manure). The better performance in these treatments is due to the improvement in soil structure, water-holding capacity and nutrient availability due to cocopeat and organic manure. Cocopeat is a well-documented effective growth medium due to its aeration and moisture retention properties (Adnan et al., 2025)and chicken manure is a readily available source of nitrogen, phosphorus and potassium essential for fruit development (Kahar, 2021).

Lower amendment levels could increase fruit elongation as compared to the control. Moderate fruit lengths obtained from C1 and C2 showed that fruit length was relatively stable across harvest ages in all treatments, which indicated that fruit elongation was determined early in fruit development, similar to the findings of (Maulida et al., 2022). In general, the combination of cocopeat and chicken manure considerably improved eggplant fruit length. The highest rates of amendment resulted in the most optimal results and supported its use as an organic growing medium to increase eggplant productivity.

Fruit Diameter

Based on the results of the ANOVA and 5% DMRT test, they are presented in Figure 8. The combination treatment of cocopeat with chicken manure significantly affected the Fruit Diameter, as demonstrated by the average Fruit Diameter of purple eggplant plants.

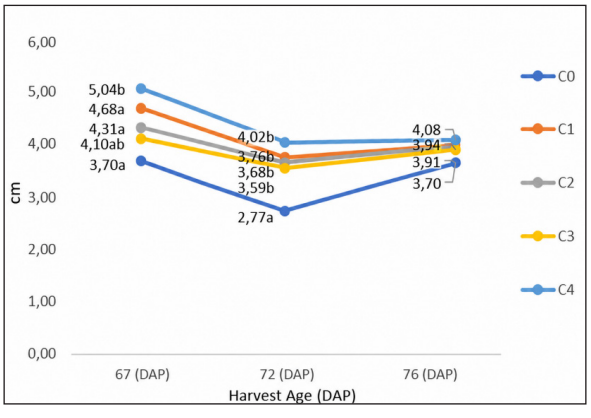

Figure 8. Shows the effect of cocopeat and chicken manure on fruit diameter. Values followed by different letters in the same chart are (DMRT) at $P \leq 0.05$

The chart shows fruit diameter of eggplant measured at 67, 72 and 76 DAP under different combinations of cocopeat-manure (C1-C4) compared with the control (C0). At 67 DAP, the fruit diameter was greater in all amended treatments (C1- C4) (4.31-5.04 cm) than in the control (3.70 cm), indicating that organic amendments improved early fruit expansion. The statistical separation (a, b) confirms the clear performance gap between the amended treatments and C0 and underlines the fact that improved soil aeration and nutrient availability stimulated early reproductive growth.

All treatments showed a reduction in fruit diameter at 72 DAP, which is commonly associated with increased fruit load and resource competition during mid-maturation. However, although this decrease was observed, the amended treatments (3.59-4.02 cm) still gave higher values than the control (2.77 cm). This confirmed that cocopeat- manure combinations still gave better fruit development during physiological stress. Fruit diameter increased again at 76 DAP in all treatments. Values stabilised at 3.91 to 4.17 cm for C1-C4, compared to 3.70 cm for the control. The constant superiority of the amended treatments suggests that the improved soil structure due to cocopeat and sustained nutrient release from manure promoted prolonged cell enlargement and fruit filling processes.

These results align with recent findings from Randi et al., (2023), who reported that organic amendments enhanced soil water retention, nutrient availability, and root-zone aeration. These factors directly improve fruit morphology. Studies indicate that cocopeat enhances porosity and water retention, whereas manure supplies necessary nutrients and stimulates microbial activity that aids nutrient mineralisation and fruit growth stability (Bahtiar et al., 2023). These synergistic effects account for the higher fruit diameters in C1-C4 compared to the unfertilised control. To summarise, the results show that the combination of cocopeat and manure significantly increases the diameter of eggplant fruits at all harvesting times, in agreement with the current literature which highlights the benefits of organic substrates on fruit size and quality.

Fruit Weight

They are presented in Figure 9, based on the results of ANOVA and the 5% DMRT test. The average fruit weight of purple eggplant plants under the combination treatment of cocopeat with chicken manure showed a significant effect on fruit weight.

The chart shows that the cocopeat-manure treatments (C1-C4) resulted in higher fruit weights than the control (C0) at all the harvest ages. At 67 DAP, the treated plants weighed 138- 156 g, which was significantly higher than the control (94.7 g), suggesting improved early fruit development. While all the treatments showed a decrease at 72 DAP, the amended groups (87- 102 g) performed better than the control (49.29 g), indicating better resilience during mid-cycle stress. At 76 DAP, fruit weights were recovered in all treatments, with C2-C4 having the highest weights (120-135 g), whereas the control was the lowest (83.03 g).

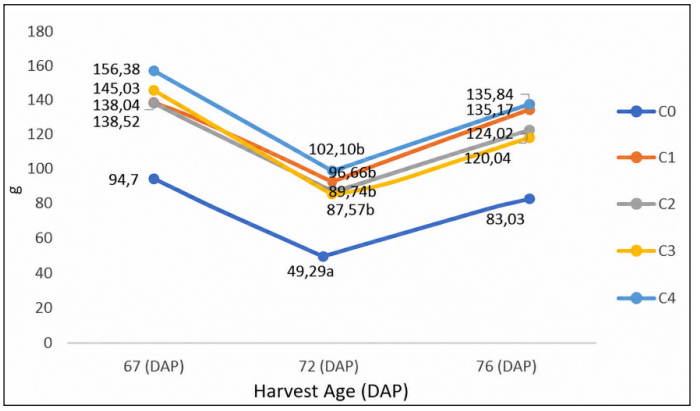

Figure 9. Effect of cocopeat and chicken manure on Fruit Weight. Values with different letters in the same chart differ (DMRT) at $P \leq 0.05$

These results indicate that the cocopeat with manure improves water retention, nutrient availability and aeration of the root zone, resulting in better fruit filling and overall yield. This trend is consistent with recent findings by Alhadi et al. (2021) that organic substrates enhance nutrient mineralisation, microbial activity and fruit biomass accumulation in eggplant and other solanaceous crops.

Interpretation of Treatment Responses

The results showed that applying a combination of cocopeat and chicken manure significantly affected vegetative growth and yield-related characteristics of purple eggplant (*Solanum melongena* L.). Among the five treatments evaluated, C4 (100 g cocopeat + 300 g chicken manure) generally showed high values for several measured parameters, including plant height, number of leaves, and selected fruit characteristics. However, responses differed among parameters and observation times. Thus, the results do not show a uniform dose-dependent increase of all growth and yield variables.

The observed responses may reflect the complementary roles of cocopeat and chicken manure. Cocopeat is widely used as a component of growing medium because of its water-holding capacity and its effect on the physical properties of the root zone. The chicken manure adds organic matter and plant nutrients. These properties offer plausible explanations for the differences identified among treatments. However, water-holding capacity, soil aeration, nutrient availability after application of the treatment, microbial activity and nutrient mineralisation were not directly measured in this experiment. Therefore, these mechanisms should be viewed as potential explanations rather than proven causes for the observed plant responses.

The number of leaves and the plant height generally increased during the observation period, but the degree of response depended on the treatment. The relatively high values

observed under C4 may suggest that this combination has provided favorable growing conditions under the experimental conditions. However, the responses should be interpreted from the statistical comparisons at each observation time and not simply from differences in the plotted means. In addition, repeated observations of the same plants have to be taken into account when evaluating treatment effects over time.

A similar caution is required for the reproductive responses. While C4 exhibited beneficial values for several fruit-related parameters, the magnitude and direction of treatment differences differed among harvest observations. Fruit number, length, diameter, and weight are all separate components of crop performance and should not be used interchangeably as measures of yield. For instance, a higher individual fruit weight does not automatically mean a higher total yield per plant if the number of fruits harvested and the total harvested mass are not taken into account too.

Furthermore, the experimental design assessed the mixtures of cocopeat and chicken manure, not the individual effects of each amendment. However, the quantities of both materials increase in parallel from C1-C4, so the effects of either can't be separated, nor can any interactions between the two. The experiment thus identifies treatment combinations linked to particular plant responses but does not establish whether cocopeat, chicken manure or their interaction was chiefly responsible for those responses.

The overall results indicate that the mixture of cocopeat and chicken manure could be a promising approach for the improvement of some growth and yield-related characteristics of purple eggplant. The evidence, however, is limited to the treatment combinations, experimental site and growing period studied. Further experiments should involve separate cocopeat and manure treatments, proper fertiliser controls, additional independent replication, and direct measurements of growing medium properties to elucidate the mechanisms underlying the observed responses and to define an agronomically and economically optimal amendment rate.

CONCLUSION

The study revealed that vegetative growth and yield-related characters of purple eggplant were associated with different combinations of cocopeat and chicken manure. The treatment C4 (100 g cocopeat + 300 g chicken manure) was generally promising for the responses of several parameters measured among the treatments evaluated. But the responses to the treatment were different for different parameters and times of observation, and the existing results do not confirm a uniform dose-dependent increase in all growth and yield variables.

The results suggest that the combination of cocopeat and chicken manure could be used as an organic growing-medium amendment for the production of eggplant. However, the effects of the single amendments and their interaction cannot be separated because both application rates were increased at the same time. The processes of water holding, aeration, nutrient availability and microbial activity were also not measured directly. The

results should thus be taken in light of the experimental conditions and not as evidence of a universally optimal treatment.

Further research should evaluate cocopeat and chicken manure alone and in combination, include appropriate unfertilised and standard-fertiliser controls, and use adequate independent replication across multiple locations and growing seasons. Direct measurements of growing-medium properties, nutrient availability, total yield per plant and production costs would strengthen the assessment of treatment effectiveness and support the development of evidence-based recommendations for sustainable eggplant production.

LIMITATIONS OF THE STUDY

When interpreting the findings, several limitations should be taken into account. First, the experiment was carried out at one experimental site and one growing period, May- July 2022. Hence, the results obtained may not be fully representative of responses in other soil conditions, climatic environments or growing seasons.

Second, the experiment was performed in three blocks, and three polybags were considered for each treatment-by-block unit. The statistical independence of the polybags should be interpreted in the light of the actual randomisation procedure. If the polybags in a treatment-by-block unit received the same treatment without independent randomisation, then they are subsamples and not independent experimental replicates. This distinction matters for estimating experimental variability and assessing the reliability of treatment comparisons.

Third, treatments were combined applications of cocopeat and chicken manure with both amendment rates increased together. The experiment did not include separate cocopeat-only and chicken-manure-only treatments, nor a standard-fertiliser control. Thus, the individual effects of the two amendments, their interaction, and their relative efficacy compared with conventional fertilisation could not be established.

Fourth, some of the proposed mechanisms to explain the observed plant responses, including changes in water retention, aeration, nutrient availability, microbial activity, and nutrient release, were not directly measured after amendment application. These mechanisms provide plausible explanations, but require further experimental validation.

Finally, the responses to the treatments were different for growth and yield parameters and harvest dates. Therefore, the reported findings need to be interpreted using validated raw data, proper statistical analyses and explicit yield measurements. Future studies should include independent replication, multiple locations and growing seasons, separate amendment treatments, standard-fertiliser controls, and direct measurements of soil and growing-medium properties. These enhancements would offer a stronger basis for determining treatment efficacy, agronomic optimum rates, and practical suggestions for eggplant cultivation.

REFERENCES

Adnan, N., Supian, M., Akpi, U. K., Francis, F., Nazir, M. Y. M., & Zaini, N. A. M. (2025). Bacterial cellulose from young coconut husk fibre hydrolysate as sustainable biomaterial. *International Food Research Journal*, *32*(4), 1174-1185

Adnan, Sondakh, R., & Alfin, M. (2023). Pengaruh kombinasi mulsa dan pupuk kandang terhadap tanaman bawang merah [The effect of mulch and manure combination on shallot plants]. *SCIENTIA: Journal of Multi Disciplinary Sciences*, *2*(2), 61-71. https://doi.org/10.62394/scientia.v2i2.55

Alhadi, B., Jamilah, J., & Hadi, A. (2021). Perlakuan sistem olah tanah dan aplikasi urin sapi terhadap pertumbuhan dan hasil tanaman terung ungu (*Solanum melongen*a L.) [Tillage system treatment and application of cow urine on the growth and yield of purple eggplant (*Solanum melongena* L.)]. *Jurnal Agroristek*, *4*(1), 6-11. https://doi.org/10.47647/jar.v4i1.407

Ardi, A., & Nuraeni, N. (2023). Pertumbuhan dan hasil tanaman seledri (Apium graveolens L.) pada pemberian pupuk organik cair [Growth and yield of celery plants (Apium graveolens L.) with liquid organic fertiliser application]. *Agrotekbis: E-Jurnal Ilmu Pertanian*, *11*(4), 972-980. https://doi.org/10.22487/agrotekbis.v11i4.1819

Bahtiar, Wasi'an, & Palupi, T. (2023). Upaya peningkatan hasil bawang merah pada tanah alluvial melalui penambahan pupuk kandang ayam dan cocopeat [Efforts to increase shallot yield in alluvial soil through the addition of chicken manure and cocopeat]. *Agrofood*, *5*(1), 12-18. https://doi.org/10.63848/agf.v05n1.2

Fernanda, Y. F., Hidayat, R., & Pribadi, D. U. (2025). Biofertiliser application of rabbit urine and eggshell powder improves purple eggplant (*Solanum melongena* L.) productivity under tropical field conditions. *Jurnal Pembelajaran dan Biologi Nukleus*, *11*(3), 1119- 1136. https://doi.org/10.36987/jpbn.v11i3.7766

Fitrianti, F., Almujihad, A., & Aliyah, M. (2023). Uji efektivitas pemberian komposisi media tanam dan aplikasi POC NASA terhadap pertumbuhan dan hasil tanaman seledri (*Apium graveolens* L.) [Effectiveness of planting media composition and NASA liquid organic fertiliser application on the growth and yield of celery (*Apium graveolens* L.)]. *Journal Peqguruang: Conference Series*, *5*(1), 1-4. https://doi.org/10.35329/jp.v5i1.3949

Kahar, K. (2021). Respon pertumbuhan dan hasil beberapa varietas tanaman tomat (S*olanum lycopersicum* L.) akibat pemberian jenis pupuk kandang [Growth and yield response of several tomato varieties (*Solanum lycopersicum* L.) to different types of manure]. *JAGO TOLIS : Jurnal Agrokompleks Tolis*, *1*(3), 60-65. https://doi.org/10.56630/jago.v1i3.164

Kamaluddin, N. N., Hindersah, R., Cahayaningrum, D. N., Purba, P. S. J., Wibawa, D. I., & Setiawati, M. R. (2022). Karakterisasi media tanam dari kombinasi cocopeat dan pupuk kandang ayam Karakterisasi media tanam dari kombinasi cocopeat dan pupuk kandang ayam [Characterisation of planting media from a combination of cocopeat and chicken manure]. *Soilrens*, *20*(1), 16-24. https://doi.org/10.24198/soilrens.v20i1.41352

Kartika, Y., Rosmaiti, R., & Syukri, S. (2024). Efektivitas penggunaan berbagai jenis pupuk kompos terhadap pertumbuhan dan produksi tanaman terung (*Solanum melongena* L.) [Effectiveness of different types of compost on the growth and production of eggplant (*Solanum melongena* L.)]. *Tumbuhan : Publikasi Ilmu Sosiologi Pertanian Dan Ilmu Kehutanan*, *1*(3), 39-56. https://doi.org/10.62951/tumbuhan.v2i1.246

Liu, Q., Chen, Z., Huang, L., Mujtaba Munir, M. A., Wu, Y., Wang, Q., Ma, L., Xu, S., Wen, Z., & Feng, Y. (2021). The effects of a combined amendment on growth, cadmium adsorption by five fruit vegetables, and soil fertility in contaminated greenhouse under rotation system. *Chemosphere*, *285,* Article 131499. https://doi.org/10.1016/j.chemosphere.2021.131499

Lukman, L., & Kusrianty, N. (2021). Kombinasi penggunaan kompos eceng gondok (*Eichhornia crassipes*) dengan pupuk kandang ayam terhadap laju pertumbuhan bibit tanaman kopi robusta (*Coffea canephora*) [Combination of water hyacinth compost (*Eichhornia crassipes*) and chicken manure on the growth rate of robusta coffee seedlings (*Coffea canephora*)]. *JST (Jurnal Sains dan Teknologi)*, *10*(2), 200-210. https://doi.org/10.23887/jstundiksha.v10i2.37615

Mansurat, A. I., Dandago, M. A., & Diya'udeen, H. B. (2023). Phytochemical contents and antioxidant potentials of eggplants from Kano State, Nigeria: A review. *Dutse Journal of Pure and Applied Sciences, 9*(1a), 160-167. https://doi.org/10.4314/dujopas.v9i1a.16

Lamasika, G., Musa, N., & Zakaria, F. (2024). Pengaruh komposisi media tanam dan konsentrasi pemberian pupuk organik cair bonggol pisang terhadap petumbuhan dan hasil tanaman tomat (*Solanum lycopersicum* L.) [Effect of planting media composition and liquid organic fertiliser concentration from banana corms on the growth and yield of tomato plants (*Solanum lycopersicum* L.)]. *Jurnal Lahan Pertanian Tropis*, *3*(2). https://doi.org/10.37159/jpa.v24i3.2185

Mostfa, Z. A., Alsawaf, A., Al-Rubaie, O. A. F., Saadi, A. M., Al-Chalabi, A. T. M., & Al-Zuhairi, F. F. A. (2025). Effects of organic and amino acid fertilisation on growth and yield of eggplant (*Solanum melongena* L.). *Organic Farming*, *11*(2), 127-134. https://doi.org/10.56578/of110205

Nasution, Y., & Tammin T. P. (2022). Pengaruh media tanam sabut kelapa (cocopeat) dan pupuk kandang terhadap pertumbuhan dan produksi tanaman cabai rawit [Effect of cocopeat growing medium and manure on the growth and production of bird's eye chilli]. *Jurnal Ilmiah Hijau Cendekia*, *7*(1), 41-45. https://doi.org/10.32503/hijau.v7i1.2257

Panjaitan, E., Sianturi, P. L. L., Sidauruk, L., & Manurung, E. Y. (2023). The effect of liquid organic fertiliser and solid organic fertiliser on the growth and production of eggplant (*Solanum melongena* L.). *Jurnal Kajian dan Penalaran Ilmu Manajemen*, *1*(3), 185-199. https://doi.org/10.59031/jkpim.v1i3.210

Poliquit, D. E. (2025). Growth and yield performance of eggplant (*Solanum melongena* L.) under bat guano tea application in potted conditions. *Thai Journal of Agricultural Science*, *58*(4), 344-360. https://doi.org/10.65764/tjas.2025.267405

Putra, M., Raksun, A., & Sedijani, P. (2025). Effect of NPK fertiliser and vermicompost on the vegetative growth of green eggplant (*Solanum melongena* L.). *Jurnal Biologi Tropis*, *25*(1), 199-210. https://doi.org/10.29303/jbt.v25i1.7861

Ramadhan, R. G., Adam, D. H., Elizabeth Mustamu, N., & Walida, H. (2024). Increasing the growth and production of eggplant (Solanum melongena L.) by providing wood biochar. *Jurnal Agronomi Tanaman Tropika (JUATIKA)*, *6*(2), 616-621. https://doi.org/10.36378/juatika.v6i2.3660

Randi, R., Rahmidiyani, R., & Zulfita, D. (2023). Pengaruh tepung cangkang telur dan pupuk NPK terhadap pertumbuhan dan hasil terung pada tanah gambut [Effect of eggshell powder and NPK fertiliser on eggplant growth and yield in peat soil]. *Jurnal Sains Pertanian Equator*, *12*(3), 676-687. https://doi.org/10.26418/jspe.v12i3.64902

Sanyang, S. E, Demba, S., & Njie, E. (2025). Growth performance of eggplant (*Solanum melongena* L.) enhanced by watering intervals and application of organic manure. *International Journal of Applied Agricultural Sciences*, *11*(1), 24-28. https://doi.org/10.11648/j.ijaas.20251101.13

Shafira, W., Akbar, A. A., & Saziati, O. (2021). Penggunaan cocopeat sebagai pengganti topsoil dalam upaya perbaikan kualitas lingkungan di lahan pascatambang di Desa Toba, Kabupaten Sanggau [Use of cocopeat as a substitute for topsoil to improve environmental quality in post-mining land in Toba Village, Sanggau Regency]. *Jurnal Ilmu Lingkungan*, *19*(2), 432- 443. https://doi.org/10.14710/jil.19.2.432-443

Shintiavira, H., Dewanti, M., Rachmawati, F., Nurlaeni, Y., Nurdina, D., Sadli, S., Ariyantika, S., & Kartikaningrum, S. (2023). Cocopeat perlite mixture as an alternative for rooted cuttings growth medium of *Impatiens hawkeri x platypetala* in Indonesia. *Caraka Tani: Journal of Sustainable Agriculture*, *38*(2), 359-370. https://doi.org/10.20961/carakatani.v38i2.73876

Sinaga, E. E., Dahang, D., & Tarigan, S. (2021). Pengaruh kombinasi pupuk kandang ayam dan pupuk kandang sapi terhadap pertumbuhan dan produksi tanaman bawang merah (*Allium ascalonicum* L.) varietas Batu Ijo [Effect of a combination of chicken manure and cow manure on the growth and production of Batu Ijo shallot (*Allium ascalonicum* L.)]. *Jurnal Agroteknosains*, *5*(1), 11-23.

Wasis, B., & Fitriani, A. S. (2022). Pengaruh pemberian pupuk kandang sapi dan cocopeat terhadap pertumbuhan *Falcataria moluccana* pada media tanah tercemar oli bekas [Effect of cow manure and cocopeat on the growth of *Falcataria moluccana* in soil contaminated with used oil]. *Journal of Tropical Silviculture*, *13*(03), 198-207. https://doi.org/10.29244/j-siltrop.13.03.198-207

Yanti, M., Setiono, & Subagiono. (2025). Pengaruh media tanam sabut kelapa (cocopeat) dan pupuk kandang kotoran ayam terhadap pertumbuhan dan hasil cabai rawit (*Capsicum frutescens* L.) varietas ORI 212 [Effect of cocopeat growing medium and chicken manure on the growth and yield of ORI 212 bird's eye chilli (*Capsicum frutescens* L.)]. *Jurnal Greenation Pertanian Dan Perkebunan*, *3*(4), 212-230. https://doi.org/10.38035/jgpp.v3i4.724

Pertanika J. Trop. Agric. Sci. 49 (5): 2461 - 2466 (2026)

PERTANIKA JOURNALS

TROPICAL AGRICULTURAL SCIENCE

Journal homepage: http://www.pertanika.upm.edu.my/

Two New Localisation Records of *Priacanthus sagittarius* (Starnes, 1988) in the Westernmost Part of the Levant Sea

Alper Yıldız[1]*, M. Tunca Olguner[2], Mehmet Gökoğlu[1], Jale Korun[1], and Mesut Yılmaz[1]

[1]Akdeniz University, Faculty of Fisheries, 07070 Antalya, Turkey
[2]Mediterranean Conservation Society, 35100 İzmir, Turkey

ABSTRACT

Two individuals of *Priacanthus sagittarius* Starnes, 1988, were recorded in the westernmost part of the Levant Sea. A single specimen (17.5 cm TL; 91.97 g W) was captured in the Gulf of Antalya at a depth of 70 m in June 2025. The fish was caught with a 25-mm trammel net off Maden Bay, the Gulf of Antalya. Another specimens (20.5 cm TL; 146 g W and 23 cm TL; 175 g W) were caught with a 45 mm gill net at Fethiye Bay, from a depth of 40-50 m. These sites mark the fish's westernmost known occurrence in the Levant. These results imply that *P. sagittarius*, a *Lessepsian* species, has likewise acclimated to the Mediterranean and is progressively spreading westward. Typically found in protected reefs, caverns, or rocky regions, this demersal species is most likely to be found farther west in the Mediterranean and Aegean Sea.

Keywords: Priacanthus, Mediterranean, Lessepsian

ARTICLE INFO

Article history:
Received: 29 June 2026
Accepted: 18 October 2026
Published: 30 October 2026

DOI: https://doi.org/10.47836/pjtas.49.5.17

E-mail addresses:
alperyildiz@akdeniz.edu.tr (Alper Yıldız)
tunca.olguner@akdenizkoruma.org.tr (M. Tunca Olguner)
gokoglu@akdeniz.edu.tr (Mehmet Gökoğlu)
jalekorun@akdeniz.edu.tr (Jale Korun)
myilmaz@akdeniz.edu.tr (Mesut Yılmaz)
* Corresponding author

INTRODUCTION

Bigeyes, also known as *Priacanthidae*, are found in tropical and subtropical waters, typically on coral reefs or rocky bottoms (Carpenter & De Angelis, 2016). According to reported studies, there are twelve recognised species in the genus Priacanthus (Oken, 1817) worldwide (Froese & Pauly, 2026). The Atlantic bigeye (Priacanthus arenatus Cuvier, 1829), the Moontail bullseye (Priacanthus hamrur; Forsskål, 1775), the Elongate bulleye (*Priacanthus prolixus* Starnes, 1988), and the Arrow

© Universiti Putra Malaysia Press

bulleye (*Priacanthus sagittarius* Starnes, 1988) are the four species of this genus that have been documented in the Mediterranean Sea so far (Alshawy et al., 2019; Ergüden et al., 2018; Gürlek et al., 2021; Goren et al., 2010; Gürlek et al., 2017). Only *P. arenatus*, one of four species found in the Mediterranean, is native to the Atlantic; the others are native to the Red Sea (Alshawy et al., 2019). The same family's *Priacanthus blochii* Bleeker, 1853, is also known to occur in the Red Sea, but to date no evidence of this species has been found in the Mediterranean (Gürlek et al., 2021). The species *Priacanthus sagittarius* inhabits the Indo-West Pacific and the Mediterranean (Froese & Pauly, 2022). It is a demersal marine fish that typically lives in rocky habitats, caves, or protected reefs (Gürlek et al., 2021). Additionally, this fish is one of the *Lessepsian* species that migrate through the Suez Canal to the Mediterranean. The species was first documented in Israel in 2010 (Goren et al., 2010) and was subsequently recorded again on the Israeli coast (Haifa) in 2011 (Golani et al., 2011). Since these reports, more specimens from the Syrian, Egyptian, Lebanese, and Israeli seas have been recorded (Golani et al., 2021).

P. sagittarius, a member of the *Priacanthidae* family, is a marine fish suitable for human consumption. The first report of this fish in Turkish waters was by Gökoğlu and Teker (2018) from the coast of Mersin/Taşucu. Subsequent reports were from Mersin Bay (Ergüden et al., 2023) and Konakcık Beach in İskenderun Bay (Gürlek et al., 2021).

This article reports on fish from the westernmost reaches of the Levant Sea, namely Maden Bay in the Gulf of Antalya and Aquarium Bay in Muğla/Dalaman.

MATERIALS AND METHODS

A fisherman named Ahmet Telçelik captured a fish he had never seen before in his net on June 13, 2025, while fishing in Maden Bay (coordinates N 36°25'57.86"; E 30°29'42.88") (Figure 3), Antalya, at a depth of 70 metres using a 25-mm trammel net. He asked for its identification. The fish sample (Figure 1) was sent to the Akdeniz University Faculty of Fisheries laboratory in an ice-cooled box. Another specimen was captured (Figure 2) in Fethiye Bay, Muğla (coordinates N 36° 39' 30.06"; E 29° 3' 52.2432") (Figure 3) at a depth of 40-50 metres using a 45-mm gill net (by a fisherman). When both fish samples were sent to our laboratory for identification, they were already dead. The species were identified after metric and meristic measurements were performed.

RESULTS AND DISCUSSION

While it is widely acknowledged that the first record of an invasive species in the Mediterranean should be published immediately, it is equally critical to publish subsequent records of the same species to confirm its establishment and distribution in its new habitat (Golani et al., 2011).



Figure 1. Priacanthus sagittarius caught in Maden Bay, the Gulf of Antalya



Figure 2. Specimens of *P. sagittarius* caught in Fethiye, Muğla



Figure 3. The points where *Priacanthus sagittarius* individuals were caught (Red pins: Present records, Black pins: Previous records)

The Gulf of Antalya is among the Mediterranean's areas with the highest prevalence of *Lessepsian* species. According to reports, there are now 71 *Lessepsian* fish species in this gulf (Yıldız & Gökoğlu, 2024). The inclusion of *P. sagittarius* in this Gulf investigation has increased the total to 72. Figures 1-2 show that the fish taken in the Gulf of Antalya measured 17.5 cm in length and weighed 91.97 g. The maximum total length reported for *P. sagittarius* is 35-37 cm (Froese & Pauly, 2026). The individual caught in the Gulf of Antalya was half the maximum reported total length for the fish and appears to be a juvenile.

The other specimens in our study were caught in Muğla's Fethiye Bay (Figure 2). The total length and weight of the fish were determined to be 20.5 cm TL; 146 g W and 23 cm TL; 175 g W, respectively. The first record of P. sagittarius on the Mediterranean coast of Turkiye was in 2018 at Tasucu (Gökoğlu & Teker, 2018). Subsequently, in 2021 and 2022, one individual of *P. sagittarius* was caught in Konacık and Yeşilovacık Bay, respectively (Ergüden et al., 2023; Gürlek et al., 2021). The recent and previous records of *P. sagittarius* on the Mediterranean coast of Türkiye are listed chronologically (Table 1).

The locations where P. *sagittarius* was caught in both the Gulf of Antalya and Muğla's Fethiye Bay represent the westernmost points of the species detected so far in the Levant Sea (Figure 3). Furthermore, Fethiye Bay lies on the border between the Aegean and Mediterranean Seas. Based on the locations where other researchers have caught the fish, it appears that *P. sagittarius* has gradually expanded its distribution westward (Farrag et al., 2016; Goren et al., 2010; Gökoğlu & Teker, 2018). The present records from Antalya

and Fethiye suggest that *P. sagittarius* is not only exhibiting a distinct westward geographic expansion but is also undergoing a vertical shift towards shallower waters of 40 to 70 metres. Furthermore, the capture of a juvenile specimen in the Gulf of Antalya, which measures only half of the species' maximum reported length, strongly supports the view that this fish is successfully establishing sustained populations in these newly occupied habitats. This demographic evidence, combined with its adaptation to shallower coastal waters, underscores the species' ongoing acclimation to the Mediterranean ecosystem. Henceforth, the fish is likely to be seen along the Aegean Sea and the coasts of Greece.

While writing this article, we learned that an individual was caught in Marmaris (Aegean Sea), confirming our view. However, because we did not receive the fish sample, the fish data could not be included in the article.

Table 1
Records of P. sagittarius *in Türkiye*

Author	Date of Record	Location	Depth (m)
Gökoğlu and Teker (2018)	2017	Tasucu	100
Gürlek et al. (2021)	2021	Konacık	80
Ergüden et al.(2023)	2022	Yesilovacık Bay	90
Present Study	2025	Antalya	70
Present Study	2025	Fethiye	40-50

CONCLUSION

Many fish species migrate from the Red Sea to the Mediterranean. Most of them are not consumed as human food and are not economically valuable. Moreover, some species, such as pufferfish, damage fishing gear and catches and complicate fishing operations. Literature on *P. sagittarius* indicates that its meat is consumed as human food, and it is also reported to be an important species for aquarium fishing (Anonymous, 2025).

ACKNOWLEDGEMENT

No funding was received from any institution or organisation for this study. The datasets generated and/or analysed during the current study are available from the corresponding author on reasonable request. The authors declare that they have no competing interests. Declarations regarding ethics approval, consent to participate, and consent to publish are not applicable, and no clinical trial number applies to this work

REFERENCES

Alshawy, F. A., Ibrahim, A., Hussein, C., & Lahlah, M. (2019). First record of arrow bulleye, *Priacanthus sagittarius Starnes*, 1988 from the Syrian marine waters (Eastern Mediterranean). *FishTaxa, 4*(2), 21-24. https://biotaxa.org/ft/article/view/4-2-1

Anonymous. (2025). *Arrow bullseye marine fish species*. Ontosight.ai. https://ontosight.ai/glossary/term/arrow-bullseye-marine-fish-species--67a26b37c445bf945af078cf

Carpenter, K. E., & De Angelis, N. (2016). *The living marine resources of the Eastern Central Atlantic: Volume 4. Bony fishes part 2 (Perciformes to Tetradontiformes) and sea turtles*. Food and Agriculture Organization of the United Nations. https://www.fao.org/3/i5715e/i5715e.pdf

Ergüden, D., Gürlek, M., & Turan, C. (2018). Confirmed occurrence of moontail bullseye, *Priacanthus hamrur* (Actinopterygii: Perciformes: Priacanthidae), in the Mediterranean Sea with first record off the coast of Turkey. *Acta Ichthyologica et Piscatoria, 48*(4), 387-391. https://doi.org/10.3750/AIEP/02415

Ergüden, D., Ayas, D., & Ergüden, S. A. (2023). Additional record of *Priacanthus sagittarius Starnes*, 1988 from the northeastern Mediterranean coast of Turkey. *Advanced Underwater Sciences, 3*(1), 15-18.

Farrag, M. M. S., Jawad, L. A., & Elhaweet, A. E. A. K. (2016). Occurrence of the arrow bulleye *Priacanthus sagittarius* (Teleostei: Priacanthidae) in the Egyptian coast of the Mediterranean Sea. *Marine Biodiversity Records, 9*, Article 6. https://doi.org/10.1186/s41200-016-0010-0

Froese, R., & Pauly, D. (Eds.). (2026). *FishBase* (version 07/2026). https://www.fishbase.org/

Goren, M., Stern, N., Galil, B. S., & Diamant, A. (2010). First record of the Indo-Pacific arrow bulleye *Priacanthus sagittarius* Starnes, 1988 in the Mediterranean Sea. *Aquatic Invasions, 5*(Suppl. 1), S45-S47. https://doi.org/10.3391/ai.2010.5.S1.011

Golani, D., Sonin, O., & Edelist, D. (2011). Second records of the Lessepsian fish migrants *Priacanthus sagittarius* and *Platax teira* and distribution extension of *Tylerius spinosissimus* in the Mediterranean. *Aquatic Invasions, 6*(Suppl. 1), S7-S11. https://doi.org/10.3391/ai.2011.6.S1.002

Gökoğlu, M., & Teker, S. (2018). Spread of the arrow bulleye *Priacanthus sagittarius* Starnes, 1988 in the Mediterranean Sea. *Acta Aquatica: Aquatic Sciences Journal, 5*(1), 1-3. https://doi.org/10.29103/aa.v5i1.455

Gürlek, M., Ergüden, D., & Turan, C. (2017). First record of elongate bulleye *Priacanthus prolixus* in the Mediterranean Sea. *Natural and Engineering Sciences, 2*(1), 44-47. https://doi.org/10.28978/nesciences.292356

Gürlek, M., Ergüden, D., & Turan, C. (2021). Range extension of *Priacanthus sagittarius* Starnes, 1988 southeastern Mediterranean coast of Turkey. *Çanakkale Onsekiz Mart University Journal of Marine Sciences and Fisheries, 4*(2), 235-239. https://doi.org/10.46384/jmsf.1018275

Yıldız, A., & Gokoglu, M. (2024). Pomacanthidae species in the Mediterranean and a new location record of the emperor angelfish *Pomacanthus imperator* (Bloch, 1787) from these species. *Thalassas: An International Journal of Marine Sciences, 40,* 1653-1657. https://doi.org/10.1007/s41208-024-00728-9

Pertanika J. Trop. Agric. Sci. 49 (5): 2467 - 2482 (2026)

PERTANIKA JOURNALS

TROPICAL AGRICULTURAL SCIENCE

Journal homepage: http://www.pertanika.upm.edu.my/

The Effect of Number of Shoots of Sorghum in First and Second Ratoon System

Avisema Sigit Saputro[1], Samanhudi[2]*, Puji Harsono[2], and Supriyono[2]

[1]Study Program of Agrotechnology, Faculty of Agriculture, Universitas Slamet Riyadi, Jl.Sumpah Pemuda 18, Joglo, Banjarsari, Surakarta, 57136 Central Java, Indonesia
[2]Study Program of Agrotechnology, Faculty of Agriculture, Universitas Sebelas Maret, Jl. Ir. Sutami 36A, Kentingan, Surakarta, 57126 Central Java, Indonesia

ABSTRACT

The ratoon cultivation system for sorghum offers various advantages, such as a short life span, minimal production costs, and the ability of the plant to grow again without the need to plant new seeds. The first objective of this research is to determine the effect of variety and number of shoots in ratoon 1 and ratoon 2, while the second objective is to determine the interaction between variety and number of shoots in the ratoon system. This research was conducted between March - August 2022 in Cabeyan, Sukoharjo, Central Java, Indonesia. Varieties used include Numbu, Super 1, Suri 3, Kawali, and Keller. The number of shoots used is up to four. The analysis of research on the 1st and 2nd ratoon was conducted as independent research with a Completely Randomized Block Design with 3 replicates. Comparison of the analysis of the 1st and 2nd ratoon. Two factors (Numbu, Super 1, Suri 3, and Keller) and the number of shoots (1, 2, 3, and 4) were used. The research results indicate that all parameters affect the variety and number of shoots in the 1st and 2nd ratoon. There was no interaction between varieties and number of shoots. All the variables were better in the 1st ratoon than in the 2nd ratoon. The first ratoon developed and performed better in terms of growth and yield than the second ratoon.

Keywords: Ratoon, shoots, sorghum, stem, yield

ARTICLE INFO

Article history:
Received: 06 August 2026
Accepted: 18 October 2026
Published: 30 October 2026

DOI: https://doi.org/10.47836/pjtas.49.5.18

E-mail addresses:
avissiip@gmail.com (Avisema Sigit Saputro)
samanhudi@staff.uns.ac.id (Samanhudi)
pharsono61@gmail.com (Puji Harsono)
supriyono_uns@yahoo.com (Supriyono)
* Corresponding author

INTRODUCTION

Sorghum is a versatile plant that can serve as both a food and an energy source across its various types and applications (Mehla et al., 2025; Stoicea et al., 2025). Sorghum stalks are often left neglected at harvest, even though they have the potential to produce ratoon shoots. The ratoon system is

© Universiti Putra Malaysia Press

established by planting the remaining parts of the harvest. The benefits of ratoon cultivation over seed-based cultivation include: a shorter life cycle, lower water use, less labour, and lower production costs. Production costs are low because it does not involve tilling or buying seeds.

Most studies on sorghum focus solely on seed production and planting material. The advantage of sorghum is that this plant can be ratooned, and the yield of ratoon one does not decrease significantly compared with yields on unratooned sorghum. Meanwhile, the yield of animal feed using ratooned sorghum was higher than that of sorghum ratooned previously. The production potential, in terms of both time and duration, can be up to 49 - 66 percent of the original performance or the initial crop (Hamaker et al., 2025). The rest of the sorghum stems are squeezed, and the 2 low outbreaks are left to produce new outbreaks. The performance of the culture at that time was also significantly and positively correlated with the main crop yield (Yali, 2026).

To achieve high yields, the number of shoots per clump in sorghum ratoon plants should be increased by using adult plants from the first ratoon. Sorghum is more drought-resistant than other cereals and is also more drought-resistant than corn. The research on the first and second ratoons was conducted separately, using the same treatments (five varieties and four types of shoots). Overall, there is no more than one ratoon in the existing research. Clarify the specific research gap and moderate the claim that no previous study has compared these ratoon cycles. Research on ratoon crops typically focuses on cultivation starting from seed and proceeding to the first ratoon.

This study addresses a research gap by examining the transition from the first to the second ratoon, as the second ratoon of sorghum has rarely been studied. This experiment will compare the growth and yield of sorghum in the first and second ratoons. The first objective of this research is to determine the effect of variety and shoot number in ratoon 1 and ratoon 2, while the second objective is to determine the interaction between variety and shoot number in the ratoon system.

LITERATURE REVIEW

Ratoon cultivation is a crop-growing technique that exploits a plant's ability to regrow after harvest, with shoots emerging from the base of the stem or other surviving parts of the plant (Wu et al., 2026). Several crops can be cultivated using the ratoon system, including rice, sorghum, sugarcane, bananas, and certain forage grasses (Cheyed et al., 2026). In the case of rice (*Oryza sativa* L.), this is known as "ratoon rice", the regrowth of shoots from the remaining stubble after harvest. This system allows farmers to obtain an additional yield within a relatively short period, as the crops do not require the stages of seedling preparation and replanting. The productivity of ratoon rice is influenced by the variety, the height at which the stalks are cut, the condition of the stubble, water availability, and fertilisation (Abirami et al., 2026).

The success of ratoon cultivation depends on a plant's tillering capacity, root system health, the availability of water and nutrients, and the variety's genetic characteristics. After the first harvest, emerging tillers must compete for light, water, growing space, and nutrients. Consequently, managing tiller numbers is critical to plant growth and productivity in a ratoon system. Regulating tiller numbers aims to balance the number of productive stalks with the resources available to each tiller (Luo et al., 2025). An excessive number of tillers intensifies competition, which can negatively affect stalk growth, panicle formation, grain filling, and biomass accumulation in individual stalks. Conversely, too few tillers may reduce the number of productive stalks per clump, thereby limiting total yield potential. Therefore, the optimal number of tillers must be determined based on production objectives and the specific characteristics of the variety being cultivated (Deng et al., 2025).

In ratoon sorghum, the response to tiller management may also differ between the first and second ratoon crops. These differences are linked to the plant's physiological state, photosynthate reserves, root development, and its capacity to regenerate after the previous harvest (Paesal et al., 2021). For this reason, research into tiller management is essential to identify a combination of tiller density and ratoon system that enhances cultivation efficiency and achieves optimal productivity. Second-ratoon cultivation in sorghum (*Sorghum bicolor* L.) is a production system that utilises the regrowth of shoots following the harvest of the main crop and the first ratoon (Zhou, 2024).

METHODS

The research was conducted from March to August 2022. The research location was in Cabeyan, Sukoharjo, Central Java, Indonesia. Materials used included herbicides, Urea fertiliser, and sorghum seeds: Numbu, Super 1, Suri 3, Kawali, and Keller. Measurement instruments included a metre, a hoe, a caliper, a hose, scales, and stationery. Each treatment combination measured 3 m in length, 1 m in width, and 30 cm in height. Planting spacing was 60 x 20 cm, with 1 m between ridges. Each ridge contained two planting rows, and each treatment plot held 20 plants (totaling 1200 plants). The planting area covered 400 m². Elevation was 104 m above sea level, and the soil type was Vertisol. Rainfall during the study period fell within the dry season, and water management relied on a rain-fed system.

This research was carried out in two ratoons, using the same experimental design in both. The two studies were conducted using a Completely Randomised Block Design with a factorial structure and 3 replicates. Analysis of Variance (ANOVA) was performed at the 5% level, after which the Duncan Multiple Range Test was used to analyse the observational data. Data analysis was conducted twice: once for the first ratoon and once for the second ratoon. The outcomes for ratoon 1 and ratoon 2 were compared for the variables. This research consisted of two factors. Factor I comprised sorghum varieties Numbu, Super 1, Suri 3, Keller and Kawali. Factor II was the occurrence of 1, 2, 3 and 4 shoots.

The experimental designs for ratoon 1 and ratoon 2 were identical, with the same treatments. The measured variables included plant height, stem diameter, weight of a bunch of seeds, number of seeds per clump, weight of 1000 seeds and seed yield per plot.

Cutting the sorghum stalks for ratoon cultivation is carried out concurrently with the harvest of the seed-grown crop. The stalks are cut at the second node above the ground. Regrowth begins seven days after cutting. By day 21, the shoots have fully emerged, allowing selection of the desired number of shoots. The same technique is used to prepare for the second ratoon crop. The sorghum is harvested 100 days after shoot selection.

RESULTS AND DISCUSSION

Plant Height

For the first ratoon, ANOVA results indicate that the variety and shoot number treatments influenced plant height; however, there was no interaction between the variety and shoot number treatments. Sorghum varieties can be useful to farmers, especially in situations where they are well-adapted to low soil fertility (Muui, 2026). According to Singh and Maiti (2026), sorghum variety diversity, the quantity, and the size of rod segments determine the height of the plants. The Numbu plant had two shoots in its normal form and four in the Kawali treatment. The Numbu cultivar was more than 2 metres in height. Sorghum variety Numbu thrived excellently in original soil at every time (Farooq et al., 2026).

Table 1
Plant height in all five varieties and in first-ratoon sorghum

Treatment	1st	2nd	3rd	4th	Average
Numbu	239.56	239.89	231.30	235.83	236.64c
Super 1	183.56	187.06	225.74	192.14	197.12b
Suri 3	195.11	213.83	195.57	190.36	198.72b
Keller	204.22	219.43	227.59	183.39	208.66b
Kawali	142.89	167.94	142.44	133.19	146.62a
Average	193.07ab	205.63c	204.53bc	186.98a	

Note. The same letter shows the absence of a significant difference at 5%
Source: Primary Data (2025)

The lowest average plant height was observed in the four-shoot group. The two-shoot treatment was more effective than either the single-shoot or four-shoot treatment. Shoot numbers are often high, causing intense competition that affects plant height. Varieties also affected plant height in ratoon 2. Numbu was the tallest, averaging 169.34 cm, followed by Keller, Super 1, Kawali, and Suri 3. The greatest shoot growth under the one-shoot treatment was 154.18 cm (Table 1). The next-highest value for shoot height was 130.75 cm under the four-shoot treatment, followed by the three- and two-shoot treatments (Table 2).

Table 2
Plant height in all five varieties and in second-ratoon sorghum

Treatment	1st	2nd	3rd	4th	Average
Numbu	206.44	152.67	163.33	154.92	169.34d
Super 1	151.33	134.33	117.85	136.91	135.11bc
Suri 3	123.11	95.22	81.91	105.16	101.35a
Keller	168.56	124.28	143.80	132.64	142.32cd
Kawali	121.44	67.56	133.02	124.11	111.53ab
Average	154.18c	114.81a	127.98a	130.75bc	

Note. The same letter shows the absence of a significant difference at 5%
Source: Primary Data (2025)

For the second ratoon, ANOVA results indicate that the variety and shoot number treatments influenced plant height; however, there was no interaction between the variety and shoot number treatments. There was a reduction in the average plant height of ratoon 2 compared with ratoon 1. This did not cause an excessive reduction in plant height. The decrease in height varied by variety. Ratoon 1-2 varieties of Numbu and Keller were high-morph. Plant height was associated with genetic characteristics. The population was negligible, which gave the best results. Examples include plant height and stem diameter. A higher population concentration tended to prevent plant growth. Leaf shading within the population caused this reduction, so only the leaves at the top received sunlight. The result was optimal photosynthetic activity in the population, thus affecting the metabolic processes of plants (Zou, 2026). An experiment using sugar cane and a raccoon system suggested that there was no significant difference between organic and inorganic fertilisers in terms of plant height (Yu et al., 2026). The same fertiliser as in ratoon 1 was used to fertilise ratoon 2. The yield in ratoon 2 was on the decline, although it was treated in the same way as ratoon 1. Vegetative character and ratoon plant production were largely related to the characteristics of ratoon plants, such as plant height, number of leaves, and stem diameter.

Stem Diameter

On the first ratoon, ANOVA results indicate that the variety and number of shoots treatments influenced stem diameter; however, there was no interaction between the variety and number of shoots treatments. The highest stem diameter was observed in the Kawali variety, with an average of 2.40 cm for 1 shoot (Table 3). The Keller variety with 4 shoots had the lowest stem diameter of 1 cm. The internode diameter character was used to show differences among varieties. The middle of the sorghum stem was usually straight and long compared with the lower and upper parts of the plant. The final segment (the end of the plant) was the longest and took the form of a panicle stalk. The internodes of sorghum were waxy, except at the ends of the stems, which were of sugar-cane type. The upper

surface wax screened the central rib of the leaves to a large extent, minimising water loss through the leaf surface and enhancing sorghum's ability to withstand drought (Santos et al., 2025). Super 1, Numbu, Suri 3, Kawali and Keller were the largest and smallest stem diameters, respectively. The species varied in their use of water, light and nutrients, which affected plant growth and development. The average stem diameter was highest with 1 shoot in ratoon 1. The lower the number of shoots, the better the growth, as there was no competition. This also had a significant influence on stem diameter, as nutrients could be taken up maximally.

Table 3
Stem diameter in all five varieties and in first-ratoon sorghum

Treatment	1st	2nd	3rd	4th	Average
Numbu	1.35	1.11	1.50	1.33	1.32a
Super 1	1.44	1.23	1.50	2.14	1.58bc
Suri 3	1.81	2.00	2.00	1.42	1.81c
Keller	1.81	2.00	1.43	1.00	1.56ab
Kawali	2.40	1.64	1.60	1.47	1.78bc
Average	1.76b	1.60a	1.61a	1.47a	

Note. The same letter shows the absence of a significant difference at 5%
Source: Primary Data (2025)

Ratoon 2 showed no variation in stem diameter across the varieties and the number of shoots. The largest stem diameter in ratoon 2 for the Kawali variety was 1.26 cm, with Super 1, Keller, Numbu and Suri 3 recording the lowest stem diameter of 0.79 cm (Table 4). The number of shoots with the largest diameter was treated as the number of shoots 1, and the lowest was treated as the number of shoots 2. Across all varieties, the average stem diameter in ratoon 2 decreased. The diameter of the rods in ratoon 2 decreased compared to ratoon 1.

Table 4
Stem diameter in all five varieties and in second-ratoon sorghum

Treatment	1st	2nd	3rd	4th	Average
Numbu	0.90	0.69	0.77	0.94	0.83a
Super 1	0.97	0.91	0.99	0.94	0.95a
Suri 3	0.98	0.74	0.57	0.88	0.79a
Keller	1.08	0.68	1.01	0.86	0.91a
Kawali	1.57	1.33	1.07	1.05	1.26a
Average	1.10c	0.87a	0.88ab	0.93ab	

Note. The same letter shows the absence of a significant difference at 5%
Source: Primary Data (2025)

There was a 50% reduction in the diameter of ratoon 2. The variety had varying growth in diameter when planted in ratoon 2. For the second ratoon, ANOVA results indicate that the variety and shoot number treatments influenced stem diameter; however, there was no interaction between them. In cases where diameter is small, yielding a smaller scale, the stems extract sap with the help of sorghum. Plant cane sugarcane farming technical efficiency averages were higher than those of ratoon cane sugarcane farming technical efficiency (Liu et al., 2025).

Seed Weight Per Clump

Seed weight per clump was influenced by treatment type and shoots number. Keller had the highest average seed weight per clump: 113.30 grams with 3 shoots. Suri 3 had the lowest, at 11.10 grams (Table 5). Variety and shoot number were interdependent (Ngidi et al., 2024). For the first ratoon, ANOVA results showed that variety and shoot number treatments influenced seed weight per clump, but there was no interaction between them. A variety is a group of plants with certain properties (morphology, physiology, cytology, chemistry, etc.) of interest to agriculture that will vary and be reproduced. The varieties had different genetic capabilities, and each sorghum type responded differently to the environment in which it was cultivated (Fadeyi et al., 2025).

Table 5
Seed weight per clump in all five varieties and in first-ratoon sorghum

Treatment	1st	2nd	3rd	4th	Average
Numbu	23.52	20.17	12.04	22.32	19.51a
Super 1	33.15	41.76	28.13	84.60	46.91b
Suri 3	26.98	26.07	11.10	70.99	33.78b
Keller	30.07	14.79	113.30	65.32	55.87c
Kawali	18.76	35.98	15.60	28.77	24.78ab
Average	26.50a	27.76a	36.03a	54.40b	

Note. The same letter shows the absence of a significant difference at 5%
Source: Primary Data (2025)

Not all cases were like those in Ratoon 2, where the quantity and varieties of shoots were not affected. In Table 6, the highest seed weight per clump in Ratoon 2 was 8.24 grams, recorded by Kawali, and the lowest seed weight per clump in Ratoon was 2.57 grams, recorded by Numbu, Suri 3, and Keller. The highest yield for two shoots was 6.47 grams, whereas the lowest for four shoots was 4.34 grams. Although they were planted in the same soil, the growth of many plant species varied. Keller Super 1, Suri 3, and Kawali seeds had the highest, middle, and lowest clump weights, respectively.

Table 6
Seed weight per clump in all five varieties and in second-ratoon sorghum

Treatment	1st	2nd	3rd	4th	Average
Numbu	7.45	6.11	9.07	5.88	7.13bc
Super 1	4.89	2.53	5.76	8.34	5.38abc
Suri 3	4.95	4.75	3.43	4.53	4.42ab
Keller	2.56	1.74	3.47	2.51	2.57a
Kawali	7.85	6,.8	7.43	11.11	8.24c
Average	5.54a	4.34a	5.83a	6.47a	

Note. The same letter shows the absence of a significant difference at 5%
Source: Primary Data (2025)

In the second ratoon, the ANOVA results indicate that variety and shoot number treatments affected seed weight per clump, but there was no interaction between them. Sorghum plants with a single stem generally produced one panicle clump. The study by Karunadhipathi et al. (2024) found that genotype had a substantial effect on all reproductive parameters, including flowering age, harvest age, panicle weight, seed weight per panicle, 1,000-seed weight, and harvest index. These parameters varied depending on the plant genotype. Genotype also influences variation in vegetative and reproductive traits, meaning that differences in the observed trait values result from genetic variation.

Number of Seeds Per Clump

The first ratoon ANOVA results indicate that the variety and shoot number treatments influenced the number of seeds per clump (Table 7). There was no interaction between the treatments. The number of seeds per clump in Kawali was 3,508.06, and in Numbu it was 2. The variety also produced different numbers of seeds per clump, as the number of seeds per panicle and the size of the seeds varied. This was due to the plant's genetics. Endalamaw et al. (2025) found that genetics and climatic and environmental factors were determinants of sorghum performance.

Table 7
Number of seeds per clump in all five varieties and in first ratoons sorghum

Treatment	1st	2nd	3rd	4th	Average
Numbu	51.90	560.49	653.70	657.44	615.81a
Super 1	995.22	1,285.43	884.47	2,302.33	1,366.86c
Suri 3	921.21	788.35	700.42	1,132.68	885.66ab
Keller	1,049.90	698.07	987.26	980.00	927.81bc
Kawali	1,818.37	3,112.60	2,752.85	3,508.06	2,797.97c
Average	1,075.26a	1,288.19a	1,195.74a	1,716.10c	

Note. The same letter shows the absence of a significant difference at 5%
Source: Primary Data (2025)

The Kawali type had the highest average seed count for its seed size, with smaller seeds and the same panicle shape as the other varieties. Competition reduced the yield component per plant when three or four plants were grown in a single planting hole, but the yield component per unit area was greater than when one or two plants were planted per hole. Experiments with plant populations indicated that high densities per hectare led to lower growth and yield per individual, but yield per hectare was larger. Sorghum ratoons require more time to emerge than rice. The ratoon then continues to grow and produces tillers.

In the Kawali variety, 2,176.78 was the highest number of seeds in a clump in ratoon 2, followed by the varieties Numbu, Keller, Super 1 and Suri 3. In the treatment, the number of shoots had the highest number of seeds. In the number of shoots, 3 was 871.76, and the lowest number of shoots was in treatment 2, which was 670.03. The varietal treatment in ratoon 2 was significant, but the number of shoots was not significant. The number of shoots had no interaction with the varietal treatment. The maximum number of seeds was realised in the Kawali variety, as high as 2,176.78, and the lowest in Suri 3 at 296.97. Shoots 3 produced the largest amount of seeds, as high as 871.76, and 2 produced the least at 670.03 (Table 8).

Table 8
Number of seeds per clump in all five varieties and in second-ratoon sorghum

Treatment	1st	2nd	3rd	4th	Average
Numbu	670.33	551.11	680.00	671.11	643.14a
Super 1	260.22	446.11	323.00	524.44	388.44a
Suri 3	268.22	457.50	139.67	322.50	296.97a
Keller	333.67	376.00	634.78	422.89	441.84a
Kawali	2,645.78	1,519.44	2,581.33	1,960.56	2,176.78b
Average	835.64a	670.03a	871.76a	780.30a	

Note. The same letter shows the absence of a significant difference at 5%
Source: Primary Data (2025)

This increase in the average number of seeds was observed only in the Numbu variety, reaching 643.14, compared with 615.18 seeds in ratoon 1. In the second ratoon, ANOVA results indicate that the variety and shoot number treatments influenced the number of seeds per clump; however, there was no interaction between the variety and shoot number treatments. Numbu has a strong capacity for tiller regeneration, allowing it to continue forming panicles and maintaining grain yield per clump even in the second ratoon crop. In contrast, the decline observed in the Super 1, Suri 3, and Keller varieties may be linked to a reduction in the number of productive tillers or a diminished ability of these tillers to produce fertile panicles. Ratoon growth depends on the condition of the root system, the base of the stem, the viability of remaining tillers, and the availability of carbohydrate

reserves and nutrients following the previous harvest. Numbu is able to maintain root function and utilise available resources relatively efficiently during the second ratoon cycle.

When this capacity is preserved, panicle formation and grain filling can proceed without a significant reduction in grain yield. Conversely, plants that experience a decline in root vigour, damage to the stem base, or a depletion of assimilate reserves may show reduced reproductive growth in subsequent ratoon cycles. This was not a substantial increase in yield, in comparison with the reduction across all varieties. Ratoon crops are environmentally sensitive. On genotypes that are able to survive stressful environmental conditions, good and stable ratoons can be produced. The stability of the main/primary plant does not necessarily correspond to the stability of the ratoon plant. Variations may occur in varietal differentiation between the main crop and the time of the plants in various locations (Utomo et al., 2025). All the vegetative quality of the period plants had lost value as compared to the main crop. Plants had a shorter time, fewer leaves and a smaller stem diameter than the plants from the seeds, even though they were fertilised with the same amount of fertiliser. The harvest age of the time plants was earlier than the main crop (Mekonen et al., 2025).

Weight of 1000 Seeds

Ratoon 1 ANOVA results indicate that the variety and shoot number treatments influenced the weight of 1000 seeds; however, there was no interaction between the variety and shoot number treatments. The average weight of 1000 seeds was greatest in Numbu, followed by the number of 1st shoots 42.24 g, and least in Kawali, with the number of 4th shoots 2.55 g (Table 9). The varieties planted in the same location exhibited varying responses to the constituents of plant growth and performance (Tian et al., 2026). The panicle and seed size of Kawali were the smallest compared with the other varieties. The weight of 100 grains determines seed size, with seed weight increasing as the weight of 100 grains increases (Nasreen et al., 2025). Seed size can determine seed weight. Advanced maturation and ageing lead to the production of the smallest seeds.

Table 9
Weight of 1000 seeds in all five varieties and in first ratoons

Treatment	1st	2nd	3rd	4th	Average
Numbu	42.24	38.59	39.41	26.10	36.59a
Super 1	33.69	38.96	24.98	36.86	33.63a
Suri 3	30.56	21.43	10.97	21.65	21.15a
Keller	29.92	32.18	26.05	24.80	28.24a
Kawali	8.46	4.54	8.11	2.55	5.92a
Average	28.98a	27.14a	21.90a	22.39a	

Note. The same letter shows the absence of a significant difference at 5%
Source: Primary Data (2025)

The seed number of the Kawali variety was the lowest among the other four varieties. When compared with the other varieties, the same amount was obtained at a lower weight. The quality of the seeds produced by the plant is related to their weight on 1000 seeds. The amount of nutrients available and the ability of plants to uptake nutrients like phosphorus during seed filling will influence the weight of 1000 seeds (Tóth et al., 2026). In ratoon 2, the various treatments and the number of shoots had no effect on the weight of 1000 seeds. The Numbu variety had the highest average yield of 30.28 grams, and Kawali had the lowest average yield of 4.25 grams (Table 10), respectively, in eight of 1000 ratoon 2 seeds. Kawali variety had the lowest average weight of 1000 seeds. Numbu is capable of maintaining effective grain filling under specific growing conditions, resulting in relatively heavy grains. The number of tillers can influence competition for light, water, nutrients, and photosynthetic products—or assimilates. If productive tillers have access to sufficient resources and the number of grains formed is relatively lower, the amount of assimilates available for each individual grain can increase, potentially leading to a higher grain weight. This result was the same as in ratoon 1. The average weight of 1000 seeds of ratoon 2 was reduced in comparison to ratoon 1. The weight loss of the 1000 ratoon seeds was also influenced by plant growth, such as reduced height and stem diameter. Genotype had a great impact on all vegetative characters of ratoon plants. The genotype of the ratoon plants influenced plant height, the number of leaves, and stem diameter.

Table 10
Weight of 1000 seeds in all five varieties and in second ratoons

Treatment	1st	2nd	3rd	4th	Average
Numbu	34.87	11.77	8.28	66.20	30.28b
Super 1	9.75	5.80	11.58	11.49	9.66ab
Suri 3	9.68	5.23	20.02	6.59	10.38ab
Keller	4.53	4.47	22.08	3.84	8.73ab
Kawali	3.58	3.08	4.71	5.61	4.25a
Average	12.48a	6.07a	13.33a	18.75a	

Note. The same letter shows the absence of a significant difference at 5%
Source: Primary Data (2025)

In the second ratoon, ANOVA results indicate that variety and shoot number treatments influenced the weight of 1000 seeds, but there was no interaction between these treatments. Ratoon growth and development are influenced by the growth of the main plant; a low generative phase is associated with low vegetative growth. The Numbu variety had the highest average 1,000-seed weight in Ratoon 2, at 30.28 grams, while Kawali had the lowest, at 4.25 grams. Among the shoot number treatments, four shoots produced the highest 1,000-seed weight at 18.75 grams, followed by three, one, and two shoots, which

had a weight of 6.07 grams. In Ratoon 2, a decrease in 1,000-seed weight was observed in all results. The plant's vegetative traits were associated with its reproductive traits, ratoon vegetative traits, and ratoon capacity. The ratoon's reproductive traits were correlated with its vegetative traits.

Seed Yield Per Plot

Seed yield per plot was the total weight of all seed of a given type in each treatment plot. Each treatment combination plot measured 3 m in length and 1 m in width, with a planting spacing of 60 x 20 cm. Consequently, a plot area of 3 m² accommodated a population of 20 plants. All plants in each plot were harvested, and the total seed weight per plot was then determined. The effect of the variety treatment was on seed yield per plot. The number of shoots had no effect on seed yield per plot within the treatment. The varietal treatment and the number of shoots did not interact. Super 1 had the highest yield of 604.33 grams, and Suri 3 had the lowest yield of 75.33 grams, with a number of shoots of 4 (Table 11). For the first ratoon, ANOVA results indicated that the variety and number of shoots treatments influenced seed yield per plot; however, there was no interaction between the variety and number of shoots treatments. The morphological and agronomic features of sorghum were highly variable, and sorghum weight varied with qualitative features of other species, such as panicle length and panicle type, the number of panicle branches, seed shape, and the number of seeds, which varied by species and by variety.

Table 11
Seed yield per plot in all five varieties and in the first ratoons

Treatment	1st	2nd	3rd	4th	Average
Numbu	262.67	130.00	146.67	182.67	180.50a
Super 1	259.33	315.00	406.33	604.33	396.25b
Suri 3	214.33	114.67	129.00	75.33	133.33a
Keller	290.67	521.33	307.67	394.33	378.50b
Kawali	147.00	119.00	100.33	146.33	128.17a
Average	234.80a	240.00a	218.00a	280.60a	

Note. The same letter shows the absence of a significant difference at 5%
Source: Primary Data (2025)

The highest yield was produced by four shoots. More shoots produce more panicles, and a greater number of panicles and sorghum grains leads to higher crop yields per plot. In Ratoon 2, average seed yield per plot did not differ significantly by variety treatment or number of shoots, and there was no interaction between these factors. The Kawali variety had the highest average yield in Ratoon 2, at 20.40 grams, while Keller had the lowest, at 4.56 grams. The highest yield among shoot-number treatments was 16.36 grams with four

shoots, while the lowest was 9.45 grams with two shoots. The best treatment was Kawali with four shoots, yielding 34.09 grams or 0.18 ton/ha. The poorest treatment was Keller with two shoots, yielding 2.54 grams or 0.13 ton/ha (Table 12).

Table 12
Seed yield per plot in all five varieties and in second ratoons

Treatment	1st	2nd	3rd	4th	Average
Numbu	8.93	17.95	27.80	16.41	17.77bc
Super 1	12.14	7.80	13.47	19.69	13.28
Suri 3	15.27	8.90	4.50	6.88	8.89ababc
Keller	2.54	1.97	9.01	4.73	4.56a
Kawali	16.89	10.64	19.99	34.09	20.40c
Average	11.15a	9.45a	14.95a	16.36a	

Note. The same letter shows the absence of a significant difference at 5%
Source: Primary Data (2025)

For the second ratoon, ANOVA results indicate that the variety and shoot number treatments influenced seed yield per plot; however, there was no interaction between the variety and shoot number treatments. These findings indicate that sorghum grain yields in the second ratoon crop declined significantly across all tested varieties. The largest decline was observed in the Keller variety (98.80%), followed by Super 1 (96.65%), Suri 3 (93.33%), Numbu (90.15%), and Kawali (84.09%). Kawali exhibited the smallest percentage decline and maintained the highest grain yield in the second ratoon crop, at 20.40 per plot. This suggests that Kawali performs relatively better in sustaining production during the second ratoon cycle compared with the other varieties. Numbu also maintained a relatively better yield than Super 1, Suri 3, and Keller, even though its percentage decline reached 90.15%. Such declines may be linked to reduced plant vigour, diminished shoot regeneration capacity, root system condition, and shifts in assimilate allocation during subsequent ratoon cycles. However, these factors remain potential explanations and require further substantiation through data on plant growth and yield components. Super-1 evolved from the selection of pure lines of local water varieties of Water Hammu White of Sumba, East Nusa Tenggara, Indonesia. Matured ICRAI (International Institute of International Plant Research) lines matured as Super-2 were a better kind of sweet sorghum, which had a potential high yield. The highest seed production was 6 ton/ ha, with a potential sap content of above 17% Brix scale.

CONCLUSION

The research results indicate that all parameters affect the variety and number of shoots in the 1st and 2nd ratoons. In the 1st ratoon, the Numbu variety had the greatest plant height,

while the Kawali variety had the largest stem diameter. Four shoots had a higher seed yield per clump and a lower plant height. There was no interaction between the characters and the varietal treatment for the number of shoots. In the 2nd ratoon, the Numbu variety was the heaviest, and Kawali had the largest stem diameter, which was the same as in ratoon 1. Super1 and Keller produced more seed per plot, but Kawali produced the best seed per clump. There was no effect of the varietal treatment on any traits in terms of shoot quantity. Ratoon 2 decreased all observational variables compared to Ratoon 1. The greatest reductions were observed in plant height and stem circumference. The counts of seeds, seed mass, weight of 1000 seeds, and seed yield per plot varied the most, with yield in Ratoon 1 decreasing by less than 10%.

IMPLICATION OF THE STUDY

This study shows that sorghum plants can be obtained from post-harvest residues by maintaining some branches. Sorghum branches only grow in ratoon systems; no branches appear in seed-grown plants. The study used five different sorghum varieties that produced varying growth and yields.

LIMITATION AND RECOMMENDATION FOR FUTURE RESEARCH

Fertiliser dosages were not compared experimentally. The use of higher fertiliser dosages is intended as a subject for future research, rather than as an established recommendation.

ACKNOWLEDGEMENT

The authors are grateful to Universitas Sebelas Maret for funding this research through the scheme of Mandatory Research (Non APBN) UNS for the fiscal year 2022, under Contract No. 254/UN27.22/PT.01.03/2022.

REFERENCES

Abirami, R., Vigneshwari, R., Malarkodi, K., Sakthivel, N., & Vanitha, K. (2026). Ratoon rice under a changing climate: Physiological responses and management strategies. *Plant Science Today, 13*(sp5). https://doi.org/10.14719/pst.16473

Cheyed, S. H., Al-Rawi, A. S. M., El-Fahdawi, W. A. T., Salih, H. A., & Rasheed, N. A. (2026). Prospects for use of ratoon agriculture in arid and semi-arid regions to achieve sustainable agriculture (Iraq as a model). *Bulgarian Journal of Agricultural Science, 32*(3), 504-512. https://doi.org/10.61308/yjy8eg50

Deng, S. -W., Abdellah, Y. A. Y., Chen, H. -Y., Gao, P. -L., Abdallah, M. M., Rana, M. S., & Wang, R. -L. (2025). Optimizing agricultural management practices to promote ratoon rice yield during ratoon crop: A comprehensive global meta-analysis. *Field Crops Research, 328*, Article 109943. https://doi.org/10.1016/j.fcr.2025.109943

Endalamaw, C., Nida, H., Tsegaye, D., van Biljon, A., Herselman, L., & Labuschagne, M. (2025). Genetics of sorghum: Grain quality, molecular aspects, and drought responses. *Planta, 261*, Article 47. https://doi.org/10.1007/s00425-025-04628-x

Fadeyi, O. J., Fabunmi, T. O., Idowu, V., Olowe, O., & Adejuyigbe, C. O. (2025). Agronomic responses of selected improved sorghum [*Sorghum bicolor* (L.) Moench] varieties to scheduled water stress. *Discover Agriculture, 3*, Article 230. https://doi.org/10.1007/s44279-025-00391-5

Farooq, U., Hussain, W., Fatima, Z., Ahmed, M., Ahmad, S., & Rashid, M. I. (2026). Kodo millet (*Paspalum scrobiculatum*): Low-input farming and ecosystem services. In M. Ahmed (Ed.), *Climate change and neglected underutilized crops* (Vol. 1, pp. 419-447). Springer Nature Switzerland. https://doi.org/10.1007/978-3-032-21005-0_15

Karunadhipathi, U. L., Malaviarachchi, M. A. P. W. K., Weerasinghe, W. M. P. B., & Mahipala, M. B. P. K. (2024). Alternative agronomic management practices through fertiliser, irrigation, and plant density adjustments for hybrid fodder sorghum (*Sorghum bicolor* L. Moench). *Journal of Agricultural Sciences-Sri Lanka, 19*(2), 275-284. https://doi.org/10.4038/jas.v19i2.10405

Ngidi, A., Shimelis, H., Abady, S., Figlan, S., & Chaplot, V. (2024). Response of *Sorghum bicolor* genotypes for yield and yield components and organic carbon storage in the shoot and root systems. *Scientific Reports, 14*, Article 9499. https://doi.org/10.1038/s41598-024-59956-x

Mehla, M. K., Palanisamy, S., Saini, D. K., & Jagadish, S. V. K. (2025). Global importance, production trends, and the need for designing the sorghum genome to address future climatic conditions. In *Designing sorghum genome for NextGen agriculture* (pp. 1-21). CRC Press. https://doi.org/10.1201/9781003623717-1

Mekonen, M., Chala, A., Tesfaye, K., Mengiste, T., Nida, H., Mekonnen, T., Tirfessa, A., Girma, G., Mehary, Z., Alemu, H., Kuru, B. & Geleta, M. (2025). Multi-location and multi-year field trials revealed broad-spectrum resistance of sorghum (*Sorghum bicolor* (L.) Moench) to anthracnose (*Colletotrichum sublineola*). *Journal of Phytopathology, 173*(2), Article e70065. https://doi.org/10.1111/jph.70065

Muui, C. W. (2026). Sorghum's potential in marginal environments: Importance, distribution, diversity, stress tolerance, and bio-enhancement with AMF and silicon. International *Journal of Bioresource Science, 13*(1), 97-113. https://doi.org/10.30954/2347-9655.01.2026.12

Nasreen, S. S., Begum, A. A., Kakon, S. S., Chowdhury, J. A., Ali, M. Z., Akther, S., Khan, M. A. H. & Mian, M. A. K. (2025). Effect of nutrient management on growth, yield and nutrient uptake in sorghum. *Bangladesh Agronomy Journal, 28*(2), 89-94. https://doi.org/10.3329/baj.v28i2.85874

Hamaker, B. R., Dabat-Partiot, M. H., vom Brocke, K., Mestres, C., & Taylor, J. R. (2025). Current and future state of sorghum in the 21st century. In *Sorghum and millets* (3rd Ed.), (pp. 1-20). Elsevier. https://doi.org/10.1016/B978-0-443-23954-0.00019-7

Liu, M., Liu, H., Zhang, H., Zhao, W., Zhao, Y., Zheng, Z., & Li, S. (2025). Comprehensive evaluation of new sorghum varieties and their light-simple and efficient production technology: A case study of Ji Niang No. 2. *Frontiers in Agronomy, 7*, Article 1518342. https://doi.org/10.3389/fagro.2025.1518342

Luo, W., Yuan, L., Yan, S., Wang, L., Yu, Y., Deng, H., Zhao, J., & Wang, R. (2025). Study on the suitable area of ratoon rice in China under climate change. *Ecology and Evolution, 15*(12), Article e72724. https://doi.org/10.1002/ece3.72724

Paesal, Syuryawati, Suarni, & Aqil, M. (2021). Sorghum cultivation of the ratoon system for increased yields in dry land. In *IOP Conference Series: Earth and Environmental Science, 911*, Article 012035. IOP Publishing. https://doi.org/10.1088/1755-1315/911/1/012035

Santos D'Almeida, C. T., Silva Oliveira, M. E. A., da Silva Lima, L. R., Carvalho, C. W. P., Mameri, H., & Ferreira, M. S. L. (2025). Sorghum. In S.A. Ceasar, S. Penna, C.W.P. Carvalho., S.M. Jain (Eds.), *Millets: Crops for climate resilience and for food and nutritional security* (pp. 239-269). Springer Nature Singapore. https://doi.org/10.1088/1755-1315/911/1/012035

Singh, V. P., & Maiti, R. K. (2026). Sorghum crop growth: Physiological insights across edapho-climatic conditions. *Farming & Management, 11*(1), 33-51. https://doi.org/10.31830/2456-8724.2026.FM-190

Stoicea, P., Iorga, A. M., David, L., & Bucur, C. G. (2025). Sorghum, the crop of the future under climate change conditions. *Scientific Papers Series Management, Economic Engineering in Agriculture & Rural Development, 25*(2), 789-803. https://managementjournal.usamv.ro/pdf/vol.25_2/Art76.pdf

Tian, R., Li, Z., Jiang, C., Yang, X., & Lu, Y. (2026). Physiological trade-offs between biomass yield and nutritional quality of sweet sorghum regulated by planting density and mowing in semiarid drylands. *Agronomy, 16*(18), Article 1814. https://doi.org/10.3390/agronomy16181814

Tóth, A., Kozma-Bognár, K., & Tóth, Z. (2026). Optimizing grain sorghum (*Sorghum bicolor* L. Moench) cultivation in Central Europe: Effects of seeding rate, nitrogen application and weed competition on hybrid performance. *Journal of Agronomy and Crop Science, 212*(4), Article e70225. https://doi.org/10.1111/jac.70225

Utomo, S. W., Lestari, F., Adiwibowo, A., & Fisher, M. R. (2025). Prediction of *Sorghum bicolor* (L.) distribution ranges provides insights on potential sorghum cultivation across tropical ecoregions of Indonesia. *BMC Plant Biology, 25*, Article 401. https://doi.org/10.1186/s12870-025-06454-5

Wu, W., Li, Z., Hassan, M. A., Xi, M., Zhou, Y., Tu, D., Wu, H., Su, H., & Li, X. (2026). Determining suitable growth period for ratoon rice cultivation in the Yangtze River basin. *BMC Plant Biology, 26*, Article 44. https://doi.org/10.1186/s12870-025-07804-z

Yali, W. (2026). Advances and challenges in sorghum breeding [*Sorghum bicolor* (L.) Moench]: Genomic tools, climate resilience and future directions. *Cogent Food & Agriculture, 12*(1), Article 2719981. https://doi.org/10.1080/23311932.2026.2719981

Yu, F., Tao, Y., Liu, L., Xie, P., Mace, E., Jordan, D., & Xie, Q. (2026). Sorghum2035: A decadal vision for sorghum functional genomics and molecular breeding. *Molecular Plant, 19*(3), 470-497. https://doi.org/10.1016/j.molp.2026.02.003

Zhou, Y., Huang, J., Li, Z., Wang, Q., Li, Y., Zhang, Y., Zhang, X. & Wu, Y. (2024). Optimal nitrogen management for high yield and N use efficiency of ratoon sorghum. *Scientific Reports, 14*, Article 19566. https://doi.org/10.1038/s41598-024-70555-8

Zou, C., Ma, J., Jin, T., Wang, X., Shi, X., Hao, Y., Guo, Z., Wei, X., Zhang, C., & Gai, Z. (2026). Physiological, metabolic, and transcriptional responses of contrasting sorghum (*Sorghum bicolor* (L.) Moench) cultivars to drought. *Plant Cell Reports, 45*, Article 57. https://doi.org/10.1007/s00299-026-03729-5

Pertanika J. Trop. Agric. Sci. 49 (5): 2483 - 2498 (2026)

PERTANIKA JOURNALS

TROPICAL AGRICULTURAL SCIENCE

Journal homepage: http://www.pertanika.upm.edu.my/

Identification and Diversity Analysis of *Uromycladium* on *Paraserianthes lophantha* subsp. *montana* Using a Multilocus Molecular Approach

I Made Mayun Maha Diputra[1], Sri Rahayu[1]*, Intan Berlian[1], and Tanaka Chihiro[2]

[1]Department of Silviculture, Faculty of Forestry, Universitas Gadjah Mada, Jalan Agro No. 1, Bulaksumur, 55281 Yogyakarta, Indonesia

[2]Terrestrial Microbiology and Systematics, Graduate School of Global Environmental Studies (GSGES), Kyoto University, Yoshida-Honmachi, Sakyo-ku, 606-8501 Kyoto, Japan

ABSTRACT

Gall rust caused by the *Uromycladium* complex is one of the most devastating diseases in forest plants. Gall rust affects several plant genera. *Paraserianthes lophantha* is one of the forest plants affected by gall rust disease. The disease also poses a serious threat to industrial forests such as *Falcataria moluccana*. However, to develop disease control strategies and risk assessments, no definitive species of *Uromycladium* associated with gall rust disease on *P. lophantha* subsp. *montana* is known in Indonesia. The research objective is to identify the existing *Uromycladium* species infecting *P. lophantha* in Indonesia using morphological identification and multilocus molecular analysis of the ITS and LSU regions. Morphological data for teliospore identification indicated that the causal agent of gall rust on *P. lophantha* was *Uromycladium tepperianum*, but molecular analysis identified it as *U. woodii.* Since the morphological features are more influenced by environmental conditions, we believed that molecular analysis was more accurate. Phylogenetic analysis showed that *U. woodii on P. lophantha* is distinctive from the *Acacia* group. These findings suggest that the *U. woodii* clade comprises several types of gall-forming rust fungi that differ by host species. Since *U. woodii* was also able to infect *F. moluccana,* an important industrial tree in Southeast Asia, monitoring and awareness of this rust fungus need to be improved.

Keywords: Gall rust, multi-gene, phylogeny, *Uromycladium woodii*

ARTICLE INFO

Article history:
Received: 24 May 2026
Accepted: 23 October 2026
Published: 30 October 2026

DOI: https://doi.org/10.47836/pjtas.49.5.19

E-mail addresses:
mayunws@gmail.com (I Made Mayun Maha Diputra)
sri.rahayu2013@ugm.ac.id (Sri Rahayu)
intanberlian@mail.ugm.ac.id (Intan Berlian)
tanaka.chihiro.6a@kyoto-u.ac.jp (Tanaka Chihiro)
* Corresponding author

INTRODUCTION

Paraserianthes lophantha (Willd.) I.C.Nielsen (syn. *Albizia lophantha*;

© Universiti Putra Malaysia Press

Fabaceae) is a leguminous shrub or small tree with a disjunct distribution. The lophantha subspecies occurs in south-western Australia, whereas subsp. *montana* (Jungh.) I.C.Nielsen is native to Indonesia, where it is found at high elevations on Sumatra, Java, Bali and Flores (Nielsen et al., 1983). Molecular phylogenetic work has confirmed that *Paraserianthes*, in the strict sense, is now restricted to *P. lophantha* and that the genus is closely related to *Acacia sensu stricto* (Brown et al., 2011). In Indonesia, *P. lophantha* colonises elevations typically above 1,500m up to 3,000+ m asl and grows along crater edges and active volcanic and gravel beds, while in Australia, *P. lophantha* subsp. lophantha naturally inhabits coastal environments (Nielsen et al., 1983). In Indonesia, villagers considered this species a high-mountain pioneer, used it for firewood, and never cultivated it as a planted tree. According to Rahayu (2014), *P. lophantha* subsp. *montana* has also been infected by *Uromycladium tepperianum*, a rust-forming gall that has caused outbreaks of gall rust diseases on *Falcataria moluccana* (sengon) in the Philippines, Sabah, Malaysia, and Java Island, Indonesia.

Gall rust disease is one of the most destructive diseases in forest plants, including *Acacia, Paraserianthes*, *Falcataria*, and *Calliandra* (Fraser et al., 2021; Pham et al., 2024; Rahayu, 2014). The rust fungus *Uromycladium* spp., native to Australia, causes the disease. There are 28 species in the genus *Uromycladium*, including *U. tepperianum*, *U. falcatarium*, *U. acaciae*, and *U. woodii*. (Doungsa-ard et al., 2015; McTaggart et al., 2015; Ryley, 2024). These rust fungi have complex life cycles that can involve up to three fruiting body types and four spore types. With the possible exception of *U. bisporum*, all *Uromycladium* species are microcyclic. *U. tepperianum* has only two spore states: pycniospores (spermatia) and teliospores. Morris (1987) reported urediniospores in the life cycle of all other species except *U. bisporum*. *Uromycladium* fungi are autoecious and require only one host to complete their life cycle. Gall rust diseases can vary by site or remain similar across vast regions, depending on complex interactions among the disease, the tree, and site- or region-specific ecology. According to Rahayu et al. (2018), more closed sites, undulating topography, fog, lower age, and higher altitude were significant local site conditions that support gall rust disease incidence and severity. High relative humidity and low wind speed promoted gall rust disease development. The most severe gall rust disease on *F. moluccana* occurred at elevations above 900 m a.s.l. at SFI, Sabah (Anonymous, 1993), while in East Timor the disease was most severe at elevations of between 700 and 900 m a.s.l. in the mountains southwest of Dili (Old & Cristovao, 2003). However, they did not explain why the disease was more severe at that elevation. According to Braza (1997), high-elevation areas, where environmental conditions appear conducive to rust development, are not considered for planting *F. moluccana* in the Philippines. At high elevations, foggy conditions usually occur. According to Hoff (1986), foggy periods with

intermittent showers induced high spore production, favoring rust infection. Uromycladium infection led to cell hyperplasia, which eventually caused tree mortality (Rahayu et al., 2010). However, researchers have also used Uromycladium as a biological control agent for the invasive *Acacia saligna* in South Africa (Morris, 1991; Wood & Morris, 2007).

McAlpine (1906) first reported gall rust disease on *P. lophantha* in Indonesia, caused by *U. tepperianum*. However, Morris (1987) described the *Uromycladium* species as highly specific to *P. lophantha* subsp. *lophantha* was *U. woodii*. Researchers collected this rust from the Porongurup Ranges, Western Australia, and maintained it on living plants at CSIRO, Australia, and the Agricultural Research Council Plant Protection Research Institute, South Africa, where they studied it as a potential biological control agent for *P. lophantha* (Impson et al., 2011). Because more than one *Uromycladium* taxon has been associated with *P. lophantha*, namely *U. woodii* in Australia and *U. tepperianum sensu lato* in Java, the relationship among these rusts in Indonesia remains to be determined. Hence, it also raises the question of how many *Uromycladium* species exist in Indonesia.

According to Doungsa-ard et al. (2018), *U. tepperianum s. lat.* was divided into 16 species. Therefore, genetic analysis of rust fungi is necessary to support the morphological identification studies. Occasionally, taxonomic identification based on morphological data alone does not align with genetic analysis results, leading to ambiguity. One extreme example of incongruence between morphology-based taxonomic relationships and Small Subunit (SSU) data is the case of the two genera in the family Pileolariaceae (*Pileolaria* and *Uromycladium*) (Cummins & Hiratsuka, 1983). These two genera appear unrelated based on SSU data, and they do not co-occur in phylogenetic trees (Wingßeld et al., 2004). To obtain accurate molecular data, multilocus analysis is required. For rust fungi, multilocus analysis is commonly used to assess diversity (Corcoran et al., 2014; Doungsa-ard et al., 2018; Zhafarina et al., 2021).

Inconsistencies between morphological identification and molecular data can also occur in rust fungi, given their high diversity and host-jump events (McTaggart et al., 2016; van der Merwe et al., 2008). Therefore, morphological identification and multilocus molecular analysis must be conducted simultaneously. In addition, the only *P. lophantha* rust sequenced so far is *U. woodii* from subsp. *lophantha* in Western Australia. *U. tepperianum sensu lato* was recorded on subsp. *montana* in Java by Magnus (1892) and Boedijn (1959), but those records are now of uncertain identity.

It is unknown whether the Indonesian rust is *U. woodii*, *U. falcatariae,* or a distinct species. This research aimed to validate the existing *Uromycladium* species infecting *P. lophantha* in Indonesia using morphological identification and multilocus molecular analysis.

MATERIALS AND METHODS

Sample Collection

Freshly mature galled tissue with mature teliospores of *P. lophantha* subsp. *montana* was collected in February 2016 from two mountains on the island of Java, Indonesia: Mount Merbabu and Mount Lawu. We also collected fresh, mature teliospores of *F. moluccana* from Mount Merapi simultaneously (Figure 1). We sampled two sites on each mountain and, at each site, collected galls from at least 3 symptomatic trees spaced 10 m apart. For each sample, we recorded GPS coordinates, elevation, the infected plant part, and gall morphology, as shown in Table 1.

We placed galled tissue in paper bags, transported it to the laboratory, dried it in an oven at 60 °C for DNA extraction, and kept it fresh for morphological examination. We identified and confirmed the host plant as *F. lophantha* subsp. *montana* using material from the herbarium at the Faculty of Forestry, Universitas Gadjah Mada, and validated by an expert botanist.

Morphological Examination

We mounted freshly collected rust spores on glass slides in 100% lactic acid and gently heated them to boiling before microscopic examination. We used ImageJ 1.46 to measure teliospore size range, germ pore width, and number of striae. We expressed teliospore size ranges as (min-max) and germ pore width as (min-max). Means and standard deviations (SD) were calculated from at least 50 spores of each host. We captured images with an EOS Kiss X5 camera attached to a DMLB Fluorescent Microscope (Leica Microsystems, Wetzlar, Germany).

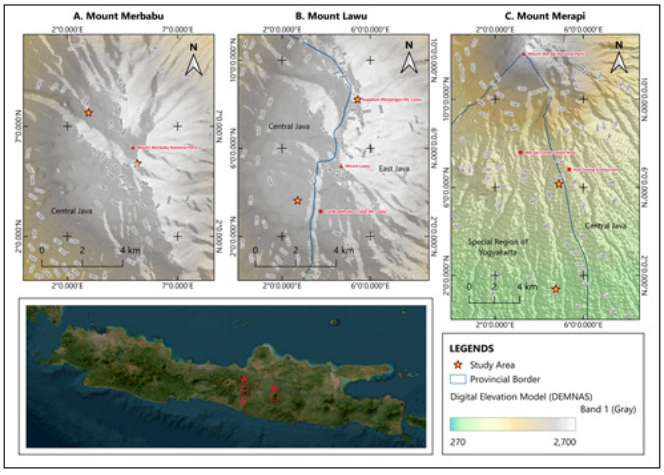

Figure 1. The study area for sample collection of (a) and (b) *Paraserianthes lophantha* subsp. *montana* forming galls infected by *Uromycladium* fungus at Mount Merbabu and Mount Lawu, (c) *Falcataria moluccana* at Mount Merapi infected by *U. falcatarium,* and (d) Their position in Java Island, Indonesia

Table 1
The location, host. elevation, infected plant part, and gall morphology of each sample

Sample	Mountain	Location	Host	Altitude m a.s.l.	Coordinates	Infected Plant Part	Gall Morphology
1	Merbabu	Boyolali Regency, Central Java	*Paraserianthes lophantha* subsp. *montana*	Pos 2, 2,507 m	-7.442683, 110.430005	branches and twigs, leaf petioles	globose, or woody convoluted masses
2	Merbabu	Boyolali Regency, Central Java	*Paraserianthes lophantha* subsp. *montana*	Kenteng Songo 3,100 m	-7.453925, 110.440491	branches and twigs, leaf petioles	globose, or woody convoluted masses
3	Lawu	Karanganyar Regency, Central Java	*Paraserianthes lophantha* subsp. *montana*	Telaga Menjangan 2,948 m	-7.612561, 111.198058	branches and twigs, leaf petioles	globose, or woody convoluted masses
4	Lawu	Karanganyar Regency, Central Java	*Paraserianthes lophantha* subsp. *montana*	Pos 3 Penggik 2,868 m	-7.635244, 111.184612	branches and twigs, leaf petioles	globose, or woody convoluted masses
5	Merapi	Cangkringan District, Yogyakarta Special Region	*Falcataria moluccana*	1,050 m	-7.589194, 110.458583	Stem and branch	as swollen, tumor-like, elongated
6	Merapi	Cangkringan District, Yogyakarta Special Region	*Falcataria moluccana*	650 m	-7.640667, 110.468639	Stem and branch	as swollen, tumor-like elongated

DNA Extraction, PCR Amplification, and Sequencing

DNA was extracted with a MagExtractor-Plant Genome Kit. Fungal nuclear rDNA was amplified by polymerase chain reaction (PCR) with LifePro Thermal Cycler version 2010-1.0 using the manufacturer-specified cycling and reaction conditions. The Large Subunit (LSU) region of rDNA was amplified with the primers Rust2inv/LR7 (Aime, 2006) and nested with the primers LR0R/LR6 (Vilgalys & Hester, 1990). The primers ITS1-F/ITS4-B were used for amplification of the Internal Transcribed Spacer (ITS) region of rDNA (Gardes & Bruns, 1993). The PCRs were performed with the following: initial denaturation at 94 ^{o}C for 2 min, followed by 40 cycles of denaturation at 94 ^{o}C for 30 s, annealing for 1 min, and extension at 72 ^{o}C for 1.5 min. The annealing temperatures were 56 ^{o}C for ITS amplification, 55 ^{o}C for initial LSU amplification, and 57 ^{o}C for nested LSU amplification. A final extension was performed at 72 ^{o}C for 7 min. PCR products were purified and subsequently sequenced by the Sanger direct sequencing method using an ABI PRISM 377 automated DNA sequencer.

Phylogenetic Analysis

Four samples in this study were sequenced, and the resulting sequences were aligned using BIOEDIT v. 7.0.9 (Hall et al., 2011). Additional ingroup sequences were selected based on BLAST searches (Altschul et al., 1990) and retrieved from GenBank based on their accession numbers listed in Table 2. A single outgroup sequence was included to root the phylogenetic trees. Maximum likelihood (ML) phylogenetic reconstruction was performed using MEGA 12 (Kumar et al., 2024). Prior to tree reconstruction, the best-fit nucleotide substitution model was determined using the model selection procedure, and the GTR+G+I model was selected for the analysis. Branch support was assessed using 1,000 bootstrap replicates (Felsenstein, 1985), and the resulting values were reported as maximum likelihood bootstrap percentages (MLBP). Bayesian inference (BI) was conducted using the BEAST software package (Bouckaert et al., 2019). The resulting phylogenetic trees were visualised using FIGTREE v. 1.4.3 (Rambaut, 2009), with Bayesian posterior probabilities (BPP) displayed as branch support values.

RESULTS AND DISCUSSION

Morphological Identification

Morphological examination showed that the rust fungi on *F. moluccana* and *P. lophantha* subsp. *montana* in Indonesia possess teliospores with converging striae and pedicellate teliospores (Figure 2). After comparing teliospore characteristics from *F. moluccana*, *Acacia* spp., and *P. lophantha* subsp. lophantha, the rust on *P. lophantha* subsp. *montana* showed striae similar to those of *Acacia* spp. (about 30-45). The striae range was broader than that of rust on *F. moluccana* (25-36). Teliospores from *P. lophantha* subsp. *montana* were

Table 2
List of rust specimens included in this study

No.	Taxon	Accession Number	Host	Genbank Accession	
				ITS Accession	LSU Accession
1	*Uromycladium brachycarpae*	BRIPa 58599	*Acacia brachycarpa*	KR994736	KR994685
2	*U. holosericeae*	BRIP 56538	*A. holosericea*	KR994740	KR994689
3	*U. farinosae*	BRIP 58154	*A. farinosa*	KR994737	KR994686
4	*U. implexae*	BRIP 57313	*A. implexa*	KR994743	KR994692
5	*U. leiocalycis*	BRIP 57285	*A. leiocalyx*	KR994746	KR994695
6	*U. ligustrinae*	BRIP 57708	*A. ligustrina*	KR994750	KR994699
7	*U. maslinii*	BRIP 57703	*A. latior*	KJ632999d	KJ632975d
8	*U. merrallii*	BRIP 58153	*A. merrallii*	KR994757	KR994711
9	*U. mitchellii*	BRIP 59355	*A. trudgeniana*	KR994836	KR994827
10	*U. morrisii*	BRIP 56963	*A. saligna*	KJ633022d	KJ632980d
11	*U. morrisii*	BRIP 57860	*A. saligna*	KJ633027d	KJ632988d
12	*U. murphyi*	BRIP 55674	*A. elata*	KR994837d	KR994828d
13	*U. murphyi*	BRIP 57629	*A. decurrens*	KR994838d	KR994829d
14	*U. murphyi*	BRIP 57929	*A. rubida*	KR994841d	KR994832d
15	*U. paradoxae*	BRIP 58152	*A. paradoxa*	KR994758	KR994712
16	*U. paradoxae*	BRIP 59221	*A. montana*	KR994761	KR994715
17	*U. paradoxae*	BRIP 59235	*A. verniciflua*	KR994762	KR994716
18	*U. tepperianum*	BRIP 57307	*A. ligulata*	KR994765	KR994719
19	*U. tepperianum*	BRIP 57707	*A. rostellifera*	KR994767	KR994721
20	*U. tepperianum*	BRIP 57742	*A. cupularis*	KR994769	KR994723
21	*U. tepperianum*	BRIP 59439	*A. xanthina*	KR994774	KR994728
22	*U. tepperianum*	BRIP 61265	*A. sclerosperma*	KR994777	KR994731

Table 2 (*continued*)

No.	Taxon	Accession Number	Host	Genbank Accession	
				ITS Accession	LSU Accession
23	*U. woodii*	BRIP 61600	*Paraserianthes lophantha*	KR994779	KR994733
24	*U. woodii*	BRIP 62249	*P. lophantha*	KR994780	KR994734
25	*Merbabu1 P. lophantha* subsp. *montana*	This study	*P. lophantha* subsp. *montana*	-	-
26	*Merbabu2 P. lophantha* subsp. *montana*	This study	*P. lophantha* subsp. *montana*	-	-
27	*Lawu1 P. lophantha* subsp. *montana*	This study	*P. lophantha* subsp. *montana*	-	-
28	*Lawu2 P. lophantha* subsp. *montana*	This study	*P. lophantha* subsp. *montana*	-	-
29	*Trachyspora intrusa*	BPI 843828	*Alchemilla vulgaris*	DQ354550	DQ354550

*Source: [d]Doungsa-ard et al. (2015)

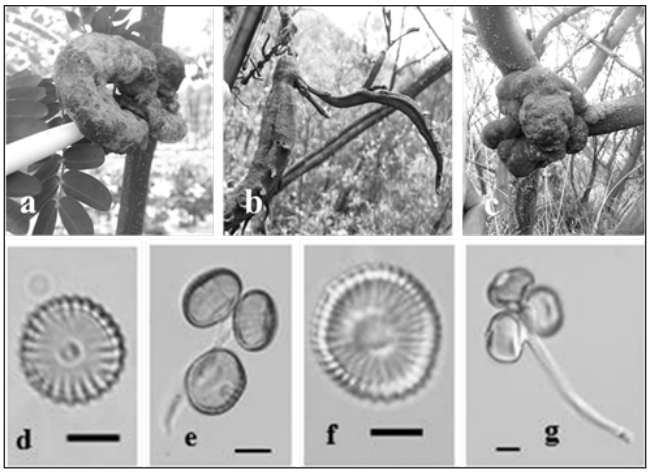

Figure 2. (a) The gall on the branch of *Falcataria moluccana*; (b) the gall on the twig; and (c) on the branch of *Paraserianthes lophantha* subsp. montana; (d) teliospores with converging striae and (e) pedicellate teliospores on *F. moluccana*; (f) teliospores with converging striae and (g) pedicellate teliospores on *Paraserianthes lophantha* subsp. montana Bar = 10 µm

bigger than those on *F. moluccana*, *Acacia* spp., and *P. lophantha* subsp. lophantha. The rust on *P. lophantha* subsp. *montana* also has larger germ pores (about 5-7 µm) than those of *F. moluccana* (2.5-4 µm), *P. lophantha* subsp. lophantha (3.5-5.5 µm), and *Acacia* spp. (3-5.5 µm) as well (Table 3).

Multi-Gene Molecular Analysis

Phylogenetic analysis based on the combined ITS and LSU rDNA sequences using Maximum Likelihood (ML) and Bayesian Inference (BI) approaches showed that the four *Uromycladium* samples obtained from *Paraserianthes lophantha* subsp. *montana* on Mount Merbabu and Mount Lawu clustered with two reference specimens of *U. woodii* (BRIP 61600 and BRIP 62249), receiving 100% ML bootstrap value (MLBP) and Bayesian posterior probability (BPP) of 1.00 (Figure 3). The two reference specimens of *U. woodii* formed a subclade supported by 90% MLBP and 1.00 BPP, while the internal relationships among the study samples showed varying levels of support. The five reference specimens of *U. tepperianum* associated with *Acacia* species formed a separate group, with support of 100% MLBP and 1.00 BPP. These results indicate that the sample in this study is more closely related to *U. woodii* than to *U. tepperianum*.

These results align with taxonomic revision by Doungsa-ard et al. (2018), who recognised *U. tepperianum sensu lato* as a species complex and described *U. woodii* as a distinct species. In that revision, *U. tepperianum sensu stricto* was restricted to hosts belonging to the *Acacia bevinosa* group, while *U. woodii* was described from *P. lophantha* subsp. *lophanta* in Western Australia (BRIP 61600 as the holotype and BRIP 62249 included

Table 3
Spore characteristics of Uromycladium *spp. on* F. moluccana, P. lophantha*, and* Acacia

Rust Species	Host	Size of Teliospores (µm)	Width of Germ Pore	Number of Striae	Colour and Shape of the Sori	Reference
U. tepperianum sensu Rahayu et al. 2010	*F. moluccana*	(18) 19-22 (24) × (17) 18-21 (22)	2-4	25-36	Cinnamon brown; depressed globose or subglobose	This study
U. tepperianum sensu Rahayu et al. 2010	*F. moluccana*	(17) 20-22 (24) × (17) 19-21 (22)	2-4	25-36	Cinnamon brown; depressed globose or subglobose	This study
U. falcatarium	*F. moluccana*	(17) 18-22 (24) × (13) 15-19 (21)	2.5-4	25-32	Cinnamon brown; depressed globose or subglobose	Doungsa-ard et al. 2015
Uromycladium sp.	*P. lophantha* subsp. *montana* sample 1	(22) 23-26 (28) × (20) 21-24 (25)	5-7	30-43	Cinnamon brown; depressed globose or subglobose	This study
Uromycladium sp.	*P. lophantha* subsp. *montana* sample 2	(22) 23-26 (29) × (21) 22-24 (25)	5-7	32-44	Cinnamon brown; depressed globose or subglobose	This study
Uromycladium sp.	*P. lophantha* subsp. *montana* sample 3	(23) 24-26 (27) × (21) 22-24 (25)	5-7	30-43	Cinnamon brown; depressed globose or subglobose	This study
Uromycladium sp.	*P. lophantha* subsp. *montana* sample 4	(21) 23-25 (28) × (20) 21-23 (25)	5-7	30-43	Cinnamon brown; depressed globose or subglobose	This study
U. tepperianum	*A. leiocalyx*[b]	(19) 20-22 (23) × (14) 14-20 (27)	4-4.5	31-38	Cinnamon brown; depressed globose or subglobose	Doungsa-ard et al. 2015
U. tepperianum	*A. implexa*	(16) 17-20 (21) × (12) 13-16 (17)	3-4.5	32-39	Cinnamon brown; depressed globose or subglobose	Doungsa-ard et al. 2015
U. tepperianum	*A. holosericea*	(18) 20-24 (24) × (16) 17-19 (20)	4-5.5	35-40	Cinnamon brown; depressed globose or subglobose	Doungsa-ard et al. 2015
U. tepperianum	*A. saligna*	(17) 18-22 (26) × (11) 14-18 (20)	4-5.5	33-40	Cinnamon brown; depressed globose or subglobose	Doungsa-ard et al. 2015
U. tepperianum	*A. latior*	(18) 20-22 (24) × (14) 16-18 (21)	4-5.5	30-44	Cinnamon brown; depressed globose or subglobose	Doungsa-ard et al. 2015

Table 3 (*continued*)

Rust Species	Host	Size of Teliospores (µm)	Width of Germ Pore	Number of Striae	Colour and Shape of the Sori	Reference
U. tepperianum	*A. coolgardiensis*	(19) 22-24 (26) × (15) 17-20 (22)	4-5.5	33-45	Cinnamon brown; depressed globose or subglobose	Doungsa-ard et al. 2015
U. tepperianum	*A. sibina*	(16) 19-22 (23) × (15) 16-18 (19)	4-5.5	33-44	Cinnamon brown; depressed globose or subglobose	Doungsa-ard et al. 2015
U. tepperianum	*A. acuminata*	(17) 19-23 (26) × (12) 15-18 (20)	4-5	33-44	Cinnamon brown; depressed globose or subglobose	Doungsa-ard et al. 2015
U. woodii	*P. lophantha* subsp. *lophantha*	(15.5)17-20 (21) × (21) 22-25(27)	3.5 - 5.5	22 - 35	Cinnamon brown; depressed globose or subglobose	Doungsa-ard et al. 2018

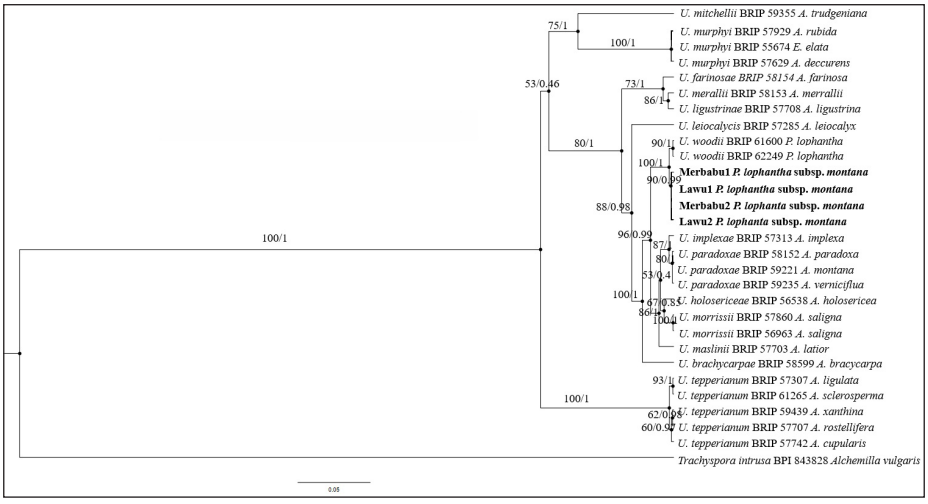

Figure 3. Phylogenetic tree using maximum-likelihood (ML) and Bayesian inference (BI) analysis. The number in each branch indicates the ML bootstrap value (MLBP) and Bayesian posterior probability values (BPP) based on ML analysis

as an additional specimen). Doungsa-ard et al. (2018) also noted that the taxonomic relationship between the rust fungus previously reported as *U. tepperianum sensu lato* on *P. lophantha* subsp. *montana* in Java and *U. woodii* remained unresolved. The present phylogenetic analysis provides a close relationship between the rust specimens collected from *P. lophantha* subsp. *montana* in Java and *U. woodii*.

We conducted phylogenetic analyses using a combined dataset of the internal transcribed spacer (ITS) region and the large subunit (LSU) rDNA, generated from an alignment of 28 ingroup and one outgroup sequences. We selected the ITS-LSU rDNA regions because they are widely used to infer phylogenetic relationships among closely related rust fungi (Aime et al., 2017; Doungsa-ard et al., 2018).

This research found that taxonomic identification varies between morphological data and multilocus molecular analysis. Based on the morphology of the *Uromycladium* rust fungus on *P. lophantha* subsp. *montana* was significantly different from those of *U. falcatarium* and *U. woodii*. The teliospores were larger, had a wider germ pore, and had a broader range of striae than those of *U. falcatarium* and *U. woodii*. The striae were similar to those of other *U. tepperianum*, except that the germ pore was larger and wider. Based on teliospore morphology, rust fungi on *P. lophantha* subsp. *montana* were identified as more closely related to *U. tepperianum*.

These size differences in *U. woodii* may be strongly related to environmental conditions. According to Loquez et al. (2025), Uromycladium teliospores increased significantly in length and width with elevation, with the largest dimensions at high elevations. Because the *U. woodii* collected by Doungsa-ard et al. (2018) came from a coastal area with higher

temperatures and lower relative humidity, whereas we collected the teliospore inoculum above 1,500 m a.s.l., where relative humidity is higher and temperatures lower, the teliospores tended to be larger. Teliospore size can vary with hydration state at the time of measurement, and lower temperatures often slow development but yield larger final cell sizes. Therefore, molecular identification based on LSU rDNA sequence data provided the most reliable species-level discrimination in this study.

Several studies have examined cross-inoculation of Uromycladium among hosts. Inoculation experiments on Acacia gall rust showed that Acacias were more susceptible to *U. tepperianum* isolates collected from the same *Acacia* species than to isolates from other species (Morris, 1987). Another study reported that teliospores collected from *F. moluccana* infected *P. lophantha* subsp. *montana* and vice versa (Rahayu, 2014). These findings suggest that *Uromycladium* diversity may include host-specific isolates that shape its genetic diversity. Thus, the occurrence of *U. woodii* in *P. lophantha* in Indonesia, which naturally grows in the highlands, poses a risk to other Fabaceae members. This study's findings illustrate Uromycladium diversity in Indonesia and raise awareness of gall rust disease, particularly at high elevations where *F. moluccana* grows near *P. lophantha*, which exhibits gall rust symptoms. Accordingly, at least three Uromycladium species have been recorded in Indonesia: *U. tepperianum*, *U. falcatarium*, and *U. woodii*.

CONCLUSION

The findings of this research showed that different identifications were based on morphological data and multilocus molecular analysis. However, molecular identification based on the combined ITS and LSU rDNA regions provided the most compelling evidence in this study. Based on multilocus analysis of the LSU and ITS regions, the causal agent of gall rust disease on *P. lophantha* subsp. *montana* was closely related to *U. woodii*. Therefore, at least three species of Uromycladium have been reported in Indonesia: *U. tepperianum*, *U. falcatarium*, and *U. woodii*.

ACKNOWLEDGEMENT

The authors thank JASSO for supporting this study through a scholarship for the Double Degree Program at Kyoto University.

REFERENCES

Aime, M. C. (2006). Toward resolving family-level relationships in rust fungi (Uredinales). *Mycoscience*, *47*(3), 112-122. https://doi.org/10.1007/S10267-006-0281-0

Aime, M. C., McTaggart, A. R., Mondo, S. J., & Duplessis, S. (2017). Phylogenetics and phylogenomics of rust fungi. *Advances in Genetics, 100*, 267-307. https://doi.org/10.1016/bs.adgen.2017.09.011

Altschul, S. F., Gish, W., Miller, W., Myers, E. W., & Lipman, D. J. (1990). Basic local alignment search tool. *Journal of molecular biology*, *215*(3), 403-410. https://doi.org/10.1016/S0022-2836(05)80360-2

Anonymous. (1993). *Gall rust disease on F. moluccana plantation in Sabah, Malaysia* [Unpublished annual report]. SSB Company.

Boedijn, K. B. (1959). The Uredinales of Indonesia. *Nova Hedwigia, 1*, 463-496.

Bouckaert, R., Vaughan, T. G., Barido-Sottani, J., Duchêne, S., Fourment, M., Gavryushkina, A., Heled, J., Jones, G., Kühnert, D., De Maio, N., Matschiner, M., Mendes, F. K., Müller, N. F., Ogilvie, H. A., du Plessis, L., Popinga, A., Rambaut, A., Rasmussen, D., Siveroni, I., Suchard, M. A., Wu, C. -H., Xie, D., Zhang, C., Stadler, T., & Drummond, A. J. (2019). BEAST 2.5: An advanced software platform for Bayesian evolutionary analysis. *PLoS Computational Biology*, *15*(4), Article e1006650. https://doi.org/10.1371/journal.pcbi.1006650

Braza, R. D. (1997). Gall rust disease of Paraserianthes falcataria in the Philippines. *Forest, Farm, and Community Tree Research Reports, 2,* 61-62.

Brown, G. K., Murphy, D. J., & Ladiges, P. Y. (2011). Relationships of the Australo-Malesian genus *Paraserianthes* (Mimosoideae: Leguminosae) identifies the sister group of *Acacia sensu stricto* and two biogeographical tracks. *Cladistics*, *27*(4), 380-390. https://doi.org/10.1111/j.1096-0031.2011.00349.x

Corcoran, P., Dettman, J. R., Sun, Y., Luque, E. M., Corrochano, L. M., Taylor, J. W., Lascoux, M., & Johannesson, H. (2014). A global multilocus analysis of the model fungus Neurospora reveals a single recent origin of a novel genetic system. *Molecular Phylogenetics and Evolution*, *78*, 136-147. https://doi.org/10.1016/j.ympev.2014.05.007

Cummins, G. B., & Hiratsuka, Y. (1983). *Illustrated Genera of Rust Fungi* (Rev. ed.). The American Phytopathological Society Press.

Doungsa-ard, C., McTaggart, A. R., Geering, A. D. W., & Shivas, R. G. (2018). Diversity of gall-forming rusts (*Uromycladium*, Pucciniales) on acacia in Australia. *Persoonia*, *40*, 221-238. https://doi.org/10.3767/persoonia.2018.40.09

Doungsa-ard, C., McTaggart, A. R., Geering, A. D. W., Dalisay, T. U., Ray, J., & Shivas, R. G. (2015). *Uromycladium falcatarium* sp. nov., the cause of gall rust on *Paraserianthes falcataria* in south-east Asia. *Australasian Plant Pathology*, *44*, 25-30. https://doi.org/10.1007/s13313-014-0301-z

Felsenstein, J. (1985). Confidence Limits on Phylogenies: An approach using the bootstrap. *Evolution*, *39*(4), 783-791. https://doi.org/10.2307/2408678

Fraser, S., McTaggart, A. R., Roux, J., Nel, J., Potgieter, J., Shuey, L. S., Somchit, C., & Wingfield, M. J. (2021). The life cycle and field epidemiology of *Uromycladium acaciae* (Pucciniales) on *Acacia mearnsii* in South Africa. *Annals of Applied Biology*, *179*(1), 21-33. https://doi.org/10.1111/aab.12677

Gardes, M., & Bruns, T. D. (1993). ITS primers with enhanced specificity for basidiomycetes - application to the identification of mycorrhizae and rusts. *Molecular Ecology*, *2*(2), 113-118. https://doi.org/10.1111/j.1365-294X.1993.tb00005.x

Hall, T., Biosciences, I. and Carlsbad, C. (2011). BioEdit: An important software for molecular biology. GERF Bulletin of Biosciences, 2, 60-61.

Hoff, R. J. (1986). *Susceptibility of pine populations to western gall rust—central Idaho* (Research Note INT-354). U.S. Department of Agriculture, Forest Service, Intermountain Research Station.

Impson, F. A. C., Kleinjan, C. A., Hoffmann, J. H., Post, J. A., & Wood, A. R. (2011). Biological control of Australian *Acacia* species and *Paraserianthes lophantha* (Willd.) Nielsen (Mimosaceae) in South Africa. *African Entomology, 19*(2), 186-207. https://doi.org/10.4001/003.019.0210

Kumar, S., Stecher, G., Suleski, M., Sanderford, M., Sharma, S., & Tamura, K. (2024). MEGA12: Molecular evolutionary genetic analysis version 12 for adaptive and green computing. *Molecular Biology and Evolution*, *41*(12), Article msae263. https://doi.org/10.1093/molbev/msae263

Loquez, M. O., Amper, C. D., Tulod, A. M., & Gilbero, D. M. (2025). Teliospore morphology characterization of *Uromycladium falcatariae* in falcata plantations at different elevations in Mindanao Island, Philippines. *Biodiversitas Journal of Biological Diversity, 26*(1), 296-305. https://doi.org/10.13057/biodiv/d260129

Magnus, P. W. (1892). Zur Kenntniss der Verbreitung einiger pilze [On the knowledge of the distribution of some fungi]. *Bericht der Deutschen Botanischen Gesellschaft, 10*, 195-200. https://www.biodiversitylibrary.org/page/36160175

McAlpine, D. (1906). *The rusts of Australia: Their structure, nature, and classification.* Government Printer. https://doi.org/10.5962/bhl.title.31958

McTaggart, A. R., Doungsa-ard, C., Wingfield, M. J., & Roux, J. (2015). *Uromycladium acaciae*, the cause of a sudden, severe disease epidemic on *Acacia mearnsii* in South Africa. *Australasian Plant Pathology*, *44*, 637-645. https://doi.org/10.1007/s13313-015-0381-4

McTaggart, A. R., Shivas, R. G., van der Nest, M. A., Roux, J., Wingfield, B. D., & Wingfield, M. J. (2016). Host jumps shaped the diversity of extant rust fungi (Pucciniales). *New Phytologist*, *209*(3), 1149-1158. https://doi.org/10.1111/nph.13686

Morris, M. J. (1987). Biology of the Acacia gall rust, *Uromycladium tepperianum*. *Plant Pathology, 36*, 100-106. https://doi.org/10.1111/j.1365-3059.1987.tb02183.x

Morris, M. J. (1991). The use of plant pathogens for biological weed control in South Africa. *Agriculture, Ecosystems & Environment*, *37*(1-3), 239-255. https://doi.org/10.1016/0167-8809(91)90153-O

Nielsen, I., Guinet, P., & Baretta-Kuipers, T. (1983). Studies in the Malesian, Australian and Pacific Ingeae (*Leguminosae-Mimosoideae*): The genera Archidendropsis, Wallaceodendron, Paraserianthes, Pararchidendron and Serianthes (Part I). *Bulletin du Muséum National d'Histoire Naturelle, Section B, Adansonia, 5*(3), 303-329. https://doi.org/10.5962/p.276287

Old, K. M., & Cristovao, C. D. S. (2003). A rust epidemic of the coffee shade tree (*Paraserianthes falcataria*) in East Timor. In H. da Costa, C. Piggin, C. J. da Cruz, & J. J. Fox (Eds.), *Agriculture: New directions for a new nation: East Timor (Timor-Leste)* (pp. 139-145). Australian Centre for International Agricultural Research.

Pham, N. Q., Wingfield, M. J., Marincowitz, S., Tanga, A. A., Tiki, K. R., Kassie, W. B., Hurley, B. P., Germishuizen, I., Lawson, S. A., Healey, M. A., & Wondafrash, M. (2024). First report of the wattle rust pathogen, *Uromycladium acaciae* (Raveneliaceae, Pucciniales) in Ethiopia. *Forestry: An International Journal of Forest Research*, *97*(2), 319-326. https://doi.org/10.1093/forestry/cpad040

Rahayu, S. (2014). *Strategi pengelolaan penyakit tanaman hutan di Indonesia: Penyakit karat tumor pada tanaman sengon (Falcataria moluccana)* [Forest plant disease management strategies in Indonesia: Gall rust disease on sengon (*Falcataria moluccana*)]. Gadjah Mada University Press.

Rahayu, S., Lee, S. S., & Shukor, N. A. A. (2010). *Uromycladium tepperianum*, the gall rust fungus from *Falcataria moluccana* in Malaysia and Indonesia. *Mycoscience*, *51*(2), 149-153. https://doi.org/10.1007/S10267-009-0022-2

Rahayu, S., See, L. S., Shukor, N. A. A., & Saleh, G. (2018). Environmental factors related to gall rust disease development on *Falcataria moluccana* (Miq.) Barneby & J. W. Grimes at Brumas Estate, Tawau, Sabah, Malaysia. *Applied Ecology and Environmental Research, 16*(6), 7485–7499. https://doi.org/10.15666/aeer/1606_74857499

Rambaut, A. (2009). FigTree v1.3.1: *Tree figure drawing tool*. Institute of Evolutionary Biology, University of Edinburgh.

Ryley, M. J. (2024). Wattle gall—the quintessential Australian plant disease. *Historical Records of Australian Science*, *35*(2), 116-129. https://doi.org/10.1071/HR230066

van der Merwe, M. M., Walker, J., Ericson, L., & Burdon, J. J. (2008). Coevolution with higher taxonomic host groups within the Puccinia/Uromyces rust lineage obscured by host jumps. *Mycological Research*, *112*(12), 1387-1408. https://doi.org/10.1016/j.mycres.2008.06.027

Vilgalys, R., & Hester, M. (1990). Rapid genetic identification and mapping of enzymatically amplified ribosomal DNA from several *Cryptococcus species*. *Journal of Bacteriology*, *172*(8), 4238-4246. https://doi.org/10.1128/jb.172.8.4238-4246.1990

Wingßeld, B. D., Ericson, L., Szaro, T., & Burdor, J. J. (2004). Phylogenetic patterns in the Uredinales. *Australasian Plant Pathology*, *33*, 327-335. https://doi.org/10.1071/AP04020

Wood, A. R., & Morris, M. J. (2007). Impact of the gall-forming rust fungus *Uromycladium tepperianum* on the invasive tree *Acacia saligna* in South Africa: 15 years of monitoring. *Biol. Control*, *41*(1), 68-77. https://doi.org/10.1016/j.biocontrol.2006.12.018

Zhafarina, S., Wibowo, A., & Widiastuti, A. (2021). Multi-genetic analysis of *Colletotrichum* spp. associated with postharvest disease of fruits anthracnose in Special Region of Yogyakarta, Indonesia. *Pakistan Journal of Biological Sciences*, *24*(1), 53-65. https://doi.org/10.3923/pjbs.2021.53.65

Pertanika J. Trop. Agric. Sci. 49 (5): 2499 - 2522 (2026)

PERTANIKA JOURNALS

TROPICAL AGRICULTURAL SCIENCE

Journal homepage: http://www.pertanika.upm.edu.my/

Aquaponics as a Sustainable Food Security Solution: Global Scholarly Trends and Intellectual Structure Analysis

Nor Azilah Husin[1,2], Amirul Syafiq Mohd Ghazali[1,2], Azni Abdul Rashid[1], Nurzalyna Mohamed Zaki[1]*, and Nasser Al Yahyaei[3]

[1]School of Business and Social Sciences, Albukhary International University, 05200 Alor Setar, Kedah, Malaysia
[2]Research Fellow, Centre for Excellence in Socio Economic Development and Innovation, Albukhary International University, Jalan Tun Razak, 05200 Alor Setar, Kedah, Malaysia
[3]Faculty of Business Studies, Arab Open University, Muscat, 130 Muscat Governorate, Oman

ASBTRACT

This study presents a comprehensive bibliometric analysis of 328 peer-reviewed journal articles retrieved from the Dimensions AI database to examine the intellectual structure, research trends, and thematic evolution of aquaponics research, with a specific focus on food security. Using a structured Boolean search strategy and defined inclusion criteria, performance analysis and science mapping techniques, including bibliographic coupling and keyword co-occurrence analysis, were employed to identify influential contributors, research networks, and emerging themes. The findings reveal substantial publication growth between 2019 and 2025, reflecting increasing scholarly interest in sustainable and resource-efficient food production. Performance analysis identifies influential authors, institutions, journals, and countries, highlighting the international development of aquaponics research. Bibliographic coupling reveals interconnected research streams addressing technological innovation, environmental sustainability, and regional food security applications. Keyword co-occurrence analysis identifies prominent themes involving water efficiency, hydroponic integration, climate resilience, community implementation, and smart agriculture. Two major knowledge domains emerge: technology-driven aquaponics optimisation and community-based food security implementation. These findings suggest a gradual shift from experimental system development towards scalable, digitally supported, and socio-economically relevant applications. Unlike previous reviews examining aquaponics broadly, this study specifically maps the intersection between aquaponics and food security, providing a more focused understanding of its intellectual and thematic development. The findings identify emerging research priorities and offer useful insights for

ARTICLE INFO

Article history:
Received: 17 July 2026
Accepted: 20 October 2026
Published: 30 October 2026

DOI: https://doi.org/10.47836/pjtas.49.5.20

E-mail addresses:
azilah.husin@aiu.edu.my (Nor Azilah Husin)
syafiq.ghazali@aiu.edu.my (Amirul Syafiq Mohd Ghazali)
azni.rashid@aiu.edu.my (Azni Abdul Rashid)
nurzalyna.zaki@aiu.edu.my (Nurzalyna Mohamed Zaki)
nasser.y@aou.edu.om (Nasser Al Yahyaei)
* Corresponding author

© Universiti Putra Malaysia Press

policymakers, researchers, and practitioners seeking to strengthen sustainable food production, resource efficiency, and long-term food security.

Keywords: Aquaponics, bibliometric analysis, bibliographic coupling, food security, science mapping, sustainable food production

INTRODUCTION

The world's food systems are increasingly challenged by rapid urbanisation, climate change, resource scarcity, and supply chain disruptions. Such pressures have increased the exploration of novel and effective solutions to agriculture, ensuring food security in the longer term. While the world is facing the issue of food insecurity, resilient and practical options in food production are much needed, especially in densely populated areas (Khan et al., 2020). In a broader framework of circular resource utilisation, aquaponics integrates a production system that focuses on resource efficiency by linking aquaculture and hydroponics. Using this system, good microorganisms convert nutrients from fish waste into forms absorbable by plants. Plants remove nutrients from the water before it is recirculated to the fish tanks. The integrated process reduces water consumption, minimises nutrient discharge and enables productive resource use, rather than being treated as waste. By incorporating circular economy principles, aquaponics transforms waste streams into valuable inputs, reducing reliance on external resources and offering an effective approach to sustainable urban food production. The overall sustainability of aquaponics systems is also dependent on crucial factors such as energy consumption, system design, nutrient management and operational costs. Singapore is using technological innovation in the application of smart food system strategies in resource-challenged settings (Mok et al., 2020). One of the emerging technologies in fish and crop production is the combination of aquaculture and hydroponics that utilises water and nutrients in the system. The research indicated that this crop could enhance sustainable food production in dry and resource-limited regions (Abusin & Mandikiana, 2020).

The increasing need for sustainable food production is largely due to the growing scarcity of natural resources, especially water and agricultural land. In circular food production, recycling and resource recovery practices reuse materials rather than discard them, offering practical ways to reduce waste and enhance resource efficiency. Exemplifying this approach, aquaponics provides a system that combines fish farming and plant cultivation, recycling water and nutrients. It offers meaningful benefits for food security, environmental protection and sustainability, although future research is required to understand its contributions, identify knowledge gaps and determine further research directions to ensure ecosystem practicality in attaining the desired outcome. Recent studies have demonstrated the potential of innovative recycling and waste-valorisation approaches to enhance resource recovery

while minimising environmental impacts. The reuse of nutrient-rich aquaculture effluent in aquaponic systems promotes water conservation, reduces dependence on synthetic fertilisers and supports sustainable agricultural production (Abd Aziz et al., 2026). The integration of aquaculture and hydroponics facilitates continuous nutrient recycling in a closed-loop production environment, highlighting the effectiveness of aqua beds in enhancing nutrient cycling, supporting plant growth, and reducing environmental impacts (Abd Aziz et al., 2025). Furthermore, their study identified alternative growing substrates, such as carbonised rice husk and cocopeat, as innovations for enhancing resource efficiency and sustainability in aquaponic farming.

The latest developments also enhance the feasibility of aquaponics due to digitalisation and precision agriculture. The use of models of artificial intelligence (AI) and machine learning has proven to be effective in controlling nutrients and irrigation processes to achieve efficiency (Dhal et al., 2022), while AI-based forecasting can be employed to boost productivity and resilience of the supply chain (Dhal & Kar, 2024). Smart systems based on IoT enable real-time monitoring of water quality and environmental parameters (Dutta et al., 2025; Kok et al., 2024). Furthermore, the use of crop diagnostic technologies (Abbasi et al., 2023) supports the detection of diseases and plant health management in aquaponic systems. The application of integrated nutrient management (INM) techniques and bio-stimulants is also used to optimise soilless cultivation systems (Ali et al., 2024). Climate resilience is increasingly emerging as a critical issue, and climate change is impacting sustainable food production systems due to technological developments (Mešić et al., 2024). Despite these changes, the previous bibliometric mapping of aquaponics was quite general and did not focus specifically on aquaponic farming and food security, with the need for a bibliometric analysis of those two areas to track the research and intellectual trends and emerging themes at that intersection. This study addresses the gap in the aquaponics literature. Basumatary et al. (2023) examined the broader development and intellectual structure of global aquaponics research, while Kushwaha et al. (2025) reviewed aquaponic configurations, operational parameters, and microbial dynamics.

These studies provide valuable foundations for understanding the technological development and scientific evolution of aquaponics. On the other hand, this study positions aquaponics within specific context of food security, zooming into the research landscape through a food-system and sustainability perspective instead of just technological or operational considerations. Bear in mind that this distinction is significant as the advancement in aquaponics technology does not necessarily translate into demonstrable improvements in food security. Challenges in technological efficiency, system productivity and operational optimisation are only part of the broader challenges, and to understand aquaponics' contribution to food security demands attention to issues of food availability, accessibility, nutritional outcomes, economic feasibility, resource sustainability, and the potential adoption by vulnerable communities.

METHODOLOGY

Bibliometric analysis examines research trends, publication patterns, and the contributions of authors, institutions, and countries, while science mapping identifies and visualises relationships among research topics and their intellectual structures. Contrastively, a systematic literature review critically examines and summarises previous studies to answer specific research questions. Therefore, this study adopts bibliometric analysis supported by science mapping techniques, including bibliographic coupling and keyword co-occurrence analysis. By examining 328 journal articles, the study identifies global research trends, key contributors, major research themes, and emerging directions in aquaponics and food security. This approach provides a clearer understanding of how research in this field has developed. This study used a bibliometric research design to conduct a systematic review of the academic literature on aquaponic farming and food security. The decision to use bibliometric analysis was based on its ability to quantify research trends, high-impact publications, and topic frameworks within a particular body of literature. In addition, the methodological framework was developed based on the previous study on sustainability and aquaponics, a concept of unity between urban agriculture, technological development and food system resilience (Khan et al., 2020; Mok et al., 2020; Pulighe & Lupia, 2020). The dataset was retrieved from the Dimensions AI database using a structured Boolean search that combined aquaponics-related terms with food security concepts. Peer-reviewed journal articles published in the specified time frame were used to achieve academic rigor and relevance.

The collected data were analysed for performance analysis and science mapping, including bibliographic coupling and occurrence of keywords. By analysing performance indicators, citations, total link strength, authorship pattern, institutional contribution and country productivity, the impact of research and collaboration networks was identified. Bibliographic coupling detected intellectual connections among studies with common references, and co-occurrence analysis revealed prevailing and emerging research topics. Network analyses were conducted using VOSviewer (version 1.6.20) (van Eck & Waltman, 2010). Our study combined performance analysis (identifying top-performing documents, authors, institutions, journals, and countries) with science mapping (bibliographic coupling and co-occurrence analyses). To ensure that only the most significant and highest-quality data were included, we set a target benchmark of 60 items as the maximum threshold for each analysis. For analyses where 60 items were available, we applied a threshold of 60; for others where fewer items met the criteria, we adjusted the threshold accordingly, down to a minimum of 36. Across all analyses, these threshold values ranged from 36 to 60. This approach allowed us to filter out weak connections and focus solely on the most impactful contributions to the field (Donthu et al., 2021). The analytical technique used herein is similar to previous empirical and review studies on aquaponics that focused on

the sustainability, water efficiency, microbiology, and feasibility of aquaponics adoption (Abisha et al., 2022; Abusin & Mandikiana, 2020; Kasozi et al., 2021).

In addition, literature covering water management (Calone et al., 2019), system adoption issues (Okomoda et al., 2022), food sovereignty (Ibrahim et al., 2023), and applications of food security in the region was employed to give theme to the clusters (Obirikorang et al., 2021). This methodological process ensured the transparency, reproducibility, and comprehensive evaluation of the knowledge base on aquaponic farming as part of the elements supporting the establishment of sustainable food systems.

Search Strings

The inclusion criteria were also formulated meticulously to ensure the bibliometric data thoroughly considers the existing scholarly input on the links between aquaponic farming and food security outcomes. The retrieval of all records was limited to the Dimensions AI database, an all-encompassing index of peer-reviewed scientific publications across multidisciplinary fields. Consistency in metadata, citation tracking, and indexing quality was achieved by using only one validated database. The time period was limited to publications from 2019-2025 to account for recent changes and advancements in aquaponic technology, sustainability practices, and food systems resilience (Table 1). This is a particularly timely issue because, in the past decade, aquaponics has emerged as an area of interest in the field of agriculture that utilises climate-friendly solutions.

Table 1
Inclusion Criteria

Dimension Database	**ALL**
Time Period	2019 to 2025; searched on 11 July 2025
Search Keywords	("aquaponic*" OR "aquaponics system*" OR "aquaponics farm*" OR "integrated aquaculture hydroponic*" OR "aquaculture-hydroponic integration" OR "recirculating aquaculture system) AND ("food security" OR "food secur*" OR "food availability" OR "food access" OR "nutrition security" OR "food self-sufficiency" OR "sustainable food production")
Publication Type	Article
Language	English
Open Access	All OA

The selection of keywords included technical and outcome-based terms. The system-oriented descriptors were combined with concepts about food security, such as “food security,” “food availability,” “food access,” “nutrition security,” “food self-sufficiency,” and “sustainable food production.” This logical approach guaranteed the conceptual compatibility of production technologies and food security effects. The inclusion criteria

included Journal articles; open-access categories were accepted to ensure maximum accessibility and transparency. These filters helped narrow the next 550 records to 328 relevant studies most suitable to the research objectives. This systematic approach to editing minimised peripheral and/or irrelevant material while preserving key empirical and theoretical contributions.

RESULTS

The PRISMA (Preferred Reporting Items for Systematic Reviews and Meta-Analyses) framework was used to offer a clear and replicable screening procedure for the final selection of the literature. PRISMA is a set of instructions that help researchers report the identification, selection, screening, and inclusion of research for systematic reviews and meta-analyses in a transparent and clear way. It ensures the research process is easy to understand, repeatable and unbiased by showing all steps of the research selection process (Moher et al., 2009; Page et al., 2021).

It began with an identification step, in which the 550 publications were identified using the given search string in the Dimensions AI database. The aim at this stage was not to be precise but to capture broadly so as not to miss potentially relevant studies. In the screening phase, non-article sources and publications that did not directly reference both aquaponic systems and food security outcomes were excluded. The eligibility phase included further screening of the remaining records, where the inclusion criteria included: the type of publication (articles only), open access (only), and time period (defined). Lastly, the inclusion stage produced 328 articles that met all the requirements. This process of identifying the final inclusion is visually displayed in the PRISMA flowchart, which shows a decrease from 550 to 328 publications (Figure 1). This transparency of the methods enhances the credibility of the bibliometric analysis and enables the researcher to conduct a similar process in the future with confidence.

Performance Analysis

Performance analysis measures the productivity and the contribution of the research outputs. It quantifies such indicators as publications, documents, citations, authors, institutions, and countries. This critique shows the most instrumental ones, up-and-coming research centers, and the scholarly impact in a given field or subject.

Publication Trend Analysis

The trend analysis provides insight into how scholars' interest in aquaponic farming as an option for improving food security has changed. With the analytical overview provided by Dimensions AI, 328 publications were reviewed within the 2019 to 2025 period (Figure 2).

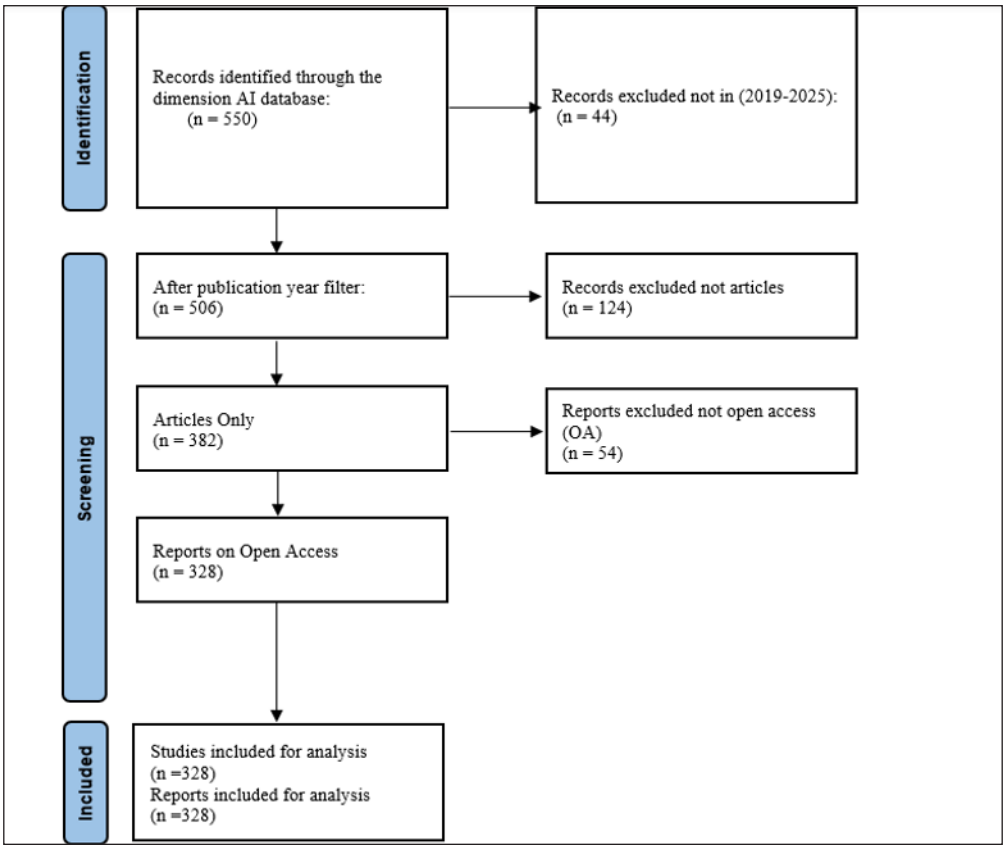

Figure 1. PRISMA flowchart

This period is when sustainable food production, urban agriculture and resource efficiency are gaining global momentum. The number of publications is slowly increasing, suggesting the experimental system of aquaponics has moved beyond the niche and has become an established area of research with possible policy and development outcomes.

The initial years of the period involved exploration, feasibility studies, and technical evaluations of the feasibility of combining aquaculture and hydroponics. As the field matures, studies moved into a variety of directions such as maximising yield, improving use of water, recycling nutrients and optimising costs. Subsequent studies focused on broader impacts, such as access to food, climate change adaptation, and participation in local food production. The rise in citation counts may represent an actual growth in production, and the influence and dissemination of knowledge within the scientific community.

The world's interest in sustainable agriculture, especially in urban and resource-limited settings, could also be a representation of the positive trend because aquaponics provides year-round production using minimal land area. The multidisciplinary collaboration of environmental scientists, agricultural engineers and food policy researchers is highlighted

in the growing literature. The fact that the publications and citations have been steadily increasing suggests that aquaponic farming is being regarded as a viable pathway to better food security and sustainable food systems.

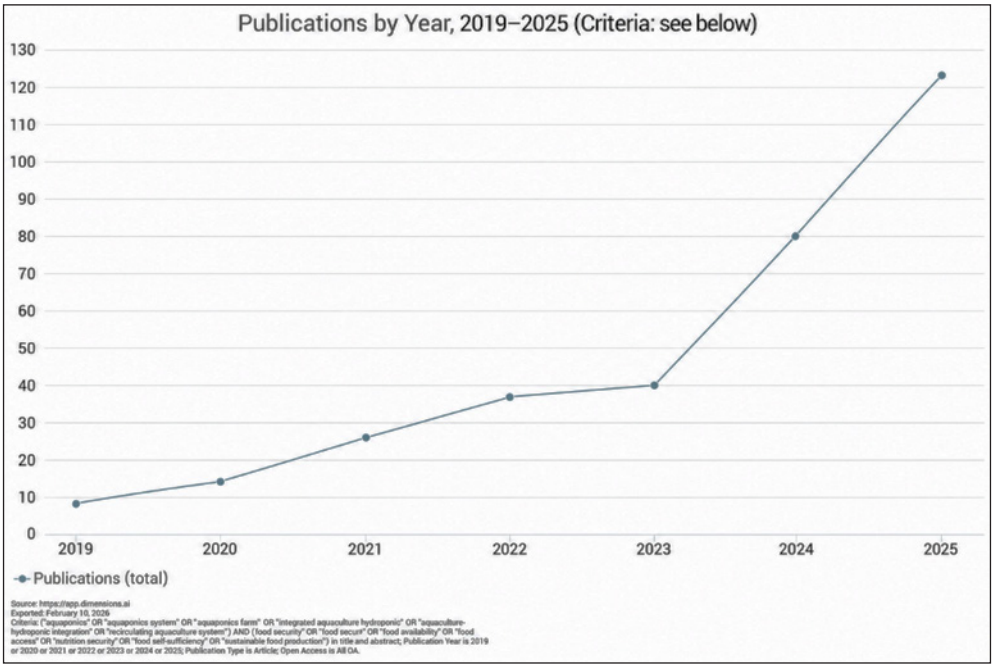

Figure 2. Quantity of publications and citations between 2019 to 2025

Documents

Document-level analysis provides information on the most influential publications in the research fields of aquaponics and food security. The number of citations reflects the impact and knowledge sharing of a study. The interest in urban agriculture during the COVID-19 crisis is evident in the most-cited journal article, which has been cited 214 times: "Food First: COVID-19 Outbreak and Cities Lockdown a Booster on a Wider Vision on Urban Agriculture," by Pulighe and Lupia (2020). It is followed by Technology Innovations in Food Security in Singapore: A Case Study of Future Food Systems in a More Natural Resource-Scarce World (141 citations), which demonstrates how technology can strengthen a country's food resilience. Similarly, during and in the aftermath of COVID-19, Urban Horticulture to Food Secure Cities emphasises the role of production systems that are city-based.

Containing more sources of reference, the other studies are in the field of aquaculture resilience and microbial ecology in aquaponics, and regional feasibility assessments. These demonstrate a balanced approach towards technical optimisation and sustainability

outcomes. The prominence of review articles is also notable, implying that synthesis papers can be crucial in terms of consolidating knowledge and establishing the path of future research. Document dissemination indicates that in many cases, the influential contributions relate aquaponics to more general topics like climate adaptation, urban agriculture, and resource efficiency. This shows that the most influential scholars in the field are not limited to systems design but rather focus on approaches to food system transformation and policy relevance (Table 2).

Table 2
Performance analysis by documents (Threshold 60)

Rank	Authors	Title	Citations
1	Pulighe and Lupia (2020)	Food First: COVID-19 Outbreak and Cities Lockdown a Booster for a Wider Vision on Urban Agriculture	214
2	Mok et al. (2020)	Technology innovations for food security in Singapore: A case study of future food systems for an increasingly natural resource-scarce world	141
3	Khan et al. (2020)	Urban Horticulture for Food Secure Cities through and beyond COVID-19	126
4	Abisha et al. (2022)	Sustainable development of climate-resilient aquaculture and culture-based fisheries through adaptation of abiotic stresses: a review	88
5	Kasozi et al. (2021)	The complex microbiome in aquaponics: significance of the bacterial ecosystem	85
6	Abusin and Mandikiana (2020)	Towards sustainable food production systems in Qatar: Assessment of the viability of aquaponics	70
7	Calone et al. (2019)	Improving water management in European catfish recirculating aquaculture systems through catfish-lettuce aquaponics	69
8	Okomoda et al. (2022)	Aquaponics production system: A review of historical perspective, opportunities, and challenges of its adoption	66
9	Ibrahim et al. (2023)	Aquaponics: A Sustainable Path to Food Sovereignty and Enhanced Water Use Efficiency	63
10	Obirikorang et al. (2021)	Aquaponics for Improved Food Security in Africa: A Review	53

Sources

With 12 publications and 442 citations, the Sustainability Journal is the first to top the list, establishing it as a site of interdisciplinary sustainability research. Other well-known journals are The Science of the Total Environment, Water, Aquaculture International, and Frontiers in Sustainable Food Systems, which have a higher citation performance with a smaller number of publications. The variety of sources establishes the interdisciplinary nature of the subject that covers environmental science, aquaculture engineering, and food

systems research. Technical publications address water management and recirculation, whereas sustainability-focused publications discuss social and policy repercussions. The total link strength values indicate that these journals have active citation networks which depict cross-disciplinary exchange of knowledge. Patterns of publication indicate that the research on aquaponics is not a niche in the aquaculture journals, but it is becoming a part and parcel of sustainability and food security studies. This extensive distribution increases exposure and speed of dissemination of research results in scientific and policy circles (Table 3).

Table 3
Performance analysis by sources (Threshold 44)

Rank	Journals	Documents	Citations	Total Link Strength
1	Sustainability	12	442	10
2	The science of the total environment	2	87	1
3	Water	3	68	12
4	Aquaculture International	4	57	11
5	Frontiers in Sustainable Food Systems	3	57	6
6	Agriculture	3	56	4
7	Annals of Animal Science	2	47	0
8	Journal of the World Aquaculture Society	2	44	10
9	Aquaculture research	3	43	1
10	Artificial Intelligence in Agriculture	2	38	3

Authors

The studies by Simon Goddek, Karel J. Keesman, R. Abbasi, R. Ahmad, and P. Martinez all resulted in three papers with relatively high citation rates and high collaboration linkage values. They tend to contribute to the optimisation of systems, their modelling, and the sustainable integration of aquaponics, implying technical leadership in the field. Large values of total link strength also indicate large co-authorship networks, which indicate collaborative and interdisciplinary research practices. This type of collaboration is necessary in aquaponics, a field that combines biology, engineering, and environmental management. The identical citation counts and link-strength values shared within the Abbasi/Ahmad/Martinez and Jaleel/Nair/Nishanth groups in Table 4 reflect tightly co-authoring teams that consistently publish together rather than a data artifact.

The other authors with moderate citations also broaden the thematic scope as they work with socio-economic adoption and regional implementation. They create centers of knowledge together, and they inform the methodological strategies and shape the future research directions. The presence of recurrent authors of various research studies with high impact suggests the development of a stable and steadily moving research community in

the domain of theoretical knowledge and practical application of aquaponics as a food security production approach.

Table 4
Performance analysis by authors (Threshold 47)

Rank	Authors	Documents	Citations	Total Link Strength
1	Goddek, Simon	3	64	5
2	Kessman, Karel J.	3	61	8
3	Abbasi, R.	3	58	11
4	Ahmad, R.	3	58	11
5	Martinez, P.	3	58	11
6	Jaleel, Abdul	3	47	10
7	Nair, Chythra Somanathan	3	47	10
8	Nishanth, Drishya	3	47	10
9	Rharrhour, Haytam	3	5	0
10	Styawati, Styawati	3	5	0

Organisations

Institutional analysis helps highlight the leading institutions for the study of aquaponics and food security. The number of citations is the highest at Sultan Qaboos University, and the involvement in sustainable agriculture in arid environments is high in the region. Other key players include Texas A&M University, University of Bologna and Wageningen University and Research, the latter having the most collaboration links, which suggests its global research collaborations. Also, the contributions of Universities like Universiti Putra Malaysia and the University of Alberta appear to be focused on developed or developing areas (Table 5). The pattern of productive organisations would suggest that aquaponics research is conducted at universities with strong agricultural, environmental and water management programmes. The link strength values are high, indicating that the institutions tend to work internationally and promote the transfer of knowledge and innovation.

Table 5
Performance analysis by organisations (Threshold 46)

Rank	Organisations	Documents	Citations	Total Link Strength
1	Sultan Qaboos University	4	139	4
2	Central Institute of Fisheries Education	2	97	2
3	Texas A&M University	3	93	2
4	University of Bologna	2	86	4

Table 5 (*continued*)

Rank	Organisations	Documents	Citations	Total Link Strength
5	Wageningen University & Research	5	84	15
6	National Water Research Center	2	67	8
7	Universiti Putra Malaysia	2	61	5
8	University of Alberta	3	58	6
9	University of the West of England	3	55	3
10	United Arab Emirates University	3	47	7

Countries

At the country level, the distribution and participation of aquaponics studies in the global context are shown. The number of citations and total number of links were significantly higher for Italy (454 and 30, respectively), with a very active and well-connected research base in sustainable agriculture and recirculating aquaculture technologies in Europe. Germany and the United States also demonstrate high output and strong collaboration due to their developed research and food-system innovation funding systems. Interestingly, India has the maximum number of documents (20), which in this context signifies the growing interest in low-cost, resource-efficient farming solutions in addressing food security issues, although the number of citations and link strength is not as high as that of Italy. Singapore and Pakistan had a few small but prominent studies that focused on urban density and climatic constraints. The closest one is Malaysia, which shows a high level of international cooperation. In the meantime, Oman and the United Kingdom are steadily contributing to the knowledge base. The distribution shows that research on aquaponics is scattered worldwide; both developed and developing countries recognise the potential of this practice to enhance sustainable food production. This international involvement enables knowledge exchange across cultures and offers the possibility of scaling up aquaponics globally (Table 6).

Table 6
Performance Analysis by Countries (Threshold 36)

Rank	Countries	Citations	Documents	Total Link Strength
1	Italy	454	12	30
2	Germany	232	11	32
3	India	217	20	29
4	United States	193	18	33
5	Canada	184	5	20
6	Singapore	173	3	4
7	Pakistan	172	2	19
8	Malaysia	143	6	41

Table 6 (*continued*)

Rank	Countries	Citations	Documents	Total Link Strength
9	Oman	139	4	10
10	United Kingdom	118	7	32

Bibliographic Coupling

Bibliographic coupling analysis describes the degree of relatedness of documents, using the number of shared references between them. When used in the context of aquaponic farming and food security, this approach can show which studies are based on similar theoretical foundations, and thus, they pertain to similar streams of knowledge. Food First: COVID-19 Outbreak and Cities Lockdown a Booster on Urban Agriculture (Pulighe & Lupia, 2020) is one of the most impactful papers in terms of citations, but with lower link strength, indicating that it is highly cited; however, it relies on a broader or more general reference base, as opposed to the same specialised aquaponics literature. In comparison, Aquaponics: A Sustainable Path to Food Sovereignty and Enhanced Water Use Efficiency (Ibrahim et al., 2023) has the highest link strength (297), which means that there is a great similarity with other core studies, and it is acting as the central node in the aquaponics knowledge network.

Likewise, Towards Sustainable Food Production Systems in Qatar: Assessment of the Viability of Aquaponics (Abusin & Mandikiana, 2020), Aquaponics for Improved Food Security in Africa: A Review (Obirikorang et al., 2021), and The Complex Microbiome in Aquaponics: Significance of the Bacterial Ecosystem (Kasozi et al., 2021), have high total link strengths, which indicate strong similarity between themes and methodological backgrounds. These articles focus on system performance, sustainability, and the application of the systems to food security at the regional level. The coupling network proposes that aquaponics research is organised around highly integrated technical and sustainability-oriented research, with review and feasibility articles serving as intellectual bridges. This interrelationship underscores the existence of a unified and fast-solidifying research field in which researchers extend shared evidence bases (Table 7).

Table 7
Bibliographic coupling most productive document (Threshold 52)

Rank	Authors	Title	Citations	Total Link Strength
1	Pulighe and Lupia (2020)	Food First: COVID-19 Outbreak and Cities Lockdown a Booster for a Wider Vision on Urban Agriculture	214	7
2	Mok et al. (2020)	Technology innovations for food security in Singapore: A case study of future food systems for an increasingly natural resource-scarce world	141	71

Table 7 (*continued*)

Rank	Authors	Title	Citations	Total Link Strength
3	Khan et al. (2020)	Urban Horticulture for Food Secure Cities through and beyond COVID-19	126	25
4	Abisha et al. (2022)	Sustainable development of climate-resilient aquaculture and culture-based fisheries through adaptation of abiotic stresses: a review	88	2
5	Kasozi et al. (2021)	The complex microbiome in aquaponics: significance of the bacterial ecosystem	85	81
6	Abusin and Mandikiana (2020)	Towards sustainable food production systems in Qatar: Assessment of the viability of aquaponics	70	113
7	Calone et al. (2019)	Improving water management in European catfish recirculating aquaculture systems through catfish-lettuce aquaponics	69	35
8	Okomoda et al. (2022)	Aquaponics production system: A review of historical perspective, opportunities, and challenges of its adoption	66	84
9	Ibrahim et al. (2023)	Aquaponics: A Sustainable Path to Food Sovereignty and Enhanced Water Use Efficiency	63	297
10	Obirikorang et al. (2021)	Aquaponics for Improved Food Security in Africa: A Review	53	108

Bibliographic Coupling by Clusters

Bibliographic coupling at the cluster level shows clear thematic groupings in the literature, showing how the field structures itself into specialised research subdomains (Figure 3). Table 8 presents the cluster analysis of Aquaponics as a Sustainable Food Security Solution, and this pattern is applied to indicate specific areas of the research focus. The largest group (Cluster 1 Red), comprising 16 articles, focuses on technological innovation and intelligent agricultural solutions. Examples of representative works include Urban Horticulture for Food Secure Cities through and beyond COVID-19 and Technology Innovations for Food Security in Singapore: a Case Study of Future Food Systems in an Increasingly Natural Resource-Scarce World, as well as works on artificial intelligence, nutrient regulation, and automated management systems. The cluster is indicative of a progressive attitude towards adopting digital solutions like IoT and machine learning to further enhance productivity and resilience in aquaponics.

Cluster 2 (Green) is less focused on performance, sustainability, economic viability and regional adoption, with 9 articles. The articles, such as Towards Sustainable Food

Table 8
Bibliographic coupling cluster on aquaponic farming and food security (Threshold 52)

Cluster No.	Cluster Labels	No. of Articles	Representative Publications
Cluster 1 (Red)	Smart/AI-Enabled Aquaponics and Urban Innovation	16	Abbasi et al. (2023); Ali et al. (2024); Dhal et al. (2022); Dhal and Kar (2024); Dutta et al. (2025); Khan et al. (2020); Kok et al. (2024); Mešić et al. (2024); Mok et al. (2020)
Cluster 2 (Green)	Sustainable Food Production and Regional Adoption	9	Abusin and Mandikiana (2020); Baganz et al. (2020); Channa et al. (2024); Gillani et al. (2022); Ibrahim et al. (2023); Karimanzira and Rauschenbach (2021); Obirikorang et al. (2021); Pinho et al. (2021)
Cluster 3 (Blue)	Techno-Economic Feasibility and Market Acceptance	7	Asciuto et al. (2019); Babatunde et al. (2023); Baiyin et al. (2020); Cifuentes-Torres et al. (2021); Eichhorn and Meixner (2020); Greenfeld et al. (2020); Okomoda et al. (2022)

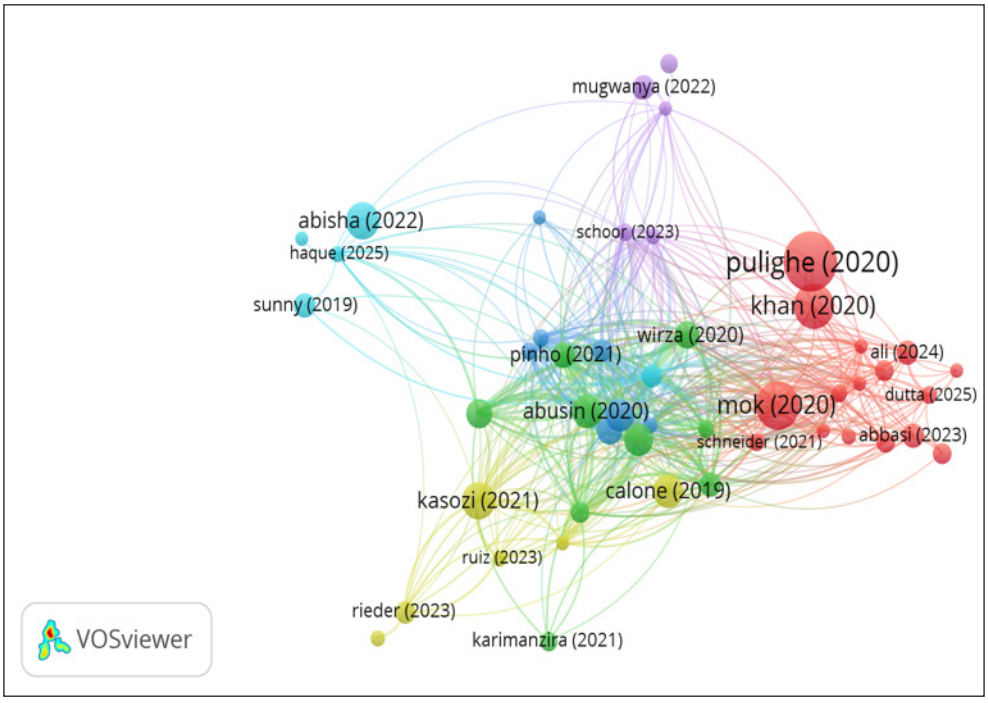

Figure 3. Bibliographic coupling analysis (VOSviewer Visualisation)

Production Systems in Qatar: Assessment of the Viability of Aquaponics, Aquaponics: A Sustainable Path to Food Sovereignty and Enhanced Water Use Efficiency and Aquaponics for Improved Food Security in Africa: A Review, are more on the practical side and the issue of food sovereignty. This cluster emphasises practice/policy implications.

In Cluster 3 (blue), there are 7 articles covering the following topics: economic feasibility, consumer acceptance and environmental sustainability evaluation. This research includes market demand, cost-benefit analysis, and urban production models. The clusters reveal the multidisciplinary nature of aquaponics research and innovation, the sustainability of aquaponics systems, and the assessment of socio-economic outcomes. This framework proposes a parallel shift of technical designs towards broader approaches to food security and adoption.

Co-Occurrence Analysis

The co-occurrence analysis of keywords provides insight into the conceptual framework and prevailing research themes in the aquaponic farming and food security literature. This process can be used to determine the most central issues and the correlation among the technological, environmental, and socio-economic aspects of the subject by analysing how often the keywords co-occur. The keywords used in the co-occurrence analysis provide an insight into the conceptual structure and predominant research trends of the aquaponic farming and food security literature. By analysing the co-occurrence of keywords, the process identifies the central issues and correlations among technological, environmental, and socio-economic aspects of the subject. The frequency of the term food security (221) indicates the major focus of the dataset on making food more available, accessible, and resilient.

Interestingly, water has one of the highest relevance scores, indicating that efficient water management and recirculation are an important research focus. Similarly, keywords such as efficiency, sustainability, and sustainable food production reflect the high level of environmental sustainability on which the literature focuses. These words demonstrate the increasing attention to resource conservation, climate adaptation, and ecological performance. Social and implementation-oriented words like the community, implementation, and activity show the growing interest in real-life adoption and local involvement. The relevance scores reported for "Community" (2.21) and "Activity" (3.12) in Table 9 are far outside the range of every other keyword (0.14 -0.74).

The co-occurrence network indicates a balanced knowledge system whereby technical production systems are well intertwined with sustainability and societal results. This convergence implies that research in aquaponics has ceased to focus on experimental design and started to engage in global food system issues. The introduction of scientific and community-oriented terminology reflects the existence of a multidisciplinary area that integrates engineering solutions with development-oriented approaches.

Table 9
The 13 most frequent keywords in the co-occurrence analysis (Threshold 56)

Rank	Keywords	Occurrences	Relevance
1	Food Security	221	0.26
2	Fish	141	0.25
3	Plant	102	0.14
4	Water	101	0.36
5	Hydroponic	99	0.30
6	Community	87	2.21
7	Efficiency	84	0.51
8	Sustainability	84	0.23
9	Research	82	0.22
10	Activity	79	3.12
11	Land	73	0.57
12	Sustainable Food Production	68	0.74
13	Implementation	62	0.25

Co-Occurrence Analysis by Clusters

Co-occurrence analysis also provides insights into how the research themes are grouped into various conceptual areas. Two large clusters are created, each of which is indicative of a different orientation of the literature. Cluster 1 (Red), with 22 keywords, may be considered a cluster related to technology and production. The keywords mentioned in the publication are horticulture, efficiency, integration, nutrient, innovations, IoT, crop, and climate change, which reflect the high priority on optimising the system and technological improvement. This cluster aims to leverage engineering solutions and smart technologies for farming to boost productivity, resource-use efficiency, and environmental resilience. The text has been incorporated into what is called the concept of innovation, which suggests that scientists are still in the process of developing an interest in automation and digital monitoring to enhance aquaponics performance under changing climatic conditions (Figure 4)

Cluster 2 (Green) (12 keywords) is on the socio-economic issues and community. The words that are associated with outputs of adoption, education and local development are associated with food security, community, implementation, program, knowledge, land and fish farming. This group highlights the use of aquaponics at grassroots and regional scales for improving livelihoods and food security. In this instance, the emphasis of the research is not primarily on technical efficiency, but on how the technology was implemented, who was involved, and what policy implications it had. Together, these clusters provide evidence of the twofold nature of the aquaponics studies: one technological innovation

and the other social application and food system benefits. All themes overlap, representing an integrated research environment where the objectives of food security in terms of engineering advancement and community development go hand in hand (Table 10).

Table 10
Co-word analysis on aquaponic farming and food security (Threshold 56)

Cluster No.	Cluster Labels	No. of Keywords	Representative Keywords
Cluster 1 (Red)	Technology-Driven Aquaponics, Efficiency, and Climate-Resilient Production	22	"Climate Change" "crop" "demand" "efficiency" "food production" "hydroponic" "innovation" "integration" "IoT" "nutrient" "paper"
Cluster 2 (Green)	Community-Based Aquaponics Adoption and Food Security Development	12	"Activity" "community" "fish" "fish farming" "food security" "implementation" "knowledge" "land" "person" "program"

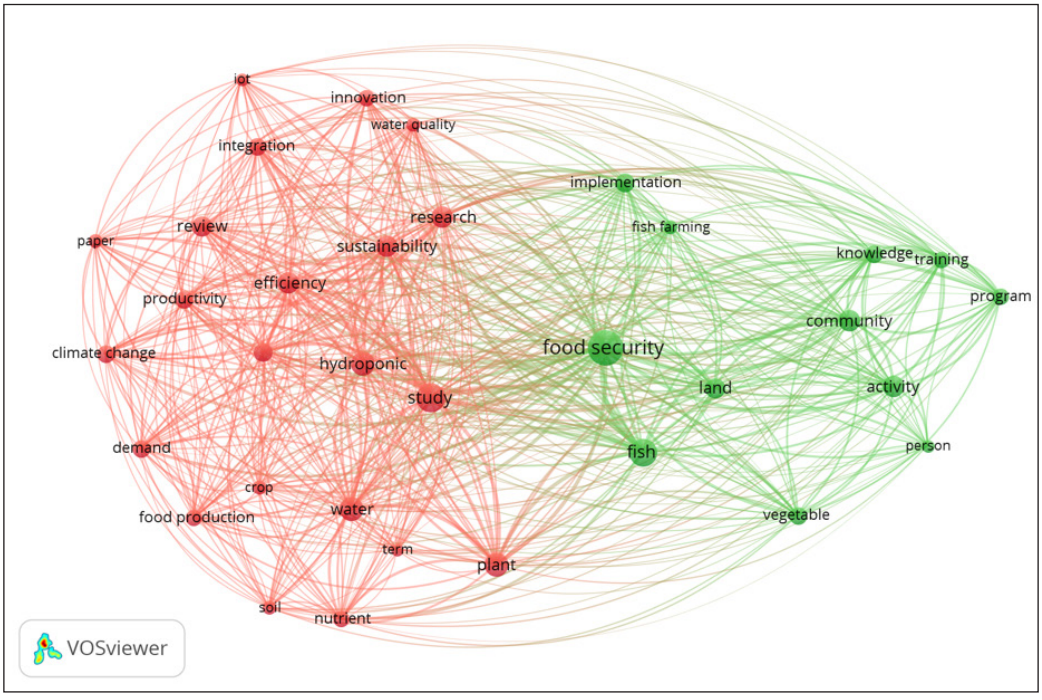

Figure 4. Co-word analysis on aquaponic farming and food security

DISCUSSION

The results of this bibliometric review demonstrate the growing multidimensional interest in aquaponics research, particularly in economic viability, technology optimisation, and

food sovereignty. Some works cited in this section (e.g., Dhal et al., 2022; Dutta et al., 2025; Mešić et al., 2024) provide contextual background and do not appear among the performance, coupling, or co-occurrence tables in Section 3; they are cited for interpretive context rather than as members of the analysed 328-document corpus. One of the major concerns about the scalability of the aquaponic systems is economic viability. It has been empirically estimated that profitability is determined by the scale of production, system design, and integration in the market (Baganz et al., 2020). The Mediterranean and African cases of financial feasibility studies also indicate that under suitable cost structure and local demand, aquaponics may make economic sense (Asciuto et al., 2019; Babatunde et al., 2023). Equally, techno-economic calculations that include renewable energy options, including photovoltaic integration, show the potential to lower operational spending and increase sustainability in arid regions (Baiyin et al., 2020). These results support the need to match technological innovation with economic performance in order to guarantee its long-term adoption.

Outside the economic aspect, technological development is now playing a bigger role in the development of aquaponics. Smart management and optimisation devices, using AI, enhance the accuracy of monitoring and control of nutrient levels and productivity (Channa et al., 2024; Karimanzira & Rauschenbach, 2021). Artificial light that is energy-efficient is also a factor in the consumption of resources and better performance of the system (Gillani et al., 2022). In addition, species selection is also vital in the success of the system, and fish species adapted to the region improve the biological compatibility and productivity (Pinho et al., 2021). Notably, aquaponics is set as a road to food sovereignty and water utilisation efficiency, especially in susceptible areas (Ibrahim et al., 2023; Obirikorang et al., 2021).

The three bibliographic-coupling clusters and two co-occurrence clusters describe an organised field. The larger, technology-oriented coupling cluster (Cluster 1, 16 articles) and the technology-driven co-occurrence cluster together indicate that a majority of the shared-reference and shared-keyword structure of the literature still centers on system optimisation, automation, nutrient regulation, and digital monitoring, rather than on food-security outcomes directly. The smaller regional-adoption coupling cluster (Cluster 2, 9 articles) and the community-based co-occurrence cluster indicate a distinct but less densely linked stream concerned with implementation, food sovereignty, and local livelihoods; its comparatively lower total link strength suggests this stream draws on a more heterogeneous and less mutually-citing set of sources than the technology cluster. The techno-economic coupling cluster (Cluster 3, 7 articles) connects these two approaches by considering the economic and social feasibility of implementing technically optimised systems. In this regard, it is important to note that in this field, the intellectual core is still maturing more quickly than the accumulation of citations, as is the case in the unusually high coupling strength of Ibrahim et al. (2023) relative to its number of citations, which indicates that,

despite not having a particularly high number of citations yet, the article serves as a kind of "nuclear point" in the shared literature evidence base.

The co-occurrence and coupling structure does reveal technological and socio-economic orientations, existing together as separate and related clusters; however, this echoes a field that has progressed beyond simple small-scale experimentation. However, the analysis does not provide a breakdown of the clusters by year, so it is not possible to conclude from it whether the field is increasingly becoming more scalable and digital in its applications over time or whether these are increasingly becoming more prevalent. The shift claim could be supported directly with a temporal decomposition of cluster membership (e.g., comparing the composition of each cluster between 2019 - 2021 and 2023 - 2025).

This bibliometric approach also carries limitations that should be considered when interpreting these findings. The corpus was drawn from a single database (Dimensions AI); although this improved metadata consistency, it also means coverage may diverge from Scopus- or Web of Science-indexed corpora, which is the choice made by the two closely related prior reviews of aquaponics bibliometrics discussed above (Basumatary et al., 2023; Kushwaha et al., 2025). No cross-database sensitivity check was performed, so the extent of this divergence in the present corpus is unknown.

CONCLUSION

This bibliometric work attests that aquaponic farming has taken a multidisciplinary and innovative form with high potential for sustainable food security. The literature has proven that aquaponics is not just a method of production but a holistic system that incorporates environmental care, technological development, and socio-economic factors. Urban aquaponics is widely recognised as a promising solution for resilient urban food systems (Wirza & Nazir, 2021), and broader reviews focus on its historical context, opportunities, and barriers to adoption (Okomoda et al., 2023). Notably, sustainability remains a focus of water research, and the use of reclaimed water under controlled conditions is supported (Cifuentes-Torres et al., 2021). Improvements in the study of microbiomes also indicate the ecological complexity and positive bacterial interactions in the aquaponic ecosystem (Ruiz et al., 2023), which supports the stability of the biological system and productivity.

In addition to environmental performance, market acceptance and consumer perception are decisive to long-term success. Research indicates that the sustainability awareness and perceived quality of aquaponic products influence willingness to pay (Eichhorn & Meixner, 2020; Greenfeld et al., 2020). Studies also suggest that aquaponic crops have similar sensory and safety qualities as traditional systems (Kralik et al., 2023). Efficiency and profitability improve through technological integration, such as IoT-based monitoring and smart nutrient management (Zamnuri et al., 2024), and through solutions like advanced foliar fertilisers, which can enhance crop performance (Frassine et al., 2025). Also, fish-plant interactions

will continue to play a vital role in the productivity and balance of water quality in a system (Loaiza et al., 2025). Taken together, these results indicate that aquaponics provides a potentially scalable, climate-sensitive, and technologically versatile avenue for enhancing the security of sustainable and resilient food systems across the globe.

ACKNOWLEDGEMENT

This research was supported by the High Community Engagement Grant (HICEG 04/2025), Albukhary International University. The authors would like to thank Albukhary International University for the institutional support and resources provided during this study. The authors declare no conflict of interest.

REFERENCES

Abd Aziz, M. A., Hairunnaja, M. A., Fatihah, N. A., & Md Isa, K. (2026). Optimising effluent reuse in aquaponics systems: Innovations for sustainable agriculture. In A. Z. Yaser, P. Tamunaidu & J. Lamaming (Eds.), *Sustainable reuse and recycling of agro-industrial effluent*. CRC Press. https://doi.org/10.1201/9781003604273-13

Abd Aziz, M. A., Nik Mu'Tasim, M. A., Wan Zainal, W. N. H., Bashari, N. A. F., Hairunnaja, M. A., Ali, M. F., Md Isa, K., Saad, S. A., & Miles, N. J. (2025). Advancements in aquaponic systems: Aqua beds and future directions. In H. L. Ong, S. J. H. Mohd Yusof, N. H. Mohd Salleh, K. F. Kasim, N. S. A. Abidin (Eds.), *Proceedings of the 4th International Conference on Biomass Utilisation and Sustainable Energy* (pp. 569–583). Springer. https://doi.org/10.1007/978-981-96-3785-0_44

Abbasi, R., Martinez, P., & Ahmad, R. (2023). Crop diagnostic system: A robust disease detection and management system for leafy green crops grown in an aquaponics facility. *Artificial Intelligence in Agriculture, 10*, 1–12. https://doi.org/10.1016/j.aiia.2023.09.001

Abisha, R., Krishnani, K. K., Sukhdhane, K., Verma, A. K., Brahmane, M., & Chadha, N. K. (2022). Sustainable development of climate-resilient aquaculture and culture-based fisheries through adaptation of abiotic stresses: A review. *Journal of Water and Climate Change, 13*(7), 2671–2689. https://doi.org/10.2166/wcc.2022.045

Abusin, S. A. A., & Mandikiana, B. W. (2020). Towards sustainable food production systems in Qatar: Assessment of the viability of aquaponics. *Global Food Security, 25*, Article 100349. https://doi.org/10.1016/j.gfs.2020.100349

Ali, A., Niu, G., Masabni, J., Ferrante, A., & Cocetta, G. (2024). Integrated nutrient management of fruits, vegetables, and crops through the use of biostimulants, soilless cultivation, and traditional and modern approaches—A mini review. *Agriculture, 14*(8), Article 1330. https://doi.org/10.3390/agriculture14081330

Asciuto, A., Schimmenti, E., Cottone, C., & Borsellino, V. (2019). A financial feasibility study of an aquaponic system in a Mediterranean urban context. *Urban Forestry & Urban Greening, 38*, 397–402. https://doi.org/10.1016/j.ufug.2019.02.001

Babatunde, A., Deborah, R. A., Gan, M., & Simon, T. (2023). Economic viability of a small-scale low-cost aquaponic system in South Africa. *Journal of Applied Aquaculture, 35*(2), 285–304. https://doi.org/10.1080/10454438.2021.1958729

Baganz, G., Baganz, D., Staaks, G., Monsees, H., & Kloas, W. (2020). Profitability of multi-loop aquaponics: Year-long production data, economic scenarios and a comprehensive model case. *Aquaculture Research, 51*(7), 2711–2724. https://doi.org/10.1111/are.14610

Baiyin, B., Tagawa, K., & Gutierrez, J. (2020). Techno-economic feasibility analysis of a stand-alone photovoltaic system for combined aquaponics on drylands. *Sustainability, 12*(22), Article 9556. https://doi.org/10.3390/su12229556

Basumatary, G., Verma, A. K., & Verma, M. K. (2023). Global research trends on aquaponics: A systematic review based on computational mapping. *Aquaculture International, 31*, 1115–1141. https://doi.org/10.1007/s10499-022-01018-y

Calone, R., Pennisi, G., Morgenstern, R., Sanyé-Mengual, E., Lorleberg, W., Dapprich, P., Winkler, P., Orsini, F., & Gianquinto, G. (2019). Improving water management in European catfish recirculating aquaculture systems through catfish-lettuce aquaponics. *Science of the Total Environment, 687*, 759–767. https://doi.org/10.1016/j.scitotenv.2019.06.167

Channa, A. A., Munir, K., Hansen, M., & Tariq, M. F. (2024). Optimisation of small-scale aquaponics systems using artificial intelligence and the IoT: Current status, challenges, and opportunities. *Encyclopedia, 4*(1), 313–336. https://doi.org/10.3390/encyclopedia4010023

Cifuentes-Torres, L., Correa-Reyes, G., & Mendoza-Espinosa, L. G. (2021). Can reclaimed water be used for sustainable food production in aquaponics? *Frontiers in Plant Science, 12*, Article 669984. https://doi.org/10.3389/fpls.2021.669984

Dhal, S. B., Bagavathiannan, M., Braga-Neto, U., & Kalafatis, S. (2022). Can machine learning classifiers be used to regulate nutrients using small training datasets for aquaponic irrigation? A comparative analysis. *PLOS ONE, 17*(8), 1-15, Article e0269401. https://doi.org/10.1371/journal.pone.0269401

Dhal, S. B., & Kar, D. (2024). Transforming agricultural productivity with AI-driven forecasting: Innovations in food security and supply chain optimisation. *Forecasting, 6*(4), 925–951. https://doi.org/10.3390/forecast6040046

Donthu, N., Kumar, S., Mukherjee, D., Pandey, N., & Lim, W. M. (2021). How to conduct a bibliometric analysis: An overview and guidelines. *Journal of Business Research, 133*, 285–296. https://doi.org/10.1016/j.jbusres.2021.04.070

Dutta, M., Gupta, D., Tharewal, S., Goyal, D., Sandhu, J. K., Kaur, M., Alzubi, A. A., & Alanazi, J. M. (2025). Internet of Things-based smart precision farming in soilless agriculture: Opportunities and challenges for global food security. *IEEE Access, 13*, 34238–34268. https://doi.org/10.1109/ACCESS.2025.3540317

Eichhorn, T., & Meixner, O. (2020). Factors influencing the willingness to pay for aquaponic products in a developed food market: A structural equation modeling approach. *Sustainability, 12*(8), Article 3475. https://doi.org/10.3390/su12083475

Frassine, D., Braglia, R., Scuderi, F., Redi, E. L., Valentini, F., Relucenti, M., Colasanti, I. A., Zaratti, C., Macchia, A., Allegrini, I., Gismondi, A., Di Marco, G., & Canini, A. (2025). Smart foliar fertilizer based

on Zn-Alg-$CaCO_3$ microparticles improves aquaponic tomato cultivation. *Scientific Reports, 15*, Article 18092. https://doi.org/10.1038/s41598-025-03136-y

Gillani, S. A., Abbasi, R., Martinez, P., & Ahmad, R. (2022). Review on energy-efficient artificial illumination in aquaponics. *Cleaner and Circular Bioeconomy, 2*, Article 100015. https://doi.org/10.1016/j.clcb.2022.100015

Greenfeld, A., Becker, N., Bornman, J. F., dos Santos, M. J., & Angel, D. (2020). Consumer preferences for aquaponics: A comparative analysis of Australia and Israel. *Journal of Environmental Management, 257*, Article 109979. https://doi.org/10.1016/j.jenvman.2019.109979

Ibrahim, L. A., Shaghaleh, H., El-Kassar, G. M., Abu-Hashim, M., Elsadek, E. A., & Hamoud, Y. A. (2023). Aquaponics: A sustainable path to food sovereignty and enhanced water use efficiency. *Water, 15*(24), Article 4310. https://doi.org/10.3390/w15244310

Khan, M. M., Akram, M. T., Janke, R., Qadri, R. W. K., Al-Sadi, A. M., & Farooque, A. A. (2020). Urban horticulture for food-secure cities through and beyond COVID-19. *Sustainability, 12*(22), Article 9592. https://doi.org/10.3390/su12229592

Karimanzira, D., & Rauschenbach, T. (2021). An intelligent management system for aquaponics. *at—Automatisierungstechnik, 69*(4), 345–350. https://doi.org/10.1515/auto-2020-0036

Kasozi, N., Abraham, B., Kaiser, H., & Wilhelmi, B. (2021). The complex microbiome in aquaponics: Significance of the bacterial ecosystem. *Annals of Microbiology, 71*, Article 1. https://doi.org/10.1186/s13213-020-01613-5

Kok, C. L., Kusuma, I. M. B. P., Koh, Y. Y., Tang, H., & Lim, A. B. (2024). Smart aquaponics: An automated water quality management system for sustainable urban agriculture. *Electronics, 13*(5), Article 820. https://doi.org/10.3390/electronics13050820

Kralik, B., Nieschwitz, N., Neves, K., Zeedyk, N., Wildschutte, H., & Kershaw, J. (2023). The effect of aquaponics on tomato (*Solanum lycopersicum*) sensory, quality, and safety outcomes. *Journal of Food Science, 88*(6), 2261–2272. https://doi.org/10.1111/1750-3841.16578

Kushwaha, J., Priyadarsini, M., Rani, J., Pandey, K. P., & Dhoble, A. S. (2025). Aquaponic trends, configurations, operational parameters, and microbial dynamics: A concise review. *Environment, Development and Sustainability, 27*, 213-246. https://doi.org/10.1007/s10668-023-03924-4

Loaiza, E. O., Avendaño, B. I. P., Burgos, L. V., Hernandez, M. F. T., Montiel, H. M. H., Reyes, J. C., & Moredia, M. S. (2025). Fish–plant interaction: Productive performance and water quality in aquaponics. *International Journal of Scientific Advances*, *6*(6). https://doi.org/10.51542/ijscia.v6i6.3

Mešić, A., Jurić, M., Donsì, F., Bandić, L. M., & Jurić, S. (2024). Advancing climate resilience: Technological innovations in plant-based, alternative and sustainable food production systems. *Discover Sustainability, 5*, Article 423. https://doi.org/10.1007/s43621-024-00581-z

Mok, W. K., Tan, Y. X., & Chen, W. N. (2020). Technology innovations for food security in Singapore: A case study of future food systems for an increasingly natural resource-scarce world. *Trends in Food Science & Technology, 102*, 155–168. https://doi.org/10.1016/j.tifs.2020.06.013

Obirikorang, K. A., Sekey, W., Gyampoh, B. A., Ashiagbor, G., & Asante, W. (2021). Aquaponics for improved food security in Africa: A review. *Frontiers in Sustainable Food Systems, 5*, Article 705549. https://doi.org/10.3389/fsufs.2021.705549

Okomoda, V. T., Oladimeji, S. A., Solomon, S. G., Olufeagba, S. O., Ogah, S. I., & Ikhwanuddin, M. (2023). Aquaponics production system: A review of historical perspective, opportunities, and challenges of its adoption. *Food Science & Nutrition, 11*(3), 1157–1165. https://doi.org/10.1002/fsn3.3154

Pinho, S. M., David, L. H., Garcia, F., Keesman, K. J., Portella, M. C., & Goddek, S. (2021). South American fish species suitable for aquaponics: A review. *Aquaculture International, 29*, 1427–1449. https://doi.org/10.1007/s10499-021-00674-w

Pulighe, G., & Lupia, F. (2020). Food first: COVID-19 outbreak and cities lockdown—a booster for a wider vision on urban agriculture. *Sustainability, 12*(12), Article 5012. https://doi.org/10.3390/su12125012

Ruiz, A., Scicchitano, D., Palladino, G., Nanetti, E., Candela, M., Furones, D., Sanahuja, I., Carbó, R., Gisbert, E., & Andree, K. B. (2023). Microbiome study of a coupled aquaponic system: Unveiling the independency of bacterial communities and their beneficial influences among different compartments. *Scientific Reports, 13*, Article 19704. https://doi.org/10.1038/s41598-023-47081-0

van Eck, N. J., & Waltman, L. (2010). Software survey: VOSviewer, a computer program for bibliometric mapping. *Scientometrics, 84*, 523–538. https://doi.org/10.1007/s11192-009-0146-3

Wirza, R., & Nazir, S. (2021). Urban aquaponics farming and cities—A systematic literature review. *Reviews on Environmental Health, 36*(1), 47–61. https://doi.org/10.1515/reveh-2020-0064

Zamnuri, M. A. H. b., Qiu, S., Rizalmy, M. A. A. b., He, W., Yusoff, S., Roeroe, K. A., Du, J., & Loh, K. -H. (2024). Integration of IoT in small-scale aquaponics to enhance efficiency and profitability: A systematic review. *Animals, 14*(17), Article 2555. https://doi.org/10.3390/ani14172555

Pertanika J. Trop. Agric. Sci. 49 (5): 2523 - 2544 (2026)

PERTANIKA JOURNALS

TROPICAL AGRICULTURAL SCIENCE

Journal homepage: http://www.pertanika.upm.edu.my/

Evaluation of the Aqueous Extracts of *Celosia argentea* L. (Plumosa Group) as a Bioherbicide for Dominant Weeds in Soybean Cultivation

Safira Nur Aini, Dyah Weny Respatie*, Aziz Purwantoro, and Qurrotul Uyun

Department of Agronomy, Faculty of Agriculture, Universitas Gadjah Mada, Jl. Flora, Bulaksumur, 55281 Sleman, Yogyakarta, Indonesia

ABSTRACT

Weed infestation is a major constraint on soybean (*Glycine max* (L.) Merrill) production, necessitating alternative weed management strategies. Plant-derived bioherbicides may offer a viable alternative. This study aims to evaluate the potential of a bioherbicide derived from *Celosia argentea* L. (Plumosa Group) against soybeans (*Glycine max* L. (Merrill)), purple nutsedge (*Cyperus rotundus* L.), and blackjack (*Bidens pilosa* L.). Two experiments were conducted: a laboratory bioassay using a completely randomised design to test extracts from the roots, stems, leaves, and flowers at concentrations of 0, 10, 20, and 40 g L^{-1}, followed by an early growth study in a greenhouse using a completely randomised block design. For the second experiment, the flower extract at a concentration of 40 g L^{-1} was selected due to its inhibitory effect on germination. The flower extract recorded the highest total phenolic content (11.77% w/w). The 40 g L^{-1} treatment reduced germination rates in soybeans (from 73.33% to 38.67%), purple nutsedge (from 84.00% to 48.00%), and blackjack (from 85.33% to 52.00%) in bioassay tests. In early growth studies, the extract affected the plants' morphological, physiological, and anatomical characteristics, such as root development, chlorophyll content, and stomata. These weed species exhibited lower stomatal aperture width and density. The results indicate that the flower extract of *C. argentea* has bioherbicidal potential, and that 40 g L^{-1} was the most effective concentration for inhibiting germination among those tested. Further research is needed to optimise application conditions and enhance weed suppression while minimising negative impacts on soybeans.

ARTICLE INFO

Article history:
Received: 24 September 2025
Accepted: 22 October 2026
Published: 30 October 2026

DOI: https://doi.org/10.47836/pjtas.49.5.21

E-mail addresses:
safira.nur.aini@mail.ugm.ac.id (Safira Nur Aini)
wenyrespatie@ugm.ac.id (Dyah Weny Respatie)
azizp@ugm.ac.id (Aziz Purwantoro)
qurrotuluyun19@gmail.com (Qurrotul Uyun)
* Corresponding author

Keywords: Soybean, *Celosia argentea*, bioherbicide, germination, total phenolic content, morphology, plant physiology

INTRODUCTION

Soybeans (*Glycine max* (L.) Merrill) are one of the most important food crops and

© Universiti Putra Malaysia Press

sources of plant-based protein in Indonesia. In 2020, per capita soybean consumption reached 11-12 kg per year, with domestic production at 0.63 million metric tons, lower than the demand of 3.29 million metric tons (Harsono et al., 2022). Soybean imports reached 2.670.086 metric tons in 2021 (Sibuea et al., 2024). Competition with weeds for water, nutrients, light, and growing space is a limiting factor for soybeans (Bidira et al., 2021). This competition can reduce crop yields by 18-76% (Setyowati et al., 2025). *Bidens pilosa* L. is a fast-growing weed that produces more than 30.000 seeds per plant (Chauhan et al., 2019). This weed has been reported to dominate soybean fields in several regions, such as Zimbabwe and the United States (Chivinge & Schweppenhauser, 1995). The leaves of C4 weeds in soybean cultivation, such as *Cyperus rotundus* L., are adapted to high light intensity (Peerzada, 2017). This weed is difficult to control because it can regrow from tubers and rhizomes (Peerzada, 2017). The allelopathic effects of purple nutsedge on the growth of other plants have been reported (Benvenuti, 2025).

Chemical herbicides are the most common way of controlling weeds. However, the overuse of herbicides can pollute air, water, and soil and affect the balance of soil microorganisms and ecosystems (Baćmaga et al., 2024). Therefore, sustainable alternatives such as plant-based bioherbicides can be developed. *Celosia argentea* L. contains bioactive compounds such as cyclic peptides, saponins, phenols, fatty acids, amino acids, and minerals (Zhang et al., 2016). Various phenolic compounds have been studied because of their different structures, from simple phenols to complex polymers (Alara et al., 2021).

Previous studies have shown that plant extracts can inhibit weed germination and growth. An extract of *Cosmos sulphureus* significantly reduced the size of the stems, roots, and leaves of purple nutsedge (Respatie et al., 2019). *Ricinus communis* extract was the most effective among extracts of *Piper tuberculatum*, *Dipteryx lacunifera,* and *Jatropha gossypiifolia* in inhibiting the germination of *Bidens bipinnata* (Lopes et al., 2022). In a study by Uyun et al. (2024), a 40% concentration of wedelia leaf extract was able to inhibit the germination and growth of purple nutsedge. Research on Wedelia extract using the same ingredients and concentration showed that it could inhibit the growth of purple nutsedge and soybeans when applied at planting (Abdillah et al., 2026). Kusumawati et al. (2026) reported that at a 10% concentration, teak leaf extract inhibited the germination of *Tridax procumbens*. Research on bioherbicides also reports that chrysanthemum stem and leaf extracts at a concentration of 40 g L^{-1} can inhibit the growth of coat button weeds (Yumna et al., 2026).

Physicochemical characteristics and biological activity of *C. argentea* extract as a potential bioherbicide. Total phenolic content was determined using the Folin-Ciocalteu method and expressed in gallic acid equivalents (Pérez et al., 2023). Measurements of physicochemical properties related to water availability and plant physiological responses,

such as pH, electrical conductivity, and osmotic potential (Mashreghi et al., 2024). Extract efficiency was assessed through germination rates and vigour indices of soybeans, purple nutsedge, and blackjack (Li et al., 2025). Early growth can be evaluated based on plant height, number of leaves, root length, root area, leaf area, fresh weight, dry root weight, and dry shoot weight (Wang et al., 2025). Leaf greenness serves as an indirect proxy for chlorophyll content, which is measured using a SPAD meter (Vishwakarma et al., 2023). Spectrophotometric estimates of chlorophyll a, chlorophyll b, and total chlorophyll were conducted to assess potential disruptions to photosynthesis (Hussain et al., 2024). Studies examining stomatal anatomy indicate that stomatal density and stomatal aperture width influence transpiration characteristics and gas regulation (Liu et al., 2024).

This study was designed to evaluate the physicochemical properties of extracts from various parts of *C. argentea* as well as the effect of flower extracts on the germination and early growth of weeds and soybeans. The hypothesis proposed is that the response of weeds and soybeans to the extract treatment will differ. The main concerns are the ability to inhibit weed growth and the potential for phytotoxicity in cultivated plants. The results of this study are expected to provide a scientific basis for the development of plant-based bioherbicides. The uniqueness of this study lies in the combination of physicochemical characterisation of the extracts with a comparative evaluation of their inhibitory effects on weeds and soybeans as bioherbicide candidates. However, the physicochemical properties of *C. argentea* require further investigation. To develop bioherbicides, studies are needed on the effects of *C. argentea* on target weeds and soybeans. This study was designed to evaluate the physicochemical properties of extracts from various parts of *C. argentea*, as well as the effects of these extracts on the germination and early growth of weeds and soybeans. The hypothesis of this study is that weeds and soybeans will respond differently to the extract treatments. The main challenges faced are estimating weed growth inhibition and the potential for phytotoxicity toward cultivated plants. It is hoped that this study will provide a scientific basis for the development of plant-based bioherbicides. The uniqueness of this study lies in the combination of physicochemical characterisation of the extracts with a comparative evaluation of their effects on the growth of weeds and soybeans.

Literature Review

The present study is in agreement with earlier reports on plants as potential bioherbicides. *Cosmos sulphureus* greatly reduced purple nutsedge growth, especially in stem and root size (Respatie et al., 2019). In addition, Lopes et al. (2022) tested several plants as bioherbicide extracts, and the Ricinus communis extract showed the highest efficiency in inhibiting the germination of Bidens bipinnata. Also, Uyun et al. (2024) show that wedelia leaf extract at 40% concentration can inhibit the germination and growth of purple nutsedge. It was reported that the extract inhibited the growth of purple nutsedge and soybean at

planting using the same material and concentration (Abdillah et al., 2026). Moreover, a 10% concentration of teak leaf extract can inhibit the germination of *Tridax procumbens* (Kusumawati et al., 2026). The buttonweed growth can be inhibited by chrysanthemum stem and leaf extracts at 40 g L-1 (Yumna et al., 2026). This study presents information on the potential of *C. argentea* extract as a bioherbicide. The objective of the present study was to determine physicochemical characteristics of red *C. argentea* and its effects on germination, early growth, and physiological characteristics of soybean, purple nutsedge, and blackjack plants. The differential sensitivities of the three species to the extract indicate the importance of evaluating weed-inhibition effectiveness and selectivity. Growth of roots and shoots, leaf area, chlorophyll content, and stomatal characteristics were also measured to elucidate the plants' response to the extract treatment and potential disturbances in physiological processes.

MATERIALS AND METHODS

Plant Cultivation

The research was conducted in September 2023 in Ngaditirto Village, Selopampang Subdistrict, Temanggung Regency, Central Java, Indonesia (7.374889° LS, 110.142852° BT) using *Celosia argentea* L. (Plumosa Group). The place is situated at an altitude of 960 m above sea level with an average temperature of 23°C. Seeds of *C. argentea* were sown in 10 × 10 cm polybags. Manure was used as a base fertiliser. *C. argentea* seedlings were transplanted to the field at 2 weeks of age with a planting spacing of 20 cm × 20 cm. NPK fertiliser was applied 30 days after planting. Pesticides were sprayed whenever pests and diseases attacked the *C. argentea* plants. The *C. argentea* plants were harvested by pulling up the roots after 120 days. Then the plant parts were separated (roots, stems, leaves, flowers). These parts were dried in an oven at 48 °C until completely dry. The dried material was ground in a grinder into a fine powder. The test plant was the Anjasmoro soybean variety, selected by mass selection from the Mansuria inbred line population. This variety is resistant to leaf rust and has pods that do not split easily. It has a flowering period of 35.7-39.4 days and a pod maturity period of 82.5-92.5 days, with a plant height of 64-68 cm. Meanwhile, purple nutsedge and blackjack weeds were collected from Tri Dharma University Experimental Garden, Banguntapan, Bantul, Special Region of Yogyakarta, which is an area with high soybean cultivation intensity.

Treatment and Experimental Design

Bioassay

The bioassay was conducted at the Crop Production Management Laboratory, Faculty of Agriculture, Gadjah Mada University. In this study, the red flowers of *C. argentea* were used

based on the results of physicochemical extract testing. This study employed a completely randomised design (CRD) with two factors: test plant species, namely soybeans and weeds (purple nutgrass and blackjack). The second factor was concentration, namely 0, 10, 20, and 40 g L^{-1}. In this study, the red flower parts of *C. argentea* were used. The results of the physicochemical analysis indicated that these parts had the greatest potential as a bioherbicide. The experiments were conducted in Petri dishes with a diameter of 6 cm. Each Petri dish contained 10 seeds. Each treatment combination was repeated three times. Each seed in every Petri dish was treated with 2 mL of extract using a measuring pipette. To maintain moisture, 5 mL of additional liquid was added per Petri dish until day 14. Germination was allowed to proceed for 14 days, after which the seeds... The bioassay was conducted at the Plant Production Management Laboratory, Faculty of Agriculture, Gadjah Mada University. In this study, the red flowers of *C. argentea* were used based on the results of physicochemical extract testing. This study employed a completely randomised design (CRD) with two factors: test plant type, namely soybeans and weeds (purple nutsedge and blackjack). The second factor was concentration: 0, 10, 20, and 40 g L^{-1}. In this study, the red flower parts of *C. argentea* were used. The results of physicochemical analysis showed that these parts had the greatest potential as a bioherbicide. The experiments were conducted in Petri dishes with a diameter of 6 cm. Each Petri dish contained 10 seeds. Each treatment combination was repeated three times. Each seed in each Petri dish was treated with 2 mL of extract using a measuring pipette. To maintain moisture, 5 mL of water was added to each Petri dish until day 14. Germination was allowed to proceed for 14 days, after which the seeds were harvested.

Early Growth Study

This early growth study was conducted in the greenhouse of the Faculty of Agriculture, Gadjah Mada University, Yogyakarta, Indonesia. The greenhouse environmental conditions included an average temperature of 31 °C, relative humidity of 60%, and light intensity of 25,000 lux. This early-growth study was conducted to determine the effects of bioherbicides on soybeans and weeds (purple nutsedge and blackjack). The experimental design used was a randomised complete block design (RCBD) with two factors. The first factor was the type of test plant, namely soybeans and weeds (purple nutsedge and blackjack). The second factor was the bioherbicide treatment with red-flowered *C. argentea* at concentrations of 0 and 40 g L^{-1}. These concentrations were selected based on recommendations from a previous bioassay indicating that 40 g L^{-1} could inhibit weed growth. Each treatment combination was replicated three times. Thus, there were 18 germination trays, each containing 25 holes. Consequently, the total number of experimental plants was 450.

In this study, *soybean* seeds of the Anjasmoro variety, uniformly sized purple nutsedge tubers (0.5 g), and blackjack seeds were used. The soil was sterilised by drying in an oven at 100 °C before being placed in the germination trays. Before use, the germination trays were tightly sealed with black tape to minimise loss of the bioherbicide solution. Next, the seedlings were transferred to the germination trays, with one seedling per hole. The bioherbicide solution was applied once at 0 DAS (days after planting) by adding 5 mL to each hole in the tray. Watering was performed every three days using a sprayer to maintain adequate soil moisture.

Extraction

The roots, stems, leaves, and flowers of red *C. argentea* were dried to a constant weight in an electric oven at 40 °C for 48 hours. After the dried plant parts were collected, they were ground into a powder and stored in airtight plastic bags. The plant material powder was extracted with 1000 mL of distilled water adjusted to predetermined concentrations: 0 grams for the control treatment, 10 grams for the 10 g L^{-1} treatment, 20 grams for the 20 g L^{-1} treatment, and 40 grams for the 40 g L^{-1} treatment. After 24 hours, the solutions were filtered using Whatman No. 1 filter paper (Uyun et al., 2024).

Analytical Procedures

Total Phenolic Content

The Folin-Ciocalteu reagent was used to measure the total phenolic content. To do this, 50 mg of the sample was mixed with 0.5 mL of the reagent and 7.5 mL of distilled water. After mixing the concoction, it was incubated for ten minutes. Next, 1.5 millilitres of 20% sodium carbonate was added. After shaking the mixture once again, the solution was allowed to stand for ten minutes. The ultimate volume was 10 mL when distilled water was added. The OD_{760} of the solution was measured after it had been diluted 25 times (Kupina et al., 2019).

pH Measurement

The pH of all extracts was measured with a calibrated pH meter to assess the acidity level.

Electrical Conductivity (EC) and Osmotic Potential (Ψs)

The EC of the extracts was measured utilising an EC meter to determine the total dissolved salt content. The Ψs were calculated by multiplying the EC value by -0.036 and expressed in megapascals (MPa) (McDonald & Wilson, 1979).

Observed and Data Collection

Germination Parameters

Germination was observed at 14 DAS during the germination and early growth studies.

The germination percentage (%) was calculated as in Equation 1 (International Seed Testing Association [ISTA], 1999):

$$Germiation\ Percentage\ (\%) = \frac{Number\ of\ total\ germinated\ seeds}{Total\ number\ of\ seeds} \times 100\% \quad [1]$$

Vigour was observed daily, and the index was ascertained using the following formula (ISTA, 1999) as in Equation 2:

$$Vigour\ Index = \sum \frac{\text{Number of sprouts on day n}}{n} \times 100\% \quad [2]$$

Growth Parameters

The plants were harvested 14 days after planting, and the following growth parameters were measured.

Plant Height

The measurement is taken from the soil surface to the highest point of the plant for soybean and the blackjack weed. The height of the purple nutsedge weed is measured from the base of the crown to the highest leaf tip.

Root Length

The length of the root is measured using a ruler with the unit in cm. The measurement is taken from the base of the root, which is the boundary between the root and the crown, to the tip of the longest root.

Number of Leaves

The quantity of leaves is monitored every day by tallying the leaves produced on each plant. The number of leaves on a soybean plant is determined by counting the trifoliate leaves, but the number of leaves on a blackjack and purple nutsedge plant is determined by counting the leaves that are created on each plant.

Number of Roots

On Soybean and Blackjack plants, observations were made by counting the roots that grow from the main root. On Purple nutsedge, the number of roots was counted based on the roots that grow from the tuber.

Leaf Area

The leaf area is measured using a leaf area meter. The leaves are arranged on white paper, then placed on the leaf area meter with sufficient lighting. Then, click on measurements to show numbers; the units of measurement on the leaf area meter are mm2.

Root Area

The root area is measured using a leaf area meter. The roots were cleaned of any remaining growing medium and then arranged on the device according to the operating procedure. The roots were placed on white paper and then positioned on the leaf area meter under adequate lighting.

Fresh Shoot Weight

The shoot parts of the plants Soybean, Blackjack, and Purple nutsedge were separated from the root parts, then weighed using an analytical balance. The measurement results are expressed in grams.

Dry Shoot Weight

The shoot part is separated from the root, then dried using an oven at 80 °C until a constant weight is achieved. After that, the samples were weighed using an analytical balance.

Fresh Root Weight

The roots of soybean, blackjack, and purple nutsedge were separated from the canopy, then weighed using an analytical balance. The measurement results are expressed in grams.

Dry Root Weight

The roots are separated from the shoot, then dried in an oven at 80 °C until a constant weight is achieved. The next sample is weighed using an analytical scale. The measurement results are expressed in mg per plant.

Physiological Parameters

Physiological parameters were observed at the final harvest (14 days after planting). Observations included leaf greenness, chlorophyll a, chlorophyll b, and total chlorophyll. Greenness of the lower, middle, and upper leaves was measured with a SPAD meter. The chlorophyll content was determined by grinding 1 g of leaf tissue with a mortar and pestle and mixing it with 20 mL of 80% acetone. The solution was filtered through a Whatman No. 1 filter paper, transferred to a test tube, and the OD_{663} and OD_{645} were measured utilising a spectrophotometer (Lichtenthaler, 1987) as in Equations 3 to 5:

$$\text{Chlorophyll a (mg g}^{-1}) = (0.0127 \times A663 - 0.00269 \times A645) \times 20 \text{ mL} \quad [3]$$

$$\text{Chlorophyll b (mg g}^{-1}) = (0.00229 \times A645 - 0.00468 \times A663) \times 20 \text{ mL} \quad [4]$$

$$\text{Total chlorophyll} = ([20.2 \times A645]) + (20 \text{ mL}/[1000 \times 1 \text{ g}]) \text{ mg g}^{-1} \text{ of leaf fresh weight.} \quad [5]$$

Leaf Anatomy

Stomata were observed at 14 DAS utilising the leaf imprinting method. The lower leaf surface was coated with nail polish and left to dry for 10 min. The dried polish layer was carefully removed using adhesive tape and placed on a glass slide. Stomatal density and opening width were observed with a microscope at 10× and 40× magnification (Paul et al., 2017).

Data Analysis

All data were analysed using analysis of variance at a significance level of $\alpha = 0.05$. We applied Tukey's honestly significant difference (HSD) test at a 95% confidence level when significant differences were detected. A contrast test was employed to compare the bioactivities of *C. argentea* flower extract with those of standard compounds. Regression analysis assessed relationships between variables and treatments. Statistical analyses were performed using the agricolae package in R software version 3.2.2 (https://cran.r-project.org/web/packages/agricolae/).

RESULTS

C. argentea, known as the cockscomb plant, is an ornamental species that is popular due to its beauty. It has a short life cycle and has potential bioherbicidal properties as it

approaches senescence. The study revealed that the flower extract of *C. argentea* had the highest phenolic content. It can be applied at planting at a concentration of 40 g L^{-1} to inhibit germination of both soybeans and weeds. The results indicate that flower extract of *C. argentea* could be a bioherbicide. However, from this study, the selectivity to soybean plants should be considered, as it can inhibit germination at planting time.

Organ Analysis

The increased bioherbicide concentrations increased the osmotic pressure, leading to hyperosmotic conditions that favored Na^+ and Cl^- accumulation, leading to physiological disturbances. Na^+ accumulation inhibits enzymes involved in photosynthetic pigment biosynthesis, leading to chloroplast membrane degradation and oxidative stress, thus reducing chlorophyll content (Laamari et al., 2023). The results of this research showed the potential of bioherbicides on the flower of *C. argentea*.

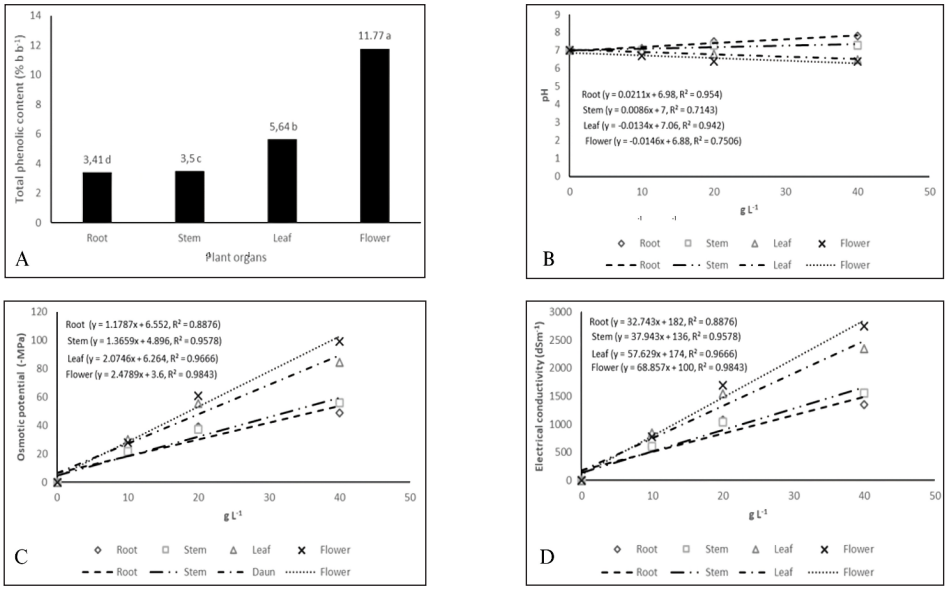

Figure 1. (A) Total phenolic content of the different plant organs (Tukey's test, $p \leq 0.05$); (B) pH; (C) osmotic potential; and (D) electrical conductivity as a function of the concentration of each *Celosia argentea* L. organ extract

Analysis of phenolic content showed that phenolic compounds were most highly concentrated in the generative parts, namely the flowers. The results of the analysis show that the red flower parts have the highest phenolic content (Figure 1A), at 11.77% w/w. In contrast, the root parts exhibit the lowest phenolic content at 3.41% w/w. The phenolic content in the stems is 3.5% w/w, while that in the leaves reaches 5.64% w/w. Differences in

phenolic content among plant parts are caused by variations in the distribution of secondary metabolites within plant tissues, indicating that each organ plays a distinct physiological role in the synthesis and accumulation of these compounds. Phenolic levels in leaves and flowers exhibited a concentration-dependent reduction with pH (Figure 1B), suggesting substantial phenolic acid levels. The flowers also demonstrated the highest EC, likely due to elevated concentrations of dissolved salts. According to Aslam et al. (2016), increased EC can induce cell leakage in plant tissues. This is attributable to the positive correlation between osmotic potential (Figure 1C) and electrical conductivity (Figure 1D).

Bioassay

The flower extracts showed the highest phenol content, EC, Ψs and the most acidic pH among all the plant organ extracts tested, indicating a strong bioherbicidal potential. In the first phase of testing, seeds of soybean, purple nutsedge, and blackjack were treated with flower extracts at 0, 10, 20 and 40 g L^{-1} (Figure 2). The extracts greatly reduced germination percentage (Figure 2A). The highest inhibition was observed at 40 g L^{-1}, corresponding to the highest phenol content. The seeds need water for imbibition during germination. Excess phenol inhibits this process and inhibits metabolic activity.

The results of the study show that increasing the concentration of the flower extract of *C. argentea* can reduce the germination percentage of soybeans, purple nutsedge, and blackjack. Based on the results, regression equations were found for the variables germination percentage (Figure 2A) and vigour index (Figure 2B). This indicates that an increase in the concentration of the flower bioherbicide *C. argentea* can reduce the germination percentage and vigour index. Li et al. (2010) showed that allelochemicals such as phenols lower cell membrane permeability, inhibit the transfer of metabolites from the endosperm to the growth points, and inhibit cell division and germination. The results show that the vigour index of the soybean is higher even with an increase in the concentration of the bioherbicide. This is because soybean seeds have a high rate of imbibition, which allows them to break dormancy quickly.

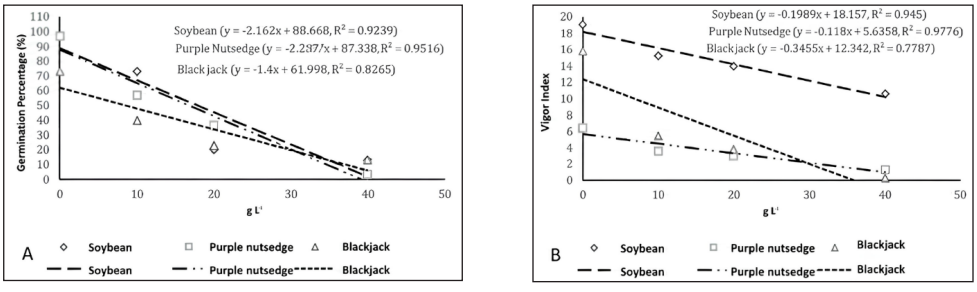

Figure 2. (A) Germination percentage (%) and (B) vigour index of soybean, purple nutsedge, and blackjack seeds under *Celosia argentea* L. extracts of different organs and concentrations. Values with varying letters indicate statistically significant differences (Tukey's test, $p \leq 0.05$)

Early Growth

Based on the germination test results, 40 g L^{-1} flower extract was identified and used as the most effective inhibitory concentration for subsequent experiments.

Germination of Soybeans, Purple Nutsedge, and Blackjack

Treatment with flower extracts significantly reduced germination rates and vigour indices in purple nutsedge and blackjack, but less and insignificantly in soybeans. This variation is attributed to higher food reserves in the latter, mitigating bioherbicide-induced stress. In contrast, germination in purple nutsedge and blackjack declined markedly, most likely due to seed coat distortions and suppressed embryonic root elongation (Liu et al., 2021).

The germination rate for soybeans decreased from 73.33% to 38.67%, for purple nutsedge from 84% to 48%, and for blackjack from 85.33% (control) to 52% (Figure 3A). Similarly, the vigour index (Figure 3B) decreased significantly in purple nutsedge (8.82) and blackjack (8.67), while soybean vigour was unaffected, remaining at 14 following application of *C. argentea* at a concentration of 40 g L^{-1} (Figure 3B). Treatment with the flower extract significantly reduced the vigour index in barnyard grass and crabgrass, but the reduction was smaller and not significant in soybeans. This variation is due to the higher protein content in soybeans, which increases the randomness of germination over a relatively short period. The high imbibition rate in soybeans causes germination to occur more rapidly, as the water absorbed by the soybean seeds breaks the dormancy present in the seeds. Water absorption in the presence of high phenolic content results in a decrease in germination percentage (Figure 3A). However, the vigour index of purple nutsedge and blackjack weeds was significantly reduced, probably because of the seed coat distortion and inhibition of embryonic root elongation (Liu et al., 2021).

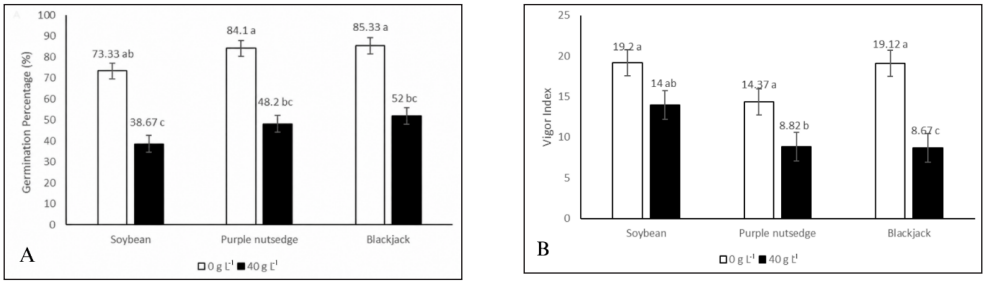

Figure 3. (A) Germination percentage (%) and (B) initial growth vigour index under treatment with 0 and 40 g L^{-1} *Celosia argentea* L. flower extracts. Values with different letters indicate statistically significant differences (Tukey's test, $p \leq 0.05$)

Effect of Bioherbicide Application on Plant Morphology

The application of 40 g L^{-1} flower extract resulted in a reduction of plant height, leaf number, leaf area, and root area in all species (Figure 4). The reduction in height is ascribed to the suppression of photosynthesis and limited biosynthesis of carbohydrates (Powles & Yu, 2010). Leaf expansion was inhibited by allelopathic compounds (Rahmawati, 2024). The extract of the red flower highly suppressed root growth, with blackjack weeds having the least root area. Oxidative stress.

Treatment with 40 g L^{-1} of cockscomb flower extract affected the height of soybean plants (Figure 4A). Soybean plants treated with a concentration of 40 g L^{-1} were shorter and had smaller roots compared to those treated with 0 g L^{-1}. The same was observed in purple nutsedge (Figure 4B), where the *C. argentea* flower extract had a significant effect on plant height. In blackjack, the canopy and root sizes were smaller compared to the 0 g L^{-1} treatment (Figure 4C). Visually, it is evident that the response to the application of *C. argentea* extract at 40 g L^{-1} was consistent across all experimental plant species. This reduction in plant height was caused by the plants' response to the herbicide, which reduced the rate of photosynthesis and, consequently, carbohydrate biosynthesis (Powles & Yu, 2010). On day 14, the number of leaves, leaf area, and root area were reduced compared to the control group.

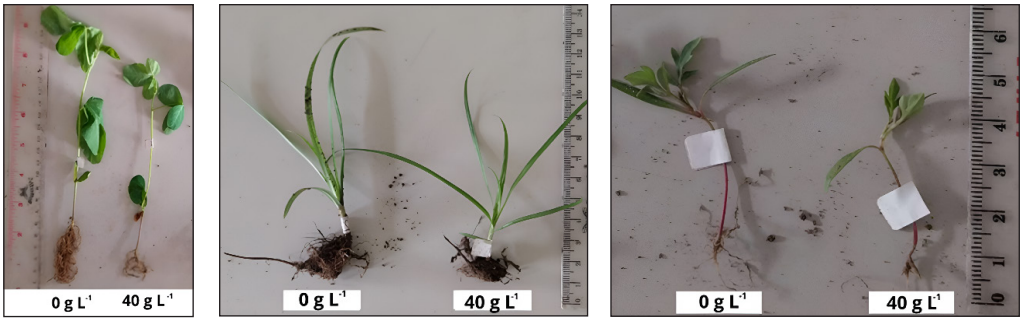

(A) (B) (C)

Figure 4. Effect of bioherbicide application on plant morphology in (A) soybean (B) purple nutsedge, and (C) blackjack. *Celosia argentea* L. flower extracts were used at 0 and 40 g L^{-1}

The application of bioherbicides affects the surface of the root hypocotyl. The thin cuticle allows phytotoxic compounds to penetrate root cells. This absorption causes changes in the cell cycle, membrane damage, and alterations in cell structure. Membrane damage results in reduced root elongation capacity (Figure 5B). In addition, the size of the metaxylem cells decreases due to these phytotoxic compounds (Hasan et al., 2021), which also disrupts cell elongation. Figure 5A shows a decrease in plant height when the bioherbicide *C. argentea* was applied at a concentration of 40 g L^{-1}. Inhibition of root

formation was caused by root damage, as evidenced by a reduction in root area (Figure 5D) and root number (Figure 5F) following treatment with flower extract at a concentration of 40 g L^{-1}. The reduction in root area resulted in decreased nutrient uptake and inhibited new leaf growth, as well as a decrease in leaf area (Figure 5C) and the number of leaves (Figure 5E).

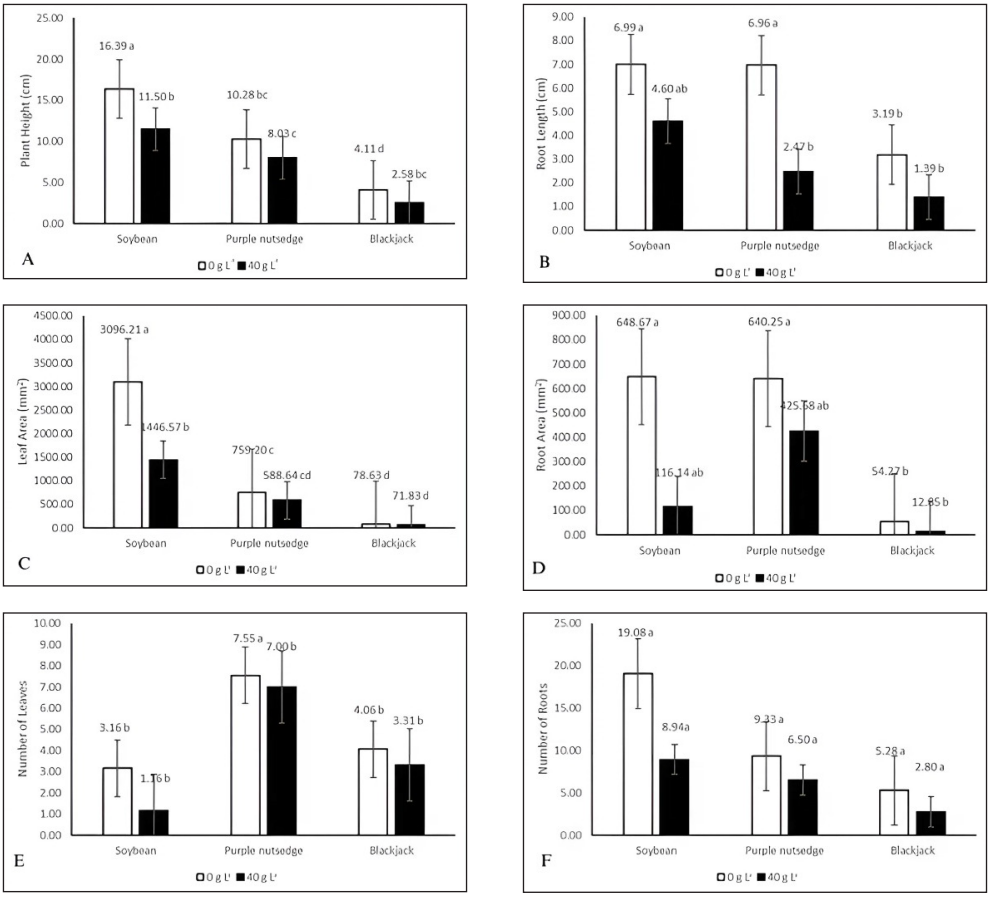

Figure 5. (A) Plant height, (B) root length (C) leaf area (D) root area (E) number of leaves, and (F) number of roots under treatment with 0 and 40 g L^{-1} *Celosia argentea* L. flower extracts. Values with varied letters indicate statistically significant differences (Tukey's test, $p \leq 0.05$)

The study results showed a reduction in fresh shoot weight, fresh root weight, dry shoot weight, and dry root weight (Figure 6). For the fresh shoot weight variable (Figure 6A), it was observed that the application of the bioherbicide derived from the flower of *C. argentea* at 40 g L^{-1} reduced the shoot weight of soybean, purple nutsedge, and blackjack, with the lowest weight observed in the blackjack weed. The decrease in fresh shoot weight

was accompanied by a decrease in fresh root weight (Figure 6B); in soybeans, fresh root weight decreased from 0.098 to 0.77 g and from 0.585 to 0.116 g when treated with 40 g L^{-1} of bioherbicide. The decrease in fresh weight of both shoots and roots reduced shoot dry weight (Figure 6C) and root dry weight (Figure 6D). This decrease in dry weight is due to the plants' inability to produce assimilates under bioherbicide stress. This decrease occurs because the compound interacts with cytoplasmic membrane components, including proteins and lipids. As a result, the apical meristem browns, which can subsequently damage the root system (Kostina-Bednarz et al., 2023).

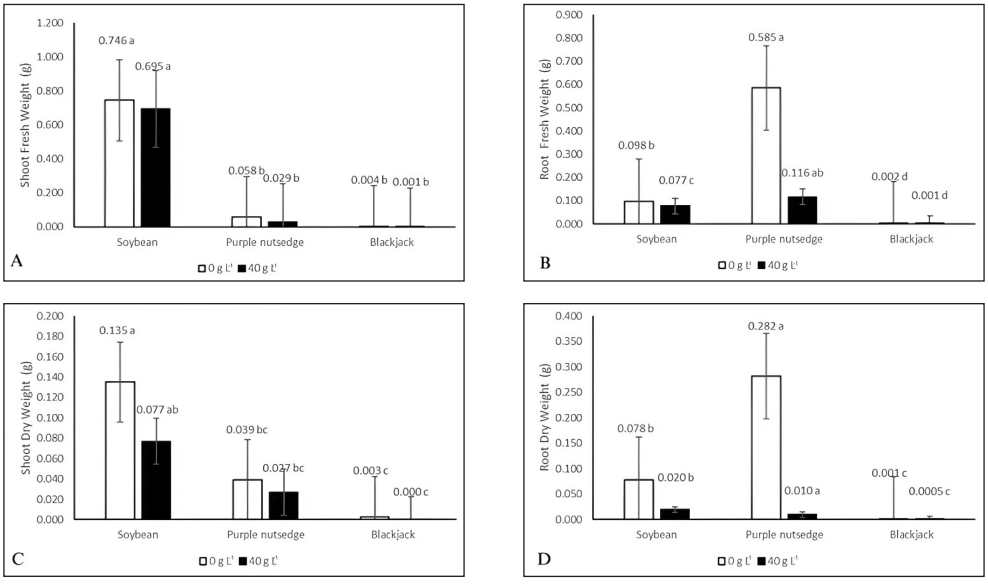

Figure 6. (A) Shoot Fresh Weight (B) root fresh weight (C) shoot dry weight and (D) root dry weights during the early growth phases of soybeans, purple nutsedge, and blackjack under treatment with *Celosia argentea* L. flower extracts at 0 and 40 g L^{-1}. Values with varied letters indicate statistically significant differences (Tukey's test, $p \leq 0.05$)

Effect of Bioherbicide Application on Plant Physiology

The application of *C. argentea* extract significantly decreased the leaf chlorophyll a, chlorophyll b, and total chlorophyll levels (Figure 7). The reduction may be due to damage to the chloroplast pigments caused by oxidative stress and hence reduced photosynthesis. Reactive oxygen species (ROS) damage the integrity of the cell membrane, leading to leakage and desiccation, ultimately causing cell death (Hasan et al., 2021).

A significant decrease in leaf greenness scores was found in blackjack, with leaf greenness at 0 g L^{-1} showing 31.34 (Figure 7A), while at 40 g L^{-1}, the greenness decreased to 30.15. The chlorophyll a variable (Figure 7B) showed insignificant results in the

combination of *C. argentea* flower extract concentration and plant type, possibly because chlorophyll a levels were less sensitive to bioherbicide stress. Variable chlorophyll b levels (Figure 7C) showed significant results that influenced the decrease in total chlorophyll levels (Figure 7D). The suppression of chlorophyll may be caused by the inhibition of the biosynthesis process or the degradation of chlorophyll components, which can be affected by allelochemicals from bioherbicides (Uyun et al., 2024).

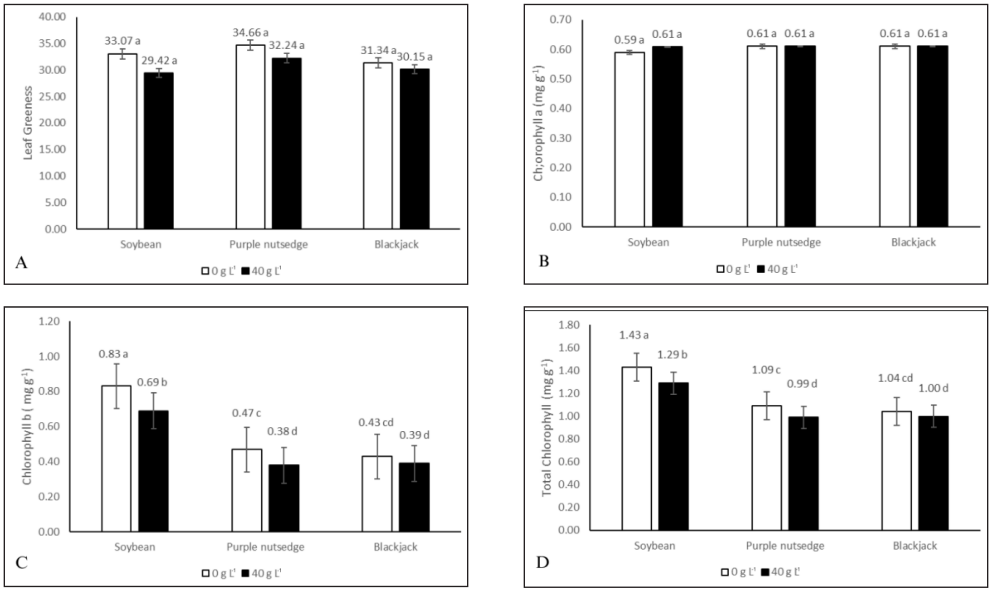

*Figure 7. (*A) Leaf greenness, (B) chlorophyll a, (C) chlorophyll b, and (D) total chlorophyll contents during the early growth phases of soybean, purple nutsedge, and blackjack treated with *Celosia argentea* L. flower extracts at 0 and 40 g L^{-1}. Values with varied letters indicate statistically significant differences (Tukey's test, $p \leq 0.05$)

Impacts of Bioherbicide Application on Leaf Anatomy

The smallest stomatal aperture width was observed in blackjack weeds treated with flower extracts, while the highest aperture width was recorded in control soybean plants (Figure 8). The higher concentrations of bioherbicide increased the stomatal resistance but reduced the stomatal density, presumably due to the reduced Ψs. Genetic factors influence the variation in stomatal density, and it is important for the regulation of photosynthetic efficiency. Lower stomatal density leads to lower uptake of photosynthetic precursors and therefore lower overall photosynthetic capacity (Yahya et al., 2025).

Such results indicated a significant reduction in the stomatal aperture width (Figure 8A) and density (Figure 8B) in all weeds treated with 40 g L^{-1} of the flower extract in comparison to the control. The higher phenolic content of the extract probably increased the diffusion resistance of the leaf and favored stomatal closure. Also, from the figure, it

can be seen that the density is affected by the width of the aperture, with lower widths corresponding to lower density.

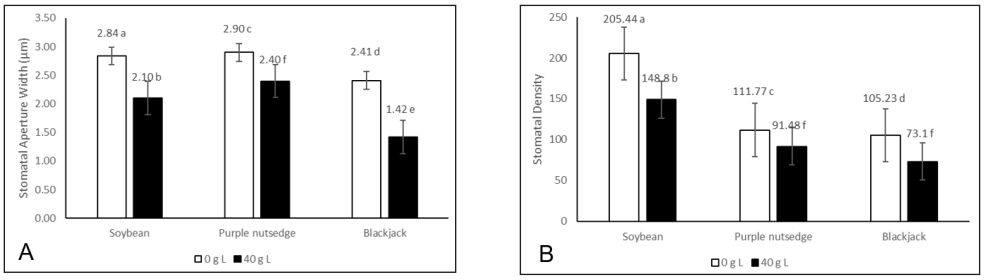

Figure 8. (A) Stomatal aperture width and (B) stomatal density during the early growth phase of soybean, purple nutsedge, and blackjack treated with *Celosia argentea* L. flower extracts at 0 and 40 g L^{-1}. Values with varied letters indicate statistically significant differences (Tukey's test, $p \leq 0.05$)

DISCUSSIONS

This finding is important in evaluating the bioherbicidal potential and possible phytotoxic effects of Celosia argentea flower extract on soybean and weeds. The bioassay and early growth responses of the test species differed, and this may give insight into their susceptibility to the extract. While many plant extracts have been reported as possible bioherbicides, the link between the physicochemical properties of *C. argentea* flower extracts and their inhibitory efficiency on weed germination and growth has not been studied.

The flower extract at 40 g L^{-1} strongly inhibited germination and early growth in soybean, purple nutsedge and blackjack weeds. The phytotoxic compounds inhibited cell division, reduced root area, and disturbed root growth, and consequently restricted nutrient absorption and leaf development. As a consequence of this, the leaf area was decreased, the chlorophyll content was decreased, and the overall productivity of the plant was decreased.

Bioherbicides can affect germination by interrupting imbibition, hydrolysing food reserves, and disturbing cell division and elongation (Wang et al., 2025). Root damage reduces water and nutrient uptake and their translocation in the vascular system (Hoang Anh et al., 2021). The inhibition of cellular respiration and ATP synthesis inhibits plant growth (Kostina-Bednarz et al., 2023). Drought stress is initiated by impaired water uptake and damage to roots and reduces stomatal conductance. Thus the chlorophyll content limits the growth of plants and accumulation of biomass.

The study results showed inhibition of germination processes in soybeans as well as weeds. Kusumawati et al. (2026) reported that the use of teak leaf bioherbicide extract at planting did not suppress soybean germination. However, it did prevent the germination of the weed T. *procumbens*. This is because of the different allelochemical content and

properties of *C. argentea* flowers and teak leaves. Since *C. argentea* produces a non-selective herbicide, it still inhibits germination of soybean when the bioherbicide is applied. Meanwhile, Abdillah et al. (2026) said that the 40% Wedelia bioherbicide is most effective when applied seven days before planting. The bioherbicide under this treatment was selective for soybean germination and inhibited the germination and growth of T. *procumbens* and Purple nutsedge. These studies indicate that soybeans and weeds have varied responses to different bioherbicide formulas and hence more research is required.

CONCLUSION

The physicochemical properties of *Celosia argentea* extracts varied among plant parts, with flower extract showing bioherbicidal potential. The extract inhibited germination and early growth of soybean, purple nutsedge, and blackjack. The early development of the plant was affected, as evidenced by the changes in root growth, leaf area, chlorophyll content, and stomatal characteristics. The results show the potential of flower extract as a weed controller and the need for crop selectivity. Application of *C. argentea* flower extract at 40 g L^{-1} can be used as a bioherbicide and may also affect the development of soybean. Further evaluation is needed to determine conditions of application under which weed suppression is achieved with minimal crop phytotoxicity. The study looked at germination and early growth in controlled conditions, and these may not completely reflect responses in the field. The roles of individual bioactive compounds and the underlying mechanisms were not fully established.

IMPLICATION OF THE STUDY

The results of the study show that *C. argentea* extract has the potential to be a bioherbicide that can inhibit weed growth in soybean crops. The most effective flower extract in suppressing germination and weed growth is C. *argentea* red flower organ extract with a concentration of 40 g L^{-1}, which shows an inhibiting effect compared to other organs and concentrations. Flower extract at this concentration can inhibit germination through a decrease in germination percentage and vigor index. In the early growth stage, it can reduce the height growth of plants, roots, and leaves. In addition, the application of these extracts can reduce the chlorophyll content and characteristics of the stomata. However, the effect of this extract still affects soybeans, so further research is needed on optimising the phytotoxic effect on weeds by minimising phytotoxic effects on soybeans. These findings are the basis for the development of weed control strategies that support environmentally friendly agriculture.

LIMITATION AND RECOMMENDATION FOR FUTURE RESEARCH

The current study has limitations that should be considered in future research. In this study, soybeans have not yet been selected for bioherbicides; therefore, research is needed to determine the right timing for applying red *C. argentea* extract. This research is still experimental in laboratories and greenhouses; therefore, field research is needed to validate the effects of *C. argentea* bioherbicides under field conditions. In addition, *C. argentea* toxicity needs to be increased through genetics, environmental conditions, and management practices that increase the secondary metabolites present in *C. argentea*. The follow-up research I recommend focuses on using nanotechnology to improve the effectiveness and efficiency of bioherbicide absorption by weeds. It is hoped that with this research, bioherbicides can be accepted by the community as environmentally friendly weed control. This follow-up research is expected to provide a comprehensive understanding of agricultural practices that use local resources for sustainable weed management strategies.

ACKNOWLEDGEMENT

The Universitas Gadjah Mada Final Project Recognition Grant (Grant No. 4971/UN1.P1/PT.01.01/2024) provided funding for this study. The authors are profoundly appreciative of the financial support provided by the Directorate of Research at Universitas Gadjah Mada for this work.

REFERENCES

Abdillah, F., Respatie, D. W., & Purwantoro, A. (2026). Application time of Wedelia trilobata leaf extract as a bioherbicide for controlling dominant weeds in soybeans. *Jurnal Agronomi Indonesia, 54*(1), 17-29. https://doi.org/10.24831/jai.v54i1.70636

Alara, O. R., Abdurahman, N. H., & Ukaegbu, C. I. (2021). Extraction of phenolic compounds: A review. *Current Research in Food Science, 4*, 200-214. https://doi.org/10.1016/j.crfs.2021.03.011

Aslam, M., Sultana, B., Anwar, F., & Munir, H. (2016). Foliar spray of selected plant growth regulator affected the biochemical and antioxidant attributes of spinach in a field experiment. *Turkish Journal of Agriculture and Forestry, 40*(2), 136-145. https://doi.org/10.3906/tar-1412-56

Baćmaga, M., Wyszkowska, J., & Kucharski, J. (2024). Environmental implication of herbicide use. *Molecules, 29*(24), Article 5965. https://doi.org/10.3390/molecules29245965

Benvenuti, S. (2025). Agroecology of *Cyperus rotundus*: Emergence dynamics as a tool for sustainable weed management. *Sustainability, 17*(21), Article 9543. https://doi.org/10.3390/su17219543

Bidira, T., Shimales, T., Adissu, M., & Eshetu, T. (2021). Weed species dominance and abundance in tea (*Camellia sinensis* L.) plantation of southwest Ethiopia. *American Journal of Plant Biology, 6*(4), 89-94. https://doi.org/10.11648/j.ajpb.20210604.14

Chauhan, B. S., Ali, H. H., & Florentine, S. (2019). Seed germination ecology of Bidens pilosa and its implications for weed management. *Scientific Reports, 9*, Article 16004. https://doi.org/10.1038/s41598-019-52620-9

Chivinge, O. A., & Schweppenhauser, A. (1995). Competition of soybean with blackjack (*Bidens pilosa* L.) and pigweed (*Amaranthus hybridus* L.). *African Crop Science Journal, 3*(1), 73-82. https://doi.org/10.4314/acsj.v3i1.54568

Harsono, A., Harnowo, D., Ginting, E., & Adi Anggraeni Elisabeth, D. (2022). Soybean in Indonesia: Current status, challenges and opportunities to achieve self-sufficiency. In J. C. Jimenez-Lopez & A. Clemente (Eds.), *Legumes research—Volume 1*. IntechOpen. https://doi.org/10.5772/intechopen.101264

Hasan, M., Ahmad-Hamdani, M. S., Rosli, A. M., & Hamdan, H. (2021). Bioherbicides: An eco-friendly tool for sustainable weed management. *Plants, 10*(6), Article 1212. https://doi.org/10.3390/plants10061212

Hoang Anh, L., Van Quan, N., Tuan Nghia, L., & Dang Xuan, T. (2021). Phenolic allelochemicals: Achievements, limitations, and prospective approaches in weed management. *Weed Biology and Management, 21*(2), 37-67. https://doi.org/10.1111/wbm.12230

Hussain, M., Hafeez, A., Al-Huqail, A. A., Alsudays, I. M., Alghanem, S. M. S., Ashraf, M. A., Rasheed, R., Rizwan, M., & Abeed, A. H. A. (2024). Effect of hesperidin on growth, photosynthesis, antioxidant systems and uptake of cadmium, copper, chromium and zinc by Celosia argentea plants. *Plant Physiology and Biochemistry, 207*, Article 108433. https://doi.org/10.1016/j.plaphy.2024.108433

International Seed Testing Association (ISTA). (1999). *International rules for seed testing*. *Seed Science and Technology, 27*(Supplement), 1-333.

Kostina-Bednarz, M., Płonka, J., & Barchańska, H. (2023). Allelopathy as a source of bioherbicides: Challenges and prospects for sustainable agriculture. *Reviews in Environmental Science and Bio/Technology, 22*, 471-504. https://doi.org/10.1007/s11157-023-09656-1

Kusumawati, F. S., Respatie, D. W., Handayani, V. D. S., & Purwantoro, A. (2026). Optimal concentration and application timing of teak leaf extract (*Tectona grandis*) as a bioherbicide against *Tridax procumbens* in soybean. *Pertanika Journal of Tropical Agricultural Science, 49*(3), 1217-1229. https://doi.org/10.47836/pjtas.49.3.11

Kupina, S., Fields, C., Roman, M. C., & Brunelle, S. L. (2019). Determination of total phenolic content using the Folin-C assay: Single-laboratory validation, first action 2017.13. *Journal of AOAC International, 102*(1), 320-321. https://doi.org/10.1093/jaoac/102.1.320

Laamari, I., Marques, I., Ribeiro-Barros, A. I., Béjaoui, Z., & Abassi, M. (2023). Can saline preconditioning enhance plant survival in degraded soils? Physiological, biochemical, and molecular responses in *Casuarina glauca* saplings. *Plant Ecology, 224*, 905-919. https://doi.org/10.1007/s11258-023-01346-w

Lichtenthaler, H. K. (1987). Chlorophylls and carotenoids: Pigments of photosynthetic biomembranes. *Methods in Enzymology, 148*, 350-382. https://doi.org/10.1016/0076-6879(87)48036-1

Li, H., Wang, J., Ning, Y., Pandey, S. P., Li, Z., & Liu, Y. (2025). Effects of whole-plant extracts of four species dominant in the Qinghai-Tibetan Plateau on their germination and growth patterns. *BMC Plant Biology, 25*, Article 1222. https://doi.org/10.1186/s12870-025-07244-9

Li, Z.-H., Wang, Q., Ruan, X., Pan, C.-D., & Jiang, D.-A. (2010). Phenolics and plant allelopathy. *Molecules, 15*(12), 8933-8952. https://doi.org/10.3390/molecules15128933

Liu, C., Huang, K., Zhao, Y., Li, Y., & He, N. (2024). A continental-scale analysis reveals the latitudinal gradient of stomatal density across amphistomatous species: Evolutionary history vs. present-day environment. *Annals of Botany, 134*(5), 877-886. https://doi.org/10.1093/aob/mcae135

Liu, T., Li, T., Zhang, L., Li, H. L., Liu, S., Yang, S., An, Q., Pan, C., & Zou, N. (2021). Exogenous salicylic acid alleviates the accumulation of pesticides and mitigates pesticide-induced oxidative stress in cucumber plants (*Cucumis sativus* L.). *Ecotoxicology and Environmental Safety, 208*, Article 111654. https://doi.org/10.1016/j.ecoenv.2020.111654

Lopes, R. W. N., Morais, E. M., de Jesus Lacerda, J. J., & da Silva asAraújo, F. D. (2022). Bioherbicidal potential of plant species with allelopathic effects on the *weed Bidens bipinnata* L. *Scientific Reports, 12*, Article 13476. https://doi.org/10.1038/s41598-022-16203-5

Mashreghi, A., Alamdari, E. G., Avarseji, Z., & Karizaki, A. R. (2024). Evaluation of the allelopathic potential of barley (*Hordeum spontaneum*) on the germination, morphophysiological, and biochemical characteristics of cress (*Lepidium sativum*). *Iranian Journal of Seed Research, 11*(1), 105-127. https://doi.org/10.61186/yujs.11.1.105

McDonald, M. B., Jr., & Wilson, D. O. (1979). An assessment of the standardization and ability of the ASA-610 to rapidly predict soybean germination. *Journal of Seed Technology,* 4(2), 1-11. https://www.jstor.org/stable/23432728

Paul, V., Sharma, L., Pandey, R., & Meena, R. C. (2017). Measurement of stomatal density and stomatal index on leaf/plant surfaces. *Indian Council of Agricultural Research (ICAR),* 27-30. https://doi.org/10.13140/RG.2.2.13426.40646

Peerzada, A. M. (2017). Biology, agricultural impact, and management of *Cyperus rotundus* L.: The world's most tenacious weed. *Acta Physiologiae Plantarum, 39*, Article 270. https://doi.org/10.1007/s11738-017-2574-7

Pérez, M., Dominguez-López, I., & Lamuela-Raventós, R. M. (2023). The chemistry behind the Folin-Ciocalteu method for the estimation of polyphenol content in food: Total phenolic intake in a Mediterranean dietary pattern. *Journal of Agricultural and Food Chemistry, 71*(46), 17543-17553. https://doi.org/10.1021/acs.jafc.3c04022

Powles, S. B., & Yu, Q. (2010). Evolution in action: Plants resistant to herbicides. Annual *Review of Plant Biology, 61*, 317-347. https://doi.org/10.1146/annurev-arplant-042809-112119

Rahmawati, N. E. D. (2024). Effect of allelopathy reed extract (*Imperata cylindrica*) on the growth of stems and flowers of cayenne pepper (*Capsicum annuum* L.). *Jurnal Global Ilmiah, 2*(3), 182-185. https://doi.org/10.55324/jgi.v2i3.150

Respatie, D. W., Yudono, P., Purwantoro, A., & Trisyono, Y. A. (2019). The potential of *Cosmos sulphureus* Cav. extracts as natural herbicides. *AIP Conference Proceedings, 2202* (1), Article 020077. https://doi.org/10.1063/1.5141690

Setyowati, N., Pujiwati, H., Rasid, R. N., Muktamar, Z., & Fahrurrozi, F. (2025). Weed control in water-saturated soybean cultivation in the coastal area. *International Journal of Agricultural Technology, 21*(1), 217-230. https://li04.tci-thaijo.org/index.php/IJAT/article/view/4156

Sibuea, F. A., Sibuea, M. B., & Safitri, S. A. (2024). Indonesian soybean import in international trade. *Jurnal Manajemen dan Agribisnis, 21*(1), 122-131. https://doi.org/10.17358/jma.21.1.122

Uyun, Q., Respatie, D. W., & Indradewa, D. (2024). Unveiling the allelopathic potential of wedelia leaf extract as a bioherbicide against purple nutsedge: A promising strategy for sustainable weed management. *Sustainability, 16*(2), Article 479. https://doi.org/10.3390/su16020479

Vishwakarma, M., Kulhare, P. S., & Tagore, G. S. (2023). Estimation of chlorophyll using SPAD meter. *International Journal of Environment and Climate Change, 13*(11), 1901-1912. https://doi.org/10.9734/ijecc/2023/v13i113348

Wang, Z. -Y., Yan, K. -L., Qin, Y. -M., Zhang, N. -C., Chen, X. -C., & Chen, M. (2025). Effects of allelochemicals from plants on seed germination. *Seed Biology, 4,* Article e023. https://doi.org/10.48130/seedbio-0025-0022

Yahya, R., Sukri, H., Nirawati, & Djarot, I. N. (2025). Responses of stomatal characteristics to environmental factors in Fabaceae trees of the urban forest in Maros Regency. *Jurnal Wasian, 12*(1), 1-9. https://doi.org/10.62142/xx0wes03

Yumna, H. S., Respatie, D. W., & Purwantoro, A. (2026). The potential of chrysanthemum (*Chrysanthemum morifolium* sp.) extract as a bioherbicide for controlling coatbuttons weeds (*Tridax procumbens*) in soybean (*Glycine max* L.) crops. *Australian Journal of Crop Science, 20*(7), 565-573. https://doi.org/10.21475/ajcs.26.20.07.pne200

Zhang, S.-M., Wang, X.-F., Feng, J., & Sun, Z.-L. (2016). Chemical constituents of the seeds of *Celosia cristata*. *Chemistry of Natural Compounds, 52*, 827-829. https://doi.org/10.1007/s10600-016-1788-z

Pertanika J. Trop. Agric. Sci. 49 (5): 2545 - 2563 (2026)

PERTANIKA JOURNALS

TROPICAL AGRICULTURAL SCIENCE

Journal homepage: http://www.pertanika.upm.edu.my/

Growth, SPAD Index, and Nitrogen Use Efficiency of Two *Axonopus compressus* Variants Under Soil Mixture Ratios and NPK Fertiliser Regimes

Ting Zeng[1, 2]*, Abdul Shukor Juraimi[1], Nazatul Shima Naharudin[1], Mahmudul Hasan[3], and Muhammad Saiful Ahmad-Hamdani[1, 3]*

[1]*Department of Crop Science, Faculty of Agriculture, Universiti Putra Malaysia (UPM), 43400 Serdang, Selangor, Malaysia*

[2]*Guangxi Cultural Tourism and Wellness Integrated Development Center, Guilin Tourism University, 541004 Guilin, China*

[3]*Institute of Plantation Studies, Universiti Putra Malaysia (UPM), 43400 Serdang, Selangor, Malaysia*

ABSTRACT

Axonopus compressus is a widely used tropical turfgrass for landscapes and sports turf systems, but appropriate substrate-fertiliser combinations for newly developed variants remain insufficiently defined. This experiment assessed the growth responses of two mutant variants, A-40 and A-46, under three soil mixture ratios: S1 = 100:0 (sand: topsoil), S2 = 0:100 (sand: topsoil), and S3 = 70:30 (sand: topsoil). Nine NPK fertilisation regimes were evaluated, including an unfertilised control and four application rates (0.5×, 0.75×, 1.0×, and 1.5× of the recommended rate) of two fertiliser blends: NPK 15-15-15 + 2S (sulfur) and NPK 12-12-17 + TE (trace elements), each applied at four rates (GF1-GF4 and BF1-BF4). In A-40, BF3 showed the highest agronomic nitrogen use efficiency AE_N = 97.10 g biomass per g N, while BF4 produced the highest SPAD index (+67.9%) and leaf colour (+17.1%) compared with the unfertilised control. In A-46, BF2 and BF3 were the most efficient (AE_N = 80.22-79.32), whereas BF4 increased SPAD by 76.6%. SPAD index showed moderate to strong positive correlations with growth and biomass traits, particularly in A-46. S3 generally created a better growing medium; BF2 and BF3 provided relatively high biomass gain per unit of nitrogen input without requiring the highest fertiliser rate. These results provide practical guidance for variant-specific substrate-fertiliser management in tropical turfgrass systems.

Keywords: Agronomic nitrogen use efficiency, biomass, mutant *Axonopus compressus*, NPK fertilisation, soil mixture ratio

ARTICLE INFO

Article history:
Received: 01 July 2026
Accepted: 09 October 2026
Published: 30 October 2026

DOI: https://doi.org/10.47836/pjtas.49.5.22

E-mail addresses:
gs64190@student.upm.edu.my (Ting Zeng)
ashukur@upm.edu.my (Abdul Shukor Juraimi)
nazatul@upm.edu.my (Nazatul Shima Naharudin)
mdmahmudul@upm.edu.my (Mahmudul Hasan)
s_ahmad@upm.edu.my (Muhammad Saiful Ahmad-Hamdani)
* Corresponding author

e-ISSN: 2231-8542

© Universiti Putra Malaysia Press

INTRODUCTION

Turfgrass is an important plant for sustainable landscapes and has a wide range of applications. *Axonopus compressus* (Sw.) P.Beauv., commonly known as Cowgrass, is a stoloniferous perennial species of the Poaceae family. Under tropical conditions, *A. compressus* is commonly used in lawns, roadsides, golf courses, and stadium fields because of its low maintenance requirements, visual quality, and tolerance to high rainfall conditions (Wahid et al., 2023). Compared to other common turfgrass species such as *Cynodon dactylon* and *Zoysia* spp., it requires relatively low fertiliser input (Petrovic et al., 2005). In addition, *A. compressus* shows adaptability to different soil conditions, including sandy, loam, and clay soils (Azuddin et al., 2023). This makes it a cost-effective turfgrass species for recreational turf systems.

The growth quality of turfgrass is influenced by fertiliser and soil texture factors (Carlson et al., 2022). Soil texture influences water retention, aeration, and nutrient availability conditions, critical to root health and canopy development in turf systems (Hamarashid et al., 2010; Roberson et al., 2021). Nitrogen (N), phosphorus (P), and potassium (K) are essential nutrients required for turfgrass growth, including root and shoot development, leaf tissue expansion, and chlorophyll synthesis (Głąb et al., 2020; Shaddox & Unruh, 2021). Compound NPK fertilisers are widely used in turfgrass management because they provide major nutrients simultaneously. In practice, different compound NPK fertilisers are used in turfgrass management. NPK 15-15-15 + 2S provides a more balanced N, P, and K ratio, whereas NPK 12-12-17 + TE contains less N and P but a higher proportion of K together with trace elements (Alif & Amira, 2023). These differences in nutrient composition may affect plant growth, chlorophyll status, root development, and physiological responses. Comparing the two formulations therefore provides a basis for identifying a more suitable fertiliser regime for *A. compressus*.

Fertiliser management should not depend only on total biomass production. Depending on the fertiliser formulation and application rate, higher fertiliser input may increase biomass or leaf greenness, but greater nutrient input does not necessarily lead to a proportional increase in biomass. Agronomic nitrogen use efficiency (AE_N), calculated as the increase in total dry biomass per unit of nitrogen applied, was used to compare fertiliser efficiency (Bhatia et al., 2023). The SPAD meter is a rapid, non-destructive indicator of relative leaf chlorophyll content (Sim et al., 2015). It has been used for chlorophyll monitoring, nitrogen status and grain yield measurement for maize (Shivashankar et al., 2025), rice (Yuan et al., 2016), wheat (Islam et al., 2014), and other horticultural crops. Its application in turfgrass has been limited, particularly for narrow and flexible leaf types. However, the relatively broad leaves of *A. compressus* allow the SPAD sensor to cover the leaf surface in a practical way and to evaluate the response of this turfgrass to different fertilisation.

Improving soil mixture and fertiliser application rate is important for balancing turfgrass growth performance and resource-use efficiency. Over-fertilisation can increase management costs and nitrate leaching (Easton & Petrovic, 2004). Furthermore, over-fertilisation may result in poorer turf density and quality in poorly nutrient-rich soils. Most previous studies have explored single management factors or traits in assessing turfgrass performance (Kopp & Guillard, 2002; Springer et al., 2014; He et al., 2021) and the real landscape may not be fully represented by these features. A-40 and A-46 are two new *A. compressus* mutants selected following gamma-ray irradiation and showed desirable morphological and turf characteristics during previous screening. However, little is known about how these two mutants perform under different root-zone substrates and fertilisation regimes. Therefore, this study evaluated responses of two variants, A-40 and A-46, to different soil mixture ratios and graded NPK fertiliser regimes. Morphological traits, SPAD index, leaf colour, biomass traits, and AE_N were assessed to identify soil-fertiliser combinations that support turfgrass growth while improving nitrogen input efficiency. The findings provide practical information for variant-specific fertiliser and substrate management in tropical turfgrass systems.

MATERIALS AND METHODS

Experimental Site and Plant Material

This study was conducted at UPM-SATIRI Turfgrass Lab, Universiti Putra Malaysia, in Serdang, Selangor, Malaysia (2°59′N, 101°44′E). The place has a tropical rainforest climate. During the experimental period from April to September 2024, monthly maximum, average, and minimum temperatures ranged from 29.0 to 29.5 °C, 27.3 to 27.8 °C, and 25.5 to 25.9 °C, respectively. Monthly rainfall ranged from 152 to 206 mm (Figure 1). Temperature and rainfall data for the experimental period were obtained from the Visual Crossing Weather API using the coordinates of the experimental site. These conditions represented a typical tropical environment for evaluating the growth and physiological performance of *A. compressus* variants. All plant materials were cultivated and not collected from the wild. Both mutants A-40 and A-46 were developed from the original accession *A. compressus* through gamma irradiation mutation breeding at the Malaysia Nuclear Agency. Briefly, the original *A. compressus*

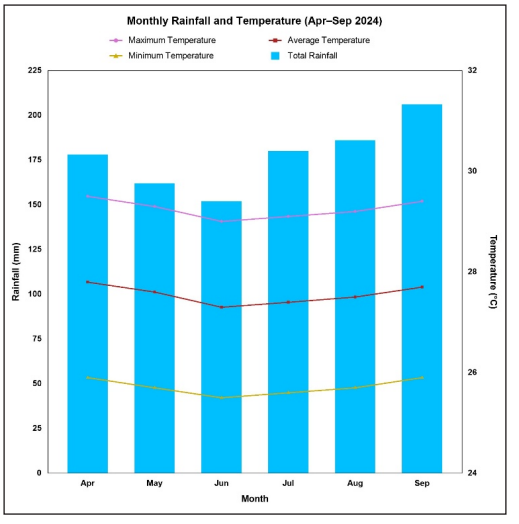

Figure 1. Monthly rainfall and temperature dynamics at the experimental site

individuals were exposed to gamma (γ) radiation at dosages of 200, 400, 600, and 800 Gy. All survivors were split into single nodes and regrown in pots at the UPM-SATIRI Turf Lab. The selection process continued until the 8th generation before the study was conducted.

Experimental Design and Treatments

The experiment was conducted in a split-plot within a randomised complete block design with three replications. Soil mixture ratio (three levels) was assigned to the main plots based on different soil mixture media: sand, topsoil, and a sand-topsoil mixture. Fertiliser treatment (nine levels) was assigned to the sub-plots based on one unfertilised control and different rates of two NPK fertiliser formulations. The experiment was conducted separately for the two variants, A-40 and A-46. Plants were established using a stolonising method. Ten stolon cuttings, each containing four internodes, were planted in plastic trays measuring 37 × 27 × 10 cm. Three soil mixture ratios were used: S1 = 100:0 (sand: topsoil), S2 = 0:100 (sand: topsoil), and S3 = 70:30 (sand: topsoil). The sand used was washed river sand with a particle diameter of <2 mm, while the topsoil was loam. Fertiliser regimes were applied across all soil mixture ratios and consisted of one unfertilised control and two NPK fertiliser formulations, each applied at four rates. NPK 15-15-15 + 2S, commonly known as NPK Green, was applied at 0.5×, 0.75×, 1.0×, and 1.5× of the recommended rate (GF1-GF4), while NPK 12-12-17 + trace elements (TE), commonly known as NPK Blue, was applied at the corresponding rates (BF1-BF4). The two compound fertilisers used in this experiment were purchased from Desyra Enterprise, Malaysia. The recommended rate was set at 0.25 kg N per 100 m² per month based on standard maintenance practice routinely used for A. *compressus* at the UPM-SATIRI Turfgrass Research Laboratory. The fertiliser amounts were calculated accordingly based on the nitrogen content (Table 1). To reduce nutrient loss caused by outdoor rainfall, trays were spaced 15 cm apart and placed on a raised, level platform lined with black plastic film.

Plants were manually watered three times daily during the first two weeks, at approximately 7:00, 10:30, and 5:00. From the third week onwards, watering was reduced to once daily at approximately 9:00 am. Fertilisation started two weeks after stolon establishment and continued every two weeks for 16 weeks. Growth parameters were recorded one week after each fertiliser application over eight sampling events, while biomass traits were measured at 20 weeks after planting. The traits included leaf length (LL), leaf width (LW), SPAD index (SPAD; relative chlorophyll content), number of leaves per plant (NLP), plant height (PH), and leaf colour (LC). At 20 weeks after planting, plants were evaluated for aboveground shoot fresh weight (SFW) and dry weight (SDW), as well as root fresh weight (RFW), root dry weight (RDW), root length (RL), and root volume (RV).

Table 1
Fertiliser formulation types, application rates, and nutrient quantities used per tray in experimental treatments

Code	NPK Fertiliser Regimes	Application Rate (× Recommended)	Single Tray Fertiliser Application Amount / Two Weeks (g)
F0	None	0×	0
GF1	(15-15-15+2S)	0.5×	0.42
GF2		0.75×	0.63
GF3		1.0×	0.84
GF4		1.5×	1.25
BF1	(12-12-17 +TE)	0.5×	0.52
BF2		0.75×	0.78
BF3		1.0×	1.04
BF4		1.5×	1.56

Note. F0 = unfertilised control; GF = NPK (15-15-15+2S); BF = NPK (12-12-17+TE). Numbers 1-4 indicate 0.5×, 0.75×, 1.0×, and 1.5× of the recommended rate, respectively

LL and LW were measured using a vernier calliper, while PH was measured using a ruler from the surface of the growing medium to the tip of the tallest leaf blade. NLP was determined by manually counting all fully expanded leaves on each selected plant. LC was evaluated with a TCM 500 NDVI Turf colour Meter (Spectrum® Technologies, Inc., USA). It was assessed using a rating scale from 1 to 9. A score of 1 represented a condition of wilting or bare ground. Scores ranging from 5 to 9 corresponded to colours from yellowish green to dark green, with a score of 5 signifying a noticeable increase in green foliage and a reduction in senescent leaves.

Determination of Relative Chlorophyll Content

Relative chlorophyll content was estimated using a SPAD meter (SPAD-502 Plus, Konica Minolta, Japan), following the general measurement approach described by Sim et al. (2015). The SPAD reading is a unitless index based on light transmittance through the leaf. Measurements were taken from the central area of the youngest fully expanded leaf to maintain consistency across samples. For each replicate, three readings were collected from different plants and averaged. All measurements were carried out in the morning between 8:30 and 9:00 under stable light conditions to reduce environmental variation and improve data reliability. SPAD index served as an indirect indicator of leaf greenness and nitrogen status during the experiment.

Determination of Biomass Parameters

All biomass traits were assessed using a randomly placed 100 cm² quadrat grid on the turf surface. Weight and root volume were expressed per unit area (g per 100 cm² and cm³ per 100 cm², respectively), while root length was expressed in centimetres (cm). At 20 weeks after planting, to determine the fresh and dry weights of the shoot and root components, samples were cleaned, and fresh weights were recorded separately. Subsequently, they were oven-dried at 65 °C for 72 hours to a constant weight. The volume of the roots was measured using a graduated cylinder and expressed in milliliters (mL), which is equivalent to cubic centimeters (cm³).

Calculation of Agronomic Nitrogen Use Efficiency

Agronomic nitrogen use efficiency (AE_N) was calculated following the general approach described by Li et al. (2023) with total dry biomass used as the biomass response variable. Total dry weight (TDW) was determined as the sum of shoot dry weight (SDW) and root dry weight (RDW) as in Equation 1:

$$TDW = SDW + RDW \quad [1]$$

Total nitrogen input for each tray was calculated using the fertiliser amount, nitrogen concentration, and number of applications. NPK 15-15-15 + 2S contained 15% nitrogen, while NPK 12-12-17 + TE contained 12% nitrogen. Since fertiliser was applied every two weeks for 16 weeks, the total nitrogen applied was calculated as in Equations 2 to 3:

$$N_{applied} = F_{amount} \times N_{concentration} \times n \quad [2]$$

$$AE_N = \frac{TDW_{fertili\ sed} - TDW_{F0}}{N_{applied}} \quad [3]$$

where F_{amount} is the fertiliser amount applied per tray at each application, $N_{concentration}$ is the nitrogen concentration of the fertiliser, and (n) is the number of fertiliser applications. For NPK 15-15-15 + 2S, ($N_{concentration}$) was 15%, whereas for NPK 12-12-17 + TE was 12%. Fertiliser was applied once every two weeks for 16 weeks; therefore, (n = 8).

Statistical Analysis

Data were analysed using analysis of variance (ANOVA) based on a split-plot design. Soil mixture ratio was used as the main-plot factor, and fertiliser regime was used as the sub-plot factor. When significant effects were detected, means were compared using the

Scott-Knott test at $p < 0.05$. When the interaction between soil mixture ratio and fertiliser regime was not significant, only the main effects were interpreted. All analyses were conducted in RStudio version 4.6.0.

RESULTS

Effects of Soil Mixture Ratio (S) and Fertiliser Regime (F) on Morphological Traits and Relative Chlorophyll Content of A-40 and A-46

The effects of fertiliser regime and soil mixture ratio on morphological traits and relative chlorophyll content of A-40 and A-46 are presented in Table 2. Fertiliser regime significantly affected all measured traits in both variants, including leaf length (LL), leaf width (LW), number of leaves per plant (NLP), plant height (PH), SPAD index, and leaf colour index (LC) ($p < 0.001$). In A-40, fertiliser regime significantly affected all measured traits. BF4 showed the highest numerical values for LL (35.55 mm), NLP (12.60), PH (4.58 cm), SPAD index (36.86), and LC (5.82). However, BF4 did not differ significantly from BF3 and GF4 for most of these traits, according to the Scott-Knott test. GF3, GF4, BF3, and BF4 were generally grouped in the highest statistical class for LL, NLP, SPAD index, and LC.

In A-46, BF4 showed the highest numerical values for LL (34.71 mm), NLP (12.62), PH (4.88 cm), SPAD index (37.62), and LC (5.89). However, several higher fertiliser treatments were statistically comparable with BF4. For example, GF3, GF4, BF2, BF3, and BF4 were not significantly different for LL, while GF3, GF4, BF3, and BF4 were grouped together for several other growth traits. BF4 was significantly higher than BF3 and GF4 only for selected traits such as SPAD index.

The soil mixture ratio had weaker effects than the fertiliser regime and significantly affected only selected traits. In A-40, soil mixture ratio significantly affected LL, LW, and LC. S3 produced the highest LL (33.44 mm), while S2 showed the highest LW (6.77 mm) and LC (5.68). In A-46, soil mixture ratio significantly affected LL, PH, and LC. S2 produced the highest LL (32.96 mm), PH (4.35 cm), and LC (5.61).

Effects of Soil Mixture Ratio and Fertiliser Regime on Biomass Traits of A-40 and A-46

Fertiliser regime significantly affected all biomass traits in both A-40 and A-46 ($p < 0.001$; Table 3). In A-40, BF4 produced the highest values for SFW (42.80 g), SDW (8.04 g), RFW (19.68 g), RDW (4.07 g), and RV (16.72 cm^3), while GF3 produced the longest RL (18.37 cm). GF4 also showed relatively high values for SFW (32.35 g), SDW (6.64 g), RFW (17.08 g), RDW (3.78 g), RV (14.08 cm^3), and RL (17.50 cm). Compared with the unfertilised control, fertiliser application clearly improved biomass accumulation in A-40.

Table 2
Main-effect means of morphological traits and SPAD index in A-40 and A-46 under fertiliser regime and soil mixture ratio

		LL (mm)		LW (mm)		NLP		PH (cm)		SPAD (Index)		LC (Index)	
Fertiliser		**A-40**	**A-46**	**A-40**	**A-46**	**A-40**	**A-46**	**A-40**	**A-46**	**A-40**	**A-46**	**A-40**	**A-46**
F	F0	28.24 c	28.20 c	6.10 c	6.07 d	5.61 c	5.26 c	2.76 c	2.81 c	21.95 d	21.30 e	4.97 c	4.46 c
	GF1	31.01 b	31.42 b	6.59 b	6.48 c	7.27 b	6.51 c	3.44 b	3.77 b	30.05 c	29.94 d	5.45 b	5.51 b
	GF2	32.34 b	31.36 b	6.82 a	6.68 b	8.44 b	8.36 b	3.72 b	4.16 b	32.88 b	32.86 c	5.59 b	5.63 b
	GF3	34.28 a	33.32 a	6.94 a	6.91 a	10.34 a	10.27 a	3.88 a	4.19 b	34.56 a	33.92 b	5.71 a	5.71 a
	GF4	35.18 a	33.98 a	6.87 a	7.07 a	12.15 a	11.62 a	4.14 a	4.67 a	35.52 a	35.51 b	5.75 a	5.86 a
	BF1	31.11 b	30.37 b	6.46 b	6.53 c	6.48 c	6.75 c	3.60 b	4.03 b	30.04 c	29.07 d	5.49 b	5.37 b
	BF2	32.14 b	32.73 a	6.53 b	6.75 b	8.36 b	8.73 b	3.99 a	4.41 a	31.73 b	32.50 c	5.46 b	5.60 b
	BF3	33.12 a	33.34 a	6.78 a	6.91 a	10.61 a	10.48 a	4.34 a	4.70 a	34.93 a	35.51 b	5.74 a	5.67 a
	BF4	35.55 a	34.71 a	6.92 a	7.04 a	12.60 a	12.62 a	4.58 a	4.88 a	36.86 a	37.62 a	5.82 a	5.89 a
	P	***	***	***	***	***	***	***	***	***	***	***	***
		LL (mm)		**LW (mm)**		**NLP**		**PH (cm)**		**SPAD (Index)**		**LC (Index)**	
Soil		**A-40**	**A-46**	**A-40**	**A-46**	**A-40**	**A-46**	**A-40**	**A-46**	**A-40**	**A-46**	**A-40**	**A-46**
S	S1	31.91 b	30.98 b	6.56 b	6.67 a	8.80 a	8.88 a	3.56 a	3.89 b	32.01 a	32.22 a	5.33 b	5.33 b
	S2	32.3 b	32.96 a	6.77 a	6.68 a	9.19 a	8.87 a	3.99 a	4.35 a	32.38 a	32.12 a	5.68 a	5.61 a
	S3	33.44 a	32.54 a	6.67 a	6.80 a	9.29 a	9.12 a	3.94 a	4.30 a	31.79 a	31.74 a	5.65 a	5.63 a
	P	*	**	*	NS	NS	NS	NS	*	NS	NS	***	***

Note. LL = leaf length; LW = leaf width; SPAD = relative chlorophyll content; NLP = number of leaves per plant; PH = plant height; LC = leaf colour rating. Soil mixture ratio means were averaged across fertiliser regimes, while fertiliser regime means were averaged across soil mixture ratios. Within each column and within the same factor section, means followed by different letters are significantly different at $p \leq 0.05$ according to the Scott-Knott test

Table 3
Main-effect means of biomass traits in A-40 and A-46 under fertiliser regime and soil mixture ratio

		SFW (g)		SDW (g)		RFW (g)		RDW (g)		RV (cm³)		RL (cm)	
Fertiliser		**A-40**	**A-46**	**A-40**	**A-46**	**A-40**	**A-46**	**A-40**	**A-46**	**A-40**	**A-46**	**A-40**	**A-46**
F	F0	2.48 e	1.79 c	0.67 d	0.51 c	1.36 c	0.80 c	0.43 b	0.23 c	1.97 c	1.03 c	8.47 c	14.50 d
	GF1	13.84 d	12.40 b	2.74 c	3.20 b	5.65 c	5.11 b	1.28 b	1.52 b	5.30 c	4.36 b	12.37 b	17.02 c
	GF2	16.20 d	14.45 b	3.34 c	3.56 b	6.83 c	7.39 b	1.44 b	1.81 b	6.29 c	6.68 b	14.82 a	19.02 c
	GF3	23.69 c	19.67 b	4.73 b	4.42 a	11.21 b	7.94 b	2.22 b	1.71 b	10.17 b	7.47 b	18.37 a	20.59 b
	GF4	32.35 b	28.78 a	6.64 a	5.54 a	17.08 a	13.91 a	3.78 a	2.23 b	14.08 a	11.03 a	17.50 a	22.10 a
	BF1	12.23 d	10.63 b	2.82 c	2.92 b	6.14 c	7.59 b	1.30 b	1.70 b	6.94 c	6.96 b	13.18 b	17.55 c
	BF2	25.50 c	17.60 b	5.69 b	4.55 a	12.12 b	10.39 a	2.46 b	2.19 b	11.18 b	9.29 a	15.02 a	20.42 b
	BF3	35.01 b	29.56 a	7.01 a	5.88 a	17.96 a	12.36 a	3.80 a	2.78 a	15.02 a	11.10 a	15.44 a	22.44 a
	BF4	42.80 a	35.43 a	8.04 a	6.25 a	19.68 a	16.01 a	4.07 a	2.91 a	16.72 a	14.82 a	14.94 a	23.25 a
	P	***	***	***	***	***	***	***	***	***	***	***	***
	SFW (g)	**SDW (g)**	**RFW (g)**	**RDW (g)**	**RV (cm³)**	**RL (cm)**	**SFW (g)**	**SDW (g)**	**RFW (g)**	**RDW (g)**	**RV (cm³)**	**RL (cm)**	**SFW (g)**
Soil		**A-40**	**A-46**	**A-40**	**A-46**	**A-40**	**A-46**	**A-40**	**A-46**	**A-40**	**A-46**	**A-40**	**A-46**
S	S1	22.85 a	14.98 b	5.06 a	3.52 a	13.04 a	7.76 a	2.57 a	1.66 a	10.80 a	7.29 a	15.61 a	22.10 a
	S2	20.73 a	19.16 a	4.35 a	4.04 a	8.34 b	9.17 a	1.87 a	2.05 a	7.46 b	7.70 a	12.61 b	17.50 c
	S3	24.45 a	22.63 a	4.48 a	4.73 a	11.30 a	10.24 a	2.49 a	1.99 a	10.96 a	9.25 a	15.15 a	19.36 b
	P	NS	**	NS	NS	**	NS	NS	NS	*	NS	*	***

Note. SFW = shoot fresh weight; SDW = shoot dry weight; RFW = root fresh weight; RDW = root dry weight; RV = root volume; RL = root length. Soil mixture ratio means were averaged across fertiliser regimes, while fertiliser regime means were averaged across soil mixture ratios. Within each column and within the same factor section, means followed by different letters are significantly different at $p < 0.05$ according to the Scott-Knott test. Mean comparisons were conducted separately for each variant

In A-46, BF4 produced high biomass rates for SFW (35.43 g), SDW (6.25 g), RFW (16.01 g), RDW (2.91 g), RV (14.82 cm^3) and RL (23.25 cm). BF3 and GF4 resulted in high biomass scores for SFW, RFW, RV and RL. This means that more fertiliser inputs, especially BF4, led to higher shoot and root biomass values in both variants. The soil mixture ratio was weaker than the fertiliser regime and affected only some biomass features. In the A-40s, soil mixture ratios are less significant than fertiliser regimes and mostly affected RFW, RV, and RL. S1 produced the highest RFW (13.04 g) and RL (15.61 cm), and S3 produced the highest RV (10.96 cm^3). In A-46, soil mixture ratio significantly affected SFW and RL. S3 produced a higher SFW (22.63 g), while S1 produced a longer RL (22.10 cm). Overall, the fertiliser regime was the dominant factor affecting biomass accumulation, whereas the soil mixture ratio mainly influenced selected root-related traits.

Agronomic Nitrogen Use Efficiency Based on Total Dry Biomass

Agronomic nitrogen use efficiency (AE_N) was calculated to assess the increase in total dry biomass per unit of applied nitrogen (Table 4). AE_N was calculated from treatment-mean total dry biomass to compare biomass gain per unit of nitrogen applied among fertiliser regimes. Values for S1, S2, and S3 are also presented to show the fertiliser responses under different soil mixture ratios.

Table 4
Agronomic nitrogen use efficiency based on total dry biomass of A-40 and A-46 under different NPK fertiliser regimes

Fertiliser	Total N Applied	S1 AE_N (g g^{-1})		S2 AE_N (g g^{-1})		S3 AE_N (g g^{-1})		Main Effect AE_N (g g^{-1})	
		A-40	A-46	A-40	A-46	A-40	A-46	A-40	A-46
GF1	0.50	44.56	66.43	97.50	89.41	30.57	81.22	57.54	79.02
GF2	0.76	43.46	61.14	67.63	61.14	34.67	61.44	48.55	61.24
GF3	1.01	73.73	47.55	49.15	42.66	50.75	70.13	57.84	53.45
GF4	1.50	67.23	38.86	66.93	44.46	51.65	57.34	61.94	46.85
BF1	0.50	54.25	48.85	59.04	57.24	67.63	127.27	60.34	77.82
BF2	0.75	86.71	78.32	64.44	88.71	130.07	73.63	93.71	80.22
BF3	1.00	124.48	55.24	70.53	100.10	96.30	82.62	97.10	79.32
BF4	1.50	90.61	51.05	60.74	58.04	68.93	59.54	73.43	56.24

Note. AE_N = agronomic nitrogen use efficiency based on total dry biomass; S1 = 100:0 (sand: topsoil); S2 = 0:100 (sand: topsoil); S3 = 70:30 (sand: topsoil). GF = NPK 15-15-15 + 2S; BF = NPK 12-12-17 + TE. Numbers 1-4 indicate 0.5×, 0.75×, 1.0×, and 1.5× of the recommended fertiliser rate, respectively. AE_N was calculated as the increase in total dry biomass per unit of nitrogen applied, relative to the corresponding unfertilised control (F0). Values are expressed as g total dry biomass increase per g N applied. F0 is not shown because AE_N cannot be calculated for unfertilised control. Values for individual soil mixture ratio-fertiliser combinations are presented for descriptive purposes only

In A-40, AE_N values varied among fertiliser regimes. Based on the fertiliser main effect means, BF3 showed the highest AE_N (97.10 g total dry biomass increase per g N applied), followed by BF2 (93.71) and BF4 (73.43). Among the NPK 15-15-15 + 2S treatments, GF4 showed the highest AE_N (61.94), followed by GF3 (57.84) and GF1 (57.54). Although BF4 produced the greatest total dry biomass, its AE_N was lower than that of BF3, indicating that the additional fertiliser input resulted in a smaller biomass gain per unit of N applied. In A-46, BF2 showed the highest numerical AE_N (80.22), followed closely by BF3 (79.32), GF1 (79.02), and BF1 (77.82). By contrast, BF4 showed a lower AE_N value (56.24), while GF4 had the lowest AE_N among the fertilised treatments (46.85).

Relationships of SPAD Index with Leaf Colour, Morphological Traits

Correlation analysis showed moderate-to-strong positive correlations among the morphological traits in both A-40 and A-46 (Figure 2). In A-40 (Figure 2a), SPAD index was strongly correlated with leaf length (LL; r = 0.88), leaf width (LW; r = 0.88), number of leaves per plant (NLP; r = 0.87), plant height (PH; r = 0.87), and leaf colour (LC; r = 0.75). In A-46 (Figure 2b), the correlations among morphological traits were generally stronger than those in A-40. SPAD index was positively correlated with LL (r = 0.85), LW (r = 0.90), NLP (r = 0.91), PH (r = 0.89), and LC (r = 0.88).

Relationships of SPAD Index with Biomass Traits

Pearson correlation analysis was conducted to evaluate the relationships between SPAD index and biomass traits, including shoot fresh weight (SFW), shoot dry weight (SDW), root fresh weight (RFW), root dry weight (RDW), root volume (RV), and root length (RL) in A-40 and A-46 (Figure 3). In A-40, SPAD index was positively correlated with all biomass traits, with correlation coefficients ranging from r = 0.67 to 0.82. The strongest correlations were observed for SDW (r = 0.82) and SFW (r = 0.81), so high SPAD values generally lead to larger shoot biomass. In A-46, SPAD showed even stronger correlations with biomass traits, ranging from r = 0.74 to 0.89, with the highest correlation observed for SDW (r = 0.89) and SFW (r = 0.85).

DISCUSSION

The fertiliser regime had a significant effect on morphological and biomass-related traits for both *A. compressus* mutant variants (A-40 and A-46). The number of leaves per plant (NLP) responded strongly to fertilisation, increasing by as much as 124.6% in A-40 and 139.9% in A-46 relative to the unfertilised controls. The results indicate that proper nutrient supply can improve tillering, canopy development and overall morpho-physiological growth of turfgrass (Kussow et al., 2012; Shaddox et al., 2017).

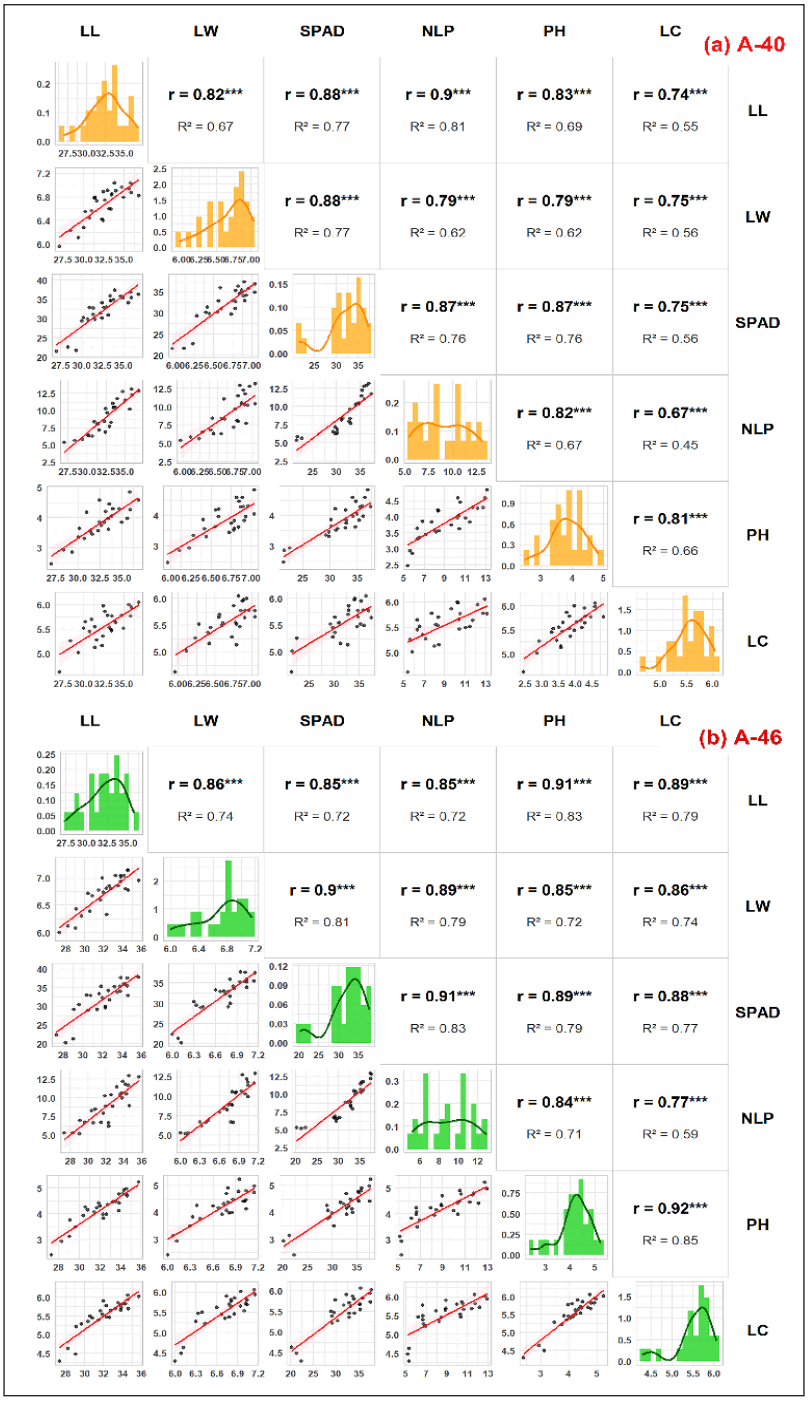

Figure 2. Relationships among SPAD index, leaf colour, and morphological traits in (a) A-40 and (b) A-46
Note. Asterisks indicate significance levels ($p < 0.05$, $p < 0.01$, $p < 0.001$). r = Pearson correlation coefficient; R^2 = coefficient of determination. LL - leaf length, LW - leaf width, SPAD - relative chlorophyll content, NLP - number of leaves per plant, PH - plant height, LC - leaf colour

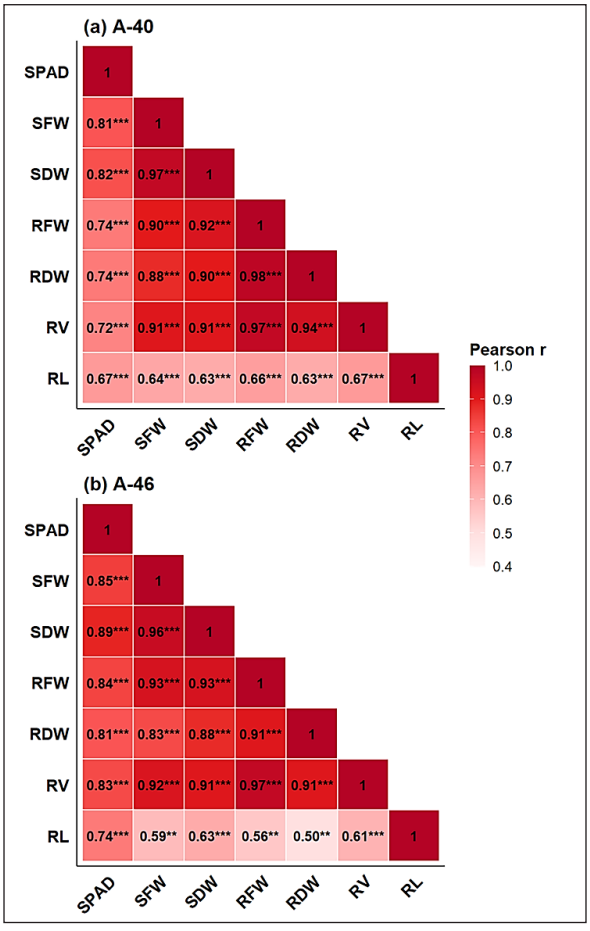

Figure 3. Relationships between SPAD index and biomass traits in (a) A-40 and (b) A-46
Note. Asterisks indicate significance levels ($p < 0.05$, $p < 0.01$, $p < 0.001$). r = Pearson correlation coefficient; R^2 = coefficient of determination. SFW - shoot fresh weight, SDW - shoot dry weight, RFW - root fresh weight, RDW - root dry weight, RV - root volume, RL - root length, SPAD - relative chlorophyll content

Both NPK fertiliser regimes improved morphological traits, but their effects varied among traits. NPK (15-15-15 + 2S), as a balanced NPK formulation, supported vegetative growth, while NPK (12-12-17 + TE) generally produced high values for SPAD index, leaf colour, and several growth traits.

In contrast, the NPK (12-12-17 + TE) fertiliser group, characterised by higher potassium and trace elements, produced greater improvements in SPAD and leaf colour, consistent with the role of potassium in chlorophyll synthesis, stomatal regulation, and stress tolerance (Johnson et al., 2022). The trace elements in NPK 12-12-17 + TE may have contributed to the greater biomass production, as micronutrients such as Fe, Mn, Zn, and Cu are involved in chlorophyll formation, enzyme activity, and photosynthesis.

Sulfur supplied by NPK 15-15-15 + 2S may support the synthesis of sulfur-containing amino acids and proteins and thereby contribute to plant metabolic activity and biomass formation. Since tissue nutrient concentrations were not measured, however, these explanations should be interpreted with caution. Compared with F0, SPAD index increased by up to 67.9% in A-40 and 76.6% in A-46 under BF4. SPAD measurements are commonly used as rapid indicators of relative chlorophyll status and leaf greenness. The availability of nitrogen is intimately associated with leaf chlorophyll since it is a component of chlorophyll and photosynthetic proteins (Fathi, 2022; Qi et al., 2025). Many studies showed that maintaining a chlorophyll content under stress is correlated with an increased tolerance to heat, drought or nutrient limitation (Poudyal et al., 2024; Pratap et al., 2025).

Although fertiliser was the main part of growth responses, soil mixture ratio also helped some traits (Chou et al., 2024; Ofori et al., 2024). S3 generally had higher growth than S1 or S2, probably due to better water retention, aeration and nutrient availability in topsoil-mixtures (see 70:30 sand: topsoil) (Brown et al., 1985; McCoy, 1998; Zhang & Han, 2019). The two mutant variants responded differently to soil mixing ratios, which indicates differences between mutants of the same species regarding their sensitivity to culture medium conditions (Huang et al., 2021). The absence of significant soil × fertiliser (S × F) interactions across all traits indicates that the relative responses to fertiliser were generally stable across soil mixture ratios. This further supports interpreting AE_N mainly based on the fertiliser main effects, while the values for S1, S2, and S3 show that the fertiliser response was generally consistent across the different soil mixture ratios. However, soil physical properties are also important for turfgrass establishment. Therefore, fertilisation should be considered together with soil substrate selection in tropical turfgrass systems.

Biomass accumulation in turfgrass was influenced by soil mixture ratio and fertiliser regime. High fertiliser rates resulted in substantial increases in shoot and root biomass. Moreover, S1 generally produced longer roots than S2 and S3, especially in A-46. A-46 had longer roots in the sandy medium. One possible reason is that the lower water and nutrient retention in this substrate encouraged greater root extension. Since root anatomy and nutrient uptake were not examined, the reason for this response remains unclear. Root elongation may have been favoured in the sandy medium, which offers little mechanical resistance to penetration but loses nutrients readily through leaching; longer roots would then allow a larger volume of substrate to be explored for nutrient uptake (Lynch, 2019). Of the fertiliser treatments, NPK 12-12-17 + TE and BF4, in particular, generally gave higher shoot and root fresh weights, along with greater root dry weight and root volume, indicating stronger stimulation of biomass accumulation. Even so, a larger plant does not by itself indicate that the fertiliser was used more efficiently. Total biomass accumulation

alone did not fully reflect fertiliser-use efficiency. In A-40, BF4 produced the highest total biomass, but AE_N was highest under BF3, showing a greater dry biomass gain per unit of nitrogen applied. In A-46, BF2 and BF3 showed the highest numerical AE_N values. These results indicate that the highest fertiliser rate did not necessarily provide the greatest biomass return per unit of nitrogen input (Springer, 2021). Although BF4 generally produced higher total dry biomass, its lower AE_N compared with BF2 or BF3 indicates that biomass gain per unit of nitrogen declined at the highest fertiliser rate. This suggests that moderate fertiliser rates may offer a better balance between turfgrass growth and nitrogen input than the highest rate (Bastidas et al., 2024). Additional nutrient input does not always lead to proportional increases in biomass. This is particularly relevant for turfgrass management, where over-fertilisation can raise costs and increase the risk of nutrient losses without providing clear benefits to growth or turf quality.

Besides soil mixture ratio and fertiliser usage, there were differences in the growth of the two variants. Growth parameters were strongly correlated between A-40 and A-46. In particular, A-46 was stronger than A-40 in leaf colour, SPAD, and biomass traits. Therefore, the relationships between SPAD and biomass traits were generally stronger in A-46 than in A-40, suggesting that SPAD may be a useful non-destructive indicator of biomass variation in A-46. Across treatments, SPAD readings closely tracked biomass, and the relationship was strongest for shoot weight: plants with greener foliage were, by and large, those that had accumulated more shoot material. Since reading takes seconds and requires no harvest, SPAD appears well suited to routine monitoring of sward growth. These results may partly explain its better potential adaptability. A clear plateau effect was observed in both fertiliser groups, beyond BF3 in the NPK (12-12-17 + TE) fertiliser group and GF2-GF3 in the NPK (15-15-15 + 2S) group, with only marginal improvements at higher levels (Supplementary Figures S1-S12). This pattern may reflect a diminishing marginal response to fertiliser input rather than a continued proportional improvement in turfgrass performance. Further fertilisation beyond the point of low marginal biomass returns may increase the risk of nutrient leaching without clear additional gains in turf functional quality (Zhu et al., 2024). Others show a similar pattern: once nutrient supply exceeds what the plant can use, each further increment of fertiliser brings progressively smaller gains in biomass (Li et al., 2023). This bears directly on input-aware fertilisation of turfgrass, where the goal is to match application to demand rather than to maximise growth. It also echoes the decline in nitrogen use efficiency documented across modern agriculture (Zhang et al., 2015). The lower AE_N at the highest fertiliser rate shows that more fertiliser does not always lead to better nutrient efficiency. Further investigation into fertiliser timing, application frequency, and soil mixture management could provide more refined turf management strategies.

CONCLUSION

This study evaluated the responses of two *A. compressus* variants, A-40 and A-46, to three soil mixture ratios and graded NPK fertiliser regimes. The results showed that fertiliser regime was the main factor affecting growth, SPAD, leaf colour, and biomass. Although BF4 produced the highest biomass, the highest agronomic nitrogen use efficiency was found under BF3 in A-40 and BF2-BF3 in A-46. SPAD index and leaf colour were positively related to morphological and biomass traits. However, this study was conducted under tray-based conditions, and soil nutrient dynamics and plant tissue nutrient concentrations were not directly measured. Future studies should validate these responses under field conditions and include soil and tissue nutrient analyses.

ACKNOWLEDGEMENT

We are grateful to Satiri Sdn. Bhd. and the UPM Industrial Research Grant (Grant No. 6300403-10201) for providing financial support to conduct this research. The authors also acknowledge the University Driven Research Program (UDRP) under the Research Framework: Technology Advancement for Economic Growth and the Research Programme: Plantation Crops - Oil Palm, Rubber, Cocoa, Kenaf (upstream and downstream), Institute of Plantation Studies, Universiti Putra Malaysia. Additional support for publication fees was provided by the GLTU Doctoral Training Research Fund (Grant No. CZ6125002), and Capacity Building Project for Science Communication on Lijiang Ecological Protection and Sustainable Landscape Utilization (Grant No. FN2600640405).

REFERENCES

Alif, A. A. A. H., & Amira, H. N. (2023). Effect of NPK green mix with different type of manure on spinach growth and yield. *IOP Conference Series: Earth and Environmental Science*, *1182*, Article 012041. https://doi.org/10.1088/1755-1315/1182/1/012041

Azuddin, N. F., Azmy, M. S. M. N., & Zakaria, L. (2023). Molecular identification of endophytic fungi in lawn grass (*Axonopus compressus*) and their pathogenic ability. *Scientific Reports*, *13*, Article 4239. https://doi.org/10.1038/s41598-023-31291-7

Bastidas, M., Vázquez, E., Villegas, D. M., Rao, I. M., Gutierrez, J. F., Vivas-Quila, N. J., Amado, M., Berdugo, C., & Arango, J. (2024). Optimizing nitrogen use efficiency of six forage grasses to reduce nitrogen loss from intensification of tropical pastures. *Agriculture, Ecosystems & Environment*, *367*, Article 108970. https://doi.org/10.1016/j.agee.2024.108970

Bhatia, A., Cowan, N. J., Drewer, J., Tomer, R., Kumar, V., Sharma, S., Paul, A., Jain, N., Kumar, S., Jha, G., Singh, R., Prasanna, R., Ramakrishnan, B., Bandyopadhyay, S. K., Kumar, D., Sutton, M. A., & Pathak, H. (2023). The impact of different fertiliser management options and cultivars on nitrogen use efficiency and yield for rice cropping in the Indo-Gangetic Plain: Two seasons of methane, nitrous oxide and ammonia emissions. *Agriculture, Ecosystems & Environment*, *355*, Article 108593. https://doi.org/10.1016/j.agee.2023.108593

Brown, K. W., Evans, G. B., & Thomas, J. C. (1985). Increased soil water retention by mixing horizons of shallow sandy soils. *Soil Science*, *139*(2), 118-121. https://doi.org/10.1097/00010694-198502000-00004

Carlson, M. G., Gaussoin, R. E., & Puntel, L. A. (2022). A review of precision management for golf course turfgrass. *Crop, Forage & Turfgrass Management*, *8*(2), Article e20183. https://doi.org/10.1002/cft2.20183

Chou, M.-Y., Pavlou, D., Rice, P. J., Spokas, K. A., Soldat, D. J., & Koch, P. L. (2024). Microbial diversity and soil health parameters associated with turfgrass landscapes. *Applied Soil Ecology*, *196*, Article 105311. https://doi.org/10.1016/j.apsoil.2024.105311

Easton, Z. M., & Petrovic, A. M. (2004). Fertiliser source effect on ground and surface water quality in drainage from turfgrass. *Journal of Environmental Quality*, *33*(2), 645-655. https://doi.org/10.2134/jeq2004.6450

Fathi, A. (2022). Role of nitrogen (N) in plant growth, photosynthesis pigments, and N use efficiency: A review. *Agrisost*, *28*, 1-8. https://doi.org/10.5281/zenodo.7143588

Głąb, T., Szewczyk, W., Gondek, K., Mierzwa-Hersztek, M., Palmowska, J., & Nęcka, K. (2020). Optimization of turfgrass fertigation rate and frequency. *Agricultural Water Management*, *234*, Article 106107. https://doi.org/10.1016/j.agwat.2020.106107

Hamarashid, N. H., Othman, M. A., & Hussain, M.-A. H. (2010). Effects of soil texture on chemical compositions, microbial populations and carbon mineralization in soil. *Egyptian Journal of Experimental Biology (Botany)*, *6*(1), 59-64.

He, L., Teng, L., Tang, X., Long, W., Wang, Z., Wu, Y., & Liao, L. (2021). Agro-morphological and metabolomics analysis of low nitrogen stress response in *Axonopus compressus*. *AoB PLANTS*, *13*(4), Article plab022. https://doi.org/10.1093/aobpla/plab022

Huang, X., Jang, S., Kim, B., Piao, Z., Redona, E., & Koh, H.-J. (2021). Evaluating genotype × environment interactions of yield traits and adaptability in rice cultivars grown under temperate, subtropical and tropical environments. *Agriculture*, *11*(6), Article 558. https://doi.org/10.3390/agriculture11060558

Islam, M. R., Haque, S., Akter, N., & Karim, M. (2014). Leaf chlorophyll dynamics in wheat based on SPAD meter reading and its relationship with grain yield. *Scientia Agriculturae*, *8*(1), 13-18. https://doi.org/10.15192/PSCP.SA.2014.4.1.1318

Johnson, R., Vishwakarma, K., Hossen, M. S., Kumar, V., Shackira, A. M., Puthur, J. T., Abdi, G., Sarraf, M., & Hasanuzzaman, M. (2022). Potassium in plants: Growth regulation, signaling, and environmental stress tolerance. *Plant Physiology and Biochemistry*, *172*, 56-69. https://doi.org/10.1016/j.plaphy.2022.01.001

Kopp, K. L., & Guillard, K. (2002). Relationship of turfgrass growth and quality to soil nitrate desorbed from anion exchange membranes. *Crop Science*, *42*(4), 1232-1240. https://doi.org/10.2135/cropsci2002.1232

Kussow, W. R., Soldat, D. J., Kreuser, W. C., & Houlihan, S. M. (2012). Evidence, regulation, and consequences of nitrogen-driven nutrient demand by turfgrass. *ISRN Agronomy*, *2012*(1), Article 359284. https://doi.org/10.5402/2012/359284

Li, B., Ma, X., Zhao, B., Wang, L., & Ata-Ul-Karim, S. T. (2023). In-season assessment of agronomic nitrogen use efficiency and its components in winter wheat using critical nitrogen dilution curve. *Frontiers in Plant Science*, *14*, Article 1128799. https://doi.org/10.3389/fpls.2023.1128799

Li, H., Zhang, Y., Sun, Y., Liu, P., Zhang, Q., Wang, X., Wang, R., & Li, J. (2023). Long-term effects of optimized fertilisation, tillage and crop rotation on soil fertility, crop yield and economic profit on the Loess Plateau. *European Journal of Agronomy*, *143*, Article 126731. https://doi.org/10.1016/j.eja.2022.126731

Lynch, J. P. (2019). Root phenotypes for improved nutrient capture: An underexploited opportunity for global agriculture. *New Phytologist*, *223*(2), 548-564. https://doi.org/10.1111/nph.15738

McCoy, E. L. (1998). Sand and organic amendment influences on soil physical properties related to turf establishment. *Agronomy Journal*, *90*(3), 411-419. https://doi.org/10.2134/agronj1998.00021962009000030016x

Ofori, B., Habteselassie, M., & Martinez-Espinoza, A. (2024). Effect of turfgrass care products on soil biological health, disease suppression, and turfgrass quality. *Applied Soil Ecology*, *201*, Article 105499. https://doi.org/10.1016/j.apsoil.2024.105499

Petrovic, A. M., Soldat, D. J., Gruttadaurio, J., & Barlow, J. (2005). Turfgrass growth and quality related to soil and tissue nutrient content. *International Turfgrass Society Research Journal*, *10*, 989-997.

Poudyal, D., Krishna Joshi, B., & Chandra Dahal, K. (2024). Insights into the responses of Akabare chili landraces to drought, heat, and their combined stress during pre-flowering and fruiting stages. *Heliyon*, *10*(16), Article e36239. https://doi.org/10.1016/j.heliyon.2024.e36239

Pratap, A., Taylor, N. L., Pal, M., Chinnusamy, V., & Siddique, K. H. M. (2025). Heat tolerance mechanisms in bread wheat: Insights from flag leaves and spike tissues. *Plant Stress*, *16*, Article 100876. https://doi.org/10.1016/j.stress.2025.100876

Qi, Z., Xu, C., Tang, R., Zhang, Q., Sun, W., Guan, C., Wang, Y., Zhang, M., Ding, J., Zhang, Y., Yang, H., Yang, Y., Liu, X., Zhang, Z., & Ling, F. (2025). Response of photosynthesis and chlorophyll fluorescence to nitrogen changes in rice with different nitrogen use efficiencies. *Plants*, *14*(10), Article 1465. https://doi.org/10.3390/plants14101465

Roberson, T. L., Badzmierowski, M. J., Stewart, R. D., Ervin, E. H., Askew, S. D., & McCall, D. S. (2021). Improving soil moisture assessment of turfgrass systems utilizing field radiometry. *Agronomy*, *11*(10), Article 1960. https://doi.org/10.3390/agronomy11101960

Shaddox, T. W., Ryan, C. D., & Tang, K. (2017). Reference ranges: A novel interpretation of turfgrass nutrient values. *Agricultural & Environmental Letters*, *2*(1), Article 160046. https://doi.org/10.2134/ael2016.12.0046

Shaddox, T. W., & Unruh, J. B. (2021). Determining nitrogen fertiliser cost using turfgrass response. *HortTechnology*, *31*(4), 470-478. https://doi.org/10.21273/HORTTECH04837-21

Shivashankar, K., Potdar, M. P., Gawdiya, S., Golshetti, A., Kanade, A. K., Balol, G., Biradar, D. P., Math, K. K., Al-Ansari, N., El-Hendawy, S., Mattar, M. A., & Salem, A. (2025). SPAD dynamics in maize crop with precision nitrogen management under rain-fed and irrigated conditions. *Scientific Reports*, *15*, Article 22842. https://doi.org/10.1038/s41598-025-05255-y

Sim, C. C., Zaharah, A. R., Tan, M. S., & Goh, K. J. (2015). Rapid determination of leaf chlorophyll concentration, photosynthetic activity and NK concentration of *Elaeis guineensis* via correlated SPAD-502 chlorophyll index. *Asian Journal of Agricultural Research*, *9*(3), 132-138. https://doi.org/10.3923/ajar.2015.132.138

Springer, R., Eudoxie, G., & Gouveia, G. (2014). Comparative evaluation of common savannah grass on a range of soils subjected to different stresses II: Root zone physical condition. *Agronomy*, *4*(1), 124-143. https://doi.org/10.3390/agronomy4010124

Springer, T. L. (2021). Effect of nitrogen fertilisation on biomass yield of sand bluestem (*Andropogon hallii* Hack.). *BioEnergy Research*, *14*, 1118-1125. https://doi.org/10.1007/s12155-020-10220-w

Wahid, M. K., Jumaidin, R., Suan, M. S. M., & Md Yusof, F. A. (2023). Characterisation of *Axonopus compressus* fibre through chemical composition, thermogravimetric behaviour, and moisture content evaluation. *Journal of Advanced Research in Fluid Mechanics and Thermal Sciences*, *110*(1), 172-181. https://doi.org/10.37934/arfmts.110.1.172181

Yuan, Z., Cao, Q., Zhang, K., Ata-Ul-Karim, S. T., Tian, Y., Zhu, Y., Cao, W., & Liu, X. (2016). Optimal leaf positions for SPAD meter measurement in rice. *Frontiers in Plant Science*, *7*, Article 719. https://doi.org/10.3389/fpls.2016.00719

Zhang, L., & Han, J. (2019). Improving water retention capacity of an aeolian sandy soil with feldspathic sandstone. *Scientific Reports*, *9*, Article 14719. https://doi.org/10.1038/s41598-019-51257-y

Zhang, X., Davidson, E. A., Mauzerall, D. L., Searchinger, T. D., Dumas, P., & Shen, Y. (2015). Managing nitrogen for sustainable development. *Nature*, *528*, 51-59. https://doi.org/10.1038/nature15743

Zhu, L., Sun, H., Liu, L., Zhang, K., Zhang, Y., Li, A., Bai, Z., Wang, G., Liu, X., Dong, H., & Li, C. (2025). Optimizing crop yields while minimizing environmental impact through deep placement of nitrogen fertiliser. *Journal of Integrative Agriculture*, *24*(1), 36-60. https://doi.org/10.1016/j.jia.2024.05.012

Pertanika J. Trop. Agric. Sci. 49 (5): 2565 - 2580 (2026)

PERTANIKA JOURNALS

TROPICAL AGRICULTURAL SCIENCE

Journal homepage: http://www.pertanika.upm.edu.my/

Classification and Prediction of Chilli Powder (*Capsicum Annuum* L.) Colour Based on Near-Infrared Spectra and Random Forest

Nafis Khuriyati[1]*, Anggoro Cahyo Sukartiko[1], Ririn Nur Alfiani[1], Tyasto Prima Ahmadi[2], and Avicenna Nur Kasih[3]

[1]Department of Agro-industrial Technology, Faculty of Agricultural Technology, Universitas Gadjah Mada, 55281 Yogyakarta, Indonesia
[2]Department of Industrial Engineering, Faculty of Engineering and Food Security, Universitas Indonesia Mandiri, 35592 Lampung, Indonesia
[3]Department of Agroindustrial Technology, Politeknik Negeri Tanah Laut, A. Yani Street, Tanah Laut, 70815 South Kalimantan, Indonesia

ABSTRACT

Colour measurements play a crucial role in the chilli industry for establishing colour standards. Limited research has been conducted on predicting colour characteristics using Near Infrared (NIR) measurements, yet none of them has been applied to chilli powder. This study aimed to classify and predict the colour intensity of chilli powder using chemometric models based on NIR spectroscopy and the random forest algorithm. This study used 84 chilli powder samples from four colour groups. NIR spectra were measured with NIRFlex N-500 at 1000 to 2500 nm. Three pretreatments were applied: Multiplicative Scatter Correction (MSC), first derivative Savitzky-Golay, and detrending. Random forest was used for classification and prediction of L*, a*, and b*. Data were split into 75% training and 25% testing, evaluated with accuracy score and root mean square error (RMSE). The machine learning method of random forest has been successfully applied for classifying and predicting the colour of chilli powder based on NIR spectroscopy. Classification of four colour groups achieved the best accuracy of 0.9524 with first derivative Savitzky-Golay, while raw spectra and MSC reached 0.7619. L* was predicted most accurately with MSC (RMSE 2.68), meanwhile a* and b* were predicted most accurately with first derivative Savitzky-Golay (RMSE 2.86 and 3.0821). The findings indicate that the most effective pretreatment varied according to colour index.

Keywords: Chilli powder, near infrared, random forest, colour, Savitzky-Golay

ARTICLE INFO

Article history:
Received: 19 August 2025
Accepted: 25 October 2026
Published: 30 October 2026

DOI: https://doi.org/10.47836/pjtas.49.5.23

E-mail addresses:
nafis.khuriyati@ugm.ac.id (Nafis Khuriyati)
cahyos@ugm.ac.id (Anggoro Cahyo Sukartiko)
ririn.nur.alfiani@mail.ugm.ac.id (Ririn Nur Alfiani)
tyasto@uimandiri.ac.id (Tyasto Prima Ahmadi)
avicennanurkasih@politala.ac.id (Avicenna Nur Kasih)
* Corresponding author

e-ISSN: 2231-8542

© Universiti Putra Malaysia Press

INTRODUCTION

Colour measurements play a crucial role in the chilli industry for establishing colour standards, whether chilli powder is used as a seasoning or as a food coating (Aşkın & Yazici, 2021). In addition to providing a distinctive spicy taste, chilli powder also provides an attractive colour to food. The colour of chilli powder can vary from green, yellow, orange, red, brown, aniline/white, and purple depending on the type and level of maturity (Swammy, 2023). The chemical content of chilli peppers, such as carotenoids, is responsible for the chilli colour. The colouration is attributed to more than 30 types of carotenoids; for example, capsanthin and capsorubin contribute to the red colour, while xanthophyll and carotene are responsible for the yellow hue (Batiha et al., 2020).

A decrease in colour values is anticipated in dried samples and powders, with reductions across all colour measurements. The colour values were assessed using L*, a*, and b* parameters. The decrease in colour values in powder form is due to the red pepper's colour darkening, likely from changes in carotenoids and the formation of browning compounds. Generally, L* values of dried pepper samples were significantly higher ($p < 0.05$) than fresh chilli (Jiménez et al., 2021). This increase is likely attributed to the varying ways in which light is reflected on wet and porous surfaces, as observed by Nowacka and Wedzik (2016). Meanwhile, the results for the a* coordinate values indicate a statistically significant decrease ($p < 0.05$) in the dried samples compared to the fresh samples before drying samples (Jiménez et al., 2021). This decline can be attributed to the oxidation and degradation of carotenoids, specifically capsanthin and capsorubin, in red pepper (Konishi et al., 2019), likely caused by the effects of heat (Liu et al., 2014).

As a result, colour plays an important role in food perception, where the brighter the red colour in food, the greater a person's arousal and appetite (Foroni et al., 2016). Existing methods for evaluating chilli colour attributes are inefficient, destructive, and often subject to inconsistency and variability. There is a need to develop fast, non-destructive, and accurate techniques. NIR spectroscopy holds promise as a foundation for such techniques, offering advantages in speed, ease of use, and minimal interference.

Over decades, NIR has been successfully applied considerably in chemical analysis of the content of chilli peppers, such as capsaicin (Jiang et al., 2018), antioxidant activity (Khuriyati et al., 2022), vitamin C and total carotene (Khuriyati et al., 2023). Those chemical contents corresponded with the colour of chilli powder. There are limited studies available on predicting colour characteristics using NIR measurements (Elmasry et al., 2012; Gabriëls et al., 2020; Wang et al., 1999). Theanjumpol et al. (2023) investigated the use of visible and near-infrared spectroscopy to predict ASTA-colour and pungency in dry red chilli powder using partial least squares (PLS) models. These studies demonstrate the potential of spectroscopic techniques for evaluating chilli quality.

NIR operates on the principle that different chemical bonds absorb or emit light at specific wavenumbers, with prominent absorption bands corresponding to hydrogen-based functional groups like C-H, C-O, O-H, and N-H (Li et al., 2019). The wavelength absorption pattern is influenced by the chemical content of the chilli, including pigments such as carotenoids and anthocyanins that determine the colour of the chilli. This was proven by Khuriyati et al. (2023) who stated that a calibration model can be developed to determine the total carotene content in chilli powder using NIR spectra. These findings suggest that NIR spectral information can also be useful for classifying chilli colour groups and predicting colour intensity. However, further investigation is needed to evaluate the use of NIR spectroscopy combined with the Random Forest algorithm for these two tasks. Accordingly, the present study evaluates both classification and colour-intensity prediction within the same analytical framework, while examining the influence of spectral pre-treatments on model performance.

Machine learning is widely used for data analysis to build the best classification and prediction models (Vidyarthi et al., 2020). Researchers commonly apply support vector machines, neural networks, and random forests for product quality evaluation (Alfiani et al., 2024; Chen et al., 2021; Younis et al., 2019). Neural networks excel at predicting non-linear data, parallel processing, and tolerance for errors, but they require large training datasets and are susceptible to overfitting (Fei et al., 2009). Support vector machines can help mitigate overfitting, although selecting optimal parameters can be challenging (Kim et al., 2019). In this context, random forests are a suitable method for measuring NIRS data because they are more robust with respect to noise as an ensemble learning method composed of decision trees (Breiman, 2001).

Therefore, this study aimed to classify and predict the level of colour in chilli powder using a combination of chemometric models based on Near Infrared (NIR) and random forest. In this research, four different levels of colour were used as samples: light green, dark green, red tinge, and red, which also indicate the level of maturity. Colour prediction in chillies has important implications for the food industry, as it can be used to optimise the quality and consistency of chilli-based products (Jiang et al., 2018). In addition, the use of NIR for chilli colour analysis can help to decrease the need for destructive and time-consuming analytical techniques (Hong & Chia, 2021). Overall, this research will contribute to the development of new and innovative methods for chilli powder colour classification with potential applications in the food industry and beyond.

MATERIAL AND METHODS

Materials and Methods

Fresh chillies were obtained from Patrowangsan Village, Candibinangun, Pakem District, Sleman Regency, Special Region of Yogyakarta, Indonesia. A total of 84 chilli powder

samples were classified into 4 colour groups of fresh chillies, using a grouping method similar to that developed by Jiang et al. (2018), including light green, dark green, red tinge, and red. The fresh chilli samples from the field were sorted, washed and dried. The drying process was carried out using a cabinet dryer at a 60°C for 10-15 hours, ground using a food processor, and sieved through a 60-mesh sieve. Then, the chilli powder was packed using a small ziplock plastic bag for further analysis.

Measurement of NIR Spectra

A 0.5 g sample was prepared in a vial tube to ensure uniformity in both surface and thickness. NIR measurements were taken across a wavelength range of 1000 to 2500 nm. The measurements were performed using the NIRFlex N-500 Fiber Optic Solids Cell (Buchi Labortechnik AG, Flawil, Switzerland). Spectra were acquired for each chilli powder sample at four different colours using near-infrared spectroscopy.

Measurement of Chilli Powder Colour

In this study, we deal with two types of colour data: qualitative and quantitative. The qualitative data originated from visual colour assessment, which categorised the colours into four groups. In contrast, the quantitative data regarding chilli powder colour were obtained through measurements using a Chroma Meter Konica Minolta CR-400 (CIELAB coordinates) in order to obtain the values of L* (lightness), a* (redness), and b* (yellowness). The calculation results were then analysed using ANOVA and further analysed using the Least Significant Difference Test (LSDT).

Spectra Analysis

The spectral data were analysed using Unscrambler X 11.0 software from Camo Analytics. Pre-treatments, including first derivative Savitzky-Golay, MSC, and detrending, were applied during data processing to enhance the detection of chemical content associated with functional groups, which serve as indicators of chilli colour characteristics, such as carotenoids or anthocyanins.

Random Forest Model

The machine learning analysis was carried out with the random forest method through Google Colab with Google Compute Engine Python 3 backend, 12.7 GB system RAM, and 107.7 GB disk. Random Forest (RF) is a machine learning model used for both regression and classification tasks. It consists of an ensemble of multiple decision tree (DT) models (Vidyarthi et al., 2020). In this instance, qualitative colour data was utilised for classification, whereas quantitative data served the purpose of prediction. Random forest was performed on the entire spectral data (input) and colour data (output), where each

factor corresponds to the potential characteristics linked to different wavelengths of the NIR data. The data were divided randomly into 75% for training and 25% for testing out of the total sample, and then the prediction results were evaluated using the accuracy score for the classification task and Root Mean Square Error (RMSE) for the regression task.

RESULTS AND DISCUSSION

Analysis of Raw Spectra

When chilli powder samples are scanned with light, the energy from the light is absorbed and reflected by the sample. The reflected light is then captured by a spectrometer and displayed on a computer. Spectra of 84 samples were recorded from 1000 nm to 2500 nm. Each spectrum displayed distinct peaks, indicating the presence of chemical bonds. The spectrum plot in Figure 1 highlights valleys (inverted peaks), which serve as signatures of specific materials in chilli powder. These valleys are observed at wavelengths of 1190-1240 nm, 1410-1490 nm, 1700-1730 nm, 1950-1960 nm, 2060-2080 nm, and 2420-2500 nm. Additionally, absorption peaks for β-carotene were identified at approximately 1235 nm, 1770 nm, 2176 nm, and 2376 nm (Chen et al., 2009). (Hagos et al., 2022) reported that the β-carotene content is associated with a wavelength of 1415 nm, which corresponds to the first overtone band of C-H stretching.

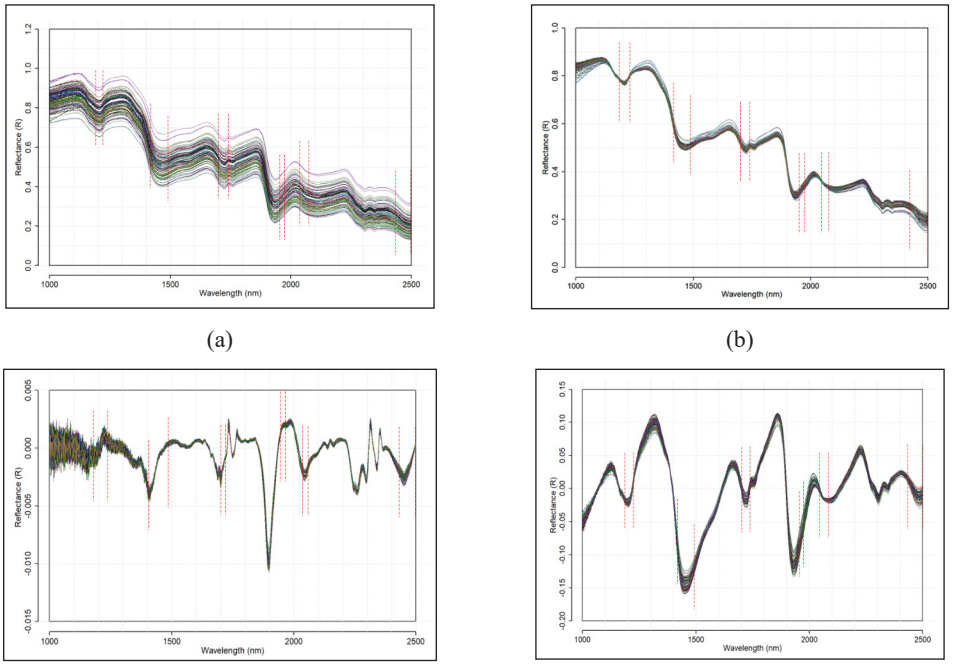

Figure 1. (a) raw spectra; (b) MSC; (c) first derivative savitzky-golay; and (d) de-trending

Pre-Treatment of Raw Spectra

Pre-treatment or preprocessing of raw NIR data serves as the initial step in model development and optimisation. This process is essential for minimising unwanted sample-to-sample variability in the measured NIR spectral data, thereby improving data quality and reliability. Spectral pre-treatment of this data is required to remove all irrelevant information such as noise, uncertainty, variability, interactions, and undetected features. Three spectral pre-treatments were applied to remove nonlinear trends in the data and reduce radio interference: MSC, first derivative Savitzky-Golay, and detrending. The differences between raw spectra and the three pre-treatment spectra are shown in Figure 1.

MSC is a widely used normalisation technique in NIR spectroscopy and other spectroscopic methods. It is designed to correct variations in both scale and offset within a set of spectra, thereby improving data consistency and accuracy (Windig et al., 2008). Multiplicative scatter correction reduced baseline variability and eliminated scatter effects. Additionally, it also reduces the number of latent variables compared to approaches that do not involve preprocessing (Khuriyati et al., 2023). The spectra of the first pre-treatment are presented in Figure 1b. The application of MSC significantly improved the spectral data, producing smoother and more uniform results compared to the raw spectra.

Additionally, the first derivative Savitzky-Golay method was employed to reduce noise while preserving the integrity of the data, effectively minimising the impact of noise on the signal (Candan & Inan, 2014). The first derivative Savitzky-Golay is performed to remove baselines that are thrown off in the spectral data and small spectral differences are amplified (Zaid et al., 2020). The first derivative Savitzky-Golay algorithm fits a polynomial to each successive segment of the curve, replacing the original values with smoother, more consistent variations (Khuriyati et al., 2023). The analysis of the first derivative revealed noticeable changes in the original data, as shown in Figure 1c, which demonstrates significant differences when compared to the raw spectra.

Detrending is a straightforward pre-treatment method used to remove baseline variations by fitting the spectrum to a polynomial of a specified degree and replacing it with the residuals of the fit. This process involves subtracting a linear or polynomial baseline fit from the original spectrum to eliminate tilted baseline variations (Roger et al., 2022).

These results demonstrate significant differences when compared to the raw spectra. Variation between valley shapes and peaks attributed to chilli powder spectra was observed. The peak and depletion spectra of the detrended spectral data showed strong and weak absorption features of chilli powder. This is likely due to the chemicals in the chilli powder. Figure 1d shows the detrended spectral results.

Colour Analysis

L*, a*, and b* values of the chilli colour group can be seen in Figure 2. The brightness value (L*) produced in the chilli colour group tends to decrease in value. The brightness value (L*) in the green group is 51.49, the dark green group is 49.07, the orange group is 48.07, and the red group is 47.24. The a* value shows that the green group has a negative value of -1.8729, the dark green, orange, and red groups have positive a* values of 2.28, 13.09, and 21.41 respectively. The a* value has an upward trend. This is in accordance with (Becker, 2016) where a positive a* value indicates a red colour tendency and a negative a* indicates a green colour. The b* value shows that all chilli colour groups have a positive b* value and have a tendency to increase in value. The b* value in the green group is 21.29, the dark green group is 22.43, the orange group is 24.65, and the red group is 25.20. Positive b* values indicate yellow colour, while negative b* values indicate blue colour (Becker, 2016). Compounds related to the colour of chilli are carotenoids and chlorophyll compounds. One of the dominant carotenoids in red chilli is β-carotene, which is an important intermediate in synthesising red xanthophyll. The concentration of these pigments usually increases when the chilli reaches maturity (Deli et al., 2001). Meanwhile, chlorophyll is known to decrease during the maturation that occurs in chilli peppers. At the beginning of chilli ripening, chlorophyll decreases significantly, while carotenoids increase because chloroplasts turn into chromoplasts which cause the appearance of red colour (Sun et al., 2018).

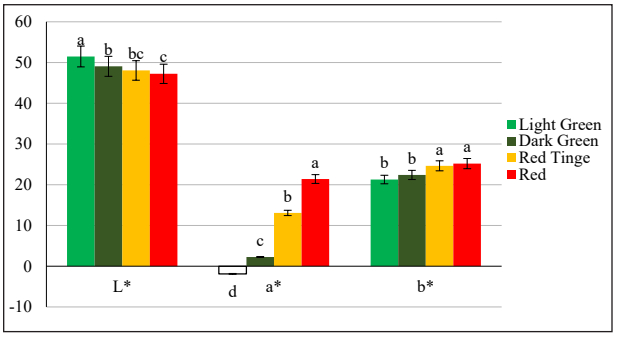

Figure 2. Colour index comparison of chilli powder

Random Forest Model

Dataset Overview

In this paper, the feature data variables (input) used are datasets of NIR spectra measurement results (raw spectra) and pre-treatment results value of raw spectra (detrending, first derivative Savitzky-Golay, and MSC). The target data variable (output) used for the Random Forest Classifier is the pre-classified colour (light green, dark green, red tinge, and red), while for the Random Forest Regressor is the colour index from the Chroma Meter measurement (L*, a*, and b* values). Furthermore, the dataset is divided into two parts, namely 75% training data and 25% testing data. In addition, data division is carried out using the same random seed to ensure consistency in data separation. The results of the dataset division are presented in Table 1.

Table 1
Data division of sample

Colour	Data Division of Samples for Each Colour		Number of Data
	Training	Testing	
Light Green	15	6	21
Dark Green	17	4	21
Red Tinge	16	6	22
Red	15	5	20
Total	63	21	84

Colour Classification Using Random Forest.

Random Forest Classifier is a machine learning algorithm used in this research and proven to be able to classify the colour of chilli powder using data on each treatment (raw spectra, de-trending, first derivative Savitzky-Golay, and MSC). The ability of each Random Forest algorithm to perform classification is interpreted in the accuracy score on evaluation using testing data. The higher accuracy score, better classification into the positive class. The evaluation results for each treatment are presented in Figure 3.

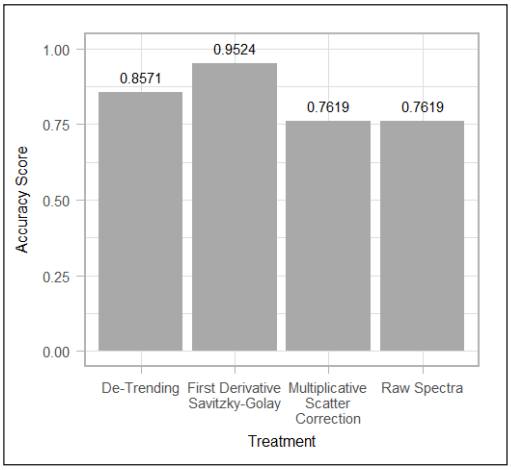

Figure 3. Accuracy scores for each treatment classification

Based on Figure 3, the accuracy score on raw spectra is 0.76, which means that the success rate of colour classification reaches 76.19%, where 16 samples are correctly identified. After applying de-trending pre-treatment on raw spectra, there was improvement in the score accuracy to 0.8571.

This indicates that the use of de-trending was able to increase the classification success to 85.71%, with the number of correctly classified samples being 18 data, although there were colour groups that experienced a decrease in the number of correct classifications. Furthermore, the use of the first derivative Savitzky-Golay pre-treatment also showed an increase in accuracy score to 0.9524, indicating that the first derivative Savitzky-Golay pre-treatment provided a classification success rate of 95.24%, with 20 properly classified samples. On the other hand, using the MSC pre-treatment did not improve the accuracy score, remaining at 0.7619, with 16 correctly classified samples. Although MSC provides a similar success rate to raw spectra, the number of correctly classified samples for each

colour group appears to be different. The details of the colour classification in each treatment are presented in Figure 4.

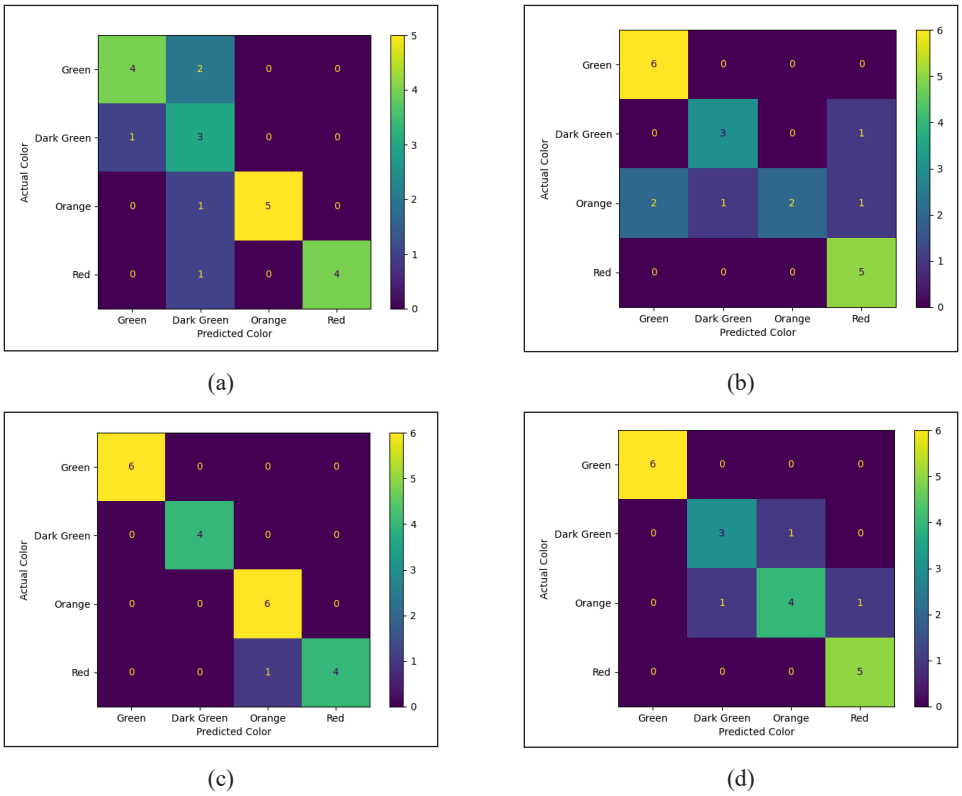

Figure 4. Confusion matrix (a) raw spectra; (b) MSC; (c) first derivative Savitzky-Golay; and (d) detrending

Colour Prediction Using Random Forest.

The need for fast and non-destructive colour measurement in the chilli industry arises because existing methods remain destructive, labour-intensive, and prone to inconsistency, while NIR spectroscopy offers a promising alternative for real-time and non-invasive colour prediction (Theanjumpol et al., 2023). Research on chilli powder colour prediction using NIR spectroscopy is still limited. The present study addresses this gap by combining spectral pre-treatments with the random forest algorithm.

Random Forest Regressor is a machine learning algorithm used in this research and proven to be suitable for predicting the L*, a*, and b* values of chilli powder colour based on the data of each treatment (raw spectra, detrending, first-derivative Savitzky-Golay, and MSC). The ability of each Random Forest algorithm to make predictions is interpreted by the RMSE value on evaluation using testing data. The smaller the RMSE value, the

better the prediction model. This is based on measuring the level of compatibility between the prediction results and the actual data. The evaluation results for each colour index are presented in Figure 5.

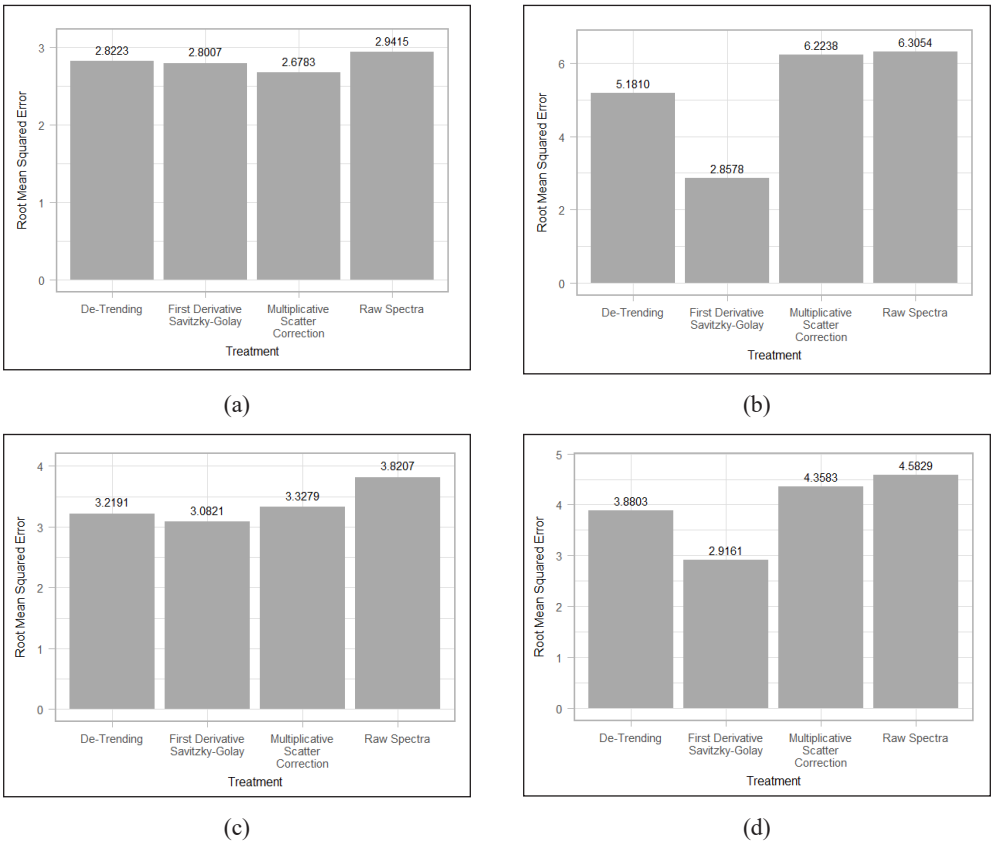

Figure 5. RMSE as an evaluation of the prediction results of the index values of (a) L*; (b) a*; (c) b*; and (d) overall

Based on Figure 5, the ability of the model to predict values of L*, a*, and b* based on NIR data with different treatments is known. Overall, the use of pre-treatment has been shown to improve the performance of the model to predict the values of the L*, a*, and b* indices, which is interpreted through the lower RMSE value. In predicting the L* index values, the best treatment was identified as Multiplicative Scatter Correction, with an RMSE of 2.68, which performed better than the first-derivative Savitzky-Golay, with an RMSE of 2.80. These results indicate that there is a better option for developing and applying a model to predict the L* index value, which is the use of the MSC pre-treatment.

First-derivative Savitzky-Golay pre-treatment achieves the best performance in predicting the a* index value, with the lowest RMSE of 2.86. The results of predicting

the a* index value using the first derivative Savitzky-Golay pre-treatment show better performance than using other treatments, especially when compared to raw spectra, which has the highest RMSE of 6.3054. In addition, first derivative Savitzky-Golay also provides the best results in predicting the b* index value with an RMSE of 3.0821, better than raw spectra, which has an RMSE of 3.8207. A comparison of the predicted and actual L*, a*, and b* index values for each treatment is presented in Figure 6.

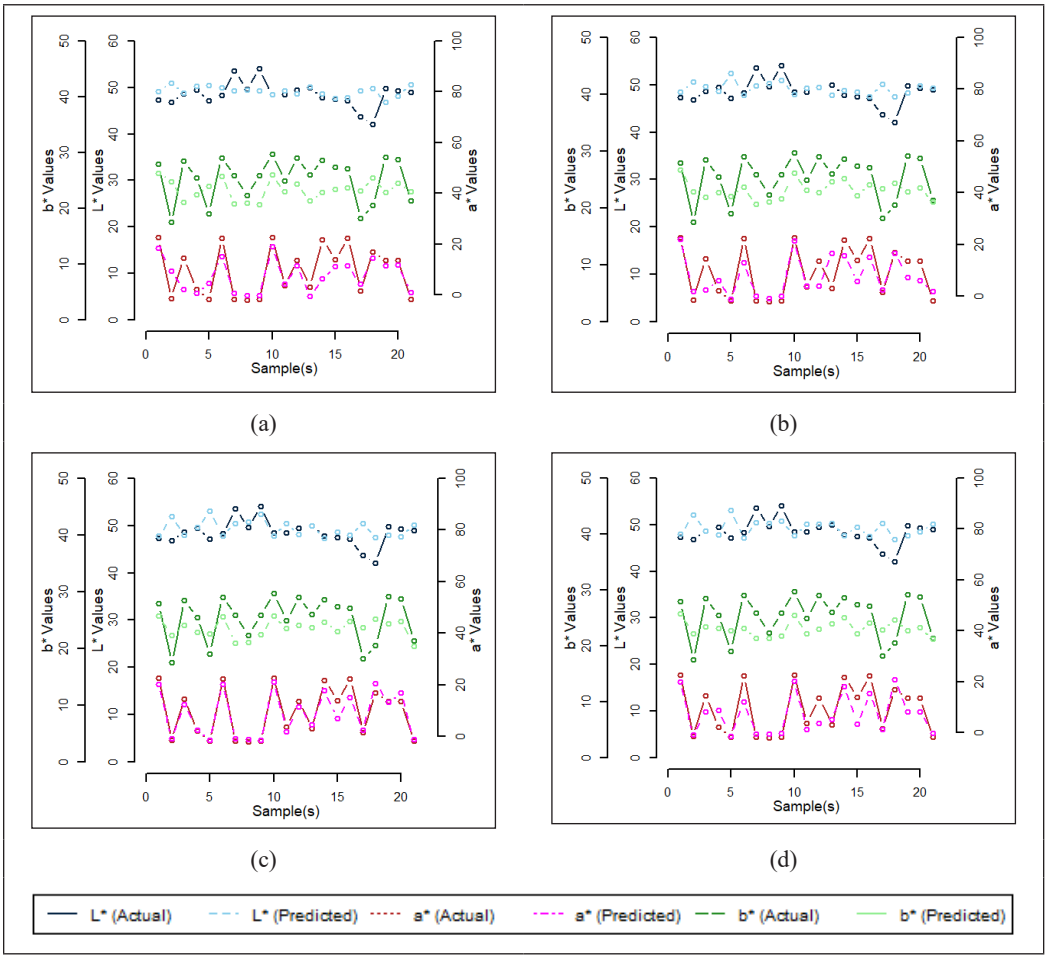

Figure 6. Colour prediction from (a) raw spectra; (b) MSC; (c) first derivative Savitzky-Golay; and (d) detrending

The difference in the best pre-treatment between L* and the other two indices can be explained by the nature of each parameter. The L* value reflects brightness, which is strongly influenced by light scattering on the powder surface, so the correction of multiplicative scatter effects by MSC is more helpful (Zhao et al., 2013).

In contrast, the a* and b* values are closely related to pigment absorption by carotenoids and chlorophyll, so baseline removal and amplification of subtle differences by first-derivative Savitzky-Golay are more effective (Zimmermann & Kohler, 2013). Accordingly, the best pre-treatment for classifying and predicting chilli powder colour depends on the parameter being estimated: first-derivative Savitzky-Golay for classification, a*and b*, and MSC for L*.

First-derivative Savitzky-Golay pre-treatment has been proven to be the best pre-treatment for colour classification and prediction of L*, a*, and b* index values in chilli powder using a Random Forest Classifier and Regressor. This selection is based on the pre-treatment's ability to classify the colour of chilli powder with a 95% success rate. In addition, overall, the first-derivative Savitzky-Golay pre-treatment predicted L*, a*, and b* index values very well, showing improved performance compared to raw spectra. This is interpreted through lower RMSE values compared to raw spectra. According to (Zimmermann & Kohler, 2013) Savitzky-Golay is able to attenuate high-frequency signals, such as noise, while at the same time tending to preserve important features of the chemical analyte signal. Therefore, first-derivative Savitzky-Golay is the most widely used smoothing algorithm in spectroscopy. According to previous research, Savitzky-Golay has also been recognised as the most effective pre-treatment method for predicting antioxidant activity, water content, total carotene, and vitamin C (Khuriyati et al., 2022, 2023).

Previous studies that applied support vector machines and neural networks for product quality assessment reported good performance, but both have limitations with NIR spectral data. Neural networks require large training datasets and are susceptible to overfitting, while support vector machines require careful parameter selection (Crone & Kourentzes, 2010; Ghasemi & Tavakoli, 2013). Random forest, as an ensemble method, is more robust to noise and does not demand complex parameter tuning, making it more suitable for NIR spectral data with a limited number of samples (Ghasemi & Tavakoli, 2013; Manneh et al., 2024).

CONCLUSION

The random forest machine learning method has been successfully applied to classify and predict the colour of chilli powder using near-infrared spectroscopy. Classification of four colour groups achieved the best accuracy of 0.9524 with the first derivative Savitzky-Golay, while raw spectra and MSC reached 0.7619. L* was predicted most accurately with MSC (RMSE 2.68), meanwhile a* and b* were predicted most accurately with first derivative Savitzky-Golay (RMSE 2.86 and 3.0821). The findings could hold significant value for industries that utilise chilli powder as an ingredient, as they can more accurately and reliably classify and predict colour using near-infrared spectroscopy and random forests. However, several limitations remain, including the relatively small sample size and the inclusion of

samples from only one region. Future research should therefore involve a larger sample size and include samples from multiple regions to improve the generalisability of the findings.

ACKNOWLEDGEMENT

The authors are grateful to the Department of Agro-industrial Technology, Faculty of Agricultural Technology, Universitas Gadjah Mada, for providing laboratory facilities to support this research.

CONFLICT OF INTEREST

The authors declare that there is no conflict of interest associated with the publication of this article. The authors confirm that the data and manuscript are free from plagiarism.

REFERENCES

Alfiani, R. N., Ushada, M., Ainuri, M., & Falah, M. A. F. (2024). Modeling consumer overall acceptance for traditional spice-based ready-to-drink using artificial neural network and Kansei engineering. *International Journal on Advanced Science, Engineering and Information Technology*, *14*(4), 1178-1184. https://doi.org/10.18517/ijaseit.14.4.19314

Aşkın, B., & Yazici, S. O. (2021). Bioactive compounds, antioxidant potential and colour properties of dried red pepper (*Capsicum annuum* L.). *International Journal of Innovative Approaches in Agricultural Research*, *5*(2), 158-171. https://doi.org/10.29329/ijiaar.2021.358.1

Batiha, G. E. -S., Alqahtani, A., Ojo, O. A., Shaheen, H. M., Wasef, L., Elzeiny, M., Ismail, M., Shalaby, M., Murata, T., Zaragoza-Bastida, A., Rivero-Perez, N., Beshbishy, A. M., Kasozi, K. I., Jeandet, P., & Hetta, H. F. (2020). Biological properties, bioactive constituents, and pharmacokinetics of some *Capsicum* spp. And capsaicinoids. *International Journal of Molecular Sciences*, *21*(15), Article 5179. https://doi.org/10.3390/ijms21155179

Becker, D. (2016). Colour measurement. In *Colour Trends and Selection for Product Design* (pp. 179-182). William Andrew Publishing. https://doi.org/10.1016/B978-0-323-39395-9.00037-2

Breiman, L. (2001). Random forests. *Machine Learning*, *45*, 5-32. https://doi.org/10.1007/978-3-030-62008-0_35

Candan, Ç., & Inan, H. (2014). A unified framework for derivation and implementation of Savitzky-Golay filters. *Signal Processing*, *104*, 203-211. https://doi.org/10.1016/j.sigpro.2014.04.016

Chen, G., Zhang, X., Wu, Z., Su, J., & Cai, G. (2021). An efficient tea quality classification algorithm based on near infrared spectroscopy and random forest. *Journal of Food Process Engineering*, *44*(1), Article e13604. https://doi.org/10.1111/jfpe.13604

Chen, X., Wu, J., Zhou, S., Yang, Y., Ni, X., Yang, J., Zhu, Z., & Shi, C. (2009). Application of near-infrared reflectance spectroscopy to evaluate the lutein and β-carotene in Chinese kale. *Journal of Food Composition and Analysis*, *22*(2), 148-153. https://doi.org/10.1016/j.jfca.2008.10.007

Crone, S. F., & Kourentzes, N. (2010). Naive support vector regression and multilayer perceptron benchmarks for the 2010 Neural Network Grand Competition (NNGC) on time series prediction. In *Proceedings of the International Joint Conference on Neural Networks*. https://doi.org/10.1109/IJCNN.2010.5596636

Deli, J., Molnár, P., Matus, Z., & Tóth, G. (2001). Carotenoid composition in the fruits of red paprika (*Capsicum annuum* var. *lycopersiciforme rubrum*) during ripening; Biosynthesis of carotenoids in red paprika. *Journal of Agricultural and Food Chemistry*, *49*(3), 1517-1523. https://doi.org/10.1021/jf000958d

Elmasry, G., Sun, D. -W., & Allen, P. (2012). Near-infrared hyperspectral imaging for predicting colour, pH and tenderness of fresh beef. *Journal of Food Engineering*, *110*(1), 127-140. https://doi.org/10.1016/j.jfoodeng.2011.11.028

Fei, S. -W., Miao, Y. -B., & Liu, C. -L. (2009). Chinese grain production forecasting method based on particle swarm optimisation-based support vector machine. *Recent Patents on Engineering*, *3*(1), 8-12. https://doi.org/10.2174/187221209787259947

Foroni, F., Pergola, G., & Rumiati, R. I. (2016). Food colour is in the eye of the beholder: The role of human trichromatic vision in food evaluation. *Scientific Reports*, *6*, Article 37034. https://doi.org/10.1038/srep37034

Gabriëls, S. H. E. J., Mishra, P., Mensink, M. G. J., Spoelstra, P., & Woltering, E. J. (2020). Non-destructive measurement of internal browning in mangoes using visible and near-infrared spectroscopy supported by artificial neural network analysis. *Postharvest Biology and Technology*, *166*, Article 111206. https://doi.org/10.1016/j.postharvbio.2020.111206

Ghasemi, J. B., & Tavakoli, H. (2013). Application of random forest regression to spectral multivariate calibration. *Analytical Methods*, *5*(7), 1863-1871. https://doi.org/10.1039/c3ay26338j

Hagos, M., Redi-Abshiro, M., Chandravanshi, B. S., & Yaya, E. E. (2022). Development of analytical methods for determination of β-carotene in pumpkin (*Cucurbita maxima*) flesh, peel, and seed powder samples. *International Journal of Analytical Chemistry*, *2022*(1), Article 9363692. https://doi.org/10.1155/2022/9363692

Hong, F. W., & Chia, K. S. (2021). A review on recent near infrared spectroscopic measurement setups and their challenges. *Measurement*, *171*, Article 108732. https://doi.org/10.1016/j.measurement.2020.108732

Jiang, J., Cen, H., Zhang, C., Lyu, X., Weng, H., Xu, H., & He, Y. (2018). Nondestructive quality assessment of chili peppers using near-infrared hyperspectral imaging combined with multivariate analysis. *Postharvest Biology and Technology*, *146*, 147-154. https://doi.org/10.1016/j.postharvbio.2018.09.003

Jiménez, D., Vardanega, R., Salinas, F., Espinosa-Álvarez, C., Bugueño-Muñoz, W., Palma, J., Meireles, M. A. A., Ruíz-Domínguez, M. C., & Cerezal-Mezquita, P. (2021). Effect of drying methods on biorefinery process to obtain capsanthin and phenolic compounds from *Capsicum annuum* L. *Journal of Supercritical Fluids*, *174*, Article 105241. https://doi.org/10.1016/j.supflu.2021.105241

Khuriyati, N., Sukartiko, A. C., & Alfiani, R. N. (2022). Non-destructive measurement of antioxidant activity and water content in chili powder (*Capsicum annuum* L.) using near-infrared spectroscopy. *International Food Research Journal*, *29*(2), 320-327. https://doi.org/10.47836/ifrj.29.2.10

Khuriyati, N., Sukartiko, A. C., Falah, M. A. F., & Alfiani, R. N. (2023). Determination of total carotene and vitamin C in chili powder (*Capsicum annuum* L.) non-destructively using near-infrared spectroscopy.

International Journal on Advanced Science, Engineering and Information Technology, *13*(1), 69-76. https://doi.org/10.18517/ijaseit.13.1.16800

Kim, N., Ha, K. -J., Park, N. -W., Cho, J., Hong, S., & Lee, Y. -W. (2019). A comparison between major artificial intelligence models for crop yield prediction: Case study of the midwestern United States, 2006-2015. *ISPRS International Journal of Geo-Information*, *8*(5), Article 240. https://doi.org/10.3390/ijgi8050240

Konishi, A., Furutani, N., Minamiyama, Y., & Ohyama, A. (2019). Detection of quantitative trait loci for capsanthin content in pepper (*Capsicum annuum* L.) at different fruit ripening stages. *Breeding Science*, *69*(1), 30-39. https://doi.org/10.1270/jsbbs.18070

Li, C., Guo, H., Zong, B., He, P., Fan, F., & Gong, S. (2019). Rapid and non-destructive discrimination of special-grade flat green tea using near-infrared spectroscopy. *Spectrochimica Acta Part A: Molecular and Biomolecular Spectroscopy*, *206*, 254-262. https://doi.org/10.1016/j.saa.2018.07.085

Liu, L., Wang, Y., Zhao, D., An, K., Ding, S., & Wang, Z. (2014). of carbonic maceration pre-treatment on drying kinetics of chili (*Capsicum annuum* L.) flesh and quality of dried product. *Food and Bioprocess Technology*, *7*(9), 2516-2527. https://doi.org/10.1007/s11947-014-1253-6

Manneh, M., Ansah, P., Tetarave, S. K., Mishra, M. R., & Kalaimannan, E. (2024). A comparative analysis of random forest and support vector machine techniques on the UNSW-NB15 dataset. In K. Daimi & A. Al Sadoon (Eds.), *Proceedings of the Third International Conference on Innovations in Computing Research (ICR'24)*, (Vol. 1058, pp. 194-203). Springer. https://doi.org/10.1007/978-3-031-65522-7_18

Nowacka, M., & Wedzik, M. (2016). Effect of ultrasound treatment on microstructure, colour and carotenoid content in fresh and dried carrot tissue. *Applied Acoustics*, *103*(Part B), 163-171. https://doi.org/10.1016/j.apacoust.2015.06.011

Roger, J. -M., Mallet, A., & Marini, F. (2022). Preprocessing NIR Spectra for Aquaphotomics. *Molecules*, *27*(20), Article 6795. https://doi.org/10.3390/molecules27206795

Sun, T., Yuan, H., Cao, H., Yazdani, M., Tadmor, Y., & Li, L. (2018). Carotenoid metabolism in plants: The role of plastids. *Molecular Plant*, *11*(1), 58-74. https://doi.org/10.1016/j.molp.2017.09.010

Swammy, K. R. M. (2023). Origin, distribution, taxonomy, botanical description, genetic diversity and breeding of capsicum (*Capsicum annuum* L.). *International Journal of Development Research*, *13*(3), 61956-61977. https://www.journalijdr.com/origin-distribution-taxonomy-botanical-description-genetic-diversity-and-breeding-capsicum-capsicum

Theanjumpol, P., Kaur, A., Muenmanee, N., Chanbang, Y., & Maniwara, P. (2023). Prediction of quality traits in dry pepper powder using visible and near-infrared spectroscopy. *International Food Research Journal*, *30*(1), 193-204. https://doi.org/10.47836/ifrj.30.1.16

Vidyarthi, S. K., Tiwari, R., Singh, S. K., & Xiao, H. -W. (2020). Prediction of size and mass of pistachio kernels using random forest machine learning. *Journal of Food Process Engineering*, *43*(9), Article e13473. https://doi.org/10.1111/jfpe.13473

Wang, D., Dowell, F. E., & Lacey, R. E. (1999). Single wheat kernel colour classification using neural networks. *Transactions of the American Society of Agricultural Engineers*, *42*(1), 233-240. https://doi.org/10.13031/2013.13200

Windig, W., Shaver, J., & Bro, R. (2008). Loopy MSC: A simple way to improve multiplicative scatter correction. *Applied Spectroscopy*, *62*(10), 1153-1159. https://doi.org/10.1366/000370208786049097

Younis, K., Ahmad, S., Osama, K., & Malik, M. A. (2019). Optimization of de-bittering process of mosambi (*Citrus limetta*) peel: Artificial neural network, Gaussian process regression and support vector machine modeling approach. *Journal of Food Process Engineering*, *42*(6), Article e13185. https://doi.org/10.1111/jfpe.13185

Zaid, A., Abu-Khalaf, N., Mudalal, S., & Petracci, M. (2020). Differentiation between normal and white striped turkey breasts by visible/near infrared spectroscopy and multivariate data analysis. *Food Science of Animal Resources*, *40*(1), 96-105. https://doi.org/10.5851/kosfa.2019.e88

Zhao, J., He, J. M., Chen, X., Zhu, X. Q., Wu, J. J., & He, G. T. (2013). A preprocessing algorithm of corn infrared spectrum based on MSC and DOSC. *Advanced Materials Research*, *734-737*, 2893-2897. https://doi.org/10.4028/www.scientific.net/AMR.734-737.2893

Zimmermann, B., & Kohler, A. (2013). Optimizing Savitzky-Golay parameters for improving spectral resolution and quantification in infrared spectroscopy. *Applied Spectroscopy*, *67*(8), 892-902. https://doi.org/10.1366/12-06723

Pertanika J. Trop. Agric. Sci. 49 (5): 2581 - 2601 (2026)

PERTANIKA JOURNALS

TROPICAL AGRICULTURAL SCIENCE

Journal homepage: http://www.pertanika.upm.edu.my/

Microbiological Quality, Antibiotic Susceptibility and Stability of Human Breast Milk Microbiota Stored at Refrigerated Temperature

Nur Hanis Salim[1], Zulfa Zakuan[1], Rashidah Sukor[1,2]*, Aliah Zannierah Mohsin[1], Yaya Rukayadi[1], Nurul Hawa Ahmad[1,2], Yu Suet Li[2], Siti Nabilah Karim[2], and Anis Shobirin Meor Hussin[1]

[1]Faculty of Food Science and Technology, Universiti Putra Malaysia, 43400 UPM Serdang, Selangor, Malaysia
[2]Laboratory of Food Safety and Food Integrity, Institute of Tropical Agriculture and Food Security, Universiti Putra Malaysia, 43400 UPM Serdang, Selangor, Malaysia

ABSTRACT

Microbiota in human breast milk is important for developing and strengthening infants' immune systems. This study aimed to identify microbial isolates, determine their antibiotic susceptibilities, and assess the microbiological quality of human breast milk during refrigerated storage. Participants (n = 19) were healthy, regularly breastfeeding mothers from Universiti Putra Malaysia with infants aged 0-24 months. Samples were manually expressed, diluted, and streaked on selective media for bacterial isolation. Isolates were identified using Gram staining and biochemical tests, then profiled for antibiotic susceptibility using the disc diffusion method. Microbiological quality was evaluated using total plate count (TPC), total Coliform count (TCC), and total *Staphylococcus* count (TSC). Eight bacterial isolates were presumptively characterised and assigned to putative genera: *Staphylococcus, Escherichia coli, Bacillus, Lactobacillus, Enterobacter, Citrobacter, Streptococcus,* and *Klebsiella*. Inhibition-zone measurements were interpreted descriptively because compliance with applicable Clinical and Laboratory Standards Institute (CLSI) testing and interpretive requirements could not be verified. During refrigerated storage, 15 of 19 samples (78.9%) consistently had TPC values below 5 $\log_{10}$ CFU/mL. TSC values also remained below 5 $\log_{10}$ CFU/mL in samples reported to meet this criterion. However, 12 samples (63.2%) had TCC values above the reference limit applied in this study. Bacterial counts generally declined during storage, although several samples had elevated coliform counts. These findings describe changes in breast

ARTICLE INFO

Article history:
Received: 22 October 2025
Accepted: 20 October 2026
Published: 30 October 2026

DOI: https://doi.org/10.47836/pjtas.49.5.24

E-mail addresses:
nurhanissalim@yahoo.com (Nur Hanis Salim)
zulfazakuan@gmail.com (Zulfa Zakuan)
rashidah@upm.edu.my (Rashidah Sukor)
aliah_mohsin@upm.edu.my (Aliah Zannierah Mohsin)
yr32@yahoo.com (Yaya Rukayadi)
nurulhawa@upm.edu.my (Nurul Hawa Ahmad)
yusuetli2001@gmail.com (Yu Suet Li)
sitinabilah2003@gmail.com (Siti Nabilah Karim)
shobirin@upm.my (Anis Shobirin Meor Hussin)
* Corresponding author

© Universiti Putra Malaysia Press

milk microbiological quality during refrigerated storage but do not establish that storage at 4 °C for seven days is microbiologically safe. They also highlight the importance of hygienic practices during milk collection, handling, and storage.

Keywords: Antibiotic susceptibility, commensal bacteria, human breast milk, refrigerated temperature, stability

INTRODUCTION

Human breast milk is considered the optimal nutrition for neonates. It is naturally sterile and responsible for the development of neonatal gut microflora, especially for the preterm infant (Xiang et al., 2023). Exclusive breastfeeding for six months for infants, and continued breastfeeding for ≧ 24 months with nutrient-dense foods for young children, has been recommended by the World Health Organization for breastfeeding mothers. Some studies have found that breast milk can protect infants against infectious diseases, such as asthma and other atopic disorders (Capra et al., 2025). Furthermore, breastfeeding has been associated with reduced childhood obesity, potentially through modulation of obesity-related genes (Danaie et al., 2024). Additionally, the synergistic effects of components in colostrum and milk such as immunocompetent cells, immunoglobulins, fatty acids, polyamines, oligosaccharides, lactoferrin, lysozyme, other glycoproteins, and antimicrobial peptides may contribute to the protective properties of breast milk (Fernández et al., 2013). Colostrum and secretory IgA in breast milk are the main providers of commensal, mutualistic, and probiotic bacteria to the infant's gut, besides conferring immunoprotection by inhibiting pathogens from adhering to or penetrating the gastrointestinal (GI) tract (Mollova et al., 2023). During breastfeeding, bacterial genera such as Lactobacillus, *Staphylococcus*, Enterococcus, and Bifidobacterium were transferred from mother to infant (Murphy et al., 2017). Furthermore, breastfeeding has been reported to benefit not only the infant's well-being but also the mother's health. Health complications such as postpartum bleeding, Type II diabetes, and breast and ovarian cancers could be prevented through breastfeeding practices (Masi & Stewart, 2024).

About 5 to 33% of lactating mothers commonly experience mastitis, or inflammation of the breast tissue. The combination of poor breast drainage, low maternal resistance, and the presence of a colonising organism makes breastfeeding mothers vulnerable to bacterial infection. Infectious mastitis is most commonly caused by bacterial strains such as *Staphylococcus aureus, Klebsiella pneumoniae, Streptococcus dysgalactiae,* and *E. coli* (Gondkar et al., 2024). Antibiotic consumption by breastfeeding mothers is one of the measures to manage mastitis. However, antibiotic resistance in bacteria is a major concern, and it is one of the food safety challenges related to public health. Bacterial species such as *Staphylococcus aureus, Acinetobacter baumannii, Pseudomonas aeruginosa, Enterobacter*

spp*., and Klebsiella pneumonia* have been frequently reported to exhibit increasing antimicrobial resistance, leading to serious infectious diseases (Mancuso et al., 2021). Moreover, current works have indicated that gut commensal bacteria can act as reservoirs for antibiotic resistance genes and may contribute to the spread of antibiotic resistance to pathogens (Despotovic et al., 2023; Lamberte & van Schaik, 2022)

According to the Australian National Health and Medical Research Council guideline (2012), the appropriate storage of human breast milk is 6-8 h at room temperature (26 °C and lower), and no more than 72 h for storage in a refrigerator (5 °C or lower). Centers for Disease Control and Prevention (2024) recommended storing freshly expressed human breast milk at room temperature (up to 26 °C) for a maximum of 4 h, in the refrigerator (at 4 °C) for up to 4 days, and in the freezer (at −18 °C or lower) for 6 to 12 months. Grazziotin et al. (2016) reported that 12 h of storage at 4-8 °C or at -20 °C for 2 weeks preserved the nutritional value and energy content of breast milk samples. Breast milk is normally stored at frozen temperature after expression. However, some mothers store the milk briefly at refrigerated temperatures to avoid freeze-thaw cycles. Hence, the microbial stability of the breast milk stored at refrigerated temperatures is mostly unknown. Therefore, this study was carried out to determine the microbiological quality, bacterial antibiotic susceptibility, and stability of human breast milk at refrigerated storage.

MATERIALS AND METHODS

Materials

MacConkey Agar (MCA), Polymyxin Mannitol Egg Yolk Phenol Red (PMYPA) Agar, Plate Count Agar (PCA), Chromocult Coliform Agar (CA), Mannitol Salt Agar (MSA), Simmon's Citrate Agar (SCA), amoxicillin, ciprofloxacin, gentamicin, penicillin, chloramphenicol, ampicillin and streptomycin were purchased from Oxoid (Hampshire, UK). Motility Agar (MA), Tryptone Broth (TB), Christensen's Urea Agar (CUA), lactose, sucrose, glucose and filter paper were purchased from Fisher (Loughborough, UK). Nutrient Agar (NA) and Nutrient Broth (NB) were purchased from Merck (Darmstadt, Germany).

Sample Collection

All participants were briefed on the study protocol (Ethic Approval No. FSTM/EXP15/P144) prior to obtaining their written consent. Healthy lactating mothers (n = 19; 24 to 36 years old) who regularly breastfed their infants aged 0 to 24 months were among staff and students of Universiti Putra Malaysia, Serdang, Selangor. Manually expressed breast milk (30- 50 mL) via hand or breast pump was collected in a sterile 120-mL polypropylene container (labelled and individually packed). Samples were immediately placed in an icebox, transported to the laboratory and stored at 4 °C. The duration of sample collection,

from breast milk expression to refrigerated storage in the laboratory, was within 4 h. Breast milk samples were coded alphabetically. Microbiological analyses were conducted within three days after sample collection.

Isolation and Identification of Bacteria

Breast milk samples were inoculated onto selective media, including MacConkey Agar (MCA), Polymyxin Mannitol Egg Yolk Phenol Red (PMYPA) Agar, Mannitol Salt Agar (MSA), and Chromocult Coliform Agar (CA), and incubated at 37 °C for 24 h for bacterial isolation using conventional culture-based methods. Briefly, 1 mL of breast milk from each coded sample was aliquoted into an Eppendorf tube and serially diluted. A volume of 0.1 mL from the appropriate dilutions was spread onto Plate Count Agar (PCA), Chromocult Coliform Agar (CA), and Mannitol Salt Agar (MSA) for the enumeration of total plate count (TPC), total coliform count (TCC), and total *Staphylococcus* count (TSC), respectively. Representative colonies were subcultured onto Nutrient Agar (NA) and incubated at 37 °C for 24 h. The isolates were then presumptively characterised using conventional biochemical tests, following the procedures described by AOAC International (2012) and Omemu et al. (2018), where applicable. The identification approach was also considered in relation to the relevant UK Standards for Microbiology Investigations (Public Health England, 2020). Because molecular or other confirmatory identification was not performed, the bacterial identities were considered presumptive. Following isolation, the bacterial isolates were presumptively characterised using colony morphology, Gram staining, and biochemical tests, including motility, indole, catalase, oxidase, urease, citrate utilisation, and sugar fermentation. The procedures were based on the laboratory methods described by Omemu et al. (2018) and, where applicable, on the relevant microbiological identification guidance. The resulting characteristics were used to assign the isolates to putative bacterial genera.

Gram Staining

Gram staining and biochemical tests, including motility, indole production, catalase, oxidase, urease, citrate utilisation, and sugar fermentation, were performed using conventional microbiological procedures. The resulting reactions were interpreted together with colony morphology and Gram-staining characteristics to support the presumptive characterisation of the bacterial isolates (AOAC International, 2012; Omemu et al., 2018). With a sterile loop, a bacterial colony from NA was smeared onto a glass slide and gently passed through the flame (heat fixation). Next, crystal violet was used to flood the smear, followed by iodine. Decolourisation was done by dropping 95% ethyl alcohol onto the smear until no dye ran. The smear was then flooded with safranin for 45 s to counterstain. Then, the smear was tissue-blotted, allowed to air-dry, and examined under the light microscope (up to 1,000× magnification). Gram-positive and Gram-negative bacteria

produced violet and pink colour, respectively. All reagents were added to the smear for 1 min and cleared with water rinsing after each step.

Biochemical Characterisation of Bacterial Isolates

Bacterial isolates obtained from 18- 24 h cultures were subjected to conventional biochemical tests, including motility, indole, catalase, oxidase, urease, citrate utilisation, and sugar fermentation tests. For these tests, bacterial growth was transferred from the culture using a sterile inoculating loop, following the respective test procedures. The inoculum was not standardised to a specified cell concentration or McFarland turbidity standard. Therefore, the amount of bacterial growth transferred was not quantitatively standardised, potentially limiting the reproducibility of the inoculation procedure. The biochemical test results were used for the presumptive characterisation of the bacterial isolates.

Motility Test

A heavy inoculum from 18 to 24 h bacterial culture was stabbed into the MA tubes. The tubes were then incubated for 24 h at 37 °C. Bacteria that grew away from the stabbed line were considered motile, and bacteria that grew along the stabbed line were considered non-motile (Aditi et al., 2017).

Indole Test

A heavy inoculum from 18 to 24 h bacterial culture was inoculated into TB and incubated at 37 °C for 18 to 24 h. Kovác's reagent (five drops) was added directly down the inner wall of the tubes to test for indole production. A positive indole test was indicated by the formation of a bright red colour at the interface of the reagent within seconds after adding the reagent. The reagent layer which remained yellow or slightly cloudy indicated negative results for the indole test (Darkoh et al., 2015).

Catalase Test

The slide method was used to perform the catalase test (Fortin et al., 2003). A heavy inoculum from an 18- to 24-h bacterial culture was smeared onto the glass slide using a sterile inoculating loop. A positive catalase test was indicated by bubble formation after addition of 3% hydrogen peroxide (H_2O_2).

Oxidase Test

The filter paper test method was used for the oxidase test (Kumar et al., 2016). Basically, 1% of freshly prepared Kovác's reagent was used to soak a small piece of filter paper and

allowed to dry. A heavy inoculum from an 18 to 24 h bacterial culture was rubbed onto the treated filter paper using a sterile cotton swab. A colour change to dark purple after 5 to 10 s indicated an oxidase-positive result.

Urease Test

The CUA slants were prepared in the Universal tubes. A heavy inoculum from an 18 to 24 h bacterial culture was streaked over the CUA slant surface and incubated with a loosened cap at 37 °C for 18 to 24 h, and the colour changes were observed. Bright pink and yellowish colour indicated the positive and negative results of the urease test, respectively (Wan et al., 2024).

Citrate Test

A heavy inoculum from 18 to 24 h bacterial culture was streaked over the SCA slant surface and incubated at 37 °C for 24 to 48 h. Citrate-positive showed visible bacterial growth on the surface and a colour change from green to intense Prussian blue (Gebremichael et al., 2024).

Sugar Fermentation Test

Three types of sugar were used for the sugar fermentation test, namely glucose, sucrose and lactose (Verma et al., 2022). A heavy inoculum from an 18 to 24 h bacterial culture was inoculated into the test tubes containing the three different sugars with a Durham tube. The test tubes were incubated at 37 °C for 24 to 48 h, and the medium was observed for colour change. Red indicated acid production, yellow or colourless indicated no fermentation and gas production was indicated by the production of a bubble in the Durham tube.

Antibiotic Inhibition Zone Assessment

The inhibition zone measurements of the bacterial isolates against seven antibiotics were assessed using the disc diffusion procedure performed in the reported study (Heller & Spence, 2019). The antibiotics evaluated were amoxicillin (25 µg), ciprofloxacin (5 µg), gentamicin (10 µg), penicillin G (6 µg), chloramphenicol, ampicillin, and streptomycin. According to Heller & Spence's (2019) experimental procedure, chloramphenicol, ampicillin, and streptomycin were prepared from antibiotic powders, and 6-mm sterile filter paper discs were loaded with 10 µL of the respective antibiotic solutions. The bacterial suspensions were prepared in 0.85% saline, adjusted to a 0.5 McFarland standard, and spread onto nutrient agar plates. The antibiotic discs were placed on the inoculated agar

surfaces, then incubated at 37 °C for 24 h. The diameters of the inhibition zones, including the disc diameter, were measured to the nearest millimetre.

The Clinical and Laboratory Standards Institute (CLSI) provides standardised guidance for antimicrobial disk diffusion testing (Clinical and Laboratory Standards Institute (CLSI, 2024). The available methodological information did not establish whether all requirements for standardised disc diffusion testing under the applicable Clinical and Laboratory Standards Institute (CLSI) guidelines were fulfilled. Therefore, the inhibition-zone measurements are presented descriptively and are not interpreted as definitive susceptible, intermediate, or resistant classifications. The findings should be considered preliminary observations of bacterial growth inhibition under the experimental conditions employed.

Microbiological Quality

The microbiological quality of the milk samples was assessed daily over seven days of storage at 4 °C. The storage temperature was monitored daily. Briefly, 1-mL of breast milk was aliquoted into an Eppendorf tube and serially diluted (10^{-1} to 10^{-5}). A volume of 0.1 mL from each dilution was spread onto Plate Count Agar (PCA), Chromocult Coliform Agar (CA), and Mannitol Salt Agar (MSA) for the enumeration of total plate count (TPC), total coliform count (TCC), and total *Staphylococcus* count (TSC), respectively. The surface-plating procedure for TPC was described with reference to the general principles of microbial colony enumeration by surface plating (International Organization for Standardization [ISO], 2013). The use of Chromocult Coliform Agar for coliform enumeration was supported by published work describing the detection and enumeration of coliforms using this medium (Stinson et al., 2022). Inoculated plates were incubated at 37 °C for 24 h, and plates containing 25- 250 colonies were used for enumeration. The resulting counts were expressed as $\log_{10}$ CFU/mL.

Statistical Analysis

Microbiological counts were expressed as $\log_{10}$ CFU/mL. Statistical analyses were conducted using the Statistical Package for the Social Sciences (SPSS), version 16.0. Analysis of variance (ANOVA) was used to assess differences in bacterial counts, with statistical significance set at $p<0.05$. Where applicable, significant differences between means were compared using Duncan's multiple range test. Microsoft Excel was used to organise the data and prepare graphs and charts. As the same milk samples were measured over multiple storage days, the statistical analysis should account for the repeated-measures structure of the data. Results below the detection limit were considered when determining the appropriate statistical approach.

RESULTS AND DISCUSSION

Isolation and identification of bacteria

Breast milk samples were collected and inoculated onto MCA, PMYPA, MSA and CA plates to isolate and identify the presence of bacteria using the conventional culture-based method. There was appearance and growth of *E.coli, Bacillus* spp., *Staphylococcus* spp. and *Coliforms*. The unknown colonies were subcultured onto NA and further examined through Gram staining and biochemical tests to observe the morphological and chemical characteristics of the bacterial isolates. Characterisation and presumptive bacterial genera isolated from human breast milk samples were performed in accordance with the UK Standards for Microbiology Investigations (Public Health England, 2020). As shown in Table 1, the presumptive bacterial genera identified included *Staphylococcus spp.*, *Streptococcus spp.*, *Lactobacillus spp.*, *Klebsiella spp.*, *Citrobacter spp.*, and *Enterobacter spp.* It was observed that the shapes of colonies of bacterial isolates were mostly small and round. The surface characteristics were smooth, and the margins of the colonies were entire and convex. The colonies, which were selected visually by naked eye, were observed to be whitish and cream-coloured. However, yellow-coloured colonies were also observed. All colonies were observed to be opaque. Among the six strains isolated, three were Gram-negative, with two displaying cocci morphology and one exhibiting a rod shape, whereas the remaining three Gram-positive strains were all rod-shaped. The bacterial isolates were presumptively characterised based on colony morphology, Gram staining, and biochemical reactions. The observed characteristics were used to assign the isolates to putative bacterial genera. As molecular or other confirmatory identification methods were not performed, the reported identities should be interpreted as presumptive rather than definitive species-level identifications.

Although human breast milk is naturally sterile, it can serve as a carrier of commensal, mutualistic, or potentially probiotic bacteria to the infant's gut, including *Staphylococcus, Streptococcus, Lactobacillus, Escherichia*, and *Enterobacter*, which is consistent with the majority of isolates identified in this study (Notarbartolo et al., 2022). It is suggested that the microbe isolated in this study may originate from the skin that was in contact with the milk during suckling or pumping (Lee et al., 2024). Furthermore, a mechanism involving gut monocytes during lactation may cause several bacteria from the maternal gut to reach the mammary gland through oromammary and enteromammary pathways. The mechanism would involve dendritic cells (DCs) and CD18 cells, which could take up bacteria from the gut lumen and carry them to other locations, including the lactating mammary gland (Mira & Rodriguez, 2017). In addition, during breastfeeding, a certain degree of milk may flow back into the mammary ducts; thus, the exchange of bacteria from the infant's mouth into the mammary gland could happen during such backflow (Wu et al., 2025). Moossavi et al. (2019) identified that breastfeeding mode is a key determinant of milk microbiota, and

Table 1
Morphological and biochemical characterization of bacterial isolates from human breast milk

Characteristics	Isolates							
	L-002	**O-01**	**N-01**	**N-02**	**Q-01**	**Q-02**	**R-01**	**R-02**
	Observation							
Margin	Smooth	Smooth	Smooth	Smooth	Smooth	Smooth	Smooth	Smooth
Colour	Creamy	Creamy	Creamy	Creamy	Creamy	Yellow	Creamy	Creamy
Shape	Small, round	Small, round	Small, round	Small, round	Small, round	Small, round	Small, round	Small, round
Cell type	Cocci	Cocci	Rod	Rod	Rod	Rod	Rod	Rod
Cell arrangement	Single	Single	Single	Single	Single	Single	Single	Single
Gram Reaction	+	+	+	−	−	−	−	−
	Sugar Fermentation Test							
Glucose	+	−	+	−	−	−	+	−
Sucrose	+	+	+	+	−	−	+	−
Lactose	+	+	+	+	−	−	+	+
	Biochemical Test							
Catalase	+	−	−	+	+	+	+	+
Oxidase	−	−	−	−	−	−	−	−
Indole	−	−	−	−	−	−	−	−
Urease	+	−	−	−	−	−	+	+
Citrate	−	+	+	+	+	+	+	+
Presumptive microorganism	*Staphylococcus epidermis*	*Streptococcus* spp.	*Lactobacillus* spp.	*Klebsiella* spp.		*Citrobacter* spp.	*Enterobacter* spp.	

pumped breast milk is a consistent source of multiple microbiota, including augmentation of potential pathogens and lessening of bifidobacteria.

Antibiotic Inhibition Zone Assessment

In this study, eight bacterial isolates from human breast milk were assessed for inhibition-zone formation in response to seven antibiotics: amoxicillin (AMX), ciprofloxacin (CIP), gentamicin (GM), penicillin G (P), chloramphenicol (C), ampicillin (AM), and streptomycin (S). As shown in Figure 1, inhibition zones ranging from 9 to 35 mm, including the 6-mm disc diameter, were observed among the isolates tested. These measurements indicate bacterial growth inhibition under the experimental conditions employed. However, because compliance with the applicable Clinical and Laboratory Standards Institute (CLSI) testing requirements and interpretive criteria could not be verified, the results should not be interpreted as definitive evidence of antibiotic susceptibility or resistance.

Differences in inhibition-zone diameters were observed among the antibiotics tested and the bacterial groups examined. For the coliform group, no statistically significant differences ($p>0.05$) were observed among AMX, CIP, and C, whereas differences were observed for the other antibiotics. For *Staphylococcus, Bacillus, Enterobacter, Citrobacter*, and *Lactobacillus,* differences in inhibition-zone diameters were also reported among the antibiotics. For *Escherichia coli,* the reported comparison involved ampicillin, AMX, and chloramphenicol; however, the statistical significance and corresponding p-values should be verified against the original analysis. Any differences in inhibition-zone diameter should

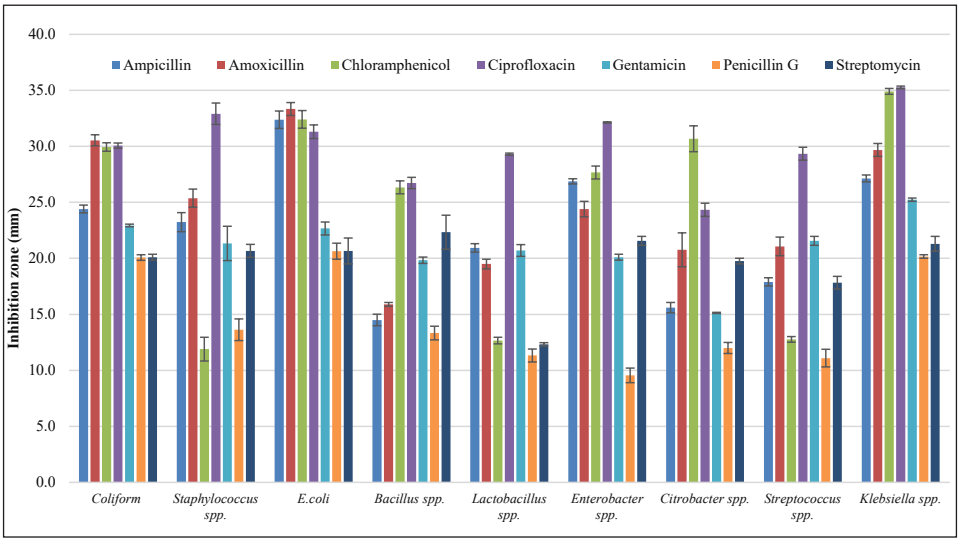

Figure 1. Inhibition-zone diameters of bacterial isolates from human breast milk in response to seven antibiotics. The measurements are presented descriptively and should not be interpreted as definitive classifications of susceptible, intermediate, or resistant. Data are expressed as mean ± SD of triplicates ($n = 3$)

be interpreted with caution, as zone sizes cannot be compared directly across different antibiotics as a measure of relative clinical effectiveness without appropriate standardised testing and organism-specific interpretive criteria.

Antibiotic resistance is an important public health concern because resistance determinants may be carried by mobile genetic elements, including plasmids and transposons, facilitating their potential dissemination among bacteria (Uddin et al., 2021). Previous studies have reported antibiotic resistance among bacteria isolated from human breast milk. For example, *Staphylococcus epidermidis* isolates from human breast milk have been reported to exhibit resistance to several antibiotics, including mupirocin, erythromycin, clindamycin, and oxacillin (Delgado et al., 2009; Begovic et al., 2013). Jiménez et al. (2013) reported virulence-associated characteristics and antibiotic resistance among *Enterococcus faecalis* and *Enterococcus faecium* isolates obtained from breast milk. Other studies have also reported resistance among breast-milk-associated *Enterococcus* spp. to selected antibiotics, including ciprofloxacin and gentamicin (Kıvanç et al., 2016). Chen et al. (2016) similarly reported resistance to antibiotics such as erythromycin, oxacillin, and clindamycin among *Enterococcus* spp. These findings highlight the importance of investigating the antimicrobial resistance characteristics of bacteria associated with human breast milk. Nevertheless, direct comparisons with the present study are limited because the bacterial species and antibiotics examined differed among studies.

Resistance patterns have also been reported among *Staphylococcus* spp*.,* although responses vary by species, antibiotic, and testing conditions. The potential clinical relevance of resistant bacteria in early life warrants attention, particularly because premature infants may receive prolonged antibiotic treatment. Such exposure may disrupt the developing gut microbiota and contribute to the selection of antimicrobial-resistant bacteria (Baker et al., 2023). However, the present study did not establish the presence or absence of antibiotic resistance in the tested isolates. Further investigation using a validated antimicrobial susceptibility testing procedure, with appropriate quality-control measures and organism-specific interpretive criteria, is therefore required to establish their susceptibility profiles and clarify the potential implications for infant health.

Stability of Human Breast Milk Microbiota at 4 °C

The microbiological quality of human breast milk during refrigerated storage was evaluated by determining the total plate count (TPC), total coliform count (TCC), and total *Staphylococcus* count (TSC). The results are presented in Tables 2, 3, and 4, respectively. Bacterial growth was detected in the TPC analysis of all samples, although no statistically significant differences ($p > 0.05$) were observed across the storage period for 10 of the 19 samples. For TCC, seven samples showed no detectable coliforms throughout the seven-day storage period, whereas the remaining 12 samples had coliform counts ranging from 2.11

Table 2
Total plate count (log_{10} CFU/mL) of human breast milk stored at refrigerated temperature (4 °C) for seven days

Sample	Aerobic Counts (log_{10} CFU/mL)							
	Day							
	0	1	2	3	4	5	6	7
1	3.60 ± 0.05^{a}	3.55 ± 0.01^{a}	3.38 ± 0.13^{ab}	3.43 ± 0.18^{a}	3.29 ± 0.21^{ab}	3.22 ± 0.35^{bc}	2.96 ± 0.05^{bc}	2.77 ± 0.00^{c}
2	5.60 ± 0.44^{a}	5.67 ± 0.42^{a}	5.09 ± 0.12^{a}	5.58 ± 0.00^{a}	4.64 ± 0.63^{a}	4.73 ± 0.00^{a}	4.81 ± 0.00^{a}	4.51 ± 0.16^{a}
3	4.21 ± 0.27^{a}	4.21 ± 0.18^{a}	4.24 ± 0.23^{a}	4.30 ± 0.17^{a}	4.19 ± 0.18^{a}	3.43 ± 0.51^{a}	3.34 ± 0.36^{a}	3.13 ± 0.32^{a}
4	5.38 ± 0.00^{de}	5.72 ± 0.10^{cde}	5.68 ± 0.34^{abc}	6.32 ± 0.03^{ab}	6.46 ± 0.23^{a}	5.38 ± 0.24^{de}	5.19 ± 0.03^{e}	5.80 ± 0.16^{bcd}
5	4.70 ± 0.03^{a}	5.14 ± 0.31^{a}	4.80 ± 0.39^{a}	4.72 ± 0.23^{a}	5.17 ± 0.23^{a}	4.69 ± 0.05^{a}	3.57 ± 0.20^{b}	3.68 ± 0.34^{b}
6	3.25 ± 0.06^{b}	3.24 ± 0.07^{b}	3.19 ± 0.38^{b}	3.22 ± 0.33^{b}	3.05 ± 0.08^{b}	5.18 ± 0.27^{a}	4.87 ± 0.05^{a}	4.51 ± 0.29^{a}
7	3.61 ± 0.25^{a}	3.39 ± 0.02^{a}	3.49 ± 0.19^{a}	3.45 ± 0.14^{a}	3.35 ± 0.15^{a}	3.33 ± 0.14^{a}	0.47 ± 0.02^{a}	3.41 ± 0.02^{a}
8	3.88 ± 0.24^{a}	3.47 ± 0.00^{ab}	3.49 ± 0.20^{ab}	3.23 ± 0.01^{bc}	2.90 ± 0.00^{bcd}	3.29 ± 0.58^{ab}	2.58 ± 0.15^{cd}	2.38 ± 0.29^{d}
9	4.39 ± 0.05^{a}	4.36 ± 0.32^{a}	4.51 ± 0.06^{a}	4.36 ± 0.24^{a}	4.23 ± 0.12^{a}	4.31 ± 0.08^{a}	0.32 ± 0.17^{a}	4.25 ± 0.12^{a}
10	3.56 ± 0.36^{a}	3.67 ± 0.16^{a}	3.51 ± 0.07^{a}	3.52 ± 0.04^{a}	3.54 ± 0.01^{a}	3.56 ± 0.38^{a}	0.34 ± 0.14^{a}	3.06 ± 0.11^{a}
11	3.77 ± 0.16^{a}	3.76 ± 0.28^{a}	3.73 ± 0.11^{a}	3.63 ± 0.09^{a}	3.69 ± 0.32^{a}	3.64 ± 0.29^{a}	3.66 ± 0.30^{a}	3.64 ± 0.33^{a}
12	5.57 ± 0.00^{a}	5.61 ± 0.00^{a}	5.24 ± 0.33^{a}	5.73 ± 0.27^{a}	5.37 ± 0.49^{a}	5.46 ± 0.44^{a}	5.25 ± 0.58^{a}	5.47 ± 0.20^{a}
13	5.02 ± 0.50^{a}	4.92 ± 0.39^{a}	4.96 ± 0.39^{a}	5.19 ± 0.47^{a}	5.85 ± 0.03^{a}	5.78 ± 0.15^{a}	5.66 ± 0.17^{a}	5.59 ± 0.15^{a}
14	4.78 ± 0.16^{ab}	4.56 ± 0.67^{b}	4.66 ± 0.13^{ab}	4.76 ± 0.16^{ab}	5.03 ± 0.49^{a}	4.82 ± 0.23^{ab}	4.75 ± 0.31^{ab}	4.63 ± 0.14^{ab}
15	3.70 ± 0.15^{a}	3.56 ± 0.17^{ab}	3.41 ± 0.06^{ab}	3.28 ± 0.14^{abc}	3.26 ± 0.13^{abc}	3.11 ± 0.00^{bc}	3.09 ± 0.08^{bc}	2.87 ± 0.12^{c}
16	3.91 ± 0.30^{a}	3.98 ± 0.22^{a}	4.00 ± 0.28^{a}	3.90 ± 0.19^{a}	3.90 ± 0.16^{a}	3.79 ± 0.03^{a}	3.77 ± 0.02^{a}	3.45 ± 0.19^{a}
17	4.16 ± 0.32^{a}	3.81 ± 0.21^{ab}	3.68 ± 0.21^{b}	3.82 ± 0.14^{ab}	3.76 ± 0.23^{ab}	3.79 ± 0.10^{ab}	3.65 ± 0.18^{b}	3.54 ± 0.12^{b}
18	4.18 ± 0.01^{a}	4.27 ± 0.00^{a}	4.37 ± 0.21^{a}	4.13 ± 0.13^{a}	4.15 ± 0.05^{a}	3.87 ± 0.00^{a}	3.73 ± 0.19^{a}	3.53 ± 0.13^{a}
19	3.60 ± 0.04^{a}	3.55 ± 0.01^{a}	3.38 ± 0.13^{ab}	3.42 ± 0.18^{abc}	3.29 ± 0.21^{abc}	3.22 ± 0.35^{ab}	2.96 ± 0.05^{abc}	2.77 ± 0.00^{c}

Note. Data are expressed as mean ± standard deviation (SD) of three experiments (n=3). Mean values with different superscripts in the same row are significantly different ($p<0.05$)

Table 3
Total coliform count (log_{10} CFU/mL) of human breast milk stored at refrigerated temperature (4°C) for seven days

Sample	log_{10} CFU/mL							
	Day							
	0	1	2	3	4	5	6	7
1	5.72 ± 0.12^{ab}	5.46 ± 0.13^{ab}	5.67 ± 0.18^{ab}	5.49 ± 0.22^{ab}	5.85 ± 0.07^{a}	5.35 ± 0.10^{b}	5.59 ± 0.12^{ab}	5.63 ± 0.11^{ab}
2	4.81 ± 0.16^{ab}	5.08 ± 0.07^{a}	4.48 ± 0.08^{abc}	4.57 ± 0.12^{abc}	4.79 ± 0.07^{ab}	3.78 ± 0.00^{c}	4.13 ± 0.24^{bc}	4.51 ± 0.15^{abc}
3	nd*	nd	nd	nd	nd	nd	nd	nd
4	5.38 ± 0.00^{ab}	5.72 ± 0.10^{a}	5.68 ± 0.34^{ab}	6.33 ± 0.04^{ab}	6.46 ± 0.23^{ab}	5.38 ± 0.24^{ab}	5.19 ± 0.03^{b}	5.80 ± 0.15^{ab}
5	3.31 ± 0.19^{a}	3.35 ± 0.29^{a}	3.06 ± 0.00^{a}	2.85 ± 0.00^{a}	2.66 ± 0.08^{ab}	3.26 ± 0.05^{a}	2.00 ± 0.43^{b}	3.28 ± 0.03^{a}
6	2.77 ± 0.00^{b}	2.58 ± 0.00^{c}	2.46 ± 0.00^{d}	2.38 ± 0.00^{f}	2.38 ± 0.00^{e}	2.28 ± 0.00^{g}	2.11 ± 0.00^{h}	3.04 ± 0.00^{a}
7	nd	nd	nd	nd	nd	nd	nd	nd
8	nd	nd	nd	nd	nd	nd	nd	nd
9	3.32 ± 0.13^{bc}	3.61 ± 0.27^{abc}	3.42 ± 0.03^{bc}	3.53 ± 0.20^{bc}	4.60 ± 0.51^{a}	4.09 ± 0.05^{ab}	3.69 ± 0.35^{bc}	2.97 ± 0.52^{c}
10	3.08 ± 0.05^{a}	3.11 ± 0.23^{a}	2.83 ± 0.18^{a}	2.80 ± 0.28^{a}	2.62 ± 0.00^{a}	2.64 ± 0.28^{a}	2.41 ± 0.16^{a}	2.46 ± 0.02^{a}
11	nd	nd	nd	nd	nd	nd	nd	nd
12	3.87 ± 0.40^{b}	3.80 ± 0.54^{b}	4.59 ± 0.56^{a}	5.59 ± 0.19^{a}	5.61 ± 0.22^{a}	5.63 ± 0.16^{a}	5.74 ± 0.29^{a}	5.52 ± 0.06^{a}
13	4.01 ± 0.24^{a}	4.25 ± 0.24^{a}	4.34 ± 0.35^{a}	3.74 ± 0.01^{a}	4.64 ± 0.09^{a}	4.85 ± 0.54^{a}	4.60 ± 0.03^{a}	4.62 ± 0.29^{a}
14	4.59 ± 0.28^{b}	3.78 ± 0.03^{c}	4.17 ± 0.08^{bc}	4.39 ± 0.11^{b}	4.81 ± 0.53^{a}	4.27 ± 0.01^{bc}	4.21 ± 0.08^{bc}	3.91 ± 0.00^{bc}
15	nd	nd	nd	nd	nd	nd	nd	nd
16	nd	nd	nd	nd	nd	nd	nd	nd
17	nd	nd	nd	nd	nd	nd	nd	nd
18	3.59 ± 0.22^{a}	3.46 ± 0.61^{ab}	3.27 ± 0.32^{ab}	2.99 ± 0.00^{ab}	2.85 ± 0.00^{ab}	2.69 ± 0.00^{b}	2.90 ± 0.00^{ab}	3.12 ± 0.00^{ab}
19	3.04 ± 0.00^{ab}	3.02 ± 0.00^{ab}	3.21 ± 0.00^{a}	2.91 ± 0.00^{b}	2.83 ± 0.00^{b}	2.30 ± 0.13^{d}	2.47 ± 0.10^{c}	2.25 ± 0.69^{cd}

Note. nd = not detected; Data were expressed as mean ± standard deviation (SD) of three experiments (n = 3). Mean values with different superscripts in the same row are significantly different ($p<0.05$)

Table 4
Total Staphylococcus *count (log_{10} CFU/mL) of human breast milk stored at refrigerated temperature (4°C) for seven days*

Sample	log_{10} CFU/mL							
	Day							
	0	1	2	3	4	5	6	7
1	nd	nd	nd	nd	nd	nd	nd	nd
2	nd	nd	nd	nd	nd	nd	nd	nd
3	nd	nd	nd	nd	nd	nd	nd	nd
4	4.44 ± 0.00^{a}	4.33 ± 0.40^{a}	4.71 ± 0.00^{a}	4.59 ± 0.14^{a}	3.51 ± 0.11^{b}	3.61 ± 0.21^{b}	3.10 ± 0.28^{b}	3.41 ± 0.03^{b}
5	nd	nd	nd	nd	nd	nd	nd	nd
6	3.12 ± 0.00^{ab}	3.07 ± 0.00^{a}	2.94 ± 0.00^{ab}	2.54 ± 0.00^{ab}	2.44 ± 0.00^{ab}	2.30 ± 0.00^{ab}	2.18 ± 0.00^{ab}	1.95 ± 0.00^{b}
7	2.92 ± 0.00^{bc}	2.72 ± 0.00^{cd}	2.74 ± 0.00^{cd}	2.74 ± 0.00^{cd}	3.07 ± 0.00^{b}	3.00 ± 0.84^{a}	2.57 ± 0.05^{d}	2.47 ± 0.06^{d}
8	2.84 ± 0.00^{b}	2.83 ± 0.00^{d}	2.77 ± 0.00^{e}	2.83 ± 0.00^{c}	2.92 ± 0.00^{a}	2.84 ± 0.00^{h}	2.76 ± 0.00^{f}	2.65 ± 0.00^{g}
9	2.92 ± 0.00^{a}	2.93 ± 0.00^{a}	3.17 ± 0.50^{a}	3.15 ± 0.44^{a}	3.44 ± 0.00^{a}	3.16 ± 0.57^{a}	2.82 ± 0.26^{a}	2.91 ± 0.43^{a}
10	3.28 ± 0.00^{a}	3.32 ± 0.00^{a}	3.55 ± 0.00^{a}	3.22 ± 0.00^{a}	3.08 ± 0.00^{a}	2.96 ± 0.00^{a}	2.78 ± 0.00^{a}	2.98 ± 0.00^{a}
11	3.37 ± 0.26^{a}	3.23 ± 0.14^{a}	3.26 ± 0.37^{a}	3.11 ± 0.36^{a}	3.16 ± 0.39^{a}	3.02 ± 0.26^{a}	3.22 ± 0.36^{a}	2.95 ± 0.60^{a}
12	3.80 ± 0.26^{a}	3.67 ± 0.07^{a}	3.58 ± 0.16^{a}	3.47 ± 0.37^{a}	3.80 ± 0.39^{a}	3.60 ± 0.20^{a}	3.66 ± 0.25^{a}	3.89 ± 0.15^{a}
13	4.91 ± 0.14^{a}	4.85 ± 0.22^{a}	4.94 ± 0.30^{a}	4.96 ± 0.30^{a}	4.37 ± 0.20^{ab}	3.72 ± 0.34^{b}	3.54 ± 0.11^{b}	3.65 ± 0.28^{b}
14	3.96 ± 0.16^{a}	4.07 ± 0.16^{a}	3.47 ± 0.35^{a}	3.49 ± 0.46^{a}	3.46 ± 0.50^{a}	3.44 ± 0.44^{a}	3.43 ± 0.43^{a}	2.83 ± 0.00^{a}
15	3.54 ± 0.09^{a}	3.51 ± 0.01^{a}	3.37 ± 0.09^{ab}	3.25 ± 0.01^{b}	3.24 ± 0.01^{b}	2.76 ± 0.01^{c}	2.25 ± 0.00^{e}	2.50 ± 0.00^{d}
16	3.18 ± 0.01^{a}	3.11 ± 0.05^{ab}	2.86 ± 0.00^{bc}	3.01 ± 0.14^{ab}	2.70 ± 0.11^{cd}	2.61 ± 0.00^{cd}	2.47 ± 0.00^{d}	2.00 ± 0.00^{e}
17	3.51 ± 0.20^{a}	3.56 ± 0.12^{a}	3.43 ± 0.03^{a}	3.32 ± 0.00^{a}	3.39 ± 0.00^{a}	2.95 ± 0.00^{a}	2.86 ± 0.00^{a}	2.97 ± 0.00^{a}
18	3.48 ± 0.17^{a}	3.32 ± 0.01^{a}	3.41 ± 0.08^{a}	2.87 ± 0.04^{b}	2.94 ± 0.00^{b}	2.53 ± 0.00^{c}	2.30 ± 0.10^{c}	1.95 ± 0.00^{d}
19	3.18 ± 0.01^{a}	3.11 ± 0.05^{ab}	2.86 ± 0.00^{bc}	3.01 ± 0.14^{ab}	2.70 ± 0.11^{cd}	2.61 ± 0.00^{cd}	2.47 ± 0.00^{d}	2.00 ± 0.00^{e}

Note. nd = not detected; Data were expressed as mean ± standard deviation (SD) of three experiments (n = 3). Mean values with different superscripts in the same row are significantly different ($p<0.05$)

to 5.85 $\log_{10}$ CFU/mL. The TSC results indicated that *Staphylococcus* was not detected in some samples; however, the number of samples with detectable and undetectable TSC values should be verified against Table 4 to ensure consistency among the samples.

Microbiological reference limits are important for interpreting the quality of milk and milk products. European Commission (2005) provides microbiological criteria for several bacterial groups, while the Malaysian Food Regulations (1985) specify microbiological limits for milk and milk products. However, these criteria should be interpreted with caution when applied to human breast milk, as the applicable regulations do not specifically establish microbiological safety limits for human breast milk in the context of this study. Using the reference criteria applied in the present study, 15 of the 19 samples (78.9%) consistently exhibited TPC values below 5 $\log_{10}$ CFU/mL throughout the seven-day storage period at 4 °C. In contrast, 12 samples (63.2%) had TCC values above the reference limit, while seven samples (36.8%) showed no detectable coliforms throughout storage. These findings indicate that the microbiological quality varied among samples and that the TCC results warrant particular attention.

Elevated TCC values may be associated with contamination introduced during milk expression, collection, handling, or storage. Potential contributing factors include inadequate hand hygiene before milk expression, insufficient cleaning of collection equipment and storage containers, and contamination during sample transfer or handling (Aliyo et al., 2022). Although sterile containers were used to collect and store the milk samples, contamination could still have occurred during other stages of collection and handling. Nevertheless, hygiene practices were not directly assessed in this study, and the source of the observed coliforms was not investigated. Therefore, poor hygiene cannot be identified conclusively as the cause of the elevated TCC values.

These findings emphasise the importance of maintaining appropriate hygiene throughout the collection and handling of human breast milk. Washing hands before milk expression, ensuring that collection equipment and containers are appropriately cleaned and sanitised, minimising contact with potentially contaminated surfaces, and handling samples carefully may help reduce the risk of contamination. Maintaining appropriate refrigeration is also important; however, refrigeration alone does not establish microbiological safety when elevated coliform counts are present. Consequently, the elevated TCC values observed in several samples warrant caution when interpreting the microbiological quality of the milk throughout the seven-day storage period.

Overall, bacterial counts declined during storage, although some samples showed minor increases or fluctuations. These observations describe changes in the measured bacterial populations under the storage conditions employed. Low temperatures can slow the growth of many microorganisms, although the response depends on the microbial species and the sample conditions (Al-Sharify et al., 2025). The observed decline in bacterial counts

should not, however, be interpreted as evidence that all microorganisms were eliminated or that the samples became microbiologically safe.

The antimicrobial properties of human breast milk may also be relevant when interpreting changes in bacterial counts during storage. Sharma et al. (2018) reported changes in the bactericidal activity of human breast milk during refrigerated storage. Lactoferrin, which binds iron and may limit its availability to microorganisms, is one of the components that contribute to the antimicrobial properties of breast milk (Kell et al., 2020). Lysozyme may also contribute to the regulation of bacterial populations through its antimicrobial activity (Aquino-Domínguez et al., 2025). However, the concentrations and activities of these components were not measured in the present study; therefore, their contribution to the observed bacterial-count trends remains speculative.

The relatively high initial bacterial counts observed in some human breast milk samples, ranging from approximately 3 to 5 log CFU/mL, may reflect bacteria originating from maternal skin or contamination introduced during milk expression and handling (Reyes et al., 2025). Although sterile containers were used in this study, their use alone cannot exclude contamination during collection or subsequent sample handling. These findings support the importance of appropriate hygiene practices and careful handling throughout the collection and storage process.

Previous research has investigated approaches to reducing the microbial load of human breast milk, including high-pressure processing and high-temperature short-time (HTST) pasteurisation (Wesolowska et al., 2019). Grazziotin et al. (2016) also discussed storage conditions in relation to the preservation of the nutritional and energy content of human breast milk. These studies provide useful context for understanding breast milk preservation; however, their findings should not be used as direct evidence of the microbiological safety of the samples examined in the present study.

In conclusion, the results describe changes in TPC, TCC, and TSC during seven days of refrigerated storage at 4 °C. Although bacterial counts generally declined, the elevated TCC values in 12 of the 19 samples highlight the need to consider hygiene during milk collection and handling and to interpret the findings cautiously. Further studies incorporating direct assessment of hygiene practices, appropriate microbiological criteria for human breast milk, and validated approaches to evaluating storage safety are needed to determine the implications of refrigerated storage duration for microbiological quality.

CONCLUSION

Eight bacterial isolates from human breast milk were presumptively characterised using conventional culture-based methods and biochemical tests, with the isolates assigned to putative bacterial genera, including *Staphylococcus, Escherichia coli, Bacillus, Lactobacillus, Enterobacter, Citrobacter, Streptococcus* and *Klebsiella*. Inhibition zone

measurements were obtained for seven antibiotics; however, these measurements were interpreted descriptively because compliance with the applicable CLSI testing and interpretive requirements could not be verified. Therefore, definitive conclusions regarding the antimicrobial susceptibility or resistance of the isolates cannot be drawn from these results.

During refrigerated storage at 4 °C for seven days, most breast milk samples exhibited total plate count (TPC) and total *Staphylococcus* count (TSC) values below the reference limits applied in this study. However, 12 of the 19 samples (63.2%) showed total coliform counts (TCC) above the reference limit. Although bacterial counts generally declined during storage, elevated coliform counts in several samples highlight the importance of hygienic practices during milk collection, handling, and storage. Overall, these findings describe changes in the microbiological quality of human breast milk under the experimental storage conditions but do not establish that storage for seven days at 4°C is microbiologically safe. Further studies using validated microbiological methods and appropriate safety criteria are needed to clarify the implications of the duration of refrigerated storage for human breast milk.

ACKNOWLEDGEMENT

This work was financially supported by the Ministry of Higher Education Malaysia through the Fundamental Research Grant Scheme [Grant number: FRGS/1/2025/STG02/UPM/02/1] and Universiti Putra Malaysia under Geran Putra [Grant number: GP/2014/9434800]. The authors would like to acknowledge University Driven Research Programs (UDRP) s: Functional Food Development and Future Food (including Cell Culture Technology), Faculty of Food Science and Technology and Food Safety (including Food Traceability and Authenticity), Institute of Tropical Agriculture and Food Security, Universiti Putra Malaysia for providing resources and facilities.

ETHICS APPROVAL

The study was approved by the Ethics Committee for Research (Ethics Approval No. FSTM/EXP15/P144)

REFERENCES

Aditi, F. Y., Rahman, S. S., & Hossain, M. M. (2017). A study on the microbiological status of mineral drinking water. *The Open Microbiology Journal, 11,* 31-44. https://doi.org/10.2174/1874285801711010031

Aliyo, A., Seyoum, A., & Teklemariam, Z. (2022). Bacteriological quality and antimicrobial susceptibility patterns among raw milk producers and vendors in Gomole district, Borena zone, Southern Ethiopia. *Infection and Drug Resistance, 15,* 2589-2602. https://doi.org/10.2147/IDR.S364578

Al-Sharify, Z. T., Al-Najjar, S. Z., Naser, Z. A., Alsherfy, Z. A. I., & Onyeaka, H. (2025). The impact of fluid flow on microbial growth and distribution in food processing systems. *Foods, 14*(3), Article 401. https://doi.org/10.3390/foods14030401

AOAC International. (2012). *AOAC INTERNATIONAL Methods committee guidelines for validation of microbiological methods for food and environmental surfaces*. https://s27415.pcdn.co/wp-content/uploads/2020/01/64ER20-7/Validation_Methods/c-aoac_validation_guidelines_for_food_microbiology.pdf

Aquino-Domínguez, A. S., Gómez-López, M., & Aguilar-Ruiz, S. R. (2025). Harmonious allies: The synergy of antimicrobial proteins and microbes in breast milk to protect neonatal health. *Hygiene, 5*(2), Article 19. https://doi.org/10.3390/hygiene5020019

Baker, S., Niranjan, R. S., Manju, K., Ranjini, H. K., & Shayista, H. (2023). Efficacy of breast milk components against microbial pathogens to combat drug-resistance. *The Microbe, 1,* Article 100010. https://doi.org/10.1016/j.microb.2023.100010

Capra, M. E., Aliverti, V., Bellani, A. M., Berzieri, M., Montani, A. G., Pisseri, G., Sguerso, T., Esposito, S., & Biasucci, G. (2025). Breastfeeding and non-communicable diseases: A narrative review. *Nutrients, 17*(3), Article 511. https://doi.org/10.3390/nu17030511

Centers for Disease Control and Prevention. (2024, May). *Breast milk storage and preparation.* https://www.cdc.gov/breastfeeding/breast-milk-preparation-and-storage/handling-breastmilk.html

Chen, P. -W., Tseng, S. -Y., & Huang, M. -S. (2016). Antibiotic susceptibility of commensal bacteria from human milk. *Current Microbiology, 72*, 113-119. https://doi.org/10.1007/s00284-015-0925-4

Clinical and Laboratory Standards Institute. (2024). *Performance standards for antimicrobial disk susceptibility tests* (14th ed.; CLSI standard M02).

Danaie, M., Yeganegi, M., Dastgheib, S. A., Bahrami, R., Jayervand, F., Rahmani, A., Aghasipour, M., Golshan-Tafti, M., Azizi, S., Marzbanrad, Z., Masoudi, A., Shiri, A., Lookzadeh, M. H., Noorishadkam, M., & Neamatzadeh, H. (2024). The interaction of breastfeeding and genetic factors on childhood obesity. *European Journal of Obstetrics & Gynecology and Reproductive Biology: X, 23*, Article 100334. https://doi.org/10.1016/j.eurox.2024.100334

Darkoh, C., Chappell, C., Gonzales, C., & Okhuysen, P. (2015). A rapid and specific method for the detection of indole in complex biological samples. *Applied and Environmental Microbiology, 81*(23), 8093-8097. https://doi.org/10.1128/AEM.02787-15

Delgado, S., Arroyo, R., Jiménez, E., Marín, M. L., del Campo, R., Fernández, L., & Rodríguez, J. M. (2009). *Staphylococcus epidermidis* strains isolated from breast milk of women suffering infectious mastitis: Potential virulence traits and resistance to antibiotics. *BMC Microbiology, 9*, Article 82. https://doi.org/10.1186/1471-2180-9-82

Despotovic, M., de Nies, L., Busi, S. B., & Wilmes, P. (2023). Reservoirs of antimicrobial resistance in the context of One Health. *Current Opinion in Microbiology, 73*, Article 102291. https://doi.org/10.1016/j.mib.2023.102291

European Commission. (2005). Commission Regulation (EC) No 2073/2005 of 15 November 2005 on microbiological criteria for foodstuffs. *Official Journal of the European Union, L 338*, 1-26. https://eur-lex.europa.eu/legal-content/EN/TXT/?uri=CELEX:32005R2073

Fernández, L., Langa, S., Martín, V., Maldonado, A., Jiménez, E., Martín, R., & Rodríguez, J. M. (2013). The human milk microbiota: Origin and potential roles in health and disease. *Pharmacological Research, 69*(1), 1-10. https://doi.org/10.1016/j.phrs.2012.09.001

Food Act 1983 (Act 281) and Food Regulations 1985. (2025). International Law Book Services.

Fortin, M., Messier, S., Paré, J., & Higgins, R. (2003). Identification of catalase-negative, non-beta-hemolytic, gram-positive cocci isolated from milk samples. *Journal of Clinical Microbiology, 41*(1), 106-109. https://doi.org/10.1128/JCM.41.1.106-109.2003

Gebremichael, D., Tadesse, A., Hailemariam, F., Hailay, B., Hadgu, H., & Kalayu, G. (2024). Investigation of microbial quality of milk and milk products and isolations of some major bacteria in the central and northwestern zones of Tigray, Ethiopia. *Veterinary Medicine International, 2024*, Article 9989527. https://doi.org/10.1155/vmi/9989527

Gondkar, P., Kumar, H., & Patel, K. (2024). Incidence and risk factors associated with human mastitis. *Health Sciences Review, 12,* Article 100191. https://doi.org/10.1016/j.hsr.2024.100191

Grazziotin, M. C. B., Grazziotin, A. L., Vidal, N. M., Freire, M. H. d. S., & da Silva, R. P. G. V. C. (2016). Analysis of the storage methods for raw human milk from mothers with infants admitted to a neonatal intensive care unit, according to Brazilian regulations. *Journal of Human Lactation, 32*(3), 446-454. https://doi.org/10.1177/0890334416647710

Heller, A. A., & Spence, D. M. (2019). A rapid method for post-antibiotic bacterial susceptibility testing. *PloS One*, *14*(1), Article e0210534. https://doi.org/10.1371/journal.pone.0210534

Jiménez, E., Ladero, V., Chico, I., Maldonado-Barragán, A., López, M., Martín, V., Fernández, L., Fernández, M., Álvarez, M. A., Torres, C., & Rodríguez, J. M. (2013). Antibiotic resistance, virulence determinants and production of biogenic amines among enterococci from ovine, feline, canine, porcine and human milk. *BMC Microbiology, 13*, Article 288. https://doi.org/10.1186/1471-2180-13-288

Kell, D. B., Heyden, E. L., & Pretorius, E. (2020). The biology of lactoferrin, an iron-binding protein that can help defend against viruses and bacteria. *Frontiers in Immunology, 11,* Article 1221. https://doi.org/10.3389/fimmu.2020.01221

Kıvanç, S. A., Kıvanç, M., & Yiğit, T. (2016). Antibiotic susceptibility, antibacterial activity, and characterisation of *Enterococcus faecium* strains isolated from breast milk. *Experimental and Therapeutic Medicine, 12*, 1732-1740. https://doi.org/10.3892/etm.2016.3545

Kumar, B., Sharma, R., Thakur, R., Barui, A. K., Rajput, Y. S., & Mann, B. (2016). Rapid lactate oxidase-based assay for lactate content in milk to ascertain its hygienic quality. *International Journal of Dairy Technology, 69*, 460-467. https://doi.org/10.1111/1471-0307.12285

Lamberte, L. E., & van Schaik, W. (2022). Antibiotic resistance in the commensal human gut microbiota. *Current Opinion in Microbiology, 68*, Article 102150. https://doi.org/10.1016/j.mib.2022.102150

Lee, S., Heo, S., Park, M. -K., Sung, M. -H., & Jeong, D. -W. (2024). Bacterial community of breast milk in breastfeeding women using culture-dependent and culture-independent approaches. *Journal of Microbiology and Biotechnology, 34*(10), 2005-2011. https://doi.org/10.4014/jmb.2407.07001

Mancuso, G., Midiri, A., Gerace, E., & Biondo, C. (2021). Bacterial antibiotic resistance: The most critical pathogens. *Pathogens, 10*(10), Article 1310. https://doi.org/10.3390/pathogens10101310

Masi, A. C., & Stewart, C. J. (2024). Role of breastfeeding in disease prevention. Microbial *Biotechnology, 17*, Article e14520. https://doi.org/10.1111/1751-7915.14520

Mollova, D., Vasileva, T., Bivolarski, V., & Iliev, I. (2023). The enzymatic hydrolysis of human milk oligosaccharides and prebiotic sugars from LAB isolated from breast milk. *Microorganisms, 11*(8), Article 1904. https://doi.org/10.3390/microorganisms11081904

Murphy, K., Curley, D., O'Callaghan, T. F., O'Shea, C. -A., Dempsey, E. M., O'Toole, P. W., Ross, R. P., Ryan, C. A., & Stanton, C. (2017). The composition of human milk and infant faecal microbiota over the first three months of life: A pilot study. *Scientific Reports, 7,* Article 40597. https://doi.org/10.1038/srep40597

Notarbartolo, V., Giuffrè, M., Montante, C., Corsello, G., & Carta, M. (2022). Composition of human breast milk microbiota and its role in children's health. *Pediatric Gastroenterology, Hepatology & Nutrition, 25*(3), 194-210. https://doi.org/10.5223/pghn.2022.25.3.194

Public Health England. (2017). *Introduction to the preliminary identification of medically important bacteria and fungi from culture* (UK Standards for Microbiology Investigations, ID 01, Issue 2). https://www.simpios.eu/wp-content/uploads/2024/04/id_1_2_en_IdentificazioneBatteriFunghi170421.pdf

Reyes, S. M., Allen, D. L., Williams, J. E., McGuire, M. A., McGuire, M. K., Rasmussen, K. M., & Hay, A. G. (2025). Pumping and hygiene practices are associated with bacterial load and microbial composition in human milk expressed at home. *Journal of Translational Medicine, 23*, Article 947. https://doi.org/10.1186/s12967-025-06967-5

Sharma, V., Sharma, C., Chauhan, S., & Kaur, S. (2018). Effect of lactation age and storage on the antibacterial potency of human breast milk against neonatal pathogens. *Journal of Pure and Applied Microbiology, 12*(3), 1307-1314. https://doi.org/10.22207/JPAM.12.3.33

Stinson, L. F., Trevenen, M. L., & Geddes, D. T. (2022). Effect of cold storage on the viable and total bacterial populations in human milk. *Nutrients, 14*(9), Article 1875. https://doi.org/10.3390/nu14091875

Uddin, T. M., Chakraborty, A. J., Khusro, A., Zidan, B. R. M., Mitra, S., Emran, T. B., Dhama, K., Ripon, M. K. H., Gajdács, M., Sahibzada, M. U. K., Hossain, M. J., & Koirala, N. (2021). Antibiotic resistance in microbes: History, mechanisms, therapeutic strategies and future prospects. *Journal of Infection and Public Health, 14*(12), 1750-1766. https://doi.org/10.1016/j.jiph.2021.10.020

Verma, R. K., Joshi, R. K., & Joshi, N. (2022). Sugar fermentation test with glucose, lactose, mannitol, maltose and sucrose for phenotypic identification of methicillin resistant *Staphylococcus aureus* (MRSA) in farm animals through nasal swab and milk samples. *Biochemical and Cellular Archives, 22*(1), 1515-1520. https://connectjournals.com/03896.2022.22.1515

Wan, Y., Xie, Z., Cao, M., Zhang, C., Feng, Z., Tian, B., & Liu, Z. (2024). Detection of urea in milk by urease-inorganic hybrid nanoflowers combined with portable colorimetric microliter tube. *Microchimica Acta, 191*, Article 679. https://doi.org/10.1007/s00604-024-06734-1

Wesolowska, A., Sinkiewicz-Darol, E., Barbarska, O., Bernatowicz-Lojko, U., Borszewska-Kornacka, M. K., & van Goudoever, J. B. (2019). Innovative techniques of processing human milk to preserve key components. *Nutrients, 11*(5), Article 1169. https://doi.org/10.3390/nu11051169

Wu, S., Luo, G., Jiang, F., Jia, W., Li, J., Huang, T., Zhang, X., Mao, Y., Su, S., Han, W., He, F., & Cheng, R. (2025). Early life bifidobacterial mother-infant transmission: Greater contribution from the infant gut to human milk revealed by microbiomic and culture-based methods. *mSystems, 10*(7), Article e00480-25. https://doi.org/10.1128/msystems.00480-25

Xiang, Q., Yan, X., Shi, W., Li, H., & Zhou, K. (2023). Early gut microbiota intervention in premature infants: Application perspectives. *Journal of Advanced Research, 51*, 59-72. https://doi.org/10.1016/j.jare.2022.11.004

Pertanika J. Trop. Agric. Sci. 49 (5): 2603 - 2611 (2026)

PERTANIKA JOURNALS

TROPICAL AGRICULTURAL SCIENCE

Journal homepage: http://www.pertanika.upm.edu.my/

Maximising Growth and Quality of *Caulerpa lentillifera* Through Multilevel Cultivation with LED Approach

Nur Amira Yasmin Mohd Nizar[1], Jamil Tajam[1]*, Non Daina Masdar[2], Zamzila Erdawati Zainol[1], Mohamad Niza Md Nor[3], Khairul Naim Abd Aziz[1], and Sharir Aizat Kamaruddin[1]

[1]Marine Research Station, Faculty of Applied Sciences, Universiti Teknologi MARA (UiTM) Perlis, 02600 Arau, Malaysia
[2]Department of Chemistry, Faculty of Applied Sciences, Universiti Teknologi MARA (UiTM) Perlis, 02600 Arau, Malaysia
[3]Department of Marketing & Entrepreneurship, Faculty of Business and Management, Universiti Teknologi MARA (UiTM) Perlis, Arau 02600, Malaysia

ABSTRACT

Caulerpa lentillifera (Laktud) is an edible green macroalga with increasing relevance in food and aquaculture. At the Kubang Badak cultivation site in Langkawi, the use of pond space is constrained by uneven light distribution across vertically arranged growing levels. This study evaluated a multilevel cultivation arrangement under white LED, pink LED and natural sunlight over 28 days. Nine cultivation plates were used, with three plates assigned to each lighting condition. Frond density, frond length, plate weight, daily growth rate (DGR) and biomass yield were recorded. At Week 4, plate W2 had the highest recorded frond density (79.33 per 100 cm²) and plate weight (1,305 g); it also had the highest reported DGR (0.018551 day^{-1}) and biomass yield (247.76 g m^{-2} day^{-1}). The longest individual fronds were recorded on sunlight-exposed plate S1 (4.628 cm), followed by white-LED plate W3 (4.017 cm). In contrast, frond density on S3 declined to 3.67 per 100 cm². The results indicate that LED lighting may help improve growth consistency across multilevel cultivation plates, although the sunlight treatment showed substantial variation among shelf positions. Further replicated experiments with measured photosynthetically active radiation and controlled shelf positions are needed to confirm the treatment effects and optimise the system for practical cultivation.

Keywords: Biomass yield, *Caulerpa lentillifera*, daily growth rate, frond density, growth multilevel cultivation

ARTICLE INFO

Article history:
Received: 17 June 2025
Accepted: 28 October 2026
Published: 30 October 2026

DOI: https://doi.org/10.47836/pjtas.49.5.25

E-mail addresses:
ysmin.nizar@gmail.com (Nur Amira Yasmin Mohd Nizar)
jamiltajam@uitm.edu.my (Jamil Tajam)
daina@uitm.edu.my (Non Daina Masdar)
zamzila396@uitm.edu.my (Zamzila Erdawati Zainol)
mohdniza@uitm.edu.my (Mohamad Niza Md Nor)
khairul87@uitm.edu.my (Khairul Naim Abd Aziz)
shariraizat@uitm.edu.my (Sharir Aizat Kamaruddin)
* Corresponding author

e-ISSN: 2231-8542

© Universiti Putra Malaysia Press

INTRODUCTION

The development of Caulerpa seaweed holds enormous promise in a variety of industries, including food, biotechnology, and environmental conservation, yet it remains understudied in Malaysia. According to a recent study by Phang et al. (2019), Malaysian seaweeds are becoming more diverse, and the Langkawi Islands are flowering with Caulerpa species. The same study stated that the increasing seaweed diversity in Malaysia is indirectly making Langkawi Island a center for several Caulerpa species. According to Phang et al. (2005), around 84 taxa of seaweeds have been identified on Langkawi Island. The species are *Padina (Phaeophyta), Halimeda, Caulerpa, Bryopsis (Chlorophyta), Gracilaria, Acanthophora, Asparagopsis, Polysiphonia,* and *Hypnea (Rhodophyta).* According to Sinurat and Fadjriah (2019), this species thrives by attaching itself to rock fragments or sand substrates. However, Zuldin et al. (2019) point out that a lack of study on cultivation methods makes it difficult for local communities to benefit from Caulerpa production. Wild stock availability is severely strained as a result of intense harvesting practices that exacerbate the strain on wild stocks (Nagappan & Vairappan, 2014). Cultivating Laktud has provided many residents with a source of income and job opportunities. However, a major issue for the local cultivation facility at Kubang Badak, Langkawi, is the underutilisation of the area in the ponds set aside for the cultivation of Caulerpa seaweed. This inefficiency results in lost opportunities to maximise Caulerpa production in the area and restricts the overall production capacity. This study therefore evaluated frond density, frond length, plate weight, daily growth rate and biomass yield over four weeks under white LED, pink LED and natural sunlight. Its practical significance lies in providing preliminary, site-specific evidence to guide the further development of multilevel Laktud cultivation in Langkawi. The novelty lies in assessing three lighting conditions within a multilevel arrangement at a local cultivation facility and reporting plate-level growth responses that reveal both promising LED performance and the variability associated with natural sunlight. Rueangnoi et al. (2025) reported that changing light intensities significantly affected the growth of sea grapes (*Caulerpa lentillifera*).

MATERIALS AND METHOD

The study was conducted in a controlled growth environment to assess the growth of Caulerpa lentillifera (Laktud) under different illumination conditions. Cultivation of Laktud was carried out for four weeks using nine plates (Figure 1) in a three-tiered cultivation system (Figure 2). Three plates were used for each illumination condition: white LED (W1, W2, W3), pink LED (P1, P2, P3) and natural sunlight (S1, S2, S3). No LED lights to allow development assessment under natural sunlight exposure.

Light intensity taken from the HOBO sensor data logger indicated light availability among cultivation sites. The highest position (S1) was 11022.3 lux in natural sunlight, while S2 and S3 were 376.7 and 150.7 lux. However, the cultivation levels with LEDs had the

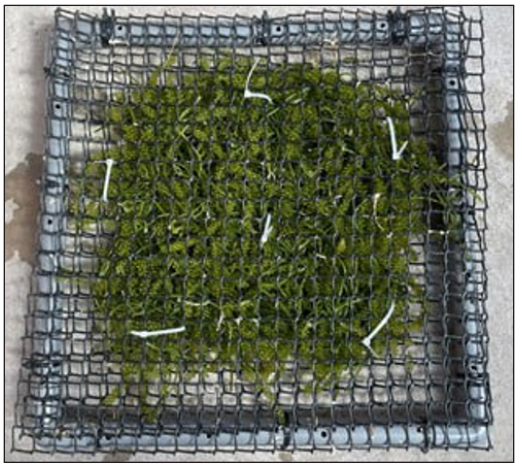

Figure 1. Plate used to cultivate Laktud



Figure 2. Multilevel cultivation with LED approach

same measured brightness. This difference is essential to the study's purpose, as natural sunlight provided more favourable illumination at the uppermost location but much reduced illumination at the lower levels. Thus, consistent LED brightness could be a practical way to improve the utilisation of vertical cultivation space. Nevertheless, the measured values in lux do not convert directly to photosynthetic photon flux density (PPFD) and so do not establish the photosynthetic light accessible to Laktud.

The data collected include biomass production, frond density, and the daily growth rate of frond length. Frond length and density were measured using a 100 cm^2 frame (Azcárate-García, 2022). The cultivation period is fixed at 4 weeks. DGR was computed as $[\ln(W_f) - \ln(W_i)]/t$ (day^{-1}), where W_i is the initial fresh weight, W_f is the final fresh weight, and t is the number of days in culture. Biomass yield was calculated as the final biomass per unit area of culture and length of cultivation (g m^{-2} day^{-1}). Fertilisation is done every two weeks (Islam et al., 2021), and a water-testing kit is used to check water quality. The optimum salinity levels should be in the range of 30 to 32 parts per thousand (ppt) and not less than 25 ppt (Fakhrulddin et al., 2021). Every two weeks, 80% of the pond's water is replaced with fresh seawater to maintain the optimum aquatic conditions.

Statistical evaluation was done to study the effectiveness of Laktud growth when exposed to light, whether it is pink LED, white LED or natural sunlight. The effects of light conditions and cultivation weeks on frond density and length were analysed by two-way analysis of variance (ANOVA). The daily growth rate (DGR) and biomass output under different illumination conditions were analysed by one-way ANOVA. The null hypothesis (H0) assumed that there were no significant variations in the evaluated growth parameters between the illumination treatments and, when relevant, the cultivation weeks. Statistical significance was defined as a P-value < 0.05.

RESULTS AND DISCUSSION

Results for frond density and frond length provide significant and important information about the overall productivity and quality of the cultivated *Caulerpa lentillifera* (Stuthmann et al., 2023). Figure 3 shows the graph of average frond density for four weeks of the cultivation period. The mean frond density for white LED light (W1, W2, W3) was the highest compared to pink LED light and natural sunlight. By week 4 (Table 1), plate W2 achieved the highest density, which was 79.33 cm2, compared to 78.67 cm^2 for pink LED light. However, natural sunlight showed a decline, with S3 at 3.67 cm^2 by week 4. This decrease may be a result of the inconsistency of natural sunlight compared to LED lighting.

Table 1
Value of density of fronds in four weeks (number per 100cm^2)

Plate	Density (cm^2)			
	Week 1	Week 2	Week 3	Week 4
P1	40.33	53.00	62.67	78.67
P2	56.33	62.67	63.33	71.00
P3	48.00	61.67	67.00	76.00
W1	45.33	58.33	64.67	70.00
W2	49.67	50.67	68.33	79.33
W3	52.00	54.33	64.67	73.67
S1	39.00	43.00	68.33	78.00
S2	13.67	18.00	13.33	9.67
S3	8.33	11.33	6.67	3.67

Table 2
Value of length of frond in four weeks

Plate	Length (cm)			
	Week 1	Week 2	Week 3	Week 4
P1	1.880	1.944	2.236	2.500
P2	1.592	2.139	2.361	2.678
P3	1.708	3.014	3.194	3.481
W1	1.667	2.139	2.694	2.922
W2	1.903	2.931	3.081	3.139
W3	2.556	3.093	3.925	4.017
S1	3.583	4.444	4.597	4.628
S2	1.700	2.125	1.955	1.886
S3	2.460	2.250	1.738	0.955

Two-way ANOVA showed significant differences in frond density between the different illumination treatments ($p<0.001$) and weeks of culture ($p = 0.004$). The frond density increased over the 4 weeks of cultivation and was higher under pink and white LED lights than under natural sunlight. This can be caused by the high demand for LED lighting to maintain constant light, where higher light intensity increases the energy available to algae for photosynthesis, leading to faster growth and possibly more ramuli (Apriliyanti et al., 2024). In the multi-level cultivation system, shading by natural sunlight can be avoided during growth.

Individual frond length at plate level was highest in S1 (4.628 cm) at Week 4, followed by W3 (4.017 cm) as shown in Figure 4. The higher frond lengths measured at S1 are probably attributable to its location at the highest point of the pond, where natural light was more favorable. The LED lighting configuration ensured uniform light intensity across all LED-illuminated cultivation levels. The lowest layers (S2 and S3) under natural sunlight had much reduced frond lengths, 1.886 cm and 0.955 cm, respectively as shown in Table 2. The results indicate a possible disadvantage of relying solely on natural sunlight

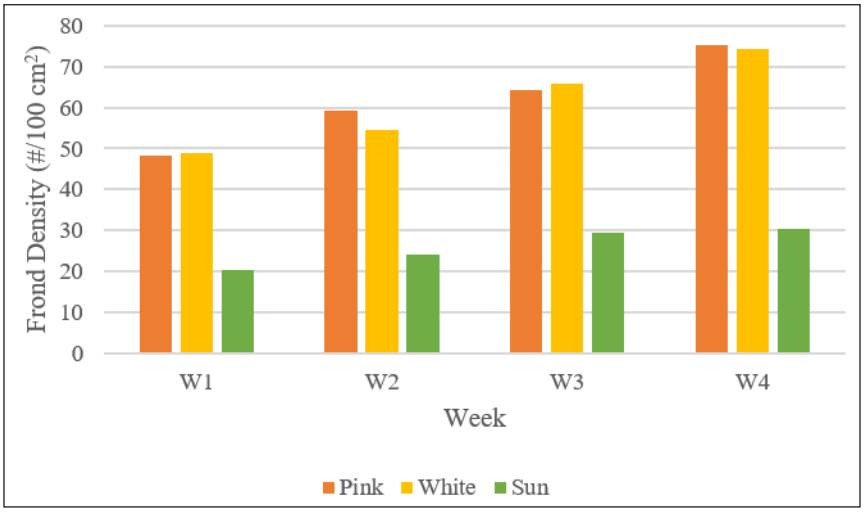

Figure 3. Average density of fronds in four weeks

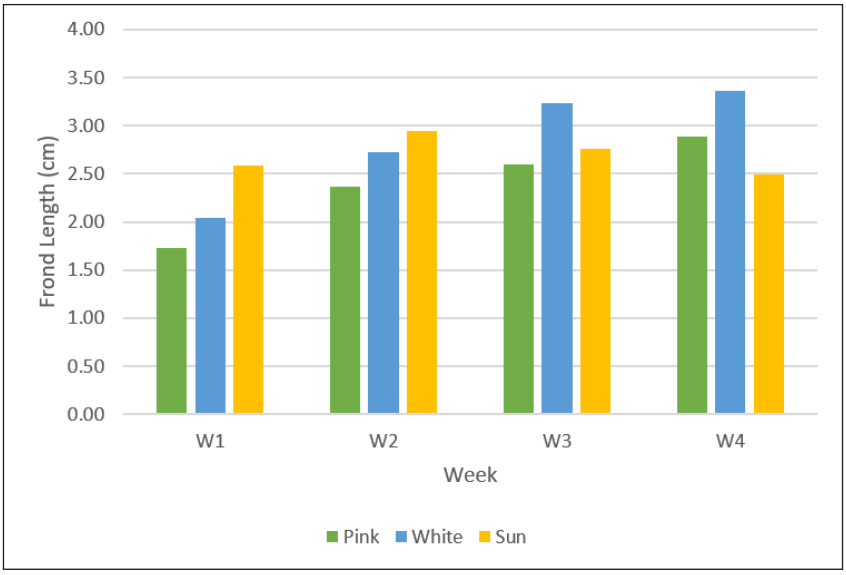

Figure 4. Average frond length over four weeks

in multilevel production systems, where ideal lighting conditions may be concentrated at the uppermost level.

Thus, the effect of LED illumination was examined as a potential means to improve lighting uniformity between culture tiers and to increase the efficiency of the available pond space for production. A broader spectrum from white LEDs may better suit Laktud's growth requirements, perhaps stimulating not only photosynthesis but also other physiological processes essential for elongation (Kim et al., 2023). This is supported by Alrajhi et al. (2023),

who found that the light spectrum significantly influenced many plant properties. However, the results should be considered as discrete observations at the plate level and not the treatment means, and further investigation is required to understand the impacts of lighting conditions and culture placement on growth performance.

However, according to the two-way ANOVA, it shows that there is no significant difference in frond length between light exposure ($p = 0.260$) and cultivation weeks ($p = 0.099$). However, the trends show that the LED light had the longest length in week 4, and the natural sunlight decreased in week 2.

The weight graph in Figure 5 illustrates the growth pattern for Laktud under all light conditions. At Week 4, the maximum weight reached was 1305 g for W2. Meanwhile, pink LED light indicated positive but slightly lower growth, with P3 reaching 1200 gram. However, natural sunlight showed inconsistent trends: S1 achieved a result similar to that under pink LED light, whereas S2 and S3 declined in weight. This underscores that Laktud received non-uniform light distribution under natural sunlight cultivation.

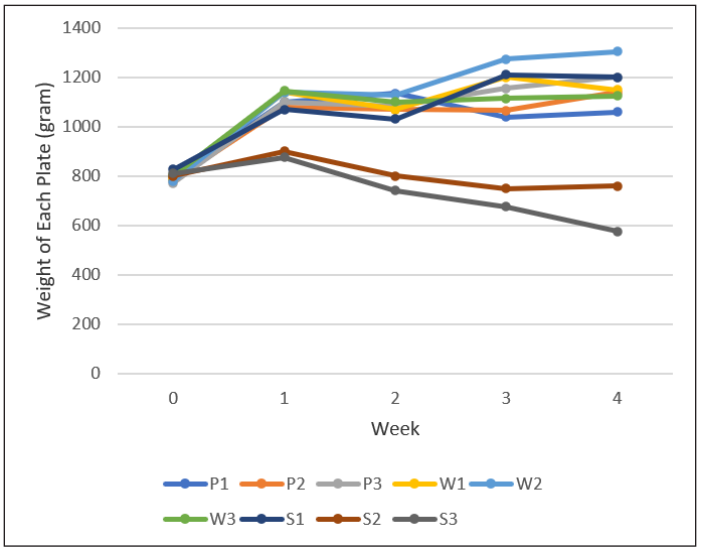

Figure 5. Weight of each plate in four weeks

White LED plates performed well, with W2 recording the highest biomass yield of 247.76 g m^{-2} day^{-1} among all plates (Figure 7). The daily growth rate (DGR) was also higher in LED-treated plates, with W2 having the highest DGR of 0.018551 day^{-1} as shown in Figure 6. These findings indicate that controlled, consistent LED lighting, particularly full-spectrum light, is significantly better for *Caulerpa lentillifera* biomass development than variable natural sunlight (Yang et al., 2022).

The one-way ANOVA showed no statistically significant differences in DGR ($p = 0.108$) or biomass yield ($p = 0.117$) between the lighting treatments. The white LED

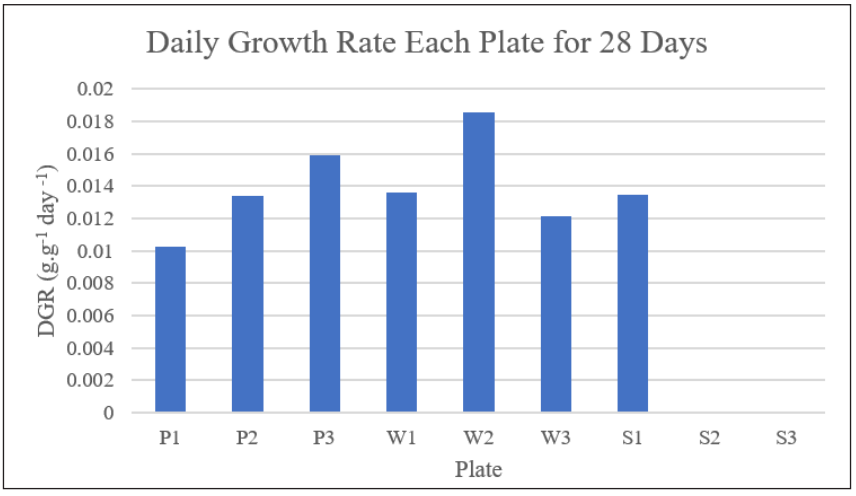

Figure 6. Daily growth rate for each cultivation plate (day^{-1})

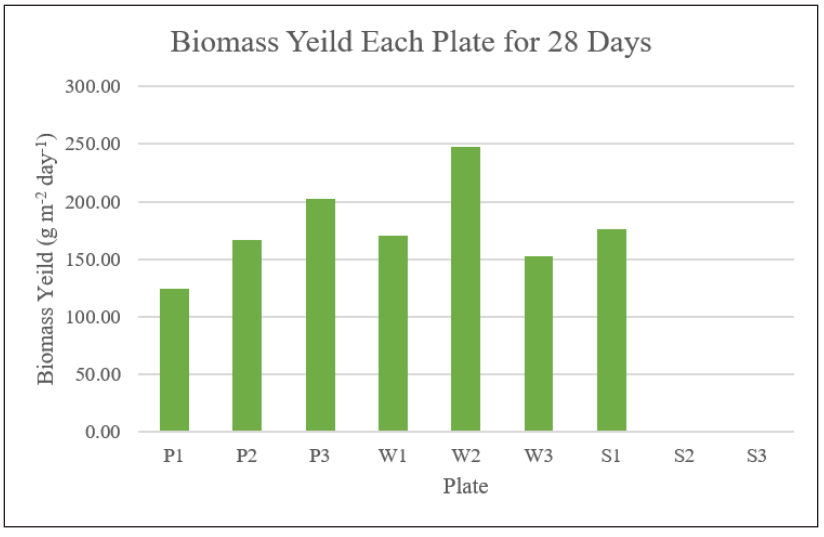

Figure 7. Biomass yield for each cultivation plate ($g\ m^{-2}\ day^{-1}$)

showed the highest mean values of both parameters, indicating its ability to induce growth and biomass yield. However, a larger sample size is needed to more accurately assess the effects of different lighting treatments on the growth performance of *Caulerpa lentillifera.*

The findings of this study underscore the potential benefits of multilevel cultivation using LED lighting for the cultivation of *Caulerpa lentillifera*. Controlled and consistent light distribution resulting from LED light offers a sustainable alternative to traditional sun-reliant cultivation and supports higher growth rate and biomass yield. Consequently, this innovation can enhance the productivity of *Caulerpa lentillifera*, which cannot meet

demand due to stock shortages resulting from overharvesting and unpredictable weather (Qudus et al., 2020).

CONCLUSION

In conclusion, multilevel cultivation with LED lighting is a feasible approach to increase the light distribution and support the growth of Laktud under land-based cultivation conditions in Kubang Badak, Langkawi. The LED lighting provides a more even distribution of light throughout the production system, unlike natural sunlight, which is affected by shade at the lower levels of cultivation. The results highlight the need for suitable lighting conditions for seaweed growth and the potential for multi-level cultivation. However, this study concentrated mainly on lighting conditions and growth performance, and the economic viability, long-term sustainability and socio-economic benefits of this cultivation technique were not directly addressed. Future studies should address the impact of different light intensities and cultivation conditions, energy consumption, production costs and economic feasibility to evaluate the feasibility of multilevel LED cultivation for sustainable seaweed production and its contribution to the development of coastal communities. This contributes to achieving the 17 United Nations Sustainable Development Goals (SDGs).

ACKNOWLEDGEMENT

The author expresses gratitude to Ts. Dr. Jamil Tajam and Dr. Non Daina Masdar for their advice and assistance, as well as the contributions of the academic and non-academic staff. Special thanks are due to UiTM Marine Research Station (MARES) and the Faculty of Applied Sciences, Universiti Teknologi MARA, Perlis Branch, Arau Campus. The author welcomes the local community's engagement and input. This study was funded by the project "Kajian Sosial: Pengembangan Produk Inovasi berasaskan Rumpai Laut untuk Komuniti Perikanan di Kampung Kelubi, Langkawi" (UiTM.800-3/2 GOV (071/2025).

REFERENCES

Alrajhi, A. A., Alsahli, A. S., Alhelal, I. M., Rihan, H. Z., Fuller, M. P., Alsadon, A. A., & Ibrahim, A. A. (2023). The effect of LED light spectra on the growth, yield and nutritional value of red and green lettuce (*Lactuca sativa*). *Plants, 12*(3), Article 463. https://doi.org/10.3390/plants12030463

Apriliyanti, F. J., Risjani, Y., Hertika, A. M. S., & Paricahya, A. F. (2024). Growth analysis of *Caulerpa lentillifera* cultivated at laboratory scale with different light intensities. *Jurnal Penelitian Pendidikan IPA, 10*(5), 2346-2353. https://doi.org/10.29303/jppipa.v10i5.6126

Azcárate-García, T., Beca-Carretero, P., Cara, C. L., Villamayor, B., Cosnett, E., Bermejo, R., Hernández, I., Brun, F. G., & Stengel, D. B. (2022). Seasonal plant development and meadow structure of Irish and southern Spanish seagrass populations. *Aquatic Botany, 183*, Article 103569. https://doi.org/10.1016/j.aquabot.2022.103569

Fakhrulddin, I. M., Harah, Z. M., Shiamala, R. D., & Azrie, A. M. (2021). Effect of salinity, light and fertilizer on Caulerpa lentillifera under culture conditions. *AIP Conference Proceedings, 2347*(1), Article 020074. https://doi.org/10.1063/5.0051569

Gao, X., Choi, H. G., Park, S. K., Sun, Z. M., & Nam, K. W. (2019). Assessment of optimal growth conditions for cultivation of the edible *Caulerpa okamurae* (Caulerpales, Chlorophyta) from Korea. Journal of Applied Phycology, 31, 1855-1862. https://doi.org/10.1007/s10811-018-1691-z

Islam, Z., Khatoon, H., Minhaz, T. M., Rahman, M. R., Hasan, S., Mahmud, Y., Hossain, M. S., & Sarker, J. (2021). Data on growth, productivity, pigments and proximate composition of indigenous marine microalgae isolated from Cox's Bazar Coast. *Data in Brief, 35*, Article 106860. https://doi.org/10.1016/j.dib.2021.106860

Kim, S.-H., Park, J.-H., Kim, E.-J., Lee, J.-M., Park, J.-W., Kim, Y.-S., Kim, G.-R., Lee, J.-S., Lee, E.-P., & You, Y.-H. (2023). White LED lighting increases the root productivity of Panax ginseng C. A. Meyer in a hydroponic cultivation system of a plant factory. *Biology, 12*(8), Article 1052. https://doi.org/10.3390/biology12081052

Phang, S. -M, Yeong, H. -Y, & Lim, P. -E. (2019). The seaweed resources of Malaysia. *Botanica Marina, 62*(3), 265-273. https://doi.org/10.1515/bot-2018-0067

Phang, S.-M., Wong, C.-L., Lim, P.-E., Yeong, H.-Y., & Chan, C.-X. (2005). Seaweed diversity of the Langkawi Islands with emphasis on the northeastern region. *Malaysian Journal of Science, 24*, 77-94. https://ejournal.um.edu.my/index.php/MJS/article/view/8823

Qudus B Aroyehun, A., Abdul Razak, S., Palaniveloo, K., Nagappan, T., Suraiza Nabila Rahmah, N., Wee Jin, G., Chellappan, D. K., Chellian, J., & Kunnath, A. P. (2020). Bioprospecting cultivated tropical green algae, *Caulerpa racemosa* (Forsskal) J. Agardh: A perspective on nutritional properties, antioxidative capacity and anti-diabetic potential. *Foods, 9*(9), Article 1313. https://doi.org/10.3390/foods9091313

Rueangnoi, W., Saoseesawat, A., Kongkaew, W., & Pattarapanyawong, N. (2025). A preliminary study on using mixed light from LED for indoor cultivation of Caulerpa lentillifera J. Agardh, 1837. *Journal of Science and Technology Kasetsart University, 14*(2). https://doi.org/10.56825/jstku.2025.1423013

Sinurat, E., & Fadjriah, S. (2019). The chemical properties of seaweed *Caulerpa lentifera* from Takalar, South Sulawesi. *IOP Conference Series: Materials Science and Engineering, 546*(4), Article 042043. https://doi.org/10.1088/1757-899X/546/4/042043

Stuthmann, L. E., da Costa, B. B., Springer, K., & Kunzmann, A. (2023). Sea grapes (*Caulerpa lentillifera* J. Agardh, Chlorophyta) for human use: Structured review on recent research in cultivation, nutritional value, and post-harvest management. *Journal of Applied Phycology, 35*, 2957-2983. https://doi.org/10.1007/s10811-023-03031-x

Yang, J., Song, J., & Jeong, B. R. (2022). Lighting from top and side enhances photosynthesis and plant performance by improving light usage efficiency. *International Journal of Molecular Sciences, 23*(5), Article 2448. https://doi.org/10.3390/ijms23052448

Zuldin, W. H., Muhamad Shaleh, S. R., & Shapawi, R. (2019). Growth, biomass yield, and proximate composition of sea vegetable, *Caulerpa macrodisca* (Bryopsidales, Chlorophyta) cultured in tank. *Philippine Journal of Science, 148*(1), 1-6. https://philjournalsci.dost.gov.ph/growth-biomass-yield-and-proximate-composition-of-sea-vegetable-caulerpa-macrodisca-bryopsidales-chlorophyta-cultured-in-tank/

REFEREES FOR THE PERTANIKA

JOURNAL OF TROPICAL AGRICULTURAL SCIENCE

Vol. 49 (5) Oct. 2026

The Editorial Board of the Pertanika Journal of Tropical Agricultural Science wishes to thank the following:

Abdul Halim Farawahida
(UTHM, Malaysia)

Ahmad Shofy Mubarak
(UNAIR, Indonesia)

Aimi Athirah Aznan
(UniMAP, Malaysia)

Ajai Kumar Tiwari
(ICAR, India)

Allah Wadhayo Gandahi
(SAU, Pakistan)

Amir Syariffuddeen Mhd Adnan
(MARDI, Malaysia)

Andri Prima Nugroho
(UGM, Indonesia)

Azmiza Syawani Jasni
(UPM, Malaysia)

Choon Yong Cheok
(UCSI, Malaysia)

Deniz Ergüden
(ISTE, Turkey)

Diaa Fliah Hasan
(UOQASIM, Iraq)

Duc Nguyen Van
(HUAF, Vietnam)

Emmanuel Daniya
(FUTMINNA, Nigeria)

Eny Ida Riyanti
(BRIN, Indonesia)

Fazleen Izzany Abu Bakar
(UTHM, Malaysia)

Ferisman Tindaon
(UHN, Indonesia)

Hesham Abozaid
(NRC, Egypt)

Intan Suhana Zulkafli
(UM, Malaysia)

Jessa Ata
(UPLB, Philippines)

Jayakrishna Kandasamy
(VIT, India)

Khairun Nisaa' Mohd Nor
(UiTM, Malaysia)

Komariah
(UNS, Indonesia)

Leonardo Airton Ressel Simões
(UFRGS, Brazil)

Md. Kamal Uddin
(UPM, Malaysia)

Mohamed Thariq Hameed Sultan
(UPM, Malaysia)

Mohammed Abdulhadi
(UODIYALA, Iraq)

Mohd Aizudin Abdul Aziz
(UMPSA, Malaysia)

Mohd Farid Ahmad
(FRIM, Malaysia)

Mohd Norsazwan Ghazali
(UPM, Malaysia)

Muhamad Hazim Nazli
(UPM, Malaysia)

Muhammad Tuseef Asghar
(UAF, Pakistan)

Nasrul Fikry Che Pa
(UTHM, Malaysia)

Norazlin Abdullah
(UTHM, Malaysia)

P. Uma Maheswara Rao
(CAPOL, India)

Purwanto
(UNSOED, Indonesia)

Rahmi Nurdiani
(UB, Indonesia)

Raihana Zahirah Edros
(UMP, Malaysia)

Raimundo Jimenez-Ballesta
(UAM, Spain)

Rawee Chiarawipa
(PSU, Thailand)

S. Chandra Mohan Reddy
(ANGRAU, India)

Saran Chaweerak
(UBRU, Thailand)

Setia Girsang
(BRIN, Indonesia)

Shahidah Md. Nor
(UPM, Malaysia)

Siti Maslizah Abdul Rahman
(UiTM, Malaysia)

Siti Saripa Rabiah Mat Lazim
(UPM, Malaysia)

Suciyono
(UNAIR, Indonesia)

Surisa Phornvillay
(UNIMAS, Malaysia)

Violijim Ranay Arangote
(SNCAT, Philippines)

Wan Fatin Amira Wan Mohd Zawawi
(UTM, Malaysia)

Wan Maznah Wan Omar
(USM, Malaysia)

Yugi R Ahadiyat
(UNSOED, Indonesia)

Zafri Hassan
(UPM, Malaysia)

Zetty Azalea Sutirman
(UTM, Malaysia)

ANGRAU	-	*Acharya N.G. Ranga Agricultural University*
BRIN	-	*National Research and Innovation Agency*
CAPOL	-	*Coromandel Agro Products and Oils Limited*
FRIM	-	*Forest Research Institute Malaysia*
FUTMINNA	-	*Federal University of Technology Minna*
HUAF	-	*Hue University of Agriculture and Forestry*
ICAR	-	*Indian Agricultural Research Institute (IARI)*
ISTE	-	*İskenderun Technical University*
MARDI	-	*Malaysian Agricultural Research and Development Institute*
NRC	-	*National Research Centre*
PSU	-	*Prince of Songkla*
SAU	-	*Sindh Agriculture University*
SNCAT	-	*Surigao del Norte College of Agriculture and Technology*
UAF	-	*University of Agriculture Faisalabad*
UAM	-	*Universidad Autónoma de Madrid*
UB	-	*Universitas Brawijaya*
UBRU	-	*Ubon Ratchathani Rajabhat University*
UCSI	-	*University College Sedaya International*
UFRGS	-	*Federal University of Rio Grande do Sul*
UGM	-	*Universitas Gadjah Mada*
UHN	-	*Universitas HKBP Nommensen*
UiTM	-	*Universiti Teknologi MARA*
UM	-	*Universiti Malaya*
UMP	-	*Universiti Malaysia Pahang*
UMPSA	-	*Universiti Malaysia Pahang Al-Sultan Abdullah*
UNAIR	-	*Universitas Airlangga*
UniMAP	-	*Universiti Malaysia Perlis*
UNIMAS	-	*Universiti Malaysia Sarawak*
UNS	-	*Universitas Sebelas Maret*
UNSOED	-	*Universitas Jenderal Soedirman*
UODIYALA	-	*University of Diyala*
UOQASIM	-	*Al-Qasim Green University*
UPLB	-	*University of the Philippines Los Baños*
UPM	-	*Universiti Putra Malaysia*
USM	-	*Universiti Sains Malaysia*
UTHM	-	*Universiti Tun Hussein Onn Malaysia*
UTM	-	*Universiti Teknologi Malaysia*
VIT	-	*Vellore Institute of Technology*

While every effort has been made to include a complete list of referees for the period stated above, however if any name(s) have been omitted unintentionally or spelt incorrectly, please notify the Chief Executive Editor, *Pertanika* Journals at executive_editor.pertanika@upm.edu.my

Any inclusion or exclusion of name(s) on this page does not commit the *Pertanika* Editorial Office, nor the UPM Press Centre or the university to provide any liability for whatsoever reason.

Two New Localisation Records of *Priacanthus sagittarius* (Starnes, 1988) in the Westernmost Part of the Levant Sea 2461
Alper Yıldız, M. Tunca Olguner, Mehmet Gökoğlu, Jale Korun, and Mesut Yılmaz

The Effect of Number of Shoots of Sorghum in First and Second Ratoon System 2467
Avisema Sigit Saputro, Samanhudi, Puji Harsono, and Supriyono

Identification and Diversity Analysis of *Uromycladium* on *Paraserianthes lophantha* subsp. *montana* Using a Multilocus Molecular Approach 2483
I Made Mayun Maha Diputra, Sri Rahayu, Intan Berlian, and Tanaka Chihiro

Aquaponics as a Sustainable Food Security Solution: Global Scholarly Trends and Intellectual Structure Analysis 2499
Nor Azilah Husin, Amirul Syafiq Mohd Ghazali, Azni Abdul Rashid, Nurzalyna Mohamed Zaki, and Nasser Al Yahyaei

Evaluation of the Aqueous Extracts of *Celosia argentea* L. (Plumosa Group) as a Bioherbicide for Dominant Weeds in Soybean Cultivation 2523
Safira Nur Aini, Dyah Weny Respatie, Aziz Purwantoro, and Qurrotul Uyun

Growth, SPAD Index, and Nitrogen Use Efficiency of Two *Axonopus compressus* Variants Under Soil Mixture Ratios and NPK Fertiliser Regimes 2545
Ting Zeng, Abdul Shukor Juraimi, Nazatul Shima Naharudin, Mahmudul Hasan, and Muhammad Saiful Ahmad-Hamdani

Classification and Prediction of Chilli Powder (*Capsicum Annuum* L.) Colour Based on Near-Infrared Spectra and Random Forest 2565
Nafis Khuriyati, Anggoro Cahyo Sukartiko, Ririn Nur Alfiani, Tyasto Prima Ahmadi, and Avicenna Nur Kasih

Microbiological Quality, Antibiotic Susceptibility and Stability of Human Breast Milk Microbiota Stored at Refrigerated Temperature 2581
Nur Hanis Salim, Zulfa Zakuan, Rashidah Sukor, Aliah Zannierah Mohsin, Yaya Rukayadi, Nurul Hawa Ahmad, Yu Suet Li, Siti Nabilah Karim, and Anis Shobirin Meor Hussin

Maximising Growth and Quality of *Caulerpa lentillifera* Through Multilevel Cultivation with LED Approach 2603
Nur Amira Yasmin Mohd Nizar, Jamil Tajam, Non Daina Masdar, Zamzila Erdawati Zainol, Mohamad Niza Md Nor, Khairul Naim Abd Aziz, and Sharir Aizat Kamaruddin

Comparative Shelf-Life Predictions of Packaged Paddy Using Water Mass-Transfer Modelling and Quality-Deterioration Kinetics Under Different Controlled Relative Humidities 2257
Astriella Awwali Maissy, Sri Rahayoe, and Hanim Zuhrotul Amanah

Visible-Near Infrared Spectroscopy for Predicting Carotenoid and Antioxidant Composition in Healthy and Bronzed Jackfruit (*Artocarpus heterophyllus* Lam. cv. Tekam Yellow) at Different Maturity Stages 2275
Kok Jeng Lim, Phebe Ding, Nazmi Mat Nawi, and Mashitah Jusoh

Review Article 2303
An In-Depth Analysis of Cottonseed Oil and Its Composition, Digestibility, Health-Promoting Properties, Industrial Relevance, Animal Feed Value, and Green Technologies
Savanam Chandra Sekhar, Degala Pushpa Sri, Mohammed Irfan, Meeravali Shaik, B. Vasantha Lakshmi, Krishna Babu Sambaru, and Palagiri Tejovathi

Comparative Phytochemical and Biological Properties of Unripe *Spondias pinnata* Fruit Extract 2323
Rattana Meekrasae, Noppadon Somphol, Wuttisak Kunu, and Supawadee Patathananone

Antioxidant Film Packaging from Red Tilapia Fish Scale Gelatin with Kesum (*Persicaria Odorata*) Powder 2343
Nur Syazwani Yusri, Roseliza Kadir Basha, Siti Nurnajihah Salahuddin, Nazatul Shima Azmi, Farah Saleena Taip, Noor Zafira Noor Hasnan, and Nor Amaiza Mohd Amin

Comparison of Plant Nutrient Requirements During the Annual Phenological Development of Young Rubber Trees (*Hevea brasiliensis* Mull. Arg.) Prior to the Rubber Tapping Process in Upland and Lowland Areas 2361
Surachart Pechkeo and Sayan Sdoodee

Integrated Effects of DAP Fertiliser, Soil Amendments, and Nano-Biostimulant Foliar Application on Growth and Yield of Wheat 2387
Maher Adhafa Drai'am Al-Aboudi, Hayyawi W. A. Al-Juthery, and Luma Abdalalah Sagban Alabadi

Microalgae for Anti-Aging Cosmeceuticals: Synergistic Bioactivities and Physicochemical Potential 2413
Felicia Stella Indarto, Sook Chin Chew, Fatimah Md Yusoff, Malinna Jusoh, and Norazira Abdu Rahman

Combination Effects of Cocopeat and Chicken Manure on the Vegetative Growth and Yield Performance of Eggplant 2439
Kahar, Rian Christian Sondakh, and Irmawati

Pertanika Journal of Tropical Agricultural Science
Vol. 49 (5) Oct. 2026

Content

Foreword xiii
Md Kamal Uddin

Review Article 2115
Synergy of *Bradyrhizobium* spp. and Co-Inoculants to Enhance Fertiliser Efficiency and Soybean Yield in Acid-Stressed Soils: A Systematic Review
Josephine Alexa Mada, Stanislaus Adhi Pramudya, Mieke Rochimi Setiawati, Fairus Hisanah Hibatullah, and Tualar Simarmata

Physiological and Metabolic Responses of Early Juvenile Blue Swimming Crab, *Portunus pelagicus*, to Dietary Deficiency 2133
Jamali Muhammad-Firdaus, Ariffin Hidir, Donald Torsabo, Hon Jung Liew, Mhd Ikhwanuddin, and Noordiyana Mat Noordin

Review Article 2155
A Review on the Use of Spices in the Blending of Malaysian Curry Powder Matrix
Chon Lok Siaw, Nyuk Ling Chin, and Nor Amaiza Mohd Amin

Biofertilisers and Micronutrients Enhance Productivity and Land-Use Efficiency of Cereal-Legume Intercropping Systems on Indonesian Drylands 2171
Yanto Surdianto, Nana Sutrisna, Muhammad Iskandar Ishaq, Bambang Susanto, Yiyi Sulaeman, Eni Maftu'ah, Dwi Purnamawati Widiastuti, Jumakir, and Agus Nurawan

Ameliorative Effects of dbcAMP and des (1-3) IGF-1 on Myogenic and Adipogenic mRNA Expression in Transdifferentiated C2C12 Myogenic Cells 2197
Muhamad Faris Ab Aziz , Zoe C.T.R. Daniel, Andrew Salter, and Tim Parr

Gallic Acid-Loaded Graphene Oxide (GAGO) Nanocomposite Attenuates Inflammatory Response in LPS-Stimulated RAW 264.7 Macrophages 2217
Nur Hazwani Norjoshukrudin, Ida May Jen Ng, Seri Narti Edayu Sarchio, Masriana Hassan, Shafinaz Abd Gani, and Suhaili Shamsi

Integrating *Brassica* spp. Residues and Bioethanol to Mitigate Disease and Enhance Potato Seed Yield in Medium-Altitude Regions 2237
Andi Muhibuddin, Zulkifli Maulana, Fatmawati, Haris Mahmud, and Andi Tenri Fada

Pertanika Editorial Office, Journal Division,
Putra Science Park,
1st Floor, IDEA Tower II,
UPM-MTDC Center,
Universiti Putra Malaysia,
43400 UPM Serdang,
Selangor Darul Ehsan
Malaysia

http://www.pertanika.upm.edu.my
Email: executive_editor.pertanika@upm.edu.my
Tel. No.: +603- 9769 1622

PENERBIT UPM
UPM PRESS

http://penerbit.upm.edu.my
Email: penerbit@upm.edu.my
Tel. No.: +603- 9769 3606

e-ISSN 2231-8542